N O T I C E

THIS DOCUMENT HAS BEEN REPRODUCED FROM
MICROFICHE. ALTHOUGH IT IS RECOGNIZED THAT
CERTAIN PORTIONS ARE ILLEGIBLE, IT IS BEING RELEASED
IN THE INTEREST OF MAKING AVAILABLE AS MUCH
INFORMATION AS POSSIBLE

1 + 15

Final Reports of U.S. Rat Experiments Flown on the Soviet Satellite Cosmos 1129

August 1981
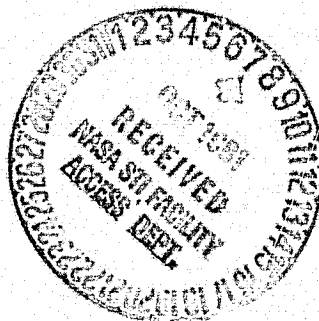
Final Reports of U.S. Rat Experiments Flown on the Soviet Satellite Cosmos 1129

Milton R. Heinrich and Kenneth A. Souza (Editors)
Ames Research Center, Moffett Field, California

NASA

National Aeronautics and
Space Administration

Ames Research Center
Moffett Field, California 94035

TABLE OF CONTENTS

PREFACE

On September 25, 1979, the Soviet Union launched Cosmos 1129, an unmanned spacecraft carrying biological and radiation physics experiments from nine countries, including fourteen from the United States. The launch marked the third time the Soviet Union has flown US experiments aboard one of its unmanned spacecraft. The first two, Cosmos 782 and 936, were launched November 1975 and August 1977, respectively.

Cooperation between the US and USSR in the area of Space Biology and Medicine began in 1971 with the signing of the US/USSR Science and Applications Agreement. A Joint Working Group for Space Biology and Medicine was established and met periodically to exchange information obtained during spaceflights and to discuss problems and topics of mutual scientific interest. In October of 1974, during the fifth meeting of the Joint Working Group, the Soviets offered to fly US experiments aboard an unmanned spacecraft which was scheduled for launch during the winter of 1975. The US accepted this offer and submitted experiment proposals to the Soviets. A group of 11 experiments was selected and subsequently flown on Cosmos 782 which remained in orbit 19.5 days. Since Cosmos 782, the US has flown seven experiments on Cosmos 936 and fourteen experiments on the most recent joint US/USSR venture, Cosmos 1129.

Cosmos 1129, like the Cosmos 782 and 936 flights, contained experiments which were directed at determining the effects of spaceflight on a variety of biological specimens, including animals, plants, and insects. Although all three of these Cosmos flights were unmanned, many of the experiments they contained focused on problems common to both man and animals during prolonged spaceflight. Rats, for example, were used to investigate alterations in normal bone chemistry, muscle structure, and general physiology resulting from spaceflight, alterations that have been observed in both astronauts and cosmonauts during and following stays in space. Rats were also used, together with a variety of other biological and nonbiological material, to measure cosmic radiation and assess its potential hazard to man during prolonged spaceflights.

The scientific results of U.S. experiments flown on Cosmos 1129 are presented in two separate volumes; one entitled, "Final Reports of U.S. Plant and Radiation Dosimetry Experiments Flown on the Soviet Satellite, Cosmos 1129," and the other entitled, "Final Reports of U.S. Rat Experiments Flown on the Soviet Satellite, Cosmos 1129." As evidenced by the scientific results presented in these volumes, the Cosmos 1129 mission has made a substantial contribution to Space Biology and Medicine. In addition, a low-cost systematic approach to the development, testing, and utilization of experimental hardware has been established which will be applied to the preparation of US biological experiments for flight aboard the Space Shuttle. But perhaps the most important result derived from the Joint US/USSR Biological Satellite Program has been the level of international cooperation achieved. American and Soviet scientists and engineers working together overcame the difficulties of language and logistics to conduct spaceflight experiments, share the results, and discuss their significance.

It has been a pleasure to have taken part in this program and, on behalf of all members of the NASA and the scientific community who participated in the Cosmos 1129 mission, I would like to extend our sincere thanks to the Soviet government for making our participation possible and to our Soviet colleagues for their devoted assistance in the execution of our experiments.

Kenneth A. Souza
Manager, Cosmos Project
NASA-ARC

COSMOS 1129 MISSION DESCRIPTION

KENNETH A. SOUZA

MANAGER, COSMOS PROJECT

BIOSYSTEMS DIVISION

NATIONAL AERONAUTICS AND SPACE ADMINISTRATION

AMES RESEARCH CENTER

MOFFETT FIELD, CA 94035

Abstract

On September 25, 1979, the Soviet Union launched Cosmos 1129, an unmanned spacecraft carrying biology and physics experiments from 9 countries including both the Soviet Union and the U.S.A. The launch marked the third time the Soviet Union has flown U.S. experiments aboard one of its unmanned spacecraft. The first was Cosmos 782 in November 1975 and the second, Cosmos 936 in August 1977. All three flights have carried a variety of biological species and remained in orbit approximately 19 days. Aboard Cosmos 1129 were: 1) 30 young male Wistar SPF rats used for a wide range of physiological studies, 2) experiments with plants, fungi, insects, and mammalian tissue cultures; 3) radiation physics experiments; 4) a heat convection study; 5) a rat embryology experiment in which an attempt was made to breed 2 male and 5 female rats during the flight; and 6) fertile quail eggs used to determine the effects of spaceflight on avian embryogenesis. After 18.5 days in orbit the spacecraft landed in Central Asia where a Soviet recovery team began experiment operations, including animal autopsies, within a few hours of landing. Seven animals were autopsied at the recovery site and the remainder returned to Moscow for readaptation studies. Specimens for US experiments were initially prepared at the recovery site or in Moscow and transferred to US laboratories for complete analyses. An overview of the mission focusing on preflight, on-orbit, and postflight activities pertinent to the fourteen US experiments aboard Cosmos 1129 is presented.

Introduction

A series of Soviet Biological Satellites has been launched at approximately 2-year intervals, beginning with Cosmos 605 in 1973. Participation of the United States began in 1975 with the third mission (Cosmos 782), by invitation of the USSR. The fifth and most recent mission, Cosmos 1129, was launched September 25 and recovered 18.5 days later on October 14, 1979 (Table I). The principal objective of the Cosmos missions is to determine the effects of spaceflight on biological materials, focusing on biomedical problems observed in both men and animals during spaceflight. Areas of special interest include muscle atrophy, space sickness, bone mineral loss, radiation, and plant growth and development. Cosmos 1129 differed from previous missions in providing an opportunity to study the progeny of rats bred during spaceflight and the development of Japanese quail embryos during weightlessness*.

Nine countries participated in the Cosmos 1129 mission. In addition to experiments from the US and USSR, the mission included experiments from

---

*Although the term "weightlessness" is used here and in other reports of this volume, it should be noted that complete weightlessness (the absence of all accelerations) was not achieved. The spacecraft rotated in orbit and imparted accelerations to experiments located at the edge of the spacecraft of 1.7×10^{-7} to 1.5×10^{-4} x g. Accelerations to rats were actually lower because rat holding units were located near the center of the spacecraft. These accelerations are generally thought to be below the threshold of biological sensitivity.

Czechoslovakia, France, Hungary, Poland, Rumania, Bulgaria, and the German Democratic Republic. Every attempt was made to maximize the scientific return from the mission and, to this end, investigators from the nine participating countries examined virtually every organ and piece of tissue from all the specimens flown. Exemplifying such attempts were the wide variety of experiments performed on the rats. Approximately 50 experiments were conducted with the rats, involving over 100 scientists. A short descriptive title and the sponsoring country for these experiments is given in Table 2. Table 3 lists the participating institutions from each country.

The involvement in the mission of scientists from countries other than the USSR was much the same. In nearly all cases, Soviet scientists were trained by the principal investigators to perform preflight and postflight procedures (e.g., drug injections, blood sample collection, tissue removal and preparation), required for various experiments. Following the flight, a team of Soviet scientists and engineers were transported to the satellite landing site where a portable field laboratory was set up. Experimental procedures at the recovery sites were designed to obtain and process tissue specimens to a point where they could be frozen or preserved and subsequently sent to the principal investigators for analysis.

In the following sections of this chapter, a general description of the Cosmos 1129 mission operations, particularly those pertinent to US experiments, is presented and will provide a foundation for understanding and interpreting the reports of US experiments contained in this volume.

The pre- and post-flight activities performed in support of non-US experiments, and which had no impact on them, will appear in the Soviet final mission report and were not included here.

THE SPACECRAFT

A modified Vostok spacecraft similar to that used for previous biological satellites, Cosmos 605, 690, 782, and 936 as well as the early Soviet manned spaceflights, was used for the Cosmos 1129 mission. It was a spherical craft approximately 2.5 meters in diameter with a 900 Kg payload and a gross weight of approximately 2250 Kg (Fig. 1). During flight, the power required by the spacecraft was supplied by batteries. The atmosphere within the craft was maintained at approximate sea level conditions. Total pressure averaged 780 mm throughout the flight, with a pO_2 of 135-212 mm mercury and a pCO_2 of up to 7 mm. Relative humidity within the spacecraft during flight was 56-66%. Gaseous impurities generated within the cabin, e.g., ammonia and methane, were kept at low levels by circulating cabin air through cannisters containing absorbent materials. Ambient temperature within the spacecraft during flight ranged from 22-25°C.

Within the spacecraft, biological specimens and experiments were contained in a variety of hardware. Of primary interest to US investigators were the rat holding units (Fig. 2). Rats were held throughout the flight in individual cages, each containing its own light, food, water, air circulating, and waste management systems. Each cylindrically shaped cage was approximately 200 mm deep and 100 mm in diameter. Light was regulated

to a 12/12 hour light/dark cycle with a 2-lux intensity within each cage. Ten-gram quantities of a special paste diet were provided to the animals four times/day at 6-hour intervals throughout the flight. This same diet was provided to both flight and ground control animals. All animals were placed on this diet approximately 10 days before launch and kept on the diet throughout the flight and 29-day recovery phases of the mission. Water was provided ad libitum at all times. Cabin air was drawn into each cage at the rear and was dispersed from the cage ceiling through a series of holes in a plastic cage liner. The air flow passed downward over the animal, forcing animal wastes and debris into a waste collection trap which rotated to present a clean trap to the animal at 2-day intervals. Air passing through the waste trap was then circulated through activated charcoal filters and returned to the cabin. Surrounding the plastic cage liner was a wire coil through which an electric current was passed and changes in current were monitored as the animal moved through the cage and the data used to determine gross motor activity during flight.

In addition to the 30 cages described above, the spacecraft contained a rodent mating chamber which housed 5 female and 2 male rats (Fig. 3). The chamber was partitioned into two sections which segregated the males from the females until day two of flight whereupon two doors in the partition were opened, permitting males and females to mingle. The dimensions of the male chamber were 17.0 cm x 20.0 cm x 16.0 cm, and of the female chamber, 48.0 cm x 20.0 cm x 16.0 cm. Within the chamber the animals had access to 8 feeding stations, each of which presented approximately 10 gram aliquots of the standard paste diet at 6 hour intervals throughout the flight. The light/dark regimen was the same as that used for the standard rat cages, 12/12 hours.

Payload

The Cosmos 1129 payload consisted of:

o Rats

Thirty male Wistar specific pathogen free (SPF) rats were obtained from the Institute of Experimental Endocrinology of the Slovakian Academy of Sciences, Bratislava, Czechoslovakia. These animals were used for a wide variety of physiological studies. The rats were approximately 85 days old and weighed an average of 300 gms at the start of the experiments.

These thirty male rats were divided into five groups:

    Group 1 - 7 rats
    Group 2 - 6 rats
    Group 3 - 7 rats
    Group 4 - 5 rats
    Group 5 - 5 rats

Following spacecraft recovery, animals in Group 1 were sacrificed 7-11 hours after the spacecraft landed; Group 2 and 3 animals were sacrificed six days postflight; Group 4 animals were sacrificed 29 days postflight; and Group 5 animals were sacrificed 32 to 37 hours postflight.

In addition, there were 5 female Wistar SPF rats and 2 males which constituted the rodent embryology experiment. Both males and females were proven breeders and their approximate weights at launch were 340 gms and 260 gms, respectively.

o **Plants and Fungi**

Carrots (*Daucus carota*) were used as a substrate for the growth of Crown Gall tumors and as a source of totipotent single cells and small plantlets. Tumor growth was used to assess the effects of spaceflight on the rate of cellular metabolism. The carrot cell culture was used to determine if spaceflight affected plant growth and development.

In addition to carrots, small sprouts (*Arabidopsis thaliana*) and corn seedlings (*Zea mays*) were flown to investigate the growth and development of these species. A multinucleated fungus, (*Physarum polycephalum*) was flown to determine if fungal migration over the solid surface of the growth medium was affected by weightlessness.

o **Insects**

A gravity-gradient experiment with the fruit fly, *Drosophila melanogaster* was designed by Soviet scientists to determine if a gravity preference could be detected in this species. Drosophila eggs were placed in a feeding dish at the hub of a centrifuge (Fig. 4). Connecting the hub to the perimeter of the centrifuge were four tubes inside of which were three food dishes placed along the tube so that

8

when the centrifuge rotated at 53 rpm the gravity levels at the three dishes were 0.3g, 0.6g and 1.0g. Flies hatched on the first day of flight were free to move along the tubes and select the feeding site of preference. Post flight the quantity of eggs and pupal cases found in each feeding dish showed that there was no gravity preference.

o <u>Japanese Quail</u>

Fertilized eggs of the Japanese Quail (<u>Coturnix</u> <u>coturnix</u>) were flown to determine the effects of spaceflight on avian embryological development.

o <u>Mammalian Cell Cultures</u>

Cultures of Chinese hamster and mouse cells were used to determine if weightlessness and/or radiation experienced during spaceflight affect their metabolism and reproduction.

o <u>Radiation Physics Experiments</u>

Radiation physics experiments consisted of dosimetry using biological and nonbiological materials to measure the radiation environment inside and outside the spacecraft, and radiation shielding studies to evaluate electrostatic and dielectric techniques for reducing the level of cosmic radiation within the spacecraft.

o <u>Heat Exchange Experiment</u>

An experiment was designed and flown to study the process of heat exchange between a heated surface and the spacecraft cabin air during spaceflight.

9

MISSION OPERATIONS

In support of the investigations aboard the spacecraft, two different types of ground controls were performed: the Synchronous Control and the Vivarium Control. The Synchronous Control attempted to provide an environment as similar as possible to that experienced by the biological specimens during spaceflight. A spacecraft mockup was loaded with all of the experiments, and specimens were housed in the same type of hardware as that used for flight (Figure 5). Food, water, lighting, temperature, humidity, and airflow were similar for both flight and control groups.

Five days after launch, the Synchronous Control was initiated (September 30, 1979). Animals were subjected to launch stresses similar to those experienced during the actual launch. The noise level was raised to 110 db and a vibration frequency of 50-70 Hz at an amplitude of 0.4 mm was applied to animal holding units for 10 minutes. Immediately following noise and vibration stresses, animals were subjected to acceleration for a period of 10 minutes with a plateau of 4 x g for 7 minutes.

After completion of the Synchronous control on October 19, 1979, reentry stresses were applied to the animals. Those in Groups 4 and 5 were first accelerated for 5 minutes to a plateau of 6 x g for 3 minutes on a centrifuge, and subsequently subjected to an impact shock with a magnitude of 50 x g and a duration of 10 msec. Animals in the embryology experiment and in Groups 1, 2, and 3 received only the 50xg impact shock. Following the application of reentry stresses, the animals as well as all other biological specimens, were handled exactly as the flight specimens.

The purpose of the Vivarium control was to provide a group of minimally stressed animals for comparison with the Flight and Synchronous Control groups. Groups 1, 2, 3 and 5 animals were housed individually in polyvinyl cages (18 x 18 x 12.5 cm) and maintained in that arrangement throughout the flight and postflight periods. Group 4 animals were housed 2-3 per standard vivarium cage (55 x 19.5 x 33 cm) during the flight and postflight phases except on days 3, 8 and 13 postflight when the animals were housed for 36 hours in special metabolic cages 18 x 18 x 12.5 cm. A paste diet identical to that provided to the Flight and Synchronous Control animals was provided to the animals once per day in 40 gm/animal quantities during the preflight and on-orbit phases of the mission; 45 gm/animal was provided once per day during the readaptation period.

In order to simplify information transfer among the many scientists conducting experiments with rats, a common identification code for the rats was established. The code, which is used extensively in the scientific reports which follow, consists of three characters, "A B C", where A is the group number (1-5), B is the test condition (F-flight, S-Synchronous Control, V-Vivarium Control, and FB or SB--a special preflight basal control group for bone experiments), and C is the rat number.

Thus, the rat designated "1-F-1" was a member of Group 1 which flew in space and was designated rat number 1.

Prelaunch Activities

Wistar SPF male rats which comprised the reservoir of experimental animals, were shipped from the Institute of Endocrinology, Slovakian Academy of

Sciences, Bratislava, Czechoslavakia to Moscow during August 1979. In Moscow the animals were placed in a vivarium at the Institute of Biomedical Problems with approximately 5 rats per cage, held at an ambient temperature of 22 ± 2°C, a relative humidity of 80 ± 5% and a 12-hour light day.

During the preflight period, Flight and Control specimens were prepared similarly, e.g., injections, surgery, etc. For example, five Group 4 flight rats and a similar number of animals in the Synchronous control had body temperature transmitters surgically implanted within their peritoneal cavities approximately 1 month before launch. Table 4 lists some of those preflight activities of general interest and those relevant to one or more US experiments.

While in the vivarium, the general health of each animal was monitored through daily examinations. Selection of the animals for the experiments consisted of an initial stage when clinically healthy animals were segregated for preparation for specific experiments. Final selection of animals was carried out during the last few days before launch, after completion of all required injections and surgery.

Approximately 2 weeks before the start of the Flight and Control experiments, all animals were switched from a pellet/seed diet fed ad libitum to the same paste diet which was used during the flight. Forty grams of the paste diet were provided once a day for each animal and water was provided ad libitum. The composition of this diet is given in Table 5.

12

On-Orbit Activities

On September 25, 1979, at 6:30 p.m. (Moscow time), Cosmos 1129 was launched into an elliptical orbit with a perigee of 226 km, an apogee of 406 km, an orbital inclination of 62.8°, and a period of 90.5 minutes. In parallel with the launch, the Vivarium Control commenced at the Institute of Biomedical Problems in Moscow. Five days later, on September 30, the Synchronous Control was initiated.

During the 18.5 day flight, animals were fed and cared for as previously described. Total gross body movement of the Flight and Synchronous Control animals was monitored for 2 hour blocks of time on odd-numbered days throughout the flight phase of the mission. Body temperature was obtained from the Group 4 animals by bio-telemetry on even-numbered flight days. On the second day of the flight, the divider separating male and female rats in the rat embryology experiment was opened and remained opened throughout the remainder of the mission. On the seventh day of flight the temperature of the quail egg incubator was elevated from the spacecraft ambient of $22-25^{\circ}C$ to approximately $37^{\circ}C$. Simultaneously, the relative humidity in the incubator was raised to about 80%. Unfortunately, the humidity control system failed in the flight incubator on day thirteen of flight resulting in a serious drop in the humidity which detrimentally affected the developing embryos.

On flight day 10, the light/dark cycle was reversed in the cages of the Group 4 animals. The reversal was accomplished by subjecting the animals to 24 hours of darkness. This shift in the light/dark cycle was performed

as part of a study to determine if spaceflight affected the biorhythm of these animals and their ability to adapt to an altered day/night cycle. After the flight, these animals were maintained at the inverted light regime.

Postflight Activities

On October 14, 1979, at 7:59 a.m. (Moscow time), Cosmos 1129 touched down near the central Asian city of Kustanay. Within several hours a recovery team consisting of Soviet scientists and engineers arrived at the scene and began assembling a field laboratory (Figs. 6 and 7). The general condition of animals postflight was good. They gained an average of 47 gms during the flight as compared to 54 and 59 gms for Synchronous and Vivarium control animals, respectively.

Only the 7 Group 1 rats were autopsied at the recovery site. Autopsies began at 1:50 p.m. and each autopsy took approximately 30 minutes. All scientific studies were completed in less than 18 hours whereupon the recovery team, specimens, and equipment departed the recovery site and arrived in Moscow in the afternoon of October 15.

During the return trip to Moscow, animals were kept individually in cages measuring 17.0 cm x 17.0 cm x 12.5 cm. The trip lasted approximately 10 hours, and during the trip the animals were provided with 45 gms/animal of the flight diet and water ad libitum. After arriving in Moscow, the Group 2 and 3 animals were transferred to individual metabolic cages 18 cm x 18 cm x 12.5 cm and housed in the Vivarium at the Institute of Biomedical

Problems. These animals continued to receive the flight paste food four times daily but with the total daily quantity increased from 40 to 45 gms. The 5 animals in Group 4 were fed one 45 gm portion per day and were housed 2-3 per cage in the standard vivarium cages (55 cm x 19.5 cm x 33 cm). However, these 5 Group 4 animals were transferred to individual metabolic cages (18 cm x 18 cm x 12.5 cm) on the evenings of postflight days 3, 8, and 13 and held in these cages for 36 hours in order to conduct a variety of metabolic studies. During this period, they were given the flight paste diet in four portions at 6 hour intervals as they had been during the flight. The corresponding control animals were treated similarly.

During hours 7-10 following landing and on days 3, 4, 5, and 6 of the readaptation period, Group 3 animals were subjected to a special stress test designed by Soviet and Czechoslovakian scientists. The animals were fixed in a prone position to a board for 2.5 hours and blood specimens taken before and after this stress. Following the stress on day 6, the animals were sacrificed. The purpose of this stress regime was to determine if animals in the flight group exhibited immediately postflight and during the 6 day readaptation period, blood chemistries indicative of acutely or chronically stressed animals; that is, does the biochemistry of the animals reflect the chronic stress of spaceflight or the more acute stress of reentry.

On October 19, the "flight" phase of the Synchronous control was completed and the same recovery team that processed the flight specimens also processed the controls. Autopsies of the Group 1 animals were begun at 10:04 a.m. and completed by 4:42 p.m. (Moscow time) and the experimental

procedures employed at the recovery site were again followed. Groups 2, 3, 4, and 5 animals were transferred to the Vivarium and treated like the flight animals throughout the readaptation period.

Following the autopsy of the rats and the unique operations required by the many investigators sharing the animals, the specimens were packed for shipment to the appropriate U.S. laboratories according to procedures worked out in advance between Soviet and US mission managers: specimens were packed in dry ice, immersed in a preservative, or brought back alive at 4°C. Specially designed shipping containers were developed to maintain the temperature requirements and integrity of the specimens during transit. On October 29, US specimens and scientists arrived in San Francisco and specimens were transferred to the laboratories of US investigators.

Two weeks after the arrival of the specimens in the US, a second group of US scientists was sent to Moscow to attend the autopsies and experimental operations on the animals (Group 4) allowed to readapt to terrestrial gravity. The same autopsy procedures and team members were utilized for both recovery and readaptation studies. Autopsies of the Flight, Synchronous Control and Vivarium Control Group 4 animals occurred on November 12, 17, and 12, respectively. Samples were again escorted by US scientists back to the US and arrived in San Francisco on November 20, 1979. Temperature recorders contained in all shipping containers indicated that the temperature in all but one container remained within specifications throughout both recovery trips. The exception occurred in a container of preserved Group 4 specimens of some bone and nasal mucosae. In this case a small quantity of dry ice was added to the shipping

container by overzealous cargo handlers in Tokyo. This resulted in the temperature dropping below the specified $0^{o}C$ for a few hours during the Tokyo to San Francisco flight. Fortunately, damage to the specimens was minimal. A summary of the above postflight operations is given in Table 6.

With the return of the experimental samples and materials on November 20, the mission operations phase was brought to an end. For the many investigators involved in the US experiments aboard Cosmos 1129, their work was just beginning, the results of which are contained in the reports which follow.

Acknowledgements

A special thanks is owed to the many individuals who contributed to the success of the US experiments flown on Cosmos 1129, especially to the extremely cooperative group of principal investigators and their experiment teams who worked so diligently in the preparation and execution of their experiments, the small but dedicated group of US Project personnel whose careful attention to detail overcame the tremendous logistics and management problems inherent in an international mission of this nature, and lastly to our Soviet colleagues for their superb assistance in the execution of the US experiments.

TABLE 1

SOVIET BIOLOGICAL SATELLITE MISSIONS

MISSION PARAMETERS	COSMOS-605	COSMOS-690	COSMOS-782*	COSMOS-936*	COSMOS 1129*
LAUNCH DATE	31 OCT '73	22 OCT '74	25 NOV '75	3 AUG '77	25 SEP '79
RECOVERY DATE	22 NOV '73	12 NOV '74	15 DEC '75	22 AUG '77	14 OCT '79
MISSION LENGTH	22 DAYS	20.5 DAYS	19.5 DAYS	18.5 DAYS	18.5 DAYS
PERIOD OF REVOLUTION	90 MIN.	89.6 MIN.	90.5 MIN.	90.7 MIN.	90.5 MIN.
APOGEE	424 KM	389 KM	405 KM	419 KM	406 KM
	(261 MI)	(241 MI)	(251 MI)	(260 MI)	(252 MI)
PERIGEE	221 KM	223 KM	226 KM	224 KM	226 KM
	(135 MI)	(137 MI)	(140 MI)	(139 MI)	(140 MI)
ORBITAL INCLINATION	62.8°	62.8°	62.8°	62.8°	62.8°

*U.S. PARTICIPATION IN MISSION

TABLE 2

DESCRIPTIVE TITLES, SPONSORING COUNTRIES, AND PRINCIPAL INVESTIGATORS

FOR THE EXPERIMENTS OF COSMOS 1129

TITLE	COUNTRY/PRINCIPAL INVESTIGATOR
I. EXPERIMENTS WITH RATS	
1. Whole Body Composition	USSR/A. Ushakov USA/G. Pitts
2. Studies of the Central Nervous System	Czechoslovakia/S. Baransky USSR/R. Tigranyan
3. Endocrine Studies	Czechoslovakia/R. Kvetnansky USSR/R. Tigranyan Bulgaria/*
4. Studies of the Cardiovascular System	Czechoslovakia/S. Baransky USSR/R. Tigranyan
5. Studies of the Musculo-Skeletal System	USSR/V. Oganov S. Oganesyan V. Nesterov E. Kovalenko G. Stupakov A. Prokhonchukov R. Tigranyan USA/ E. Morey-Holton L. Kazarian D. Simmons C. Cann Hungary/T. Szilagyi
6. Blood and Bone Marrow Studies	Czechoslovakia/N. Ahlers E. Mishurova N. Chernaya I. Alers A. Bacek USSR/R. Tigranyan L. Serova V. Korol'kov Bulgaria/*

---

*Principal Investigator not known

19

TABLE 2 (Continued)

7. Studies of Lymphoid Organs

Czechoslovakia/I. Alers
    E. Mishurova
USSR/I. Egorov
    L. Serova

8. Studies of Connective Tissue

USSR/L. Serova
    Bulgaria/*

9. Studies of the Hepatic System

USA/ S. Abraham
USSR/R. Tigranyan
    I. Egorov
Czechoslovakia/I. Alers

10. Excretory System Studies

USSR/M. Natochin
    A. Pankova

11. Adipose Tissue Studies

Czechoslovakia/I. Alers
USSR/R. Tigranyan

12. Studies of the Gastrointestinal Tract

USSR/K. Smirnov
Rumania/P. Groza

13. Studies of Sensory Organs and Mucosae

USSR/F. Sushkov
USA/ L. Kraft

14. Embryological Studies

USSR/L. Serova
    N. Chel'naya
    V. Yagodovsky
    V. Oganov
    Yu. Natochin
    Z. Apanasenko

15. Embryological Studies

USA/ J. Keefe
    S. Abraham
    E. Sabelman
Bulgaria/A. Vyglenov
Poland/V. Stodolnik-
    Baranskaya
    S. Kozlovsky
    K. Ostrovsky

II. EXPERIMENTS WITH PLANTS

1. Studies of Carrot Crown Gall Tumor
    Growth

USA/ R. Baker
USSR/M. Gusev

2. Studies of Carrot Tissue Culture
    Morphogenesis

USA/ A. Krikorian

*Principal Investigator not known

TABLE 2 (Continued)

3. Studies of Higher Plant Morphogenesis   USSR/M. Tairbekov

4. Studies of Fungal Surface Migration   USSR/M. Tairbekov

III. EXPERIMENTS WITH INSECTS

1. Drosophila melanogaster Gravity   USSR/*
   Preference

IV. EXPERIMENTS WITH BIRDS

1. Study of Embryogenesis in the   USSR/Y. Shepelev
   Japanese Quail   USA /J. Keefe

V. EXPERIMENTS WITH MAMMALIAN CELL CULTURES

1. Cytological Studies of Mammalian Cell   USSR/*
   Cultures

VI. RADIOBIOLOGICAL RESEARCH

1. Bioblock Studies   USSR/E. Kovalev
       France/Planel

2. Radiation Dosimetry   USSR/E. Kovalev
       USA/ E. Benton

---

*Principal Investigator not known

TABLE 3

LIST OF SCIENTIFIC INSTITUTIONS PARTICIPATING IN THE

EXPERIMENTS OF COSMOS 1129

INSTITUTION	COUNTRY
NASA-Ames Research Center	USA
Colorado State University	USA
University of Delaware	USA
State University of New York, Stony Brook	USA
University of California, San Francisco	USA
Veterans Administration Hospital, American Lake	USA
University of Utah	USA
Baylor University Medical Center	USA
University of the Pacific Dental School	USA
Columbia University	USA
Wright-Patterson Air Force Base	USA
University of Southern California Medical Center	USA
Jet Propulsion Laboratory	USA
University of San Francisco	USA
Washington University School of Medicine	USA
Yale University	USA
Children's Hospital Medical Center, Oakland	USA
Biospace Incorporated, Ohio	USA
University of Virginia	USA
University of California, Berkeley	USA
University of California, Davis	USA
Institute of Medical and Biological Problems, USSR Ministry of Health	USSR
Institute of Evolutionary Physiology and Biochemistry, USSR Academy of Sciences	USSR
Bach Institute of Biochemistry, USSR Academy of Sciences	USSR
Pavlov Institute of Physiology, USSR Academy of Sciences	USSR
Central Dental Research Institute, USSR Ministry of Health	USSR
Priorov Central Institute of Traumatology and Orthopedics Research, USSR Ministry of Health	USSR
Central Institute of Gastroenterology Research, Moscow Municipal Executive Committee of the Council of Workers' Deputies	USSR
Institute of Medical Radiology, USSR Academy of Medical Sciences	USSR
Institute of Nutrition, USSR Academy of Medical Sciences	USSR
Sklifasovsky Central First Aid Institute, RSFSR Ministry of Health	USSR
Institute of Cardiology, Armenian SSR Ministry of Health	USSR
Bratislava Institute of Experimental Endocrinology, Slovakian Academy of Sciences	Czechoslovakia
Shafarik State University, Kosice	Czechoslovakia
Military Institute of Aviation Medicine, Warsaw	Poland

TABLE 3 (Continued)

INSTITUTION	COUNTRY
Bucharest Institute of Physiology	Romania
Institute of Roentgenology and Radiobiology, Sofia Medical Academy	Bulgaria
Institute of Physiology, Debrecen Medical College	Hungary
Institute of Pathophysiology, Debrecen Medical College	Hungary
Szeged Institute of Biochemistry	Hungary
Humboldt University	GDR

TABLE 4

PRELAUNCH EXPERIMENT ACTIVITIES

DATE (1979)	ACTIVITY
July 3-5	Date of birth of experimental animals
August 15 (approx.)	Temperature transmitters implanted intraperitoneally into Group 4 Flight and Synchronous Control animals
September 2	Carrot tumor preparations loaded into flight hardware at Colorado State University
September 3	Carrot tissue preparation loaded into flight hardware at State University of New York, Stony Brook
September 10	Approximate start of cage training: animals complete 30 hours of training before launch
September 14	Animals transferred from standard vivarium diet to 40 gms/animal/day of flight diet given once each day
September 15	U.S. plant experiments and radiation dosimeters shipped to Moscow
September 22	The bone label, Declomycin, was injected intraperitoneally into all Flight, Synchronous Control and Vivarium Control animals
September 22	Flight animal and other experimental material loaded into spacecraft
September 25	Launch: 6:30 p.m. Moscow time, North Cosmodrome, Plesetsk, USSR
September 25	Start of the Vivarium Control
September 30	Start of the Synchronous Control

TABLE 5

COMPOSITION OF THE PASTE DIET FED TO RATS DURING THE COSMOS 1129 MISSION

INGREDIENTS*

NAME	QUANTITY IN GRAMS
Casein (Milk)	3.0
Cornstarch	3.0
Sucrose	6.7
Sunflower Seed Oil	1.7
Dry Brewers Yeast	1.0
Salt Mixture	0.6
Water	24.0

FOOD CONTENT

NAME	QUANTITY IN GRAMS
Protein	3.06
Fats	1.79
Carbohydrates	9.61

MINERAL CONTENT

NAME	QUANTITY IN MG.
Sodium	60.9
Chlorine	15.5
Potassium	67.1
Phosphorus	86.3
Calcium	84.26
Iron	3.19
Iodine	0.07
Zinc	0.08
Copper	0.08
Cobalt	0.008
Fluorine	0.13
Aluminum	0.0008
Magnesium	6.96
Sulfur	11.17
Manganese	0.90

VITAMIN CONTENT

NAME	QUANTITY IN μ GRAMS
B_1	64.8
B_2	62.4
B_6	50.5
Pantothenic Acid	240.0
Nicotinic Acid	493.6
E	1380.0
A	20.0
D	6.0
Folic Acid	32.0
Inosine	800.0
B_{15} Biotin	16.0
P-Amino Benzoic Acid	800.0
B_{12}	0.48 mg
Choline	16000.0
K	16.0

*Sorbic Acid 0.5% to Weight of Feed Added as Preservative

NOTE: Quantities are those provided by Soviet scientists and are for 40 gm of diet, wet weight.

TABLE 6

POSTFLIGHT CHRONOLOGY OF MAJOR EVENTS

DATE (1979)	EVENT
Oct. 14	(7:59 a.m., Moscow time) Spacecraft landed near Kustanay in Central Asia
	Autopsies of Flight Group 1 animals commence (1:50 p.m., Moscow time)
Oct. 15	Specimens arrive at the Institute of Biomedical Problems, Moscow
	Autopsies of Group 5 Flight animals
Oct. 17	Autopsies of Vivarium Control Group 1 animals
	Autopsies of Vivarium Control Group 5 animals
Oct. 19	Termination of "Flight" phase of Synchronous Control
	Autopsies of Synchronous Control Group 1 animals
Oct. 20	Autopsies of Synchronous Control Group 5 animals
	Autopsies of Flight Group 2 and 3 animals
Oct. 22	Autopsies of Vivarium Control Group 2 and 3 animals
Oct. 25	Autopsies of Synchronous Control Group 2 and 3 animals
Oct. 29	Experimental Material Arrives in USA
Nov. 12	Autopsies of Flight Group 4 animals
	Autopsies of Vivarium Control Group 4 animals
Nov. 17	Autopsies of Synchronous Control Group 4 animals
Nov. 20	Experimental material arrives in USA

27
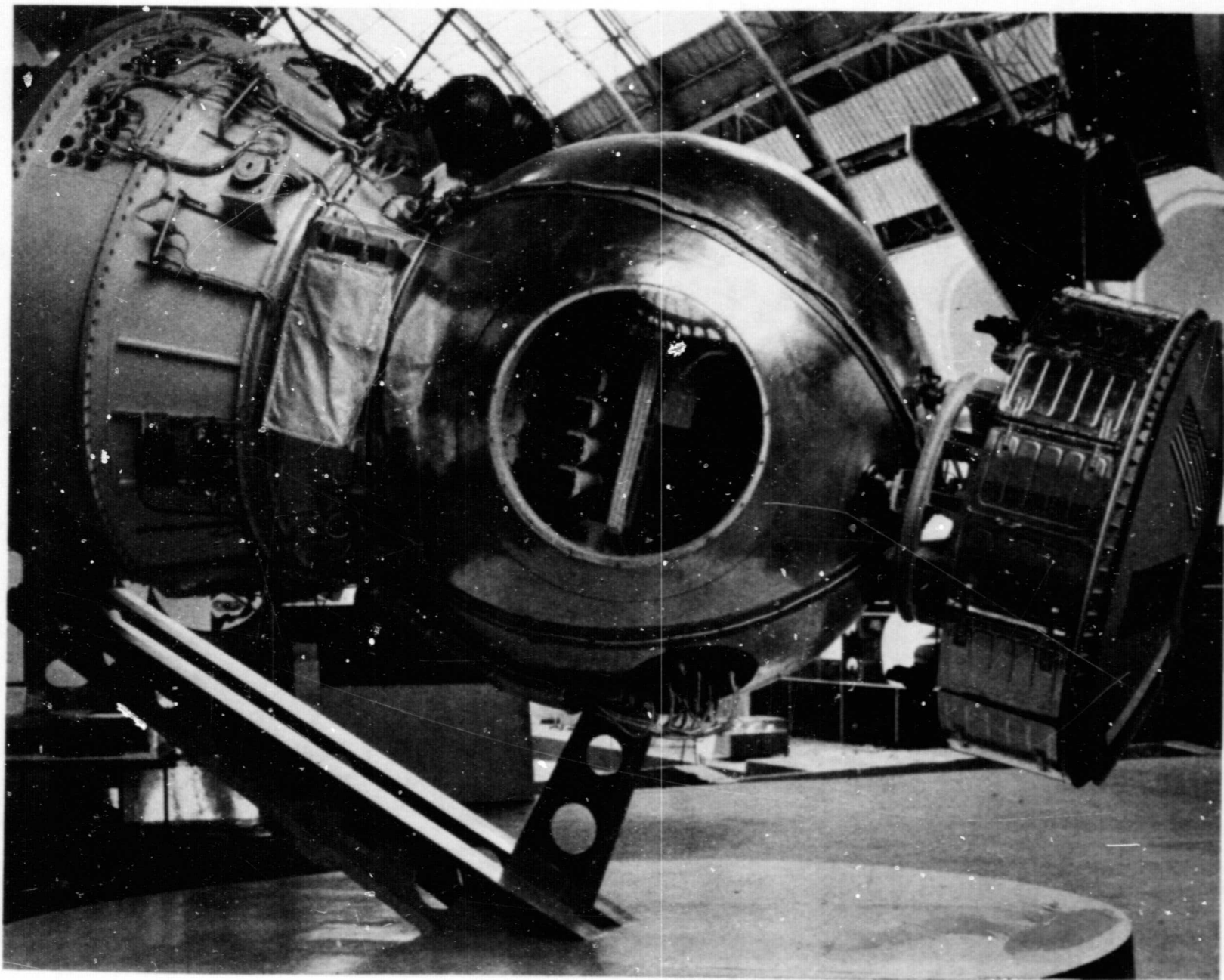
Figure 1.   Cosmos 782 Spacecraft on display in the Space Museum.   Astakeno, USSR.   A circular viewport was installed in the spherical craft when placed on display in the museum.
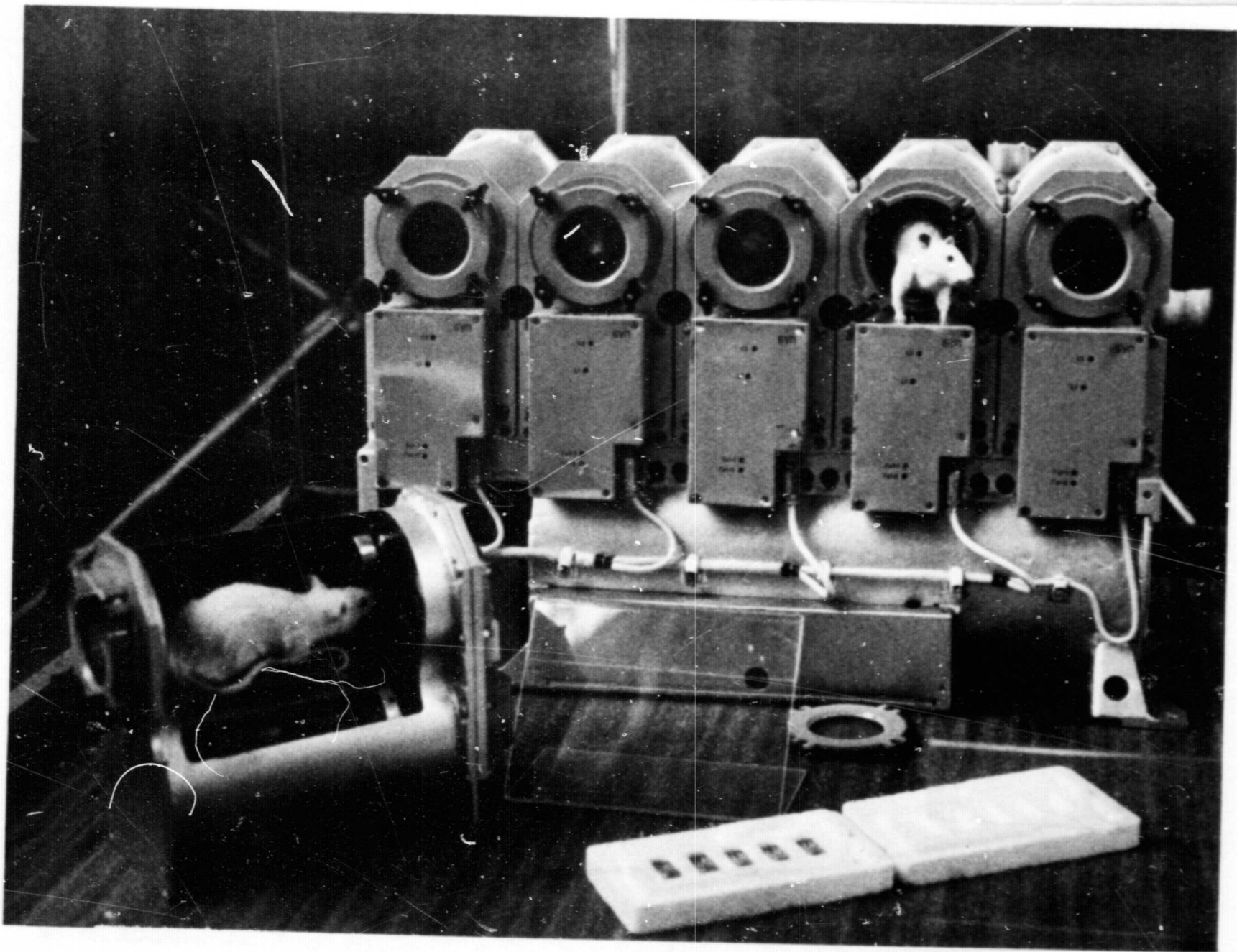
Figure 2. Rat cages of the type flown on Cosmos 1129. Cages are placed aboard
the spacecraft in blocks of five cages. The cages in a block share
food and water reservoirs.
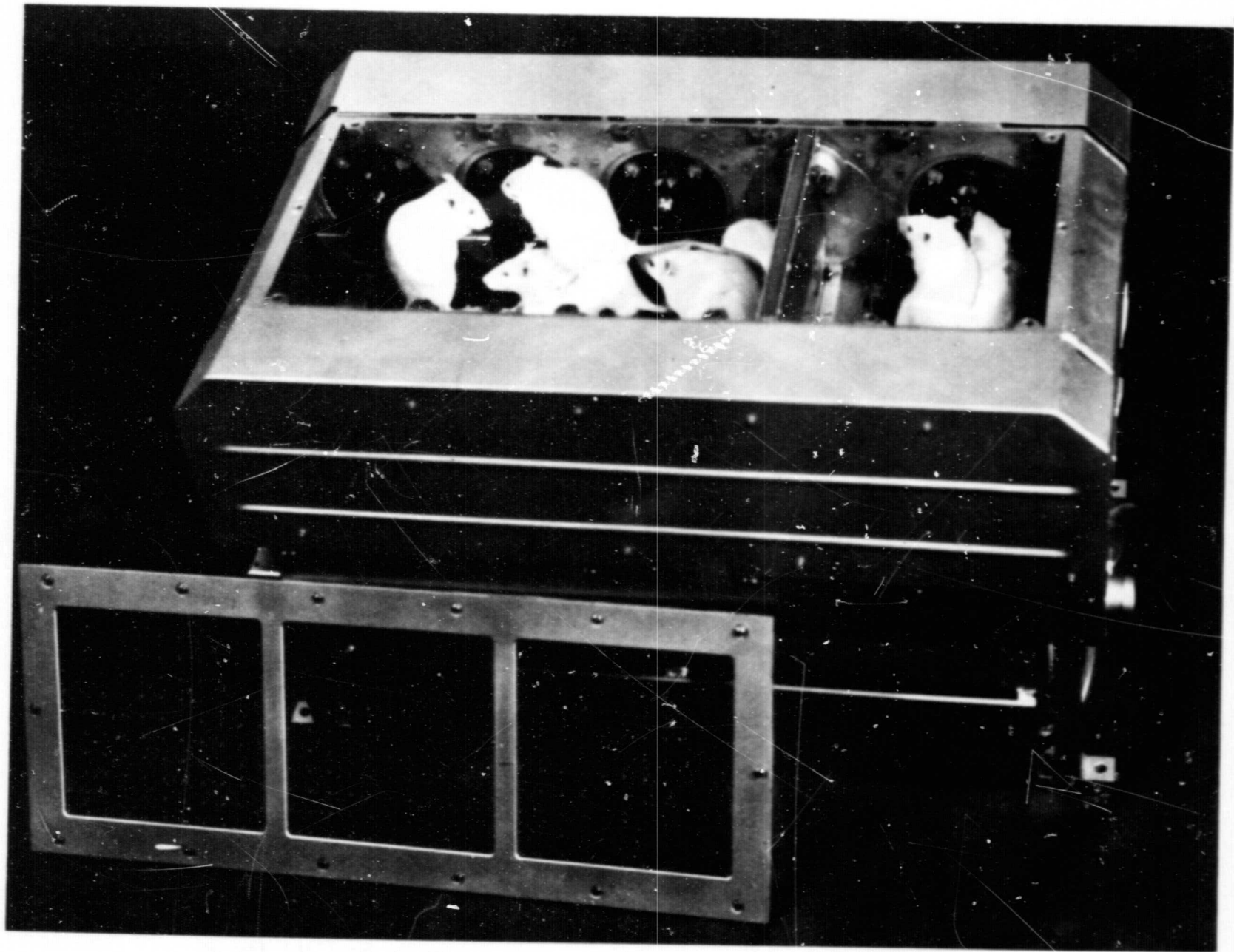
Figure 3. Rat breeding chamber of the type flown on Cosmos 1129.

29
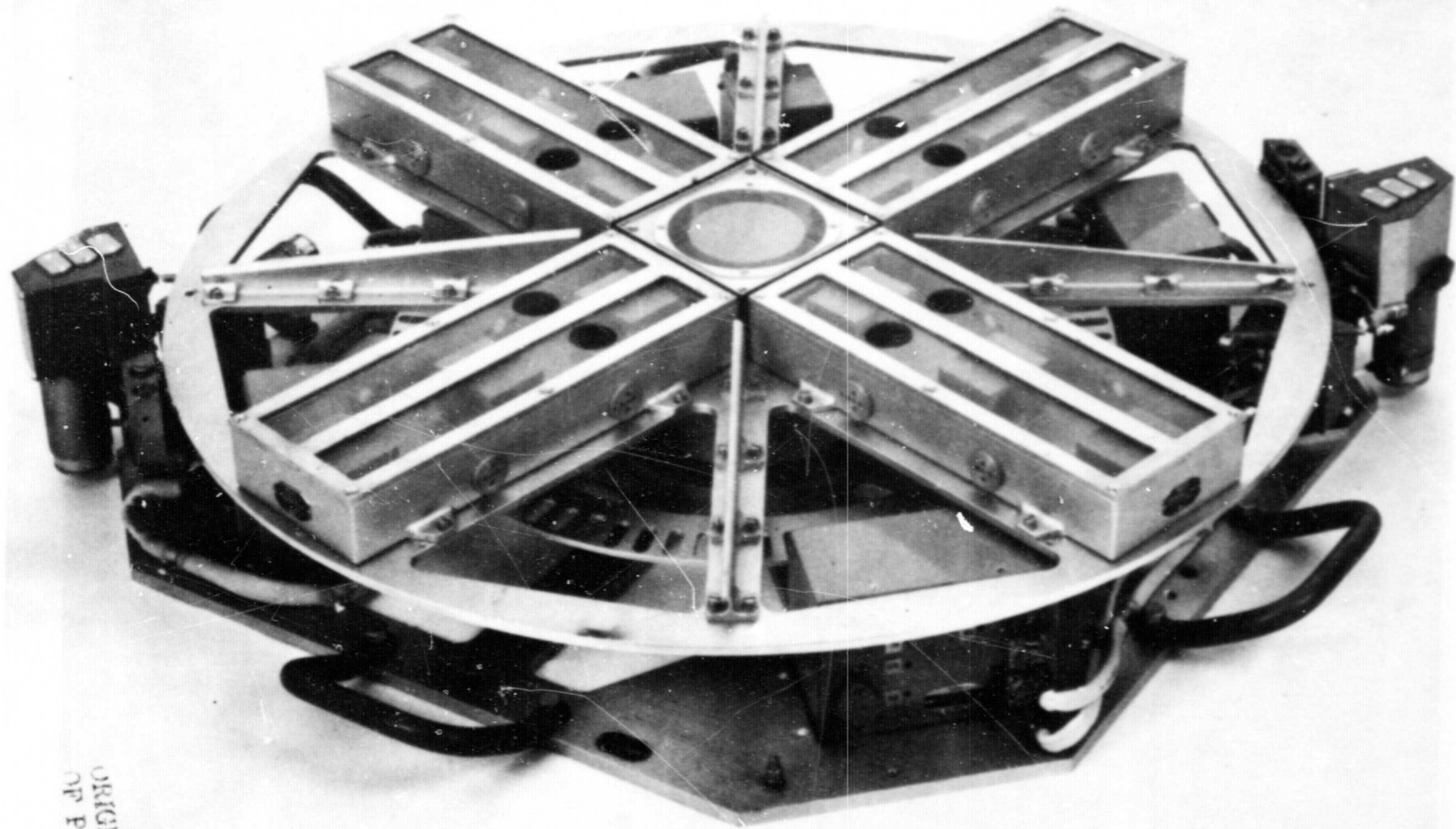
Figure 4. Cosmos 1129 centrifuge used to create a gravity gradient for an experiment with the fruit fly, Drosophila melanogaster.
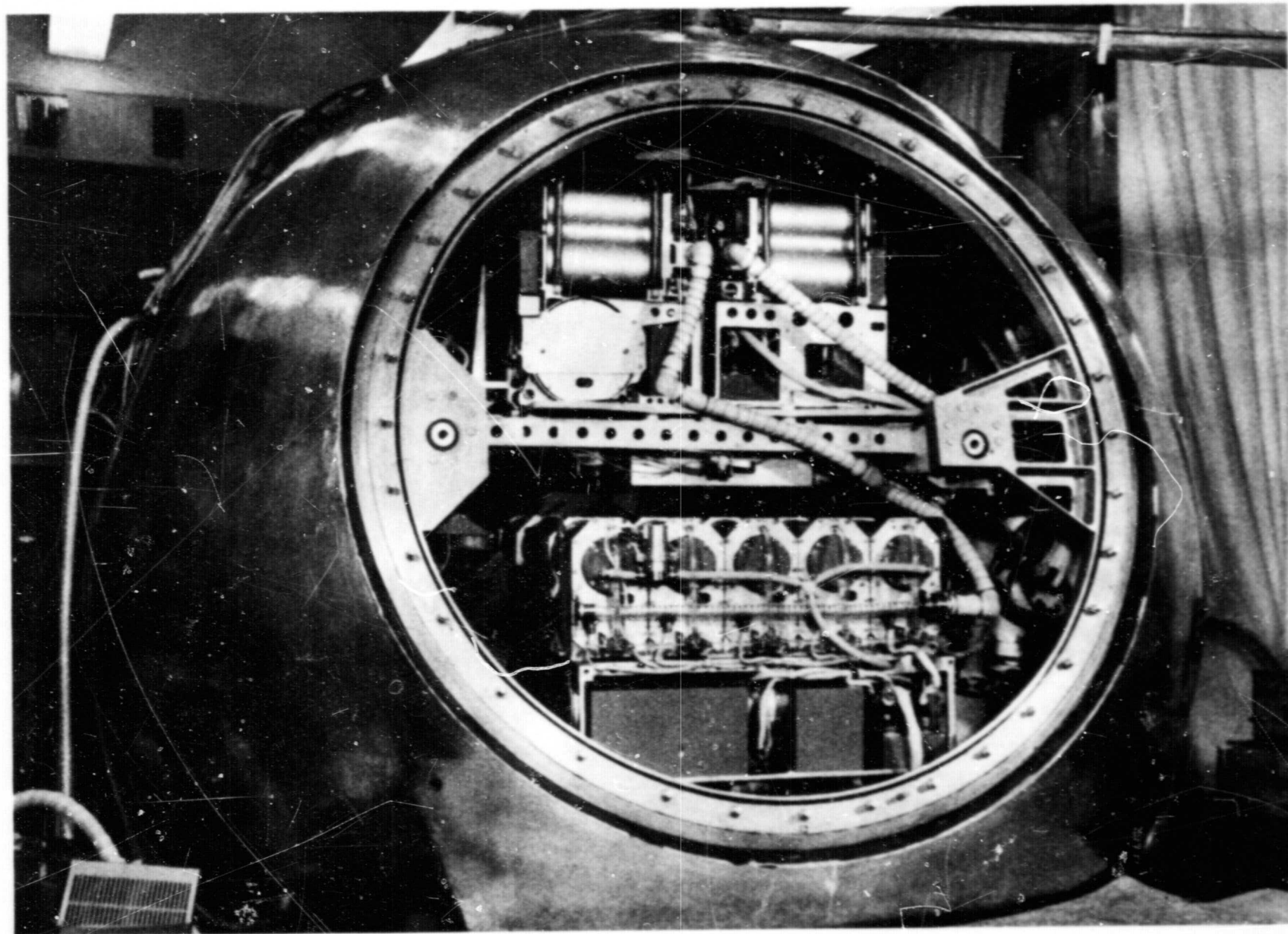
Figure 5. Spacecraft mockup used to conduct the Synchronous ground control.
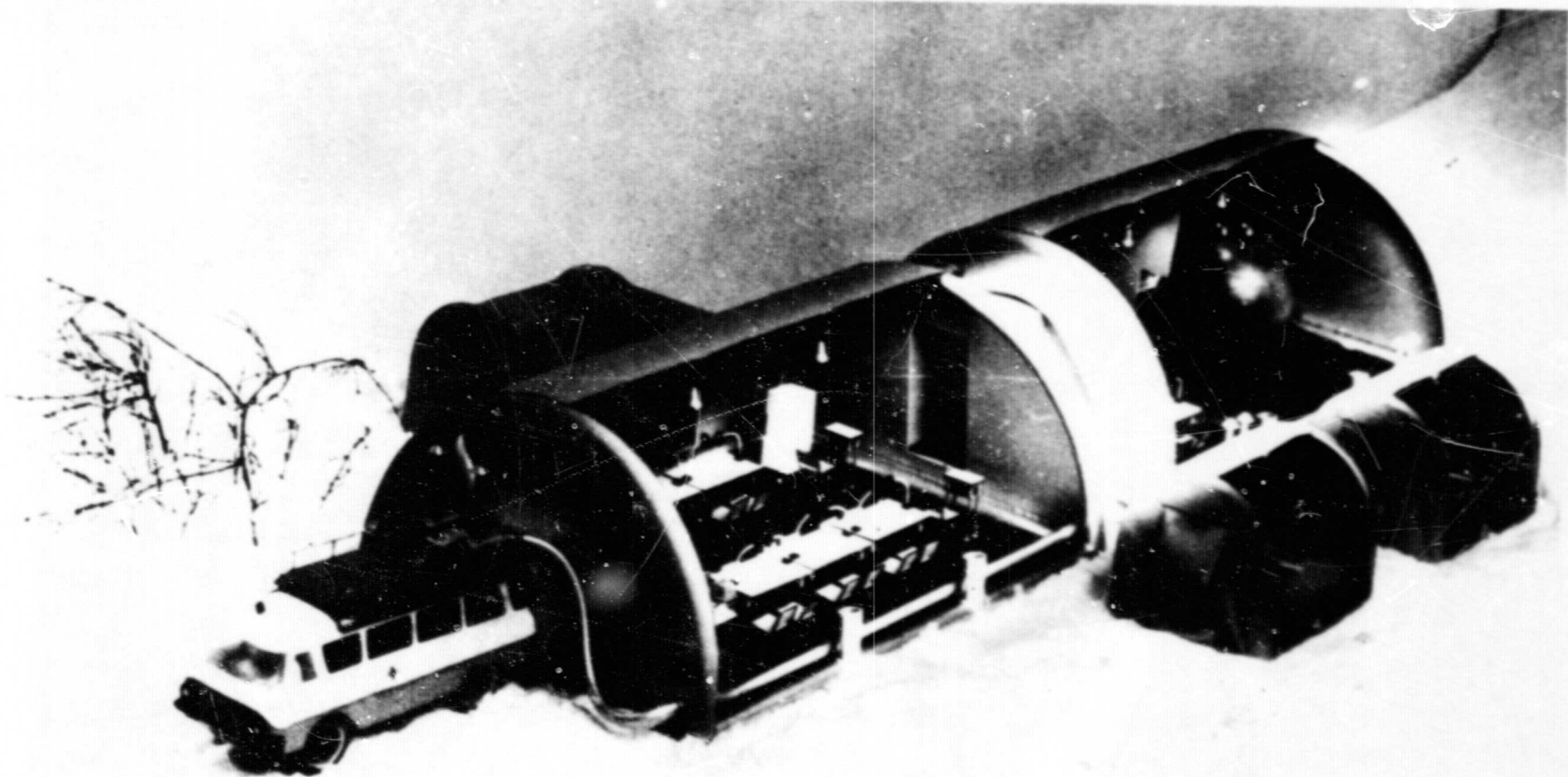
Figure 6 - Model of the field laboratory set up at the
spacecraft recovery site. Electric generators and environmental
control equipment provide the necessary conditions
for the initial observation and examinations of biological
specimens.

32

Figure 7 - Recovery team in the process of performing an autopsy and experimental procedures following the completion of the Synchronous Control experiment.

Experiment K304

STUDIES OF SPECIFIC HEPATIC ENZYMES AND LIVER CONSTITUENTS INVOLVED IN THE CONVERSION OF CARBOHYDRATES TO LIPIDS IN RATS EXPOSED TO PROLONGED SPACE FLIGHT

Principal Investigators:

S. Abraham[*] and H. P. Klein[+]

Collaborating Investigators

C. Y. Lin[*], C. Volkmann[+]
R. A. Tigranyan[++] and E. G. Vetrova[++]

[*] Bruce Lyon Memorial Research Laboratory, Children's Hospital Medical Center of Northern California, 51st and Grove Streets, Oakland, California 94609.

[+] National Aeronautics and Space Administration, Ames Research Center, Moffett Field, California 94035.

[++] Institute of Medical and Biological Problems, Moscow, U.S.S.R.

PRECEDING PAGE BLANK NOT FILMED

SUMMARY

We have investigated the effects of space flight on the activities
of 26 enzymes concerned with carbohydrate and lipid metabolism in hepa-
tic tissue taken from male Wistar rats flown in Earth orbit for 18.5
days aboard the Cosmos 1129 biosatellite. These activities were mea-
sured in the various hepatic cell compartments, i.e., cytosol, mitochon-
dria and microsomes. In addition, the levels of glycogen, total lipids,
phospholipids, triglycerides, cholesterol, cholesterol esters, and the
fatty acid composition of the rat livers were also examined and quanti-
fied. A similar group of ground-based rats (synchronous controls) treat-
ed in an identical manner served as controls. Both flight and synchro-
nous control rats were sacrificed at three time intervals: R_0, 7-11 hours
after recovery; R_{+6}, after 6 days; $R_{+6(S)}$, after 6 days (having undergone
2-5 hour periods of fixed stress in a "backupward" position on days 0, 3,
4, 5 and 6) and R_{+29}, after 29 days post-flight.

Although most of the enzyme activities and the amounts of liver con-
stituents studied were unaffected by the period of "weightlessness", some
significant differences were observed. Generally, all of our new findings
agree well with our previous observations in the livers of rats kept in
the weightless condition aboard Cosmos 936 flown during August 1977. A
statistically greater amount of liver glycogen was observed in flight rats
than in synchronous control rats sacrificed at R_0. In addition, in con-
firmation of our results aboard Cosmos 936, a significant difference was
again found in the ability of flight animals to complex long-chain fatty
acids. Thus, both the microsomal diglyceride acyltransferase and microso-

36

mal cholinephosphotransferase of the flight rats showed reduced activities when compared with synchronous controls at R_0.

The activity of one hepatic enzyme concerned with gluconeogenesis, glutamate-pyruvate transaminase found in the cytosol, was increased in the livers of rats in the weightless group sacrificed at R_0. On the other hand, the activities of two mitochondrial enzymes which function in the terminal oxidative sequence (Krebs Cycle), isocitrate dehydrogenase and aconitase, were significantly depressed as a result of the weightless condition at this same time after flight.

Stressing the flight rats for 6 days after space flight produced changes in some of the parameters we measured. Increases in the amounts of total lipids and of phospholipids as well as an elevation in the activity of glutamate-pyruvate transaminase were noted. On the other hand, stress was responsible for lowering the activities of the following: a) soluble enzymes: (cytosolic) glucokinase, hexokinase, and fatty acid synthetase, and b) microsomal enzymes: diglyceride acyltransferase, cholinephospho-transferase, and both the palmitoyl-CoA and the stearoyl-CoA desaturases.

As a result of our experiments aboard Cosmos 936 and Cosmos 1129 we have concluded that a) weightlessness can indeed affect metabolic pathways concerned with lipid and carbohydrate metabolism by influencing the activities of specific enzymes, b) these metabolic changes are in some cases independent of stresses other than weightlessness which are involved in space flight, and c) flight rats react more dramatically to imposed stress than their synchronous controls.

37

INTRODUCTION

Examination of liver, blood, muscle and skeletal tissues from rats aboard earlier Cosmos flights, indicated changes in the lipid and the carbohydrate levels of these tissues in response to space flight (1-5). After the Cosmos 936 space mission, we observed (6,7) specific alterations in hepatic enzyme activities (diglyceride acyltransferase, palmitoyl-CoA desaturase and glycogen phosphorylase) as well as changes in liver glycogen and the levels of specific fatty acids in the livers of flight rats but not in comparable animals subjected to continuous 1 x g centrifugation during the flight. These metabolic alterations, both in enzyme levels and in hepatic constituents, appeared to be unique to the weightless condition. In addition, our previous data seem to justify the conclusion that centrifugation during flight is equivalent to terrestrial gravity (6,7).

The present study (Cosmos 1129) was designed to reinvestigate some of our earlier observations (Cosmos 936) and to extend the range of inquiry to include additional hepatic microsomal and mitochondrial enzymes, as well as other liver constituents (total lipids, triglycerides, phospholipids and sterols) not included in our original Cosmos 936 protocol.

MATERIALS AND METHODS

Our experiment aboard the Cosmos 1129 biosatellite called for the use of 25 male Wistar rats caged individually within the spacecraft. Seven rats were sacrificed at 7-11 hours after recovery (R_0), and 5 rats after 29 days (R_{+29}). Of the remaining flight rats, 7 were stressed by immobilization in a "backupward" position for 2-5 hour periods on days 0, 3, 4, 5 and 6 after recovery, and were sacrificed ($R_{+6(S)}$), after the final stress on day 6. The other 6 rats served as unstressed flight controls and were also sacri-

38

ficed on day 6 (R_{+6}). Synchronous control rats, housed and fed in the
same manner as the flight animals were included in the experimental de-
sign. Analogous to this scheme a similar number of vivarium control rats
housed 3-4 per cage in standard laboratory cages and fed the same diet,
but with a different schedule than flight and synchronous control rats,
were also sacrificed and their livers processed. Table 1 lists the con-
ditions of our experiment and gives the number of rats in each group.
The specific details for the flight conditions (duration 18.5 days) are
given elsewhere in this volume.

Sacrifice of the animals, preparation of the liver homogenates, and
separation of the homogenate into supernatant and mitochondria were done
in the Soviet Union. These procedures followed the general plan as given
below.

Tissue and Homogenate Preparation. All rats were sacrificed by decapita-
tion and their livers removed as quickly as possible and immediately
placed in ice-cold 0.25 M sucrose solution. Two small pieces of liver
(about 200 mg each) were taken for glycogen, total lipid, and fatty acid
analysis. These were wrapped in aluminum foil and frozen in dry ice.

Four-gram portions of each liver were minced and individually homo-
genized in a Potter-Elvehjem-type tissue grinder with exactly 12.0 ml of
fresh ice-cold 0.25 M sucrose solution as given previously (8). All sub-
sequent procedures were carried out at 0-4°C. Nuclei and cell debris were
sedimented at 800 x g for 10 minutes (8,000 g. min, 2,400 rpm) in a refri-
gerated centrifuge (Beckman). The mixed pelleted fractions were discarded
and the supernatant fractions (obtained with the aid of a disposable pipet
from under the free floating fat) retained. These supernatant fractions

39

were again subjected to centrifugation at 4,500 x g for 30 min (135,000 g. min, 5,700 rpm) to separate the cytosol plus microsome fraction (supernatant) from the mitochondria (pellet). The cytosol plus microsome fractions were frozen immediately to -80°C. The pellets containing the crude mitochondria were washed by resuspension in fresh 0.25 M sucrose solution and sedimented by centrifugation at 4,500 x g for 30 minutes (135,000 g. min, 5,700 rpm). The supernatant solution was discarded, and the washed mitochondria were frozen for shipment to the United States at -80°C. (These procedures are depicted in Figure 1).

Extensive preliminary experiments with rats of the same strain coming from the same source (Institute of Experimental Endocrinology, Slovakian Academy of Sciences) and fed the identical diet [Soviet paste diet (6)] demonstrated that all of the activity of each enzyme assayed was stable under the conditions of storage used (i.e., at -80°C) (6). In addition, all enzyme activities were retained in the appropriate cellular location, even after freezing of the post-mitochondrial supernatant fractions for as long as two months. Thus, the data contained in the pertinent Tables represent the specific activity values for enzymatic activities in the livers of the rats at the time of sacrifice.

When the liver homogenate samples, which arrived frozen from the Soviet Union, were gently thawed in our laboratories, in preparation for the isolation of the cytosol and microsomal fractions, most of the fractions appeared to have large amounts of particulate material which sedimented on standing. We have recorded our impressions for each fraction and these appear in column 4 of Tables III A-D under the heading condition of homogenate. Thus, we found it necessary to clarify all homoge-

nate fractions by an additional centrifugal spin at 8,000 x g for 10 minutes (80,000 g. min, Spinco Ultracentrifuge). The resulting pellets were stored at -80°C for further biochemical analysis. The supernatant fractions thus cleared of the large particulates, were centrifuged in a Spinco Ultracentrifuge at 100,000 x g for 60 minutes at 0-4°C. The cytosol (particle-free supernatant fraction) and the microsomes (pellet) were separated. The cytosol fractions from each rat liver were divided into several small aliquots which were placed into individual plastic test tubes, quick frozen, and stored at -80°C until used for enzymatic analysis. Once thawed, the sample was immediately used for the assay of its enzymatic activity and was not repeatedly frozen and thawed. The microsomal and mitochondrial fractions were treated in a similar manner.

The washed mitochondria fractions were kept frozen at -80°C until used for analysis of enzyme activity. When needed, mitochondria containing about 50 mg protein were suspended in 7.5 ml of 10 mM Tris-phosphate buffer, pH 7.5, by means of a Teflon pestle fitted into the centrifuge tube. After standing at 0°C for 5 minutes, during which time the mitochondria undergo swelling, 2.5 ml of a solution containing 1.8 M sucrose, 2 mM ATP, and 2 mM MgSO$_4$ were added to the suspension. After another 5 minutes at 0°C, the suspension was subjected, in aliquots of 3.5 ml, to sonic oscillation at 3 amperes with a Branson Sonifier for 15 seconds at 0°C (9). The resulting material was used immediately for enzyme analysis.

Total Lipid, Fatty Acid and Glycogen Analysis. Samples of frozen liver were thawed, weighed (50 mg), and extracted for total lipids (10). Total lipids were extracted from the tissues with chloroform:methanol (2:1, v/v)

41

and washed with Folch upper phase (10). Lipid classes were separated by thin-layer chromatography on 0.25 mm silica gel plates (Whatman) with the solvent mixture of petroleum ether:diethyl ether:acetic acid (85:15:1.5). The phospholipid and triglyceride fractions were extracted from the silica gel and saponified. Aliquots of the fatty acid fractions were taken for quantitation and others were subjected to esterification in the manner given below.

Total lipids were determined gravimetrically. The phospholipid and triglyceride fractions isolated by thin-layer chromatography were quantitated by measuring the fatty acid contents of these fractions, by the method of Ho (11) which employs ^{63}Ni. Cholesterol was determined by the method of Zlatkis and Zak (12) as modified by Rudel and Morris (13).

Total hepatic fatty acids were isolated by refluxing small pieces of tissue (100 mg) with 1 ml of 30% KOH:methanol (1:1) overnight at 85°C. Hydroquinone (0.01%) was added to retard the oxidation of unsaturated fatty acids. Sterols and unsaponifiable material were removed by extraction with petroleum ether (30-60°C) and after acidification, fatty acids were extracted with hexane and the fatty acid methyl esters were prepared with diazomethane (14). Gas chromatography was carried out in a Varian aerograph (model 3700) equipped with a flame ionization detector and a stainless-steel column (6 ft. x 1/8 in.) packed with 10% DEGS-PS on Supelcoport (Supelco, Bellefonte, PA).

Fatty acid methyl esters were identified by means of their chromatographic retention times with the use of appropriate standards. The percentage fatty acid composition was determined with a Varian model CDS111 data system. The heat program had an initial temperature of 110°C and

at 2 min. after sample injection the temperature was increased at a rate of 10°C/min. to a temperature of 185°C. At 28 min. the temperature was elevated to 190°C at a rate of 10°C/min. and stayed at that temperature for the remainder of the analysis.

Other liver samples (100 mg) were taken for the analysis of glycogen contents by the anthrone procedure as given previously (15).

Enzyme Assays. All enzyme assays, unless otherwise noted, were performed with a) the 100,000 x g supernatant fraction (cytosol), or b) the pellet (microsomes) obtained from this centrifugation after removal of the mito-chondria, or c) the purified mitochondria. Enzyme activities were deter-mined by following the changes in optical density of the reaction mixtures at 30°C with a Gilford automatic recording spectrophotometer. In all en-zyme assays, concentrations of substrates and of added enzymes (where needed) were at least 10 times those required to yield maximal activities. Absorbancy changes were measured with reference to reaction mixtures, de-void either of substrates or of coenzymes. The reactions were started by additions of substrates, after a brief period of preincubation of the en-zymes in the reaction mixtures. Measurements of initial velocities were made under conditions in which kinetics were zero-order, and activities were proportional to enzyme concentrations.

Specific activities of the cytosol enzymes are reported as nanomoles, either of pyridine nucleotide oxidized or reduced, or of substrate con-verted to product, per milligram of protein per minute, whereas those for the mitochondrial and the microsomal enzymes are given in the footnotes to the Tables. The following extinction coefficients were used in the calcu-lations: reduced NADP (NADPH) and NADH (340 nm), 6.22×10^3 liter x mole^{-1}

cm^{-1} (16); cis-aconitate (240 nm), 3.54×10^3 liter $\times$ mole^{-1} $\times$ cm^{-1} (17).
Protein was determined by the microbiuret method of Goz (18).

Enzymes were measured according to well-established methods or modifications of currently used techniques, as indicated below.

a) Cytosolic Enzymes -   Hexokinase and glucokinase (19), glucose-6-phosphate dehydrogenase (20), 6-phosphogluconate dehydrogenase (20), glycogen synthetase (21), glycogen phosphorylase (22), isocitrate dehydrogenase (23), fatty acid synthetase (19), aconitase (24), glutamate-oxaloacetate transaminase (25), glutamate-pyruvate transaminase (26), glutamate dehydrogenase (27), malate dehydrogenase (28) and lactate dehydrogenase (29).

b) Mitochondrial Enzymes =   Cytochrome oxidase (30), glutamate dehydrogenase (27), aconitase (24), isocitrate dehydrogenase (23) and malate dehydrogenase (28).

c) Microsomal Enzymes -   Palmitoyl-CoA and stearoyl-CoA desaturase activities were measured as given for palmitoyl-CoA desaturase as follows: The complete system contained 30 nmoles of either palmitoyl-1-^{14}C-CoA or stearoyl-1-^{14}C-CoA (saturated fatty acid), 0.3 µmoles Tris-MgCl$_2$ buffer, pH 7.5 and sufficient microsomal protein to yield a linear rate of desaturation in a total volume of one ml. The enzyme and buffer mixture were equilibrated in air at 37°C for 2 min., and the reaction was started by the addition of the substrate. At the end of 5 minutes of incubation, the reaction was stopped by the addition of 0.5 ml of saturated KOH. The samples were then saponified, and the fatty acids were extracted and methylated as reported previously (31). After methylation, methyl palmitate (C-16) and methyl palmitoleate (C-16:1) were separated by gas chromatography (32), and

the radioactivity associated with each peak was counted. Enzyme activity is calculated as nanomoles of palmitoleic acid produced as follows: [cpm in methyl C-16:1/cpm in methyl C-16 + methyl C-16:1] times the initial amount C-16-CoA used in nanomoles and is expressed per 5 minutes per mg protein.

The 3-hydroxy-3-methylglutaryl-coenzyme A reductase activity was assayed according to the procedure described by Goodwin and Margolis (33).

α-Glycerolphosphate acyltransferase and diglyceride acyltransferase activities of hepatic microsomes were measured according to the procedures reported previously (34,35). Phospholipid transferases were assayed by an established procedure (36) modified in our laboratory. Since in both cases (for PC and for PE) our modifications were substantial and allow for a more rapid analysis, we present them here.

PHOSPHORYLCHOLINE (PC) OR PHOSPHORYLETHANOLAMINE (PE)

GLYCERIDE-TRANSFERASE ASSAY PROCEDURES

Constituents for Assay System	µmoles/assay	ml/assay
Tris-HCl, (0.5 M, pH 8.0)	25	0.050
Dithiothreitol, (0.05 M)	1	0.020
$MgCl_2$, (0.5 M)	10	0.020
EDTA, (0.1 M)	5	0.050
^{14}C-CDP-choline, or ^{14}C-CDP-ethanolamine, (7.25 mM)	0.150	0.020
Bovine serum albumin, (5 mg/ml)	0.25	0.050
Water	-	0.140
		0.350
Diglyceride preparation (14 µmoles/ml) sonicated in 0.25% Tween 20 for 10 minutes	0.700	0.050
Start assay with enzyme preparation; 5 mg/ml suspension (0.02 M Tris-HCl, pH 7.5, 0.001 M EDTA)	0.25 or 0.5 mg	0.100
TOTAL VOLUME		0.500

After 30 minutes of incubation at 37°C, the reaction is arrested with 1.5 ml of 95% ethanol. Following centrifugation, the supernatant fraction is removed and combined with three subsequent 1.5 ml ethanol extractions of the protein precipitate. The precipitate is macerated by grinding with a small amount of micromesh glass beads prior to each ethanol extraction. Ethanol extracts (6.0 ml) are combined with 2.5 ml of CCl_4 and washed twice with 10 ml of 2 M KCl and once with 10 ml of water. The CCl_4 phase is removed from beneath the water phase and transferred to a 20 ml scintillation vial. One ml of CCl_4 is added to the wash water phase and after vortexing and centrifugation, the CCl_4 is removed from beneath the water phase and combined with the first extract in the vial. After evaporating the CCl_4 under an airstream, 10 ml of scintillator solution 0.5% PPO (2,5-diphenyloxazole), 2 parts toluene, 1 part 2-ethoxyethanol are added to the vial and the contents of the vial is assayed for ^{14}C in a liquid scintillation spectrometer (37).

Chemicals. All chemicals were obtained from commercial sources and were of the highest purity available. ATP, glucose-6-phosphate dehydrogenase, 6-phosphogluconate, phosphoenolpyruvate, were purchased from Boehringer Mannheim Corp., San Francisco, CA. Glucose-6-phosphate, NAD^+, NADPH $NADP^+$, NADPH, ethylenediaminetetraacetate (EDTA), coenzyme A, CDP-choline and CDP-ethanolamine were purchased from Sigma Chemical Co., St. Louis, MO. Dithiothreitol, ADP, α-glycerol-3-phosphate were purchased from Cal-biochem, San Diego, CA. Acetyl-CoA, malonyl-CoA and HMG-CoA were purchased from P-L Biochemical, Milwaukee, Wisconsin. Palmitoyl-1-^{14}C-CoA, stearoyl-1-^{14}C-CoA, ^{14}C-CDP-choline, ^{14}C-CDP-ethanolamine, 3-hydroxy-3-methyl glutaryl-^{14}C-CoA (^{14}C-HMG-CoA) were obtained from New England Nuclear Corp. Boston, Mass., and ICN, Irvine,

CA. PPO (2,5-diphenyloxazole) was purchased from the Fisher Scientific Company, Fair Lawn, N.J.

RESULTS AND DISCUSSION

Individual values for some specific liver constituents from rats sacrificed at R_0, R_{+6}, $R_{+6(S)}$, and R_{+29} are given in Table II A-D. It should be noted that livers from flight rats at R_0 were generally larger than those of either the synchronous or vivarium controls. These differences were highly significant ($P < 0.01$).

Tables II through VIII list the individual values for the liver constituents and the hepatic enzyme activities that were examined in this study. Each group average and its standard deviation is given in Table IX. The statistical significance of the differences found between groups are presented in Table X.

When the values for each animal within a group were compared, we noted that the standard deviations were greater than one would expect from a normal group sampling of rat liver tissue. In addition, several microsomal enzymes (specifically, the acyltransferases) had specific activities which were from 1/10 to 1/20 those previously found in the liver of normal ratsor of those flown aboard the Cosmos 936 biosatellite. This great variability in enzyme activity within a group and the low specific activity of certain enzymes might be a result of the presence, in the frozen homogenate fractions, of the easily sedimentable large particulates which we removed. Subsequent biochemical analysis of these contaminating particles showed that they had considerable cytochrome oxidase activity (Figure 2). Since this enzyme is found exclusively in the mitochondrial fraction of liver homogenates these data suggest that hepatic lysosomes would also be present.

47

We have previously noted that such contamination of the cytosol and micro-somal fractions could adversely affect certain enzyme activities. In view of these observations, we are cautious in interpreting our Cosmos 1129 enzyme activity results.

Further, although values for the vivarium control rats are presented in the tables, we question the advisability of using these data, since there appear to be many anomalies in the results obtained with these rats. This is very dramatically illustrated when one compares the levels of hepatic glycogen for the vivarium control rats sacrificed at various times (Table II A-D). Whereas those killed at R_0 and at R_{+29} gave values of $0.23\pm0.06\%$ and $0.34\pm0.18\%$ wet weight respectively (Table II A and Table II D), those sacrificed at R_6 and $R_{6(S)}$ yielded levels of 3.6 ± 1.1 and $2.56\pm0.92\%$ wet weight respectively (Table II B and Table II C). Although the values at R_0 and R_{29} were similar, and those after 6 days post-flight whether stressed or not stressed were similar, these two groups were vastly different from each other. It would suggest, therefore, that the conditions of these vivarium animals were not the same at all periods studied. Thus, we feel that the most meaningful comparisons are those between the flight animals and the rats that served as ground-based synchronous controls.

Given these constraints, the data, when compiled and statistically evaluated, did generally confirm many of our Cosmos 936 findings. The activities of most of the hepatic enzymes and liver constituents were unaffected by space flight (Table X). A statistically significant difference was seen between the flight and synchronous control rats at R_0 with respect to their contents of liver glycogen (Table X) (Figure 3). The livers of the flight rats had 30% more glycogen than those of the synchronous controls. This

finding confirms our previous observations aboard Cosmos 936. The actual increases in hepatic glycogen, however, were not as great as those recorded for the Cosmos 936 flight rats. In addition, the Cosmos 1129 flight animals showed no significant changes in the activities of glycogen synthetase or of phosphorylase at R_0 that could fully explain the increased glycogen contents (Table III). The glycogen of the flight animals also did not return to normal levels within the post-flight recovery period as did the glycogen of the Cosmos 936 rats. Indeed, the hepatic glycogen of the flight rats on this mission decreased to abnormally low levels 29 days after recovery, while the synchronous controls were virtually unchanged (Table II D, Figure 3). To explain such a marked decrease in glycogen levels, one would have to postulate either a change in the dietary regimen or the application of additional stress on the flight animals. The glycogen phosphorylase activities (enzyme concerned with glycogen breakdown) of the flight rats did increase 58% after the 29 day readaptation period, and thus biochemically, could account for the decreased liver glycogen observed in the flight animals (Table III).

In confirmation of our results aboard Cosmos 936, a significant difference was found in the ability of the flight animals to complex long-chain fatty acids (Table X, Figures 4 and 5). Both the diglyceride acyltransferase and the cholinephosphotransferase of the flight rats showed reduced activities when compared with the synchronous controls at R_0. However, these decreased enzyme activities did not appear to affect the hepatic lipid values (Table II A). The triglyceride and phospholipid contents were similar for the flight and synchronous control rats at R_0. The apparent discrepancy between the observed decrease in transferase activities

49

and the normal triglyceride and phospholipid values most probably reflects the fact that we were not able to measure a dynamic metabolic process under the conditions of this experiment. It is conceivable, however, that the decreased transferase activities could precede a measurable change in metabolic end products. All transferase activities returned to normal values after 29 days post-flight (Table III D).

The values for total fatty acids in the individual livers as well as those for the triglycerides and phospholipids isolated by our thin-layer chromatographic procedures are given in Tables VI A through D and VII A and B. The pertinent ratios of 16/16:1, 18/18:1 and 18:2/20:4 are given in Tables VIII A through D. It is interesting to note that the values for the ratios of 16/16:1 and 18/18:1 for the total fatty acids are very similar to those found with the phospholipid and triglyceride fatty acids for the animals sacrificed at R_0 (Tables VII A and B).

It is also interesting that the activity of one hepatic enzyme concerned with gluconeogenesis, namely, glutamate-pyruvate transaminase, was increased in the livers of the weightless group sacrificed at R_0 when compared to the synchronous controls (Tables III A and X). On the other hand, mitochondrial enzyme activities for isocitrate dehydrogenase and aconitase were significantly depressed as a result of the period the rats spent in the weightless condition (Tables V and X) (Figures 6 and 7).

Stressing the flight rats, after space flight, produced changes in the levels of liver constituents not seen in the R_0 flight animals (Table II B, II C and X). Total lipids and phospholipids increased in the flight rats after stress while the control groups showed no differences (Table X and Figure 8). Several enzyme activities were affected. We observed lower activities for the soluble enzymes, glucokinase (Figure 9), hexokinase (Figure 10),

50

fatty acid synthetase, and for the microsomal enzymes diglyceride acyl-transferase (Figure 11), phosphatidylcholine (Figure 12) and phosphatidyl-ethanolamine (Figure 13) transferases, palmitoyl-CoA (Figure 14) and stea-royl-CoA desaturases. The cytosolic glutamate-oxaloacetate transaminase, however, was increased (Figure 15) in the flight stressed group vs. non-stressed group at R_{+6}. In a few instances the stressed synchronous controls for the R_{+6} were affected by the applied stress. Glycogen (Figure 16), hexokinase, glucokinase and PE acyltransferase activities were all depressed in these animals. However, the response of these control animals to stress was less pronounced than the response of the rats that had been exposed to weightlessness (Table X). We may conclude, therefore, that the flight rats react more strongly to stress than their synchronous controls.

It is also clear from our data that the particular type of stress administered to the rats, whether applied to flight or synchronous control animals, caused a decrease in the levels of hepatic glycogen. Since we observed that weightlessness caused an increase in hepatic glycogen values in the rats sacrificed at R_0 in both Cosmos 936 (6,7) and Cosmos 1129, we have concluded that the environmental conditions of spaceflight may not be similar to those of the applied stress, at least with regard to hepatic glycogen levels.

It would appear, from the data presented in this report and from our results with rats aboard Cosmos 936 (6,7) that weightlessness can indeed affect metabolic pathways concerned with lipid and carbohydrate metabolism, and that such metabolic changes are in some cases independent of stresses, other than weightlessness which are involved in spaceflight.

ACKNOWLEDGEMENTS

REFERENCES

1.   Berry, C. A. Weightlessness. In Bioastronautics Data Book,
     2nd Ed., Chap. 8, pp. 349-415. Washington, D. C., NASA 1973
     (NASA SP-3006).

2.   Belitskaya, R. A. Carbohydrate and lipid content of rat liver
     tissue following a 22-day space flight. Space Bio. and Aero-
     space Med. 4: 97-99, 1977.

3.   Yakovleva, V. I. Arkhiv. Anat. Gistologii i Embriologii, 73:
     39, 1977.

4.   Preliminary reports from KOSMOS 690.

5.   Tigranayan, R. A. KOSMOS 782 Post-flight biochemical studies
     of various organs and tissues of rats. 1976.

6.   Abraham, S., H. P. Klein, C. Y. Lin and C. Volkmann. The effects
     of spaceflight on some liver enzymes concerned with carbohydrate
     and lipid metabolism in the rat. In Final Reports of U. S. Experi-
     ments flown on the Soviet Satellite COSMOS 936, ed. by S. N.
     Rosenzweig and K. A. Souza, NASA Tech. Memorandum 78526, Sept.
     1978, pp. 78-134.

7.   Abraham, S., C. Y. Lin, H. P. Klein and C. Volkmann. The effects
     of spaceflight on some liver enzymes concerned with carbohydrate
     and lipid metabolism in rats. The Physiologist, 21: No. 4, 1978.

8.   Abraham, S., K. J. Matthes and I. L. Chaikoff. Fatty acid syn-
     thesis from acetate by normal and diabetic rat liver homogenate
     fractions. I. A comparison of cofactor requirements. J. Biol.
     Chem. 235: 2551-2559, 1960.

9.   Sottocasa, G. L., G. Kuylenstierna, L. Ernster and A. Bergstrand.

Separation and some enzymatic properties of the inner and outer membranes of rat liver mitochondria. Meth. Enzymol. 10: 448-463, 1967.

10. Folch, J., M. Lees and G. H. Sloane-Stanley. A simple method for the isolation and purification of total lipids from animal tissues. J. Biol. Chem. 226: 497-509, 1957.

11. Ho, R. J. Radiochemical assay of long-chain fatty acids using ^{63}Ni as tracer. Anal. Biochem. 36: 105-113, 1970.

12. Zlatkis, A. and B. Zak. Study of a new cholesterol reagent. Anal. Biochem. 29: 143-148, 1969.

13. Rudel, L. L. and M. D. Morris, Determination of cholesterol using ophthalaldehyde. J. Lipid Res. 14: 364-366, 1973.

14. Abraham, S., K. J. Matthes and I. L. Chaikoff. Factors involved in synthesis of fatty acids from acetate by a soluble fraction obtained from lactating rat mammary gland. Biochim. Biophys. Acta 49: 268-285, 1961.

15. Hassid, W. Z. and S. Abraham. Chemical procedures for analysis of polysaccharides. I. Determination of glycogen and starch. Meth. Enzymol. 3: 34-78, 1957.

16. Horecker, B. L. and A. Kornberg. The extinction coefficients of the reduced band of pyridine nucleotides. J. Biol. Chem. 175: 85-390, 1948.

17. Rauen, H. M. Biochemisches Taschenbuch. p. 988, Springen Verlag, Berlin. 1956.

18. Goz, J. Microbiuret method for protein determination. Scand. J. Clin. Lab. Invest. 5: 218, 1953.

19. Smith, S., H. T. Gagné, D. R. Pitelka and S. Abraham. The effect of dietary fat on lipogenesis in mammary gland and liver from lactating and virgin mice. Biochem. J. 115: 807-815, 1969.

20. Kornberg, A. and B. L. Horecker. Glucose-6-phosphate dehydrogenase. Meth. Enzymol. 1: 323-326, 1955.

21. Mendicino, J., H. Abou-Issa, R. Medicus and N. Kratowich. Fructose-1,6-diphosphatase, phosphofructokinase, glycogen synthetase, phosphorylase, and protein kinase from swine kidney. I. Isolation and properties of glycogen synthetase. Meth. Enzymol. 42: 375-381, 1975.

22. Mendicino, J., H. Abou-Issa, R. Medicus and N. Kratowich. Fructose-1,6-diphosphatase, phosphofructokinase, glycogen synthetase, phosphorylase, and protein kinase from swine kidney. IV. Purification and properties of phosphorylase. Meth. Enzymol. 42: 389-394, 1975.

23. Ochoa, S. Isocitric dehydrogenase system (TPN) from pig heart. Meth. Enzymol. 1: 699-704, 1955.

24. Racker, E. Spectrophotometric measurements of the enzymatic formation of fumaric and cis-aconitic acids. Biochim. Biophys. Acta 4: 211-214, 1950.

25. Bergmeyer, H. and E. Bernt. Glutamate-oxaloacetate transaminase. In: Methods of Enzymatic Analysis (H. Bergmeyer, ed.), Academic Press Inc., New York, pp. 837-845 1963.

26. Bergmeyer, H. and E. Bernt. Glutamate-pyruvate transaminase. In: Methods of Enzymatic Analysis (H. Bergmeyer, ed.), Academic Press, Inc., New York, pp. 846-853, 1963.

27. Schmidt, E. Glutamate dehydrogenase. In: Methods of Enzymatic Analysis (H. Bergmeyer, ed.), Academic Press, Inc., New York, pp. 650-656, 1974.

28. Ochoa, S. Malic dehydrogenase from pig heart. Meth. Enzymol. 1: 735-739, 1955.

29. Yoshida, A. and E. Freese. Lactate dehydrogenase from Bacillus subtilis. Meth. Enzymol. 41: 304-309, 1975.

30. Smith, L. In: Methods of Biochemical Analysis (D. Glick, ed), Wiley (Interscience), New York, pp. 427-434, 1955.

31. Klein, H. P. Synthesis of lipids in resting cells of Saccharomyces cerevisiae. J. Bacteriol. 69: 620-627, 1955.

32. Klein, H. P. Nature of particles involved in lipid synthesis in yeast. J. Bacteriol. 90: 227-234, 1965.

33. Goodwin, C. D. and S. Margolis. Improved methods for the study of hepatic HMG-CoA reductase: one step isolation of mevalonolactone and rapid preparation of endoplasmic reticulum. J. Lipid Res. 17: 297-303, 1976.

34. Lin, C. Y., S. Smith and S. Abraham. Acyl specificity in triglyceride synthesis by lactating rat mammary gland. J. Lipid Res. 17: 647-656, 1976.

35. Tanioka, H., C. Y. Lin, S. Smith and S. Abraham. Acyl specificity in glyceride synthesis by lactating rats. Lipids 9: 229-234, 1974.

36. Young, D. L. and F. Lynen. Enzymatic regulation of 3-sn-phosphatidyl-choline and triacylglycerol synthesis in states of altered lipid metabolism. J. Biol. Chem. 244: 377-383, 1969.

37. Bartley, J. C. and S. Abraham. Improved methods for liquid scintillation assay of (A) C^{14}-compounds on paper chromatograms and (B)

C^{14}-protein. In: Advances in Tracer Methodology (S. Rothchild, ed.), Plenum Press, New York, pp. 69-79, 1966.

TABLE I

COSMOS 1129: EXPERIMENT K304

Rat Group	Number of Rats per Group			
	R_0	R_{+6}	$R_{+6(S)}$	R_{+29}
Flight, F	7	6	7	5
Synchronous Control, S	7	6	7	5
Vivarium Control, V	7	6	7	5
Sacrificed on:				
F	10-14-79	10-20-79	10-20-79	11-12-79
S	10-19-79	10-25-79	10-25-79	11-17-79
V	10-17-79	10-21-79	10-21-79	11-12-79
Arrived In:				
USA	10-29-79	10-29-79	10-29-79	11-20-79
BLMRL*	11-05-79	11-05-79	11-05-79	11-29-79

* Bruce Lyon Memorial Research Laboratory, Children's Hospital Medical Center, Oakland, California.

TABLE II A

INDIVIDUAL VALUES FOR LIVER CONSTITUENTS FROM RATS SACRIFICED AT R_0

Group	Rat No. USSR	Rat No. USA	Weight at Sacrifice Carcass (grams)	Liver (grams)	Liver as % carcass	Liver Constituents (mg/100mg Tissue) Glycogen	Total lipids	Phospho-lipids	Triglycer-ides	Free cholesterol	Cholesterol esters	Total cholesterol
Flight	IF-1	42	329	14.10	4.29	5.3	4.0	2.3	1.1	0.31	0.25	0.46
	IF-2	43	331	12.83	3.88	3.7	4.4	2.5	1.4	0.28	0.22	0.41
	IF-3	14	343	14.15	4.13	6.0	4.9	2.4	2.0	0.24	0.27	0.40
	IF-4	48	321	11.95	3.72	5.5	3.4	2.4	0.67	0.22	0.12	0.30
	IF-5	50	341	13.25	3.89	4.6	3.4	2.2	0.67	0.30	0.23	0.44
	IF-6	8	318	12.18	3.83	4.5	3.9	2.6	0.82	0.27	0.22	0.40
	IF-7	18	328	13.05	3.98	3.3	2.9	2.0	0.76	0.14	0.08	0.19
	Ave. ± S.D.		330±9.3	13.07±0.85	3.96±0.19	4.7±0.97	3.8±.68	2.3±0.2?	1.1±0.49	0.25±0.06	0.20±0.07	0.37±0.09
Synchronous Control	IS-1	20	332	11.95	3.60	3.1	3.7	2.3	1.1	0.26	0.14	0.35
	IS-2	45	344	12.68	3.69	3.7	4.4	2.5	1.4	0.22	0.26	0.38
	IS-3	9	340	12.71	3.74	4.6	3.9	2.5	1.0	0.27	0.14	0.35
	IS-4	3	306	11.00	3.59	2.2	3.7	2.7	0.60	0.26	0.13	0.34
	IS-5	44	324	11.55	3.56	3.2	3.8	2.5	0.73	0.27	0.35	0.48
	IS-6	40	356	12.50	3.51	3.7	4.4	2.8	0.96	0.34	0.33	0.54
	IS-7	24	355	12.40	3.49	2.6	2.1	1.5	0.39	0.34	0.41	0.59
	Ave. ± S.D.		337±17.8	12.1±0.64	3.60±0.09	3.3±0.79	3.7±0.77	2.4±0.43	0.87±0.33	0.28±0.04	0.25±0.12	0.43±0.10
Vivarium Control	IV-1	1	336	10.70	3.18	0.23	4.1	3.0	0.55	0.35	0.21	0.47
	IV-2	12	362	12.27	3.39	0.30	4.1	2.8	0.77	0.31	0.22	0.44
	IV-3	4	364	12.78	3.51	0.32	3.6	2.3	0.71	0.33	0.26	0.49
	IV-4	7	355	10.75	3.03	0.17	5.0	3.0	1.4	0.38	0.33	0.58
	IV-5	38	364	12.02	3.30	0.15	4.1	2.7	0.83	0.34	0.23	0.48
	IV-6	27	356	11.67	3.33	0.23	4.7	2.6	1.4	0.33	0.32	0.52
	IV-7	30	376	13.32	3.01	0.20	5.1	3.1	1.5	0.31	0.25	0.46
	Ave. ± S.D.		359±12.3	11.67±0.78	3.25±0.19	0.23±0.06	4.4±0.55	2.8±0.28	1.0±0.39	0.34±0.02	0.26±0.05	0.49±0.05

TABLE II B

INDIVIDUAL VALUES FOR LIVER CONSTITUENTS FROM RATS SACRIFICED AT R_{+6}

Group	Rat No. USSR	Rat No. USA	Weight at Sacrifice Carcass (grams)	Liver (grams)	Liver as % carcass	Glycogen	Liver Constituents (mg/100mg Tissue) Total lipids[1]	Phospholipids	Triglycerides	Free cholesterol	Cholesterol esters[2]	Total cholesterol
Flight	2F-1	31	330	11.50	3.48	3.6	3.4	2.1	0.71	0.29	0.29	0.47
	2F-2	10	350	12.43	3.55	4.5	2.6	1.7	0.64	0.15	0.09	0.21
	2F-3	28	335	12.00	3.58	4.1	3.2	1.8	1.1	0.16	0.17	0.27
	2F-4	56	348	11.57	3.32	2.1	2.9	1.8	0.68	0.16	0.11	0.23
	2F-5	57	334	10.87	3.25	3.5	3.5	2.4	0.72	0.32	0.07	0.36
	2F-6	58	375	11.75	3.13	2.7	4.8	2.7	1.5	0.34	0.27	0.50
	Ave. ± S.D.		345±16.6	11.69±0.52	3.39±0.18	3.4±0.89	3.4±0.78	2.1±0.40	0.89±0.34	0.24±0.09	0.17±0.09	0.32±0.10
Synchronous Control	2S-1	16	346	10.35	2.97	3.0	5.0	3.4	1.1	0.26	0.23	0.40
	2S-2	47	380	13.67	3.60	3.6	3.2	2.3	0.46	0.25	0.13	0.33
	2S-3	51	366	11.85	3.24	3.7	4.0	3.1	0.51	0.25	0.12	0.32
	2S-4	25	400	13.62	3.41	2.7	4.2	2.7	1.1	0.29	0.18	0.40
	2S-5	6	336	10.62	3.16	1.6	3.5	2.4	0.63	0.26	0.16	0.36
	2S-6	17	358	12.30	3.44	2.6	3.7	2.5	0.67	0.34	0.25	0.49
	Ave. ± S.D.		365±22.9	12.07±1.42	3.30±0.23	2.9±0.77	3.9±0.63	2.7±0.43	0.75±0.29	0.28±0.04	0.18±0.05	0.38±0.07
Vivarium Control	2V-1	52	380	12.82	3.37	3.0	5.0	2.3	2.1	0.32	0.35	0.53
	2V-2	60	372	14.43	3.88	5.5	3.8	2.4	1.1	0.27	0.10	0.33
	2V-3	19	382	13.75	3.60	3.5	3.4	2.6	0.59	0.25	0.09	0.31
	2V-4	26	358	9.85	2.75	(0.8)[3]	4.2	2.4	1.3	0.28	0.21	0.40
	2V-5	59	350	12.95	3.70	3.4	4.4	2.8	1.1	0.28	0.16	0.37
	2V-6	13	362	12.57	3.47	2.7	3.5	2.7	0.51	0.28	0.09	0.33
	Ave. ± S.D.		367±12.8	12.73±1.57	3.46±0.39	3.6±1.1	4.1±0.61	2.5±0.20	1.1±0.57	0.28±0.02	0.17±0.10	0.38±0.08

TABLE II C

INDIVIDUAL VALUES FOR LIVER CONSTITUENTS FROM STRESSED RATS SACRIFICED AT R+6(S)

Group	Rat No. USSR	Rat No. USA	Weight at Sacrifice Carcass (grams)	Liver (grams)	Liver as % carcass	Liver Constituents (mg/100mg Tissue) Glycogen	Total lipids[1]	Phospholipids	Triglycerides	Free cholesterol	Cholesterol esters[2]	Total cholesterol
Flight	3F-1	37	320	8.37	2.61	0.68	-	-	1.3	-	-	-
	3F-2	5	336	10.07	3.00	0.36	4.6	2.7	2.3	0.34	0.30	0.52
	3F-3	15	315	8.95	2.84	0.51	5.1	2.3	0.67	0.28	0.15	0.37
	3F-4	32	305	8.44	2.77	0.19	4.1	2.8	1.7	0.36	0.20	0.48
	3F-5	21	305	8.82	2.89	0.48	5.1	2.7	0.48	0.34	0.41	0.59
	3F-6	33	310	10.25	3.30	0.43	3.6	2.7	1.4	0.33	0.18	0.44
	3F-7	23	346	14.28	4.13	(2.96)[3]	4.0	2.2		0.22	0.15	0.31
	Ave. ± S.D.		320±15.8	9.88±2.08	3.08±0.51	0.44±0.16	4.4±0.62	2.6±0.25	1.3±0.67	0.31±0.05	0.23±0.10	0.45±0.10
Synchronous Control	3S-1	11	328	10.18	3.10	1.39	3.5	2.0	0.89	0.27	0.32	0.47
	3S-2	34	342	9.50	2.78	1.35	6.6	4.1	2.0	0.25	0.22	0.39
	3S-3	35	326	9.20	2.82	0.78	2.9	1.8	0.65	0.26	0.20	0.38
	3S-4	39	327	8.87	2.71	1.49	5.9	3.2	2.1	0.37	0.25	0.52
	3S-5	40	318	8.57	2.69	1.37	5.2	2.2	2.6	0.19	0.22	0.32
	3S-6	36	352	10.47	2.97	1.79	4.8	2.3	1.8	0.28	0.38	0.51
	3S-7	61	332	8.75	2.64	(0.26)[3]	6.3	2.5	3.1	0.34	0.39	0.58
	Ave. ± S.D.		332±11.4	9.36±0.73	2.82±0.17	1.36±0.35	5.0±1.4	3.6±0.80	1.9±0.87	0.28±0.08	0.28±0.08	0.45±0.09
Vivarium Control	3V-1	22	352	12.17	3.46	4.15	2.7	2.2	0.35	0.16	0.04	0.18
	3V-2	46	340	10.75	3.16	3.22	4.0	2.7	0.83	0.30	0.14	0.38
	3V-3	41	350	11.86	3.39	2.73	4.2	2.8	0.83	0.34	0.27	0.50
	3V-4	29	338	10.75	3.18	2.15	4.5	2.5	1.4	0.28	0.29	0.45
	3V-5	54	356	11.42	3.21	2.33	5.0	2.8	1.6	0.35	0.28	0.52
	3V-6	53	340	12.22	3.49	1.92	5.0	2.8	1.5	0.44	0.34	0.64
	3V-7	55	349	13.82	3.96	2.39	3.2	2.1	0.49	0.30	0.12	0.49
	Ave. ± S.D.		348±6.9	11.86±1.06	3.41±0.28	2.56±0.92	4.1±0.9	2.6±0.30	0.96±0.56	0.31±0.08	0.21±0.11	0.45±0.14

61

TABLE II D

INDIVIDUAL VALUES FOR LIVER CONSTITUENTS FROM RATS SACRIFICED AT R_{+29}

Group	Rat No. USSR	Rat No. USA	Weight at Sacrifice Carcass (grams)	Liver (grams)	Liver as % carcass	Glycogen	Liver Constituents (mg/100mg Tissue) Total lipids[1]	Phospholipids	Triglycerides	Free cholesterol	Cholesterol esters[2]	Total cholesterol
Flight	4F-1	93	400	10.12	2.53	0.15	4.6	3.4	0.53	0.47	0.28	0.64
	4F-2	101	370	9.65	2.61	0.24	3.6	2.6	0.52	0.35	0.17	0.45
	4F-3	87	350	9.86	2.73	0.07	4.0	2.8	0.59	0.38	0.22	0.51
	4F-4	99	440	10.92	2.48	0.22	4.7	3.1	0.54	0.44	0.30	0.62
	4F-5	104	400	10.02	2.51	0.21	4.6	3.0	0.84	0.46	0.27	0.62
	Ave. ± S.D.		392±34.2	10.05±0.54	2.57±0.10	0.18±0.07	4.3±0.48	3.0±0.30	0.66±0.15	0.42±0.05	0.25±0.05	0.57±0.08
Synchronous Control	4S-1	91	465	14.12	3.04	2.0	4.9	2.9	1.3	0.45	0.28	0.62
	4S-2	103	425	11.95	2.81	2.4	4.2	3.0	0.72	0.35	0.22	0.48
	4S-3	97	385	11.15	2.90	3.1	4.5	3.0	0.93	0.34	0.22	0.47
	4S-4	90	455	14.80	3.25	2.7	4.2	2.7	0.95	0.29	0.23	0.43
	4S-5	94	505	16.72	3.31	4.5	4.1	2.6	0.92	0.34	0.22	0.47
	Ave. ± S.D.		447±44.9	13.75±2.24	3.06±0.22	2.9±0.93	4.4±0.33	2.8±0.18	0.96±0.21	0.35±0.06	0.23±0.03	0.49±0.07
Vivarium Control	4V-1	98	365	10.05	2.75	0.37	5.3	3.1	1.5	0.41	0.28	0.58
	4V-2	88	430	16.87	2.53	0.08	3.9	2.9	0.44	0.35	0.16	0.49
	4V-3	92	410	10.17	2.48	0.48	4.3	2.9	0.73	0.42	0.25	0.57
	4V-4	100	375	9.44	2.52	0.42	4.9	3.2	0.56	0.48	0.25	0.63
	4V-5	89	345	10.66	3.10	-	3.6	2.4	0.68	0.28	0.23	0.42
	Ave. ± S.D.		385±34.5	10.24±0.56	2.68±0.26	0.34±0.18	4.4±0.70	2.9±0.31	0.86±0.40	0.39±0.07	0.24±0.04	0.52±0.08

TABLE III A

INDIVIDUAL VALUES FOR CYTOSOLIC HEPATIC ENZYMES FROM RATS SACRIFICED AT R_0

Group	Rat No. USSR	Rat No. USA	Condition of Homogenate[4]	Cytosol Protein (mg/ml)	Cytosolic Enzymes (nmoles/min/mg)[5] GS	GP	GK	HK	G6PDH	6PGDH
Flight	IF-1	42		20.7	9.5	26.5	36.1	7.1	30.7	16.3
	IF-2	43	E	21.1	8.9	31.5	22.4	3.5	38.7	13.7
	IF-3	14	E	18.7	7.1	27.9	13.9	4.2	9.7	12.6
	IF-4	48	E	19.4	9.5	19.8	29.8	5.3	42.9	15.1
	IF-5	50		22.7	7.1	26.7	31.9	4.1	22.5	18.6
	IF-6	8	E	22.0	10.6	27.2	31.5	4.4	18.7	15.4
	IF-7	18	E	20.0	11.8	31.0	40.2	5.1	29.2	16.4
	Ave. ± S.D.			20.7±1.4	9.2±1.7	27.2±3.9	29.4±8.8	4.8±1.2	27.5±11.5	16.3±2.3
Synchronous Control	IS-1	20		20.8	6.3	30.0	23.0	3.4	7.2	15.1
	IS-2	45	E	21.2	11.8	26.9	38.4	5.2	15.8	16.1
	IS-3	9	D,E	20.6	13.7	24.1	34.3	3.5	30.4	17.4
	IS-4	3	D,E	23.0	9.6	21.7	34.9	7.4	23.4	12.7
	IS-5	44	E	23.0	8.1	31.6	38.7	5.3	17.8	14.0
	IS-6	49	E	25.4	5.9	28.1	30.8	5.2	18.5	16.4
	IS-7	24		24.3	8.0	36.3	55.4	5.6	30.2	20.9
	Ave. ± S.D.			22.6±1.8	9.1±2.9	28.4±4.9	36.5±9.9	5.2±1.4	20.5±8.3	16.1±2.6
Vivarium Control	IV-1	?	A,B,C,D,E	18.1	8.8	38.0	2.2	4.0	47.4	24.2
	IV-2	?	A,B,C,E	21.1	8.7	45.4	22.6	3.2	37.9	15.8
	IV-3	4	A,E	21.2	9.0	35.4	5.9	3.6	63.8	21.8
	IV-4	7	A,B,C,E	23.3	8.3	56.4	21.5	3.5	87.6	20.4
	IV-5	38	C,E	24.4	4.9	42.1	31.7	3.9	64.1	17.2
	IV-6	27	A,B,C,E	25.0	6.4	53.7	13.5	3.0	84.6	23.4
	IV-7	30	A,C,D,E	20.5	10.8	44.6	4.5	2.1	96.8	33.8
	Ave. ± S.D.			21.9±2.4	8.1±1.9	44.2±6.5	14.6±11.1	3.3±0.7	68.9±21.8	22.5±5.7

63

TABLE III A (CONTINUED)

INDIVIDUAL VALUES FOR CYTOSOLIC HEPATIC ENZYMES FROM RATS SACRIFICED AT R_0

Group	Rat No. USSR	Rat No. USA	Cytosolic Enzymes (nmoles/min/mg)[5] FAS	AC	GPT	GOT	ICDH	LDH	MDH	GDH
Flight	IF-1	42	8.8	67.3	565.8	395.8	328.1	6378	5931	6.1
	IF-2	43	10.1	77.7	702.0	426.3	297.6	5601	5055	6.8
	IF-3	14	2.8	71.3	544.5	418.6	260.4	6388	5370	4.2
	IF-4	48	11.5	45.2	732.4	559.1	346.5	5145	6048	6.4
	IF-5	50	6.4	71.3	721.7	383.9	307.6	9149	4522	4.7
	IF-6	8	10.8	39.7	622.0	546.1	295.5	5635	4830	20.5
	IF-7	18	18.1*	58.3	537.4	520.2	421.6	7535	6410	2.9
	Ave. ± S.D.		9.8±4.7	61.5±14.4	632.3±85.8	464.3±74.7	330.2±56.2	6547±1384	5452±697	7.4±6.0
Synchronous Control	IS-1	20	5.0	75.6	615.4	418.9	386.1	6401	4654	14.2
	IS-2	45	9.0	67.7	605.7	309.5	408.2	6425	5212	2.2
	IS-3	9	13.2	54.1	508.0	424.0	410.3	7378	5735	3.3
	IS-4	3	5.5	72.2	462.0	403.4	445.4	6020	4918	2.1
	IS-5	44	9.8	65.7	581.0	451.5	364.0	6174	5373	11.6
	IS-6	49	7.8	56.9	465.9	351.0	271.0	6085	5419	5.3
	IS-7	24	15.0	38.9	492.5	434.4	357.5	6375	5293	2.5
	Ave. ± S.D.		9.3±3.7	61.6±12.6	532.9±66.1	399.0±50.6	377.5±55.7	6408±457	5229±352	5.9±5.0
Vivarium Control	IV-1	1	2.2	51.3	640.4	483.7	452.5	7098	6115	11.9
	IV-2	12	10.9	51.1	412.0	349.1	393.0	5387	5074	3.6
	IV-3	4	11.4	63.0	525.9	310.4	491.7	5468	6341	9.0
	IV-4	7	11.9	84.1	385.2	288.5	494.9	6827	5977	21.5
	IV-5	38	12.6	57.9	397.5	339.0	449.5	6400	4908	8.6
	IV-6	27	18.3	54.5	373.5	309.9	435.5	5921	4267	3.2
	IV-7	30	5.6	61.0	410.3	230.7	486.0	7272	6263	19.0
	Ave. ± S.D.		10.4±5.2	60.4±11.4	449.3±98.2	330.2±77.9	457.6±36.8	6343±764	5564±808	11.0±7.1

64

TABLE III B

INDIVIDUAL VALUES FOR CYTOSOLIC HEPATIC ENZYMES FROM RATS SACRIFICED AT R_{+6}

Group	Rat No. USSR	Rat No. USA	Condition of Homogenate	Cytosol Protein (mg/ml)	Cytosolic Enzymes (nmoles/min/mg)[5] GS	GP	GK	HK	G6PDH	6PGDH
Flight	2F-1	31	C	22.1	8.7	34.8	17.7	5.7	76.6	23.2
	2F-2	10	E	20.9	10.0	31.6	42.4	7.5	74.9	20.2
	2F-3	28	E	20.4	8.7	32.4	15.0	5.0	29.2	15.6
	2F-4	56	C	22.9	9.5	39.2	25.7	4.0	41.1	26.9
	2F-5	57		22.9	9.3	36.4	28.2	6.1	28.2	27.9
	2F-6	58		24.2	5.8	19.0	(1.0)[3]	3.4	39.7	28.8
	Ave. ± S.D.			22.2±1.4	8.7±1.5	32.2±7.0	25.8±10.8	5.3±1.5	48.3±21.9	23.8±5.1
Synchronous Control	2S-1	16		21.1	12.0	31.4	29.7	4.4	28.3	16.9
	2S-2	47	E	21.0	13.1	33.7	36.7	4.6	28.3	12.8
	2S-3	51	E	19.9	11.3	39.3	25.9	7.1	19.7	22.5
	2S-4	25		22.3	9.8	29.7	29.4	7.7	32.5	17.0
	2S-5	6	A,C	21.8	9.4	35.0	28.9	7.0	22.2	14.8
	2S-6	17		25.6	9.3	30.7	40.8	6.8	36.0	15.6
	Ave. ± S.D.			22.0±2.0	10.8±1.6	33.3±3.5	31.9±5.6	6.3±1.4	27.8±6.1	16.6±3.3
Vivarium Control	2V-1	52	E	23.0	9.5	26.9	35.3	5.2	56.2	17.7
	2V-2	60		23.2	11.0	25.9	28.2	5.7	55.0	20.6
	2V-3	19		22.5	9.1	29.0	35.6	4.9	81.3	18.9
	2V-4	26		24.9	5.0	34.3	44.6	5.5	47.7	13.2
	2V-5	59		24.2	7.2	29.2	19.0	3.6	47.7	13.7
	2V-6	13	D,E	24.0	5.8	27.8	27.0	4.4	60.0	19.6
	Ave. ± S.D.			23.6±0.9	7.9±2.3	28.9±3.0	31.6±8.8	4.8±0.8	58.0±12.4	17.3±3.1

TABLE III B (CONTINUED)

INDIVIDUAL VALUES FOR CYTOSOLIC HEPATIC ENZYMES FROM RATS SACRIFICED AT R_{46}

Group	Rat No. USSR	Rat No. USA	Cytosolic Enzymes (nmoles/min/mg)[5] FAS	AC	GPT	GOT	ICDH	LDH	MDH	GDH
Flight	2F-1	31	16.6	55.1	661.1	318.7	416.2	5522	6320	0.5
	2F-2	10	19.8	51.5	939.7	338.9	406.4	6810	6740	16.9
	2F-3	28	7.3	84.4	382.7	325.6	430.1	7498	5968	7.6
	2F-4	56	14.5	36.9	752.3	456.1	342.7	4710	5308	1.4
	2F-5	57	13.2	76.3	520.3	529.9	409.5	7734	7241	5.0
	2F-6	58	9.8	76.2	417.5	291.9	372.3	8156	7119	2.6
	Ave. ± S.D.		13.5±4.5	63.4±18.4	595.6±185.0	376.9±94.2	396.2±32.5	6738±1355	6449±736	5.7±6.1
Synchronous Control	2S-1	16	8.6	88.4	541.8	419.7	450.2	7188	5322	4.4
	2S-2	47	8.2	28.8	624.9	377.6	412.1	7575	6229	1.9
	2S-3	51	10.5	42.5	507.7	594.6	503.6	7734	5663	2.5
	2S-4	25	11.8	41.8	536.1	339.3	407.0	7119	5406	4.0
	2S-5	6	8.7	68.4	459.7	352.6	439.4	5450	5908	30.1
	2S-6	17	9.5	47.6	671.4	448.9	367.9	6201	4638	4.2
	Ave. ± S.D.		9.6±1.4	52.9±21.6	556.9±77.8	422.1±94.0	430.0±46.1	6878±880	5528±548	7.9±11.0
Vivarium Control	2V-1	52	20.7	84.7	505.7	363.1	437.5	4648	5320	4.1
	2V-2	60	22.8	54.6	645.4	391.2	386.9	4962	5465	3.9
	2V-3	19	21.5	74.9	701.2	309.5	398.0	7900	5295	8.4
	2V-4	26	11.9	52.3	827.6	432.4	355.6	5121	4857	61.2
	2V-5	59	20.9	36.4	520.6	462.4	348.6	5682	5256	21.0
	2V-6	13	17.9	77.6	744.6	445.3	405.9	5930	5601	24.8
	Ave. ± S.D.		19.3±4.0	63.4±18.5	657.5±126.8	400.7±57.7	388.8±33.1	5707±1173	5239±252	20.6±21.8

TABLE III C

INDIVIDUAL VALUES FOR CYTOSOLIC HEPATIC ENZYMES FROM RATS SACRIFICED AT $R_{+6(S)}$

Group	Rat No. USSR	Rat No. USA	Condition of Homogenate[f]	Cytosol Protein (mg/ml)	Cytosolic Enzymes (nmoles/min/mg)[5] GS	GP	GK	HK	G6PDH	6PGDH
Flight	3F-1	37	A,B,C,D,E	21.5	11.9	36.9	4.1	3.2	39.9	20.8
	3F-2	5	A,E	16.3	13.5	43.7	3.3	3.2	35.9	28.6
	3F-3	15	A,B,C,D,E	20.0	9.7	38.2	6.3	2.5	18.3	13.1
	3F-4	32	A,B,C,D,E	19.4	12.9	47.5	3.0	1.7	44.3	29.6
	3F-5	21	A,B,C,E	24.3	8.0	44.2	2.8	1.7	15.1	18.1
	3F-6	33	D,E	20.9	11.7	20.8	2.7	1.3	87.2	42.4
	3F-7	23	A,C,E	21.8	8.4	24.5	4.1	4.7	32.9	22.4
	Ave. ± S.D.			20.6±2.5	10.9±2.2	36.5±10.2	3.8±1.3	2.6±1.2	39.1±23.8	25.0±9.6
Synchronous Control	3S-1	11	E	22.3	6.9	31.6	23.5	6.1	15.3	10.9
	3S-2	34	E	24.2	11.6	46.2	8.5	2.7	41.5	20.5
	3S-3	35	D,E	23.9	9.0	42.8	18.5	4.8	36.6	16.8
	3S-4	39	C,D	23.7	6.3	47.6	5.9	2.6	21.7	16.7
	3S-5	40	C,E	20.9	3.6	39.9	6.4	3.5	36.9	22.9
	3S-6	36		23.9	9.4	33.2	16.5	4.9	36.2	14.4
	3S-7	61		25.0	4.5	49.6	35.7	4.0	106.9	17.6
	Ave. ± S.D.			23.4±1.4	7.3±2.8	41.4±6.8	16.4±10.8	4.1±1.3	42.2±30.1	17.1±3.9
Vivarium Control	3V-1	22		21.4	9.5	26.5	21.1	4.6	38.5	17.3
	3V-2	46		22.0	7.2	35.1	14.3	3.1	45.8	18.5
	3V-3	41	D,E	22.8	10.9	26.8	23.3	4.9	24.1	15.1
	3V-4	29	D,E	21.2	11.3	28.6	20.1	3.3	18.5	13.2
	3V-5	54		22.5	7.5	43.3	40.1	5.6	28.9	18.2
	3V-6	53	E	23.8	6.6	32.8	23.6	3.5	43.4	22.4
	3V-7	55		22.8	9.7	25.4	31.0	5.6	81.0	18.6
	Ave. ± S.D.			22.4±0.90	9.0±1.9	31.2±6.4	24.8±8.4	4.4±1.1	40.0±20.7	17.6±2.9

TABLE III C (CONTINUED)

INDIVIDUAL VALUES FOR CYTOSOLIC HEPATIC ENZYMES FROM RATS SACRIFICED AT $R_{+6(S)}$[5]

Group	Rat No. USSR	USA	FAS	AC	GPT	GOT	ICDH	LDH	MDH	GDH
							Cytosolic Enzymes (nmoles/min/mg)[5]			
Flight	3F-1	37	5.5	62.8	743.5	638.2	404.4	7126	7230	12.2
	3F-2	5	1.8	80.0	743.5	360.9	514.9	7625	5729	11.7
	3F-3	15	3.3	89.6	666.2	532.3	342.1	6987	6792	16.3
	3F-4	32	0.5	75.8	842.4	714.7	534.3	7535	7842	6.2
	3F-5	21	2.8	59.2	356.1	604.6	434.0	7818	5516	10.0
	3F-6	33	0.3	99.6	822.3	745.3	450.7	6024	7703	9.8
	3F-7	23	13.7	55.8	716.4	450.5	326.8	6041	6462	3.3
	Ave. ± S.D.		4.0±4.6	74.5±16.4	698.2±162.5	616.6±101.4	429.6±79.1	7022±734	6753±911	9.9±4.2
Synchronous Control	3S-1	11	11.4	71.0	444.0	267.1	362.8	6122	4133	1.4
	3S-2	34	10.6	70.1	553.8	323.5	446.6	6134	6121	6.2
	3S-3	35	12.5	90.7	680.4	482.5	457.2	6669	5894	1.2
	3S-4	39	6.1	56.7	404.2	472.1	405.1	7350	6250	8.6
	3S-5	40	6.5	85.8	741.4	458.3	417.9	7565	7183	7.5
	3S-6	36	8.6	56.0	798.2	340.2	428.6	6790	6442	0
	3S-7	61	6.5	31.4	386.4	370.3	455.6	6079	5828	1.1
	Ave. ± S.D.		8.9±2.6	66.0±20.1	572.6±168.8	387.7±84.0	424.8±33.6	6672±608	5983±930	3.7±3.6
Vivarium Control	3V-1	22	10.7	73.9	821.9	335.7	410.0	6937	6649	9.8
	3V-2	46	9.1	45.7	938.5	558.9	374.1	8811	7135	5.3
	3V-3	41	5.2	84.1	752.0	415.7	432.5	6384	3778	10.3
	3V-4	29	7.2	71.6	617.0	-	506.0	6865	5278	6.3
	3V-5	54	8.0	70.6	672.6	443.6	407.9	6154	6458	2.6
	3V-6	53	17.8	42.4	705.2	353.5	412.7	4952	5598	21.3
	3V-7	55	14.5	78.9	609.0	308.9	404.3	5847	5737	4.9
	Ave. ± S.D.		10.4±4.4	66.7±16.2	730.9±118.1	402.7±91.6	421.1±41.2	6564±1197	5805±1106	8.6±6.2

TABLE III D

INDIVIDUAL VALUES FOR CYTOSOLIC HEPATIC ENZYMES FROM RATS SACRIFICED AT R_{+29}

Group	Rat No. USSR	Rat No. USA	Condition of Homogenate[4]	Cytosol Protein (mg/ml)	Cytosolic Enzymes (nmoles/min/mg)[5] GS	GP	GK	HK	G6PDH	6PGDH
Flight	4F-1	93	E	21.3	(0.5)[3]	51.2	8.6	3.2	36.7	14.8
	4F-2	101	E	20.5	10.1	48.9	1.8	3.4	52.7	14.1
	4F-3	87	E	21.2	7.0	48.9	10.6	2.8	45.0	14.4
	4F-4	99	E	25.0	7.5	52.0	5.5	2.9	76.7	18.6
	4F-5	104	E	22.0	12.1	53.1	4.9	5.2	53.9	15.4
	Ave. ± S.D.			22.0±1.8	9.2±2.4	50.8±1.9	6.3±3.4	3.7±1.4	53.0±14.9	15.5±1.8
Synchronous Control	4S-1	91	E	19.5	10.4	22.7	2.3	7.2	79.5	23.1
	4S-2	103	E	18.3	15.2	21.3	2.4	8.5	64.0	12.7
	4S-3	97	E	18.1	10.3	20.5	8.3	6.4	63.9	19.1
	4S-4	90	E	20.0	9.6	25.1	6.5	5.1	73.1	18.8
	4S-5	94	E	20.6	9.6	17.2	10.6	14.8	32.8	12.6
	Ave. ± S.D.			19.3±1.1	11.0±2.4	21.4±2.9	6.0±3.7	8.4±3.8	62.7±17.9	17.3±4.5
Vivarium Control	4V-1	98	E	21.5	9.7	49.1	7.4	1.4	65.1	21.9
	4V-2	88	E	22.0	11.4	49.6	6.3	4.9	66.0	20.1
	4V-3	92	E	20.8	7.6	30.5	7.5	4.8	92.8	30.0
	4V-4	100	E	23.9	10.4	42.8	9.7	1.9	43.2	13.9
	4V-5	89	E	19.6	7.3	16.1	16.3	6.4	66.8	17.8
	Ave. ± S.D.			21.6±1.6	9.3±1.8	37.6±14.3	9.4±4.0	3.9±2.1	66.8±17.6	20.7±6.0

TABLE III D (CONTINUED)

INDIVIDUAL VALUES FOR CYTOSOLIC HEPATIC ENZYMES FROM RATS SACRIFICED AT R_{+29}

Group	Rat No. USSR	Rat No. USA	Cytosolic Enzymes (nmoles/min/mg)[5] FAS	AC	GPT	GOT	ICDH	LDH	MDH	GDH
Flight	4F-1	93	9.4	45.7	593.3	444.1	408.2	7090	6255	1.4
	4F-2	101	13.6	42.8	634.2	438.8	343.6	7869	5223	0
	4F-3	87	15.3	49.1	600.0	526.9	406.3	5081	5601	13.3
	4F-4	99	13.7	60.0	544.2	361.4	400.1	6595	6070	2.9
	4F-5	104	8.7	69.9	678.8	449.2	374.1	7260	6678	7.3
	Ave. ± S.D.		12.1±2.9	53.5±11.3	610.1±50.1	444.1±58.6	386.5±27.6	6779±1053	5965±567	5.0±5.4
Synchronous Control	4S-1	91	12.6	63.3	619.2	314.8	389.1	4970	6419	5.0
	4S-2	103	10.7	103.1	554.3	298.0	398.1	6414	6796	8.8
	4S-3	97	13.0	81.5	727.2	332.5	462.5	7116	7072	6.4
	4S-4	90	12.2	29.5	450.8	357.2	374.3	7036	7084	6.3
	4S-5	94	10.9	71.9	404.5	207.1	473.8	6159	6018	3.1
	Ave. ± S.D.		11.9±1.0	69.9±27.0	551.2±129.6	301.9±57.4	419.6±45.3	6339±866	6678±457	5.9±2.1
Vivarium Control	4V-1	98	11.8	46.2	769.4	393.1	437.1	6544	5729	2.1
	4V-2	88	16.4	73.4	587.3	391.5	446.4	7304	6202	2.2
	4V-3	92	10.5	63.3	727.6	399.6	452.8	7291	6695	2.8
	4V-4	100	10.0	70.3	754.5	359.6	409.2	7181	6046	3.8
	4V-5	89	17.2	57.8	1008.3	481.6	516.5	6933	7085	3.2
	Ave. ± S.D.		13.2±3.4	62.2±10.8	769.4±151.8	405.1±45.5	452.4±39.5	7051±320	6351±538	2.8±0.7

TABLE IV A

INDIVIDUAL VALUES FOR MICROSOMAL ENZYMES FROM LIVERS OF RATS SACRIFICED AT R_0

Group	Rat No. USSR	Rat No. USA	Acyltransferase[a] αGP	Acyltransferase[a] DG	Glyceride-transferase[b] PC	Glyceride-transferase[b] PE	Desaturase[c] Palmitoyl-CoA	Desaturase[c] Stearoyl-CoA	HMG-CoA[a] Reductase
Flight	1F-1	42	13.6	43.7	1.00	0.55	2.1	4.8	11
	1F-2	43	14.4	76.6	0.94	0.51	2.8	5.6	18
	1F-3	14	8.0	53.8	0.95	0.47	0.5	0.6	19
	1F-4	48	4.6	12.8	0.46	0.27	1.9	2.4	15
	1F-5	50	23.7	(1796.2)[3]	0.78	0.51	1.9	2.0	20
	1F-6	8	9.9	31.5	1.04	0.50	1.5	4.4	55
	1F-7	18	15.4	17.5	1.13	0.50	4.2	5.9	31
	Ave. ± S.D.		12.8±6.2	39.3±23.9	0.90±0.22	0.47±0.09	2.1±1.2	3.7±2.0	24±15
Synchronous Control	1S-1	20	32.4	60.9	1.40	0.54	2.3	3.0	21
	1S-2	45	15.8	17.5	0.95	0.52	0.4	2.1	55
	1S-3	9	10.2	201.2	1.32	(0.25)[3]	4.6	8.1	39
	1S-4	3	15.0	108.6	1.12	0.44	1.5	2.3	24
	1S-5	44	18.2	177.0	0.91	0.64	2.6	8.5	15
	1S-6	49	36.5	189.0	1.10	0.66	4.1	8.8	10
	1S-7	24	23.1	176.3	1.35	0.56	7.6	0.1	25
	Ave. ± S.D.		21.6±9.7	132.9±71.6	1.16±0.20	0.56±0.08	3.3±2.4	4.7±3.6	27±15
Vivarium Control	1V-1	1	0.0	14.5	0.12	0.05	0.4	0.3	15
	1V-2	12	0.6	0.0	0.64	0.30	2.0	2.9	20
	1V-3	4	0.0	15.8	0.51	0.20	3.1	5.4	24
	1V-4	7	3.8	30.9	0.36	0.14	1.9	3.6	17
	1V-5	38	1.4	1.2	0.43	0.14	2.2	2.7	13
	1V-6	27	-	-	-	-	4.2	5.4	-
	1V-7	30	0.4	0.3	0.09	0.04	1.6	1.9	15
	Ave. ± S.D.		1.0±1.5	10.5±12.3	0.36±0.22	0.15±0.10	2.2±1.2	3.2±1.8	17±4

Microsomal Enzyme[5,6]

71

TABLE IV B

INDIVIDUAL VALUES FOR MICROSOMAL ENZYMES FROM LIVERS OF RATS SACRIFICED AT R_{+6}

Group	Rat No. USSR	Rat No. USA	Acyltransferase[a] αGP	Acyltransferase[a] DG	Glyceride-transferase[b] PC	Glyceride-transferase[b] PE	Desaturase[c] Palmitoyl-CoA	Desaturase[c] Stearoyl-CoA	HMG-CoA[a] Reductase
Flight	2F-1	37	26.5	429.8	0.93	0.44	7.2	1.2	19
	2F-2	10	(0.9)[3]	(5.2)[3]	0.38	0.15	4.4	4.6	11
	2F-3	28	18.5	180.4	1.11	0.42	3.1	3.7	15
	2F-4	56	20.7	83.2	1.15	0.53	4.3	7.3	13
	2F-5	57	18.7	106.8	0.97	0.46	3.4	10.6	19
	2F-6	58	26.7	167.9	1.36	0.58	4.9	11.2	12
	Ave. ± S.D.		22.2±4.1	193.6±138.2	0.98±0.33	0.43±0.15	4.6±1.5	6.4±4.0	15±3
Synchronous Control	2S-1	16	45.7	267.1	1.68	0.76	(0.1)[3]	0.8	50
	2S-2	47	25.7	272.4	0.95	0.54	1.3	2.7	24
	2S-3	51	49.8	522.6	0.98	0.55	2.9	6.5	11
	2S-4	25	17.2	78.0	1.27	0.58	3.3	6.1	18
	2S-5	6	19.9	30.2	1.33	0.65	2.0	2.6	15
	2S-6	17	14.3	133.8	1.27	0.52	4.5	5.9	22
	Ave. ± S.D.		28.8±15.2	217.4±179.0	1.25±0.27	0.60±0.09	2.8±1.2	4.1±2.4	23±14
Vivarium Control	2V-1	52	11.6	196.6	0.77	0.42	3.6	6.7	14
	2V-2	60	34.5	203.3	1.31	0.57	10.6	17.9	25
	2V-3	19	19.9	114.7	1.12	0.54	7.6	11.0	15
	2V-4	26	63.0	(1658.4)[3]	1.27	0.56	1.3	1.0	18
	2V-5	59	20.2	57.7	1.21	0.53	5.8	11.5	10
	2V-6	13	26.5	57.7	1.05	0.47	1.7	2.5	36
	Ave. ± S.D.		29.3±18.2	126.0±71.4	1.12±0.20	0.52±0.05	5.1±3.6	8.4±6.3	20±9

Microsomal Enzyme[5,6]

TABLE IV c

INDIVIDUAL VALUES FOR MICROSOMAL ENZYMES FROM LIVERS OF RATS SACRIFICED AT $R_{+6}(S)$

Group	Rat No.		Microsomal Enzyme [5,6]						
			Acyltransferase[a]		Glyceride-transferase[b]		Desaturase[c]		HMG-CoA[a] Reductase
	USSR	USA	αGP	DG	PC	PE	Palmitoyl-CoA	Stearoyl-CoA	
Flight	3F-1	37	24.3	8.4	0.90	0.31	0.3	1.2	15
	3F-2	5	3.4	8.2	0.19	0.10	0.1	0.3	14
	3F-3	15	5.3	12.4	0.52	0.18	0.1	0.3	14
	3F-4	32	37.8	13.9	0.29	0.13	0.6	0.2	18
	3F-5	21	27.5	8.4	0.67	0.24	0.1	0.1	9
	3F-6	33	43.8	8.1	0.04	0.06	0.9	0.9	8
	3F-7	23	67.0	18.5	0.56	0.21	(3.8)[a]	6.8	21
	Ave. ± S.D.		29.9±22.3	11.1±4.0	0.45±0.30	0.18±0.109	0.35±0.33	1.4±2.4	14±5
Synchronous Control	3S-1	11	20.8	37.0	1.55	0.68	3.0	4.2	20
	3S-2	34	35.7	70.7	0.90	0.35	1.6	1.6	14
	3S-3	35	40.6	347.6	1.11	0.37	2.7	2.6	22
	3S-4	39	50.5	495.8	1.15	0.53	0.2	0.1	16
	3S-5	40	44.0	330.5	1.26	0.54	0.3	1.7	23
	3S-6	36	38.0	272.5	1.16	0.45	0.2	1.9	18
	3S-7	61	18.1	34.7	0.95	0.33	1.9	0.7	8
	Ave. ± S.D.		35.4±11.9	227.0±181.2	1.15±0.21	0.46±0.13	1.4±1.2	1.8±1.3	17±5
Vivarium Control	3V-1	22	30.3	122.6	1.15	0.44	3.0	4.8	16
	3V-2	46	58.4	(2800.9)[3]	1.05	0.59	0.9	1.7	17
	3V-3	41	15.2	27.1	0.53	0.29	0.5	0.4	19
	3V-4	29	10.7	19.2	0.68	0.27	1.2	1.0	14
	3V-5	54	26.6	347.5	1.02	0.67	1.2	1.9	36
	3V-6	53	64.6	644.4	1.18	0.64	2.6	3.8	25
	3V-7	55	37.3	269.5	1.36	0.52	4.1	7.9	30
	Ave. ± S.D.		34.7±20.4	238.4±238.2	1.00±0.29	0.49±0.16	1.9±1.3	3.1±2.6	22±8

73

TABLE IV D

INDIVIDUAL VALUES FOR MICROSOMAL ENZYMES FROM LIVERS OF RATS SACRIFICED AT R_{+29}

Group	Rat No. USSR	Rat No. USA	Acyltransferase[a] αGP	Acyltransferase[a] DG	Glyceride-transferase[b] PC	Glyceride-transferase[b] PE	Desaturase Palmitoyl-CoA	Desaturase Stearoyl-CoA	HMG-CoA[a] Reductase
					Microsomal Enzyme[5,6]				
Flight	4F-1	93	13.1	31.9	1.03	0.51	1.5	2.9	23
	4F-2	101	6.0	19.6	0.77	0.36	1.3	2.0	13
	4F-3	87	39.1	54.3	0.42	0.38	1.0	2.5	13
	4F-4	99	14.6	63.6	1.11	0.54	0.4	0.5	10
	4F-5	104	11.3	25.9	1.12	0.49	0.4	0.1	14
	Ave. ± S.D.		16.8±12.9	43.1±26.1	0.89±0.30	0.46±0.08	0.9±0.5	1.6±1.2	15±5
Synchronous Control	4S-1	91	7.8	40.2	0.74	0.32	2.6	3.6	31
	4S-2	103	6.3	8.9	0.76	0.36	0.7	1.9	91
	4S-3	97	11.9	16.9	0.93	0.44	1.5	3.6	34
	4S-4	90	41.8	40.7	0.82	0.35	1.7	2.5	57
	4S-5	94	9.6	70.0	1.09	0.46	2.4	3.9	145
	Ave. ± S.D.		15.9±14.9	35.3±23.9	0.87±0.14	0.39±0.06	1.8±0.8	3.1±0.9	72±48
Vivarium Control	4V-1	98	11.9	9.9	0.59	0.48	1.0	1.0	16
	4V-2	88	20.3	29.1	1.07	0.52	0.4	2.0	18
	4V-3	92	3.9	2.6	0.50	0.19	1.0	1.3	18
	4V-4	100	12.9	112.3	1.41	0.60	0.4	1.9	24
	4V-5	89	8.8	6.0	0.42	0.20	2.2	10.2	37
	Ave. ± S.D.		11.6±6.0	32.0±46.1	0.80±0.43	0.40±0.19	1.0±0.7	3.3±3.9	23±9

TABLE V

INDIVIDUAL VALUES FOR MITOCHONDRIAL ENZYMES
FROM LIVERS OF RATS SACRIFICED AT R_0

Group	Rat No. USSR	Rat No. USA	Mitochondrial Enzymes (nmoles/min/mg)[5] GDH	ICDH	AC	MDH
Flight	1F-1	42	802	66.1	12.0	1668
	1F-2	43	1307	38.3	2.7	2043
	1F-3	14	249	34.4	5.7	682
	1F-4	48	404	32.6	3.9	862
	1F-5	50	272	34.0	3.5	797
	1F-6	8	657	76.6	10.0	2118
	1F-7	18	532	34.2	6.7	806
	Ave. ± S.D.		603±369	45.2±18.2	6.4±3.5	1282±636
Synchronous Control	1S-1	20	1041	63.1	13.7	1477
	1S-2	45	790	57.8	8.1	1580
	1S-3	9	554	55.2	15.3	1160
	1S-4	3	567	66.1	20.6	1444
	1S-5	44	788	52.3	6.6	1477
	1S-6	49	1251	65.8	13.2	1909
	1S-7	24	762	73.4	15.8	1775
	Ave. ± S.D.		822±250	62.0±7.3	13.3±4.8	1546±243
Vivarium Control	1V-1	1	1411	72.9	3.4	2969
	1V-2	12	1859	85.9	14.8	3273
	1V-3	4	853	60.1	9.9	1795
	1V-4	7	867	51.5	9.2	1806
	1V-5	38	1096	61.3	8.2	2968
	1V-6	27	861	67.1	11.6	2128
	1V-7	30	743	60.3	3.2	1793
	Ave. ± S.D.		1099±403	65.6±11.1	8.6±4.2	2390±654

TABLE VI A

HEPATIC TOTAL LIPID FATTY ACID COMPOSITION OF RATS SACRIFICED AT R_0

Group	Rat No. USSR	USA	\	\	\	\	\	Percent of Total Fatty Acids[5] As:	\	\	\	\	\	\
			12:0	14:0	16:0	16:1	18:0	18:1	18:2	18:3	20:2	20:3(ω6)	20:4	22:%
Flight	1F-1	42	0.1	0.4	19.1	2.2	15.9	14.1	21.1	0.5	0.9	1.1	23.1	1.5
	1F-2	43	0	0.5	19.3	2.5	14.6	15.6	25.9	0.4	0.8	1.2	21.0	1.2
	1F-3	14	0	0.2	22.0	2.1	11.9	15.9	31.5	0.1	0.5	0.4	15.0	2.0
	1F-4	48	0.1	0.3	17.7	2.2	15.0	11.6	21.0	0.4	1.0	1.5	22.7	5.4
	1F-5	50	0.1	0.5	19.6	2.3	13.2	16.8	23.6	0.1	0.4	0.4	20.1	3.1
	1F-6	8	0	0	21.0	1.9	16.7	13.0	21.5	0.2	0.4	0.8	24.6	1.7
	1F-7	18	0	0.6	20.6	3.0	12.5	16.6	23.7	0.1	0.7	0.8	20.1	1.4
	Ave. ± S.D.		0.1±0.03	0.4±0.2	19.9±1.4	2.3±0.4	15.9±2.0	14.8±2.0	24.0±3.8	0.2±0.2	0.7±0.3	0.9±0.4	20.9±3.1	2.3±1.5
Synchronous Control	1S-1	20	0	0.4	20.7	2.5	13.6	15.4	26.0	0.1	0.8	0.6	18.9	1.1
	1S-2	45	0.1	0.3	17.5	1.4	13.3	12.3	28.6	0.6	1.4	1.3	18.9	4.5
	1S-3	9	0	0.3	20.7	2.6	15.2	16.0	22.7	0.2	0.5	0.4	21.3	0.5
	1S-4	3	0	0.3	5.3	1.4	2.6	15.1	29.9	0.1	1.0	0.8	42.5	1.0
	1S-5	44	0	0.2	19.0	2.8	14.2	15.1	22.2	0.2	0.5	1.2	22.0	1.8
	1S-6	49	0	0.6	20.2	2.3	13.7	14.7	24.7	0.1	0.7	0.7	21.1	1.4
	1S-7	24	0	0.4	20.4	3.4	14.0	15.0	20.2	0	0.6	0.8	23.5	1.7
	Ave. ± S.D.		0	0.4±0.2	17.7±5.6	2.3±0.7	12.4±4.4	14.8±1.2	24.9±3.5	0.1±0.1	0.8±0.4	0.8±0.3	24.1±8.3	1.3±0.5
Vivarium Control	1V-1	1	0	0.2	21.3	1.4	18.9	12.1	20.7	0	0.3	0.3	26.5	0.1
	1V-2	12	0	0.3	22.5	1.8	17.0	14.0	25.1	0.1	0.4	0.3	18.2	2.0
	1V-3	4	0	0.3	21.5	2.2	15.6	13.6	19.2	0	0.4	0.4	26.4	0.3
	1V-4	7	0	0.2	22.9	1.6	17.0	14.4	22.8	0.1	0.4	0.2	20.4	0.2
	1V-5	38	0	0.3	23.6	1.4	20.3	11.3	23.3	0	0.3	0.2	17.8	1.5
	1V-6	27	0	0.3	22.7	1.9	13.6	17.2	24.8	0.1	0.3	0.3	17.7	0.9
	1V-7	30	0	0.3	22.4	1.6	14.8	15.8	24.8	0	0.3	0.2	19.5	1.2
	Ave. ± S.D.		0	0.3±0	22.4±0.8	1.7±0.3	16.7±2.3	14.0±2.0	22.9±2.3	0.1±0	0.3±0.1	0.3±0.1	20.7±3.5	0.9±0.7

TABLE VI B

HEPATIC TOTAL LIPID FATTY ACID COMPOSITION OF RATS SACRIFICED AT R_{+6}

Group	Rat No. USSR	Rat No. USA	Percent of Total Fatty Acids[5] As: 12:0	14:0	16:0	16:1	18:0	18:1	18:2	18:3	20:2	20:3(ω6)	20:4	22:4
Flight	2F-1	31	0	0.5	21.5	3.1	16.2	12.9	18.9	0.1	0.5	0.7	24.4	1.4
	2F-2	40	0	0.3	21.4	1.4	18.8	12.3	20.8	0	0.3	0.3	24.2	0.2
	2F-3	28	0	0.3	19.0	1.5	14.4	13.6	29.0	0	0.6	0.3	15.6	1.7
	2F-4	56	0	0.2	17.6	2.8	13.4	15.3	20.8	0.8	0.5	0.6	26.8	1.7
	2F-5	57	0	0.5	18.2	2.3	14.3	14.2	21.2	0.8	1.1	1.0	24.7	1.7
	2F-6	58	0	0.5	18.8	2.5	12.2	16.0	23.7	0.3	0.8	1.1	23.0	1.2
	Ave. ± S.D.		0	0.4±0.1	19.4±1.6	2.3±0.7	14.9±2.3	14.1±1.4	22.4±3.6	0.2±0.1	0.6±0.3	0.7±0.3	23.8±2.4	1.3±0.6
Synchronous Control	2S-1	16	0	0.1	21.2	2.4	16.5	11.2	24.2	0	0.3	0.2	22.1	0.7
	2S-2	47	0	0.5	19.4	2.1	15.5	12.7	19.0	0	0.6	1.1	27.1	1.7
	2S-3	51	0	0.3	19.5	1.9	15.7	13.0	19.9	0	0.7	1.0	26.4	1.4
	2S-4	25	0	0.3	20.8	2.7	15.3	14.4	23.3	0	0.4	0.4	20.1	2.0
	2S-5	6	0	0.2	21.4	1.6	19.4	9.8	19.8	0	0.6	0.5	26.5	0.3
	2S-6	17	0	0.5	22.2	2.7	17.5	14.2	17.1	0	0.3	1.0	24.2	1.9
	Ave. ± S.D.		0	0.3±0.1	20.7±1.1	2.2±0.5	16.5±1.2	12.6±1.8	20.5±2.7	0	0.5±0.2	0.7±0.4	24.4±2.8	1.3±0.7
Vivarium Control	2V-1	52	0.1	0.4	18.3	4.6	8.5	20.3	24.5	0	0.5	1.1	19.5	1.9
	2V-2	60	0	1.0	24.1	6.8	12.9	16.5	14.9	0.1	0.3	0.9	20.2	2.1
	2V-3	19	0	0.5	23.0	3.3	15.3	14.5	17.6	0	0.5	1.4	22.1	1.2
	2V-4	26	0	0	20.4	1.6	19.8	11.6	20.2	0	0.2	0.3	23.6	2.1
	2V-5	59	0	0.5	21.6	3.8	13.1	16.5	20.0	0	0.6	1.6	21.3	1.4
	2V-6	13	0	0.3	22.5	2.3	18.7	12.7	17.9	0	0.5	0.7	22.9	1.6
	Ave. ± S.D.		0	0.5±0.3	21.7±2.1	3.8±1.8	14.7±4.2	15.3±3.1	19.2±3.3	0	0.4±0.2	0.9±0.4	21.6±1.6	1.7±0.4

TABLE VI C

HEPATIC TOTAL LIPID FATTY ACID COMPOSITION OF RATS SACRIFICED AT $R_{+6(S)}$

Group	Rat No. USSR	Rat No. USA	Percent of Total Fatty Acid[b] As: 12:0	14:0	16:0	16:1	18:0	18:1	18:2	18:3	20:2	20:3(ω6)	20:4	22:4
Flight	3F-1	37	0	0.3	22.7	1.2	18.0	10.3	25.9	0.1	0.3	0.1	20.4	0.8
	3F-2	5	0	0.3	24.7	2.3	17.8	14.6	21.1	0.3	0.2	0.3	18.4	0
	3F-3	15	0	0.5	22.9	1.7	10.0	13.2	36.2	0.2	0.3	0.2	13.3	1.5
	3F-4	32	0	0.4	20.7	1.6	17.2	12.0	23.8	0	0.3	0.3	22.0	1.4
	3F-5	21	0	0.3	19.7	1.0	15.1	12.3	29.6	0.1	0.3	0.4	19.6	1.6
	3F-6	33	0	0.4	19.7	1.7	20.7	11.8	20.8	0	0.2	0.3	23.1	1.0
	3F-7	23	0	1.4	30.8	8.7	8.8	19.3	18.2	0.1	0.2	0.7	11.0	0.7
	Ave. ± S.D		0	0.6±0.4	23.0±3.9	2.6±2.7	15.1±4.4	13.4±3.0	25.2±5.7	0.1±0.1	0.2±0.1	0.4±0.2	14.5±6.3	1.0±0.6
Synchronous Control	3S-1	11	0	0.2	21.1	1.2	17.0	11.7	22.9	0	0	0.3	22.7	1.6
	3S-2	34	0	0.3	21.2	1.5	17.5	12.0	24.4	0.1	0.3	0.5	21.0	1.3
	3S-3	35	0	0.4	21.3	1.5	18.2	11.4	21.6	0	0.3	0.6	23.2	1.3
	3S-4	39	0	0.3	23.0	1.3	17.0	11.4	25.6	0.1	0.2	0.3	19.4	1.4
	3S-5	40	0	0.3	21.8	1.4	12.5	12.4	30.3	0.1	0.3	0.5	18.2	1.8
	3S-6	36	0	0.4	20.9	1.4	19.9	9.3	21.1	0.1	0.3	0.5	25.0	1.2
	3S-7	61	0	0.4	23.7	1.3	10.2	14.9	31.9	0	0.3	0.3	15.7	1.3
	Ave. ± S.D		0	0.3±0.1	21.9±1.1	1.4±0.1	16.1±3.4	11.9±1.7	25.4±4.2	0.1±0	0.3±0	0.4±0.1	20.8±3.2	1.4±0.2
Vivarium Control	3V-1	22	0	0.4	21.6	2.1	15.0	13.7	24.8	0.1	0.5	0.7	19.9	1.2
	3V-2	46	0	0.3	18.3	1.3	18.4	10.5	24.6	0	0.4	0.3	24.2	1.7
	3V-3	41	0	0.4	16.9	1.8	9.7	14.4	32.3	0	0.5	0.5	21.6	1.9
	3V-4	29	0	0.2	9.8	1.8	4.5	16.2	39.0	0	0.7	0.6	25.5	1.9
	3V-5	54	0	0.3	19.7	1.4	15.2	12.9	27.1	0.1	0.5	0.5	20.5	1.7
	3V-6	53	0	0.3	19.8	2.5	17.2	13.6	18.9	0	0.3	0.4	22.7	1.8
	3V-7	55	0	0.4	21.4	1.7	18.6	11.4	21.9	0	0.4	0.8	21.1	1.3
	Ave. ± S.D		0	0.3±0.1	18.2±4.1	1.8±0.4	14.1±5.2	13.2±1.9	26.9±6.8	0	0.5±0.1	0.6±0.2	22.2±2.0	1.6±0.3

TABLE VI D

HEPATIC TOTAL LIPID FATTY ACID COMPOSITION OF RATS SACRIFICED AT R_{+29}

| Group | Rat No. | | Percent of Total Fatty Acids [5] As: | | | | | | | | | | | |
	USSR	USA	12:0	14:0	16:0	16:1	18:0	18:1	18:2	18:3	20:2	20:3(ω6)	20:4	22:6
Flight	4F-1	93	0.1	0.2	14.6	0.8	18.3	7.3	24.8	0.5	0.5	0.6	30.3	2.1
	4F-2	101	0.1	0	17.4	2.9	20.1	7.0	19.4	0.8	0.7	0.5	27.5	2.9
	4F-3	87	0	0.2	16.9	0.8	26.1	6.5	20.7	0.4	0.5	0.7	21.9	5.3
	4F-4	99	0.3	0.2	16.6	0.9	22.1	7.7	21.4	0.3	1.4	1.1	23.3	4.8
	4F-5	104	0.1	0.3	17.7	1.3	18.0	10.2	22.3	0.3	0.5	0.4	19.4	3.7
	Ave. ± S.D.		0.1±0.1	0.2±0.1	16.6±1.2	1.3±0.9	20.9±3.4	7.9±1.4	22.9±3.9	0.5±0.2	0.7±0.4	0.7±0.3	24.5±4.4	3.8±1.3
Synchronous Control	4S-1	91	0.1	0.2	19.2	0.8	18.6	10.0	28.5	0.5	0.7	0.5	18.7	3.2
	4S-2	103	0.1	0.2	18.2	0.7	20.2	7.8	21.3	0.3	1.1	1.1	22.3	6.7
	4S-3	97	0.3	0.2	17.8	0.8	17.3	7.1	19.6	0.1	1.9	1.9	23.6	9.5
	4S-4	90	0	0.3	16.5	2.3	13.3	12.4	26.5	0.5	0.7	0.9	23.9	2.7
	4S-5	94	0	0.3	19.6	0.9	17.3	9.2	22.7	0.3	0.8	1.0	20.5	6.9
	Ave. ± S.D.		0.1±0.1	0.2±0.1	18.3±1.2	1.1±0.6	17.4±2.5	9.3±2.1	23.7±3.7	0.3±0.2	1.3±0.6	1.1±0.5	21.8±2.2	5.8±2.9
Vivarium Control	4V-1	98	0	0.3	17.2	1.3	13.2	11.4	26.9	0.1	0.7	1.2	23.7	4.6
	4V-2	88	0	0.1	17.4	1.8	25.4	6.5	17.3	0.5	0.5	0.6	26.3	4.5
	4V-3	92	0	0.1	17.5	0.9	22.5	7.7	21.2	0.4	0	0.4	22.1	6.7
	4V-4	100	0	0.2	17.0	0.8	22.3	8.0	22.0	0.3	0.6	0.7	22.2	7.6
	4V-5	89	0	0.5	23.5	3.4	16.3	14.6	21.1	0.4	0.8	1.2	12.8	4.4
	Ave. ± S.D.		0	0.2±0.2	18.5±2.8	1.4±1.1	19.9±5.0	9.7±3.3	21.7±3.4	0.3±0.1	0.6±0.1	0.8±0.3	21.4±5.1	5.6±1.5

79

TABLE VII A

HEPATIC PHOSPHOLIPID FATTY ACID COMPOSITION OF RATS SACRIFICED AT R_0

Group	Rat No. USSR	Rat No. USA	Percent of Phospholipid Fatty Acid[5] As: 12:0	14:0	16:0	16:1	18:0	18:1	18:2	18:3	20:2	20:3(ω6)	20:4	22:4
Flight	IF-1	42	0	0	16.6	1.1	23.3	7.4	14.9	0.4	0.9	1.3	27.6	6.6
	IF-2	43	0	0.3	18.8	1.5	21.0	9.3	17.3	0.8	0.9	1.7	24.2	4.1
	IF-3	14	-	-	-	-	-	-	-	-	-	-	-	-
	IF-4	48	0.1	0.2	16.5	1.2	22.0	7.0	15.4	0.4	0.3	1.2	29.7	6.1
	IF-5	50	0.1	0.2	19.8	1.0	27.0	5.5	16.8	0.4	0.6	0.9	23.0	5.0
	IF-6	8	0.1	0.2	18.9	1.2	23.5	6.8	15.0	0.4	0.5	1.1	31.2	1.4
	IF-7	18	0	0.3	18.9	1.6	21.6	9.1	16.3	0.5	0.7	1.0	30.6	0.8
	Ave. ± S.D.		0.1±0.1	0.2±0.1	18.2±1.4	1.3±0.2	23.1±2.1	7.5±1.5	16.0±1.0	0.5±0.2	0.7±0.2	1.2±0.3	27.7±3.4	4.0±2.4
Synchronous Control	IS-1	20	0.2	0.3	18.1	1.5	20.3	9.3	18.4	0.6	0.9	0.9	27.8	1.7
	IS-2	45	0	0.2	16.9	0.8	25.3	6.7	17.2	0.6	1.1	0.9	27.9	3.1
	IS-3	9	0	0.2	17.9	1.2	22.0	7.9	16.0	0.5	0.7	0.9	29.8	2.6
	IS-4	3	-	-	-	-	-	-	-	-	-	-	-	-
	IS-5	44	0.1	0.3	17.9	1.5	16.9	8.8	16.8	0.6	1.0	1.1	27.8	5.1
	IS-6	49	0	0.2	18.0	0.9	23.2	6.7	16.3	0.6	1.1	0.7	30.3	1.7
	IS-7	24	0	0.3	20.1	1.7	22.2	8.4	13.4	0.4	0.7	1.2	28.4	2.8
	Ave. ± S.D.		0	0.2±0.1	18.1±1.1	1.3±0.4	22.0±2.2	8.0±1.1	16.4±1.7	0.5±0.1	0.9±0.2	1.0±0.2	28.7±1.1	2.8±1.2
Vivarium Control	IV-1	1	-	-	-	-	-	-	-	-	-	-	-	-
	IV-2	12	-	-	-	-	-	-	-	-	-	-	-	-
	IV-3	4	-	-	-	-	-	-	-	-	-	-	-	-
	IV-4	7	0	0.1	17.2	0.6	25.5	5.7	14.3	0.5	0.8	0.9	32.2	2.3
	IV-5	38	0.2	0.2	10.1	0.7	22.1	8.5	17.5	0	1.5	0.6	33.2	3.1
	IV-6	27	0.2	0.2	17.5	1.2	23.5	6.0	15.6	1.1	0.5	0.9	30.5	3.0
	IV-7	30	0.1	0.1	17.6	0.6	27.3	5.2	14.9	0.4	0.5	0.7	29.7	3.4
	Ave. ± S.D.		0.1±0.1	0.2±0.0	15.6±3.7	0.8±0.3	24.6±2.3	6.3±1.5	15.5±1.4	0.6±0.4	0.8±0.5	0.7±0.2	31.4±1.6	3.0±0.5

TABLE VII B

HEPATIC TRIGLYCERIDE FATTY ACID COMPOSITION OF RATS SACRIFICED AT R_3

Group	Rat No. USSR	USA	Percent of Triglyceride Fatty Acids As: 12:0	14:0	16:0	16:1	18:0	18:1	18:2	18:3	20:2	20:3(ω6)	20:4	22:4
Flight	1F-1	42	0.2	1.0	25.0	4.7	2.8	25.8	35.7	0.9	0.5	1.0	5.8	3.0
	1F-2	43	0.1	0.9	22.0	4.7	1.9	24.0	37.4	0.8	0.6	0.9	3.7	3.0
	1F-3	14	-	-	-	-	-	-	-	-	-	-	-	-
	1F-4	48	0.1	0.9	22.2	4.5	2.2	24.4	34.9	0.2	0.4	1.0	4.1	4.5
	1F-5	50	0.7	0.9	30.9	3.1	2.6	20.2	28.9	0.3	0.5	0.9	3.3	-
	1F-6	8	0.6	0.9	23.2	3.0	3.3	24.2	36.3	0.5	0.5	0.7	4.2	2.5
	1F-7	18	0.4	1.1	21.9	5.7	1.3	26.8	33.1	0.8	0.9	0.9	4.0	3.3
	Ave. ± S.D.		0.4±0.3	1.0±0.1	24.2±3.5	4.3±1.0	2.4±0.7	24.2±2.3	34.4±3.1	0.6±0.3	0.6±0.2	0.9±0.1	4.2±0.9	3.3±3.8
Synchronous Control	1S-1	20	0.1	0.9	22.0	6.8	3.0	25.6	37.4	1.4	0.9	0.4	5.0	2.0
	1S-2	45	0.1	0.7	22.2	2.2	1.8	20.9	44.2	0.5	0.7	0.5	3.2	3.0
	1S-3	9	0.1	0.9	2.5	4.4	2.1	25.0	35.4	0.5	0.7	0.7	3.6	5.7
	1S-4	3	-	-	-	-	-	-	-	-	-	-	-	-
	1S-5	44	0.1	1.0	21.1	4.4	2.1	24.8	36.8	0.6	0.6	0.6	3.1	4.4
	1S-6	49	0.1	0.8	24.1	2.5	2.9	19.4	42.1	0.7	0.6	0.1	4.2	1.9
	1S-7	24	0.1	1.0	19.7	6.5	1.8	25.9	30.1	0.7	1.1	1.1	3.9	-
	Ave. ± S.D.		0.1±0	0.9±0.1	21.6±1.5	4.5±1.9	2.3±0.6	23.6±2.8	37.7±5.0	0.7±0.4	0.8±0.2	0.6±0.4	3.8±0.7	3.4±1.5
Vivarium Control	1V-1	1	-	-	-	-	-	-	-	-	-	-	-	-
	1V-2	12	-	-	-	-	-	-	-	-	-	-	-	-
	1V-3	4	-	-	-	-	-	-	-	-	-	-	-	-
	1V-4	7	0.2	1.0	26.9	3.8	4.6	25.4	36.2	0.4	0.2	0.3	3.4	1.8
	1V-5	38	0	0.8	24.0	2.0	3.2	22.4	41.1	0.6	0.4	0	3.4	1.6
	1V-6	27	0.2	0.6	25.9	2.2	2.2	27.8	38.4	0.7	0.3	0.1	2.2	2.2
	1V-7	30	0	0.7	22.5	1.7	2.5	25.2	37.1	0.2	0.2	0.2	2.8	3.4
	Ave. ± S.D.		0.1±0.1	0.8±0.2	25.3±1.3	2.4±0.9	3.1±1.1	25.2±2.2	38.2±2.2	0.5±0.2	0.3±0.1	0.1±0.1	3.0±0.5	2.2±0.8

TABLE VIII A

INDIVIDUAL VALUES FOR SPECIFIC LIPID RATIOS FROM LIVERS OF RATS SACRIFICED AT R_0

Group	Rat No. USSR	Rat No. USA	Ratio Fatty Acids[5] 16/16:1	18/18:1	18:2/20:4	Cholesterol/Cholesterol ester	Phospholipids/Triglycerides
Flight	IF-1	42	8.7	1.13	0.91	1.24	2.09
	IF-2	43	7.63	0.75	1.24	1.27	1.79
	IF-3	14	10.45	0.75	2.10	0.89	1.20
	IF-4	48	8.21	1.29	0.93	1.83	3.58
	IF-5	50	8.69	0.79	1.17	1.30	3.28
	IF-6	8	11.26	1.29	0.87	1.23	3.17
	IF-7	18	6.87	0.76	1.18	1.75	2.63
	Ave. ± S.D.		8.89±1.54	0.97±0.26	1.20±0.42	1.36±0.33	2.53±0.88
Synchronous Control	1S-1	20	8.28	0.88	1.37	1.86	2.09
	1S-2	45	12.86	1.08	1.51	0.85	1.79
	1S-3	9	7.95	0.95	1.07	1.93	2.50
	1S-4	3	3.71	0.17	0.70	2.00	4.50
	1S-5	44	6.85	0.94	0.C?	0.77	3.42
	1S-6	49	8.96	0.93	1.17	1.03	2.92
	1S-7	24	18.89	1.23	1.51	0.83	3.05
	Ave. ± S.D.		9.64±4.90	0.88±0.34	1.19±0.30	1.32±0.57	3.01±0.97
Vivarium Control	1V-1	1	14.97	1.56	0.84	1.67	5.45
	1V-2	12	12.30	1.21	1.37	1.41	3.64
	1V-3	4	9.73	1.14	0.73	1.27	3.24
	1V-4	7	14.29	1.18	1.11	1.15	2.14
	1V-5	38	17.36	1.80	1.31	1.48	3.25
	1V-6	27	11.99	0.79	1.40	1.03	1.86
	1V-7	30	13.89	0.94	1.27	1.24	2.07
	Ave. ± S.D.		13.60±2.44	1.23±0.35	1.15±0.27	1.32±0.22	3.09±1.25

TABLE VIII B

INDIVIDUAL VALUES FOR SPECIFIC LIPID RATIOS FROM LIVERS OF RATS SACRIFICED AT R_{+6}

Group	Rat No.		Ratio				
			Fatty Acids[5]			Cholesterol	Phospholipids
	USSR	USA	16/16:1	18/18:1	18:2/20:4	Cholesterol ester	Triglycerides
Flight	2F-1	31	6.95	1.25	0.77	1.00	2.96
	2F-2	10	14.84	1.53	0.86	1.67	2.65
	2F-3	28	12.86	1.06	1.48	0.94	1.64
	2F-4	56	6.20	0.87	0.78	1.45	2.65
	2F-5	57	7.85	1.01	0.86	4.57	3.33
	2F-6	58	7.57	0.76	1.03	1.26	1.80
	Ave. ± S.D.		9.38±3.57	1.08±0.28	0.96±0.27	1.82±1.38	2.51±0.66
Synchronous Control	2S-1	16	8.66	1.48	1.10	1.13	3.09
	2S-2	47	9.38	1.22	1.43	1.92	5.00
	2S-3	51	10.18	1.21	0.75	2.08	6.08
	2S-4	25	7.81	1.06	1.16	1.61	2.45
	2S-5	6	13.69	1.88	0.25	1.63	3.01
	2S-6	17	8.14	1.18	0.71	1.36	3.73
	Ave. ± S.D.		9.64±2.16	1.34±0.30	0.90±0.29	1.62±0.35	4.03±1.32
Vivarium Control	2V-1	52	4.00	0.42	1.26	0.91	1.10
	2V-2	60	3.55	0.78	0.74	2.70	2.18
	2V-3	19	5.97	1.05	0.80	2.75	4.41
	2V-4	26	12.46	1.71	0.86	1.33	1.85
	2V-5	59	5.72	0.80	0.94	1.75	2.55
	2V-6	13	9.99	1.47	0.78	3.11	5.29
	Ave. ± S.D.		6.95±3.53	1.04±0.48	0.90±0.19	2.10±0.89	2.90±1.61

TABLE VIII C

INDIVIDUAL VALUES FOR SPECIFIC LIPID RATIOS FROM LIVERS OF STRESSED RATS SACRIFICED AT $R_{+6(S)}$

Group	Rat No. USSR	Rat No. USA	Ratio Fatty Acids[5] 16/16:1	18/18:1	18:2/20:4	Cholesterol / Cholesterol ester	Phospholipids / Triglycerides
Flight	3F-1	37	18.27	1.75	1.27	-	-
	3F-2	5	10.64	1.21	1.15	1.13	1.54
	3F-3	15	13.37	0.76	2.71	1.87	1.00
	3F-4	32	13.18	1.43	1.08	1.80	4.18
	3F-5	21	18.89	1.23	1.51	0.83	1.59
	3F-6	33	11.67	1.76	0.90	1.83	5.63
	3F-7	23	3.54	0.45	1.66	1.47	1.57
	Ave. ± S.D.		12.79±5.15	1.23±0.49	1.47±0.60	1.49±0.43	2.59±1.07
Synchronous Control	3S-1	11	18.32	1.45	1.01	0.84	2.25
	3S-2	34	13.86	1.46	1.16	1.14	2.05
	3S-3	35	14.03	1.60	0.93	1.30	2.77
	3S-4	39	18.09	1.49	1.32	1.48	1.52
	3S-5	40	15.15	1.01	1.66	0.66	0.85
	3S-6	36	15.36	2.16	0.85	0.74	1.28
	3S-7	61	18.09	0.69	2.04	0.87	0.91
	Ave. ± S.D.		16.13±1.98	1.41±0.46	1.28±0.43	1.01±0.26	1.65±0.74
Vivarium Control	3V-1	22	10.16	1.20	1.25	4.00	6.29
	3V-2	46	14.63	1.75	1.02	2.14	3.25
	3V-3	41	9.57	0.68	1.49	1.26	3.37
	3V-4	29	5.51	0.27	1.53	0.97	1.79
	3V-5	54	14.48	1.18	1.32	1.25	1.75
	3V-6	53	8.09	1.27	0.83	1.29	1.87
	3V-7	55	12.28	1.63	1.03	2.50	4.29
	Ave. ± S.D.		10.69±3.35	1.14±0.52	1.21±0.26	1.92±1.07	3.23±1.66

TABLE VIII D

INDIVIDUAL VALUES FOR SPECIFIC LIPID RATIOS FROM LIVERS OF RATS SACRIFICED AT R_{+29}

Group	Rat No. USSR	Rat No. USA	Ratio — Fatty Acids[5] 16/16:1	Ratio — Fatty Acids[5] 18/18:1	Ratio — Fatty Acids[5] 18:2/20:4	Cholesterol / Cholesterol ester	Phospholipids / Triglycerides
Flight	4F-1	93	19.41	2.50	0.82	1.68	6.42
	4F-2	101	5.98	2.59	0.71	2.06	5.00
	4F-3	87	20.08	4.04	0.95	1.73	4.75
	4F-4	99	18.86	2.88	0.92	1.47	3.88
	4F-5	104	14.05	1.77	1.45	1.70	3.57
	Ave. ± S.D.		15.68±5.92	2.76±0.83	0.97±0.28	1.73±0.21	4.72±1.12
Synchronous Control	4S-1	91	22.89	1.86	1.52	1.61	2.23
	4S-2	103	26.03	2.60	0.95	1.59	4.17
	4S-3	97	22.01	2.45	0.83	1.55	3.23
	4S-4	90	7.34	1.07	1.11	1.26	2.84
	4S-5	94	22.97	1.88	1.01	1.55	2.83
	Ave. ± S.D.		20.25±7.37	1.97±0.60	1.08±0.26	1.51±0.14	3.06±0.72
Vivarium Control	4V-1	98	13.55	1.16	1.14	1.46	2.07
	4V-2	88	21.18	3.88	1.52	2.11	6.59
	4V-3	92	19.88	2.91	0.97	1.68	3.97
	4V-4	100	21.49	2.78	0.99	1.92	3.33
	4V-5	89	6.92	1.11	1.65	1.22	3.53
	Ave. ± S.D.		16.60±6.30	2.37±1.20	1.25±0.31	1.68±0.35	3.90±1.66

TABLE IX A

AVERAGE VALUES[7] FOR RATS SACRIFICED AT R_0

Measurement[5,6]		Groups		
			Control	
Parameter	Units[6]	Flight	Synchronous	Vivarium
Weights				
Carcass	grams	330 ± 9.3	337 ± 17.8	359 ± 12.3
Liver	grams	13.07± 0.85	12.10± 0.64	11.67± 0.78
Liver/carcass	%	3.96± 0.19	3.60± 0.09	3.25± 0.19
Liver Constituents				
Cytosol protein	mg/ml	20.7 ± 1.4	22.6 ± 1.8	21.9 ± 2.4
Glycogen	% tissue wt.	4.7 ± 0.97	3.3 ± 0.79	0.23± 0.06
Total Lipids	% tissue wt.	3.8 ± 0.68	3.7 ± 0.77	4.4 ± 0.56
Phospholipids	% tissue wt.	2.3 ± 0.20	2.4 ± 0.43	2.8 ± 0.28
Triglycerides	% tissue wt.	1.1 ± 0.49	0.87± 0.33	1.0 ± 0.39
Free cholesterol	% tissue wt.	0.25± 0.06	0.28± 0.04	0.34± 0.02
Cholesterol esters	% tissue wt.	0.20± 0.07	0.25± 0.12	0.26± 0.05
Total cholesterol	% tissue wt.	0.37± 0.09	0.43± 0.10	0.49± 0.05
Ratio:				
Cholesterol/cholesterol esters		1.36± 0.33	1.32± 0.57	1.32± 0.22
Phospholipids/triglycerides		2.53± 0.88	3.01± 0.97	3.09± 1.25
Fatty acids				
16/16:1		8.89± 1.54	9.64± 4.90	13.50± 2.44
18/18:1		0.97± 0.26	0.88± 0.34	1.23± 0.35
18:2/20:4		1.20± 0.42	1.19± 0.30	1.15± 0.27
Enzyme Activity				
1. Cytosolic				
GS	b	9.2 ± 1.7	9.1 ± 2.9	8.1 ± 1.9
GP	b	27.2 ± 3.9	28.4 ± 4.9	44.2 ± 6.5
GK	b	29.4 ± 8.8	36.5 ± 9.9	14.6 ± 11.1
HK	b	4.8 ± 1.2	5.2 ± 1.4	3.3 ± 0.7
G6PDH	b	27.5 ± 11.5	20.5 ± 8.3	68.9 ± 21.8
6PGDH	b	16.3 ± 2.3	16.1 ± 2.6	22.5 ± 5.7
FAS	b	9.8 ± 4.7	9.3 ± 3.7	10.4 ± 5.2
AC	b	61.5 ± 14.4	61.6 ± 12.6	60.4 ± 11.4
GPT	b	632.3 ± 85.8	532.9 ± 66.1	449.3 ± 98.2
GOT	b	464.3 ± 74.7	339.0 ± 50.6	330.2 ± 77.9
ICDH	b	330.2 ± 56.2	377.5 ± 55.7	457.6 ± 36.8
LDH	b	6547 ±1384	6408 ± 457	6343 ± 764
MDH	b	5452 ± 697	5229 ± 352	5464 ± 808
GDH	b	7.4 ± 6.0	5.9 ± 5.0	11.0 ± 7.1
2. Microsomal				
Acyl transferase				
a. αGP	a	12.8 ± 6.2	21.6 ± 9.7	1.0 ± 1.5
b. DG	a	39.3 ± 23.9	132.9 ± 71.6	10.5 ± 12.3
Glyceride-transferase				
a. PC	b	0.90± 0.22	1.16± 0.20	0.36± 0.22
b. PE	b	0.47± 0.09	0.56± 0.08	0.15± 0.10
Desaturase				
a. Palmitoyl-CoA	c	2.1 ± 1.2	3.3 ± 2.4	2.2 ± 1.2
b. Stearoyl-CoA	c	3.7 ± 2.0	4.7 ± 3.6	3.2 ± 1.8
HMG-CoA reductase	a	24 ± 15	27 ± 15	17 ± 4
3. Mitochondrial				
GDH	b	603 ± 369	822 ± 250	1099 ± 403
ICDH	b	45.2 ± 18.2	62.0 ± 7.3	65.6 ± 11.1
AC	b	6.4 ± 3.5	13.3 ± 4.8	8.6 ± 4.2
MDH	b	1282 ± 636	1546 ± 243	2390 ± 654

TABLE IX B

AVERAGE VALUES[7] FOR RATS SACRIFICED AT R_{+6}

Measurement [5,6]		Groups		
			Control	
Parameter	Units[6]	Flight	Synchronous	Vivarium
Weights				
Carcass	grams	345 ± 16.6	365 ± 22.9	367 ± 12.8
Liver	grams	11.69± 0.52	12.07± 1.42	12.73± 1.57
Liver/carcass	%	3.39± 0.18	3.30± 0.23	3.46± 0.39
Liver Constituents				
Cytosol protein	mg/ml	22.2 ± 1.4	22.0 ± 2.0	23.6 ± 0.9
Glycogen	% tissue wt.	3.4 ± 0.89	2.9 ± 0.77	3.6 ± 1.1
Total lipids	% tissue wt.	3.4 ± 0.78	3.9 ± 0.63	4.1 ± 0.61
Phospholipids	% tissue wt.	2.1 ± 0.40	2.7 ± 0.43	2.5 ± 0.20
Triglycerides	% tissue wt.	0.89± 0.34	0.75± 0.29	1.1 ± 0.57
Free cholesterol	% tissue wt.	0.24± 0.09	0.28± 0.04	0.28± 0.02
Cholesterol esters	% tissue wt.	0.17± 0.09	0.18± 0.05	0.17± 0.10
Total cholesterol	% tissue wt.	0.32± 0.10	0.38± 0.07	0.38± 0.08
Ratio:				
Cholesterol/cholesterol esters		1.82± 1.38	1.62± 0.35	2.10± 0.89
Phospholipids/triglycerides		2.51± 0.66	4.03± 1.32	2.90± 1.61
Fatty acids				
16/16:1		9.38± 3.57	9.64± 2.16	6.95± 3.53
18/18:1		1.08± 0.28	1.34± 0.30	1.04± 0.48
18:2/20:4		0.96± 0.27	0.98± 0.29	0.90± 0.19
Enzyme Activity				
1. Cytosolic				
GS	b	8.7 ± 1.5	10.8 ± 1.6	7.9 ± 2.3
GP	b	32.2 ± 7.0	33.3 ± 3.5	28.9 ± 3.0
GK	b	25.8 ± 10.8	31.9 ± 5.6	31.6 ± 8.8
HK	b	5.3 ± 1.5	6.3 ± 1.4	4.9 ± 0.8
G6PDH	b	48.3 ± 21.9	27.8 ± 6.1	58.0 ± 12.4
6PGDH	b	23.8 ± 5.1	16.6 ± 3.3	17.3 ± 3.1
FAS	b	13.5 ± 4.5	9.6 ± 1.4	19.3 ± 4.0
AC	b	63.4 ± 18.4	52.9 ± 21.6	63.4 ± 18.5
GPT	b	595.6 ±185.0	556.9 ± 77.8	657.5 ± 126.8
GOT	b	376.9 ± 94.2	422.1 ± 94.0	400.7 ± 57.7
ICDH	b	396.2 ± 32.5	430.0 ± 46.1	388.8 ± 33.1
LDH	b	6738 ±1355	6878 ±880	5707 ±1173
MDH	b	6449 ±736	5528 ±548	5299 ± 252
GDH	b	5.7 ± 6.1	7.9 ± 11.0	20.6 ± 21.8
2. Microsomal				
Acyl transferase				
a. αGP	a	22.2 ± 4.1	28.8 ± 15.2	29.3 ± 18.2
b. DG	a	193.6 ±138.2	217.4 ±179.0	126.0 ± 71.4
Glyceride-transferase				
a. PC	b	0.98± 0.33	1.25± 0.27	1.12± 0.20
b. PE	b	0.43± 0.15	0.60± 0.09	0.52± 0.05
Desaturase				
a. Palmitoyl-CoA	c	4.6 ± 1.5	2.8 ± 1.2	5.1 ± 3.6
b. Stearoyl-CoA	c	6.4 ± 4.0	4.1 ± 2.4	8.4 ± 6.3
HMG-CoA reductase	a	15 ± 3	23 ± 14	20 ± 9

TABLE IX C

AVERAGE VALUES[7] FOR RATS SACRIFICED AT $R_{+6(S)}$

Measurement[5,6]		Groups		
			Control	
Parameter	Units[6]	Flight	Synchronous	Vivarium
Weights				
Carcass	grams	320 ± 15.6	332 ±11.4	348 ± 6.9
Liver	grams	9.88± 2.08	9.36± 0.73	11.86± 1.06
Liver/carcass	%	3.08± 0.51	2.82± 0.17	3.41± 0.28
Liver Constituents				
Cytosol protein	mg/ml	20.6 ± 2.5	23.4 ± 1.4	22.4 ± 0.90
Glycogen	% tissue wt.	0.44± 0.16	1.06± 0.33	2.56± 0.92
Total lipids	% tissue wt.	4.4 ± 0.62	5.0 ± 1.4	4.1 ± 0.9
Phospholipids	% tissue wt.	2.6 ± 0.25	2.6 ± 0.80	2.6 ± 0.30
Triglycerides	% tissue wt.	1.3 ± 0.67	1.9 ± 0.87	0.96± 0.56
Free cholesterol	% tissue wt.	0.31± 0.05	0.28± 0.06	0.31± 0.08
Cholesterol esters	% tissue wt.	0.23± 0.10	0.28± 0.08	0.21± 0.11
Total cholesterol	% tissue wt.	0.45± 0.10	0.45± 0.09	0.45± 0.14
Ratio:				
Cholesterol/cholesterol esters		1.49± 0.43	1.01± 0.26	1.92± 1.07
Phospholipids/triglycerides		2.59± 1.87	1.65± 0.74	3.23± 1.66
Fatty acids				
16/16:1		12.79± 5.15	16.13± 1.98	10.69± 3.35
18/18:1		1.23± 0.49	1.41± 0.46	1.14± 0.52
18:2/20:4		1.47± 0.60	1.28± 0.43	1.21± 0.26
Enzyme Activity				
1. Cytosolic				
GS	b	10.9 ± 2.2	7.3 ± 2.8	9.0 ± 1.9
GP	b	36.5 ± 10.2	41.4 ± 6.8	31.2 ± 6.4
GK	b	3.8 ± 1.3	16.4 ± 10.8	24.8 ± 8.4
HK	b	2.6 ± 1.2	4.1 ± 1.3	4.4 ± 1.1
G6PDH	b	39.1 ± 23.8	42.2 ± 30.1	40.0 ± 20.7
6PGDH	b	25.0 ± 9.6	17.1 ± 3.9	17.6 ± 2.9
FAS	b	4.0 ± 4.6	8.9 ± 2.6	10.4 ± 4.4
AC	b	74.5 ± 16.4	66.0 ± 20.1	66.7 ± 16.2
GPT	b	698.2 ±162.5	572.6 ±168.8	730.9 ± 118.1
GOT	b	616.6 ±101.4	387.7 ± 84.0	402.7 ± 91.6
ICDH	b	429.6 ± 79.1	424.8 ± 33.6	421.1 ± 41.2
LDH	b	7022 ±734	6672 ±608	6564 ±1197
MDH	b	6753 ±911	5983 ±930	5805 ±1106
GDH	b	9.9 ± 4.2	3.7 ± 3.6	8.6 ± 6.2
2. Microsomal				
Acyl transferase				
a. αGP	a	29.9 ± 22.3	35.4 ± 11.9	34.7 ± 20.4
b. DG	a	11.1 ± 4.0	227.0 ±181.2	238.4 ± 238.2
Glyceride-transferase				
a. PC	b	0.45± 0.30	1.15± 0.21	1.00± 0.29
b. PE	b	0.18± 0.09	0.46± 0.13	0.49± 0.16
Desaturase				
a. Palmitoyl-CoA	c	0.35± 0.33	1.4 ± 1.2	1.9 ± 1.3
b. Stearoyl-CoA	c	1.4 ± 2.4	1.8 ± 1.3	3.1 ± 2.6
HMG-CoA reductase	a	14 ± 5	17 ± 5	22 ± 8

TABLE IX D

AVERAGE VALUES[7] FOR RATS SACRIFICED AT R_{+29}

Measurement[5,6]		Groups		
			Control	
Parameter	Units[6]	Flight	Synchronous	Vivarium
Weights				
Carcass	grams	392 ± 34.2	447 ± 44.9	385 ± 34.5
Liver	grams	10.05± 0.54	13.75± 2.24	10.24± 0.56
Liver/carcass	%	2.57± 0.10	3.06± 0.22	2.68± 0.26
Liver Constituents				
Cytosol protein	mg/ml	22.0 ± 1.8	19.3 ± 1.1	21.6 ± 1.6
Glycogen	% tissue wt.	0.18± 0.07	2.90± 0.93	0.34± 0.18
Total lipids	% tissue wt.	4.3 ± 0.48	4.4 ± 0.33	4.4 ± 0.70
Phospholipids	% tissue wt.	3.0 ± 0.30	2.8 ± 0.18	2.9 ± 0.31
Triglycerides	% tissue wt.	0.66± 0.15	0.96± 0.21	0.86± 0.40
Free cholesterol	% tissue wt.	0.42± 0.05	0.35± 0.06	0.39± 0.07
Cholesterol esters	% tissue wt.	0.25± 0.05	0.23± 0.03	0.24± 0.04
Total cholesterol	% tissue wt.	0.57± 0.08	0.49± 0.07	0.52± 0.08
Ratio:				
Cholesterol/cholesterol esters		1.73± 0.21	1.51± 0.14	1.68± 0.35
Phospholipids/triglycerides		4.72± 1.12	3.06± 0.72	3.90± 1.66
Fatty acids				
16/16:1		15.68± 5.92	20.25± 7.37	16.60± 6.30
18/18:1		2.76± 0.83	1.97± 0.60	2.37± 1.20
18:2/20:4		0.97± 0.28	1.08± 0.26	1.25± 0.31
Enzyme Activity				
1. Cytosolic				
GS	b	9.2 ± 2.4	11.0 ± 2.4	9.3 ± 1.8
GP	b	50.8 ± 1.9	21.4 ± 2.9	37.6 ± 14.3
GK	b	6.3 ± 3.4	6.0 ± 3.7	9.4 ± 4.0
HK	b	3.7 ± 1.4	8.4 ± 3.8	3.9 ± 2.1
G6PDH	b	53.0 ± 14.9	62.7 ± 17.9	66.8 ± 17.6
6PGDH	b	15.5 ± 1.8	17.3 ± 4.5	20.7 ± 6.0
FAS	b	12.1 ± 2.9	11.9 ± 1.0	13.2 ± 3.4
AC	b	53.5 ± 11.3	69.9 ± 27.0	62.2 ± 10.8
GPT	b	610.1 ± 50.1	551.2 ±129.6	769.4 ±151.8
GOT	b	444.1 ± 58.6	301.9 ± 57.4	405.1 ± 45.5
ICDH	b	386.5 ± 27.6	419.6 ± 45.3	452.4 ± 39.5
LDH	b	6779 ±1053	6339 ±866	7051 ±320
MDH	b	5965 ±567	6678 ±457	6351 ±538
GDH	b	5.0 ± 5.4	5.9 ± 2.1	2.8 ± 0.7
2. Microsomal				
Acyl transferase				
a. αGP	a	16.8 ±12.9	15.9 ±14.9	11.6 ± 6.0
b. DG	a	43.1 ± 26.1	35.3 ± 23.9	32.0 ± 46.1
Glyceride-transferase				
a. PC	b	0.89± 0.30	0.87± 0.14	0.80± 0.43
b. PE	b	0.46± 0.08	0.39± 0.06	0.40± 0.19
Desaturase				
a. Palmitoyl-CoA	c	0.9 ± 0.5	1.8 ± 0.8	1.0 ± 0.7
b. Stearoyl-CoA	c	1.6 ± 1.2	3.1 ± 0.9	3.3 ± 3.9
HMG-CoA reductase	a	15 ± 5	72 ± 48	23 ± 9

TABLE X

SIGNIFICANCE OF DIFFERENCES FOUND IN VALUES FOR LIVERS OF RATS
SACRIFICED AT R_0, R_{+29}, R_{+6} (NON-STRESSED) AND $R_{+6(S)}$ (STRESSED)

	Comparisons Between:			
	At R_0	At R_{+29}	Flight	Synchronous
Measurement [5]	Flight vs. Synchronous	Flight vs. Synchronous	(R_{+6S}) vs. (R_{+6})	(R_{+6S}) vs. (R_{+6})
Liver Constituent				
Glycogen	+70% < 0.02	-94% < 0.001	-87% < 0.001	-53% < 0.01
Total lipids	none	none	+23% < 0.05	none
Phospholipids	none	none	+95% < 0.05	none
Total cholesterol	none	none	none	none
Triglycerides	none	-31% < 0.05	none	+61% < 0.02
Fatty acids				
16/16:1	none	none	none	+40% < 0.001
18/18:1	none	none	none	none
18:2/20:4	none	none	none	none
Enzyme activity				
1. Cytosol				
GS	none	none	none	-32% < 0.05
GP	none	+58% < 0.001	none	+20% < 0.05
GK	none	none	-85% < 0.001	-49% < 0.01
HK	none	-56% < 0.05	-51% < 0.01	-35% < 0.02
G6PDH	none	none	none	none
6PGDH	none	none	none	none
FAS	none	none	-70% < 0.01	none
AC	none	none	none	none
GPT	+16% < 0.05	none	none	none
GOT	none	none	+39% < 0.001	none
ICDH	none	none	none	none
LDH	none	none	none	none
MDH	none	none	none	none
2. Mitochondria				
GDH	none	-	-	-
ICDH	-27% < 0.05	-	-	-
AC	-52% < 0.01	-	-	-
MDH	none	-	-	-
3. Microsome				
αGP acyl trans.	none	none	none	none
DG acyl trans.	-70% < 0.01	none	-94% < 0.01	none
PC transferase	-22% < 0.05	none	-54% < 0.02	none
PE transferase	none	none	-58% < 0.01	-23% < 0.05
Pal-CoA Desat.	none	none	-92% < 0.001	none
Stear-CoA Desat.	none	none	-78% < 0.02	-73% < 0.05
HMG-CoA Red.	none	-79% < 0.05	none	none

FOOTNOTES TO TABLES II THROUGH X.

1. Total lipids: sum of triglycerides + phospholipids + cholesterol esters; the small amounts of other constituents, free fatty acids, monoglycerides and diglycerides are not included.

2. Cholesterol esters = cholesterol + FA; ÷ by 1.67 to get cholesterol value. Total cholesterol = (free cholesterol) + $\frac{(cholesterol\ ester)}{1.67}$.

3. (   ) value not used to calculate average.

4. Condition of Homogenate:

Code for appearance of post-mitochondrial supernatant fractions obtained in U.S.A.

    A = Large particulates in homogenates (pellet on standing at 1 x g).
    B = Foamy homogenate.
    C = Small amount of fat layer.
    D = No microsomal pellet obtained; pellet used to be a mitochondrial subfraction.
    E = Presumption of mitochonria or other large particles (pellet at 8,000 x g for 10 min).

5. Abbreviations used are: 12:0 for laurate; 14:0 for myristate; 16:0 for palmitate; 16:1 for palmitoleate; 18:0 for stearate; 18:1 for oleate; 18:2 for linoleate; 18:3 for linolenate; 20:2 for eicosadienoate; 20:3 for eicosatrienoate ($\omega6$); and 20:4 for arachidonate; GS for glycogen synthetase; GP for glycogen phosphorylase; GK for glucokinase; HK for hexokinase; G6PDH for glucose-6-phosphate dehydrogenase; 6PGDH for 6-phosphogluconate dehydrogenase; FAS for fatty acid synthetase; AC for aconitase; GPT for glutamate-pyruvate transaminase; GOT for glutamate-oxaloacetate transaminase; ICDH for isocitrate dehydrogenase; LDH for lactate dehydrogenase; MDH for malate dehydrogenase; GDH for glutamate dehydrogenase; αGP for α-

glycerol phosphate; DG for diglyceride; PC for phosphatidyl
choline; PE for phosphatidyl ethanolamine; Pal-CoA for palmi-
toyl-CoA; stear-CoA for stearoyl-CoA and HMG-CoA Red. for 3-
hydroxy-3-methyl-glutaryl-CoA reductase.

6. Units of Enzymatic Activity:

    a = pmoles/min/mg protein
    b = nmoles/min/mg protein
    c = nmoles/unsaturated fatty acid/5 min/mg protein.

7. Each value is presented as the mean ± standard deviation.

C-2
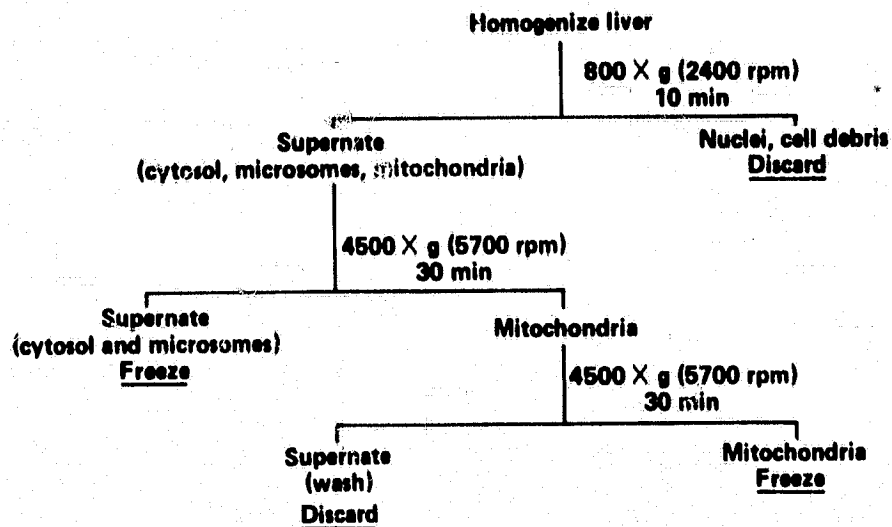
Figure 1.- Procedure for liver homogenate fractionation.

CYTOCHROME OXIDASE ACTIVITY
OF 80,000 g min. PELLETS
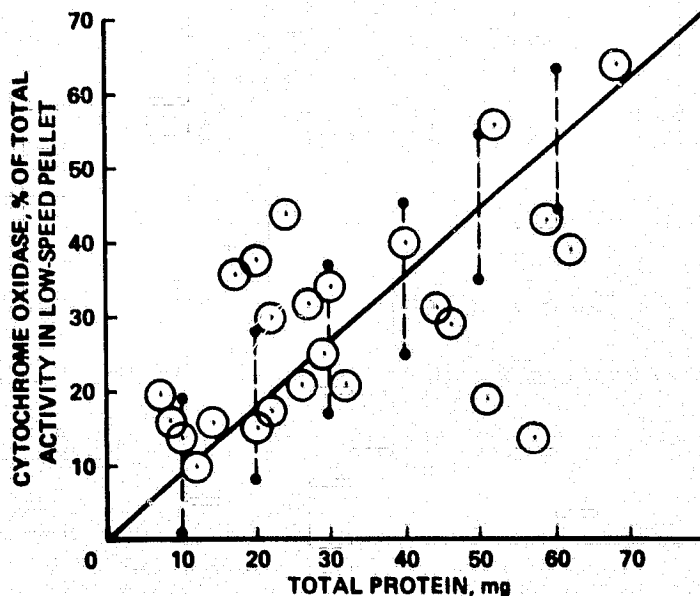
Figure 2.- Each point represents a different sample; all had considerable activity, and some samples had as much as 70% of all the hepatocyte cytochrome oxidase activity.
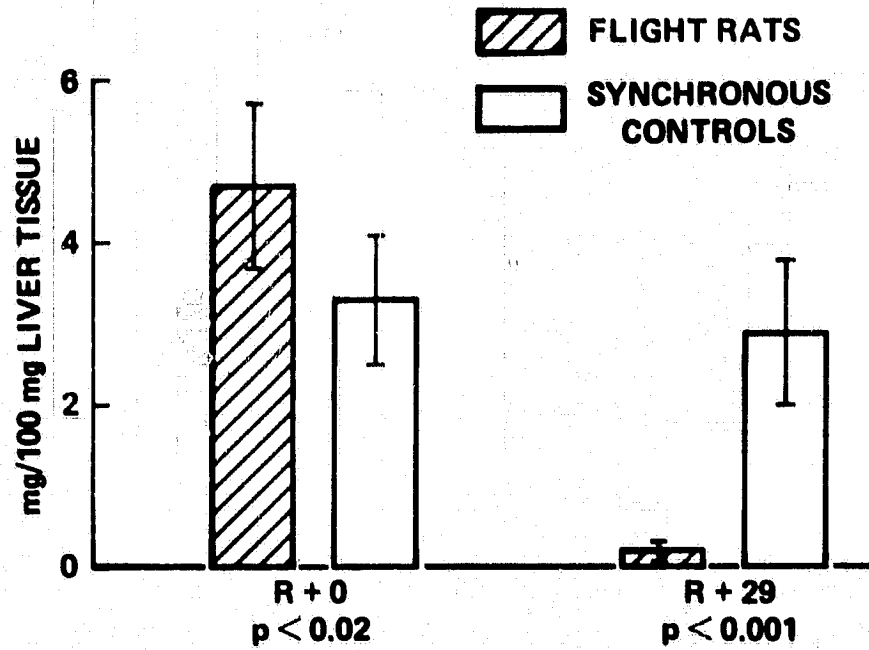
Figure 3.- Glycogen.
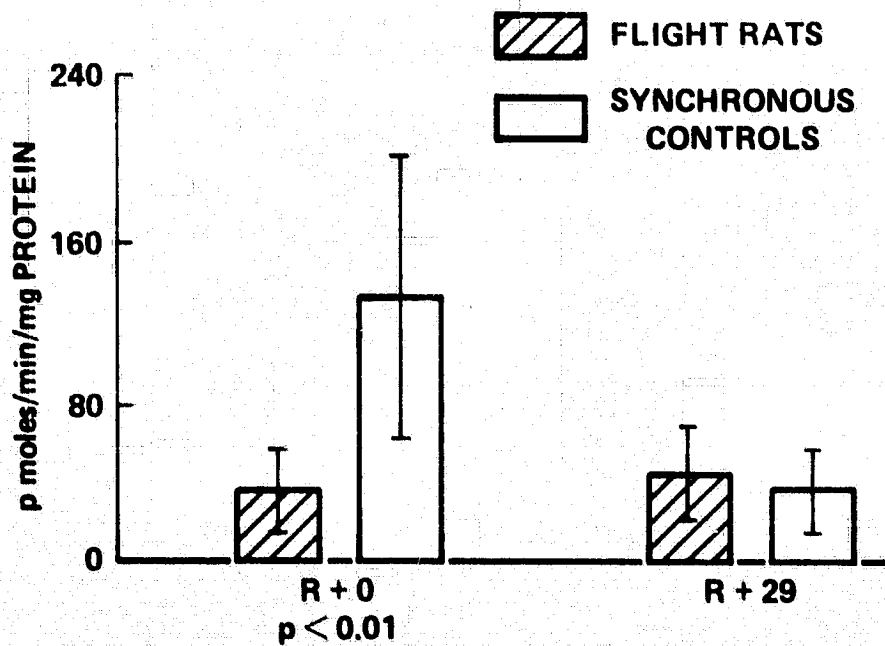
Figure 4.- Diglyceride acyltransferase.

94

PC - GLYCERIDE TRANSFERASE
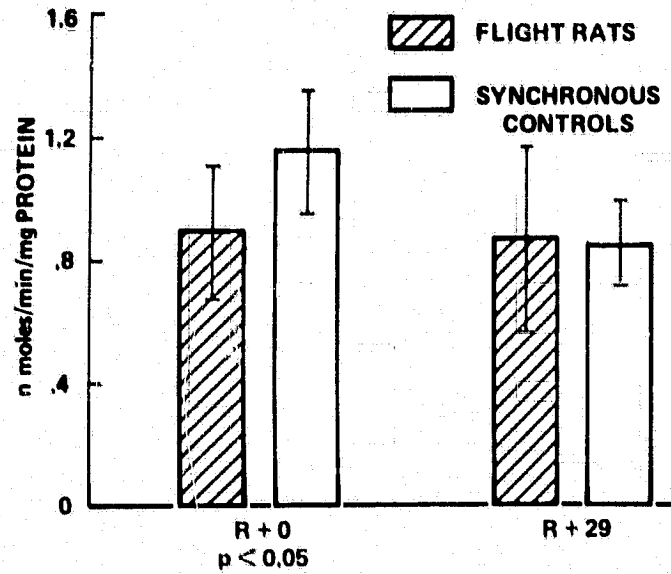
Figure 5

ICDH (MITOCHONDRIAL)
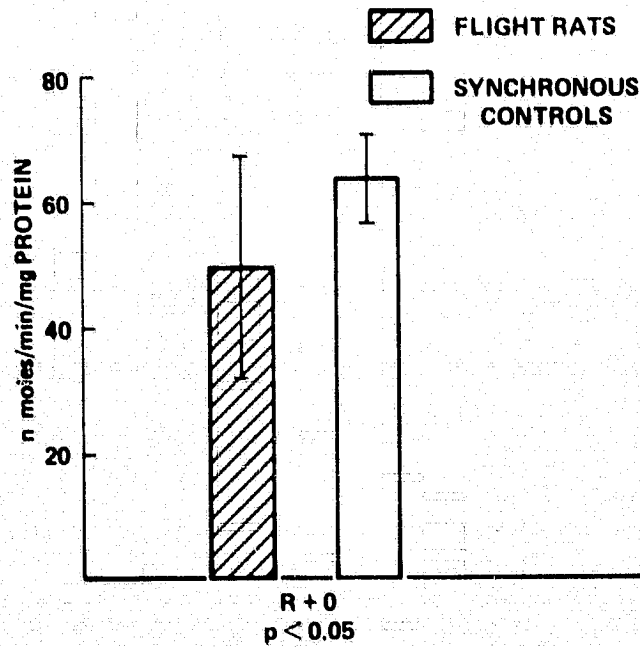
Figure 6

ACONITASE (MITOCHONDRIAL)
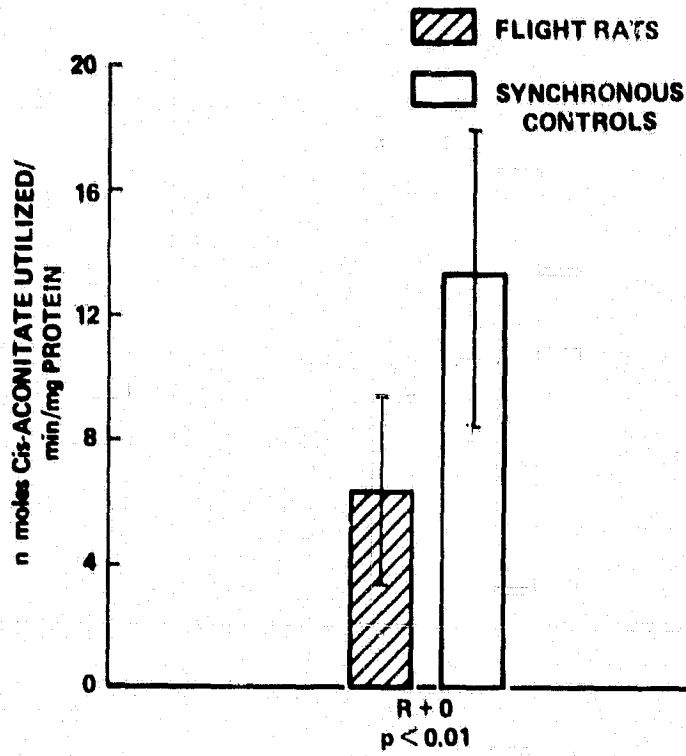
Figure 7

TOTAL LIPIDS

Figure 8

GK

Figure 9

HK

Figure 10

97
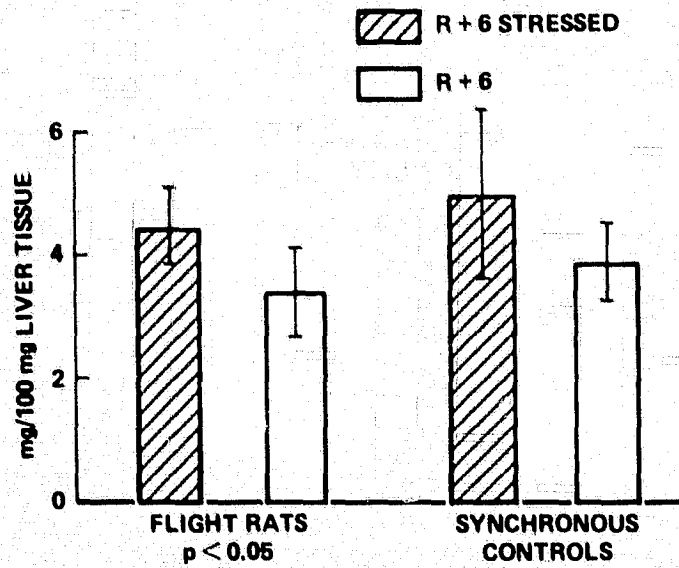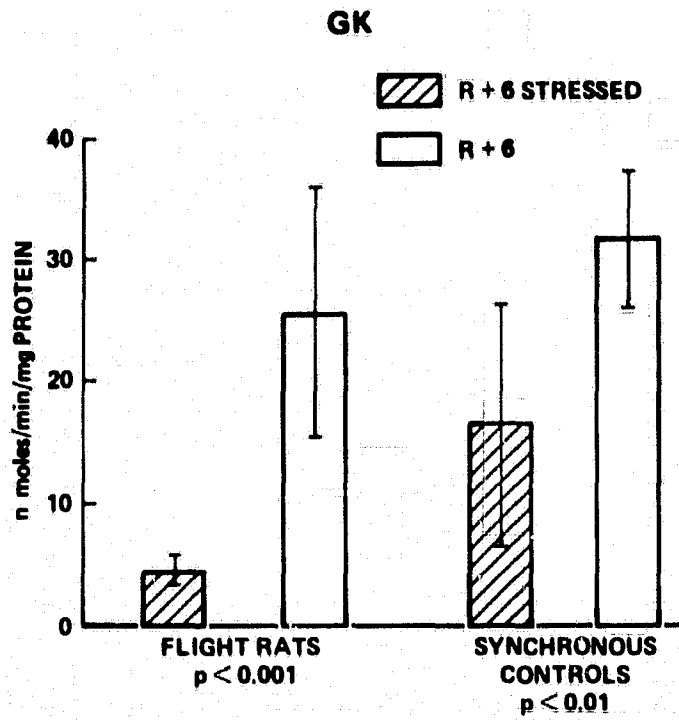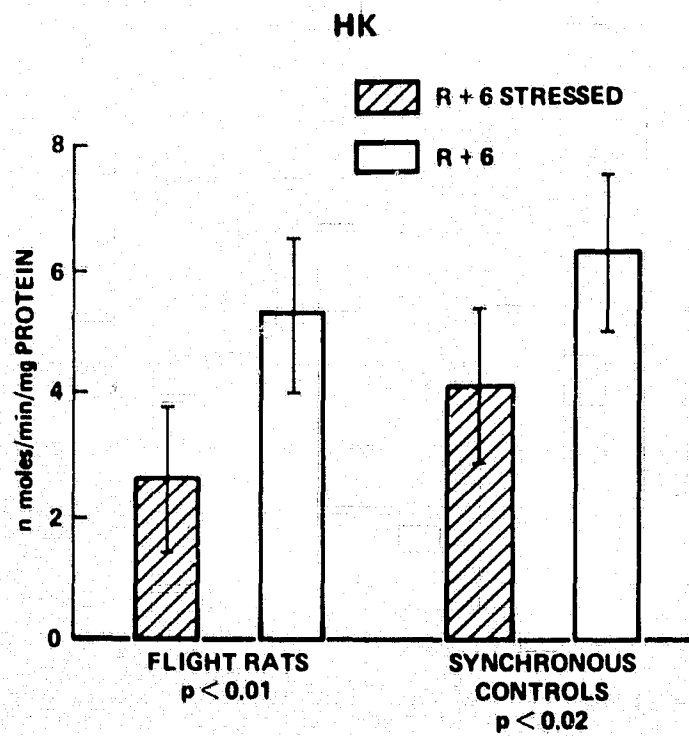
DIGLYCERIDE
ACYL TRANSFERASE
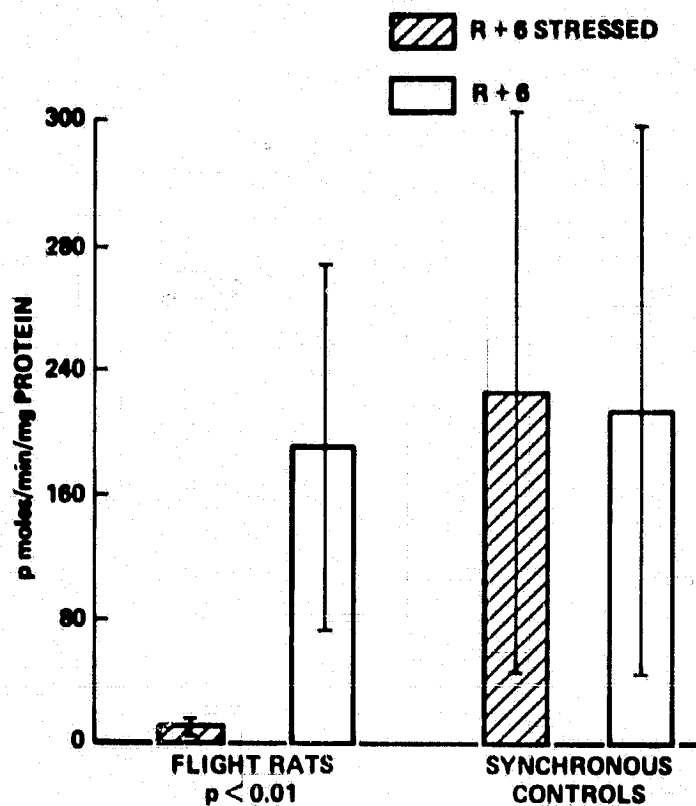
Figure 11

PC · GLYCERIDE
TRANSFERASE

Figure 12

98
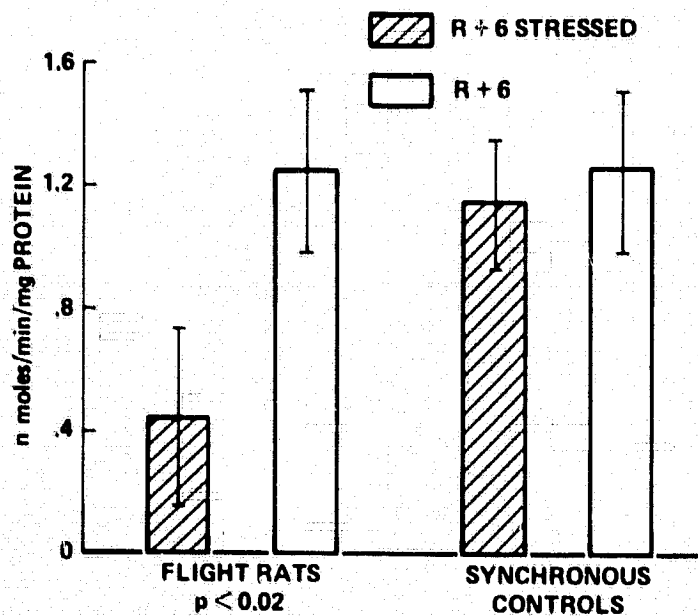
PE – GLYCERIDE TRANSFERASE
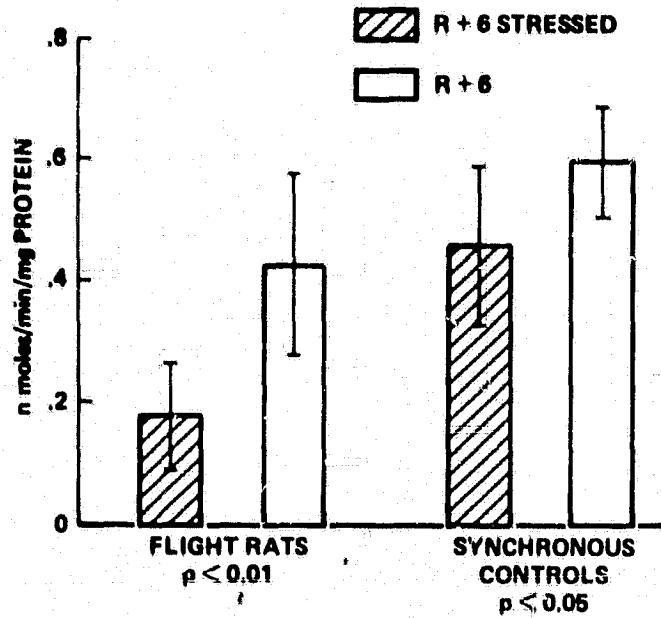
Figure 13

PALMITOYL — CoA DESATURASE

Figure 14

GOT

Figure 15

GLYCOGEN

Figure 16

D_2
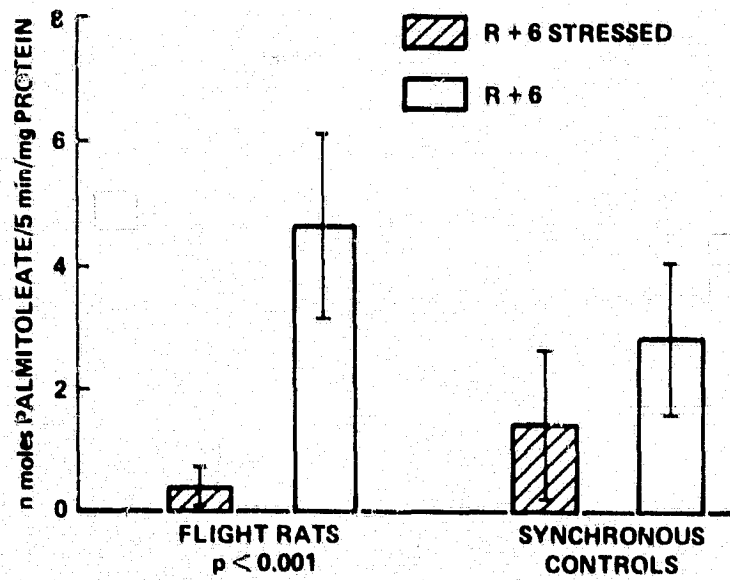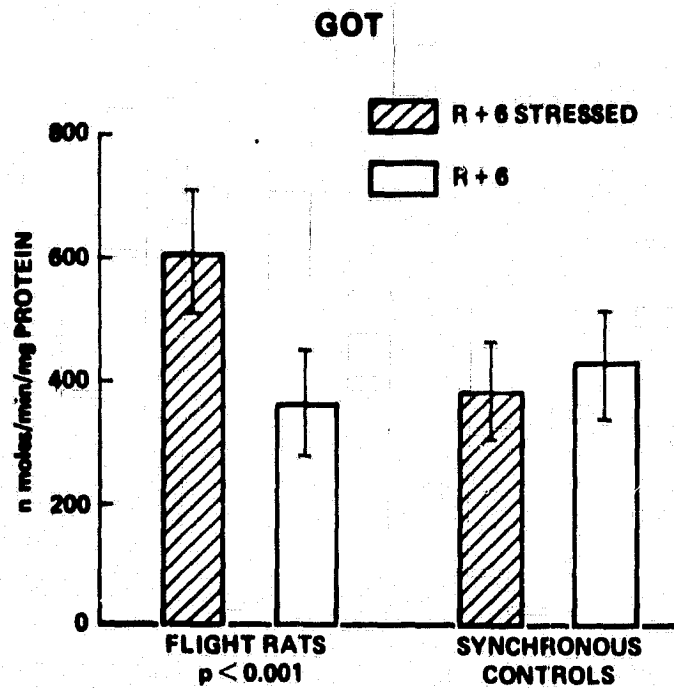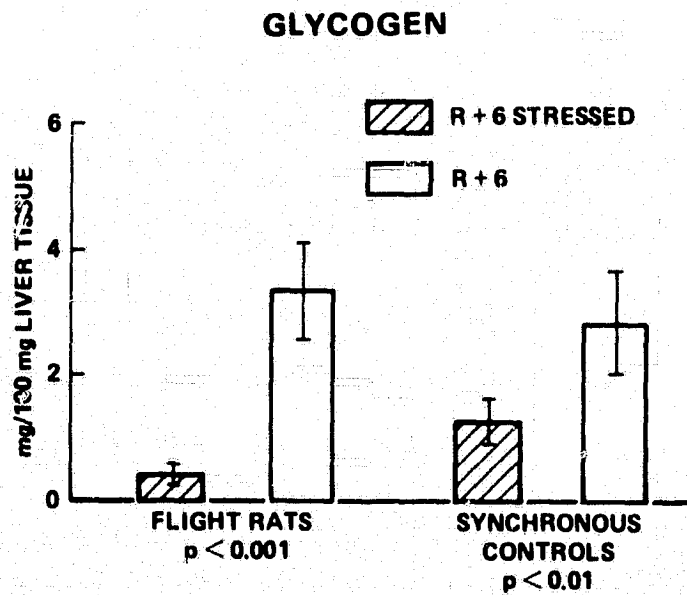
K305: QUANTITATIVE ANALYSIS OF SELECTED BONE PARAMETERS

Thomas J. Wronski, Emily Morey-Holton
NASA-Ames Research Center
Moffett Field, CA 94035

Christopher E. Cann, Claude D. Arnaud
University of California Medical School
San Francisco, CA

David J. Baylink, Russell T. Turner
American Lake VA Medical Center
Tacoma, WA

Webster S. S. Jee
University of Utah College of Medicine
Salt Lake City, UT

SUMMARY

The skeletal alterations induced by space flight were determined to be a reduced rate of periosteal bone formation in the tibial and humeral diaphyses, and a decreased trabecular bone volume and an increased fat content of the bone marrow in the proximal tibial metaphysis. An increased incidence of arrest lines in flight animals suggested that periosteal bone formation may have ceased during space flight. Endosteal bone resorption was not affected markedly.

INTRODUCTION

Changes in calcium homeostasis have been noted during space flight. Metabolic studies of the Skylab astronauts indicated that a significant increase in urinary calcium (1), similar to bed rest immobilization, occurred in flight (2, 3). No change in hydroxyproline was observed (4). Bone density determinations in the Skylab astronauts showed a significant decrease in the os calcis density after 84 days of flight while no change in the radius or ulna was detected (2). Such data suggest that loss of bone mineral is more prevalent in the weight-bearing bones.

Microscopic examination of the metaphysis of the long bones of young Wistar rats after a 22-day space flight aboard the Soviet biological satellite Cosmos 605 suggested that an inhibition of bone growth occurred during flight but returned to normal by 27 days postflight; no gross changes were observed in the diaphysis (5).

Following Cosmos 782, a significant inhibition of periosteal bone formation was noted in the tibial diaphysis of the flight rats (6). A significant decrease in cross sectional area and medullary canal area in the femoral diaphysis was also noted (7). The ash content of the femoral epiphysis was decreased 13%, while the humeral epiphyseal ash content decreased 8% and no change was noted in the radius or ulna ash content (8). $^{45}CaCl_2$, injected 4 hours prior to sacrifice of rats following Cosmos 782, showed an increase in uptake in the epiphysis of the femur and humerus with a decreased surface uptake in the diaphysis of the femur, ulna, and radius (8).

Following Cosmos 936, more information was obtained concerning the decreased bone formation during flight (9). Mean periosteal bone formation rate was decreased about 45% and was not corrected by on-board centrifugation. No gross change in endosteal bone resorption was noted during flight or postflight. The cessation of bone formation was calculated to occur sometime after the eleventh day of flight and continued until the second postflight day. Although centrifugation did not correct the defect in periosteal bone formation rate during flight, it appeared to hasten the recovery following flight. Postflight, all flight rats corrected the defect in periosteal bone formation rate. Following Cosmos 936, about a 30% decrease in femur stiffness was detected in the flight animals, but the defect was corrected by centrifugation (9).

A significant decrease in the weight of soleus (32%) and extensor digitorum longus (12%) muscles were reported after Cosmos 605 while nonsignificant decreases in the gastrocnemius or quadriceps muscles and no change in the biceps brachii or diaphragm muscles were noted (10). Similar results were found following Cosmos 782 (7). Mechanical forces imposed by muscle utilization and gravity are known to influence bone turnover; therefore, differential bone responses to space flight might be predicted. Such a differential response may be evident in the rat, a quadriped, since the rear limbs are used primarily for weight-bearing while the front limbs are used for grasping, grooming, and feeding. According to the above space flight results, differential effects are noted not only between weight-bearing and non-weight-bearing bones, but also are seen within different regions of the same bone. Therefore, one of the objectives of this study is to determine growth at the periosteum in different regions

both in weight-bearing (tibia) and non-weight-bearing (rib) bones.

Following both Cosmos 782 and 936, an arrest line was found in all flight rats and was both more distinct and more extensive than in control rats (6, 9). The arrest line stains with thionin suggesting that it contains acid polysaccharide or a basic substance which is not fat extracted (9). Osteocyte lacunae and walls of canaliculi stain similarly. Another objective of this study is to obtain more precise measurements and further define the arrest line.

MATERIALS AND METHODS

Specific pathogen-free, male Wistar rats from the Institute of Experimental Endocrinology of the Slovakian Academy of Sciences were approximately 83 days of age and weighed an average of 290 grams at the beginning of the experimental period. The rats were divided into three groups. The flight animals were placed in orbit in individual cylindrical cages aboard a modified Soviet Vostok spacecraft for a period of 18.5 days. There were two groups of ground-based controls. The synchronous control rats were also housed individually in a modified Vostok spacecraft and subjected to the conditions associated with launch and reentry. An attempt was made to simulate as closely as possible the spacecraft environment experienced by the flight animals. The vivarium control rats were housed in animal quarters and were not subjected to flight conditions. The first group of flight, synchronous control, and vivarium control rats were sacrificed at the end of the 18.5 day flight period. The second and third groups were sacrificed at 6 and 29 days postflight, respectively.

All rats were injected intraperitoneally with 1 mg/kg body weight of Declomycin three days prior to launch. Declomycin is a tetracycline derivative which labels areas of bone formation (11). A second Declomycin injection was administered to the postflight group 5 days after flight. The rats were decapitated at the end of the experimental periods and the left tibia and humerus were removed. The bone lengths were measured with a vernier caliper, after which the bones were placed in a fixative composed of paraformaldehyde, glutaraldehyde, and diflourodinitrobenzene. The vials containing the bones were refrigerated and shipped to the United States.

The bones were sawed into three parts corresponding to the proximal, middle, and distal thirds. The proximal tibia was dehydrated in increasing concentrations of acetone and embedded undecalcified in methyl methacrylate. Multiple sections of approximately 5μ m thickness were cut parallel to the longitudinal axis of the bone with a Jung model K microtome. Following removal of the plastic with xylene, the sections were stained according to the von Kossa method (12).

The fractional area of trabecular bone and the fractional area of fat in the bone marrow were quantified in a 2 by 2.5 mm area of the proximal tibial metaphysis with the aid of a Merz grid (13). This grid consists of 6 semicircular lines and 36 points within a square. The number of points superimposed over bone and bone marrow were counted at a magnification of 160 X. The fractional area of trabecular bone was calculated by dividing the number of points lying over bone by the total number of points lying over bone and bone marrow. The fractional area of fat in the bone marrow was quantified in a similar manner.

Portions of the tibial and humeral diaphyses were processed for ultraviolet microscopy of fluorescent tetracycline labels. The bone specimens were dehydrated in a series of acetone and ether changes and embedded undecalcified in a styrene monomer which polymerizes into a polyester resin (Tap Plastic Inc., San Jose, CA). The portions of the tibial diaphysis immediately proximal to the tibiofibular junction and the portion of the humeral diaphysis immediately distal to the deltoid tuberosity were sawed into 50 μm thick cross-sections with a Gillings-Hamco thin sectioning machine.

The Merz grid was also used to quantify the rate of periosteal bone formation in the tibial and humeral diaphyses. In a growing rat, the periosteal surface is forming bone and will therefore be labeled with tetracycline. The number of points superimposed over the newly formed bone between the fluorescent tetracycline label and the periosteal surface was counted at a magnification of 160 X under ultraviolet illumination. The area was calculated by multiplying the number of points by the constant d^2, with d equal to the distance between points. The rate of periosteal bone formation was calculated by dividing the volume of newly formed bone (assuming that the cross-sections were 1 mm thick) by the time interval between administration of the tetracycline label and sacrifice. The medullary area in cross-sections of the tibial and humeral diaphyses was also quantified by point counting with a Merz grid.

Polaroid photographs were taken of cross-sections of the tibial and humeral diaphyses at a magnification of 25 X. The arrest line lengths of the postflight group were quantified with a map measure (Dietzgen Corp., Santa

Clara, CA). The distance between units of the map measure was calibrated with a 25 X photograph of a stage micrometer.

Additional cross-sections of the tibial diaphysis were used for chemical characterization of the arrest lines. The sawed sections were hand ground to a final thickness of about 30 μm. The following procedures were used:

1) Unstained: unstained, mineralized ground sections were mounted in Abopon (Valmor Corp., Brooklyn, NY) a water soluble mounting medium.

2) Nuclear fast red: mineralized ground sections were stained for 1 min. with 1% nuclear fast red (aq.).

3) Toluidine blue: mineralized and demineralized (15 min. in 0.2 M acetate buffer, pH 4) ground sections were stained for 10 min. with 0.02% toluidine blue.

4) Sudan black: mineralized and demineralized ground sections were stained with 1% Sudan black-B in 70% EtOH for 10 min.

5) Methylene blue: mineralized and demineralized ground sections were stained with 1% alkaline methylene blue for 15 min.

A segment of the tibial diaphysis was demineralized and embedded in glycol methacrylate. Thin sections (approximately 5 μm thick) were stained for acid phosphatase enzyme (14), counter stained with aqueous methyl

green-thionine in citrate buffer, and then mounted in Fluoromount (E. Gurr Ltd., London, S.W.N., England).

RESULTS

The body weights and weight gain data are shown in Table 1. The weight gained by the rats sacrificed immediately following flight (Group 1) was significantly less than that gained by the synchronous ($p=0.01$) or the vivarium ($p<0.005$) control rats; the rate of gain was significantly less in the flight as compared to the vivarium ($p<0.025$) but not as compared to the synchronous due to the larger variability in the latter control group. The non-stressed animals killed 6 days after flight appeared to gain weight during that period following flight; however, the flight animals still gained significantly less weight than either the synchronous ($p<0.05$) or vivarium ($p<0.001$) control group. Again, the rate of weight gain was less in the flight group than the vivarium groups ($p<0.001$) but not significantly less than the synchronous rats due to the large variability in this control group. In the stressed animals sacrificed 6 days following flight, the control groups appeared to maintain their weight as compared to Group 1 rats while the flight rats lost weight ($p<0.05$); all groups showed a decrease in the rate of weight gain as compared with Group 1 rats. The decreased weight gain of the 3F group was significantly different from that of either the synchronous ($p<0.001$) or vivarium ($p<0.001$) groups and the rate of weight gain was significantly less than either control group ($p<0.001$ vs either control). The Group 4 rats did not gain as much weight during the flight period as did the Group 1 rats; this difference is probably related to a weight loss during the 5 days after flight since the

108

4S group weighed 385+26.4 gms on 10/19 and only 369+20.4 on 10/24. The weight loss during this 5 day period may be attributed to the volume of physiological studies performed during this time period. The synchronous controls in Group 4 gained weight at a higher rate than did the other groups; the reason for this is unknown. However, since the Group 4 animals weighed more than any other group, at the beginning of the experiment, these animals may have been somewhat immobilized during the flight period as indicated by the increased length of the arrest line in these rats (Table 4).

Table 2 lists values for the length of the left tibia and humerus and the bone cross-sectional area of the tibial and humeral diaphyses. The bone lengths for the three experimental groups were approximately the same for both the tibia and humerus. The bone cross-sectional area of both the tibial and humeral diaphyses was significantly decreased in flight animals relative to vivarium control animals immediately following flight. This difference was not significant in the animals sacrificed at 29 days postflight.

Values for periosteal bone formation rate in the tibial and humeral diaphyses and the rib are listed in Table 3. During the flight period, the flight rats exhibited a reduced rate of periosteal bone formation in the tibial and humeral diaphyses in comparison to both synchronous control and vivarium control rats. These differences were evaluated by means of Student's t-test and, in the tibia, found to be highly significant at the level of $P < 0.001$. There was also a reduced rate of periosteal bone formation in the humerus during spaceflight, but it was not as marked as in

the tibia. The value for the flight rats was significantly different from the flight control rats at the level of $P < 0.01$, and from the vivarium control rats at the level of $P < 0.001$. Periosteal bone formation rate in the rib did not appear to be affected by spaceflight conditions.

During the postflight period, the flight rats exhibited an increased rate of periosteal bone formation in the tibia in contrast to the reduced rate which was observed during the flight period. This increase was significant at the level of $P < 0.025$ and $P < 0.05$ from synchronous control and vivarium control values, respectively. A similar increase was not observed in the humerus.

The mean medullary area in cross-sections of the tibial and humeral diaphyses and the rib did not exhibit significant differences among the three experimental groups.

The arrest line data are shown in Table 4. In the animals sacrificed at 29 days postflight, the length of the arrest lines in the humeral diaphysis was significantly greater ($P < 0.025$) in the flight group in comparison to both control groups. In the tibia, there was also a significant difference ($P < 0.001$) in arrest line lengths between the flight and vivarium animals, but not between the flight and synchronous control animals.

The staining characteristics of the arrest lines are listed in Table 5. Arrest lines in mineralized ground sections were not stained or were only weakly stained by Nuclear fast red, Toluidine blue, and Sudan black. In contrast, arrest lines in demineralized ground sections were stained by

several procedures: Sudan black, methylene blue and Toluidine blue. The most intense staining was achieved with Sudan black. In addition to staining arrest lines the above procedures also stained cement lines, osteocyte lacunae and osteocyte canaliculi. When ground sections were stained with Sudan black and viewed under oil, it was clear that most osteocyte canaliculi terminated at the arrest line. Acid phosphatase activity was not observed at the arrest line in 5µ sections. In contrast, acid phosphatase was observed at cement lines and in osteoclasts. Arrest lines as well as cement lines were stained by thionine.

The fractional area of trabecular bone, commonly referred to as trabecular bone volume, is plotted vs. time in Figure 1. There appears to be a trend for a reduced trabecular bone volume in the proximal tibial metaphysis in flight rats. This parameter was significantly lower in the flight group relative to the vivarium control group at all time periods. The flight rats also had a consistently lower trabecular bone volume in comparison to the synchronous control rats. This difference was not significant (P<0.10) at days 19 (R+0) and 25 (R+6) but there was a significant difference (P<0.05) at day 48 (R+29). The trabecular bone volume remained relatively constant in each of the three groups throughout the experimental period. If the data from all three time periods were combined, the trabecular bone volume in the flight group was significantly different from both the synchronous control (P<0.025) and the vivarium control (P<0.001) groups.

Figure 2 is a similar plot of the fractional area of fat in the bone marrow vs. time. The data suggest that the fat content of the bone marrow in the

proximal tibial metaphysis increased during spaceflight. The difference in fat content at day 19 (R+0) between the flight group and both control groups was significant at the level of P<0.05. By the end of the postflight period (day 48), there were no significant differences among the three groups.

DISCUSSION

The flight animals gained about 35% less weight and at a rate about 25% lower than either control group (Table 1). If the food consumption of the flight and control animals was equivalent, these data confirm the findings of previous Cosmos experiments (9) that the rat gains less weight per gram of food consumed while in space. The greatest difference between flight and control animals occurred in the animals stressed postflight and killed at R+6 days. This suggests that the flight animals were less able to compensate for the immobilization stress than were the controls. Extensive handling of the R+29 animals postflight appears to mask the differential response in weight between flight and control animals; weights taken immediately postflight, rather than at R+6, in this group would probably be more consistent with other groups and would aid in the interpretation of the postflight effects on weight gain.

This study demonstrates that periosteal bone formation in the tibial and humeral diaphyses was inhibited during orbital flight aboard the Soviet Cosmos 1129 biological satellite. A similar effect was observed in the tibia during previous Cosmos experiments (15), but the humerus was not included in prior investigations. The inhibition of periosteal bone

112

formation in the humerus was not as dramatic as in the tibia. This may be due to the lower rate of periosteal bone formation in the humerus relative to the tibia. The decrease in bone cross-sectional area in the tibial and humeral diaphyses may be related to the inhibition of periosteal bone formation. The rate of periosteal bone formation in the rib was not significantly decreased during spaceflight, possibly due to its non-weight-bearing nature. Also, the periosteal bone formation rate in the rib may be too low to exhibit a significant change during the relatively short flight period.

The rebound in periosteal bone formation rate in the tibia during the postflight period has also been previously observed. The humerus did not exhibit a similar rebound, but periosteal bone formation did return to normal during the postflight period.

The results from Cosmos 782 (6) and Cosmos 936 (9) demonstrate that arrest lines are greatly increased during space flight. The results of the present study add further support to that conclusion. Interestingly, the length of the arrest line in flight and synchronous groups (Table 4) was more extensive than that noted in previous flights (Cosmos 782: flight, 5.3 mm; synchronous, 2.1 mm; Cosmos 936: flight, 4.0 mm; synchronous, 1.6 mm). The dramatic increase in the extent of the arrest line, particularly in the synchronous animals, in Cosmos 1129 may have been related to the larger size of the rats confined to a small space. The starting weight of the flight rats for the two previous missions was about 220 gms while the synchronous groups weighed about 190 gms; for Cosmos 1129, the 4F rats had an initial weight of about 320 gms while the corresponding synchronous

group had an average mass of about 310 gms. This increased initial mass of around 100 gms in Cosmos 1129 rats may have somewhat immobilized them; rats for all missions were housed in cylindrically shaped cages which were approximately 8.12 inches deep and 3.75 inches in diameter. Conversely, the vivarium animals for all flights had similar arrest line lengths (Cosmos 782 = 1.5 mm; Cosmos 936 = 1.6 mm; Cosmos 1129 = 1.6 mm). For Cosmos 936, the vivarium animals (205 gms) were housed 5/cage in standard polyvinyl cages (450 x 310 x 160 mm) while for Cosmos 1129, the vivarium controls (305 gms) were housed 3-4/cage in similar cages (550 x 330 x 195 mm). Thus, cage restraint may increase the length of the arrest lines, but weightlessness even with cage restraint increases the length of the arrest line greater than cage restraint alone.

Formation of arrest lines appears to be associated with a temporary cessation of bone formation. Arrest lines clearly differed from cement lines. The latter were highly irregular in appearance and exhibited acid phosphatase activity. Arrest lines were smooth and showed no residual acid phosphatase from prior osteoclast activity. The staining properties of arrest lines (lack of staining by mineralized ground sections and no selective staining by a variety of methods in demineralized ground sections) and the demonstration that osteocyte canaliculi rarely pass through arrest lines suggest that arrest lines represent a cessation of bone matrix formation followed by reinitiation of bone formation at a later time.

There were no significant differences among the three experimental groups in cross-sectional medullary area in the tibial and humeral diaphyses and

the rib. The predominant activity along the endosteal surface of the medullary canal in growing rats is bone resorption. An alteration in bone resorption during spaceflight would presumably be accompanied by a change in the dimensions of the medullary canal. Since this did not occur, these data suggest that no gross changes in endosteal bone resorption occurred during spaceflight. However, subtle changes in bone resorption may not be revealed by this technique.

A decreased trabecular bone volume and an increased fat content of the bone marrow in the proximal tibial metaphysis appear to be a consequence of spaceflight. However, these parameters are difficult to evaluate due to a great deal of variability within groups. A decreased mass of trabecular bone in the femoral and tibial metaphysis has been reported in half of the rats subjected to spaceflight aboard the Soviet Cosmos 605 biosatellite (5). A marked elevation of triglycerides in the bone marrow of flight rats during the Cosmos 936 experiment (16) supports our finding of an increased fat content in the bone marrow.

In summary, the findings in this study demonstrate: 1) the rate of periosteal bone formation in the tibial and humeral diaphyses decreased during the spaceflight period; 2) the decrease in formation may be due, in part, to a cessation of bone formation, as evidenced by the increased incidence of arrest lines in flight animals; 3) endosteal bone resorption was not affected markedly by spaceflight conditions; 4) the trabecular bone volume in the proximal tibial metaphysis decreased during the flight and postflight periods; 5) the fat content of the bone marrow in the proximal tibial metaphysis increased during spaceflight.

ACKNOWLEDGEMENTS

REFERENCES

1. Whedon, C. D., L. Lutwak, P. C. Rambaut, M. W. Whittle, M. C. Smith, J. Reid, C. S. Leach, C. R. Stadler, and D. D. Sanford. Mineral and nitrogen metabolic studies, experiment M071 in Biomedical Results from Skylab (NASA SP-377), p. 164.

2. Vogel, J. M., M. W. Whittle, M. C. Smith, and P. C. Rambaut. Bone mineral measurement - experiment M078, Biomedical Results from Skylab (NASA SP-377), p. 183.

3. Donaldson, C. L., S. B. Hulley, J. M. Vogel, R. S. Hattner, J. H. Bayers, and D. E. McMillan. Effect of prolonged bed rest on bone mineral. Metab. 19:1071-1084 (1970).

4. Claus-Walker, J., J. Singh, C. S. Leach, D. V. Hatton, C. W. Hubert, and N. DiFerrante. The urinary excretion of collagen degradation products by quadriplegic patients and during weightlessness. J. Bone Jt. Surg. 59A:209 (1977).

5. Yagodovsky, V. S., L. A. Triftanidi, and G. P. Gorokhova. Space flight effects on skeletal bones of rats (light and electron microscopic examination). Aviation Space Environ. Med. 47: 734-738 (1976).

6. Holton, E. Morey and D. J. Baylink. Quantitative analysis of selected bone parameters, Final Reports of US Experiments Flown on the Soviet Satellite Cosmos 782 (NASA TM-78525, 1978), p. 321.

7. Yagodovskiy, V. S. and G. P. Gorokhova. Changes in bones of the skeleton, The Effect of Dynamic Factors of Space Flight on Animal Organisms, A. M. Genin, Ed. (NASA TM-75692, 1979), p. 158.

8. Prokhonchukov, A. A., A. G. Kolesnik, N. A. Komissarova, L. L. Novikov, and N. N. Sirotkina. Mineral exchange in calcified tissues, The Effect of Dynamic Factors of Space Flight on Animal Organisms, A. M. Genin, Ed. (NASA TM-75692, 1979) p. 154.

9. Holton, E. Morey, R. T. Turner, and D. J. Baylink. Quantitative analysis of selected bone parameters, Final Reports of US Experiments Flown on the Soviet Satellite Cosmos 936 (NASA TM-78536, 1978), p. 135.

10. Ilyina-Kakueva, E. I., V. V. Portugalov, and N. P. Krivenkova. Space flight effects on the skeletal muscles of rats. Aviation Space Environ. Med. 47:700-703 (1976).

11. Milch, R. A., D. P. Rall, and J. E. Tobie. Bone localization of the tetracyclines. J. Nat. Cancer Inst. 19:87-03 (1957).

12. McManus, J. F. A. and R. W. Mowry. Staining Methods, Histological and Histochemical. Paul B. Hoeber, Inc. New York, New York, p. 201 (1960).

13. Merz, W. A., and R. K. Schenk. Quantitative structural analysis of human cancellous bone. Acta Anat. 75:54-66 (1970).

14. Thompson, E. R., D. J. Baylink, and J. E. Wergedal. Increases in number and size of osteoclasts in response to calcium or phosphorus deficiency in the rat. Endocrinology. 92:283-289 (1975).

15. Morey, E. R., and D. J. Baylink. Inhibition of bone formation during spaceflight. Science 201:1138-1141 (1978).

16. Ahlers, I., R. A. Tigranyan, and M. Praslicka. The effect of artificial gravitation on rat plasma and tissue lipids: The Cosmos 936 experiment. Abstracts for the Twenty-Third Plenary COSPAR Meeting. Budapest, Hungary, p. 493 (1980).

TABLE 1

GROUP	N	WEIGHT (g)	WEIGHT (g)	# DAYS	WEIGHT CHANGE (g)	Δ% controls	RATE OF WEIGHT GAIN (g/day)	Δ% controls
1F	7	287±6.5*	336±8.8	22	48±9.1	-33	2.2±0.41	-21
1S	7	270±17.7	344±18.3	27	74±18.9		2.7±0.70	
1V	7	297±16.9	367±12.8	25	70±9.4		2.8±0.38	
2F	6	291±13.3	354±17.0	28	63±7.6	-36	2.2±0.27	-30
2S	6	274±18.6	373±23.4	33	99±33.3		3.0±1.01	
2V	6	277±9.7	376±13.0	30	99±10.5		3.3±0.35	
3F	7	291±11.5	326±15.8	28	34±10.8	-51	1.2±0.39	-45
3S	7	268±13.5	337±12.6	33	69±8.1		2.1±0.25	
3V	7	285±13.0	355±6.9	30	70±12.1		2.3±0.40	
4F	5	317±18.6	356±21.9	27	39±6.7		1.4±0.25	
4S	5	311±28.8	369±20.4	32	58±15.2		1.8±0.48	
4V	5	307±27.3	348±25.1	27	41±5.5		1.5±0.20	
4F'	5	356±21.9	392±34.2	24	36±15.2		1.5±0.63	
4S'	5	369±20.4	447±44.9	24	78±24.6		3.3±1.03	
4V'	5	348±25.1	385±34.5	24	37±2.7		1.5±0.11	

*mean±1S.D.

The first weight was taken upon the first injection of tetracycline in all
  groups except 4' which was taken upon the second injection of tetracycline.

The second weight was taken upon sacrifice of the rats in all groups
  except 4 which was taken upon the second injection of tetracycline.

N = number of rats

119

TABLE 2

BONE DIMENSIONS

GROUP	N	LENGTH (cm) LEFT TIBIA	LENGTH (cm) LEFT HUMERUS	BONE CROSS-SECTIONAL AREA (mm^2) LEFT TIBIA	BONE CROSS-SECTIONAL AREA (mm^2) LEFT HUMERUS
GROUP 1 (R+0)					
FLIGHT	7	3.80* ±0.06	2.71 ±0.09	3.68** ±0.17	3.31** ±0.18
SYNCHRONOUS CONTROL	7	3.77 ±0.09	2.69 ±0.06	4.10 ±0.47	3.43 ±0.29
VIVARIUM CONTROL	7	3.90 ±0.09	2.79 ±0.07	4.09 ±0.33	3.64 ±0.27
GROUP 4 (R+29)					
FLIGHT	4	3.97 ±0.05	2.77 ±0.10	4.23 ±0.34	3.76 ±0.25
SYNCHRONOUS CONTROL	5	4.08 ±0.11	2.93 ±0.10	4.75 ±0.48	3.94 ±0.52
VIVARIUM CONTROL	5	3.90 ±0.12	2.85 ±0.06	4.51 ±0.38	4.03 ±0.48

* Mean±1 S.D.
** Significantly different from vivarium control values (P< .025).

120

TABLE 3

EFFECT OF SPACEFLIGHT ON BONE TURNOVER

GROUP	N	PERIOSTEAL BONE FORMATION RATE (10^{-3} mm^3/DAY)			N	MEDULLARY CROSS-SECTIONAL AREA(mm^2)		
		TIBIA	HUMERUS	RIB*		TIBIA	HUMERUS	RIB*
GROUP 1 (R+0)								
FLIGHT	11	10.0** $\pm$2.1	10.9** $\pm$2.2	3.66 $\pm$1.45	7	0.99 $\pm$0.19	1.11 $\pm$0.12	0.09 $\pm$0.04
SYNCHRONOUS CONTROL	11	17.9 $\pm$2.7	14.2 $\pm$2.8	4.52 $\pm$2.06	7	0.92 $\pm$0.13	1.18 $\pm$0.17	0.08 $\pm$0.03
VIVARIUM CONTROL	11	22.6 $\pm$4.7	17.9 $\pm$5.3	–	7	0.99 $\pm$0.13	1.21 $\pm$0.32	–
GROUP 4*** (R+29)								
FLIGHT	4	18.4** $\pm$2.1	11.7 $\pm$1.4	–	4	0.92 $\pm$0.08	1.43 $\pm$0.12	–
SYNCHRONOUS CONTROL	4	12.6 $\pm$2.4	10.7 $\pm$2.4	–	5	0.88 $\pm$0.14	1.45 $\pm$0.18	–
VIVARIUM CONTROL	4	14.5 $\pm$2.3	12.3 $\pm$3.0	–	5	0.79 $\pm$0.13	1.20 $\pm$0.14	–

* Each value for the rib is the mean $\pm$ the standard deviation of 5 animals.

** Significantly different from control values (see text).

*** Although 5 rats were used for each group, only 4 were analyzed since rat 4F-3 appeared to have traumatized his tibia and was forming woven bone following flight and rats 4S-4 and 4V-5 did not label when given their second tetracycline injection.

TABLE 4

EFFECT OF SPACEFLIGHT ON FORMATION OF ARREST LINES

GROUP	N	ARREST LINE LENGTH (mm) TIBIA	HUMERUS
GROUP 4	(R+29)		
FLIGHT	4	7.3* ±0.6	6.0* ±1.1
SYNCHRONOUS CONTROL	5	6.1 ±1.4	4.0 ±0.7
VIVARIUM CONTROL	5	1.6 ±1.2	4.1 ±0.2

*Significantly different from control values (see text)

TABLE 5

Staining Properties of Arrest Lines

STAIN	INTENSITY[1]
Nuclear Fast Red (mineralized)	0
Toluidine Blue (mineralized)	0
Toluidine Blue (demineralized)	**
Sudan Black (mineralized)	0
Sudan Black (demineralized)	***
Methylene Blue (mineralized)	0-*
Methylene Blue (demineralized)	**

---

[1]Relative staining intensity; 0 to *** are increasing
values
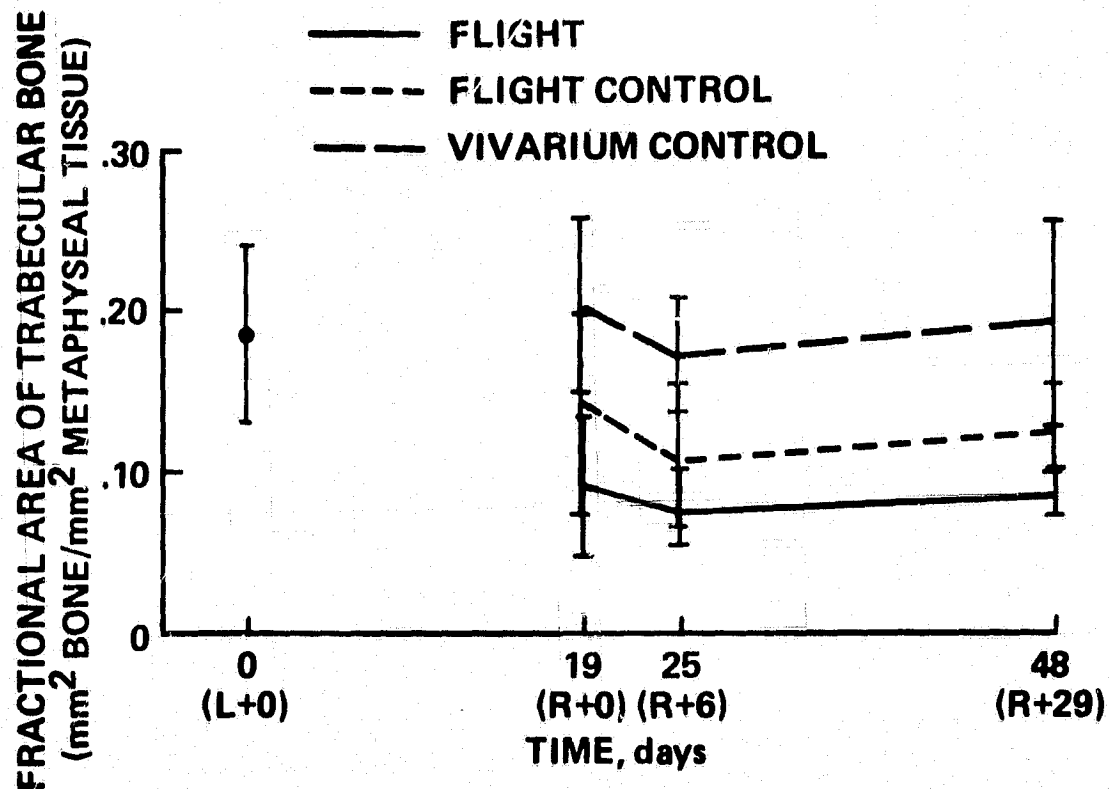
Figure 1. The fractional area of trabecular bone (trabecular bone volume) in the proximal tibial metaphysis vs. time. The spacecraft was launched on day 0, and recovered on day 19. Day 25 is equivalent to recovery + 6 days, and day 48, the end of the postflight period, is equivalent to recovery + 29 days. Each point is in the mean of 7 animals at day 19, 6 animals at day 25, and 5 animals at day 48. The vertical lines represent the standard deviations. The point at day 0 is the mean of 10 basal control rats ± the standard deviation. These rats were housed in animal quarters and sacrificed at the beginning of the flight period. The flight control group is equivalent to the synchronous control group.
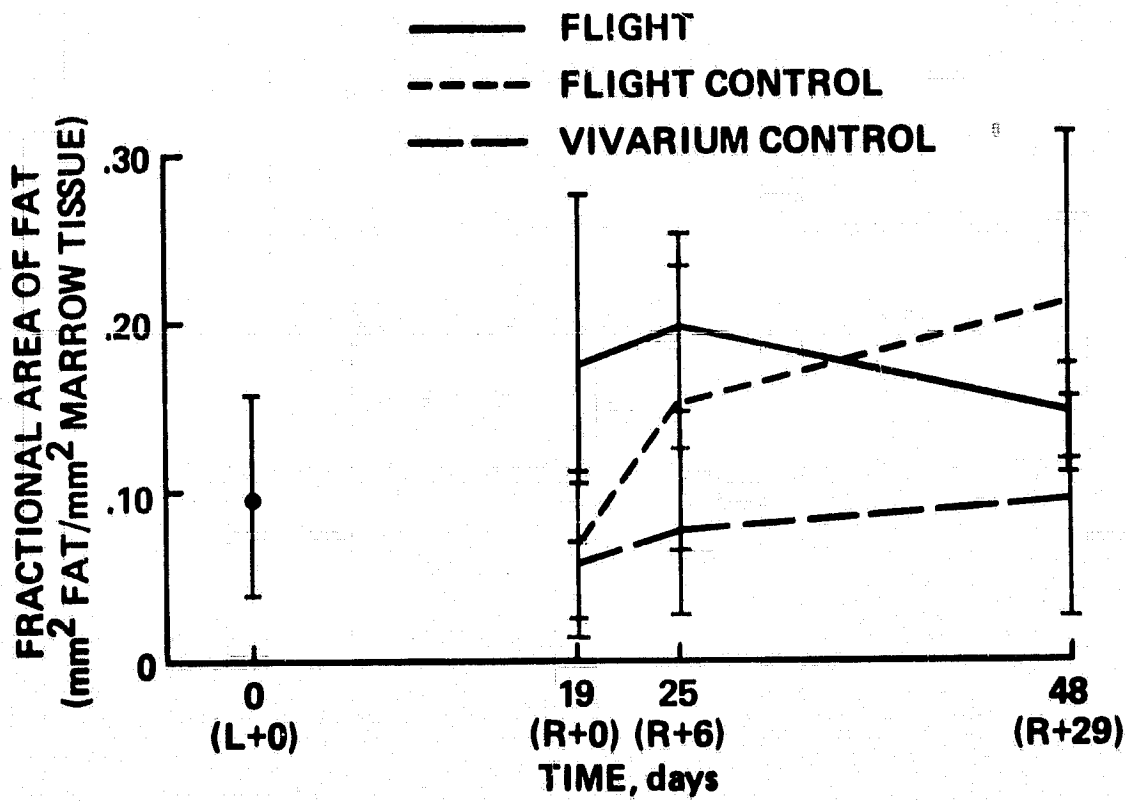
Figure 2. The fractional area of fat in the bone marrow in the proximal tibial metaphysis vs. time. See the legend for Figure 1 for a detailed description.

K305:   QUANTITATIVE ANALYSIS OF SELECTED BONE PARAMETERS

Supplemental Report 1:   Effects of Weightlessness on Osteoblast

Differentiation in Rat Molar Periodontium

W. Eugene Roberts and Peter G. Mozsary
University of the Pacific Dental School
San Francisco, CA

Emily Morey-Holton
NASA-Ames Research Center
Moffett Field, CA 94035

SUMMARY

Periodontal ligament (PDL), the osteogenic interface between tooth and bone, was morphometrically analyzed in rats subjected to 18.5 days of weightlessness. Immediately post-flight, PDL width and total cell number were decreased. Frequency distributions of nuclear volume revealed that presumptive preosteoblasts (nuclei $\geq 130 \mu m^3$) were particularly depressed. Depleted numbers of preosteoblasts may be an important factor in the mechanism of inhibited bone formation during weightlessness.

INTRODUCTION

Marked depression or arrest of bone formation is associated with space flight and simulated weightlessness (6,7). The mechanism of this suppression of osteogenesis is unclear, but probably involves altered induction.

The maxilla is not a weight-bearing bone and is not directly subjected to antigravity posturing as are the long bones. Thus, alveolar bone of the maxillary periodontium is an interesting experimental contrast to the axial skeleton to determine whether the depression of bone formation is a generalized, systemic effect.

Using cytomorphometric methods, fibroblast-like cells in the rat PDL are separated into four compartments (A, B, C, D) according to increasing nuclear volume. "D" fraction nuclei ($\geq 175\,\mu m^3$) are the first to proliferate following osteogenic stimulus and are the immediate kinetic precursors of osteoblasts. "A" fraction nuclei, the smallest in the series ($\leq 80\,\mu m^3$), are less differentiated cells which are the source of D fraction nuclei (15). These data indicate that nuclear volume frequency distributions are an effective means of assaying preosteoblast differentiation in a population of connective tissue cells.

Thus, the objective of this experiment was to determine whether spaceflight would alter cellular induction in the fibroblast-like cells in the rat PDL.

MATERIALS AND METHODS

Specific pathogen-free, male Wistar rats from the Institute of Experimental
Endocrinology of the Slovakian Academy of Sciences were approximately
83 days of age and weighed an average of 290 grams at the beginning
of the experimental period. The flight animals were placed in orbit in
individual cylindrical cages aboard a modified Soviet Vostok spacecraft for
a period of 18.5 days. There were two types of ground-based controls. The
synchronous control rats were housed identically like the flight animals and
subjected to the conditions associated with launch and reentry. An attempt
was made to simulate as closely as possible the spacecraft environment
experienced by the flight animals. The vivarium control rats were housed in
animal quarters and were not subjected to flight conditions.

The rats were divided into four groups. The first group of flight,
synchronous control, and vivarium control rats were sacrificed at the end of
the 18.5 day flight period. The second and fourth groups were sacrificed at
6 and 29 days postflight, respectively. The third group, which was sub-
jected to immobilization stress and sacrificed 6 days after flight, was not
analyzed in this experiment. All rats were injected intraperitoneally with
1 mg/kg body weight of Declomycin three days prior to launch. Declomycin is
a tetracycline derivative which labels areas of bone formation (7). A
second Declomycin injection was administered to the postflight group 5 days
after flight. The rats were decapitated at the end of the experimental
periods, and skulls were preserved in triple-fix (3).

Maxillary left first molars and surrounding periodontium were dehydrated in
a series of acetone and ether changes and embedded undecalcified in a
styrene monomer which polymerizes into a polyester resin (Tap Plastic Inc.,
San Jose, CA). The mesial root of the maxillary left first molar was sawed
in the midsagittal plane into 50 μm thick sections with a Gillings-Hamco
thin sectioning machine. Fluorescent tetracycline labels were observed at
160X under ultraviolet illumination.

Maxillary right first molars and surrounding periodontium were demineralized in 10% EDTA (pH 7.4) for two weeks, embedded in modified methyl methacrylate (5), and serially sectioned at 3 μm. The mesial root of the maxillary first molar was cut in the mid-sagittal plane, parallel to the long axis of the root. Serial sections were mounted on gelatinized slides and stained with hematoxylin and eosin/phloxine.

The region studied was a 300 μm length of midroot PDL on the mesial aspect of the mesial root of the maxillary first molars. Under oil immersion at 1000X, the length (2a) and width (2b) of the nuclei of all fibroblast-like PDL cells were measured with an ocular micrometer. Since nuclei in the area studied are prolate spheroid (width approximating depth, correlation of r = 0.9) and are 90-95% oriented in the midsagittal plane, nuclear volume of each nucleus was calculated according to $V = 4/3 \pi ab^2$. Replication error, for determining nuclear volume with this method, is inversely related to width and ranges from ± 5 to $\pm 15\%$. For groups of 100 to 1000 nuclei, reproducibility of relative frequency distributions is ± 5 to $\pm 10\%$, inversely related to sample size.

Each nucleus was categorized according to location within the PDL. Zone I is within 25 μm of bone, Zone II is further than 25 μm but within the bone half of the PDL, Zone III is on the cementum side but further than 25 μm from the root surface, and Zone IV is within 25 μm of the cementum surface. As previously described, about 90% of PDL vascularity in this area is located in Zone II (10).

Volumes for 100 nuclei from throughout the width of the PDL were determined for each animal. Five animals were quantitated for a total sample of 500 nuclei per subgroup (i.e., flight, vivarium, or synchronous).

Frequency distributions of nuclear volume for each of the nine subgroups were calculated (Tables I-III). Means and standard deviations are given in

130

Table IV. Table V is a statistical comparison of subgroups utilizing Student's t-test. Table VI is mean nuclear volume according to histological zones and Table VII is interzone statistical comparisons (t-test with p<.05 considered significant).

RESULTS

In general, the alveolar bone surface adjacent to the area of PDL studied (mesial aspect of maxillary first molar) was a bone forming surface, as revealed by tetracyline labels. Compared to vivarium controls (1V), frequency distributions of nuclear volume (intervals of 10 μm^3) for the 18.5 day flight subgroup (1F) sacrificed at recovery revealed a relative increase in smaller nuclei ($\leq$ 80 μm^3) at the expense of larger nuclei ($\geq$ 130 μm^3) In contrast, synchronous controls (1S) showed a relative increase in larger nuclei compared to either the flight or vivarium controls (Table I, Figure 1).

These observations were confirmed by comparing the nuclear volume means for subgroups 1F, 1S, 1V in Table IV. Relative to the vivarium controls (1V), a significant (p < 0.001) <u>decrease</u> in mean nuclear volume was observed for flight (1F), while synchronous controls (1S) displayed a significant (p < 0.001) <u>increase</u> (Table V). At 6 and 29 days after flight, mean nuclear volume (all zones combined) of post-flight animals (2F, 4F) and synchronous controls (2S, 4S) were no longer significantly different from vivarium controls (2V, 4V) (Tables IV and V). Figure 2 depicts the nuclear volume frequency distributions of the flight animals at the three different time periods and shows that a shift in the curve toward normal is obvious by 6 days after return to 1G.

No significant differences in interzone mean nuclear volumes were observed for Groups 2 or 4 (6 or 29 days post-flight, respectively). Compared to vivarium controls (1V), Zone I nuclei of synchronous controls (1S) were significantly (p < .02) larger, while those of flight rats (1F) were significantly (p < .01) smaller (Table VI and VII). Synchronous controls were

significantly (p<.01) larger than animals exposed to weightlessness (1F).
The only significant difference in Zone II was a smaller mean nuclear size
of flight (1F) versus synchronous controls (1S). In Zone III, 1S nuclei
were significantly larger than either the 1F or 1V subgroups. Flight rats
(1F) had significantly smaller mean nuclear volume than vivarium controls
(1V).

As shown in Table VIII, width of the midroot PDL was significantly (p < .01)
less for flight (1F) animals than for either control group. However, there
were no significant differences in PDL nuclear density of fibroblast-like
cells for the 1F, 1S and 1V subgroups (Table IX).

Compared to the vivarium control range (mean ± 1 standard deviation of all
zones at all time periods), mean nuclear volumes in Zones II, III, and IV of
1F rats recovered, to near control values, by 6 and 29 days after flight.
Zone I is no longer significantly different at 6 days and is within the
control range by 29 days (Figure 3). Synchronous controls, which have
significantly (p <.01) larger mean nuclear size in Zone I immediately after
flight, are back in the control range by 6 and 29 days (Figure 4).

DISCUSSION

Bone formation, adjacent to the area of the PDL studied in this experiment,
is an interesting observation because similar rats maintained on a standard
pellet diet normally resorb bone in this area. Roberts (9) attributed the
resorbing surface to mesial movement of the first molar roots in response to
physiological approximal drift. As the interdental areas are abraded,
the first molar tips distally to maintain contact with the second molar.
This general growth pattern for rats and mice has been confirmed by bone
labeling studies (2,18). The low grit, paste diet for the present study may
cause less approximal attrition and distal tipping of the first molar. The
net effect is a tendency toward bone formation as the tooth extrudes in

response to intermaxillary growth. Thus, bone formation on the mesial (rather than the distal) surface of the maxillary first molar is probably a diet effect.

In contrast to previous studies of formalin fixed tissue (14,15), control frequency distributions are about 25% smaller, overall. Since the relative distributions are quite similar, this probably reflects a difference in tissue processing shrinkage associated with the "triple fix" used in these studies. Consequently, the immediate precursors of osteoblasts, previously described as $\geq 175 \mu m^3$ (15) are probably $\geq 130 \mu m^3$ in the present study. Relatively undifferentiated (germinal) precursor would be expected in the $< 80 \mu m^3$ range (15).

The most extensively studied cell kinetic model of mechanically induced bone formation is experimental orthodontics (1,8,12,13,16,20,21). The specific osteogenic response in PDL is increased conversion of small to large nuclei within 8 hours (15) and recruitment of fibroblast-like cells into DNA synthesis beginning at about 21 hours after application of orthodontic force (17). Subsequent kinetic studies have confirmed that cells of the large nuclear fraction are the immediate precursors of osteoblasts (15).

These studies suggest that the shift in nuclear volume (from < 80 to $> 130 \mu m^3$), independent of DNA synthesis, is a critical, mechanical stress mediated event in osteoblast differentiation. As shown in Figure 1, synchronous controls (1S) show a significant increase in presumptive preosteoblasts (nuclei $> 130 \mu m^3$). This may reflect high endogenous corticosteroid levels in response to the physiological stress of simulated space flight and confinement in a rather small cage. These data are consistent with more rapid, orthodontically induced bone formation in cortisol treated rats (11). Apparently corticosteroids enhance formation of preosteoblasts, and may be an important factor in the change in genomic expression, which is manifest by an increase in nuclear volume, independent of DNA synthesis (15).

It is possible that the enhanced preosteoblast maturation associated with corticosteroids is mediated by parathyroid hormone because the secondary hyperparathyroid effect of corticosteroids is well established (4, 19), and parathyroid extract specifically stimulates proliferation of the large nuclear fraction (14).

Weightlessness appears to deplete preosteoblasts, as evidenced by significantly ($p < 0.001$) decreased mean nuclear volume in PDL from rats killed immediately after space flight, compared to either synchronous or vivarium controls (Table V). Frequency distributions (Table I-III and Figures 1 and 2) confirm a lower proportion of cells with larger nuclei, while numbers of smaller nuclei are relatively increased. This may be a generalized systemic effect on bone since the PDL/maxilla complex is not weightbearing.

An interesting dichotomy between simulated (synchronous) and actual space flight is evident. Enhanced preosteoblast formation, subsequent to physiological stress, may be blocked by lack of mechanical stress during weightlessness. The critical step may be the failure to convert cells with smaller, less differentiated nuclei to "preosteoblasts", which are characterized by relatively large nuclei. This is a key mechanism in the first hours of orthodontically induced osteogenesis (15), and could be a differentiation event that is inhibited in a weightless environment.

This explanation would predict normal and possibly elevated rates of bone formation during early stages of space flight, with rapidly decreasing bone accretion as the supply of viable osteoblasts is exhausted. Return to a terrestrial environment reverses the suppression of preosteoblast production, as evidenced by increased mean nuclear volumes at 6 days (2F) and 29 days (4F) after flight. Frequency distributions (Figure 2) confirm recovery of the relative number of presumptive preosteoblasts (nuclear volume ≥ 130 μm^3) at 6 and 29 days.

Studies of orthodontically induced osteogenesis have shown that new
osteoblasts are produced and bone formation initiated in about 40-48 hours.
Since the overall cell census, as well as relative number of preosteoblasts,
is depressed immediately following space flight, cell replenishment would be
expected to require an additional 20-32 hours (15). This cell kinetic data
predicts a minimum of 60-80 hours to reestablish significant bone formation
following space flight, which is essentially identical to the three day
estimate calculated from tetracycline labeling studies of tibias from
Cosmos rats (Table X).

The 29% decrease in PDL width of flight rats (Table VIII) may be related to
the 36.2% reduction in extracellular water observed in the same animals
(22). Since a major portion of PDL is ground substance, which is pre-
dominantly water, the decrease in thickness is probably a relative
dehydration. The loss of water apparently does not affect nuclear size,
because the overall range of nuclear volume for flight versus control ani-
mals is unchanged (Figures 1 and 2). Thus, tissue shrinkage in the PDL
appears to involve primarily extracellular matrix and/or cytoplasm.
Assuming the total census of PDL cells is unchanged between groups, cell den-
sity should increase as the PDL width decreases. In fact, cell density is
not significantly different in flight rats (Table IX), even though PDL width
is less (Table VIII). This indicates a net loss of cells during
weightlessness. Therefore, the preferential loss of preosteoblasts (large
nuclei) probably involves not only a block in differentiation, but a failure
of proliferation and/or enhanced cell death, as well.

This morphometric study suggests that depleted numbers of preosteoblasts may
be an important factor in the arrest of bone formation during
weightlessness. Data are consistent with either a defect in proliferation
and/or differentiation. Additional cell kinetic studies utilizing
^{3}H-thymidine are needed to define the mechanism of this important aerospace
problem.

135

REFERENCES

1. Baumrind, S. and D. L. Buck. Rate changes in cell replication and protein synthesis in the periodontal ligament incident to tooth movement. Am. J. Orthod. 57:109-131 (1970).

2. Cleall, J. F. Growth of the palate and maxillary dental arch. J. Dent. Res. 53:1226-1234 (1974).

3. Corbett, R., D. E. Philpott, and S. Black. Prolonged fixation studies for space flight. Ann. Proc. Electron Microscopy Soc. Am. 31:332-333, 1973.

4. Fucik, R. F., S. C. Kureja, G. K. Hargis, E. N. Bowser, W. J. Henderson, and G. A. Williams. Effect of glucocorticoids on function of the parathyroid glands in man. J. Clin. Endocrinol. Metab. 40:152 (1975).

5. Kimmel, D. B. and W. S. S. Jee. A rapid plastic embedding technique for preparation of three micron thick sections of decalcified tissue. Stain Technol. 50:83-86 (1975).

6. Morey, E. R. Spaceflight and bone turnover; correlation with a new rat model of weightlessness. BioSci. 29:168-172 (1979)

7. Morey, E. R. and D. J. Baylink. Inhibition of bone formation during space flight. Science, 201:1138-1141 (1978).

8. Roberts, W. E. Advanced techniques for quantitating bone cell kinetics and cell population dynamics. In: Proceedings of the First Workshop on Bone Morphometry, Z. F. G. Jaworski, S. Klosevych, and E. Cameron (eds.), University of Ottawa Press, Ottawa, p. 310-314 (1976).

9. Roberts, W. E. Cell kinetic nature and diurnal periodicity of the rat periodontal ligament. Archs. Oral Biol. 20:465-471 (1975).

10. Roberts, W. E. Cell population dynamics of peridontal ligament stimulated with parathyroid extract. Am. J. Anat. 143:363-370, 1975.

11. Roberts, W. E. The effects of cortisol on the cellular kinetics and cell population dynamics of periodontal ligament bone cells. Ph.D. Thesis, Department of Anatomy, University of Utah, Salt Lake City, Utah (1979).

12. Roberts, W. E. and D. C. Chase. Cell kinetics of orthodontically stimulated osteogenesis. Calc. Tiss. Res. 20:(Suppl) 439-441 (1977).

13. Roberts, W. E., D. C. Chase, and W. S. S. Jee. Contents of labeled mitoses in orthodontically stimulated periodontal ligament. _Arch. Oral Biol._ 19:665-670 (1974).

14. Roberts, W. E., D. J. Ferguson, and D. C. Chase. Nuclear volume distribution of ^{3}H-Thymidine labeled cells in periodontal ligament (PDL) stimulated with parathyroid extract (PTE). In: _Proc. 6th Parathyroid Conf._, Vancouver, Talmadge, R. V., et. al. (eds.), Excerpta Medica, Amsterdam, p. 358 (1978).

15. Roberts, W. E., W. C. Goodwin, and S. R. Heiner. Cellular response to orthodontic force. Dental Clin. North Amer., in press.

16. Roberts, W. E. and W. S. S. Jee. Cell kinetics of orthodontically-stimulated and non-stimulated periodontal ligament in the rat. _Arch. Oral Biol._ 19:17-21 (1974).

17. Smith, R. K. and W. E. Roberts. Cell kinetics of the initial response to orthodontically induced osteogenesis in rat molar periodontal ligament. _Calc. Tiss. Internat._ 30:51-56 (1980).

18. Tonna, E. A. Application of the ^{3}H-proline topographic method to dental tissues. _J. Periodont. Res._ 10:357-368 (1975).

19. Williams, G. A., W. C. Peterson, E. N. Bower, W. J. Henderson, G. K. Hargis, and N. J. Martinez. Interrelationship of parathyroid and adrenocortical function in calcium homeostasis in the rat. _Endocrinology_, 95:707-712 (1974).

20. Yee, J. A. Response of periodontal ligament cells to force. _Anat. Rec._ 194:603-613, 1979.

21. Yee, J. A., D. B. Kimmel, and W. S. S. Jee. Periodontal ligament cell kinetics following orthodontic tooth movement. _Cell Tissue Kinet._ 293-302, (1976).

22. Ushakov, A. S., T. A. Smirnova, G. C. Pitts, N. Pace, and A. H. Smith. Effects of weightlessness on body composition in the rat. _In:_ Final Reports of U. S. Rat Experiments on Cosmos 1129, NASA-Ames Research Center, Moffett Field, CA 94035.

TABLE I. R+O

NUCLEAR VOLUME FREQUENCY DISTRIBUTIONS
(Mean ($\bar{x}$) and Standard Deviation (SD) at each 10 μm^3 interval)

Nuclear Volume (μm^3)	1F $\bar{x}$	SD	1S $\bar{x}$	SD	1V $\bar{x}$	SD
up to 40	1.40	0.89	0.40	0.55	1.20	2.68
41 - 50	7.60	2.97	3.60	1.67	4.40	1.34
51 - 60	11.20	2.17	6.20	3.63	10.00	4.06
61 - 70	13.60	2.07	5.60	1.82	6.40	1.34
71 - 80	12.40	2.97	6.80	2.49	11.20	2.28
81 - 90	10.20	4.49	7.60	0.55	8.40	2.07
91 - 100	10.40	2.51	9.80	2.28	7.80	1.30
101 - 110	8.20	0.55	9.00	2.92	13.20	1.79
111 - 120	6.80	2.59	1.20	5.40	7.60	2.07
121 - 130	3.80	1.95	3.60	1.52	5.20	1.64
131 - 140	4.00	2.00	7.20	0.84	6.20	1.92
141 - 150	2.60	1.14	6.80	3.35	4.00	1.87
151 - 160	4.80	1.48	9.20	3.49	6.60	0.89
161 - 170	1.20	0.84	2.80	1.79	1.20	0.45
171 - 180	1.20	1.64	4.00	2.35	2.60	2.07
181 - 190	1.00	0.71	2.40	1.82	1.20	0.84
191 - 200	-	-	1.20	1.10	2.00	1.22
201 - 210	0.20	0.45	.80	0.84	0.40	0.55
211 - 220	-	-	-	-	-	-
221 - 230	-	-	0.80	0.84	0.40	0.55

R = recovery

Sample size (n) is 100 nuclei for each specimen (animal), with five animals (500 total nuclei) for each subgroup (1F, 1S, 1V).

TABLE II. R+6

NUCLEAR VOLUME FREQUENCY DISTRIBUTIONS
(Mean ($\bar{x}$) and Standard Deviation (SD) at each 10 μm^3 interval)

Nuclear Volume (μm^3)	2F $\bar{x}$	2F SD	2S $\bar{x}$	2S SD	2V $\bar{x}$	2V SD
up to 40	1.20	1.30	0.20	0.45	0.40	0.55
41 - 50	3.40	1.52	5.00	2.00	1.60	0.55
51 - 60	8.40	3.85	7.20	2.28	8.40	2.07
61 - 70	7.40	6.11	5.40	2.19	6.60	1.32
71 - 80	8.20	1.48	9.00	1.87	11.40	4.72
81 - 90	7.80	2.28	6.80	1.64	6.20	1.79
91 - 100	9.80	4.15	9.60	1.95	10.40	4.04
101 - 110	12.40	3.44	14.80	3.27	12.80	2.59
111 - 120	10.80	2.68	9.60	3.13	12.80	2.05
121 - 130	4.20	1.30	6.00	2.24	7.20	1.30
131 - 140	7.60	2.30	8.60	1.95	7.40	1.67
141 - 150	5.40	1.14	4.40	1.14	2.60	1.14
151 - 160	8.80	3.42	5.80	0.84	6.40	2.07
161 - 170	1.40	1.14	2.80	2.49	1.80	1.10
171 - 180	1.80	0.84	2.80	0.45	1.40	1.34
181 - 190	0.80	1.10	0.60	0.55	0.80	1.30
191 - 200	0.20	0.45	1.20	1.30	1.20	0.84
201 - 210	0.40	0.89	0.20	0.45	0.20	0.45
211 - 220	-	-	-	-	0.20	0.45
221 - 230	-	-	-	-	0.20	0.45

R = recovery

Sample size (n) is 100 nuclei for each specimen (animal), with five animals (500 total nuclei) for each subgroup (2F, 2S, 2V).

TABLE III. R+29

NUCLEAR VOLUME FREQUENCY DISTRIBUTIONS
(Mean (x) and Standard Deviation (SD) at each 10 μm^3 interval)

Nuclear Volume (μm^3)	4F $\bar{x}$	4F SD	4S $\bar{x}$	4S SD	4V $\bar{x}$	4V SD
up to 40	1.20	0.80	0.84	0.45	0.40	0.55
41 - 50	3.40	2.30	3.80	1.30	3.40	1.95
51 - 60	7.80	3.56	9.80	4.44	7.00	1.87
61 - 70	8.20	3.90	7.00	0.71	6.60	2.97
71 - 80	11.80	0.45	9.20	1.92	9.80	2.68
81 - 90	9.40	3.58	8.00	2.74	7.60	3.29
91 - 100	9.60	2.61	7.00	2.92	10.60	2.19
101 - 110	11.60	2.41	12.60	0.89	10.60	0.89
111 - 120	8.40	4.04	8.40	2.70	11.40	2.79
121 - 130	4.40	3.05	5.60	0.89	6.60	3.71
131 - 140	6.00	2.35	7.00	2.12	6.00	2.45
141 - 150	4.60	0.89	5.00	2.24	4.60	0.89
151 - 160	7.20	2.86	8.00	3.08	8.40	0.89
161 - 170	1.60	1.34	1.00	1.22	1.20	1.30
171 - 180	1.40	1.14	4.20	1.64	2.60	3.13
181 - 190	0.60	0.89	1.40	0.55	0.40	0.55
191 - 200	1.00	1.00	0.60	0.55	1.80	0.84
201 - 210	0.20	0.45	0.40	0.55	0.60	0.55
211 - 220	-	-	-	-	-	-
221 - 230	1.00	1.00	0.20	0.45	-	-

R = recovery

Sample size (n) is 100 nuclei for each specimen (animal), with five
animals (500 total nuclei) for each subgroup (4F, 4S, 4V).

TABLE IV

NUCLEAR VOLUME OF PERIODONTAL LIGAMENT FIBROBLAST-LIKE CELLS FOR SPACE FLIGHT (F), SYNCHRONOUS CONTROL (S) AND VIVARIUM CONTROL (V) RATS*

TOTAL SAMPLE*

Time After Flight	Group	$\bar{x}$	SD	n
0 days	1F	85.90	19.41	500
(Group 1)	1S	112.69	41.13	500
	1V	101.96	38.10	500
6 days	2F	103.41	36.41	500
(Group 2)	2S	105.25	36.02	500
	2V	104.57	34.75	500
29 days	4F	100.51	38.46	500
(Group 4)	4S	104.92	38.78	500
	4V	105.00	36.02	500

*Mean ($\bar{x}$), standard deviation (SD), and sample size (n) for the total sample (all frequency distribution intervals) of each subgroup, based on quantitation of 100 nuclei from each of five animals (5 x 100 = 500)

TABLE V - TESTS FOR STATISTICAL SIGNIFICANCE*

Intergroup Comparisons

Post-flight Sacrifice Times		n	t	p
0 days (Group 1)	1F vs. 1S	500	13.20	<.001
	1F vs. 1V	500	8.41	<.001
	1S vs. 1V	500	4.23	<.001
6 days (Group 2)	2F vs. 2S	500	0.35	-
	2F vs. 2V	500	0.22	-
	2S vs. 2V	500	0.15	-
29 days (Group 4)	4F vs. 4S	500	0.74	-
	4F vs. 4V	500	0.81	-
	4S vs. 4V	500	0.01	-

Intragroup Comparisons

		n	t	p
1F/2F/4F	1F vs. 2F	500	9.46	<.001
	1F vs. 4F	500	7.57	<.001
	2F vs. 4F	500	1.22	-
1S/2S/4S	1S vs. 2S	500	1.25	-
	1S vs. 4S	500	1.22	-
	2S vs. 4S	500	0.17	-
1V/2V/4V	1V vs. 2V	500	0.49	-
	1V vs. 4V	500	0.62	-
	2V vs. 4V	500	0.09	-

* n is sample size (100 nuclei x 5 animals); t refers to Student's t-test; p is probability based on 499 degrees of freedom

TABLE VI - NUCLEAR VOLUME OF PDL FIBROBLAST-LIKE CELLS DIVIDED INTO FOUR HISTOLOGICAL ZONES*

		ZONE I			ZONE II			ZONE III			ZONE IV		
	n	Mean	SD	SEM	Mean	SD	SEM	Mean	SD	SEM	Mean	SD	SEM
FLIGHT + 0 Days													
1F	5	85.61	10.10	4.52	86.33	6.39	2.86	87.37	10.49	4.69	94.27	5.89	2.63
1S	5	123.42	9.32	4.17	107.57	13.85	6.19	110.72	6.95	3.11	105.11	12.11	5.42
1V	5	101.70	6.39	2.86	99.22	14.64	6.55	96.71	9.56	4.28	104.62	5.15	2.30
FLIGHT + 6 days													
2F	5	96.58	13.42	6.00	110.90	13.27	5.93	99.74	10.26	4.59	112.75	11.15	4.98
2S	5	107.86	10.91	4.88	110.57	18.51	8.28	96.35	17.52	7.84	106.20	2.26	1.01
2V	5	107.50	4.14	1.85	104.03	9.62	4.30	101.93	5.42	2.43	104.83	10.29	4.60
FLIGHT + 29 days													
4F	5	97.46	14.44	6.46	98.87	11.03	4.93	107.30	8.60	3.85	104.62	4.38	1.96
4S	5	116.88	15.84	7.08	92.42	10.70	4.79	104.91	6.89	3.08	105.55	11.90	5.32
4V	5	110.03	7.84	3.51	106.97	5.03	2.25	105.58	10.74	4.80	98.78	9.98	4.46

*Zone I is within 25μm of bone, Zone II is further than 25μm but within the bone half of the PDL, Zone III is on the cementum side but further than 25μm from the root surface, and Zone IV is within 25μm of the cementum surface.

143

TABLE VII – T-TESTS FOR INTERZONE COMPARISONS OF NUCLEAR VOLUME

		GROUP 1 (Flight + 0 days)				GROUP 2 (Flight + 6 days)				Group 4 (Flight + 29 days)		
		t	D.F	p		t	D.F	p		t	D.F	p
ZONE I	1F vs. 1S	6.15	4	<.01	2F vs. 2S	2.24	4	—	4F vs. 4S	2.03	4	—
	1S vs. 1V	4.30	4	<.02	2S vs. 2V	0.07	4	—	4S vs. 4V	0.87	4	—
	1F vs. 1V	3.01	4	<.05	2F vs. 2V	2.69	4	—	4F vs. 4V	1.71	4	—
ZONE II	1F vs. 1S	3.11	4	<.05	2F vs. 2S	0.03	4	—	4F vs. 4S	0.94	4	—
	1S vs. 1V	0.93	4	—	2S vs. 2V	0.70	4	—	4S vs. 4V	2.75	4	—
	1F vs. 1V	1.81	4	—	2F vs. 2V	0.94	4	—	4F vs. 4V	1.49	4	—
ZONE III	1F vs. 1S	4.15	4	<.02	2F vs. 2S	0.37	4	—	4F vs. 4S	0.48	4	—
	1S vs. 1V	2.65	4	<.05	2S vs. 2V	0.68	4	—	4S vs. 4V	0.12	4	—
	1F vs. 1V	1.47	4	—	2F vs. 2V	0.42	4	—	4F vs. 4V	0.28	4	—
ZONE IV	1F vs. 1S	1.80	4	—	2F vs. 2S	1.29	4	—	4F vs. 4S	0.16	4	—
	1S vs. 1V	3.08	4	—	2S vs. 2V	0.29	4	—	4S vs. 4V	0.97	4	—
	1F vs. 1V	2.96	4	<.05	2F vs. 2V	1.17	4	—	4F vs. 4V	1.20	4	—

TABLE VIII

MIDROOT PDL WIDTH OF ANIMALS
KILLED IMMEDIATELY AFTER FLIGHT

PDL Width (μm)

	MEAN	SD	SEM	n
1F	106.00	6.52	2.92	5
1S	148.75	7.40	3.31	5
1V	147.50	17.50	7.83	5

Intergroup t-tests

	t	D.F.	p
1F vs. 1V	4.97	4	<.01
1V vs. 1S	0.10	4	-
1F vs. 1S	9.69	4	<.001

TABLE IX

PDL NUCLEAR DENSITY OF ANIMALS KILLED
IMMEDIATELY AFTER FLIGHT

Nuclei/100μm^2 of Midroot PDL

	MEAN	S.D.	SEM	n
1F	0.292	0.011	0.005	5
1S	0.289	0.014	0.006	5
1V	0.282	0.006	0.002	5

Intergroup t-tests

	t	D.F.	p
1F vs. 1V	1.667	4	-
1V vs. 1S	1.000	4	-
1F vs. 1S	0.375	4	-

145

TABLE X

CALCULATED TIME AFTER RETURN TO 1G FOR BONE FORMATION TO BE REINITIATED

COSMOS 782		3.5 days
COSMOS 936		2.3 days
COSMOS 1129		2.8 days
	average	2.9 days

These data are from cross-sections of rat tibia at the tibiofibular junction and were taken from Cosmos experiments K005, K205, and K305; bone formation rate was measured using tetracycline labeling. The calculations were based on the amount of bone area formed in those animals sacrificed immediately following flight versus the amount of bone formed in those animals which received a second tetracycline label following return to earth (3 days postflight in Cosmos 782, 4 days postflight in Cosmos 936, and 5 days postflight in Cosmos 1129). The difference between these 2 values was divided by the rate of bone formation of the synchronous rats for the flight period to give the number of days of bone formed during this period. To determine when bone formation was reinitiated, the latter value was subtracted from the number of days between recovery and the second tetracycline injection. Interestingly, Cosmos 782 rats injected postflight formed slightly less bone during the flight period than did those animals sacrificed immediately following flight; however, a very faint second label given 3 days after flight suggested that bone formation was, indeed, just being reinitiated.
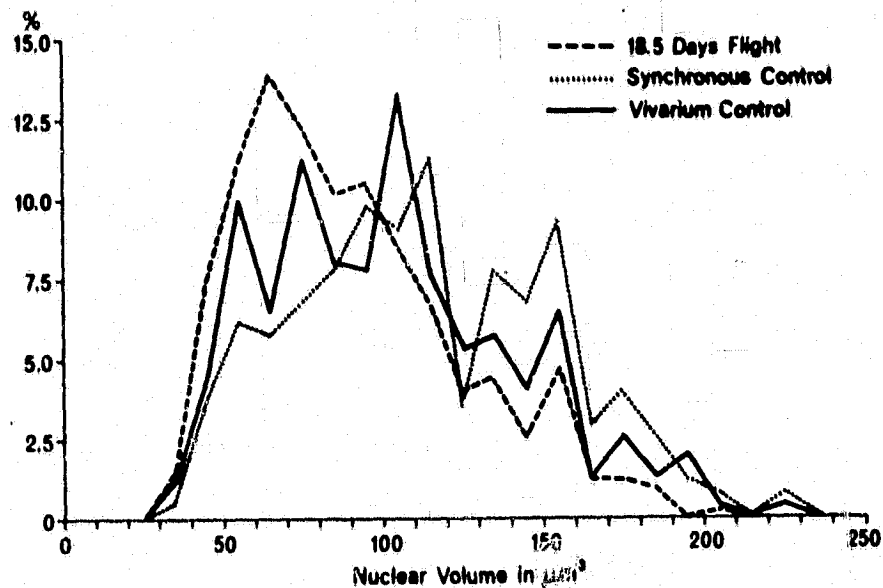
Figure 1 - Frequency distributions of nuclear volume for Group 1, killed immediately after 18.5 days of space flight. The 18.5 days flight, synchronous control and vivarium control curves correspond to the 1F, 1S and 1V subgroups, respectively (Tables I-III). The sample size for each distribution is 500 (5 animals x 100 nuclei).
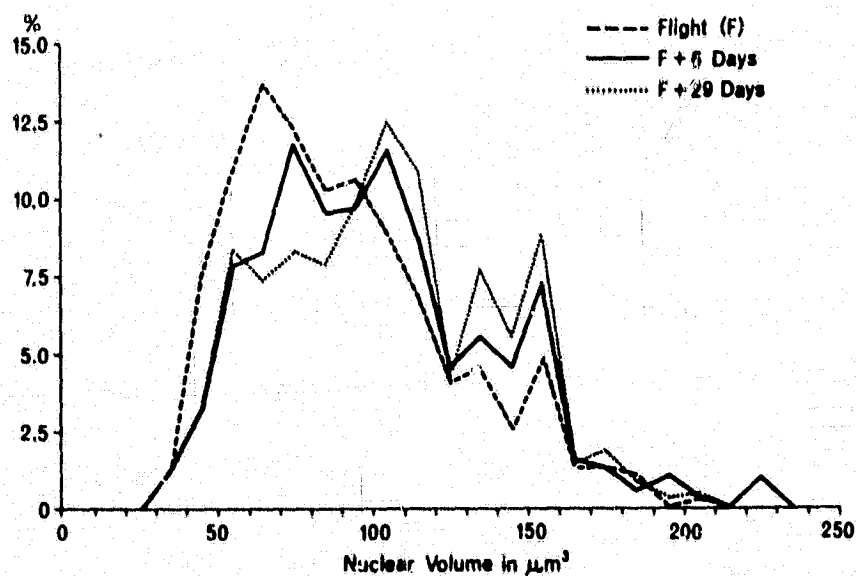
Figure 2 - Frequency distributions of nuclear volume for all flight animals. The flight, F+6 days and F+29 days curves correspond to the 1F, 2F, and 4F subgroups, respectively (Tables I-III). The sample size for each distribution is 500 (5 animals x 100 nuclei).

147
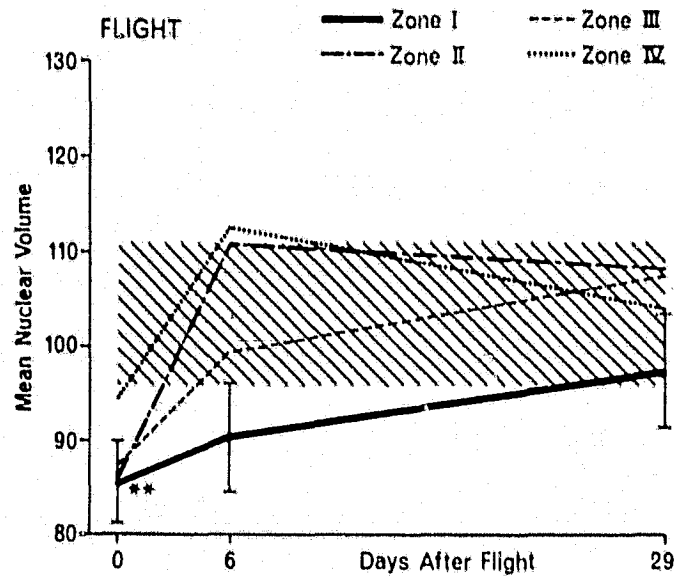
Figure 3 - Mean nuclear volume for the four histological zones of the PDL from rats exposed to 18.5 days of weightlessness. The crosshatched area is the vivarium control range, which is the mean ± 1 standard deviation of all four zones combined. Immediately after flight (0 days), zones I, II, and III are significantly (p < .01) less than vivarium controls.
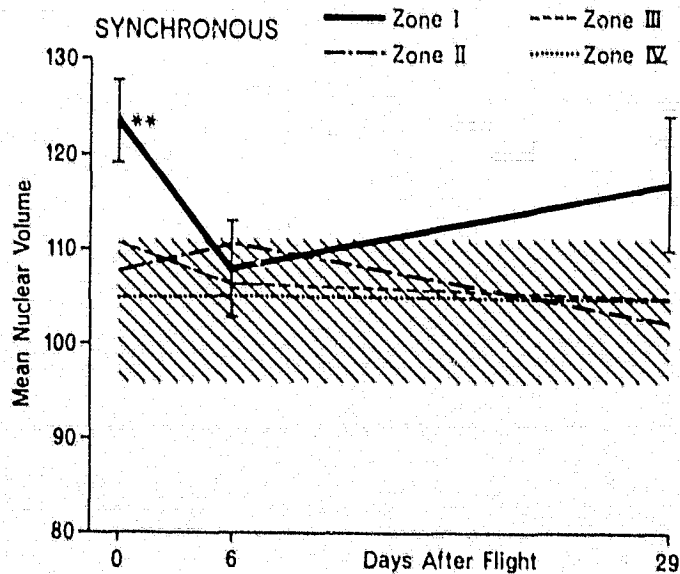
Figure 4 - Mean nuclear volume for the four histological zones from synchronous control rats. The crosshatched area is the vivarium control range, which is the mean ± 1 standard deviation of all four zones combined. Immediately after flight (0 days), mean nuclear volume of zone I is significantly (p < .01) greater than vivarium controls.

148

K 305: QUANTITATIVE ANALYSIS OF SELECTED BONE PARAMETERS

SUPPLEMENTAL REPORT 2: BONE ELONGATION RATE AND BONE MASS IN

METAPHYSIS OF LONG BONES

W.S.S. Jee, D.B. Kimmel, C. Smith, and R.B. Dell

Division of Radiobiology, Department of Pharmacology

Bldg. 351, University of Utah

Salt Lake City, UT 84112

SUMMARY

The proximal humeral metaphysis of rats from time periods recovery plus zero days (R+0), recovery plus six days (R+6), and recovery plus twenty nine days (R+29) was analyzed. The volume of calcified cartilage and bone in flight and synchronous controls was reduced in groups R+0 and R+6, but was normal in group R+29. The number of functional bone cells (osteoblasts and osteoclasts) was decreased in proportion to the amount of bone in the early groups, and was normal in the last group. The fatty marrow volume was increased only in flight animals of groups R+0 and R+6, but was normal in the R+29 group. Accumulation of excess fatty marrow was seen only in flight animals. The decreased amount of bone and calcified cartilage is believed to be the result of a temporarily slowed or arrested production of calcified cartilage as a substrate for bone formation. This would have resulted from slowed bone elongation during flight and synchronous control conditions. Bone elongation returned to normal by twenty nine days after return.

INTRODUCTION

The purpose of this study is to determine whether bone elongation rate and bone cell number in the metaphysis of long bones are altered by Cosmos 1129 spaceflight. The proximal humeral metaphysis from animals of groups killed at recovery plus zero days (R+0), recovery plus six days (R+6), and recovery plus twenty-nine days (R+29) was measured using quantitative light microscopic techniques (1). An attempt was made to measure the rate of bone elongation directly in the proximal tibial metaphysis by the use of tetracycline labeling.

MATERIALS AND METHODS

Specimen Processing

Upon receipt of the left proximal humerus, a parasagittal slice containing growth plate and adjacent metaphysis was cleaved for electron microscopic studies (see Supplemental Report 3A). The remaining portion was decalcified, trimmed to one cm in length and parasagittally halved, and embedded for parasagittal sectioning. Sections were then prepared, all as previously described (1).

The tibia was trimmed to leave only the most proximal one cm. A frontal cut was made to expose the epiphysis, growth cartilage, metaphysis, and marrow cavity. These specimens were gradually dehydrated in increasingly concentrated acetone, and then embedded in methyl methacrylate. Fifteen ten-micron thick frontal sections were prepared with a motor-driven Jung microtome (2). They were affixed to glass slides with Haupt's adhesive. Coverslips were affixed to the unstained sections with Permount.

150

The remainder of the embedded sample was sent to the bone laboratory at NASA-Ames where 100 μm sections were cut with a Gillings-Hamco thin sectioning machine. The sections were returned to Utah, where microradiographs were prepared (12 kV, 25 mA, 3 minutes; Spectroscopic Plates #649-0, Eastman Kodak, Rochester, NY). The microradiographs were shipped to Dr. Judy at Baylor for laser analysis (see Supplemental Report 3B).

Microscopic Examination

One section of the proximal humerus of each animal was randomly selected, blind-coded, and subjected to quantitative histologic analysis by a trained operator. The method is identical to that previously described (1). In addition, the number of Merz grid points over fatty and red bone marrow was counted. It resulted in presentation of various quantitative histologic parameters from a series of metaphyseal tissue bands of increasing age, whose physical locations were 0.108, 0.324, 0.768, 1.182, 1.620, 2.052, 2.484, 2.916, 3.348, and 3.780 mm on center from the growth cartilage-metaphyseal junction (GCMJ). Previously established criteria of bone cell identification were used (1).

The following parameters were calculated for each band analyzed in the metaphysis: 1) fractional bone volume, 2) fractional calcified cartilage volume, 3) osteoblast number, 4) osteoprogenitor cell number, 5) osteoclast nucleus number, 6) osteoblast number/surface area of bone, 7) osteoprogenitor cell number/surface area of bone, 8) osteoclast nuclei/surface area of bone, and 9) fractional fatty marrow volume.

The 10 μm sections of the proximal tibia were examined under ultra-violet light for the location of tetracycline label, with the intent of measuring the amount of longitudinal growth which had occurred since the time of administration of the label.

Data Processing

The raw data from each individual field of each band of each bone was coded into a Hewlett-Packard 9825 desktop computer and stored on tape. The values for each parameter for each group in each band were compared. Paired t-tests were done for each of the calculated parameters from the different groups. Figures comparing quantities of the various parameters as a function of distance from the GCMJ are presented (Figs. 1-15).

RESULTS

The tetracycline label was present, but of such low intensity that it was inadequate to allow measurement of the bone elongation rate.

For each parameter, the important changes in the minds of the investigators are described.

Bone Volume (Figs. 1-3)

All vivarium control animals showed a marked maximum for bone volume in the area 0.3-0.8 mm from the GCMJ. The flight animals showed no such maximum in the R+0 and R+6 groups. However, in the R+29 group, there was no apparent difference between the vivarium controls and the flight group. The synchronous controls showed an intermediate trend which tended to resemble that of the flight animals more than that of the vivarium controls.

Calcified Cartilage Volume (Figs. 4-6)

As with bone volume, there was less calcified cartilage in the 0.3-1.1 mm region, in the flight animals of Groups R+0 and R+6, when compared to the vivarium controls. Again, in Group R+29, there were no appreciable differences between vivarium control and flight groups. The synchronous animals again tended to resemble the flight group.

Osteoblast Numbers (Figs. 7-9)

In flight animals of Group R+0 and R+6, there were fewer osteoblasts in the area between 0.108 and 0.768 mm of the GCMJ, where most bone formation activity is normally found. In Group R+29, there was no such difference. It was not clear where the synchronous group fell.

Osteoprogenitor Cell Numbers (Figs. 10-12)

There was no convincing difference in osteoprogenitor cell number among any groups at any time. There was an overall tendency for there to be fewer osteoprogenitor cells in flight and synchronous controls, when compared to vivarium controls.

Osteoclast Nucleus Number (Figs. 13-15)

There were fewer osteoclast nuclei in the flight and synchronous animals of Groups R+0 and Group R+6, than in the vivarium controls, while there were no differences in Group R+29.

Fatty Marrow Volume (Figs. 16-18)

There was more marrow space occupied by fat in flight animals of Group R+0, than in either synchronous or vivarium controls. This was less marked in Group R+6, and no longer noticeable in Group R+29. It is particularly of note that the flight and synchronous controls were

different for this parameter, while they were similar for hard tissue mass and cell numbers.

Cells and Nuclei per Bone Surface

In all cases, when cells were evaluated based on the perimeter of bone surface available, there was no difference from the interpretations which were based upon cells and nuclei/area of tissue.

DISCUSSION

It is our interpretation that the study demonstrates a reduction in bone and calcified cartilage volume in flight and synchronous animals, in a region of the metaphysis where a maximum is seen in controls (0.3-0.8 mm from the GCMJ). This is associated with a decreased number of functional bone cells (osteoblasts and osteoclasts) in both flight and (probably) synchronous groups. There was an increased amount of fatty marrow in flight animals when compared to both synchronous and vivarium controls. These changes persist at six days after recovery, but seem to have subsided by twenty nine days after recovery, when the appearance of the metaphysis had returned essentially to normal.

The decreased amount of bone and calcified cartilage is probably due to a decreased production rate of calcified cartilage coupled with a normal or mildly decreased rate of removal. Though it is conceivable that the decreased amount of either calcified cartilage or bone could be due to a normal rate of production coupled with an increased rate of removal, the reduction in function of bone cell population sizes makes this an unlikely explanation. The most likely explanation

is that the function of the growth cartilage in providing calcified cartilage as a substrate for bone formation has been temporarily slowed or arrested by the experimental treatment of flight and synchronous control animals. This leads to the conclusion that the growth cartilage is functioning at a slower rate, which results in a slower rate of bone elongation. This is not an unreasonable conclusion because inhibition of bone elongation and a reduction in primary spongiosa hard tissue mass have been reported in two previous Cosmos experiments (4,5).

The impression is that the synchronous group shows changes quite similar to those of the flight group. It is unfortunate that the proper statistical analysis of the data, one which considers the trend of a particular parameter through the complete metaphysis (6), is not available at the present time. If this synchronous group did indeed prove to show significant changes quite similar to the flight animals, this would indicate that the general stress as well as the flight itself, had an effect on the rate of bone elongation. The appearance of excess fatty marrow in flight animals and not in synchronous controls is at least one specific effect of flight over and above the synchronous conditions.

It is also clear that the metaphysis has returned to normal by the end of the twenty nine day recovery period. It is reasonable to assume that the bone elongation rate, which was slowed or arrested during flight, resumed shortly after the return and after several weeks provided sufficient calcified cartilage that bone formation

could begin anew and metaphyseal bone mass could again approach that of controls. It is vitally important to point out that the recovery of bone mass in these animals is associated with a resumption of activity of a growth cartilage. It is recommended that all future experiments dealing with growing animals should be designed to determine directly the rate of bone elongation. The fact that these growing animals recovered bone mass in the month following spaceflight has no relationship to what might happen in a mature animal where epiphyseal growth cartilages have long since closed.

REFERENCES

1. Kimmel, D.B. and W.S.S. Jee. A quantitative histologic analysis of the growing long bone metaphysis. _Calcif. Tiss. Res._, 32:113-122 (1980).

2. Arnold, J.S. and W.S.S. Jee. Embedding and sectioning undecalcified bone and its application to radioautography. _Stain Technol._, 29:225-234 (1954).

3. Sokal, R.R. and F.J. Rohlf. _Biometry_, Freeman, San Francisco (1969).

4. Yagodovsky, V.S., L.A. Triftanidi and G.P. Gorokhova. Spaceflight effects on skeletal bones of rats (light and electron microscopic examination). _Aviat. Space Environ. Med._, 47:734-738 (1976).

5. Yagodovsky, V.S. and G.P. Gorokhova. Changes in bones of the skeleton. In "The Effect of Dynamic Factors of Space Flight on Animal Organisms". A.M. Genin (ed.), NASA TM-75692, pp. 158-167 (1979).

6. Takahashi, M., M.L. Mendelsohn and J.D. Hogg. The automatic analysis of FLM curves. _Cell Tiss. Kinet._ 4:505-518 (1971).
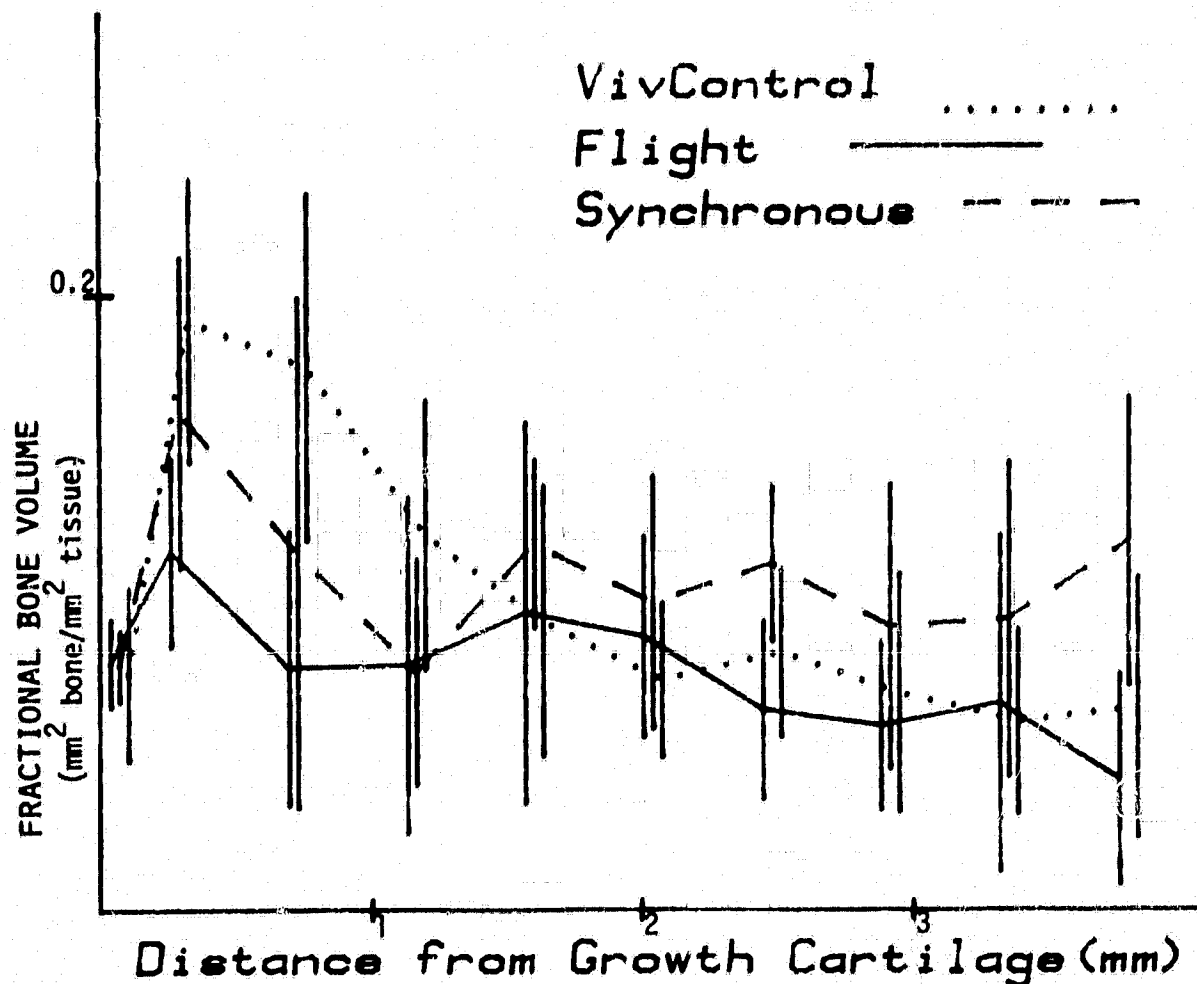
Figure 1. Bone Volume as a function of distance from the growth cartilage metaphyseal junction is plotted for Group R+O. Control animals show a marked maximum in the 0.324 - 0.768; synchronous animals show a less marked maximum, while flight animals show still less.
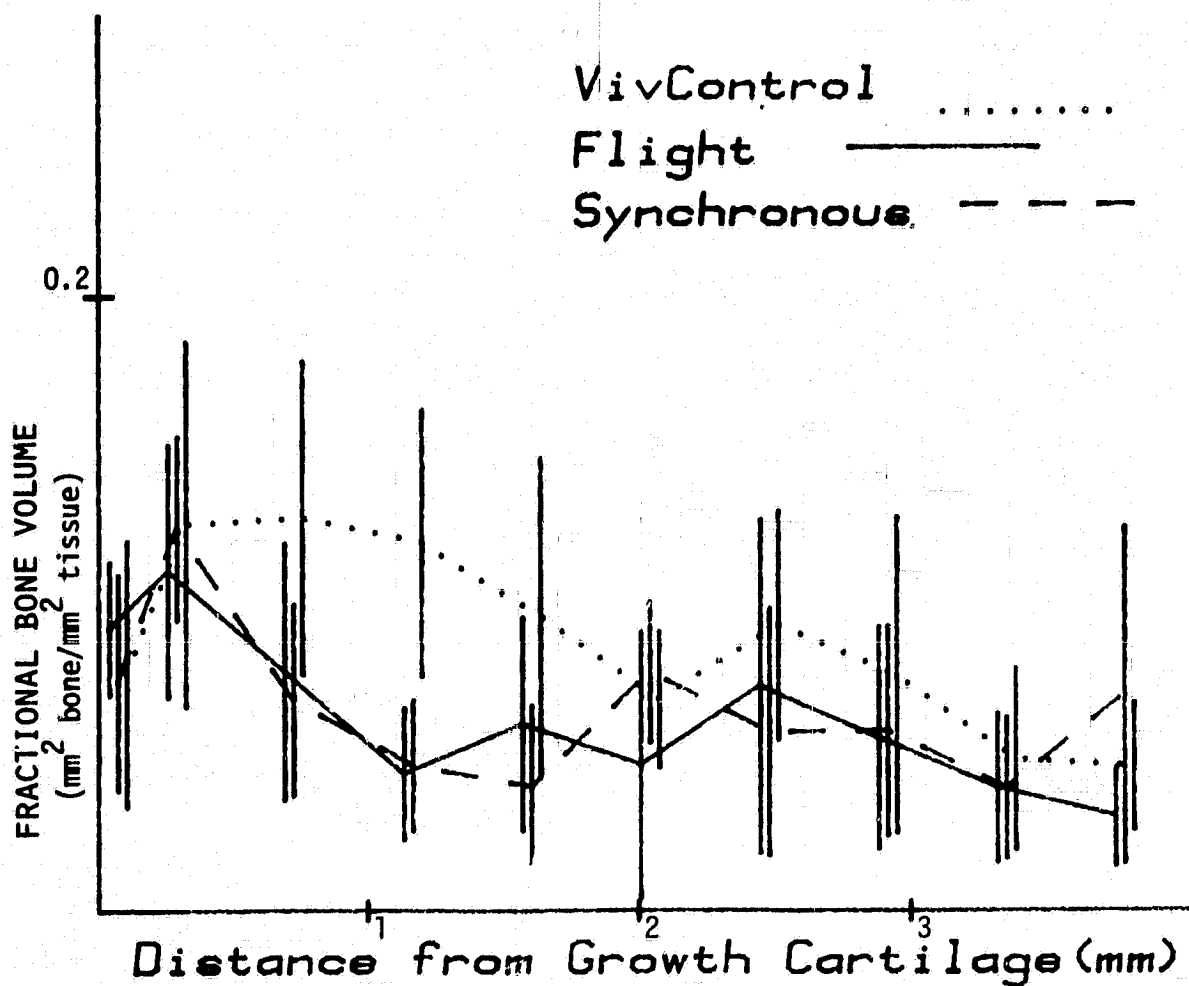
Figure 2. Bone Volume as a function of distance from the growth cartilage metaphyseal junction is plotted for Group R+6. Bone volume in both synchronous and flight animals is decreased in the 0.768 - 1.620 regions.
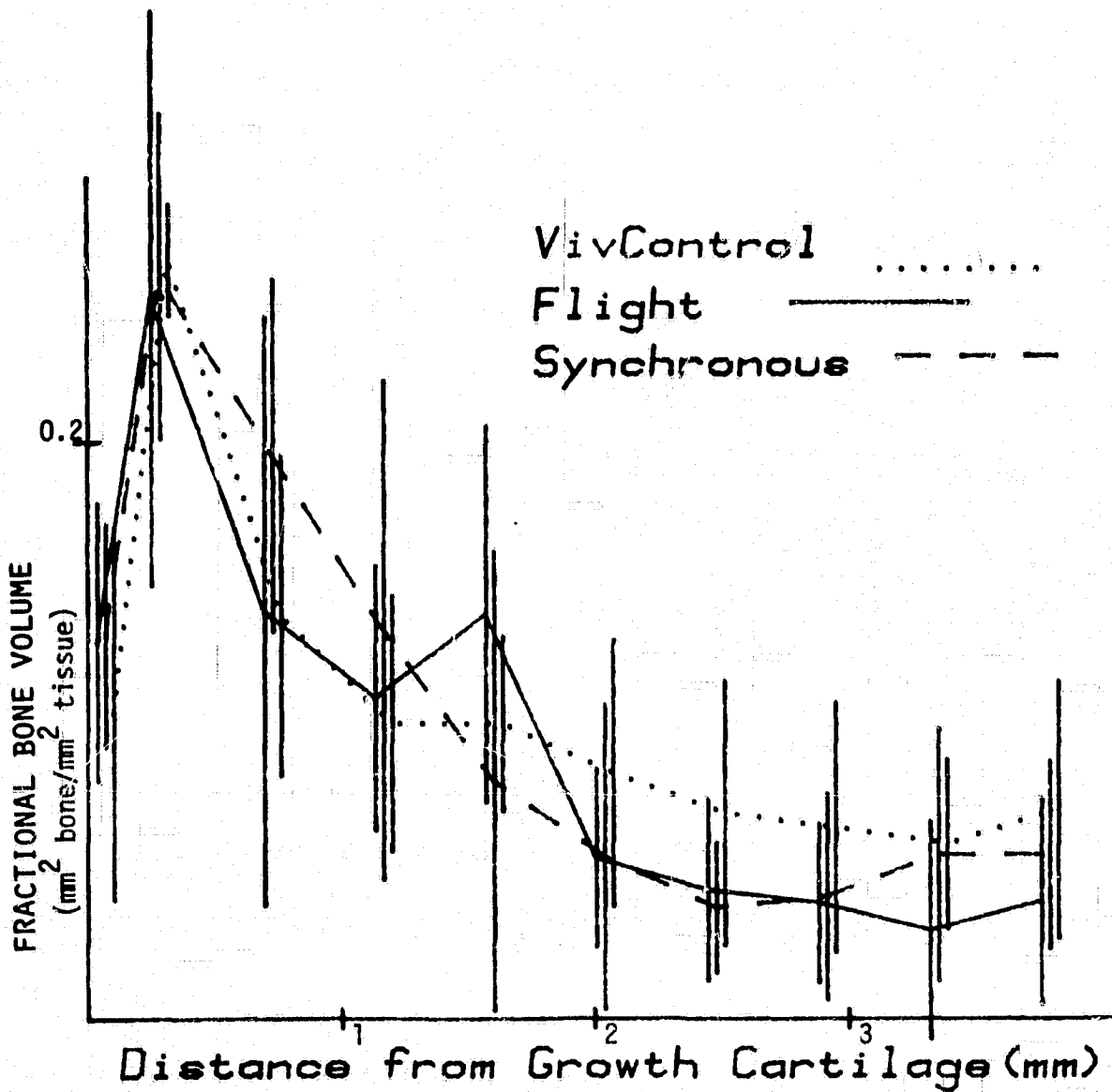
Figure 3. Bone Volume as a function of distance from the growth cartilage metaphyseal junction is plotted for Group R+29. All curves assume basically a similar shape, which is interpreted to mean that the bone volume of the metaphysis is basically normal.
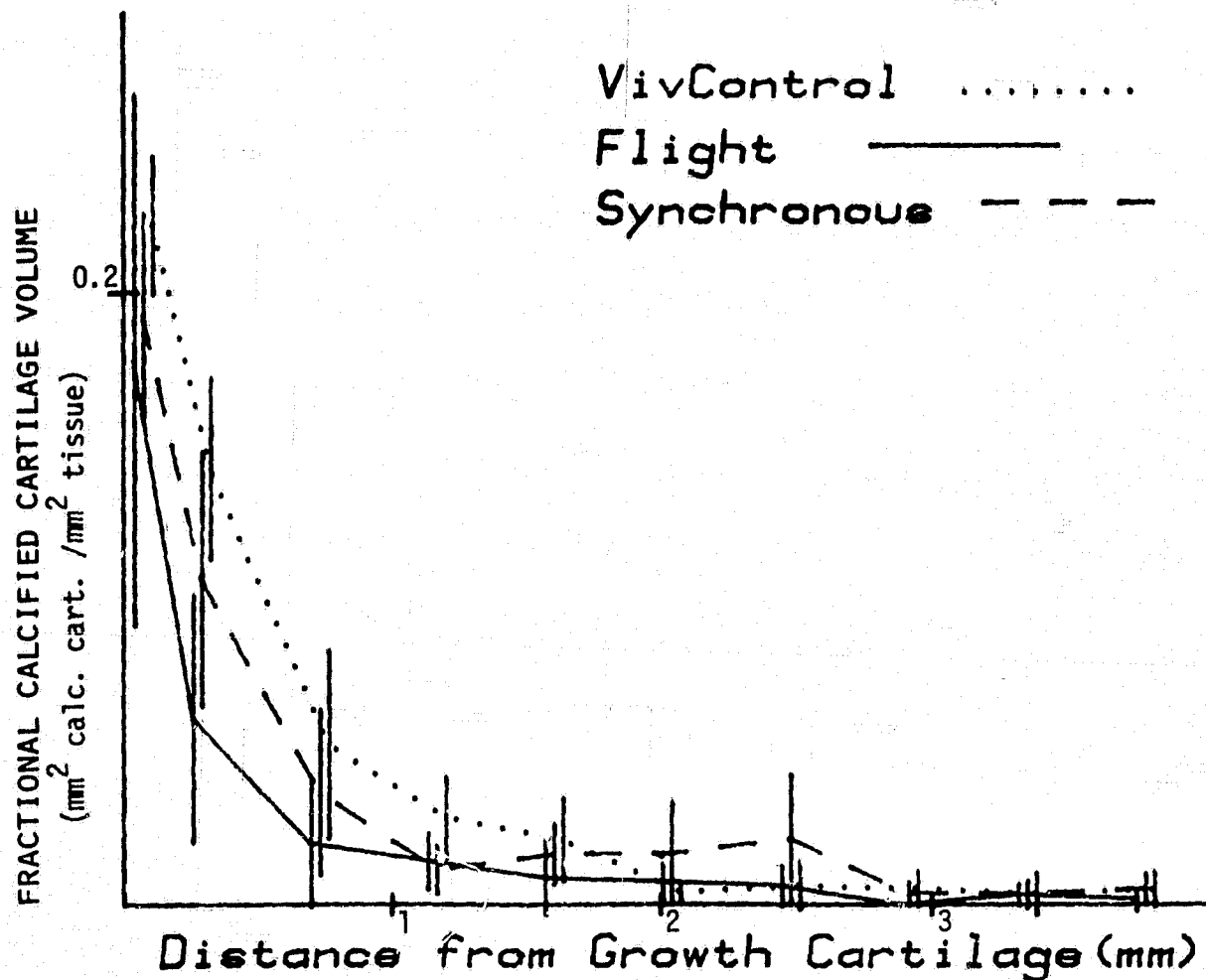
Figure 4. Calcified Cartilage Volume as a function of distance from the growth cartilage metaphyseal junction is plotted for Group R+0. The flight and synchronous animals appear to have less calcified cartilage in the 0.324 - 0.768 region when compared to the controls.
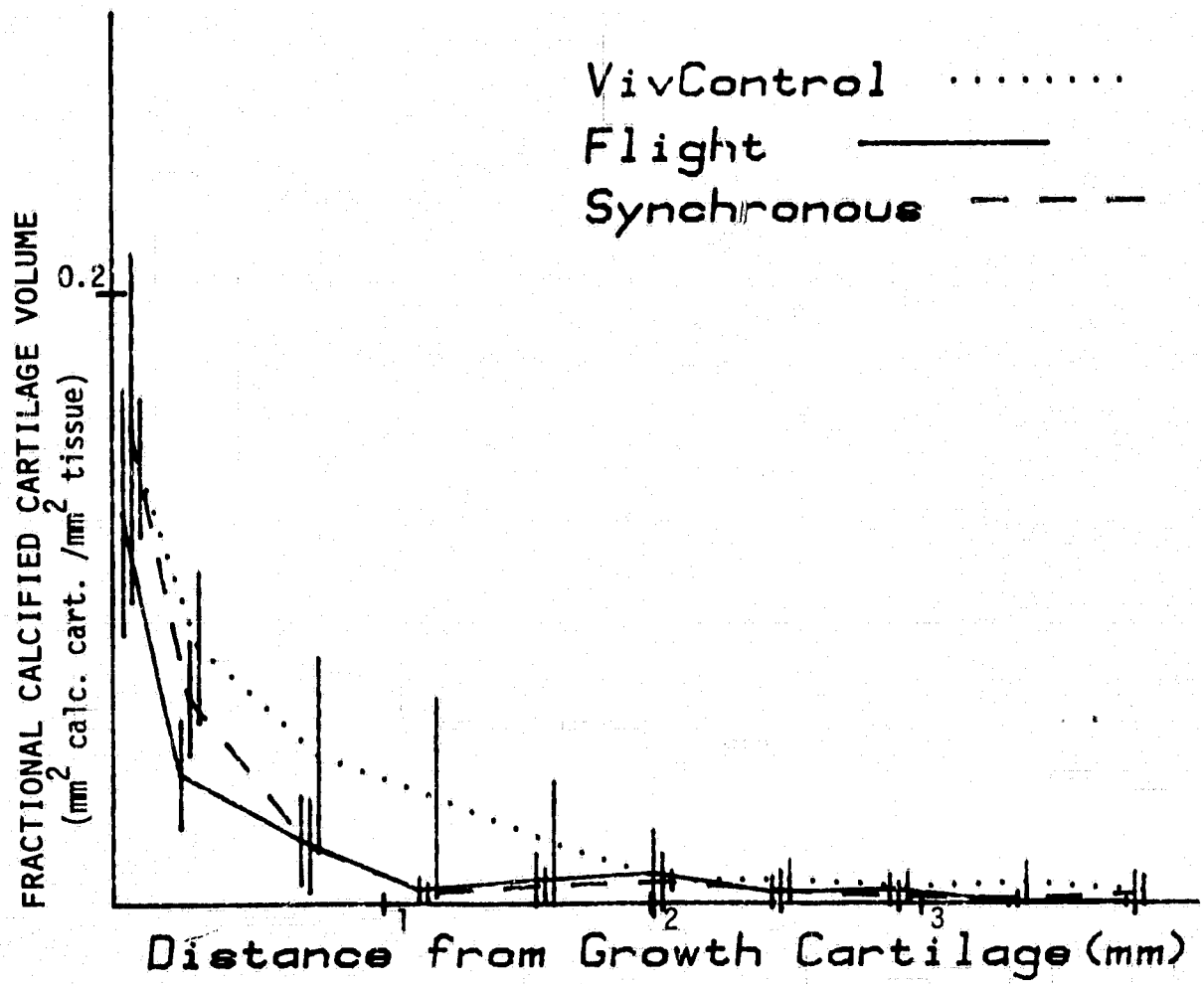
Figure 5. Calcified Cartilage Volume as a function of distance from the growth cartilage metaphyseal junction is plotted for Group R+6. Calcified cartilage volume in the 0.324 - 1.62 regions of both the synchronous and flight controls is again low when compared with controls.
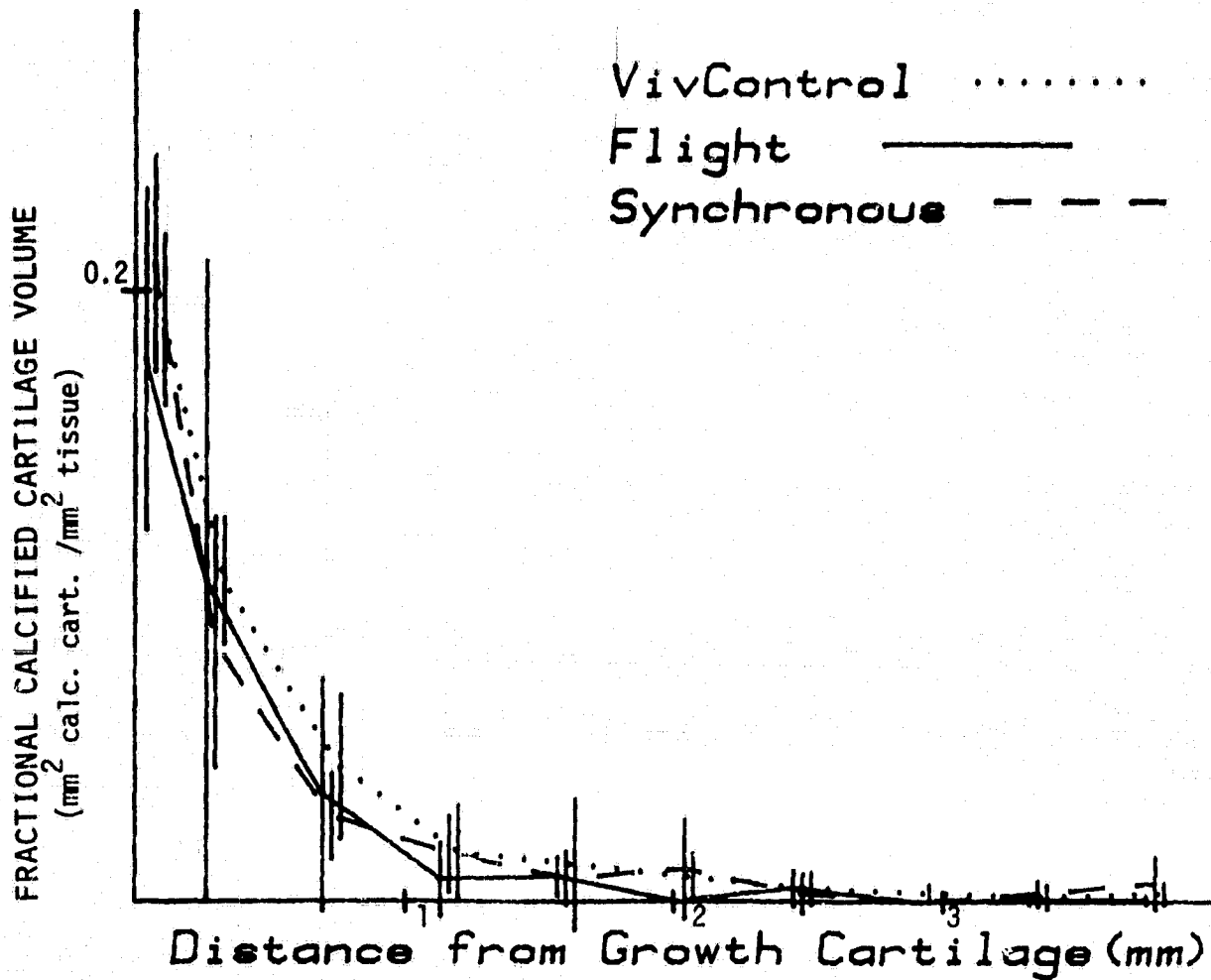
Figure 6. Calcified Cartilage Volume as a function of distance from the growth cartilage metaphyseal junction is plotted for Group R+29. There is essentially no difference in the curves, indicating calcified cartilage volume of the metaphysis is normal.
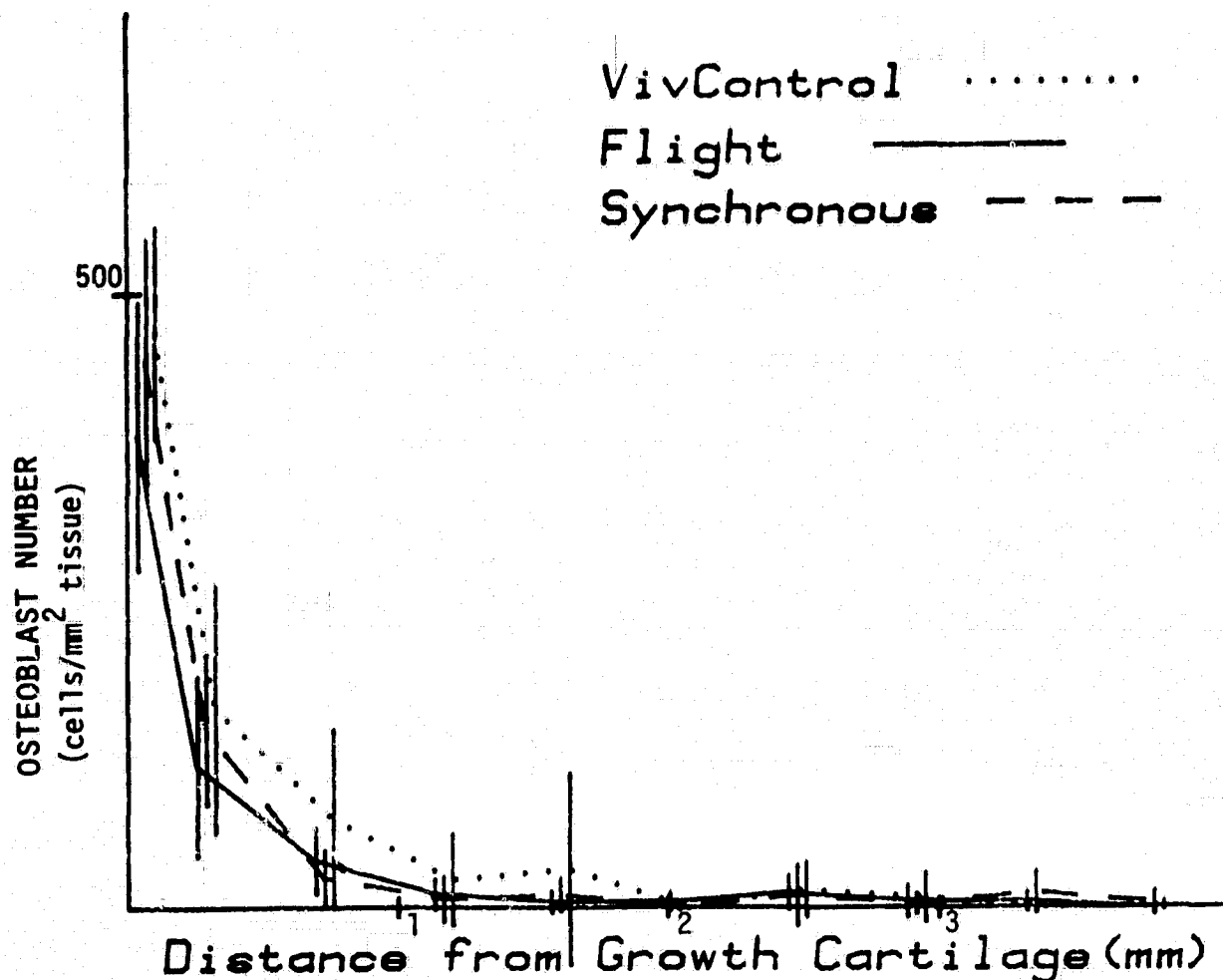
Figure 7. Osteoblast Number as a function of distance from the growth cartilage metaphyseal junction is plotted for Group R+0. There are somewhat fewer osteoblasts in both flight and synchronous groups in the 0.108 - 0.768 regions when compared to the controls.
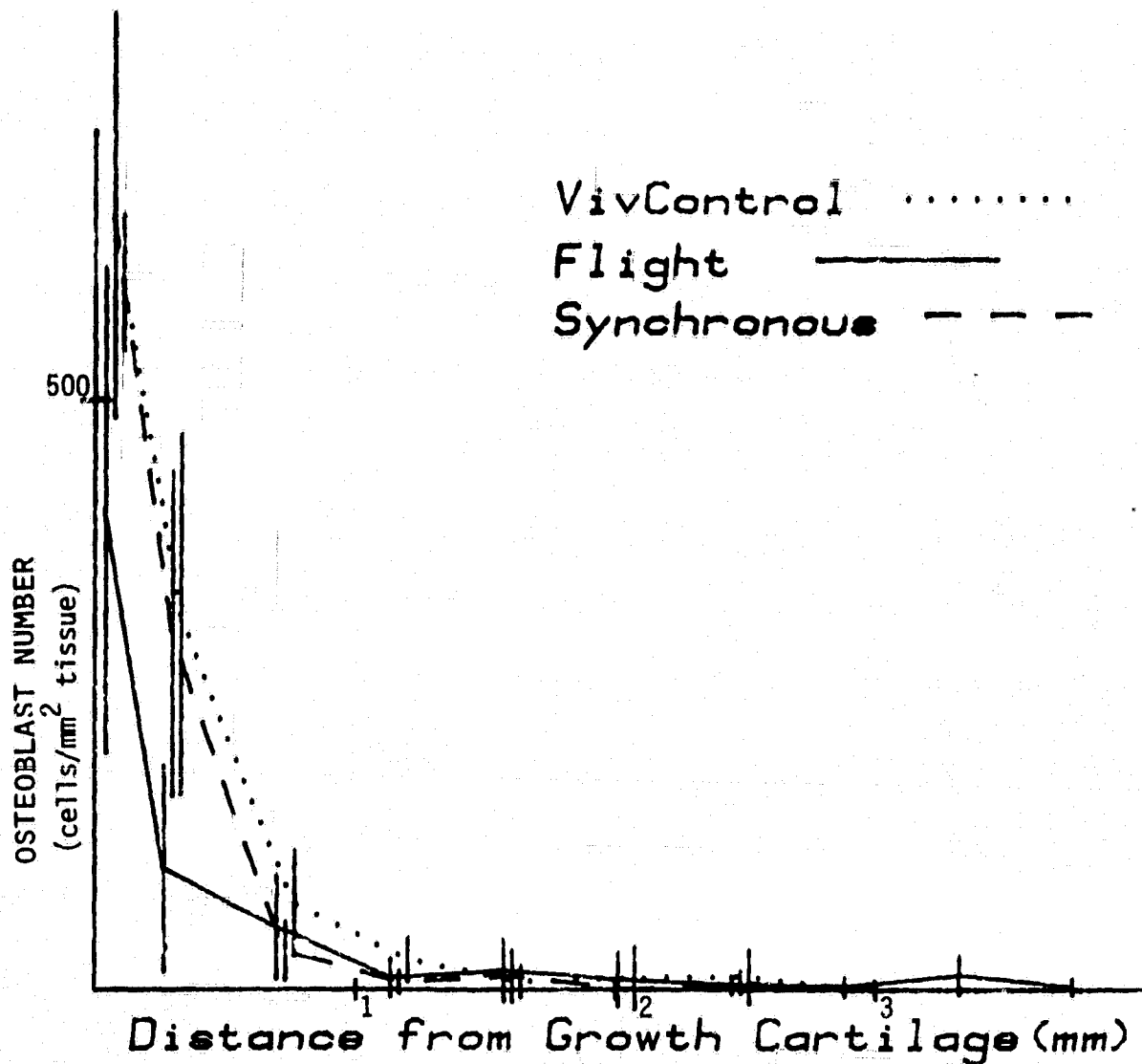
Figure 8. Osteoblast Number as a function of distance from the growth cartilage metaphyseal junction is plotted for Group R+6. There are still fewer osteoblasts in the flight animals (0.108 - 0.768 mm) when compared to the controls. The synchronous animals now appear more similar to controls.
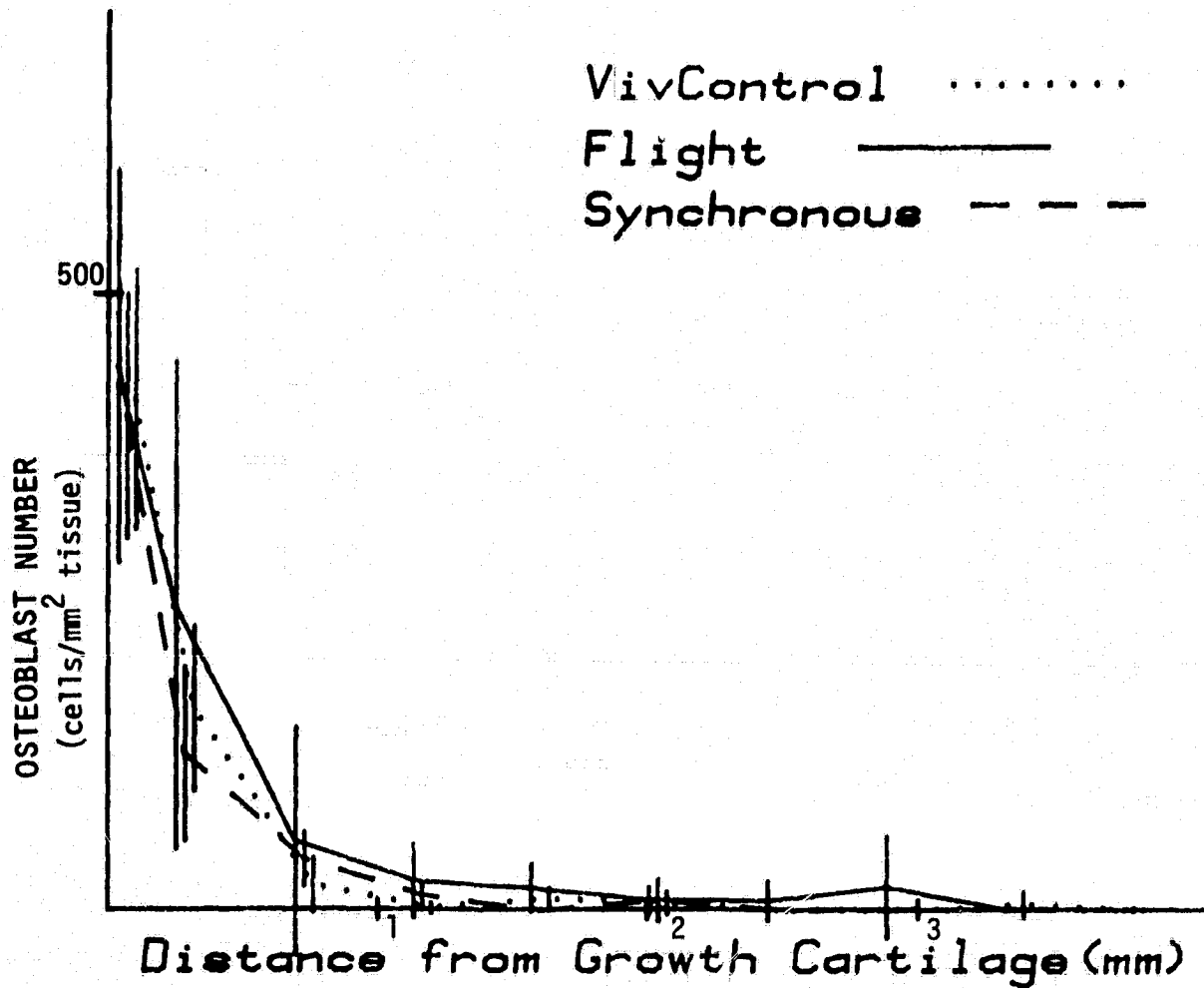
Figure 9. Osteoblast Number as a function of distance from the growth cartilage metaphyseal junction is plotted for Group R+29. All curves appear basically similar, suggesting that the metaphysis has returned to normal.
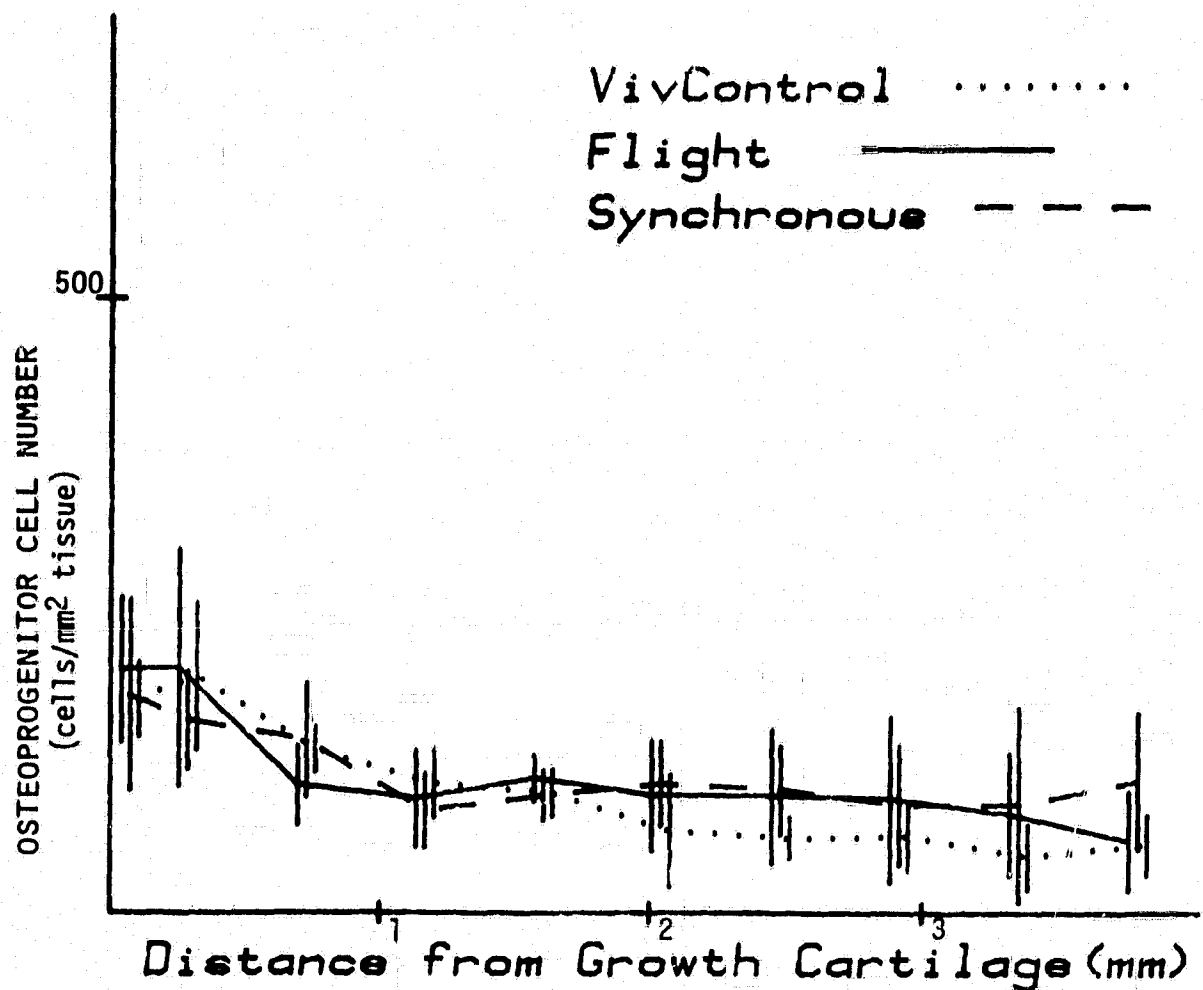
Figure 10. Osteoprogenitor Cell Number as a function of distance from the growth cartilage metaphyseal junction is plotted for Group R+O. The shapes of all the curves are basically similar. It is suggested that there is no real difference among the three groups.
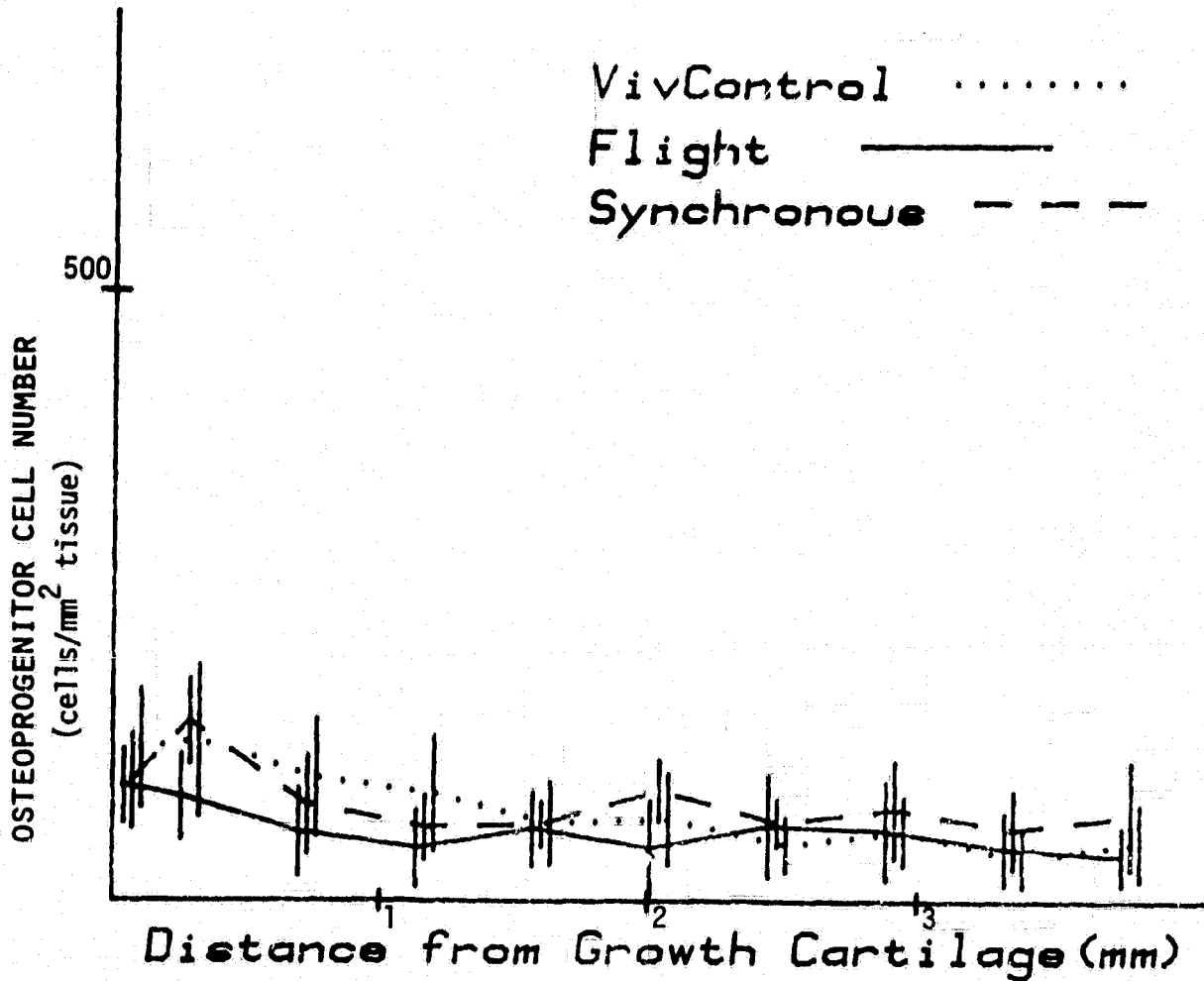
Figure 11. Osteoprogenitor Cell Number as a function of distance from the growth cartilage metaphyseal junction is plotted for Group R+6. There is some suggestion that the osteoprogenitor cell number in the 0.324 - 1.168 mm region is low in flight animals when compared to controls, but it is also possible that there is no real difference.
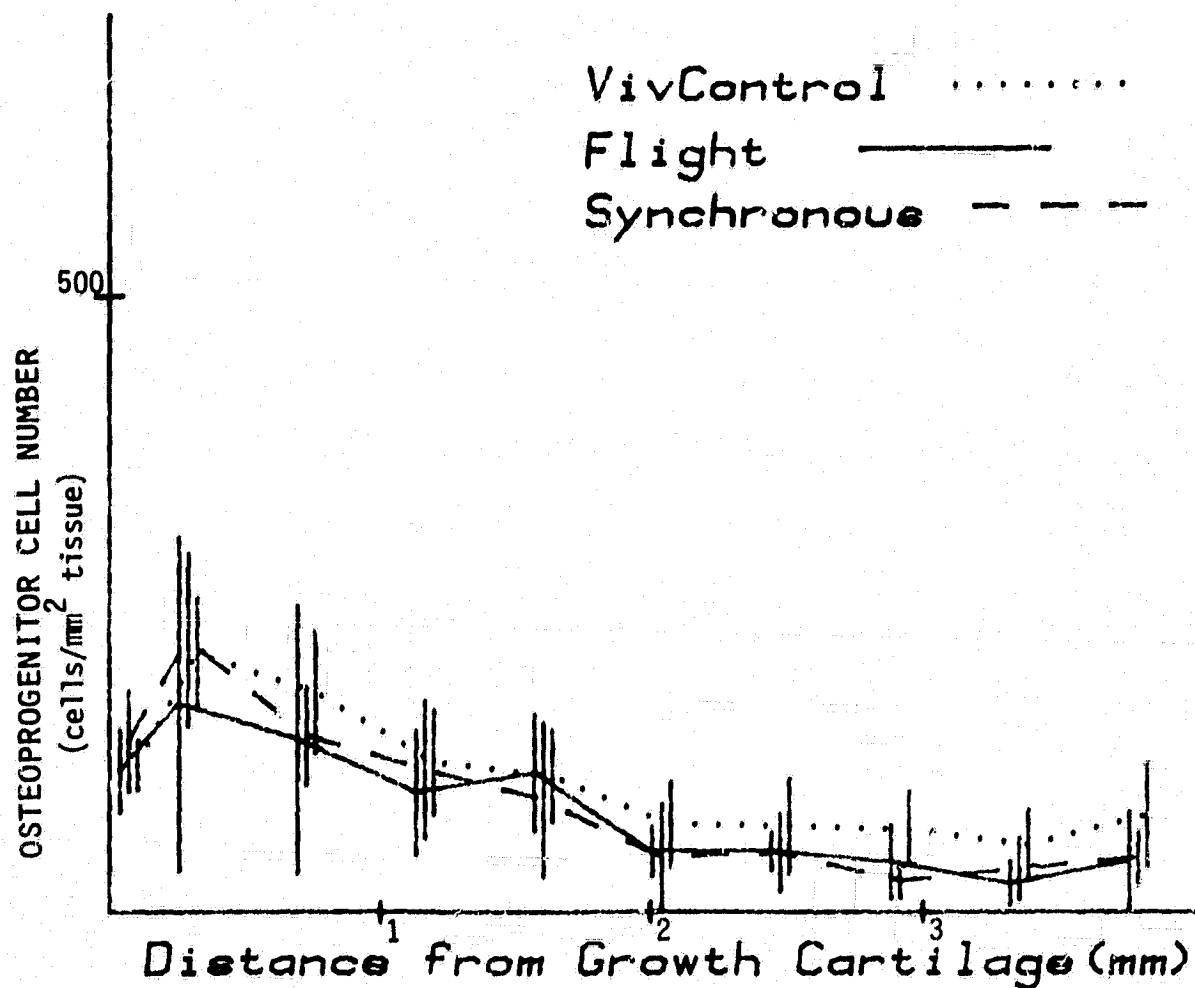
Figure 12. Osteoprogenitor Cell Number as a function of distance from the growth cartilage metaphyseal junction is plotted for Group R+29. There is essentially no difference among the curves.
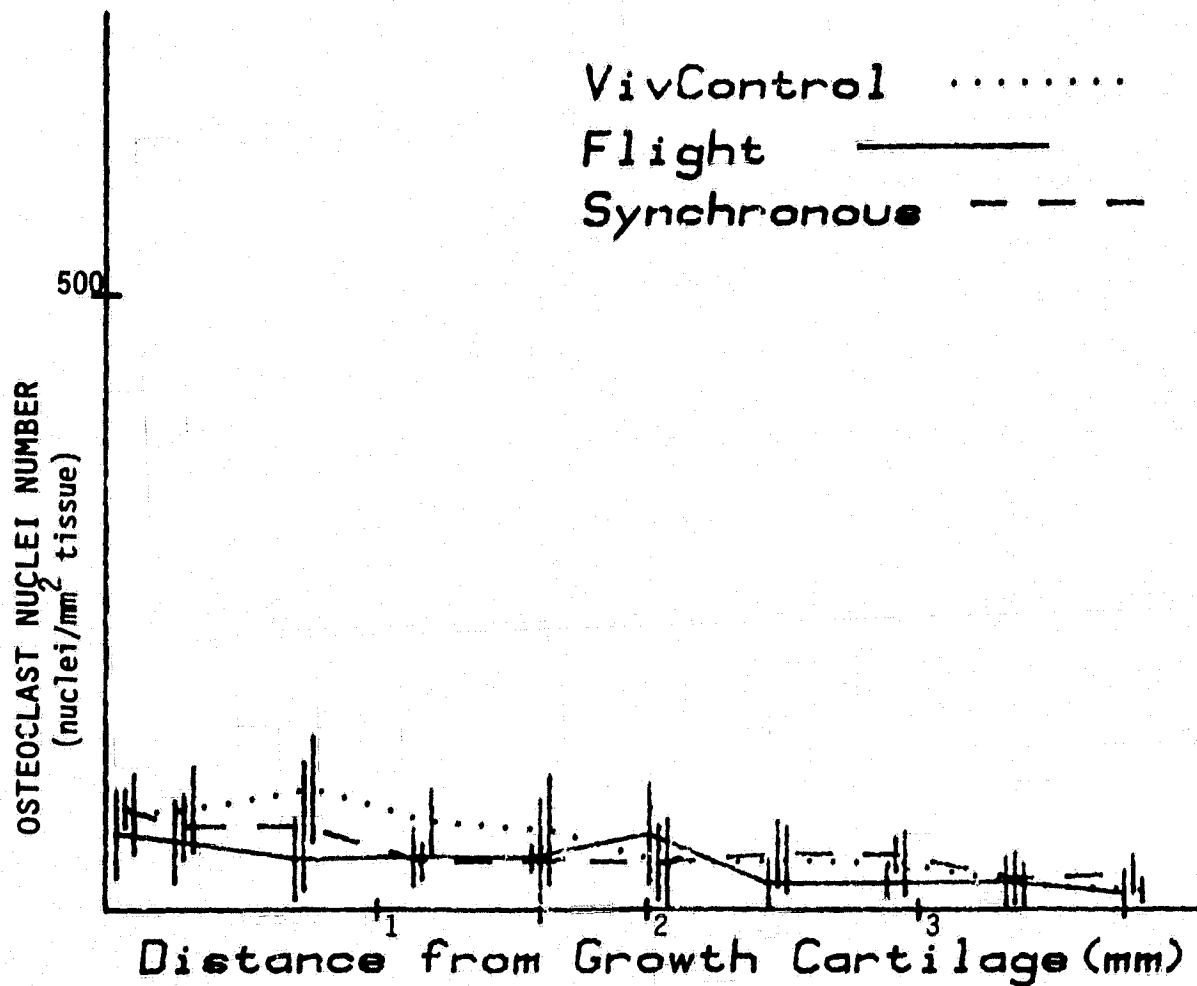
Figure 13. Osteoclast Nucleus Number as a function of distance from the growth cartilage metaphyseal junction is plotted for Group R+0. The osteoclast nucleus number in both flight and synchronous controls is probably somewhat low in the 0.324 - 1.62 mm region, when compared to controls.
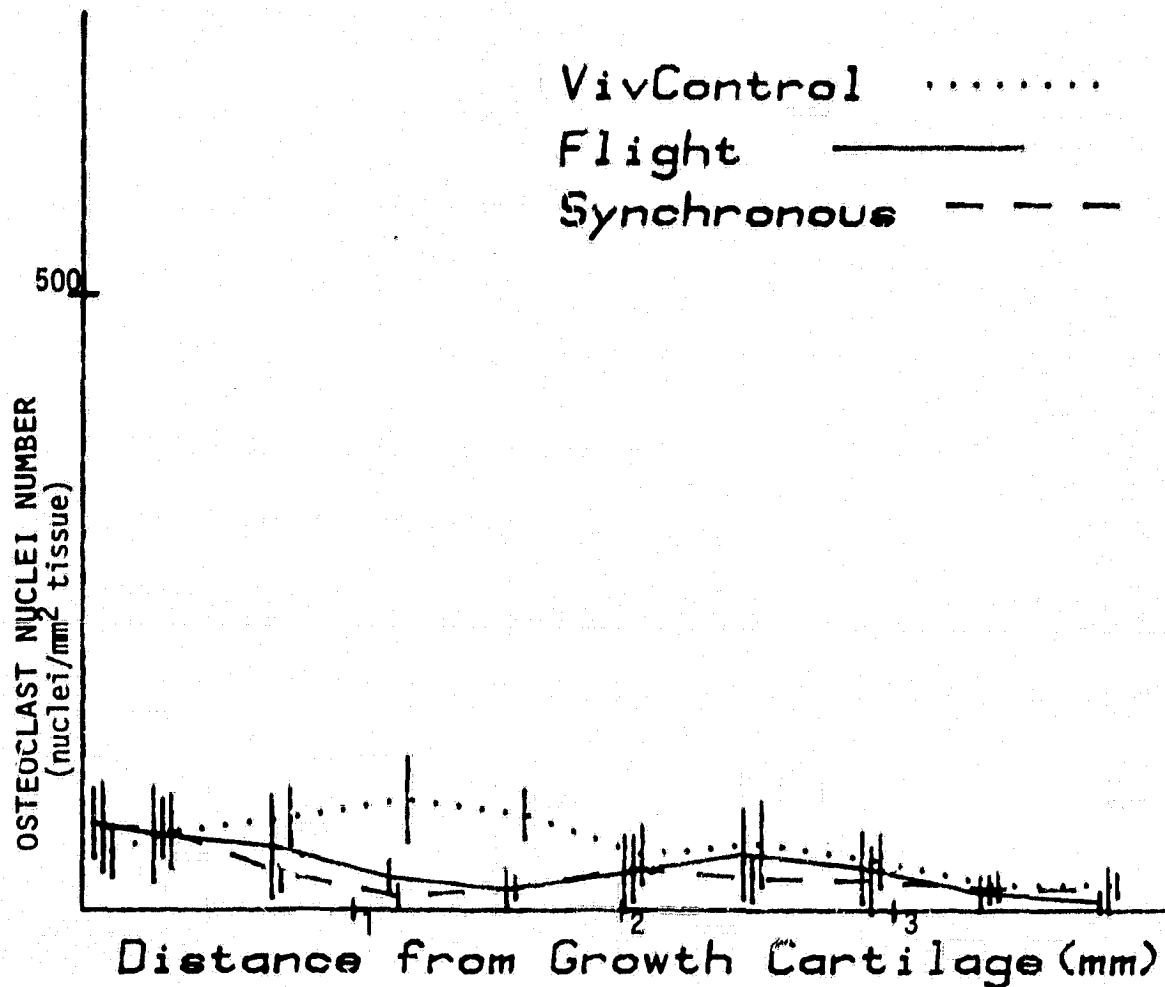
Figure 14. Osteoclast Nucleus Number as a function of distance from the growth cartilage metaphyseal junction is plotted for Group R+6. The osteoclast number remains basically low in the flight and synchronous animals (0.768 - 1.62 mm) when compared to the controls.
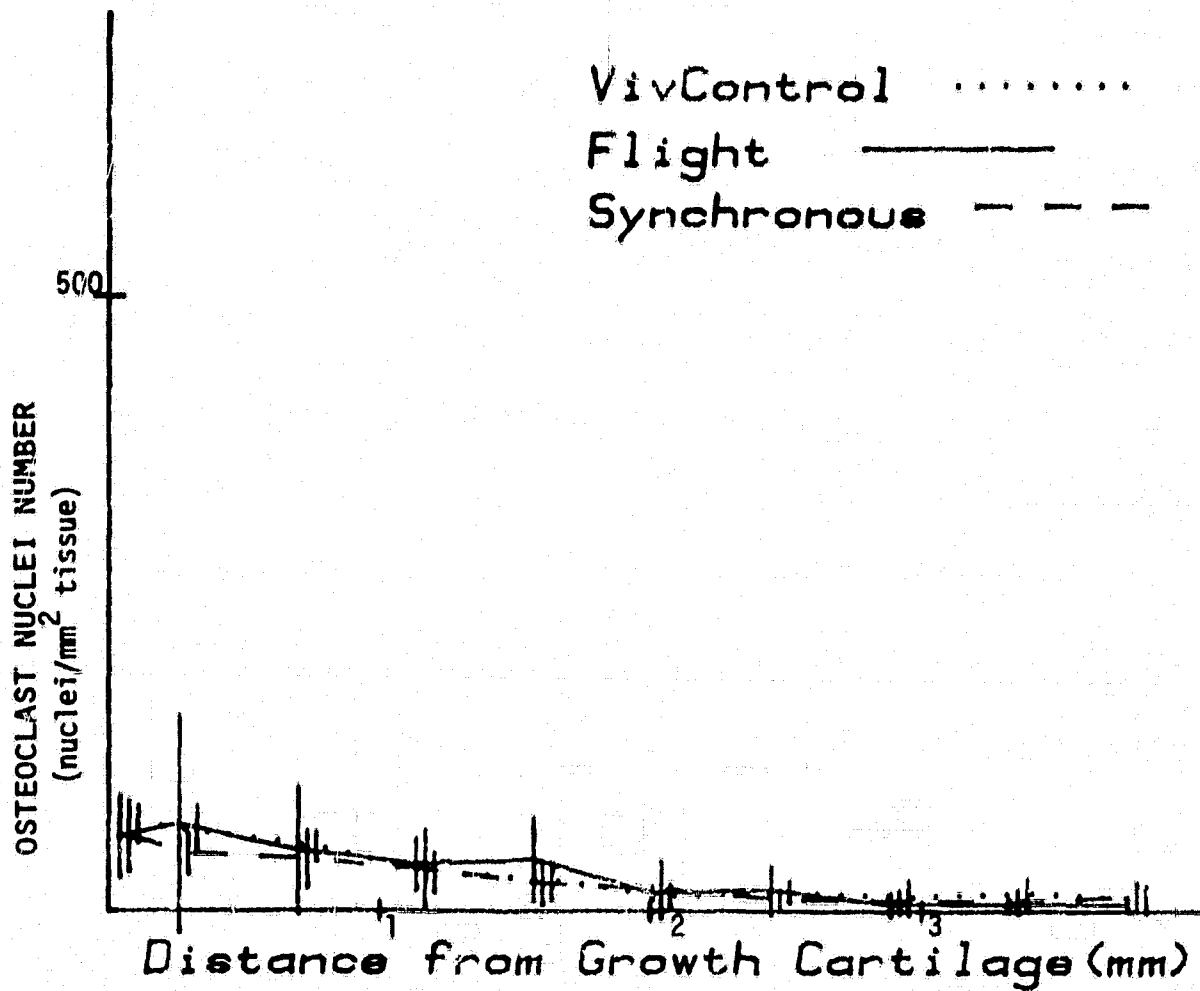
Figure 15. Osteoclast Nucleus Number as a function of distance from the growth cartilage metaphyseal junction is plotted for Group R+29. There is essentially no difference in the curves now, indicating that the appearance of the metaphysis is relatively normal.
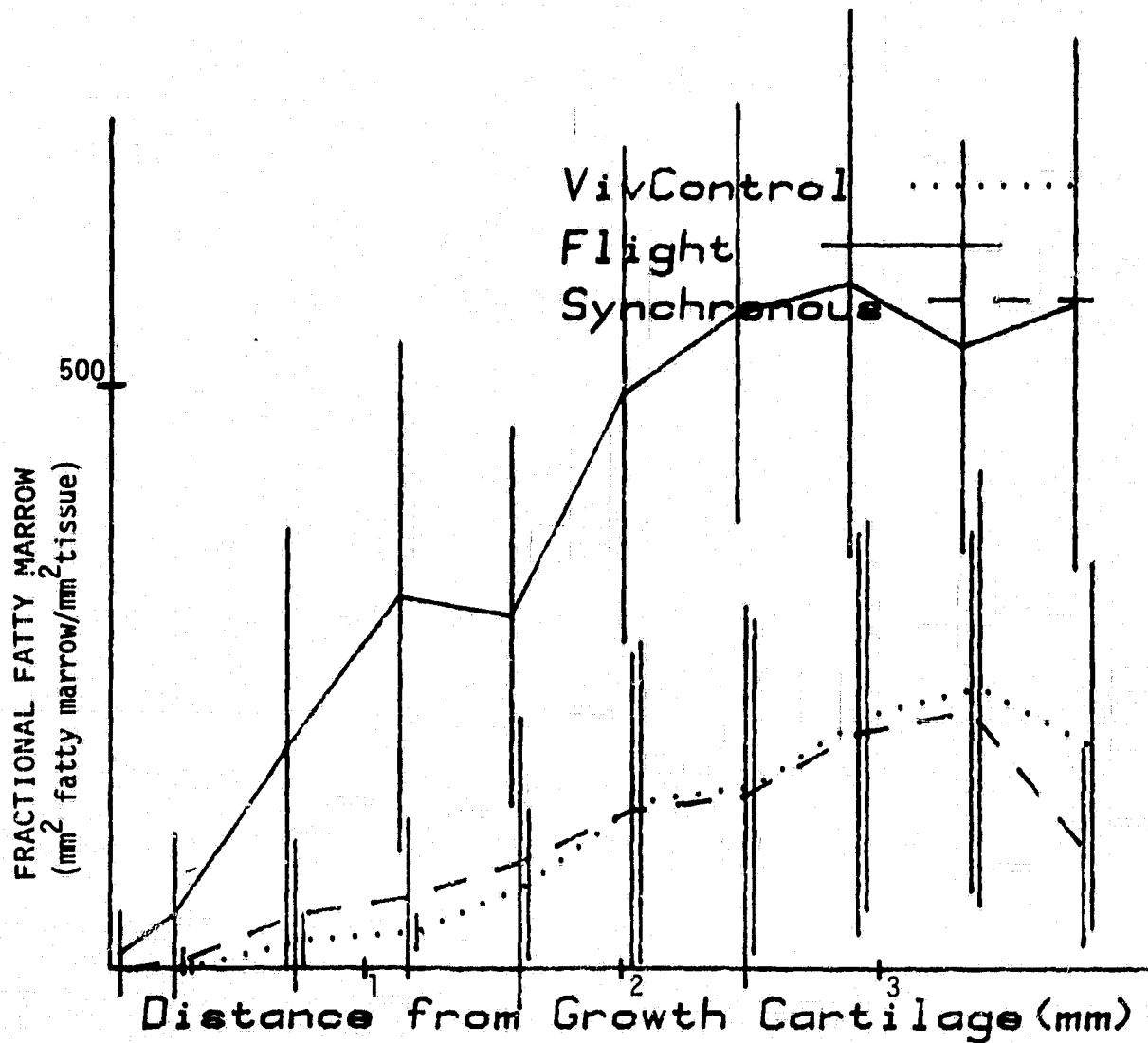
Figure 16. Fraction of Metaphysis Occupied by Fatty Marrow as a function of distance from the growth cartilage metaphyseal junction is plotted for Group R+0. There is markedly more fat in the marrow of flight animals than in either synchronous or control animals all through the metaphysis.
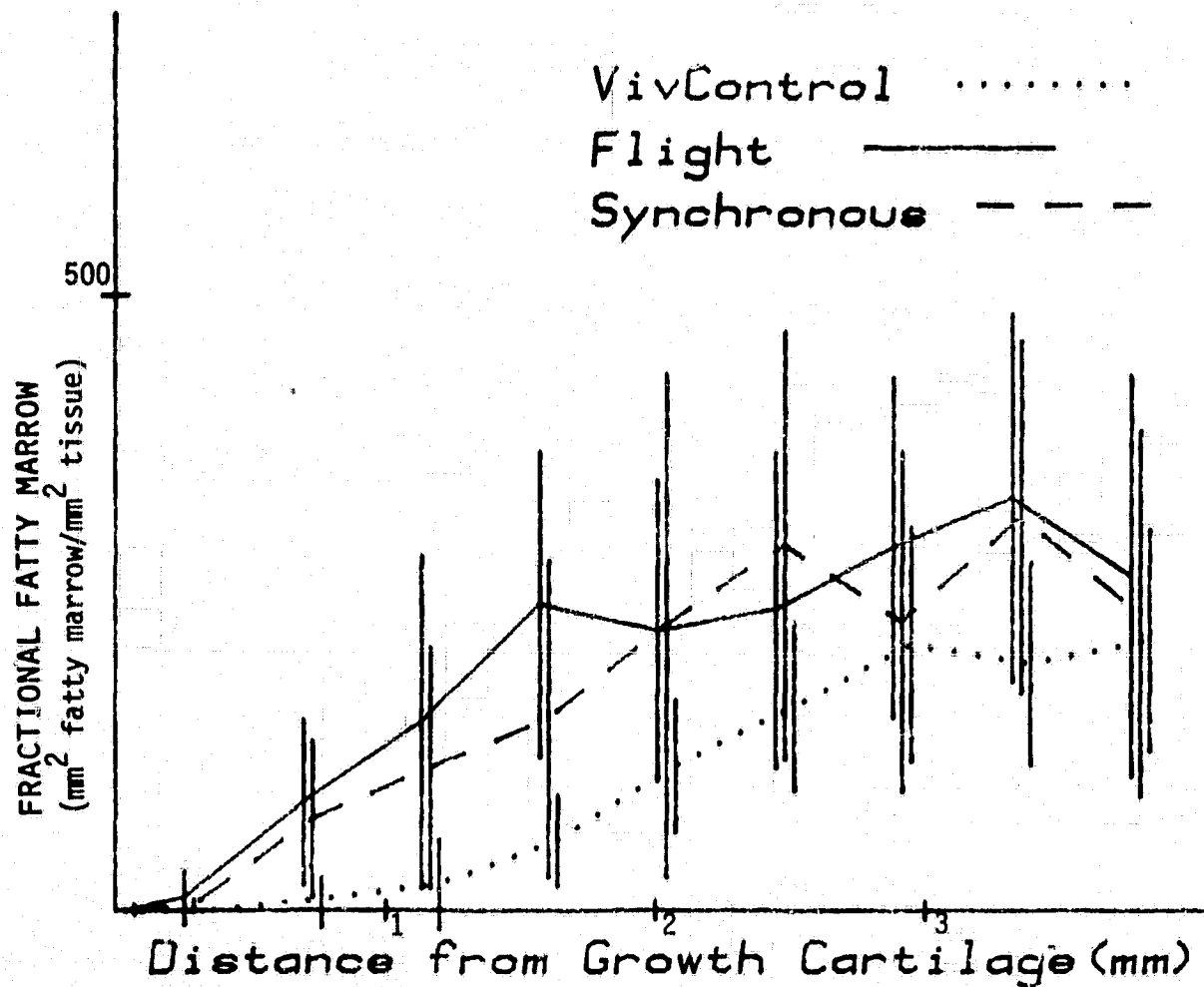
Figure 17. Fraction of Metaphysis Occupied by Fatty Marrow as a function of distance from the growth cartilage metaphyseal junction is plotted for Group R+6. The curves are more similar than those in Figure 16; the volume of fatty marrow is markedly reduced in flight animals, but is probably somewhat above control levels.

174
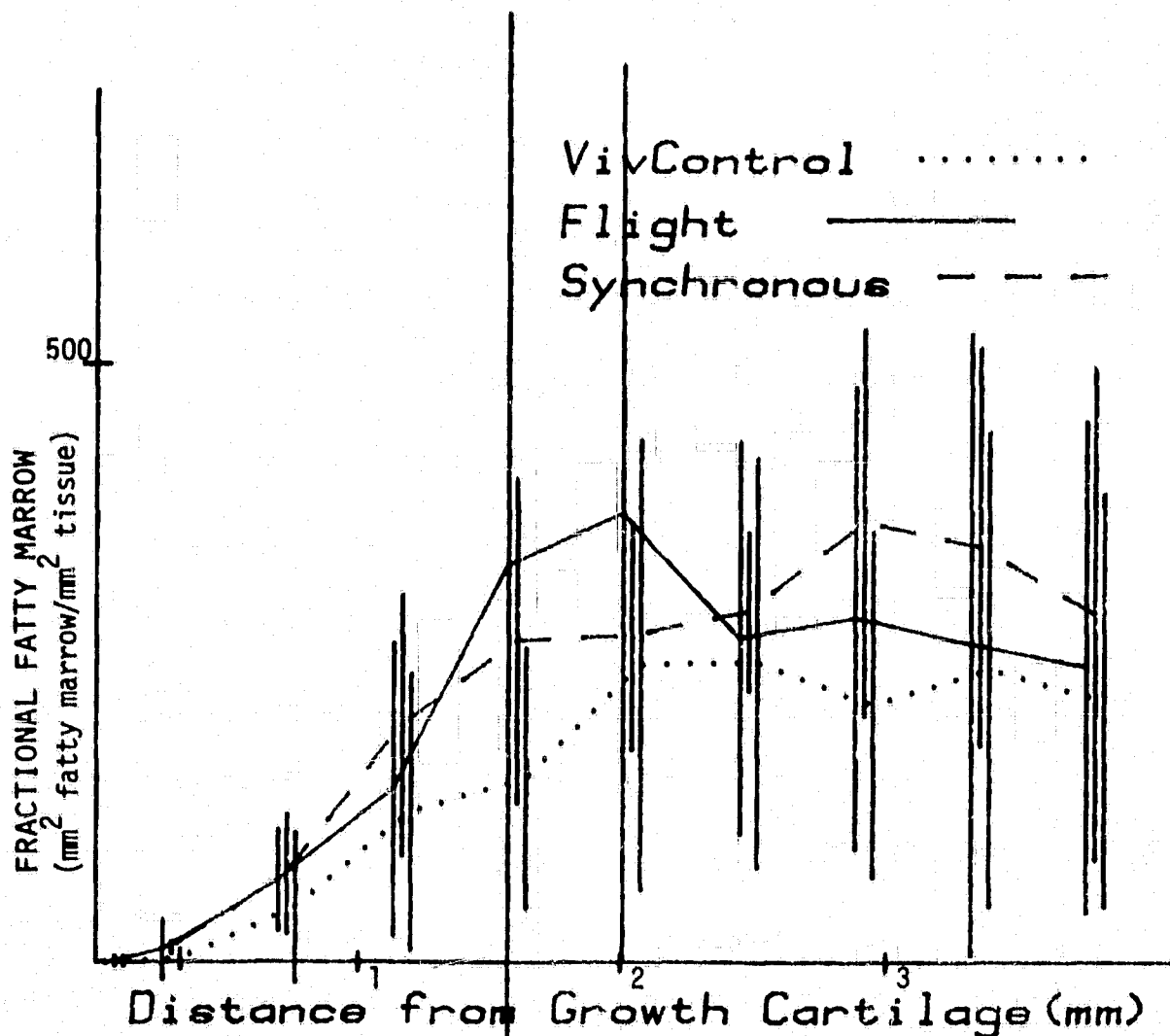
Figure 18. Fraction of Metaphysis Occupied by Fatty Marrow as a function of distance from the growth cartilage meta- physeal junction is plotted for Group R+29. The curves probably do not show any real differences at this point.

K305: QUANTITATIVE ANALYSIS OF

SELECTED BONE PARAMETERS

SUPPLEMENTAL REPORT 3A:

TRABECULAR SPACING AND ORIENTATION IN

THE LONG BONES

M. M. JUDY, DEPARTMENT OF PATHOLOGY,

BAYLOR UNIVERSITY MEDICAL CENTER,

DALLAS, TEXAS U.S.A.

SUMMARY

Values of mean trabecular spacing computed from optical diffraction patterns of 1:1 x-ray micrographs of tibial metaphyses and those obtained by standard image digitization techniques show excellent agreement. Upper limits on values of mean trabecular orientation deduced from diffraction patterns and the images are also in excellent agreement. Values of the ratio of mean trabecular spatial density in a region $300\ \mu$m distal to the downwardly directed convexity in the cartilage growth plate to the value adjacent to the plate determined for flight animals sacrificed at recovery were significantly smaller ($P \leq 0.2$) than values for vivarium control animals. No significant differences were found in proximal regions. No significant differences in mean trabecular orientation were detected. Decreased values of trabecular spatial density and of both osteoblastic activity and trabecular cross-sectional area noted in collateral researches suggest decreased modeling activity under weightlessness.

INTRODUCTION

The primary objective of this research was to quantitatively determine, by optical diffraction techniques, changes in trabecular spacing, (i.e., areal density) and orientation under effects of weightlessness. One major goal of the proposed research was to study changes throughout the area and height of both primary and secondary spongiosa in a trabecular region which is primarily weight supporting. The second research goal was comparison of measured values of changes in metaphyseal trabecular cross-sectional area, and metaphyseal osteoclastic activities, determined in collateral researches with the changes in trabecular spacing and orientation determined from this research.

BACKGROUND AND RATIONALE

Radiographic measurements of bone density in Skylab astronauts [1] showed significant bone loss in os calcis after 59 and 84 days of flight; no density changes were detected in radius or ulna. These data suggest mineral loss is prevalent in weight bearing bones.

Optical micrographic studies of the metaphyses of young rats after 22 days of space flight showed significant decrease in number of trabeculae within the primary spongiosa [2]. However, no quantification of changes in trabecular spacing or orientation were performed.

Optical diffraction techniques, both experimental and theoretical, for determining mean trabecular spacing and orientation have been developed (3). These techniques are applicable to trabecular bone because plastic imbedded sections and x-ray micrographs of sections behave optically as quasi-periodic diffraction gratings. In the case of the actual thin sections, the grating is comprised of alternating regions of different refractive index and, in the case of the x-ray micrographs, it is comprised of alternating regions of emulsion having different optical transmissivities.

One advantage of the use of optical diffraction to determine mean trabecular spacing and orientation over image scanning techniques is that a single diffraction pattern contains unique information about these parameters for all trabeculae in the field sampled by the incident light beam. Furthermore, for trabecular arrays in which the spacing and orientation are quasi-periodic and characterized by distribution functions, an additional important advantage of optical diffraction techniques is that the contribution to the diffracted light intensity from each diffracting element (e.g. trabecula) is correctly weighted according to its position in the distribution function mathematically describing the variation of the structural parameter about mean values. This weighting arises from the integration of the diffracted light intensity over the distribution function (4). Additionally, the shape and height characteristics of diffraction peaks along the meridional direction from approximately periodically spaced diffracting arrays (e.g. trabeculae or myofibrillar sarcomeres) have been shown to depend directly on the standard deviation of the distribution

function describing their spacing and the correlation of spacing between serially arranged diffracting elements (4). Further work (5) has shown that the presence of tilting of the diffracting elements relative to each other and the distribution function describing the variation of the angle of tilt about its mean value uniquely affect peak height and width along the equatorial direction (perpendicular to the meridional direction) of the diffraction pattern. These results suggest that the distribution functions characterizing trabecular spacing and orientation can be characterized from analysis of diffraction peak shape.

METHODS

We use optical diffraction measurements to determine the magnitudes of changes in mean trabecular spacing and in mean trabecular orientation. The trabecular region immediately below the inferiorly directed convexity of the cartilage growth plate which is functionally related predominantly to sustaining mechanical forces of weight bearing and locomotion was studied.

Longitudinal plastic imbedded sections of tibia and 1:1 x-ray micrographs of these sections were used in the optical diffraction measurements. Both 100 μm and 3-5 μm thick sections, unstained and stained with Wilder's stain (6) to darken the bone relative to cartilage and plastic were studied. The x-ray micrographs studied were of the 100 μm thick sections and were obtained at 5 kv using 1.25 min exposure times. Sections and x-ray micrographs obtained from

vivarium control and flight animals sacrificed at recovery were used in this study.

The optical diffraction measurements and their analysis have been described previously (3). The measurements were performed using the optical diffractometer shown schematically in Figure 1. The helium-neon laser provided monochromatic light of 632.8 nm wavelength. The intensity of the light incident upon the sample was modulated by the polarizing optics. The light diffracted by the sample was focused upon the target of the detector vidicon by the Fraunhoffer lens. Use of lenses of up to 133 cm focal length ensured that Fraunhoffer or far-field diffraction conditions (7) were met for trabecular arrays with spacing less than 160μ m. Under these diffraction conditions analysis of diffraction patterns for mean trabecular spacing using equations (3, 4, 8) derived using straightforward Kirchoff scalar field diffraction theory (9) is valid. The detector electronics were modified (3) so that the diffraction pattern could be displayed on a monitor and the diffracted light intensity along any one of 256 scan lines could be displayed on the oscilloscope and routed to the PDP-11 computer of the associated data acquisition system for signal averaging to reduce effects of random noise due to detector dark current and laser light intensity fluctuations. Reproducible patterns with acceptable signal to random noise levels were obtained as the average of 10-20 line scans for all samples studied.

The sample could be moved in the plane perpendicular to the incident light beam so that various regions of the trabecular array could be

positioned opposite to the 100 μ m x 1mm slit used to limit the areal extent of the incident light. In this way, any region of the trabecular array, 100 μ mx 1mm in size, could be chosen for study. For this research each sample was placed so that diffraction patterns were obtained from four contiguous regions, each 100 μ m in height and located sequentially away from the cartilage plate. The trabecular area denoted by Region A was located so that the 1 mm long upper edge of the slit was tangent to the apex of the contour of the downwardly directed convexity of the cartilage growth plate. Region B through D in order were located at 100 μ m increments away from the initial position of A. In this way mean trabecular spacing was determined at distances of 0, 100, 200, and 300 μ m away from the tangency point of Region A and the cartilage plate.

For all of the measurements the nominal orientation of the trabeculae was parallel to the height of the slit and thus perpendicular to the tangent line at the cartilage plate. Therefore, the region of the trabecular array of each sample defined by the slit at each measurement position behaved as a linear grating because of the alternating optical refractive index properties of trabeculae and plastic in the case of the actual sections and alternating clear and darkened areas of emulsion in the case of the x-ray micrographs.

Previously developed theory (4, 5, 8) has shown that the location of the centroid of major order meridional diffraction peaks is directly proportional to the inverse of the mean value of the spacing between regions of alternating refractive index or optical transmission, hence, to the inverse of mean trabecular spacing. The proportionality constant

182

LONG FOCAL LENGTH
OPTICAL DIFFRACTOMETER
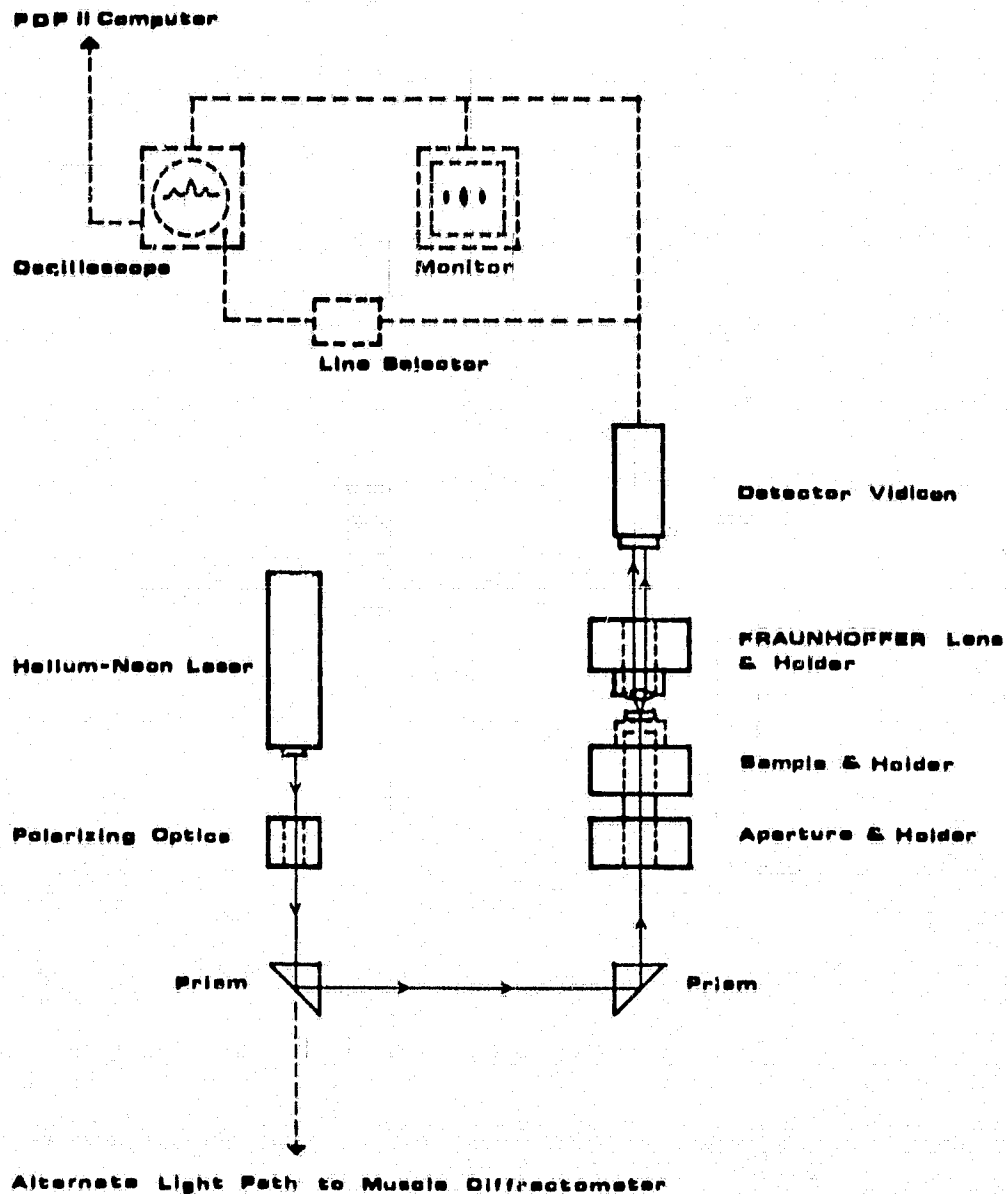
Figure 1. Schematic diagram of long focal length diffractometer used to determine mean trabecular spacing and orientations.

depends on the known values of the focal length of the diffractometer and the wavelength of the monochromatic laser light incident upon the sample (10). Accordingly mean trabecular spacing for each region was computed from the distance between the centroid of the first order diffraction peak and the zero-order peak or undiffracted beam (3).

The amount of displacement or smearing of meridional peak intensity in the perpendicular equatorial direction has been shown to depend directly on the mean angular orientation of the diffracting elements of trabeculae relative to the vertical axis of the slit (5). For small angular tilt the equatorial displacement was found to scale directly with the mean tilt angle, this being zero for zero mean tilt.

For purposes of comparison with results of diffraction measurements, values of mean trabecular spacing were obtained from projected images of 10x optical micrographs of the 1:1 x-ray micrographs using standard digitizing techniques. Care was taken to include only those trabeculae actually within each region as defined by the slit for the diffraction measurements. Accuracy of the digitized values is estimated to be 1% for a trabecular spacing of 30 μm and 0.3% for a value of 100μm. This uncertainty is attributed to the 100μm resolution of the position of the digitizing cursor during operation.

RESULTS AND DISCUSSION

Diffraction patterns obtained from 100μm thick sections, both heavily stained with Wilder's stain and unstained, were extremely noisy

184

and contained no recognizable diffraction peaks with uniform spacing which related to trabecular spacing or orientation. Polishing of both surfaces of the plastic embedded sections and/or immersing the section in a uniform thickness of oil having the same refractive index (1.49) as the plastic resulted in a less noisy pattern, but recognizable diffraction peaks were not obtained. This result is attributed to intense geometrical scattering (11) by interlayered calcified cartilage and bone in these thick sections.

Both unstained and Wilders stained 3-5 μ m thick sections surrounded with refractive index matching oil have yielded diffraction patterns which were noisy but contained recognizable diffraction peaks with uniform spacing uniquely related to trabecular spacing in the secondary spongiosa. Patterns from the primary spongiosa in both stained and unstained sections contained no recognizable diffraction peaks.

Diffraction peak amplitudes in patterns obtained from the secondary spongiosa in unstained bone were very small indicating a very small difference in refractive index, and hence, optical path difference (12), between bone and plastic. Peaks in patterns obtained from the secondary spongiosa of intentionally overstained bone sections (3) were larger in amplitude, indicating that, at least in part, the trabecular bone was behaving as a linear diffraction grating comprised of alternating dark and light areas. However, noise due to scattering from small size organic and mineral constituents (13), and from optical path differences due to uneven bone thickness, severely reduced the precision with which trabecular spacing could be determined.

185

Lack of recognizable diffraction peaks from the primary spongiosa
of stained and unstained sections is attributed to a combination of noise
due to scattering as described above, and small amplitude of diffraction
peak due to the closeness in dimensions of trabecular spacing and width
of marrow cavity. This closeness in values of the dimensions leads to
a small value near zero for the amplitude of the pattern of light
diffracted by each marrow cavity (14) in the vicinity of the diffraction
peak.

Judged on the basis of signal to noise ratio of the diffracted
light intensity, the diffraction patterns of best quality were obtained
from the x-ray micrographs. Those obtained from micrographs of bone
from flight animals were usually less noisy than those obtained from
micrographs of vivarium control animal sections. This is attributed to
the presence of fewer grey regions in the flight animal micrographs.
As a consequence, these images of the trabecular array better approximate
a true amplitude grating in which light transmissive areas alternate
with completely light absorbing areas. However, the noise present in
patterns obtained from vivarium control animals was not of sufficient
magnitude to prevent their use in computing mean values of trabecular
spacing or in estimating mean trabecular orientation. Typical
diffraction patterns obtained from x-ray micrographs of flight and
vivarium control animals are shown in Figures 2 and 3.

Examination of the diffraction patterns shows that the single first
order diffraction peak of the hypothetical trabecular array with per-
fectly periodic spacing has split into subpeaks. This phenomenon,

186
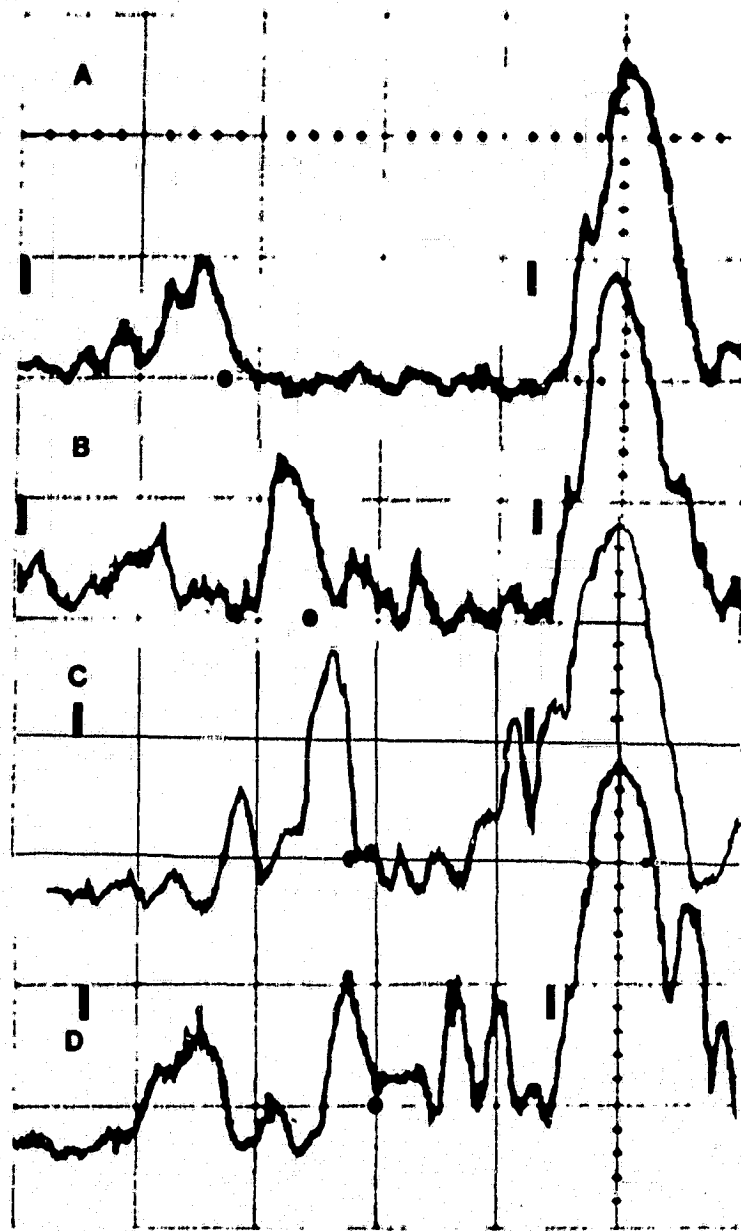
Figure 2.   Optical diffraction patterns from four contiguous regions,
A through D of tibial metaphysis of vivarium control animal 6.   The
regions were located at 0, 100, 200, and 300 μ m distal to the
downwardly directed convexity of the growth plate.   The dots on the
horizontal axis of each pattern locate the centroid of the first order
diffraction peak comprised of all subpeaks between vertical bars.

< - 3
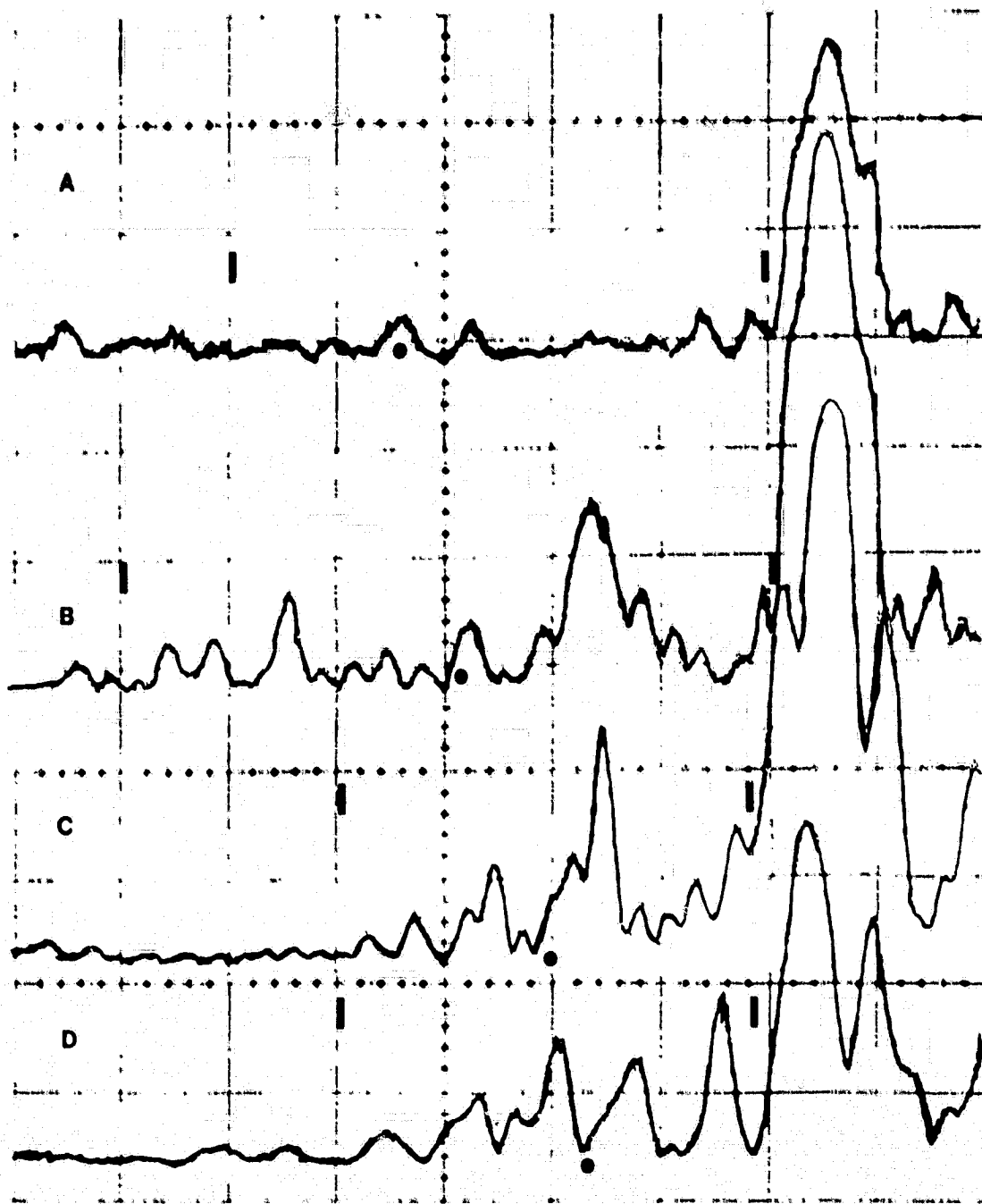
Figure 3. Optical diffraction patterns from four contiguous regions, A through D of tibial metaphysis of flight control plus zero animal 7. The regions were located at 0, 100, 200 and 300 μm distal to the downwardly directed convexity of the growth plate. The dots on the horizontal axis of each pattern locate the centroid of the first order diffraction peak comprised of all subpeaks between vertical bars.

188

typical of all sections studied, shows that the trabecular array is only quasi-periodic in these samples. Additionally, splitting into subpeaks suggests spatial correlation between serially arrayed trabeculae (4). Preliminary analysis of the digitized data shows that values of trabecular spacing near the middle of the array within the optical slit during diffraction are usually smaller than those for trabeculae located nearer each end of the slit. Thus, these trabeculae are roughly arranged into three serial zones with at least the middle one having a different mean value of trabecular spacing. We are currently extending our previous theoretical treatment of diffraction by an array of serial domains with different characteristic values of diffractor spacing to include effects of statistical fluctuations in spacing about mean values in hopes that a complete analysis of the diffraction pattern for values of modality, population fraction, and standard deviation can be obtained in order to characterize not only mean trabecular spacing but also its distribution function.

Values of mean trabecular spacing calculated from the position of the centroid of first order diffraction peaks and values obtained by digitization of the micrographic images are presented in Tables I and II for vivarium control and flight animals, respectively. Values of the standard deviation computed from digitized data accompany each mean value. These typically are large compared to an uncertainty of 1% or less in the mean value introduced by digitization error. Values of mean trabecular spacing $\overline{X}$ computed from diffraction patterns are stated within an estimated error given by

$$2 E_h \overline{X} / A$$

in which E_h is the error in the average subpeak height and A is the
integrated area of the first order diffraction peak. The quantity E_h
is estimated to be of the order of .01 times the average subpeak height.
This error equation was derived by straight-forward application of the
theory of propagation of errors to the defining integral equation for the
centroid.

The data of Tables I and II show values of mean trabecular spacing
obtained by optical diffraction technique and values obtained by image
digitization to be in excellent agreement. This result and that obtained
previously (3) suggests that the use of optical diffraction measurements
gives reliable values of mean trabecular spacing.

Examination of Tables I and II show that for each animal mean
trabecular spacing increases with distance away from the cartilage plate
in both vivarium control and flight animals. However, values of mean
trabecular spacing in Regions A through D averaged for all vivarium
control and all flight animals have not been directly compared. This is
because of the unknown relationship between the plane of the longitudinal
tibial section and the two directions of maximum lateral packing
density of the trabecular array. If the plane of the section were to
contain one of the directions parallel to tightest packing, then the
measured value of mean trabecular spacing would be its minimum. If,
however, the section were to be oriented along the diagonal to this
tightest packing direction then the value obtained would be a maximum.
In order to provide a basis for comparison of trabecular spacing in
control and flight animals, the ratio of mean trabecular spacing

190

TABLE I

MEAN TRABECULAR SPACING $\overline{X}$

VIVARIUM CONTROL, R + 0

Animal	Metaphyseal Region			
	a,b A	B	C	D
1.	53.6 ± 1.1 53.0 ± 12.4	67.8 ± 1.5 65.6 ± 16.8	89.8 ± 1.1 91.3 ± 19.4	109.9 ± 1.3 110.2 ± 26.4
2.	36.7 ± 1.4 34.8 ± 12.7	43.0 ± 1.0 40.6 ± 21.1	53.4 ± 2.0 51.4 ± 20.1	61.3 ± 1.5 58.9 ± 12.9
3.	40.1 ± 2.0 39.8 ± 17.5	52.0 ± 1.6 50.7 ± 17.5	58.6 ± 2.4 56.1 ± 19.9	68.4 ± 1.5 66.9 ± 16.9
4.	42.3 ± 1.9 40.8 ± 13.2	46.3 ± 1.7 44.7 ± 23.5	60.6 ± 2.0 61.9 ± 19.5	90.9 ± 1.8 88.2 ± 31.2
5.	53.8 ± 2.0 54.8 ± 10.4	59.7 ± 1.3 59.9 ± 28.6	71.7 ± 1.4 70.4 ± 24.6	85.8 ± 1.2 85.2 ± 32.5
6.	53.5 ± 1.9 51.9 ± 19.3	72.8 ± 1.3 76.6 ± 22.7	80.3 ± 1.6 78.4 ± 24.7	90.5 ± 0.9 91.1 ± 22.9
7.	50.7 ± 2.6 48.8 ± 19.3	60.4 ± 1.3 61.5 ± 18.7	88.6 ± 2.8 87.4 ± 32.0	97.0 ± 2.13 95.9 ± 40.4

a. Values are given in microns; first value is from diffraction data ($\overline{X} \pm$ E); second is from digitized image ($\overline{X} \pm$ S. D.).

b. Regions A through D respectively are located 0, 100, 200, and 300 microns distal to the downwardly directed convexity in the cartilage plate.

TABLE II

MEAN TRABECULAR SPACING

FLIGHT ANIMALS, R + O

Animal	Metaphyseal Region			
	A [a,b]	B	C	D
1.	49.4 ± 1.1	60.1 ± 1.4	64.7 ± 1.3	91.5 ± 3.6
	50.1 ± 21.1	61.5 ± 15.7	63.3 ± 21.7	88.0 ± 40.4
2.	41.7 ± 2.2	58.6 ± 2.4	62.5 ± 1.7	75.4 ± 1.0
	39.2 ± 12.1	57.9 ± 22.9	63.9 ± 27.1	76.0 ± 37.4
3.	44.8 ± 1.4	49.9 ± 1.4	61.0 ± 1.9	66.5 ± 1.3
	45.2 ± 22.3	48.8 ± 15.1	61.5 ± 21.7	65.1 ± 23.5
4.	35.2 ± 1.5	54.8 ± 1.6	58.7 ± 2.3	124.7 ± 1.2
	36.2 ± 10.3	53.7 ± 20.5	59.7 ± 18.7	126.7 ± 37.4
5.	46.0 ± 2.2	53.3 ± 1.5	62.9 ± 1.3	84.3 ± 3.7
	45.2 ± 16.0	52.4 ± 16.9	62.1 ± 19.3	82.0 ± 33.2
6.	45.6 ± 2.3	55.0 ± 1.3	76.5 ± 1.1	207.7 ± 6.3
	47.0 ± 19.3	56.7 ± 22.3	77.2 ± 30.1	208.0 ± 83.0
7.	45.0 ± 2.3	52.3 ± 1.9	67.0 ± 2.5	89.2 ± 1.0
	42.2 ± 11.5	50.7 ± 23.5	67.5 ± 24.1	91.1 ± 16.3

a. Values are given in microns; first value is from diffraction data $(\overline{X} \pm E)$; second is from digitized image $(\overline{X} \pm S. D.)$.

b. Regions A through D respectively are located 0, 100, 200, and 300 microns distal to the downwardly directed convexity in the cartilage plate.

TABLE III

RATIOS OF MEAN TRABECULAR SPACING

$$(\overline{X}_K/\ \overline{X}_A),\ K = A,\ B,\ C,\ D.$$

VIVARIUM CONTROL, R + O

Animal		Metaphyseal Region		
	A^a	B	C	D
1	1	1.26	1.68	2.05
2	1	1.17	1.46	1.67
3	1	1.30	1.46	1.70
4	1	1.09	1.43	2.15
5	1	1.19	1.33	1.59
6	1	1.36	1.50	1.69
7	1	1.19	1.75	1.91
Mean ±S.D.	1	1.21 ± 0.16	1.52 ± 0.19	1.82 ± 0.25

a. Regions sequentially distal at 0, 100, 200, 300 microns to the downwardly directed convexity in the growth plate.

TABLE IV

RATIOS OF MEAN TRABECULAR SPACING

$$(\overline{X}_K/\overline{X}_A), \quad K = A, B, C, D$$

FLIGHT ANIMALS, R + O

Animal	Metaphyseal Region			
	A^a	B	C	D
1	1	1.22	1.31	1.85
2	1	1.41	1.50	1.93
3	1	1.10	1.36	1.49
4	1	1.55	1.66	3.54
5	1	1.16	1.37	1.81
6	1	1.21	1.68	4.56
7	1	1.16	1.49	1.98
Mean ±S.D.	1	1.26±0.15	1.48 ± 0.17	2.46 ± 1.0

a. Regions sequentially distal at 0, 100, 200, 300 microns to the downwardly directed convexity in the growth plate.

determined in each region, A through D, to the value determined for Region A was computed for each animal. This ratio does not depend upon the angular orientation of the section plane and the tightest packing direction provided that the lattice of trabeculae does not twist about a direction parallel to the trabecular axis with distance from the cartilage plate. The long relatively straight trabecular contours evident in the micrographs suggest this provision is met in the samples studied. Value of the ratios of trabecular spacing in vivarium control and flight animals, respectively, are presented in Tables III and IV.

It is worthwhile to call attention to the physical picture described by these ratios. They not only mirror the increase in mean trabecular spacing with increasing distance away from the downwardly directed convexity in the cartilage plate but their inverse represents the decrease in mean trabecular density. Thus, ratio values for, say, the hypothetical average flight animal show that for every 10 contiguous trabeculae arrayed over the distance $10 \bar{X}_A$, where $\bar{X}_A$ is mean trabecular spacing in Region A, there are approximately 8,7, and 4 arrayed over the same distance at distances of 100, 200, and 300 μm away from the cartilage plate. Therefore, mean trabecular density has decreased respectively to approximate values of $8/(10\bar{X}_A)$, $7/10\bar{X}_A)$, and $4/(10\bar{X}_A)$.

Comparison of values averaged over the vivarium control and flight animal group shows a significant increase ($P \leq 0.2$, student-t test) in the value of the ratio of mean trabecular spacing in Region D (300 μm distal to Region A) to that in Region A for flight animals relative to vivarium control animals. Differences between ratios computed for

195

Regions B and C (100 and 200 μm distal to A) were judged to be insignificant (P $\leq$ 0.8).

Values of mean angular trabecular orientation were found to deviate by less than $\pm$ 5 deg. from alignment perpendicular to the tangent line to the apex of the inferiorly directed convexity of the cartilage plate for all vivarium control and flight samples studied. This upper limit to angular misorientation was established by noting that angular shifting of any first order diffraction peak or of the mean trabecular trajectory in the micrographic image was less than 5 deg. relative to cursors on the diffractometer monitor and digitizing table.

The increase in the ratio of trabecular spacing at 300 μm distal to that at the cartilage plate in the flight animals means that the linear trabecular density at this distance decreased under the reduced loading of weightlessness. This decrease and that notable in more distal regions by even casual visual observation probably reflects decreased modeling activity under weightlessness as evidenced by decreased osteoblastic activity (15) and decreased trabecular area (16) in this and proximal regions.

REFERENCES

1. Vogel, J. M., Whittle, M. W., Smith, M. C., and P. C. Rambaut. Bone mineral measurements - Experiment M078. In: Biomedical Results from Skylab, NASA SP-377, 183-190, 1977.

2. Yagodovsky, V. S., Triftanidi, L. A., and G. P. Gorokhova. Space flight effects on skeletal bones of rats (Light and electron microscope examination). _Aviation, Space, and Environ. Med._ 47: 734-738 (1976).

3. Judy, M. M., LeConey, T. R., Matthews, J. L., and W. S. S. Jee. Measurement of trabecular spacing and orientation by optical diffraction. In: _Bone Histomorphometry, Third International Workshop_, 1980 (In press).

4. Judy, M. M., Summerour, V., LeConey, T. L., and G. H. Templeton. Differences in optical diffraction by uni- and multimodal sarcomere length populations. _Fed. Proc._ 39: 1731 (1980).

5. Judy, M. M., Summerour, V, LeConey, T. L., and G. H. Templeton. Effects of z-plate _can_-registry on optical diffraction patterns of muscle. (In preparation).

6. Humason, G. L. _Animal Tissue Techniques_, W. H. Freeman Company, San Francisco, p. 195, 1967.

7. Haskill, J. D., _Linear Systems, Fourier Transforms and Optics_, J. Wiley and Sons, New York, p. 375, 1978.

8. Judy, M. M., Computations of the mean spacing of a one-dimensional quasi-periodic diffracting array from positions of the centroids of major order diffraction peaks. (In preparation).

9. Born, M. and E. Wolf. _Principles of Optics_, Pergamon Press, New York. .p. 382-392, 1975.

10. Ibid, p. 402, 1975

11. Van de Hulst, H. C., _Light Scattering by Small Particles_, John Wiley and Sons, New York, p. 200-227, 1957.

12. Born, M. and E. Wolf. Ibid, p. 401, 1975.

13. Ibid, p. 654-655, 1975.

14. Ibid, p. 392, 1975.

15. Matthews, J. b. Mineralization in the long bones. In: NASA Report K305. Quantitative Analysis of Selected Bone Parameters, Supplemental Report 3B, 1980.

16. Jee, W. W. W., Kimmel, D. B., Smith, C., and R. B. Bell. Growth rate and histology of long bones. In: NASA Report K305. Quantitative Analysis of Selected Bone Parameters, Supplemental Report 2, 1980.

K305

<u>QUANTITATIVE ANALYSIS OF SELECTED BONE PARAMETERS</u>

SUPPLEMENTAL REPORT 3B: Mineralization in the Long Bones

J. L. Matthews, Ph.D., Baylor University Medical Center

INTRODUCTION

The major objectives of this project were:

1. A microscope study of growth plates and metaphyseal trabeculae to assess the type and functional state of bone cells and to characterize the zone of calcification of the cartilagenous growth plate, particularly the presence and condition of matrix vesicles.

2. An optical birefringent study of the trabeculae in order to assess trabecular number, size, shape, and orientation as it is presumed that this metabolically active bone will reflect subtle changes that may result from a zero-gravity condition.

METHODS

Thin slices (less than 1 um thick) have been fixed in aldehyde fixatives immediately following sacrifice and bone dissection. Thin slices of trabecular bone and longitudinal slices of growth plate were post-osmicated in buffered osmium-tetroxide, washed, dehydrated in an alcohol series and embedded in spur media in preparation for ultra thin sectioning on a Porter Blum microtome. Half micron thick sections were made and stained with Paragon to permit orientation and study with the light microscope. Adjacent ultra-thin sections were made with a Sorvall MT-2 ultra-microtome, and stained with uranyl acetate and lead citrate in preparation for examination with the Phillips 300 transmission electron microscope. The attached check list of cell organelles, inclusions, and ultrastructural features were used during examination of all tissue sections in an effort to give a complete descriptive profile of the bone cells and matrix of representative sections of all experimental bones from both flight and ground control animals. The

same check list was used to characterize cells of the cartilage growth plate including study of the resting zone, zone of proliferation, zone of matrix synthesis, zone of cell hypertrophy, zone of provisional calcification, and zone of ossification. Matrix vesicle conditions were examined in each of the lower 4 zones. Emphasis on matrix vesicles is felt to be important, as these structures are associated with the initiation of hydroxyapatite crystal formation in the longitudinal septa of the cartilage. These structures form by budding from the adjacent cells. (1) They possess high phosphatase activity and the first crystals are observed within these membrane-limited structures. Bones made "rachitic" by treating the animals with diphosphonate compounds, especially ethane hydroxy diphosphonate (EHDP), show numerous but empty matrix vesicles. The state of these mineral associated vesicles in both bone and cartilage of zero gravity animals is not presently known.

RESULTS

Ultrastructural Studies

Specimens of tibial metaphysis and epiphyseal growth plate were received in fixative from NASA - Ames Research Center. Following routine processing, embedding, ultra thin sectioning, and staining of twenty randomly selected diced pieces from each control and immediate post flight groups, sections were viewed with a Phillips 300 transmission electron microscope and the following scoring was made by averaging observations from all viewed specimens of each study group. The following descriptions are of R + 0 - time flight and from comparable age synchronous and vivarium control groups. (No significant differences were noted between the ultrastructure of these two control groups.)

A. Osteoblasts on surface of primary and secondary metaphyseal trabeculae.

	Flight Group (R + 0) (Figure 1-3)	Control Group (Both Synchronous & Vivarium) (Figure 4-7)
1. Cell size and shape	Flattened cells 6-10 um high	Large cuboidal pyramidal cells 12-16 um high
2. Nucleus	rounded configuration, pronounced peripheral clumping of heterochromatin, little euchromatin, intact nuclear pores. Perinuclear space dilated, no inclusions, one irregular shaped nucleolus reduced to 78% of control size. No nuclear inclusions noted.	Nucleus is round to oval, centrally positioned in the cell. Heterochromatin is seen at nuclear margins but euchromatin is also dispersed in nucleus. Nucleolus is single, large, and eccentrically located. Nuclear membrane has nuclear pores. Perinuclear space is dilated (a likely artifact of fixation). No nuclear inclusions, nor perichromatin granules, were present.
3. Cytoplasm	Cytoplasm has low optical density, dilated mitochondria, sparse endoplasmic reticulum, few dilated cysternae of granular endoplasmic reticulum, Golgi complex occupies area comparable to control, Golgi vesicles on mature face and assembled lamellae are reduced in number but are more widely dispersed, single vesicles are larger than in control, free ribosomes were not different from control, glycogen granules sparse, no unusual lipid inclusions on crystals were noted. Phagosomes	Cytoplasm density higher than experimental group, mitochondria are dilated and comparable in number, granular endoplasmic reticulum is distributed throughout cell, and cysternae of rough endoplasmic reticulum are dilated containing electron dense substance. Golgi complex occupies basilar or basi-lateral position, is large, and consists of stacks of lamellae with vesicles on the formative or maturing face. Glycogen granules sparse, no unusual lipid inclusions noted. No phagosomes noted, some lysosomes are randomly located, pinocytotic vesicles are abundant on cell surface. Gap

	Flight Group	Control Group
Cytoplasm cont.	not noted, few lysosomal bodies noted, no coated vesicles, few pinocytotic vesicles. Gap junctions between adjacent osteoblasts not commonly found, no detectable cell lamina.	junctions were not regularly observed.
4. Matrix	Adjacent osteoid matrix contains sparse number of collagen fibers with axial periodicity. Fibers are randomly directed. Few processes of basilar osteoblast cells penetrate or extend into the osteoid. Few mineralization nodules noted, mineralized surface shows an irregular contour. The osteoid thickness is less than 50% of control.	Osteoid consists of bundles of collagen fibers, irregularly placed, but closely packed. Mineralized surface shows regular contour, microvilli of osteoblast and elongated cell processes penetrate osteoid. Mineralization nodules are abundant in osteoid close to mineral front.

Summary of differences in osteoblasts:

All of the differences noted: reduced nucleolus, increase in heterochromatin, dispersion of Golgi components, reduction in number but increase in size of golgi vesicles (fusion?), reduction in rough surfaced endoplasmic reticulum, reduction in number and size of rough endoplasmic reticulum cysternae, reduction in evidence of pinocytotic activity, and overall flattening of the cell characterize a reduction in cell metabolic activity, particularly its protein synthesizing and secreting activity. This is further confirmed by a thinning of the osteoid with a reduction in number of mature collagen fibers. Reduction of new mineral nodules and irregularity of mineral surface contour suggests that the newly secreted osteoid is immature.

B. Osteoclasts on trabecular surfaces.

	Flight Group (Figure 6-7)	Control Group (Figure 8-9)
1. Nucleus	Nuclei are rounded to ovoid with peripheral clumping of heterochromatin. Nuclei number per section range from 6-9; nucleoli are single when observed. Nuclear pores are present. The nuclear membranes are dilated. Few smooth surfaced membranes are attached to nuclear membrane. No significant nuclear inclusions observed.	Nuclei are round to oval. Heterochromatin predominates; some dispersed euchromatin; nuclei number 4-7/section. A single nucleolus is present in most nuclei, nuclear membranes are dilated, smooth surfaced membranes are present at nuclear membrane. No significant nuclear inclusions observed.
2. Cytoplasm	Numerous dilated mitochondria are found throughout cytoplasm, approximately 20% of 44 cells are not directly associated with bone surfaces. These unassociated cells contain sparse vacuoles, few invaginations of plamsa membrane, and sparse microvilli are present. 17 of 44 cells touched the bone but their brush border width is less than 30 μm; infoldings between microvilli are present terminating in dilations in an apical region containing some vacuoles. These vacuoles are typically involved in endocytotic activity and represent less that half the number of vacuoles observed in control bone. No special filaments, crystals, inclusions or evidence of cell deterioration was noted.	Numerous dilated mitochondria are found throughout the cell. All but three osteoclasts of 51 observed were found associated with bone resorption surfaces. A clear zone bounding the resorption edge was present surrounding a microvillus brush border width in excess of 40 μm. Numerous infoldings of plasma membrane occur between microvilli forming vacuoles that occupy a large part of apical cell cytoplasm. No special inclusions are noted.

Summary of Observations on Osteoclasts.

Larger numbers of nuclei per cell, reduction in brush border and cytoplasmic vacuoles in the flight group are indicative of a reduction of activity for each osteoclast. If histomorphometric data confirm that osteoclast numbers are the same in control and flight groups, then resorption reduction in flown animals should still be expected as each clast reflects reduced activity. Some resorption activity is noted, however, and shallow matrix resorption cavities in flight bone are observed. Whether each clast ultimately resorbs the same bone volume, simply requiring more time, will have to be established by double tetracycline labeling studies.

C. Osteocytes Summary

No ultrastructural differences were noted between osteocytes of flown and control group other than the reduction in number of osteocytes, due likely to smaller size of trabeculae. No differences in osteocyte spacing or axial orientation was noted.

D. Cartilagenous Growth Plate

Chondrocytes and cartilage matrix were examined. Each growth plate was divided into classic zones, i.e., resting zone, zone of proliferation, zone of matrix synthesis, zone of cell hypertrophy, zone of provisional calcification, zone of ossification. Particular attention was given to the distribution of matrix vesicles, site of onset of mineralization, and maturation of mineral clusters.

Flown	Control
(Figures 10-14 and 19-25)	(Figures 15-18 and 26-29)

Resting Zone

Multiple chondrocytes occupy ovoid   same
lacunae surrounded by cartilage
matrix of thin collagen filaments
and ground substance. No vesicles
are present in matrix. Cells are
small, irregular in shape, and
contain some rough surfaced endo-
plasmic reticulum, a small Golgi
complex. Few cytoplasmic pro-
cesses are seen. Mitochondria
are dilated. No special inclusions
are noted in cells.

Zone of Proliferation

Multiple cells occupy lacunae.   same
The cells are flattened and
arranged in stacks oriented in rows
parallel to the central bone axis.
The nuclei are ovoid and contain
both euchromatin and heterochro-
matin and a prominent nucleolus.
Rough surface endoplasmic reticu-
lum occupies the periphery of the
cells. A Golgi complex is situated
in a juxtanuclear position. A few
electron dense prematrix inclusions
are seen at secretory face. Nests
are surrounded by a filamentous
matrix. Little or no matrix is
seen between cells within one
lacuna. The cell surface shows
some irregularity, bearing short
protoplasmic extensions.

Zone of Matrix Synthesis

Single large, more rounded chondro-	Single large, more rounded
cytes occupy matricial lacunae.	chondrocytes occupy matrical
The rough surfaced endoplasmic reti-	lacunae. The rough surfaced
culum occupies more of cytoplasm.	ER is extensive with dilated
The nuclei are large, centrally	cisternae. The nuclei are
positioned. The chromatin is pri-	large, oval and show primar-
marily euchromatin with some margin-	ily euchromatin formation.
ation of heterochromatin. The	The Golgi complex is large,
nucleolus is smaller than in prolif-	sometimes cleaved, juxtanu-
erative zone. The Golgi complex is	clear, and contains many

Flown	Control

Zone of Matrix Synthesis
cont.

juxtanuclear, large, containing many vesicles with granular material within them. Many vesicles appear fused and irregular leaving voids in the cell. This was also observed in this and subsequent zones in both flight and control animals and is suggestive of poor infiltration of initial fixative into this avascular tissue. Only short cell processes and microvilli are observed. The matrix surrounding the cells contains few or no vesicles or cell processes. The matrix consists of collagen filaments and granular ground substance.	vesicles - some coalesced. Mitochondria are randomly located. No special inclusions are noted. The cell surface is irregular with some showing bulbous ends. The matrix contains many vesicles at each cell level.

Zone of Hypertrophy

Cells are irregular in shape, containing vacuoles and distended Golgi vesicles. The rough surfaced endoplasmic reticulum is widely scattered. The mitochondria are located peripherally. Some short cytoplasmic processes extend into the lacunae. Matrix vesicles are isolated, 2-5/cell. The nuclei are oval showing some heterochromatin and euchromatin. No special inclusions are noted.	Cells are large, scalloped, and processes from cells extend to matrix. The nucleus has both heterochromatin and euchromatin. The Golgi vesicles are large, irregular and show fixation artifact. No special changes in mitochondria or inclusions are noted. Matrix vesicles are distributed in matrix - 10 per cell.

Zone of Provisional Calcification

Only 2-3 cells in a column are bounded by mineralized cartilage matrix. The matrix has many small needle-like clusters of hydroxyapatite that converge as the metaphysis is reached. Numerous vesicles are observed in the lacunae and lacunar boundary in the first two cells of column. The cells are distended, irregular and contain sparse organelles and vesicles and vacuoles.	A gradient of 4-8 cells occupies a cell column bounded by mineralized matrix beginning with mineral clusters of needles progressing to convergence of clusters into relatively solid calcified cartilage trabeculae in the longitudinal axis. Cells contain vacuoles, are irregular shaped and the lower cells show deterioration.

Summary of observations on cartilage.

The significant differences between flight and control cartilage are the location of onset of mineralized matrix and the distribution of matrix vesicles. The latter appear first in the hypertrophic zone and only become prominent in the zone of mineralization as compared with control bone where matrix vesicles bud from chondrocytes beginning in the zone of matrix synthesis. The difference in mineral distribution can be accounted for in two ways: 1) Matrix vesicles initiate mineral deposition and are not extended from processes or released from cells in flight bones at development times comparable to control. However, no differences are found between flight and control groups at R + 29 (Figures 30-32). 2) The matrix of flight bones is less dense, as it has fewer collagen bundles that show axial periodicity, hence matrix maturation appears to lag. Cell division does not appear to differ significantly as total cell column height is not significantly different from control. Rates of synthesis of matrix products should be studied with isotope labeled precursors to assess matrix production capability and histochemical studies of enzymes alkaline phosphatase, ATPase, and/or pyrophosphatase should be done on future experiments to help delineate location of onset of mineralization activity.

C. Work remaining to be done.

At present, specimens of animals killed immediately post flight and both vivarium and synchronous control groups have been completed. Flight and control group specimens obtained from later recovery periods are embedded, thin sectioned, and their examination is in progress. The oldest flight group (R + 29) shows no difference in ultrastructure, vesicle numbers, distribution of mineral, or organellar content, or cell shape from control.

Thus, a "recovery" is noted within 29 days. Intermediate stages are now being studied in an effort to establish the time of first noticeable change of flight group structure during the earlier recovery stages.

REFERENCE

Anderson, H. C., Introduction to the second conference on matrix vesicle calcification. Metab. Bone Dis. & Rel. Res. 1, 83-87 (1978).

Figure Legends

1. Electron micrograph of osteoblasts from R + 0 flight group. Note paucity of osteoid and flattened cells, often tapering to zones where cell thickness is less than 2 μm. (2 μm scale)

2. Electron micrograph of osteoblasts from R + 0 flight group. Osteoid is irregular and shows zonation of collagen bundles. No new nodules of mineralization are found in osteoid. Basilar processes of osteoblast are sparse and short. Cell morphology is flat. The endoplasmic reticulum is condensed. (2 μm scale)

3. Electron micrograph of osteoblast of R + 0 flight group. Some regions of bone are covered only by thinned cell margins. (2 μm scale)

4. Electron micrograph of osteoblast of vivarium rat group 1. Osteoid shows mature collagen fibers throughout and includes nodules of new mineral initiation. Cells are cuboidal and show dilated endoplasmic reticulum. (2 μm scale)

5. Electron micrograph of osteoblast of synchronous control group 1. Osteoid is mature and some mineral nodules are present. The cell has a well developed Golgi complex and the endoplasmic reticulum is dilated into cysternae. Cells meet at well demarked intercellular junctions. (2 μm scale)

6. Electron micrograph of osteoclast of R + 0 flight group. There is no ruffled border. No vacuoles are noted within cell. Flattened osteoblasts are interposed between bone and osteoclast. Cytoplasm of a single nucleated clast-like cell lies adjacent to blood vessel wall. (2 μm scale)

7. Electron micrograph of osteoclast from R + 0 flight group. A limited brush border is seen at lower right. Few vacuoles are noted. (5 μm scale)

8. Electron micrograph of osteoclast of synchronous control group. A wide brush border bounded by a clear zone is shown. Intracellular vacuolation indicative of resorptive activity is noted. Some mineral is found in vacuoles. (2 μm scale)

9. Electron micrograph of osteoclast from vivarium control group 1. Active brush borders, wide clear zones, and vacuolation typify osteoclasts of this group. (2 μm scale)

10. Electron micrograph of zone of cell proliferation of flight group R + 0. New matrix separates cells in common lacunae indicative of continued matrix synthesis. No vesicles are noted. (5 μm scale)

11. Electron micrograph of chondrocyte in zone of matrix synthesis of R + 0 flight group. Matrix is mature but cell processes are short and vesicles, if present, are limited to cell margins. (2 μm scale)

12. Electron micrograph of chondrocyte in zone of matrix synthesis of R + 0 flight group. Matrix is mature but cell processes are short and vesicles, if present, are limited to cell margins. (2 μm scale)

13. Electron micrograph of chondrocyte in zone of matrix synthesis of R + 0 flight group. Matrix is mature but cell processes are short and vesicles, if present, are limited to cell margins. (2 μm scale)

14. Electron micrograph of chondrocyte in zone of matrix synthesis of R + 0 group. This animal showed greatest amount of matrix vesicles in this zone being more comparable to control that rest of flight group which showed a paucity of matrix vesicles. (2 μm scale)

15. Electron micrograph of chondrocytes of zone of matrix synthesis in group 1 of vivarium control. Cell processes extend well into matrix and some matrix vesicles are present. (2 μm scale)

16. Electron micrograph of chondrocytes and matrix of group 1 vivarium control. Note vesicle formation in matrix above zone of cell hypertrophy. (2 μm scale)

17. Electron micrograph of chondrocyte of hypertrophic zone of group 1 vivarium control. Vesicles are prominent among connective tissue fibers in longitudinal septa. (2 μm scale)

18. Electron micrograph of intercellular septa in zone of hypertrophy of group 1 synchronous control group. Note vesicles in matrix in hypertrophic zone and beginning of mineral clusters about vesicles in the zone of provisional calcification. (1 μm scale)

19. Electron micrograph from R + 0 flight group showing zone of cell hypertrophy and provisional calcification. The matrix is lacking new sites of mineral clusters. Vesicles are limited to the lacunar space of adjacent cells and are absent from cells on layer above. (5 μm scale)

20. Electron micrograph of zone of cell hypertrophy and provisional calcification of R + 0 flight rat. Note vesicle release occurs from cells nearest matrix mineralization. (5 μm scale)

21. Electron micrograph of zone of provisional calcification of R + 0 flight rat showing limited matrix mineral deposits. Vesicles and cell processes lie close to cell. (2 μm scale)

22. Electron micrograph of zone of provisional calcification of R + 0 flight rat showing limited matrix mineral deposits. Vesicles and cell processes lie close to cell. (2 μm scale)

23. Electron micrograph of zone of hypertrophy of R + 0 flight rat showing paucity of matrix vesicles. (2 μm scale)

24. Electron micrograph of chondrocyte in zone of provisional calcification in flight group R + 0. Note vesicles in lacunae and absence of matrix vesicles in more distal region. (2 μm scale)

25. Electron micrograph of zone of provisional calcification of R + 0 flight rat. Only a limited number of vesicles are noted in zones between adjacent cell columns of hypertrophic zone. (2 μm scale)

26. Electron micrograph of zone of provisional calcification and hypertrophy of group 1 of vivarium control. Extensive new matrix mineral sites are noted. No vesicles remain in lacunae. (2 μm scale)

27. Electron micrograph of zone of provisional calcification and hypertrophy of group 1 of vivarium control. Extensive new matrix mineral sites are noted. No vesicles remain in lacunae. (2 μm scale)

28. Electron micrograph of zone of cell hypertrophy and provisional calcification of group 1 vivarium control. Extensive new matrix mineral sites are noted as compared to sparse distribution in flight group. (5 μm scale)

29. Electron micrograph of hypertrophic chondrocyte of synchronous group control. New mineral sites are seen here and maturing granules are fused into septa in zone of provisional calcification. (2 μm scale)

30. Electron micrograph of flight group R + 29. Note mature collagen bundles in longtudinal septa and 50+ matrix vesicles prior to onset of mineralization of septa. Vesicles were not noted in this site in R + 0 group. (2 μm scale)

31. Electron micrograph of flight group R + 29 zone of mineralization. Note vesicles in matrix and new sites of mineral formation. No vesicles are noted within lacunae as seen in R + 0 group. (2 μm scale)

32. Electron micrograph of zone of provisional calcification - cell hypertrophy of flight group R + 29. New mineralizing vesicle sites are noted. (2 μm scale)
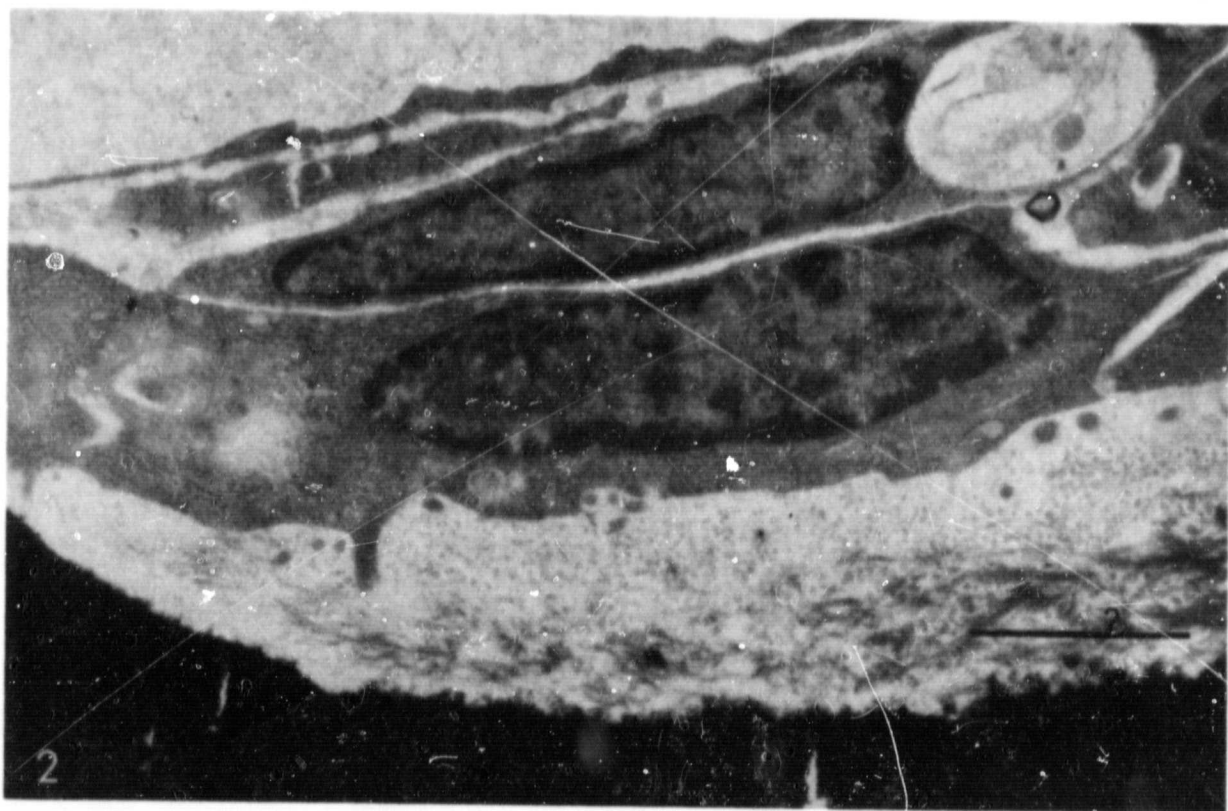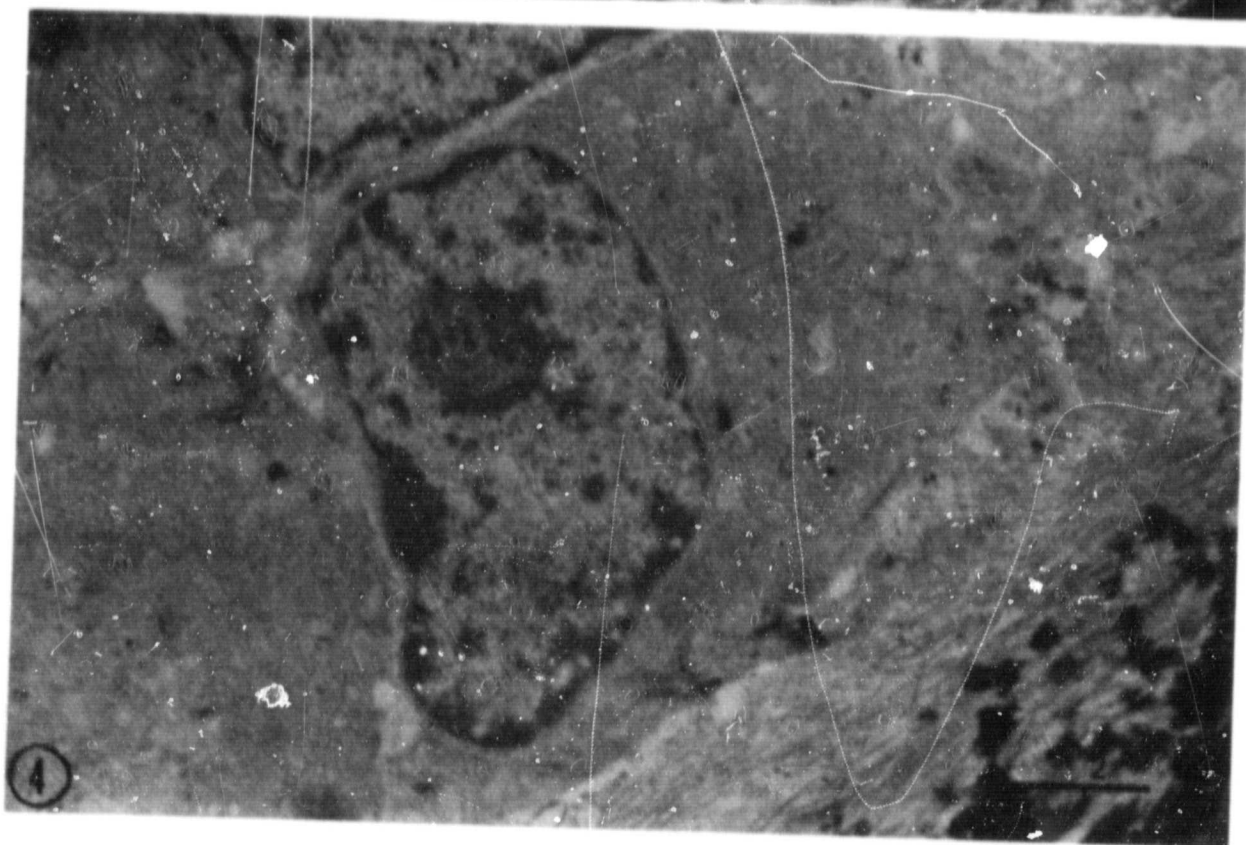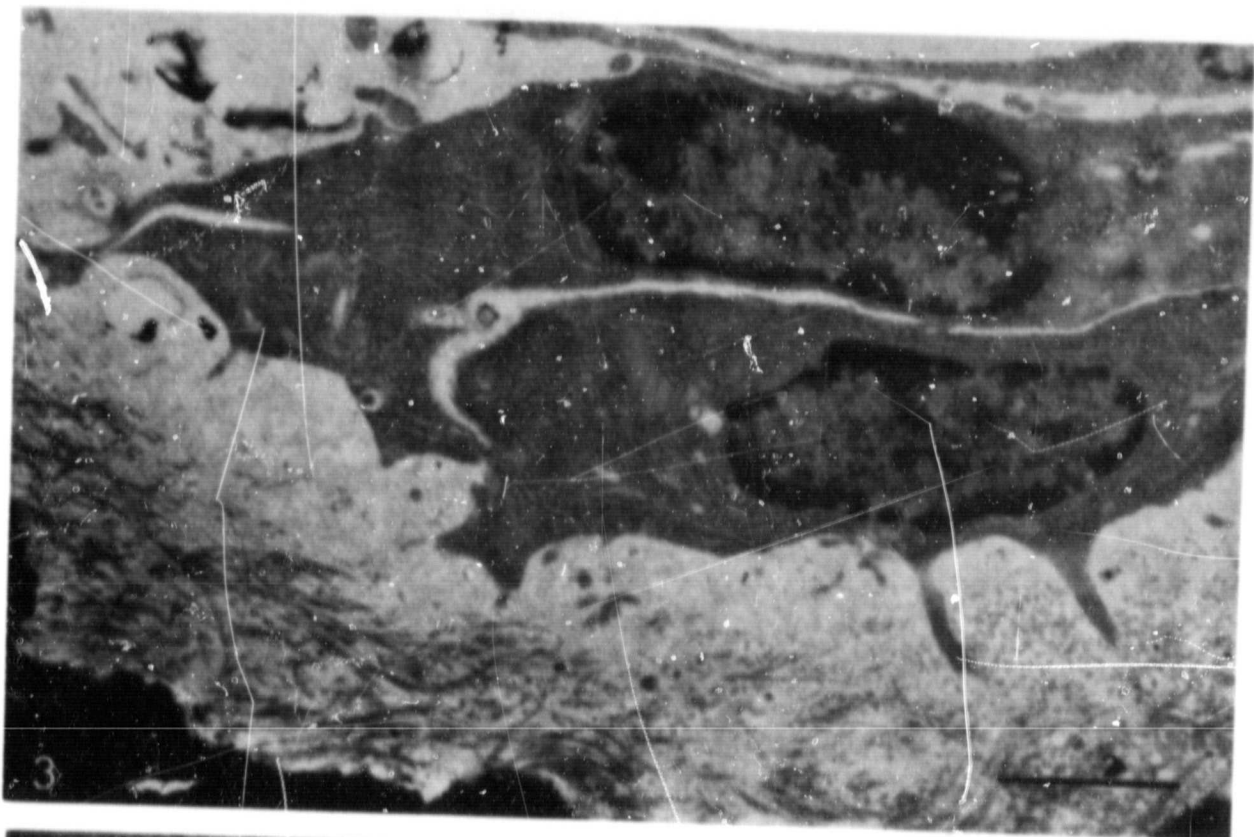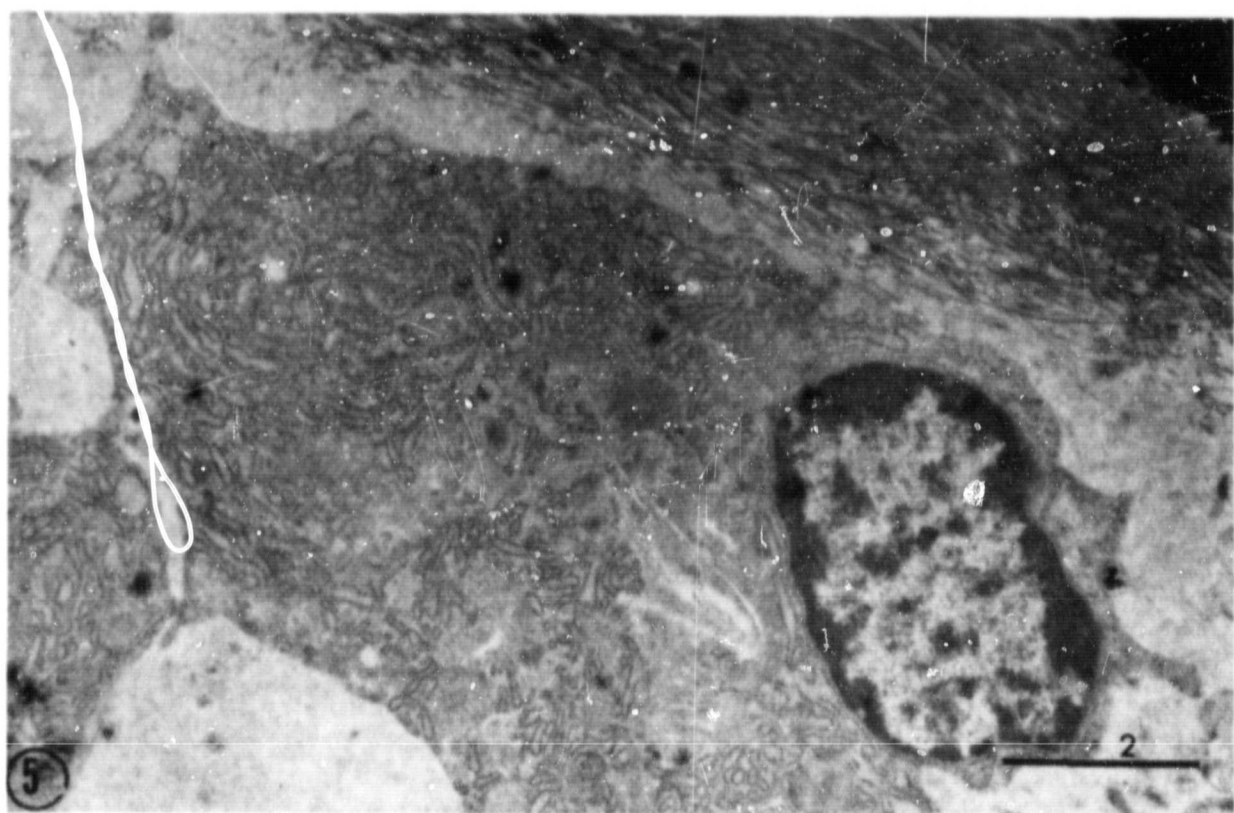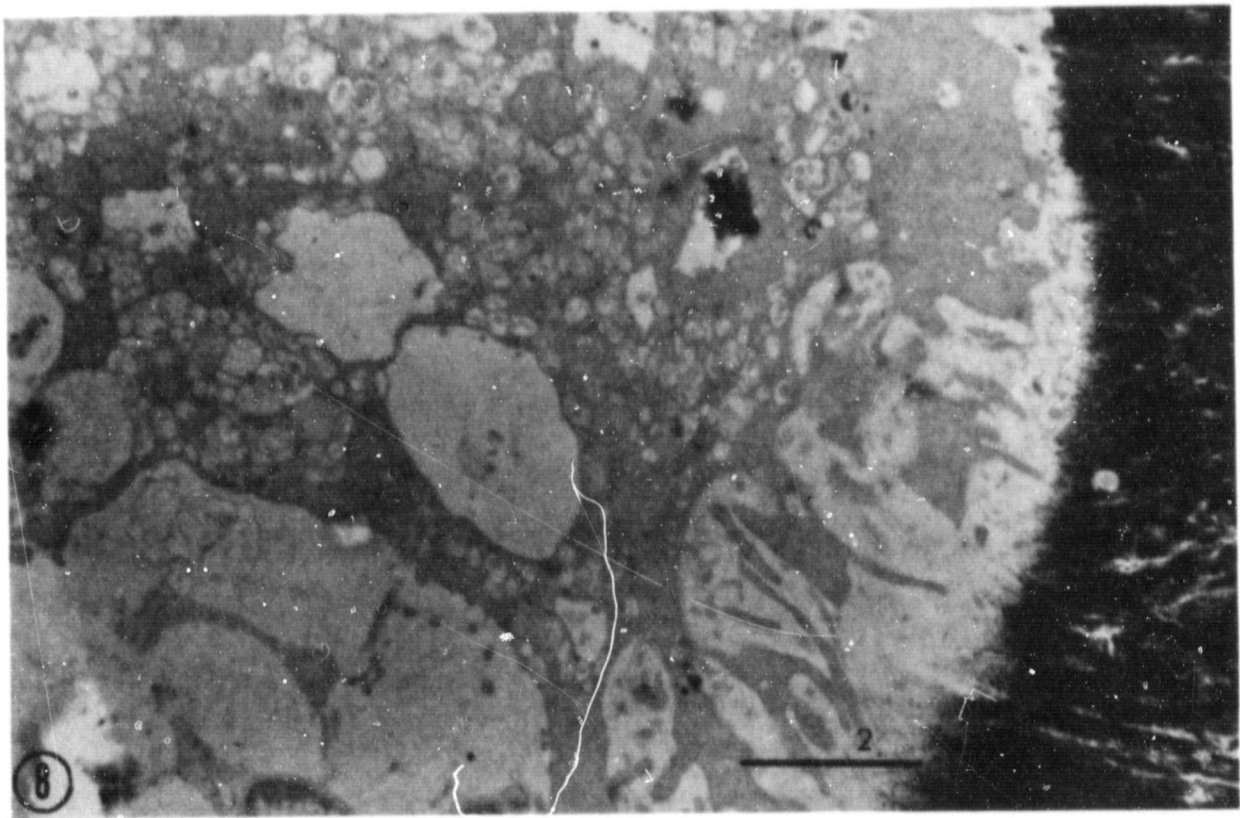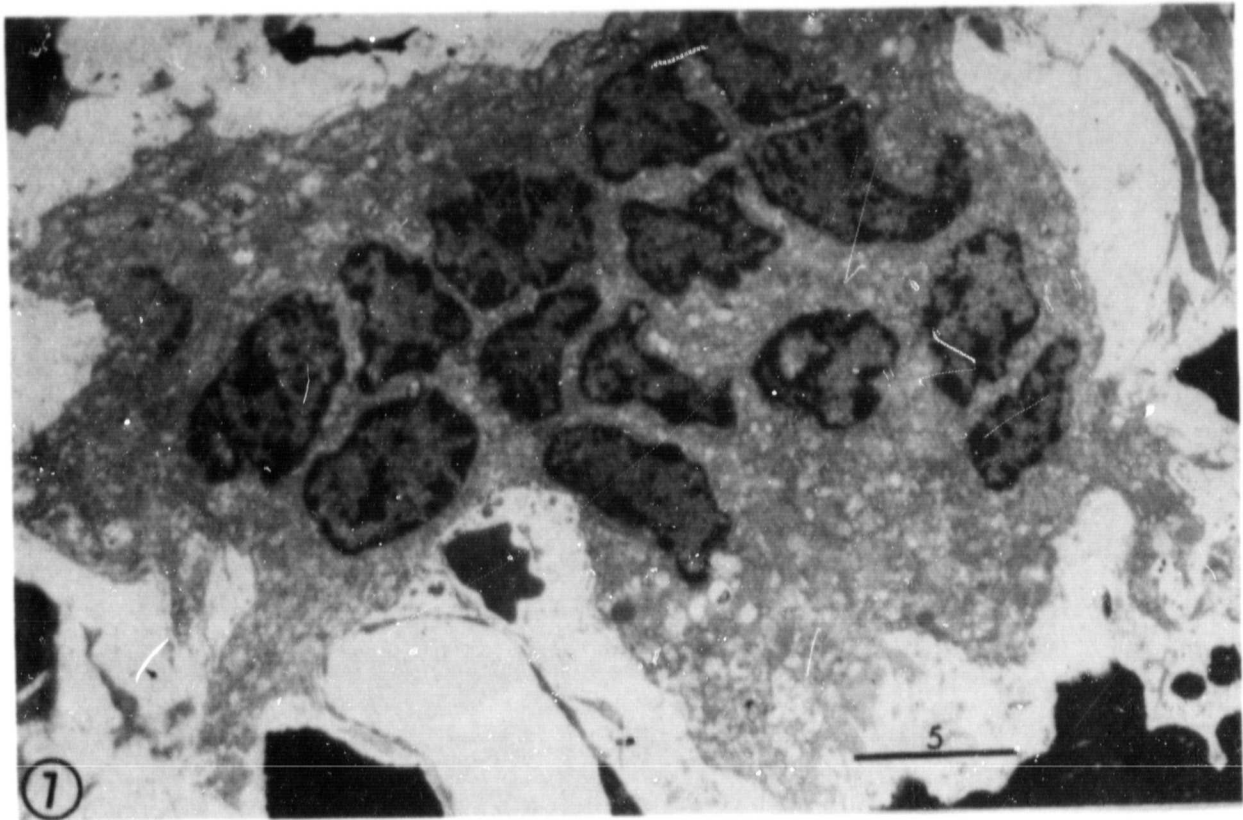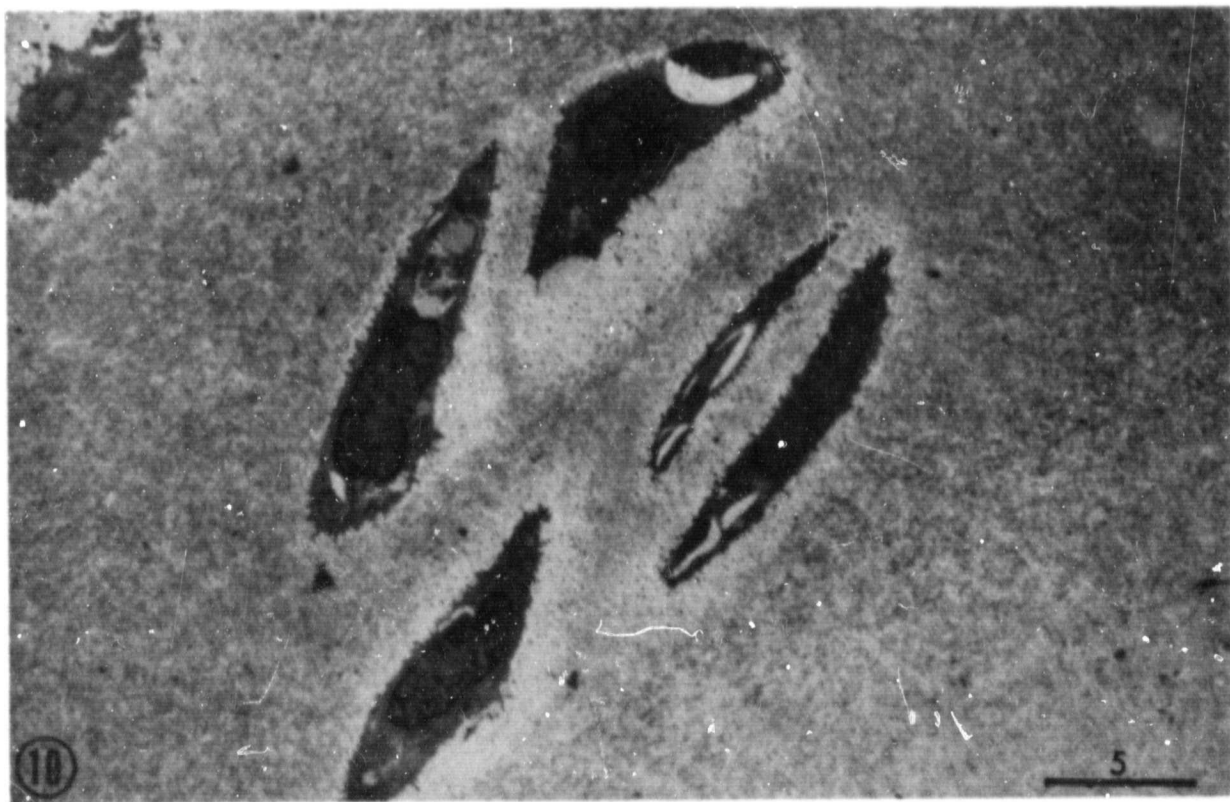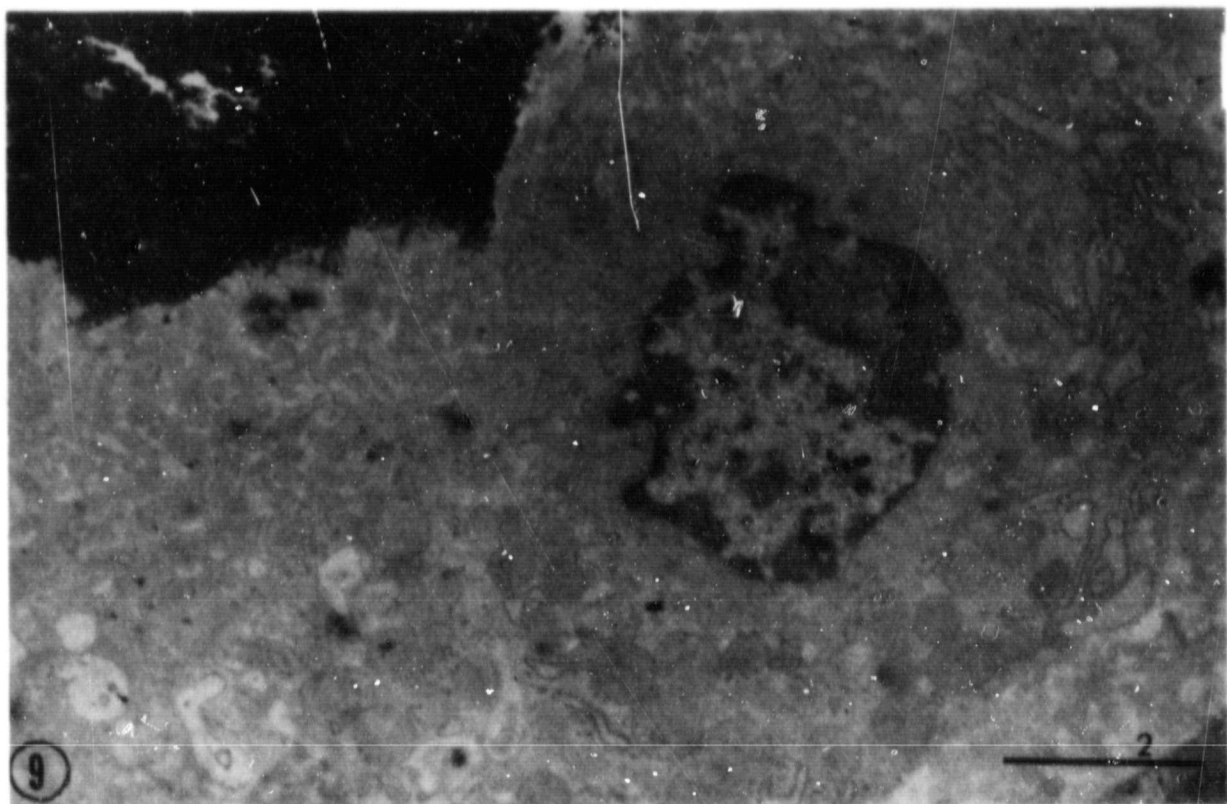
213

215

217

219

15

16

221

(21)

2

(22)

2

223

23

24

27

28

(31)

(32)
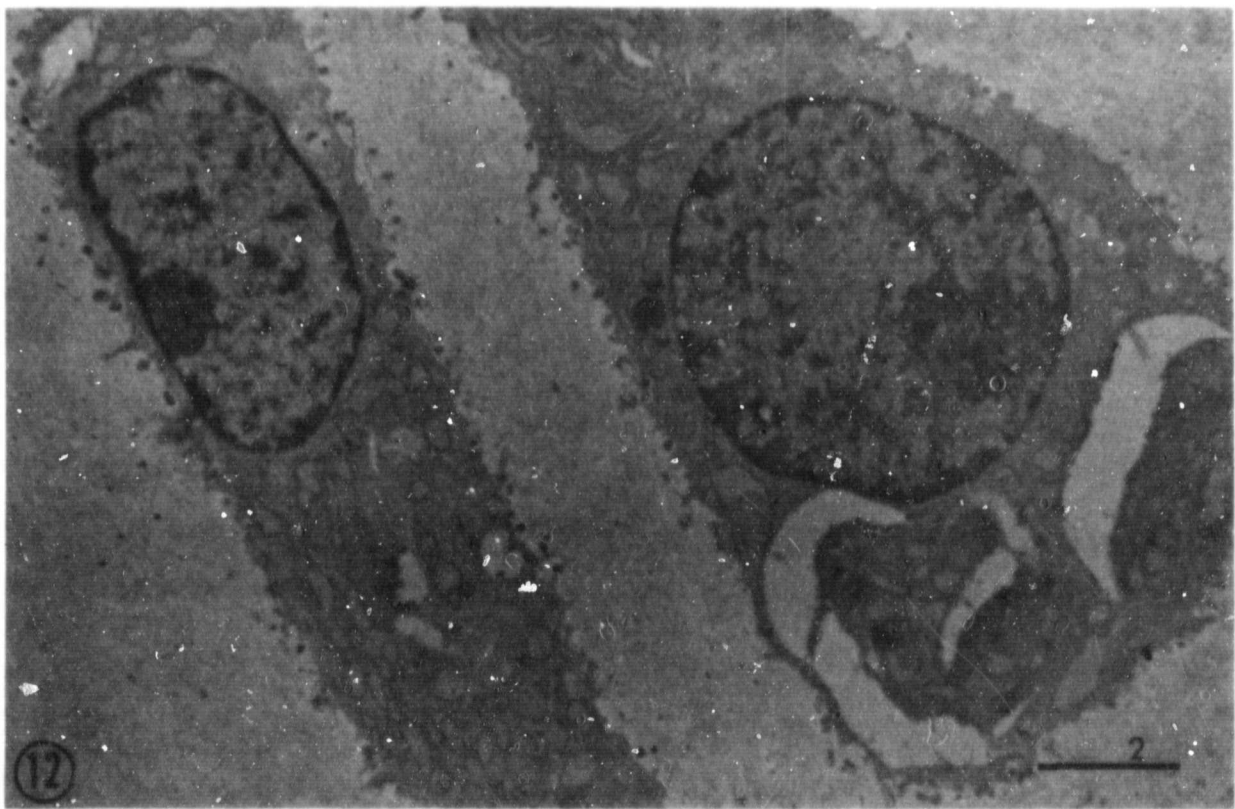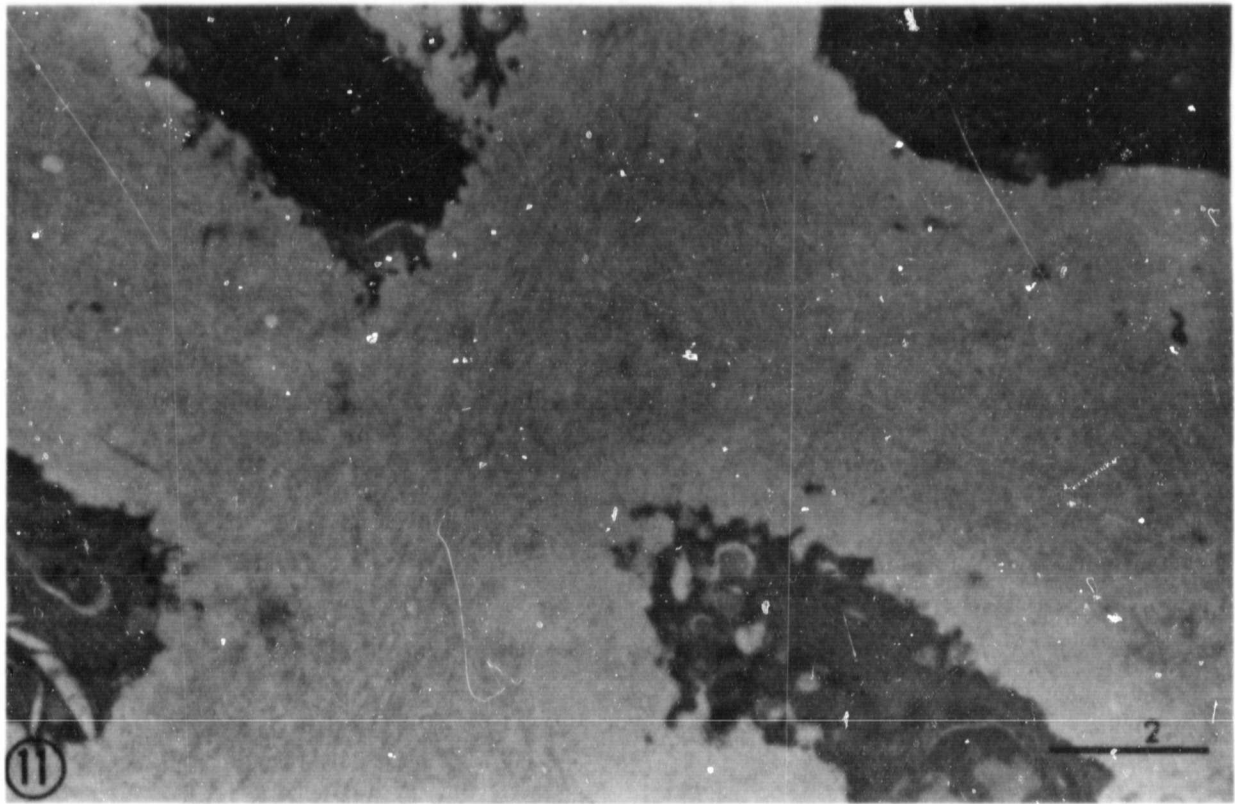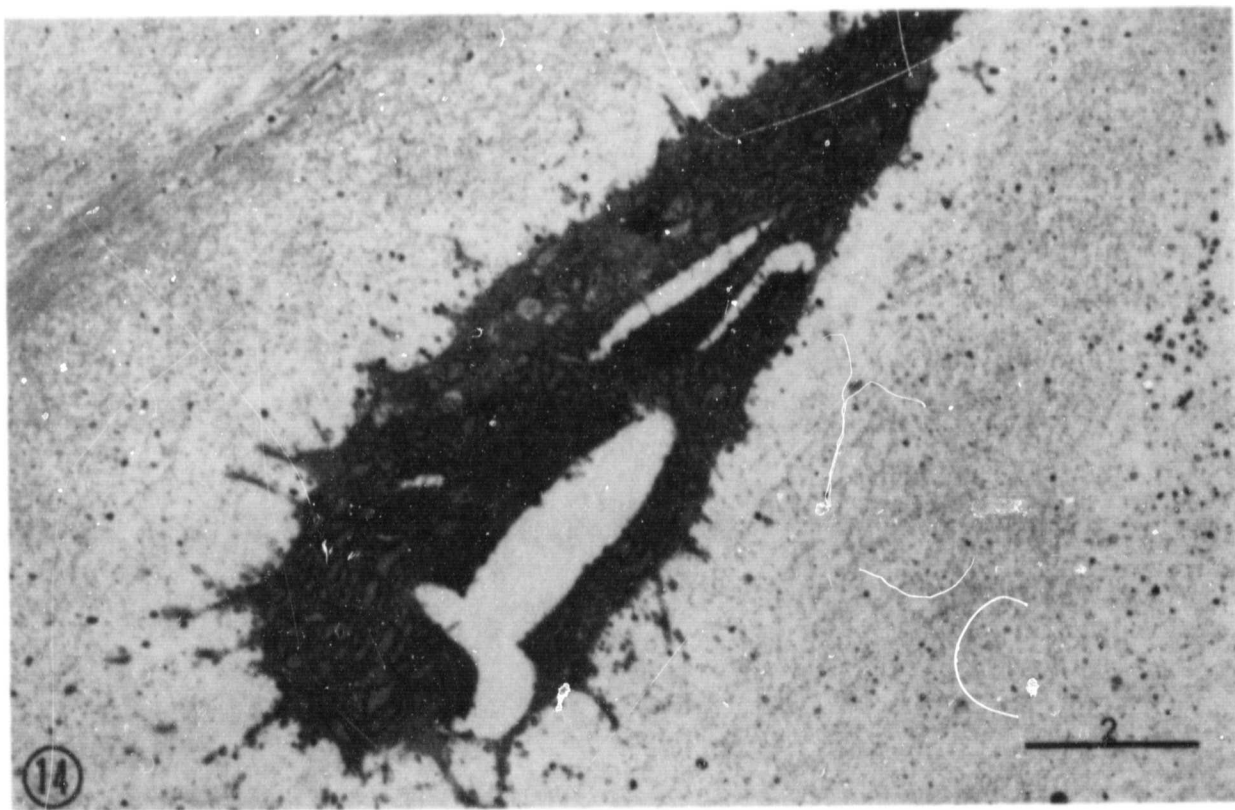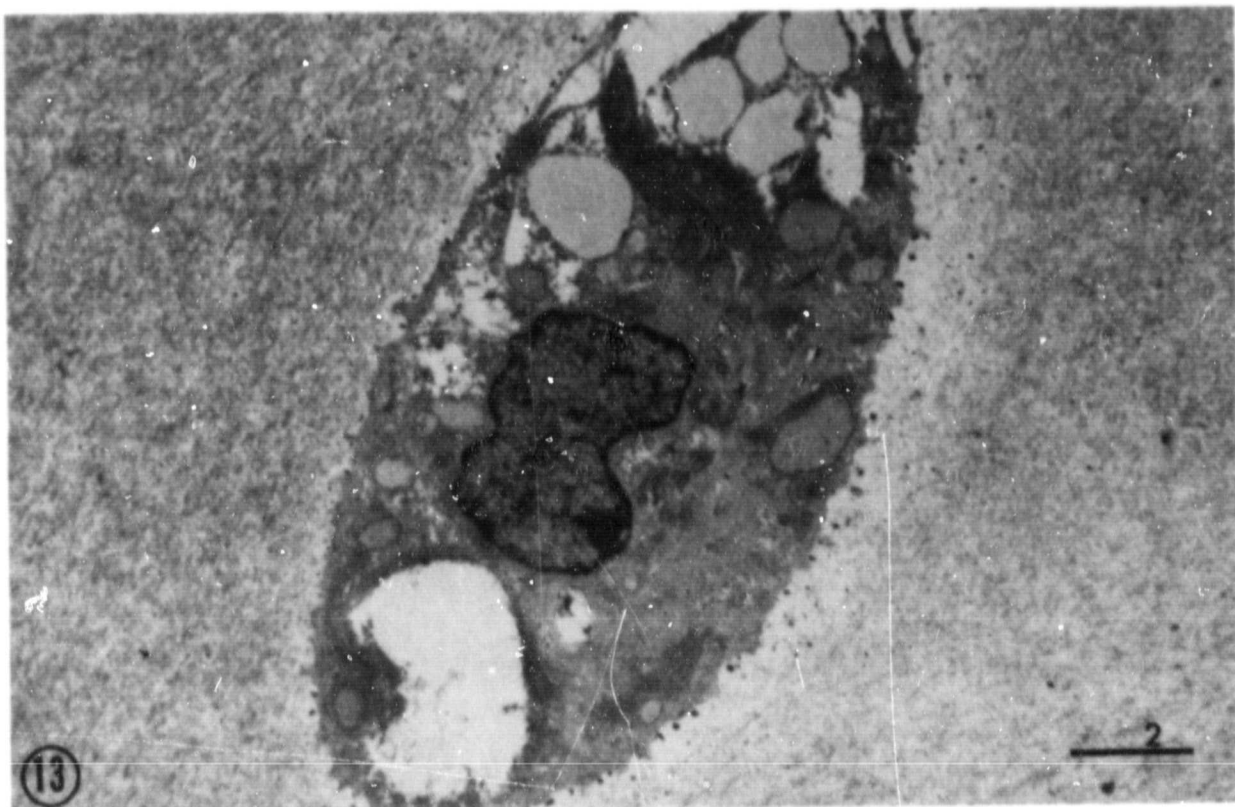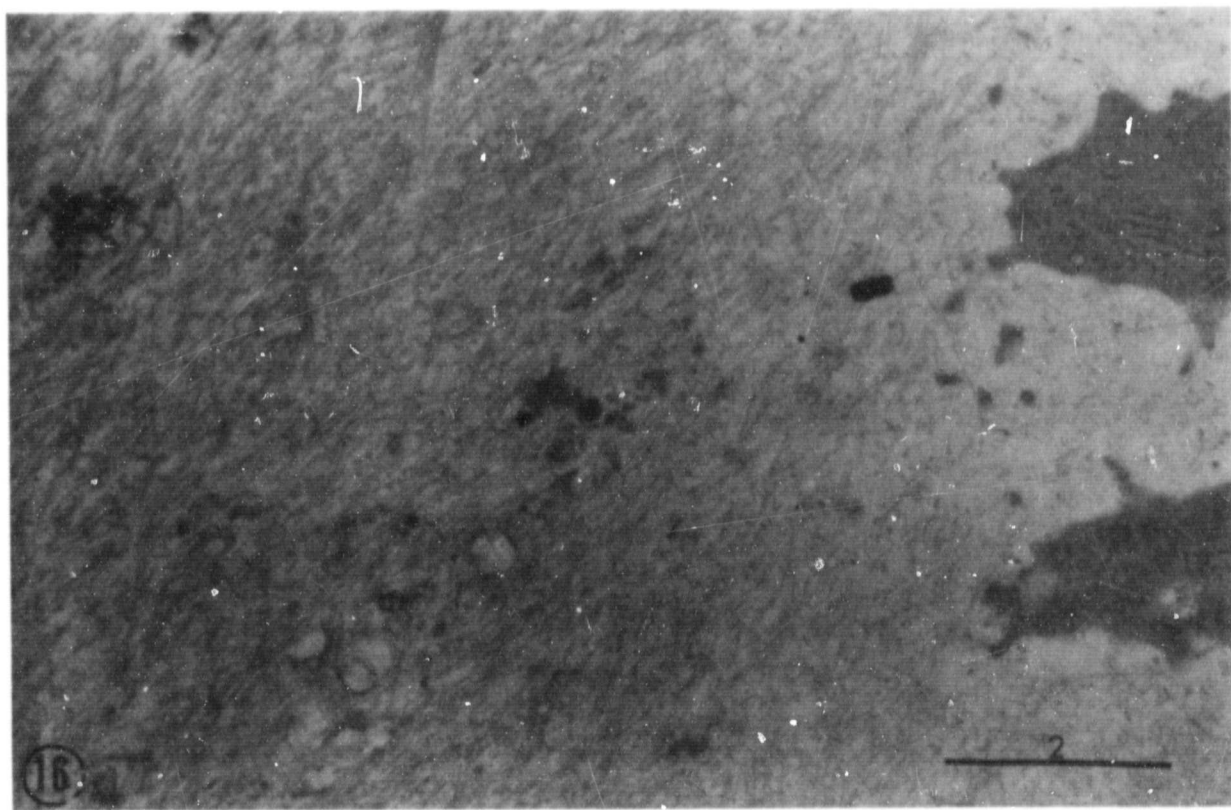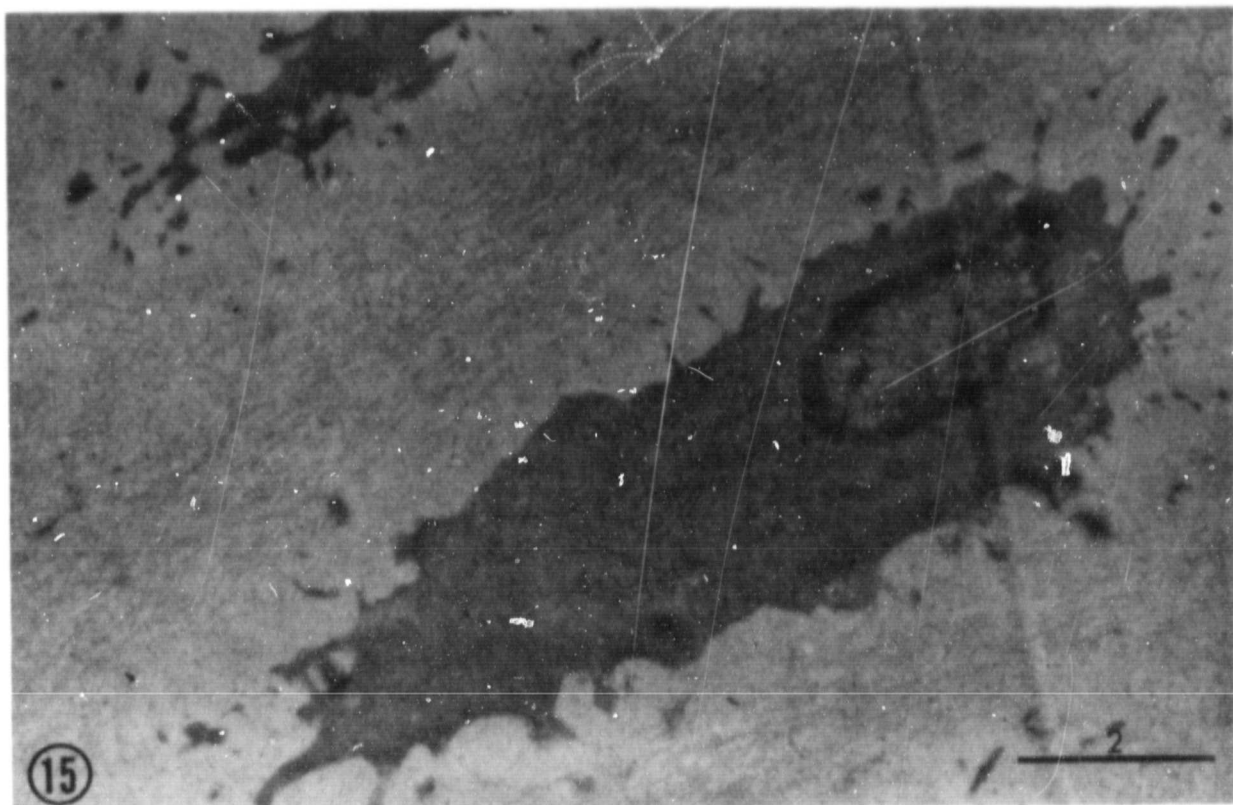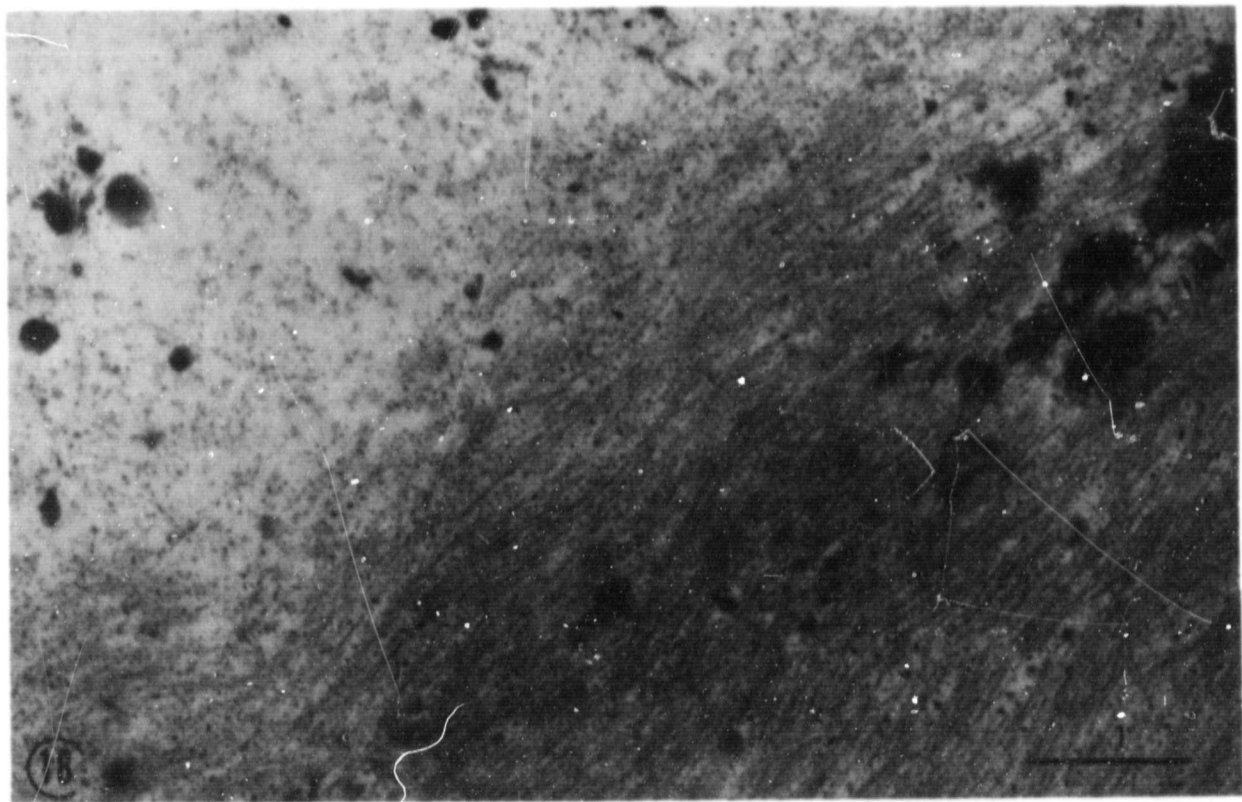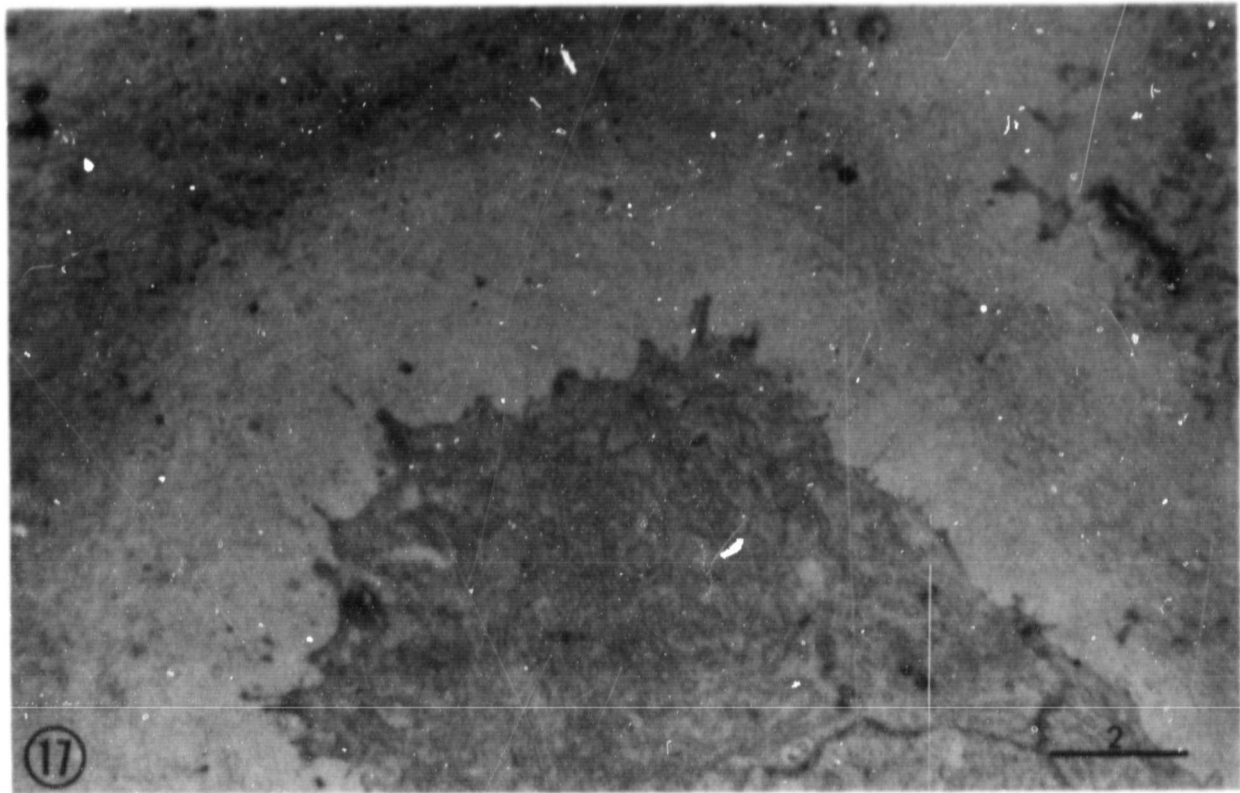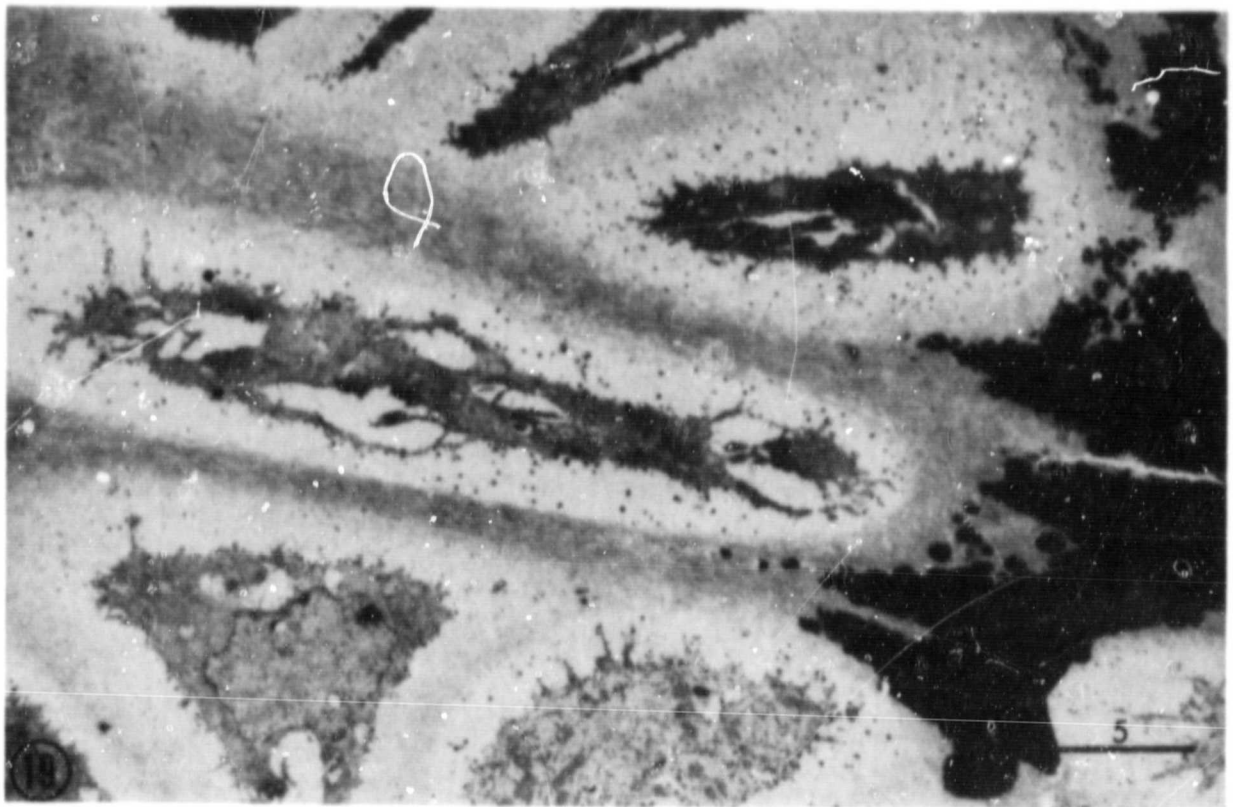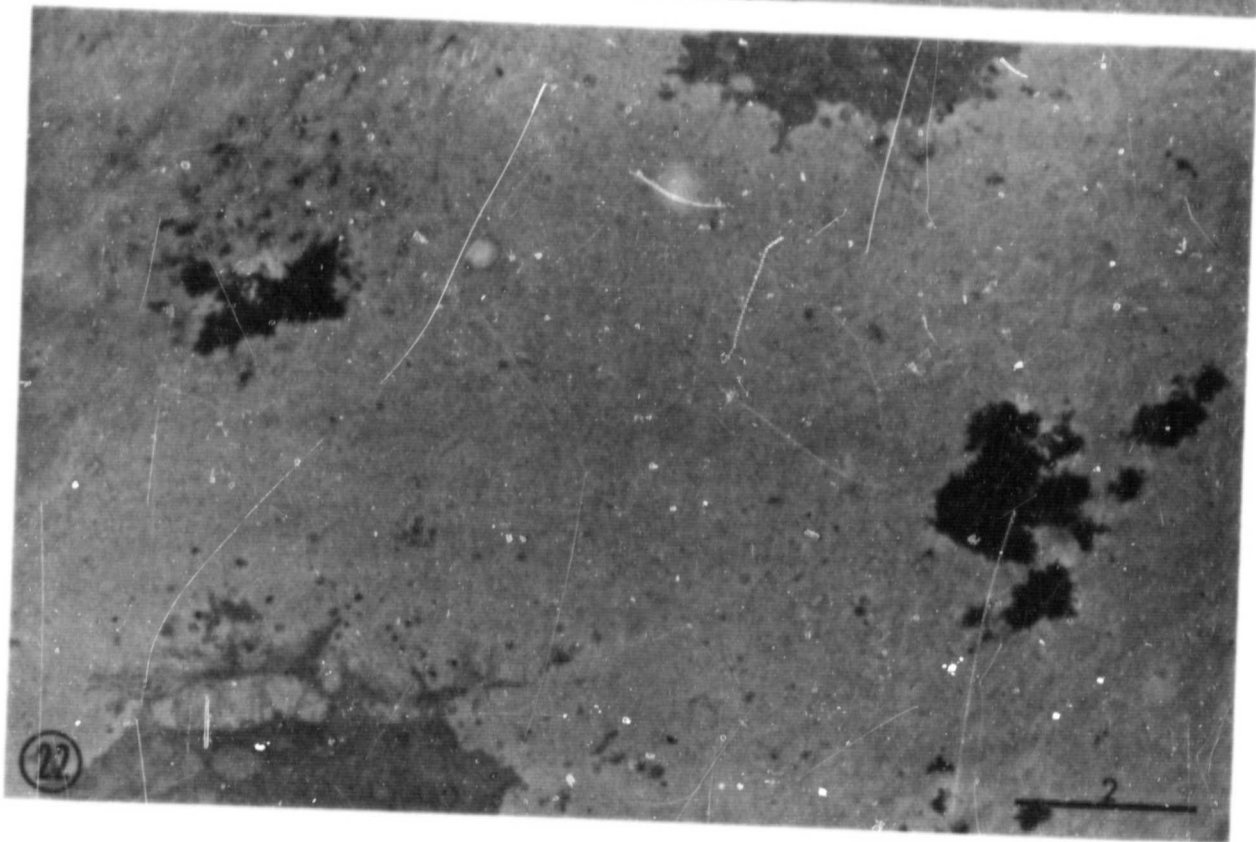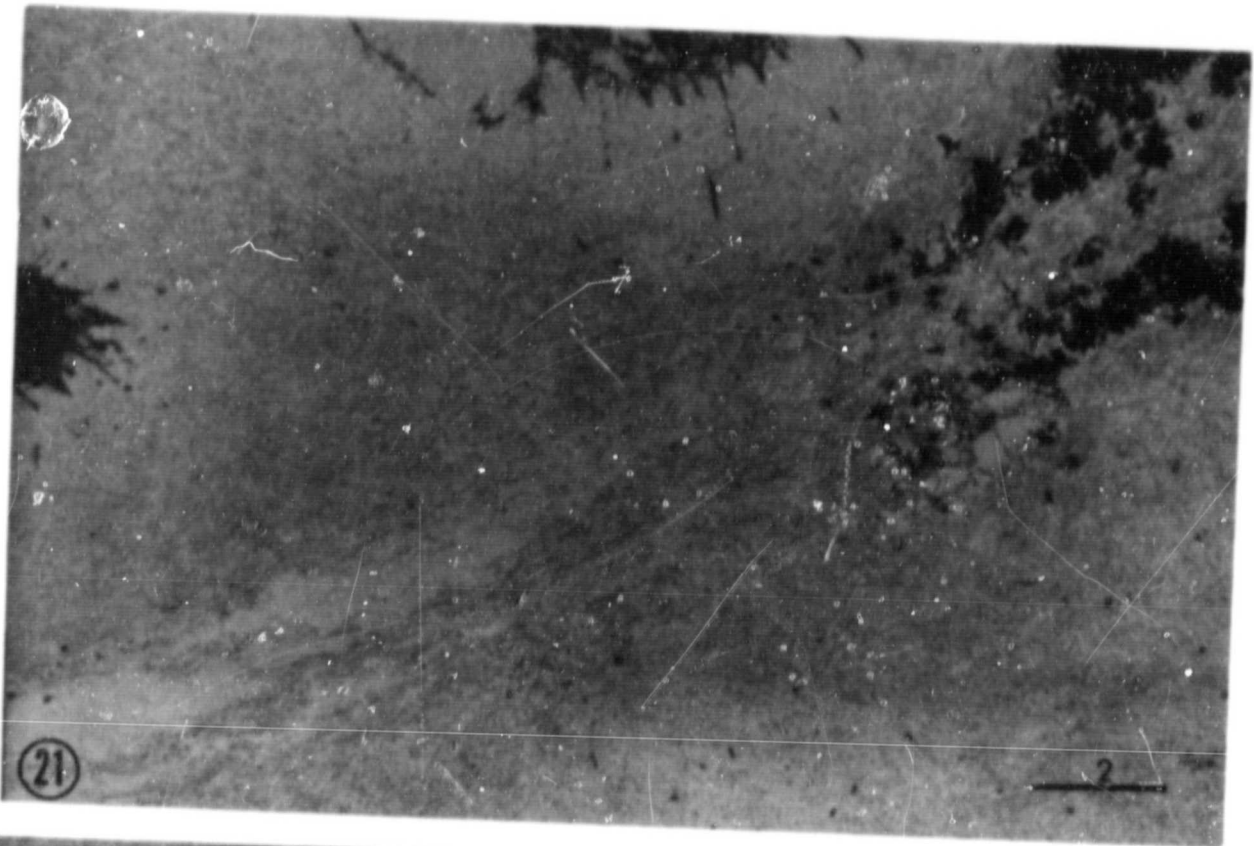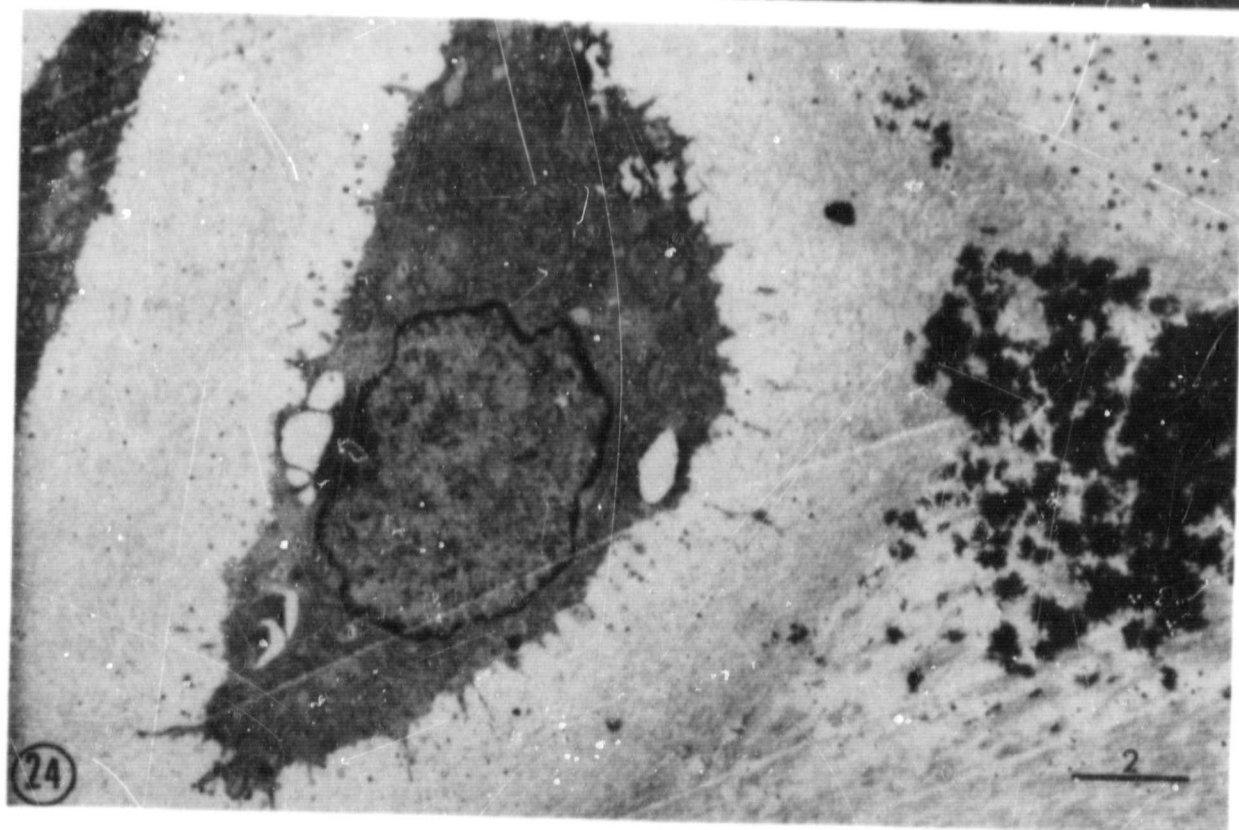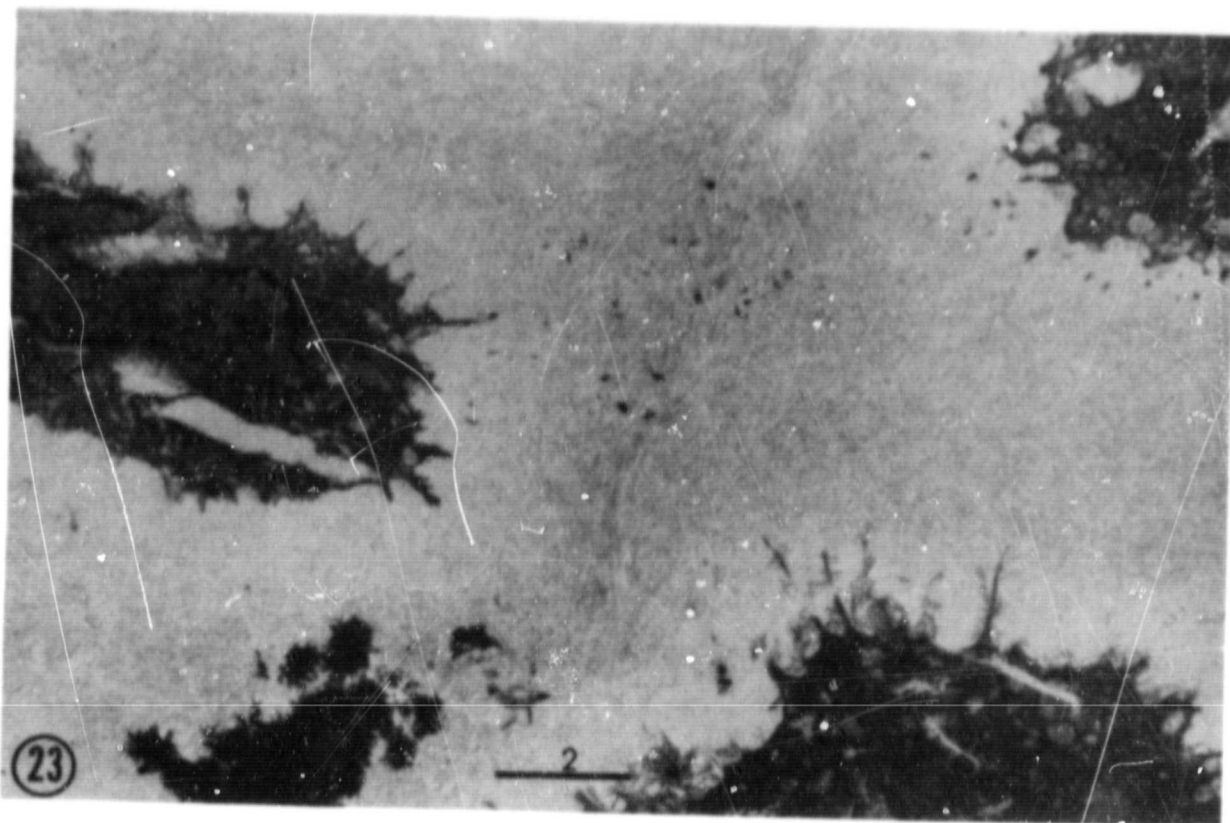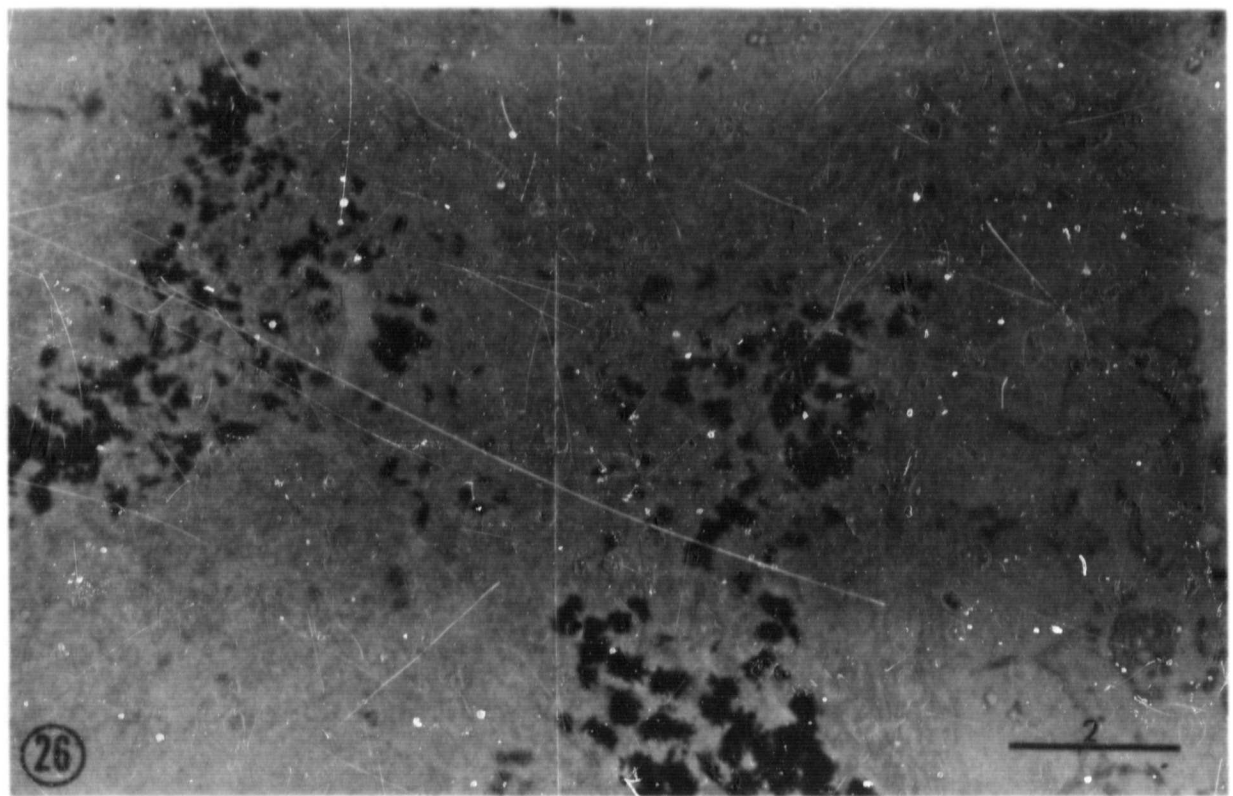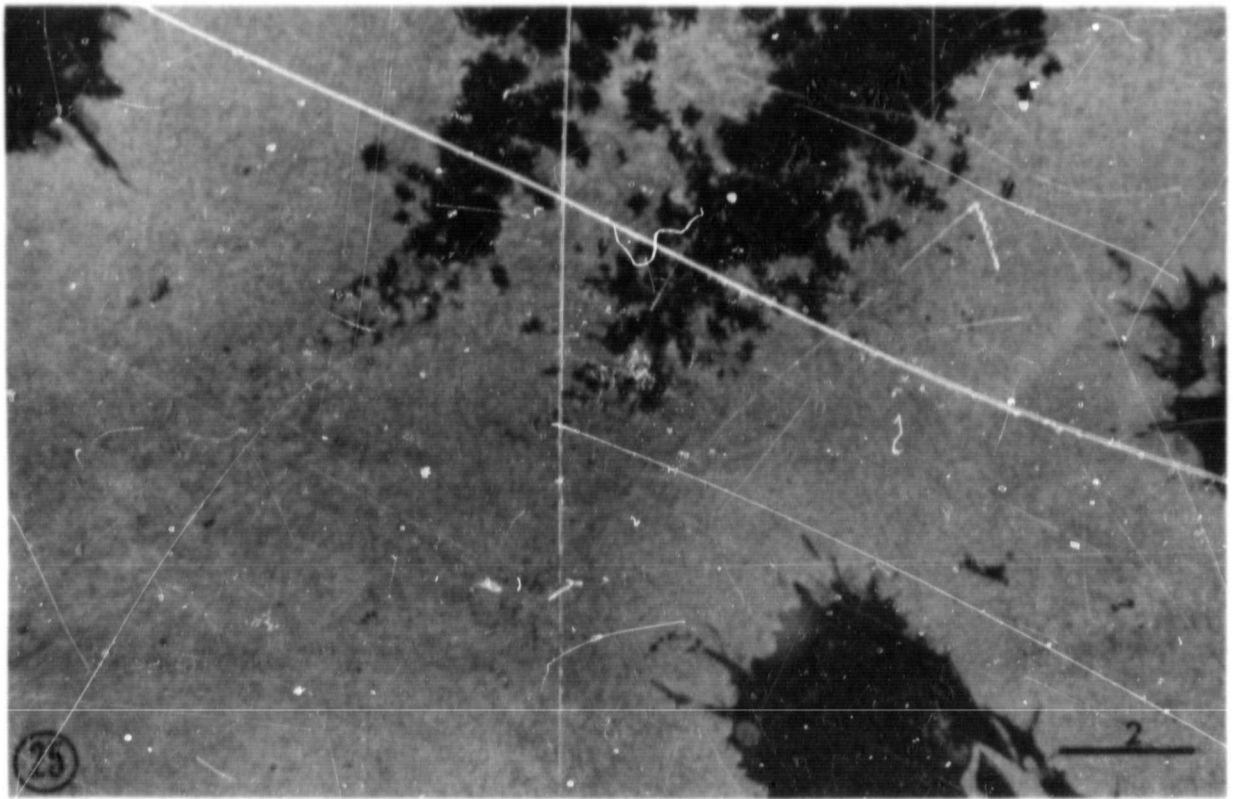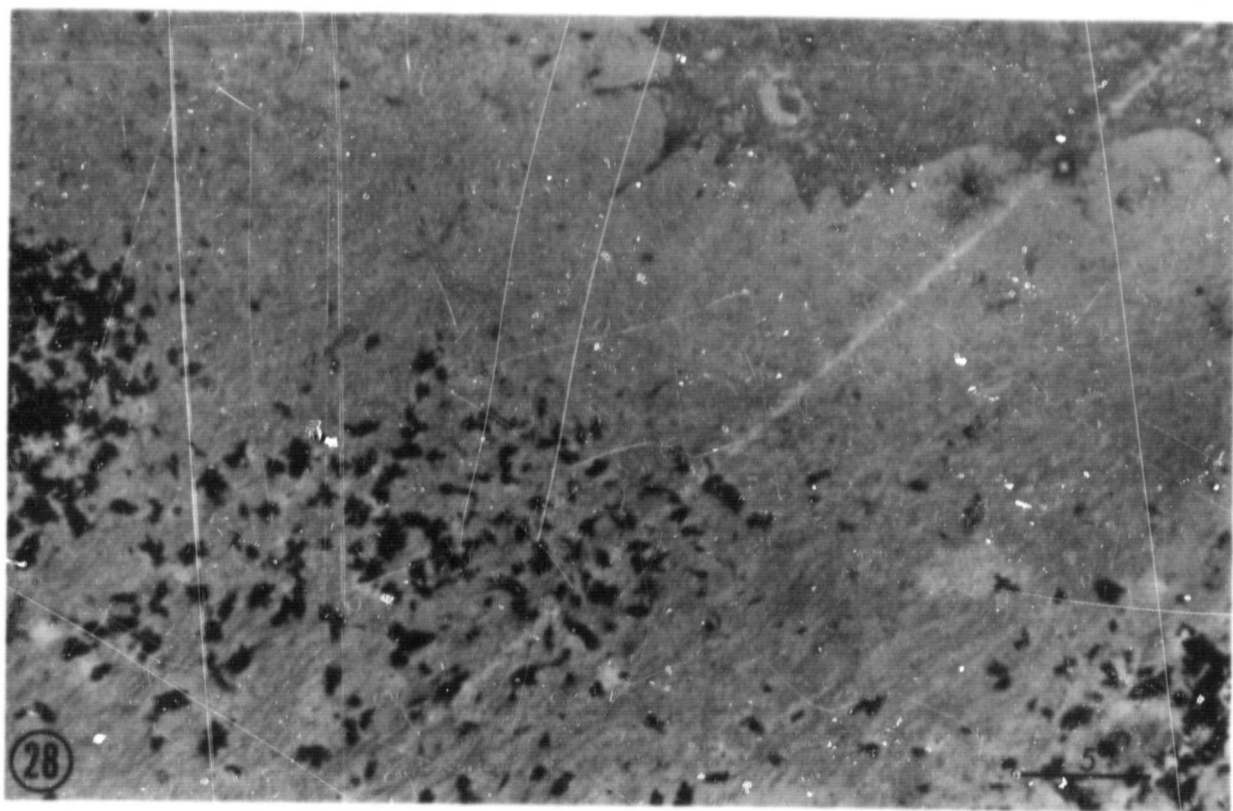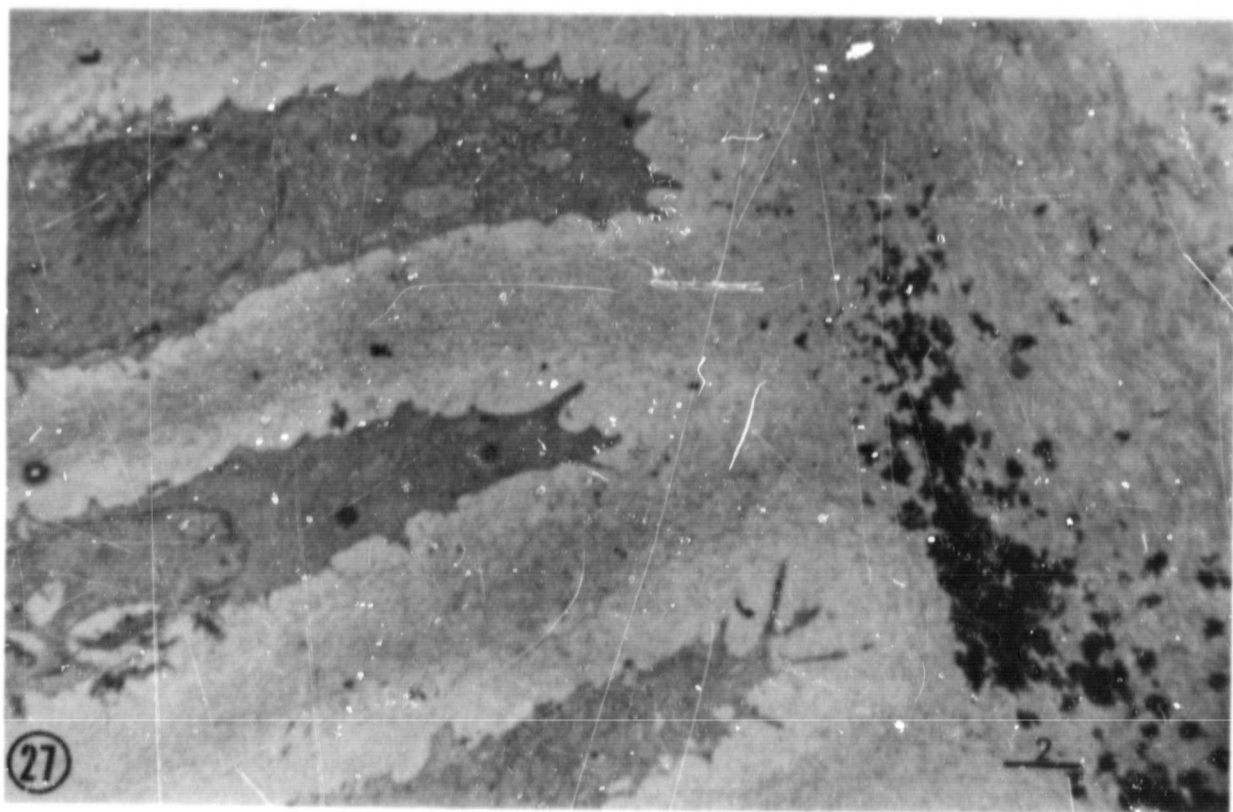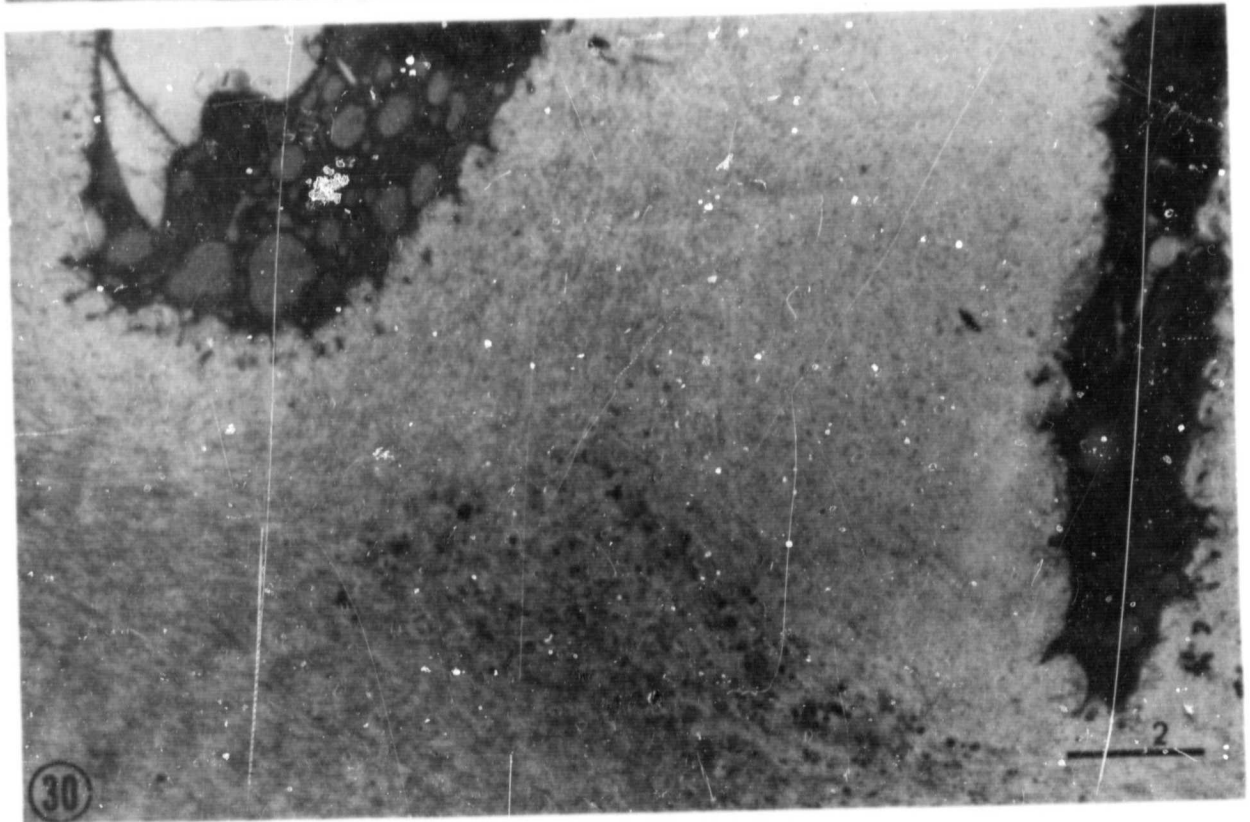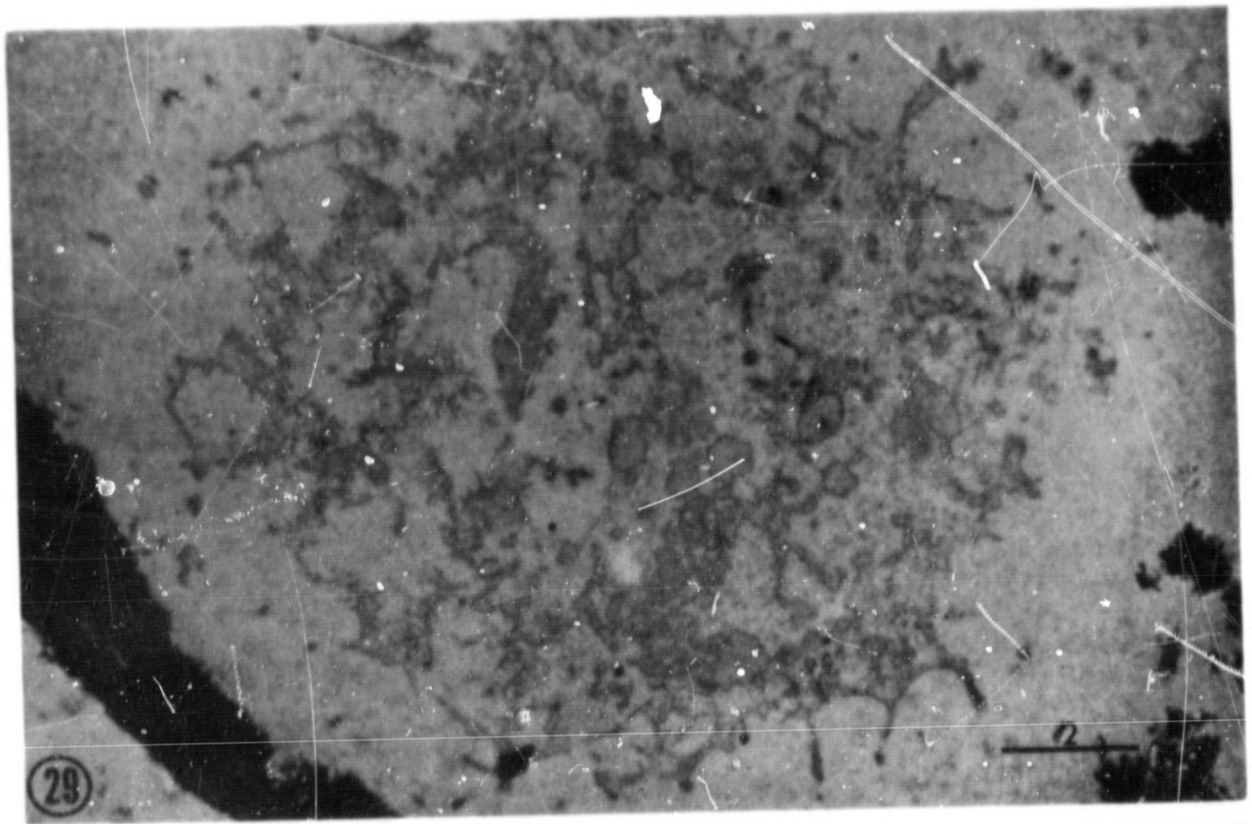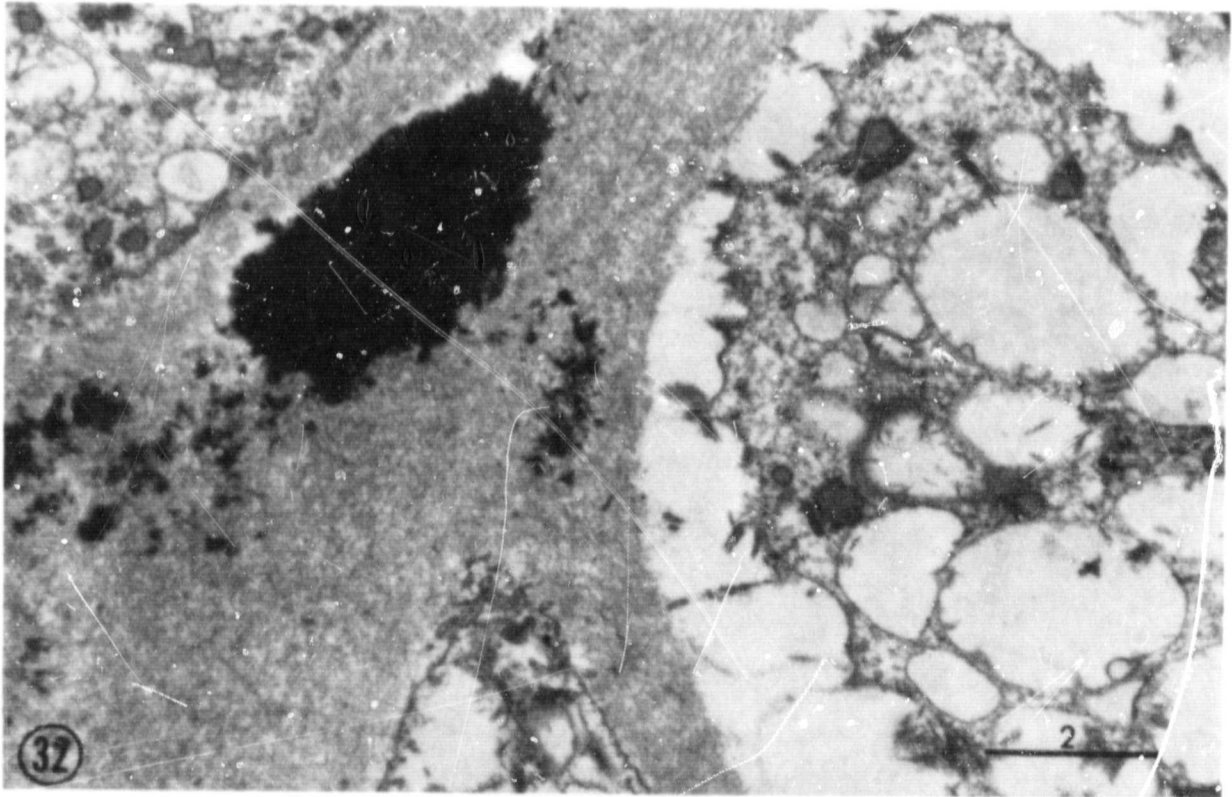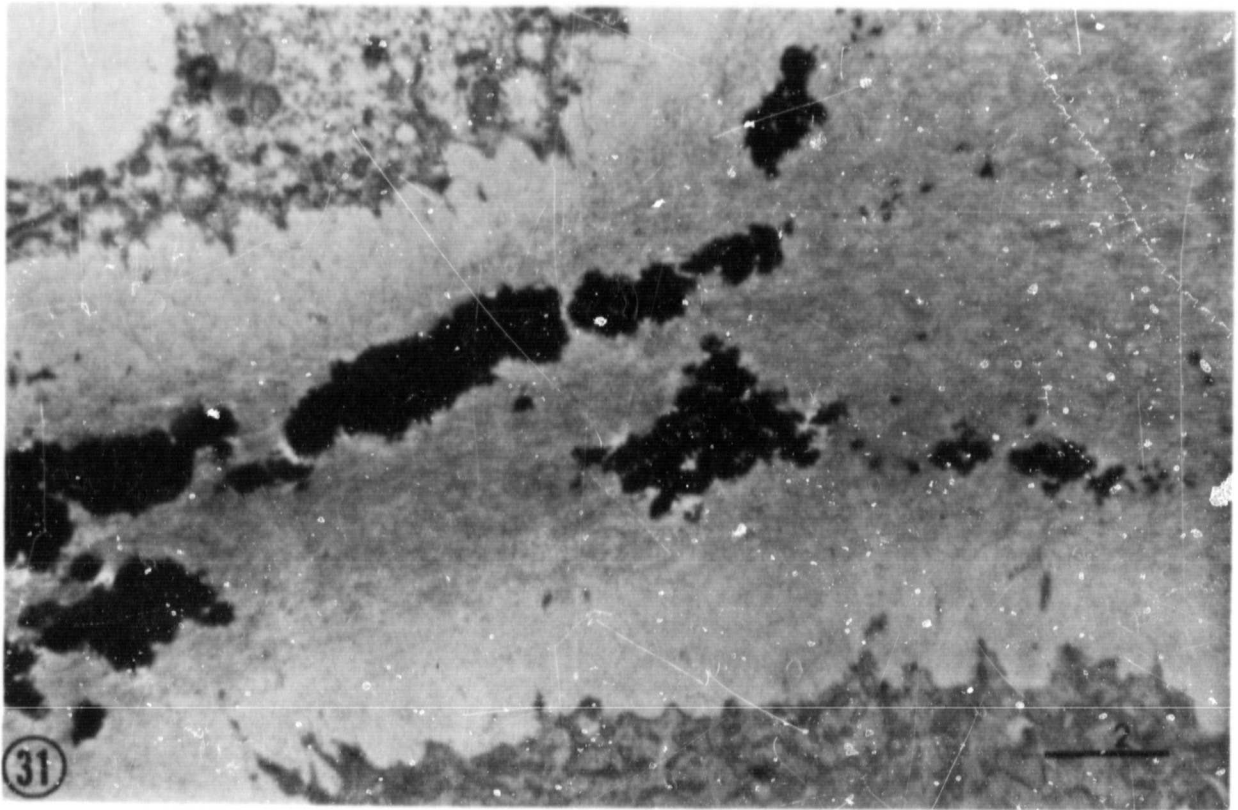
K-307 - VERTEBRAL BODY STRENGTH OF RAT SPINAL COLUMNS

LEON E. KAZARIAN, Dr.Ing.

BIODYNAMIC EFFECTS BRANCH
BIODYNAMICS & BIOENGINEERING DIVISION
AIR FORCE AEROSPACE MEDICAL RESEARCH LABORATORY
WRIGHT-PATTERSON AIR FORCE BASE, OHIO

Summary

The effects of space flight on vertebral body bone strength excised

from male Wistar rats flown in earth orbit for 18.5 days aboard COSMOS

1129 have been investigated. This report describes results of comparative

biomechanical investigations of vertebral body strength for flight,

synchronous, and vivarium rats following spacecraft recovery (R+0), at

R+6 and R+29 days post flight recovery. The groups for which differences

are analyzed were formed by different combinations of environment, spinal

column position and three different loading rates. Statistical analyses

are presented for the mechanical properties of stiffness, ultimate load,

displacement to ultimate load, and energy to ultimate load. At R+0 all of

the above properties show that the vertebral body exhibits an increasing

susceptibility to fracture. The reduction of bone strength is

inhomogeneous and dependent on vertebral level. The R+6 recovery data was

inconclusive since it varied above and below the R+0 data. At R+29

ultimate load values showed a statistically significant increase in

bone strength approaching that of the vivarium or control group.

INTRODUCTION

This report provides a comparative analysis of biomechanical property data of rat vertebral bodies following 18.5 days exposure to earth orbital space flight. The purpose of this report is to shed light on the effects of environment, relative vertebral body position and loading rate on groups of rats killed immediately at spacecraft recovery (R+0), at 6 days (R+6) and 29 days (R+29) post flight.

MATERIALS / METHODS

Specific pathogen free, male Wistar rats from the Institute of Experimental Endocrinology of the Slovakian Academy of Sciences, Bratislava, Czechoslovakia were used. The animals were approximately 83 days of age and ranged in weight between 270-320 grams at the beginning of the experimental period. The rats were divided into three groups.

Flight (F): The flight animals were placed in earth orbit in individual cylindrical containers aboard a modified Soviet Vostok spacecraft for a period of 18.5 days.

Synchronous Control (S): The synchronous control rats were caged individually in a modified Vostok spacecraft and subjected to environmental conditions associated with launch, reentry, pressure, light cycle, air temperature, humidity etc. An attempt was made to simulate as closely as possible the spacecraft environment exposure by the flight animals.

Vivarium (V): The vivarium control rats were housed in animal quarters and not subjected to the flight conditions.

Following the experiment, the animals were sacrificed in three phases: A group of flight, synchronous and vivarium rats were sacrificed at the end of the 18.5 day flight period (shortly following ground landing

impact). A second and third group of rats was sacrificed 6 days post flight and a fourth group at 29 days post flight. The sacrifice schedule is shown in Table 1.

Table 1

Sacrifice Schedule - Flight, Synchronous, and Vivarium Rats

(R=space craft recovery)

Group	Group Number	Rat Number	Sacrifice Schedule	Number of Rats
Flight	1	F 1 - 7	R + 0	7
	2	F 8 - 13	R + 6	
	3*	F 14 - 20	R + 6	13
	4	F 21 - 25	R + 29	5
	Total number of rats = 25			
Synchronous	1	S 1 - 7	R + 0	7
	2	S 8 - 13	R + 6	
	3*	S 14 - 20	R + 6	13
	4	S 21 - 25	R + 29	5
	Total number of rats = 25			
Vivarium	1	V 1 - 7	R + 0	7
	2	V 8 - 13	R + 6	
	3*	V 14 - 20	R + 6	13
	4	V 21 - 25	R + 29	5
	Total number of rats = 25			

There are two groups of R+6 rats. Group Number 3(*) of the R+6 rats were handled differently than groups 1, 2, and 4. Group 3 rats underwent readaptation functional tests just following and for several days after spacecraft recovery. Since this group was handled differently than the others, the results of vertebral compression tests on this group of animals are not reported for R+6 or R+29.

The animals were decapitated at the end of the prescribed experimental period and their vertebral column and sacrum grossly dissected. The specimens were frozen, refrigerated, and forwarded to the AFAMRL. Upon arrival, each vertebral column was radiographed, the number of vertebral bodies in the respective thoracic and lumbar regions identified.

Preparation and Testing

The individual vertebral centra were disarticulated from one another by slicing through the mid section of the intervertebral disk, the articular capsules were sectioned and the vertebral bodies were cut away. Each vertebral centrum was cleaned of all soft tissue clinging to its surface. The individual vertebrae in the spinal column were assigned the following groupings.

Column Position	Assigned Vertebral Levels
P_1	T_2-T_3-T_4
P_2	T_5-T_6-T_7
P_3	T_8-T_9-T_{10}
P_4	T_{11}-T_{12}-L_1
P_5	L_2-L_3-L_4
P_6	L_5-L_6-L_7

The test matrix is shown in Table 2.

The Test Machine

Vertebral centra properties were determined by subjecting the specimens to simple compression loading using an Instron Model TTC-L; this screw gear test machine applies a load in compression by the motion of a movable crosshead. Details regarding the operation of the test machine are given in manufacturers catalogs.

For this particular test matrix the column groupings were assigned so that compression loading could be conducted at three separate and distinct loading rates. These rates were selected to be

$$8,467 \times 10^{-4} \text{ m/s} = 2.0 \text{ in/min}$$

$$4,233 \times 10^{-4} \text{ m/s} = 1.0 \text{ in/min}$$

$$4,233 \times 10^{-5} \text{ m/s} = 0.1 \text{ in/min}$$

K307 RAT TEST MATRIX

GROUP 1 GROUP 2 GROUP 3 GROUP 4 GROUP 5 GROUP 6 GROUP 7 GROUP 8 GROUP 9 GROUP 10 GROUP 11 GROUP 12

RATE 1 = 8.467×10⁻⁴ M/S   RATE 2 = 4.233×10⁻⁴ M/S   RATE 3 = 4.233×10⁻⁵ M/S

Table 2

The Force-Displacement Curve - Data Reduction Methodology

The values of stiffness, ultimate load, displacement to ultimate load, and energy to ultimate load were analyzed. Each of these parameters was defined and/or determined from individual load-displacement curves.

A typical load displacement curve is shown in Figure 1.
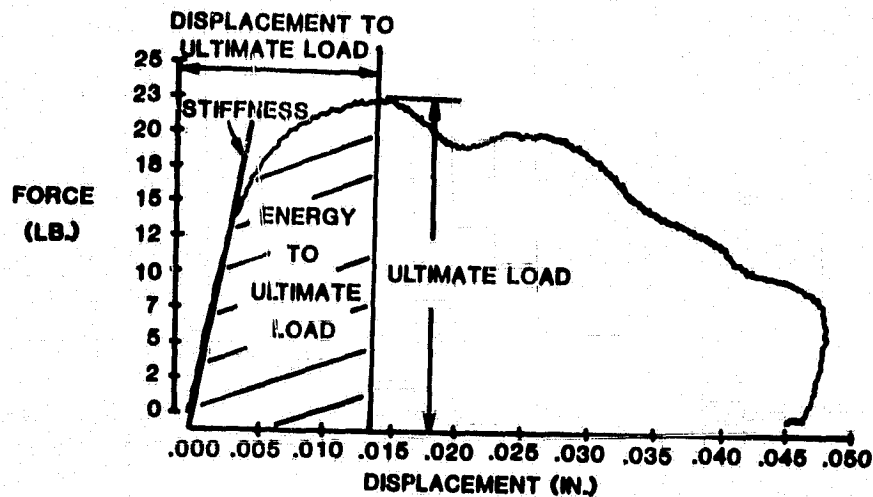
SUBJECT 10	=RAT R+63F5
COLUMN POSITION	=4
VB LEVEL	=11
DISPLACEMENT RATE	=2.009 IN./MIN.
MAXIMUM STRAIN	=0.3000 IN./IN.
SPECIMEN PRETEST LENGTH	=0.1500 IN.
SPECIMEN PRETEST AVERAGE AREA	=1.0200E-02 SQ.IN.

Figure 1

The test specimen load is plotted on the ordinate versus the cross head displacement on the abscissa. Each of the above material properties was extracted directly from the test curves.

The initial portion on the load-displacement curve, following the apparent elastic section, where the tangent to the curve becomes parallel to the displacement axis is defined as the ultimate load. Ultimate load has to do with the maximum compressive load developed by the specimen. The ultimate load can be looked upon as the load at which the specimen has become permanently deformed and/or structurally damaged. The displacement

at this point is defined as the _displacement to ultimate load_.

The _energy to ultimate load_ is defined as the area under the load versus displacement curve, from the point of zero displacement up to the displacement at ultimate load; the capacity of a specimen to absorb or store energy.

The specimen _stiffness_ (loading slope) is determined by fitting the apparent linear elastic section of the load displacement curve with a least squares linear fit. Stiffness has to do with the relative deformability of a specimen under load.

Statistical Analysis

Two procedures were used for analyzing the experimental results: (1) Analysis of variance (ANOVA) and (2) Duncan's Multiple Range test. The ANOVA was used to test for a difference in means among several different groups. If the ANOVA procedure indicated a difference, Duncan's multiple range test was used to give an indication of which groups differ from the others.

The groups for which differences were being analyzed were formed by different combinations of environment, spinal column position, and loading rate. Different types of differences were analyzed within these combinations and identified as interaction and main effects.

An interaction occurs when there is a difference in means for different values of one variable, but the difference depends on one or more of the other variables. For example, if for two loading rates the ultimate load were higher for the vivarium group than for the synchronous or flight group, but for the third loading rate the synchronous and flight groups were higher than the vivarium group, then we say there is an interaction between these two variables. (Note this is for explanatory purposes only.

235

This effect did not happen in the data.) If an interaction occurs, it does not make statistical significance to look at one of the variables involved without taking the others into account. For these data there could be two way interactions (two variables involved) or three way interactions (all three variables involved).

An interaction term reflects the fact that although a particular variable is statistically significant it is also related to, or interacts with, another variable to a high statistical significance. The smaller the number of inter-action terms associated with a particular material property, the easier the data can be interpreted.

Main effects are environment, column position and loading rate. That is, we are interested in whether or not each of these variables has an effect on the parameters measured, without regard to the other two. If the ANOVA procedure detects a difference, the effect was identified as a significant main effect.

Statistical analysis of the K-307 (COSMOS) vertebral body rate data was prepared on the following dependent material parameters:

1) Stiffness - N/M (Newton/Meters)

2) Ultimate Load - N (Newtons)

3) Displacement to Ultimate Load - M (Meters)

4) Energy to Ultimate Load - J (Joules)

For all parameters an analysis of variance table reflects those independent variables which were significant to the 95% level of confidence or above (α less than 0.05). The independent variables of environment (ENV), column position (CP) and loading rate (LR) were analyzed along with their associated cross-products or interaction terms (ENV*CP, ENV*LR, CP*LR, ENV*CP*LR).

236

RESULTS (R+0)

STIFFNESS

The stiffness analysis of variance data are presented in Table 3.

TABLE 3

ANALYSIS OF VARIANCE FOR STIFFNESS (N/M)

Source of Variation	Degrees of Freedom	Mean Square	F Ratio	Probability of > F
ENV	2	7.84227×10^{11}	6.98	< 0.01
AN(ENV)+	18	1.12319×10^{11}	2.00	0.01
CP	5	5.40023×10^{11}	9.60	< 0.01
LR	2	1.28709×10^{11}	2.29	0.10
ENV*CP	10	7.77499×10^{10}	1.38	0.19
ENV*LR	4	3.10750×10^{10}	0.55	0.70
CP*LR	10	8.65246×10^{10}	1.54	0.13
ENV*CP*LR	20	5.43643×10^{10}	0.97	0.50
ERROR	281	5.62702×10^{10}		

+AN(ENV) mean square was used as the error term to compute the ENV F ratio.

The effects due to both environment and column position were significant at the α = .01 level. The loading rate effect was not significant and there were no significant interaction terms. Further analysis of the stiffness means using the Duncan's Multiple Range test showed that at the α = .05 level, the flight and synchronous means were significantly larger than the vivarium mean. Very little difference in stiffness was noted between the flight and synchronous groups. Similarly, the mean stiffness for the first three column positions (P_1, P_2 and P_3) was significantly greater than for the last three column positions (P_4, P_5 and P_6). These results

are illustrated in Figure 2, which is a plot of average stiffness over all loading rates for the flight, synchronous, and vivarium groups for each column position.

RAT VERTEBRAL BODIES - K307 R-0 OVER ALL LOADING RATES
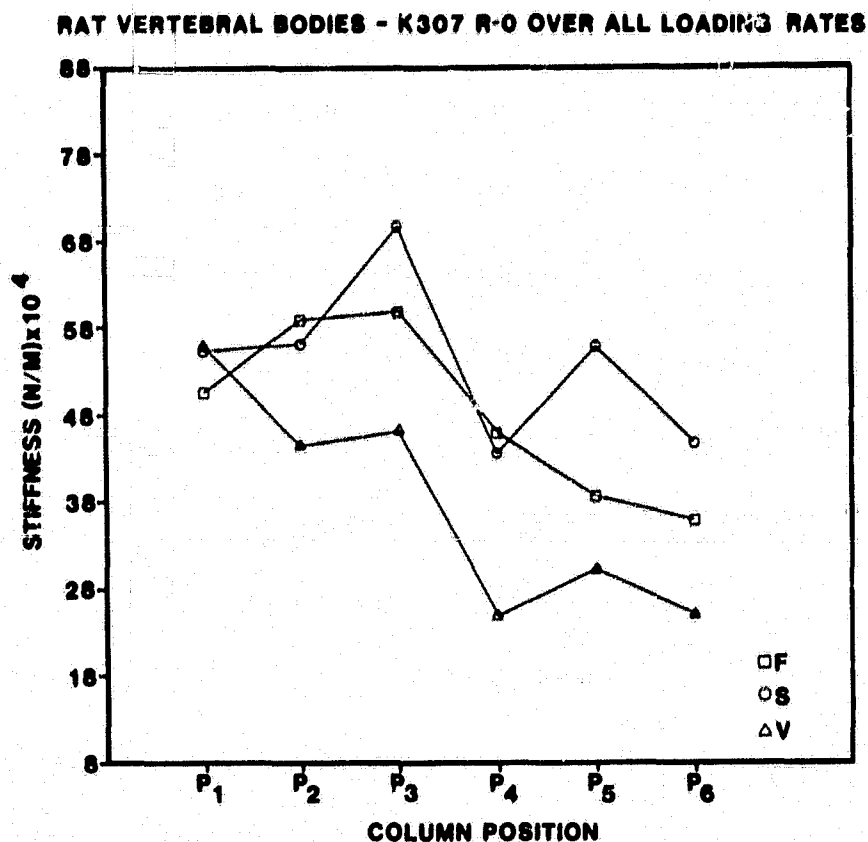
Figure 2

The plots in Figure 2 are in agreement with the above statistical results, excepting for the first column position (P_1). For this column position the vivarium and synchronous rats constantly exhibited larger stiffness values than the flight rats. The values of stiffness appear to decrease with increasing column position; however, this decrease in stiffness is not consistent over all column positions. Rather, it appears that stiffness as a function of column position can be divided into two levels, with the first three column positions (P_1, P_2 and P_3) at one

level and the last three (P_4, P_5 and P_6) at a second sharply lower level. (The geometry of the vertebral bodies also exhibits a comparative change at these levels. The vertebral bodies at the P_1, P_2, P_3 levels are comparatively shorter than those in the lower spinal column.)

ULTIMATE LOAD

The ultimate load analysis of variance data are presented in Table 4.

TABLE 4

ANALYSIS OF VARIANCE FOR ULTIMATE LOAD (N)

Source of Variation	Degrees of Freedom	Mean Square	F Ratio	Probability of > F
ENV	2	43642.32	10.15	< 0.01
AN(ENV)+	18	4298.08	6.28	< 0.01
CP	5	56718.74	82.92	< 0.01
LR	2	22122.39	32.34	< 0.01
ENV*CP	10	1140.13	1.67	0.09
ENV*LR	4	599.98	0.88	0.48
CP*LR	10	606.69	0.89	0.55
ENV*CP*LR	20	375.57	0.55	0.94
ERROR	281	684.04		

+AN(ENV) mean square was used as the error term to compute the ENV F ratio.

The effects due to environment, loading rate and column position were significant. Further testing of the ultimate load means using the Duncan's Multiple Range test indicated the following at the α = .05 level.

(a) the vivarium mean was significantly larger than the synchronous mean which in turn was significantly larger than the flight

mean,

(b) the ultimate load means for the two larger loading rates (R_1 = 8.467 x 10^{-4} and R_2 = 4.233 x 10^{-4} meters/second) were significantly larger than the ultimate load mean for the slowest loading rate (R_3 = 4.233 x 10^{-5} meters/second),

(c) the column position ultimate load means were approximately the same for P_1 and P_2 but increased significantly for each of the remaining column positions (P_1 = P_2 < P_3 < P_4 < P_5 < P_6).

These results are presented in Figure 3 which is a plot of average ultimate load over all loading rates for each vertebral level and for environment at each column position.

RAT VERTEBRAL BODIES – K307 R+O OVER ALL LOADING RATES
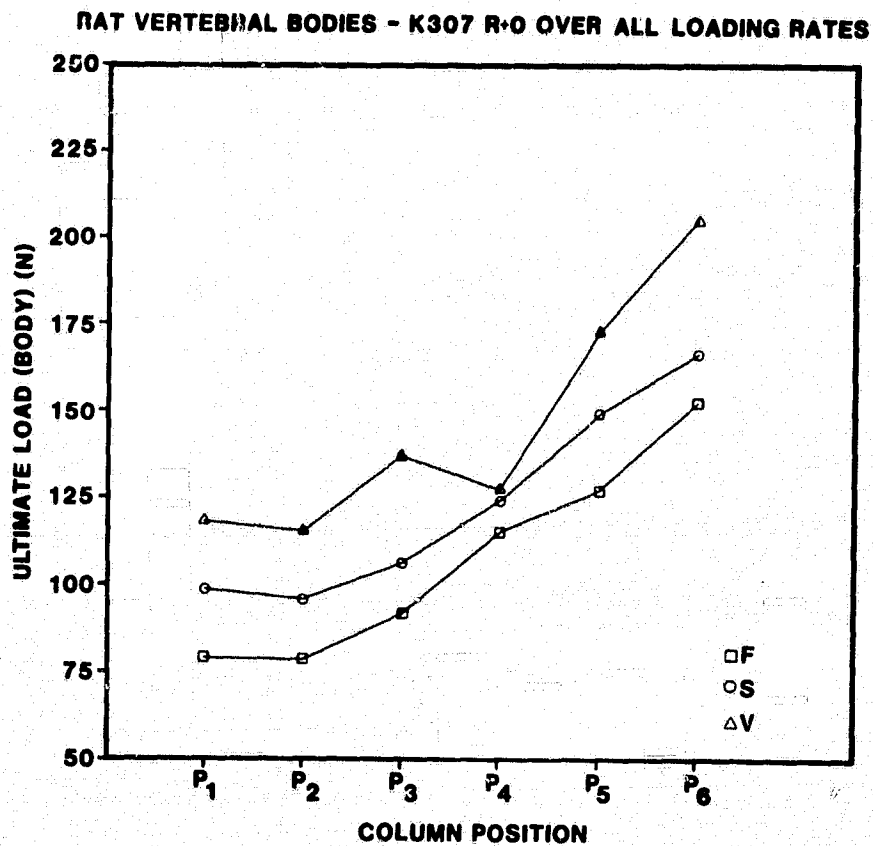
Figure 3

Figure 4 which is a plot of average ultimate load over all environments for each level of loading rate at each column position.

RAT VERTEBRAL BODIES - K307 R·O OVER ALL ENVIRONMENTS
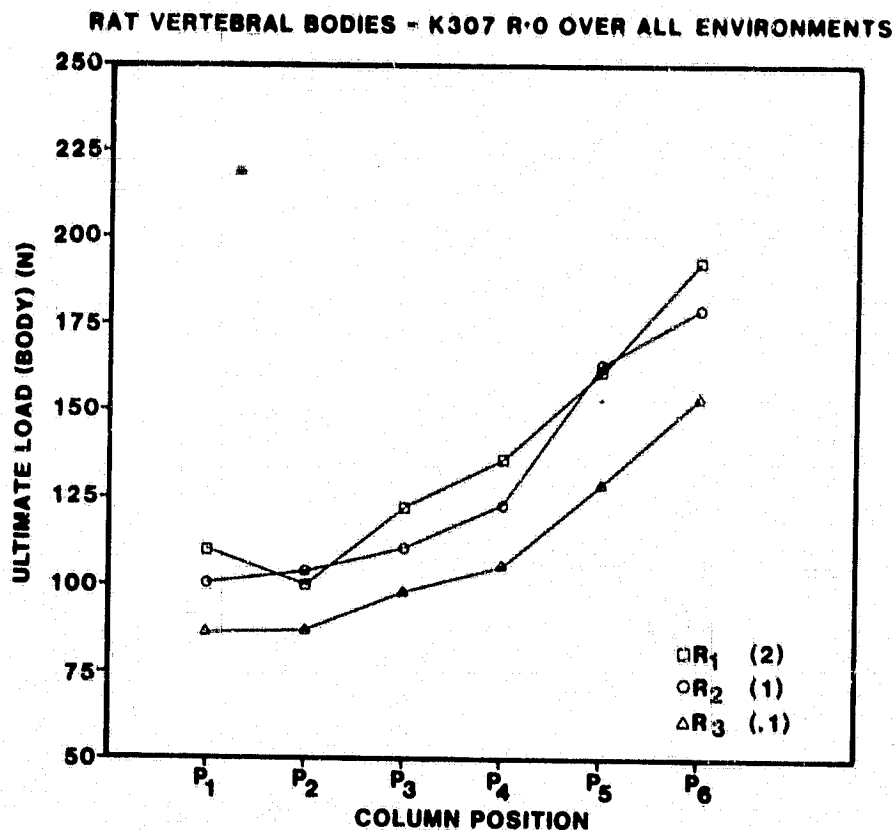
Figure 4

Figures 3 and 4 are consistent with the statistical results. Figure 3 indicates that ultimate load was the lowest for the flight vertebrae and the highest for the vivarium vertebrae with the synchronous data falling approximately midway in between. Figure 4 shows that the ultimate load was loading rate sensitive, that is, the ultimate load for the R_3 loading rate was clearly less than the ultimate load for the two larger loading rates (R_1 and R_2). Loading rate R_1 was only a factor or two larger than R_2. This difference was insufficient to demonstrate a significant change in the resulting ultimate load.

241

Both figures clearly illustrate that vertebral body ultimate load increases from column positions P_1 to P_6. The results indicate a decrease in bone strength for the flight and synchronous groups. 13.5 days of space flight appears to weaken bone structure.

DISPLACEMENT TO ULTIMATE LOAD

The displacement to ultimate load analysis of variance data are presented in Table 5.

TABLE 5

ANALYSIS OF VARIANCE FOR DISPLACEMENT TO ULTIMATE LOAD (M)

Source of Variation	Degrees of Freedom	Mean Square	F Ratio	Probability of > F
ENV	2	6.140×10^{-7}	9.56	< 0.01
AN(ENV)	18	6.440×10^{-8}	2.24	< 0.01
CP	5	2.602×10^{-6}	90.58	< 0.01
LR	2	4.750×10^{-7}	16.60	< 0.01
ENV*CP	10	3.300×10^{-8}	1.14	0.34
ENV*LR	4	5.500×10^{-8}	1.92	0.11
CP*LR	10	6.100×10^{-8}	2.11	0.02
ENV*CP*LR	20	2.550×10^{-8}	0.88	0.61
ERROR	280	3.0×10^{-8}		

+AN(ENV) mean square was used as the error term to compute the ENV F ratio.

The effects due to environment, and to the interaction between column position and loading rate were significant. Because of this interaction, the effects of loading rate and column position were not considered separately. Testing of the displacement to ultimate load means, using the Duncan's Multiple Range test at the α = .05 significance level, showed that

the displacement to ultimate load for the vivarium rats was significantly greater than for the synchronous or flight rats.

The significant interaction means that, although both loading rate and column position effects were significant, the displacement to ultimate load did not respond the same over column position for the three loading rates. That is, displacement to ultimate load response over column position was dependent on loading rate. Because of this loading rate dependence, the displacement to ultimate load data were not averaged over all loading rates. The effect of environment at each loading rate is presented in Figures 5, 6, and 7.

RAT VERTEBRAL BODIES - K307 R+O AT LR=8.467E-04 M/S

Figure 5

243
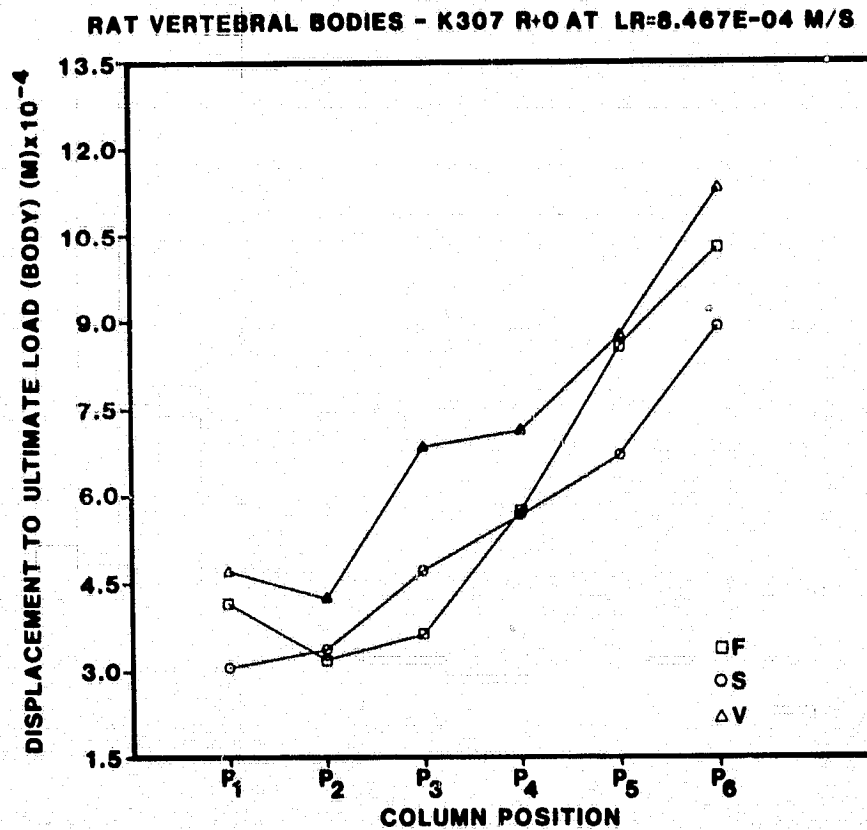
RAT VERTEBRAL BODIES – K307 R+0 AT LR-4.233E-05 M/8
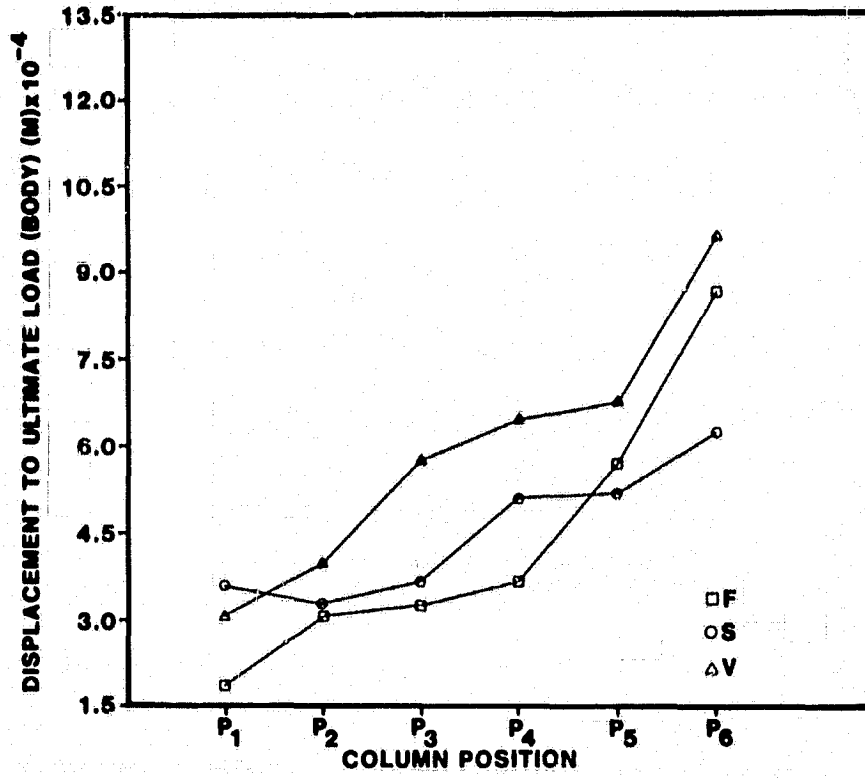
Figure 6

RAT VERTEBRAL BODIES – K307 R+0 AT LR-4.233E-04 M/S

Figure 7

244
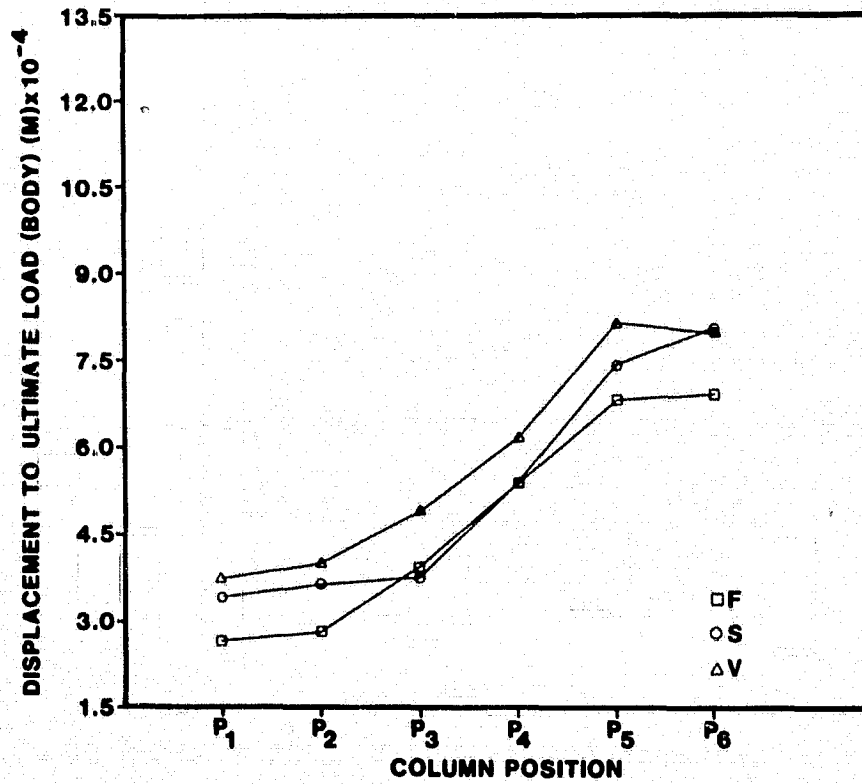
The displacement to ultimate load was consistently larger for the vivarium vertebrae. The overall mean displacements for synchronous and flight were approximately the same; no consistent trends were evident.

The inconsistent slope of the response curve from column positions 5 to 6 in these three plots is typical of the type response which will result in a significant interaction between column position and loading rate. That is, the three slopes for the two extreme loading rates (fastest and slowest) are reasonably consistent; however, the slopes for the 4.233×10^4 meters per second loading rate show a very different rate of change of displacement with column position. The effects of loading rate is shown in Figure 8 which is a plot of displacement to ultimate load versus column position for each loading rate averaged over all environments.

RAT VERTEBRAL BODIES - K307 R+O OVER ALL ENVIRONMENTS

Figure 8

245
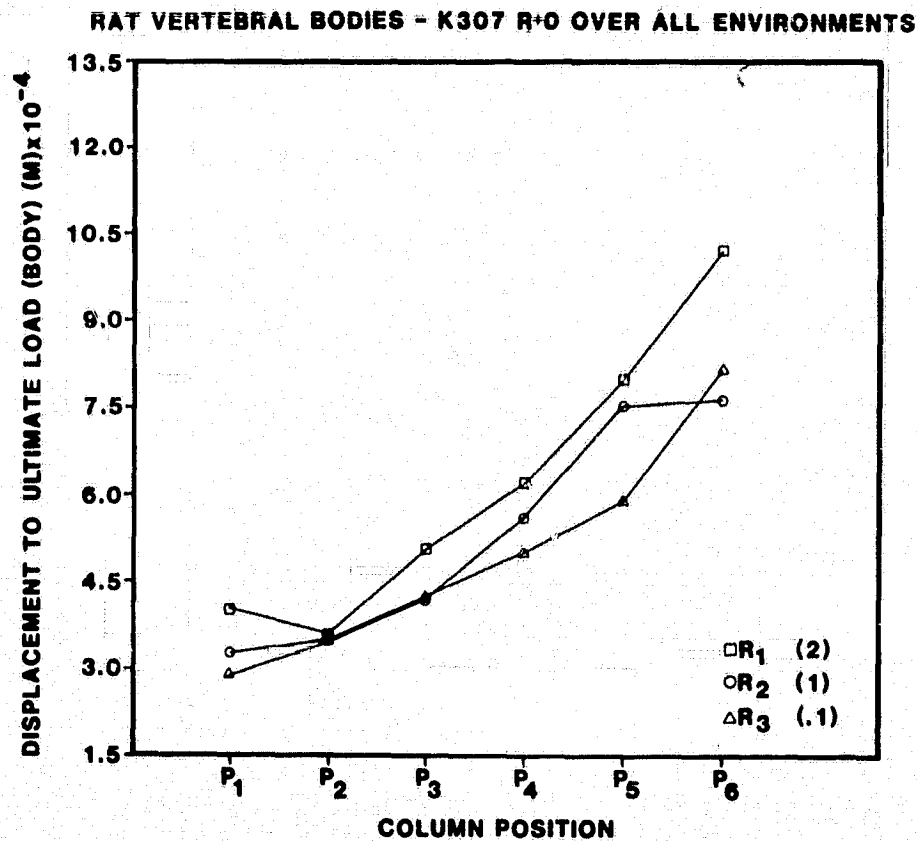
The displacement for the 8.467 x 10^4 meters/second loading rate was greater than for the two slower loading rates. All four figures clearly demonstrate the increase in displacement with increasing column position. These results also show that less displacement was necessary to fail the hypogravity exposed rats indicating a loss in bone strength which correlates to the ultimate load results.

ENERGY TO ULTIMATE LOAD

The energy to ultimate load analysis of variance data are presented in Table 6.

TABLE 6

ANALYSIS OF VARIANCE FOR ENERGY TO ULTIMATE LOAD (JOULE)

Source of Variation	Degrees of Freedom	Mean Square	F Ratio	Probability of > F
ENV	2	1.31144 x 10^{-2}	7.81	< 0.01
AN(ENV)	18	1.67845 x 10^{-3}	2.47	< 0.01
CP	5	5.34479 x 10^{-2}	78.57	< 0.01
LR	2	1.34479 x 10^{-2}	21.45	< 0.01
ENV*CP	10	5.43855 x 10^{-4}	0.80	0.63
ENV*LR	4	3.22155 x 10^{-4}	0.47	0.76
CP*LR	10	1.73723 x 10^{-3}	2.55	< 0.01
ENV*CP*LR	20	5.15330 x 10^{-4}	0.76	0.76
ERROR	280	6.8024 x 10^{-4}		

+AN(ENV) mean square was used as the error term to compute the ENV F ratio.

The effects due to environment and the interaction of loading rate and column position were significant. Further testing of the energy to ultimate load means, using the Duncan's Multiple Range test at the α = .05

significance level, showed that the energy to ultimate load for the vivarium and sychronous vertebrae was significantly greater than for the flight vertebrae. The effects of environment are presented in Figures 9, 10, and 11.

RAT VERTEBRAL BODIES – K307 R+O AT LR=8.467E-04 M/S
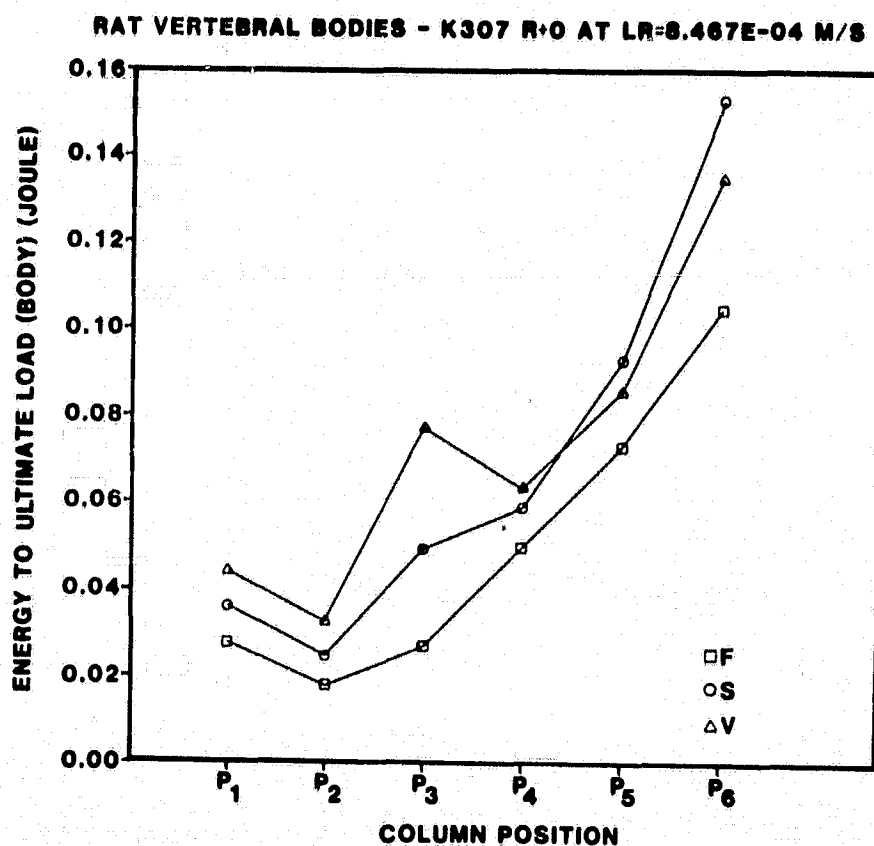
Figure 9

RAT VERTEBRAL BODIES – K307 R·0 AT LR=4.233E–04 M/S
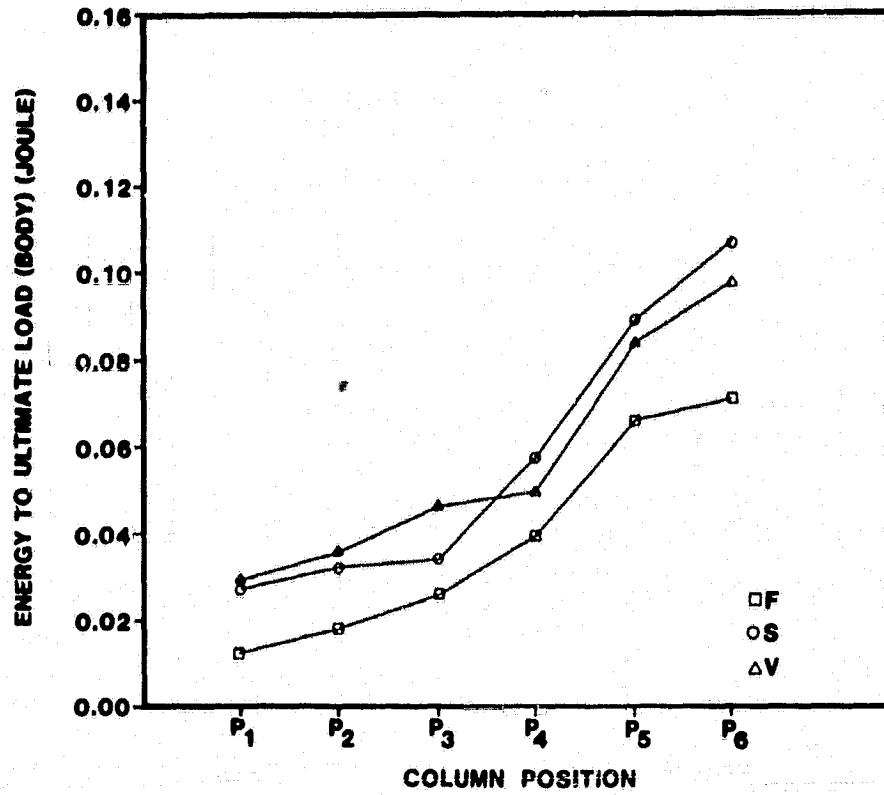
Figure 10

RAT VERTEBRAL BODIES – K307 R+0 AT LR=4.233E–05 M/S

Figure 11

248
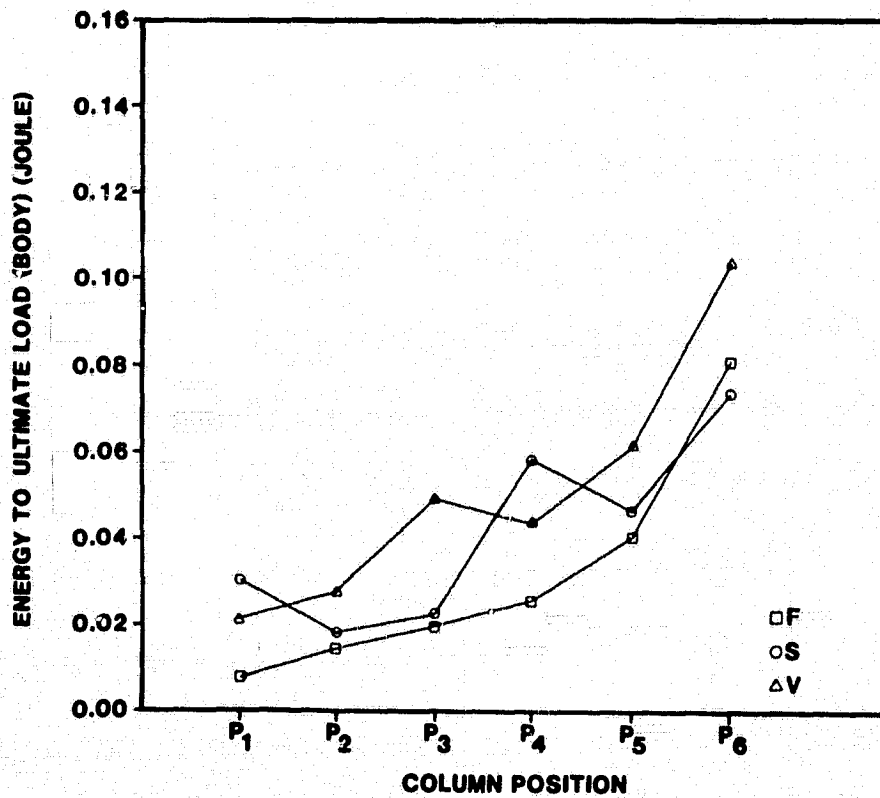
Due to the loading rate interaction with column position, a separate plot is presented for each loading rate. The energy to ultimate load for the vivarium and synchronous vertebrae were inconsistent over loading rate and column position; however, the energy for both was greater than for the flight vertebrae.

These three plots provide a good graphic demonstration of the meaning of a significant interaction. In general, energy to ultimate load increases with column position and also with increasing loading rate; however, this increase is not consistent over all column positions and loading rates. This is evident from the wide variation in the slope of the corresponding curves at each loading rate. The effect of loading rate is presented in Figure 12 which is a plot of energy to ultimate load for each loading rate averaged over all environments.

RAT VERTEBRAL BODIES - K307 R+O OVER ALL ENVIRONMENTS
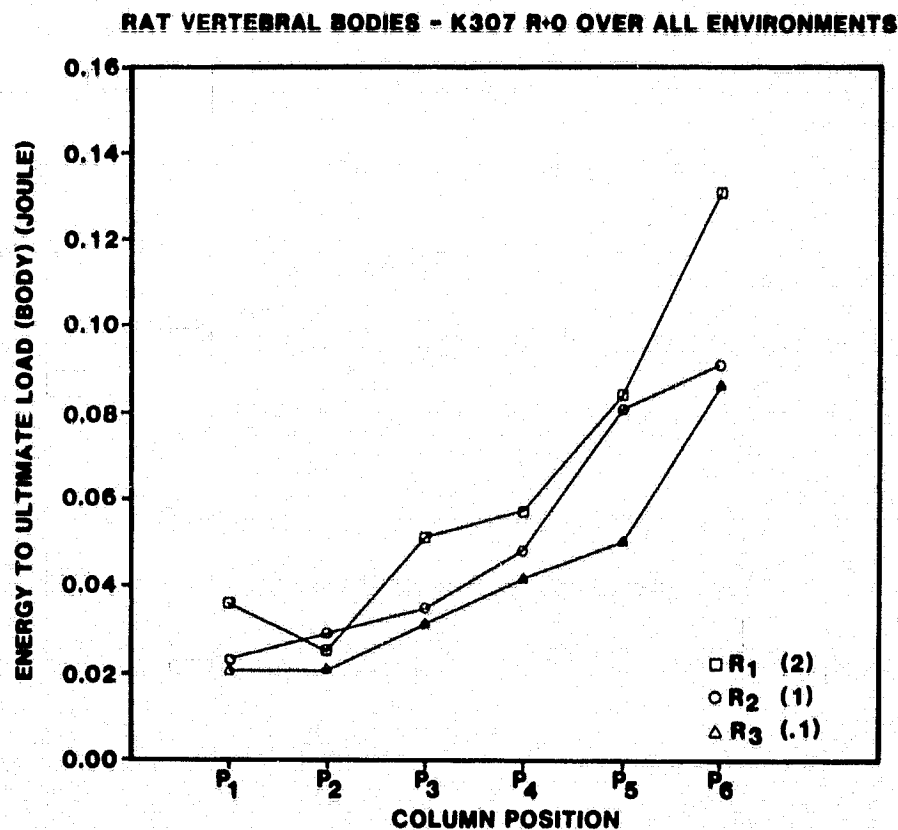
Figure 12

This plot shows that the energy increases with increasing loading rate.

All four figures show that energy increases with column position. In all cases the vivarium group required more energy to ultimate load failure than the flight groups. The synchronous group was not conclusive, but averaged between the flight and vivarium groups. These results correlate with the previous parameter analysis, in that there was a probable loss of bone strength due to space flight since less energy was required to fail the flight specimens.

RECOVERY TIME EFFECTS

Due to the number of recovery time/environment interaction effects that were statistically significant in the R+0 analysis, it was decided to break the data down into three groups by environment. This can be done since the data showed that environment had a statistically significant effect on the rat vertebral strength. The previous (R+0) original analysis indicated a decrease in bone strength for the Flight and Synchronous groups. One additional change was also made to the original test matrix. Test group 3 consisting of seven rats was removed from each of the three environments at the R+6 recovery period. This resulted in a more balanced test matrix whereby seven rats were run at R+0, six at R+6 and five at R+25.

ULTIMATE LOAD

Only the material property of ultimate load is presented. The other material properties also indicated significant recovery time effects, but are not presented in this report to simplify the analysis. For ultimate load, an analysis-of-variance table reflects those independent variables which were significant to the 95% level of confidence or above (α less than 0.05). The independent variables of

250

recovery time (RT), column position (CP) and loading rate (LR) were analyzed along with their associated interaction terms (RT*LR, RT*CP, CP*LR, RT*CP*LR). The following summarize the results within the three environments of vivarium, synchronous and flight.

VIVARIUM

The ultimate load analysis of variance data for the V group is shown in Table 7.

TABLE 7

ANALYSIS OF VARIANCE FOR VIVARIUM GROUP ULTIMATE LOAD (N)

Source of Variation	Degrees of Freedom	Mean Square	F Ratio	Probability of > F
RT	2	378.88	0.07	0.9286
AN(RT)+	15	5092.25	4.84	0.0001
LR	2	18269.92	17.36	0.0001
CP	5	70186.16	66.69	0.0001
RT*LR	4	190.34	0.18	0.9482
RT*CP	10	1039.52	0.99	0.4547
CP*LR	10	781.03	0.74	0.6843
RT*CP*LR	19	918.42	0.87	0.6177
ERROR	233	1052.35		

+AN(RT) mean square was used as the error term to compute the RT F ratio.

The main effects due to loading rate and column position were all significant at the 95% level of confidence. These results are presented

in Figure 13, which is a plot of average ultimate load over all loading rates for each level of recovery time, at each column position, and Figure 14, which is a plot of average ultimate load over all recovery times, for each level of loading rate, at each column position.
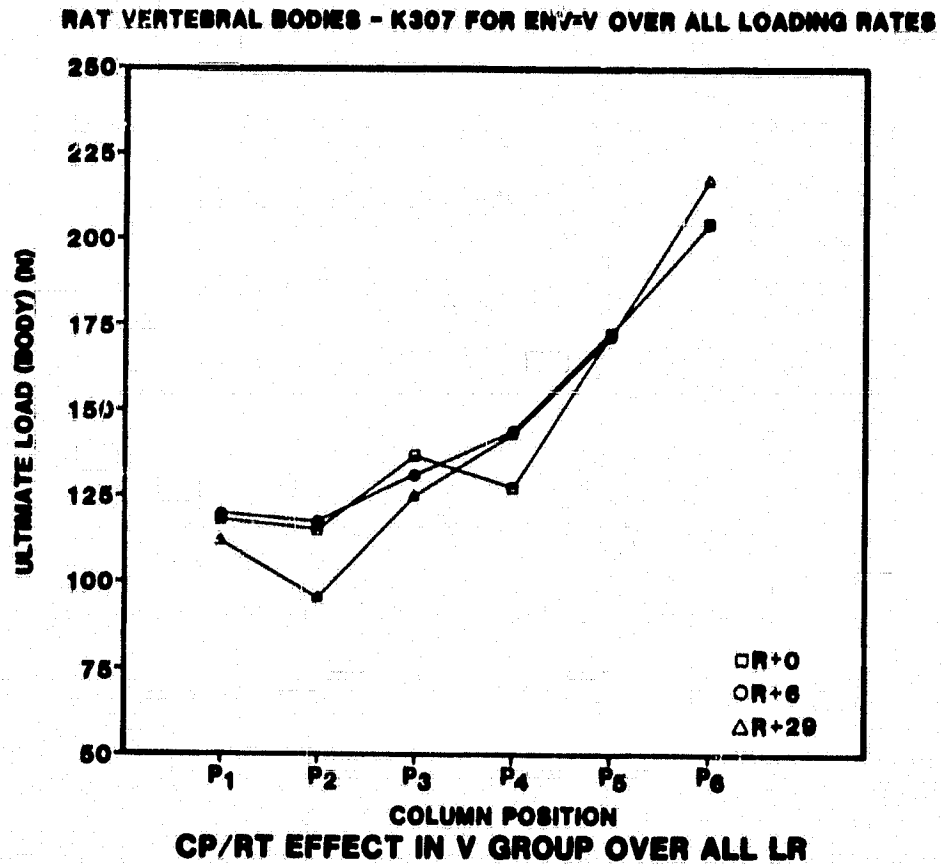
RAT VERTEBRAL BODIES - K307 FOR ENV=V OVER ALL LOADING RATES

Figure 13

LR/CP EFFECT IN V GROUP OVER ALL RT
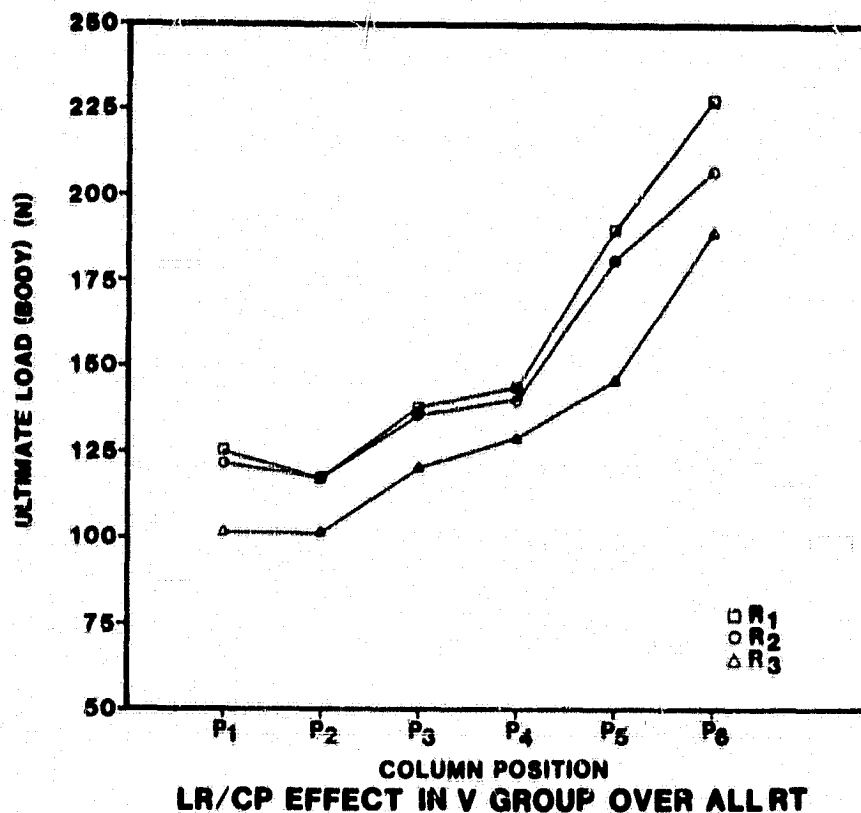
Figure 14

Figures 13 and 14 are consistent with the statistical results. Figure 13 shows, as would be expected since the vivarium group is a control group, that there is no significant effect due to recovery time since the R+0, R+6, and R+29 curves are essentially the same. Figure 14 shows that the ultimate load was loading rate sensitive. The ultimate load for the slowest rate (R_3) was clearly less than the two larger loading rates (R_1 and R_2). Loading rate R_1 was only a factor of two larger than R_2. This difference was insufficient to demonstrate a significant change in the resulting ultimate load. Both figures clearly illustrate how vertebral body ultimate load increases from column position P_1 to P_6.

SYNCHRONOUS

The ultimate load analysis of variance data for the Synchronous group is shown in Table 8.

TABLE 8

ANALYSIS OF VARIANCE FOR SYNCHRONOUS GROUP ULTIMATE LOAD (N)

Source of Variation	Degrees of Freedom	Mean Square	F Ratio	Probability of > F
RT	2	43865.11	4.84	0.0232
AN(RT)+	15	8975.12	13.87	0.0001
LR	2	24320.11	37.59	0.0001
CP	5	59934.23	92.63	0.0001
RT*LR	4	534.26	0.83	0.5094
RT*CP	10	2281.26	3.53	0.0002
CP*LR	10	1317.08	2.04	0.0307
RT*CP*LR	20	580.78	0.90	0.5904
ERROR	235	646.99		

+AN(RT) mean square was used as the error term to compute the RT F ratio.

There were no independent significant main effects, but there were significant interaction effects between recovery time and column position, and loading rate and column position. These interaction effects were significant to the 95% level of confidence (α = 0.05).

The RT*CP interaction effect is presented in Figures 15, 16, and 17.

RAT VERTEBRAL BODIES – K307 FOR ENV=S AT LR=8.467E-04 M/S

RT/CP EFFECT FOR S GROUP
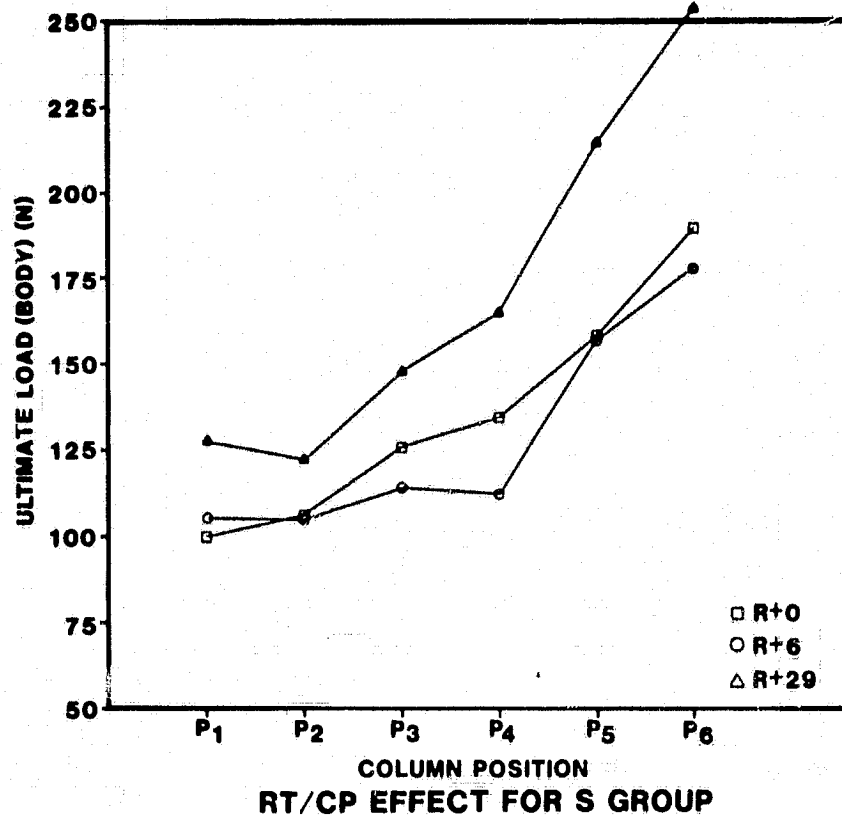
Figure 15

RAT VERTEBRAL BODIES – K307 FOR ENV=S AT LR=4.233E-04 M/S

RT/CP EFFECT FOR S GROUP

Figure 16

255

RAT VERTEBRAL BODIES - K307 FOR ENV-S AT LR=4.233E-05 M/S

RT/CP EFFECT FOR S GROUP
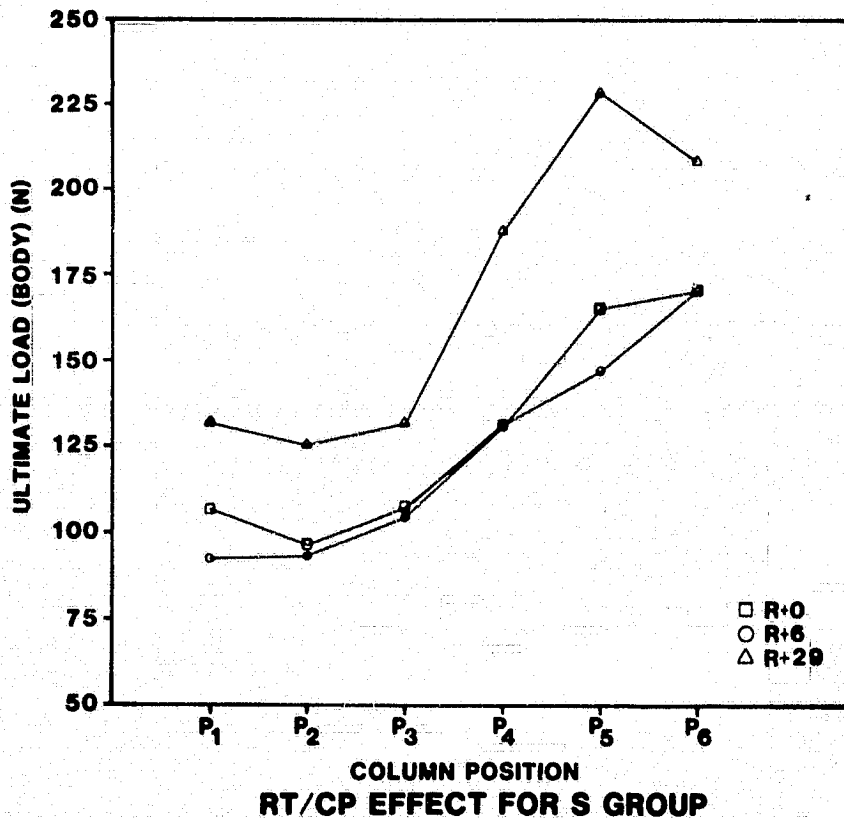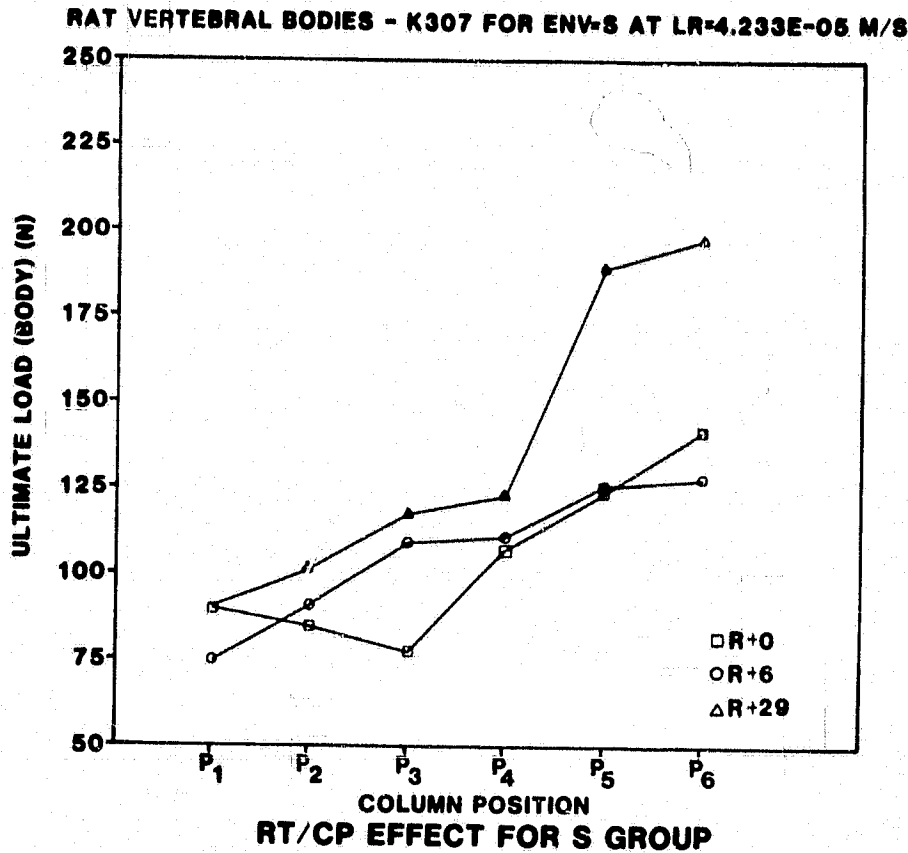
Figure 17

Because of the additional interaction terms of LR*CP the effect of RT data can not be averaged over all loading rates, but must be presented as separate plots at each of the three loading rates of R_1, R_2, and R_3 ($R_1 = 8.467 \times 10^{-4}$ M/S, $R_2 = 4.233 \times 10^{-4}$ M/S, $R_3 = 4.233 \times 10^{-5}$ M/S). The ultimate load at R+29, in all cases, was greater than the ultimate load at R+6, and R+0. The ultimate load data at R+6 was inconclusive, since it varied above and below the R+0 ultimate load curve. These curves indicate that an increase in bone strength, relative to the R+0 level, was apparent at the R+29 level. These curves also demonstrate the increase in ultimate load with increasing column position.

The LR*CP interaction effect is presented in Figures 18, 19, and 20.

RAT VERTEBRAL BODIES - K307 FOR ENV=S AT R+0

LR/CP EFFECT FOR S GROUP
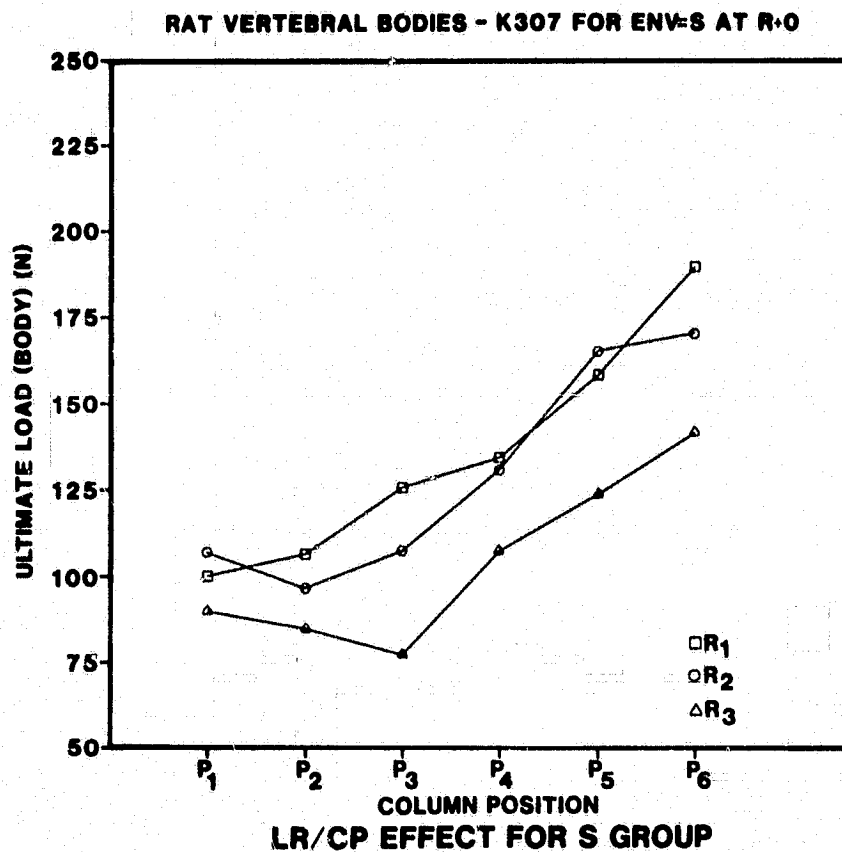
Figure 18

RAT VERTEBRAL BODIES - K307 FOR ENV=S AT R+6

LR/CP EFFECT FOR S GROUP
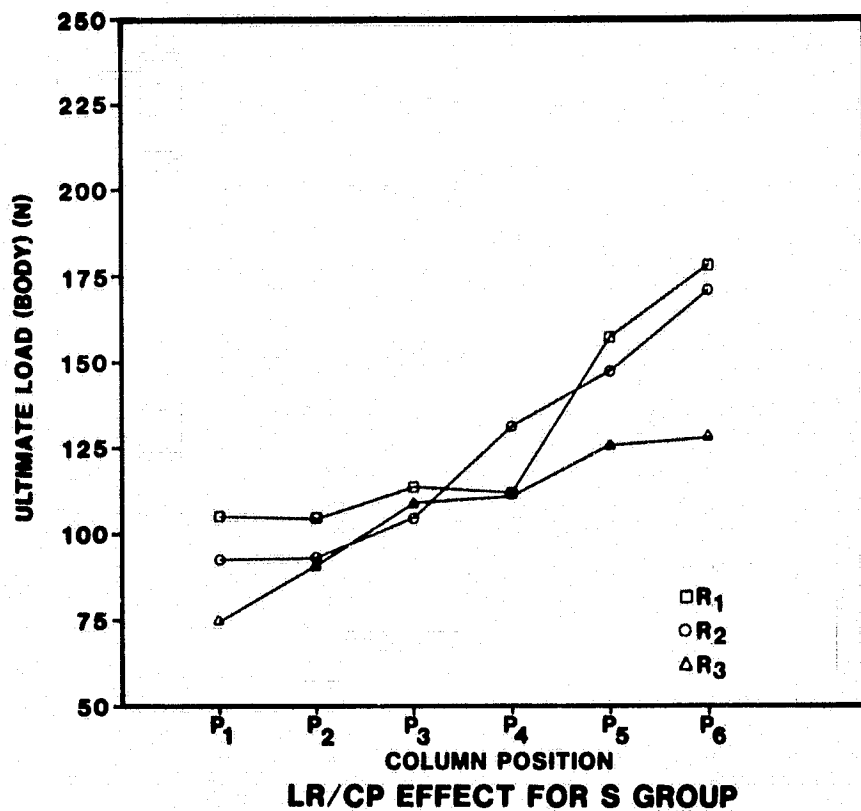
Figure 19

RAT VERTEBRAL BODIES - K307 FOR ENV=S AT R+29

LR/CP EFFECT FOR S GROUP

Figure 20

258
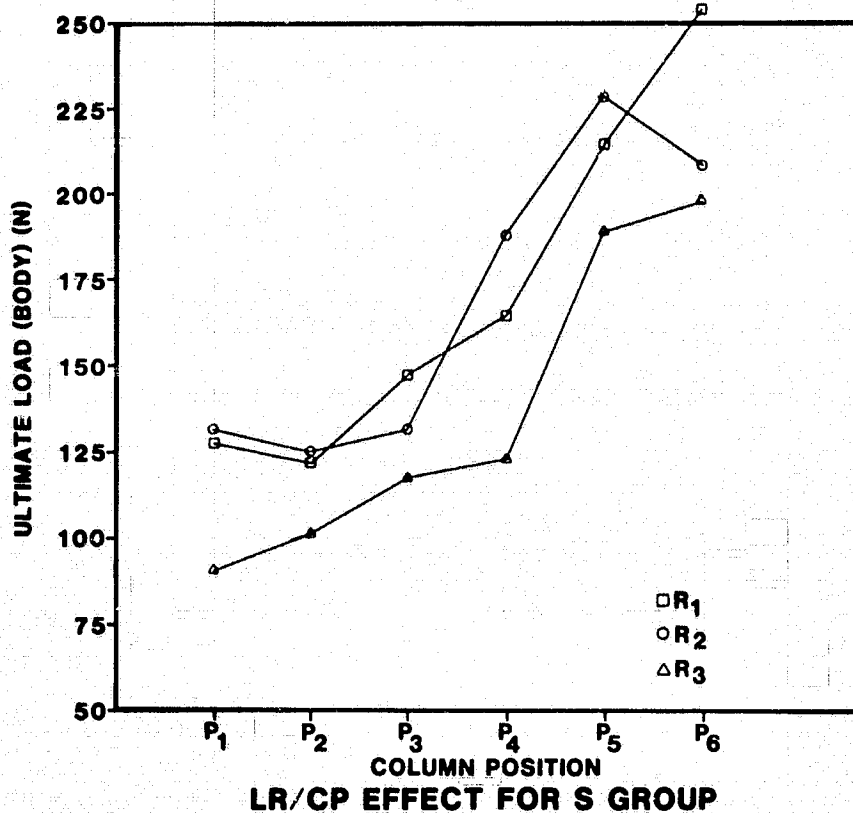
Again, because of the additional interaction term of RT*CP, the effect of loading rate can not be averaged over all recovery times, but must be presented as separate plots at each RT level (R+0, R+6, R+29). The ultimate load was lowest at the R_3 loading rate, while the R_1 and R_2 loading rates showed an ultimate load greater than that at R_3. No conclusive trends were noted between R_1 and R_2 loading rates. These plots also show the increase in ultimate load as column position increased from P_1 to P_6.

FLIGHT

The ultimate load analysis of variance data for the Flight group is shown in Table 9.

TABLE 9

ANALYSIS OF VARIANCE FOR FLIGHT GROUP ULTIMATE LOAD (N)

Source of Variation	Degrees of Freedom	Mean Square	F Ratio	Probability of > F
RT	2	11293.95	4.21	0.0355
AN(RT)	15	2685.34	5.87	0.0001
LR	2	15059.84	32.92	0.0001
CP	5	55508.96	121.35	0.0001
RT*LR	4	1117.04	2.44	0.0475
RT*CP	10	1243.09	2.72	0.0035
CP*LR	10	732.59	1.60	0.1069
RT*CP*LR	20	274.45	0.60	0.9110
ERROR	236	475.43		

+AN(RT) mean square was used as the error term to compute the RT F ratio.

There were no independent significant main effects, but there were significant interaction effects between recovery time and column position, and recovery time and loading rate. These interaction effects were all significant to the 95% level of confidence ($\alpha = 0.05$).

The RT*CP interaction effect is shown in Figures 21, 22, and 23.

RAT VERTEBRAL BODIES - K307 FOR ENV=F AT LR=8.467E-04 M/S
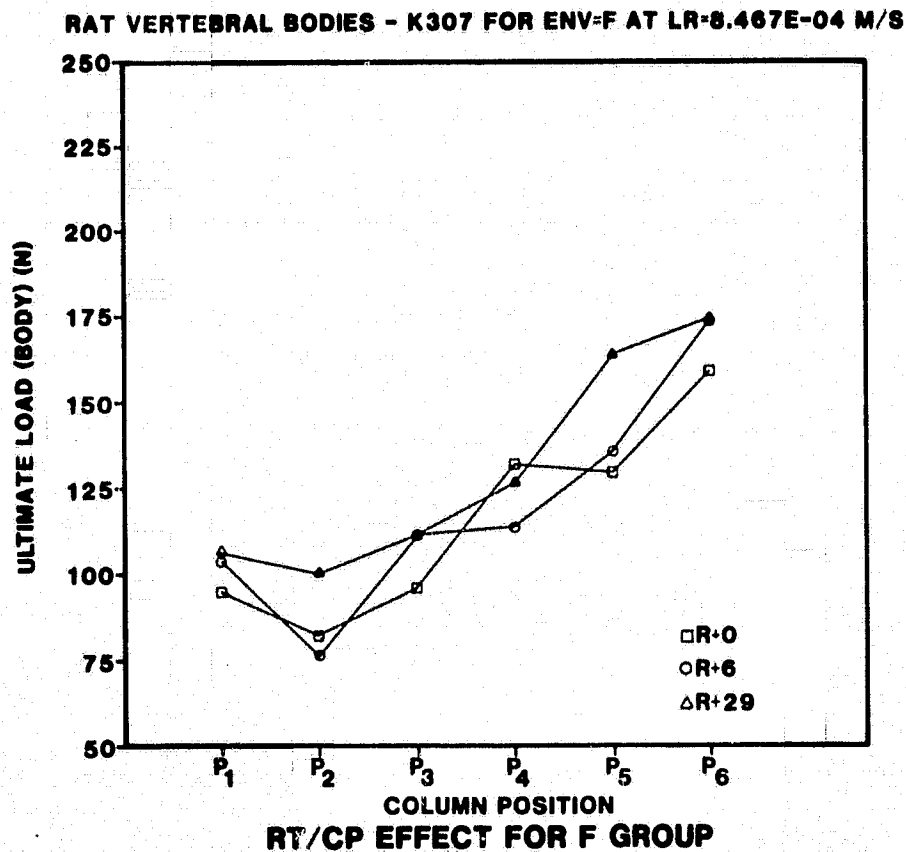
Figure 21

RAT VERTEBRAL BODIES - K307 FOR ENV=F AT LR=4.233E-04 M S

RT/CP EFFECT FOR F GROUP
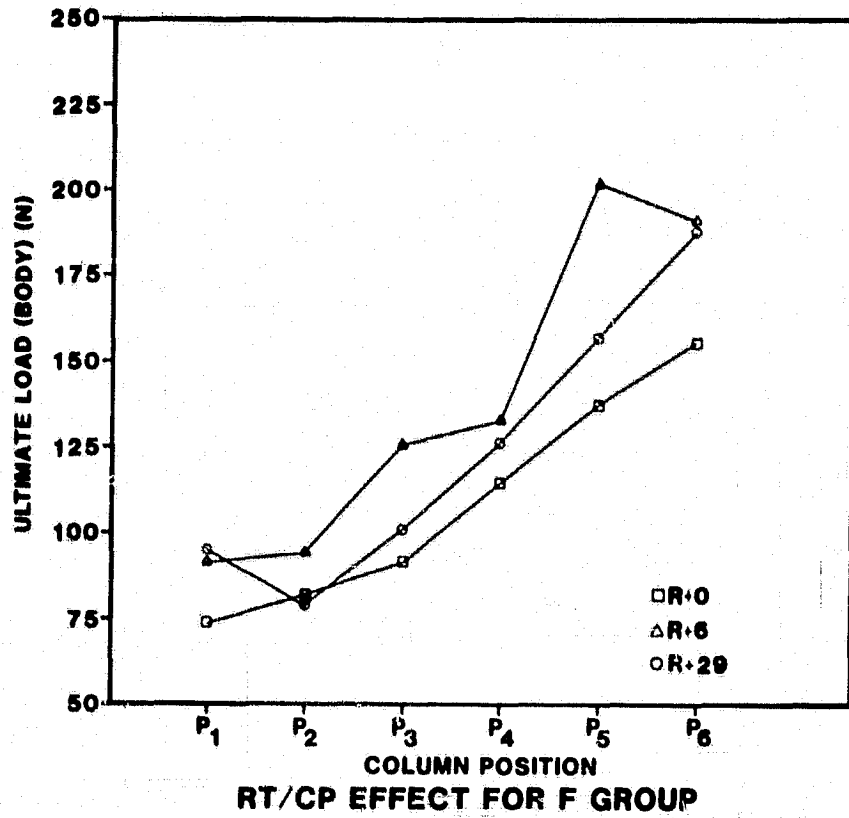
Figure 22

RAT VERTEBRAL BODIES - K307 FOR ENV=F AT LR=4.233E-05 M/S

RT/CP EFFECT FOR F GROUP

Figure 23

261
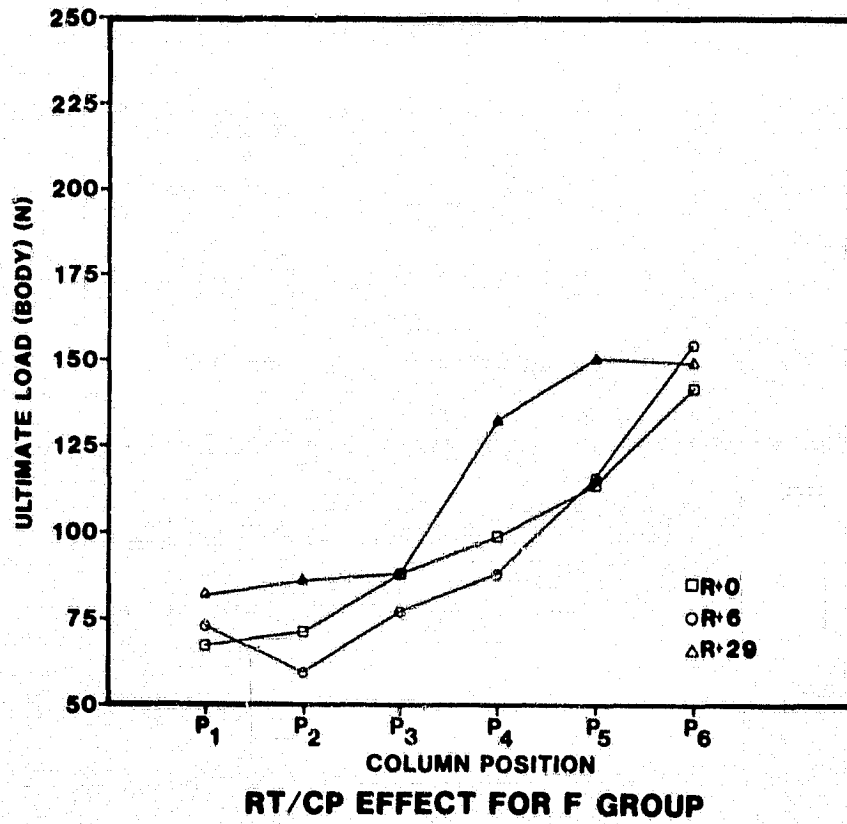
Because of the additional interaction term of RT*LR the effect of RT can not be averaged over all loading rates, but must be presented as separate plots at each of the three loading rates. The ultimate load at R+29 was greater than the ultimate load at R+6, and R+0. However, the ultimate load data at the R+6 level was inconclusive, since it varied above and below the R+0 ultimate load curve. As with the synchronous data, these plots indicate an increase in bone strength, relative to the R+0 level, at R+29. These curves also demonstrate the increase in ultimate load with increasing column position.

The RT*LR interaction effect is presented in Figures 24 thru 29.

RAT VERTEBRAL BODIES - K307 FOR ENV=F FOR CP=1

RT/LR EFFECT FOR F GROUP
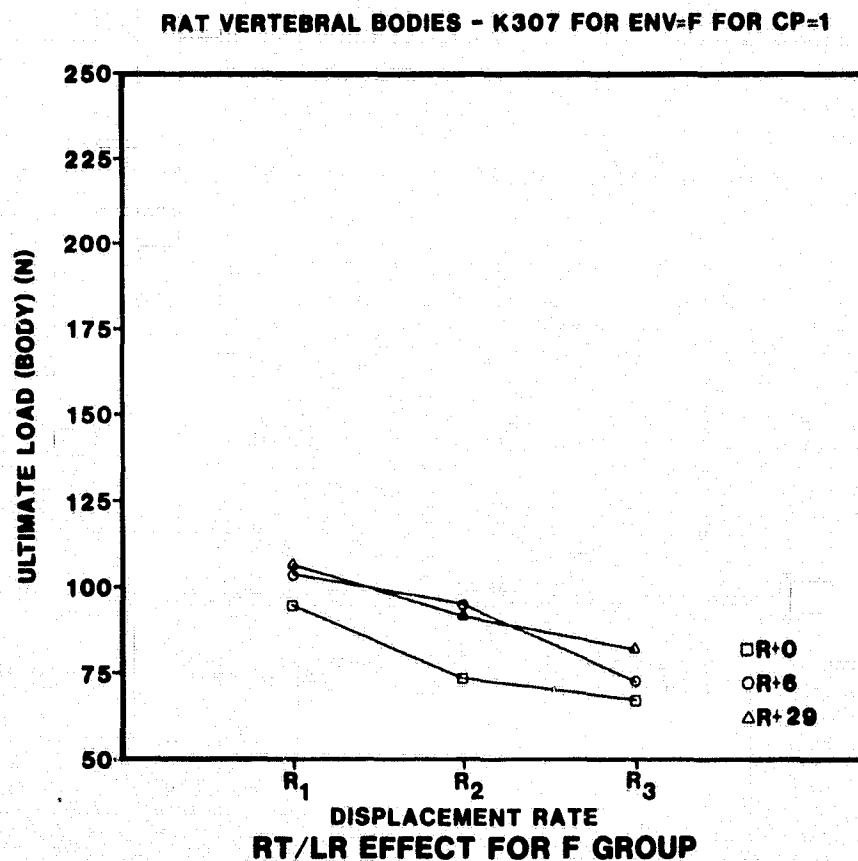
Figure 24

RAT VERTEBRAL BODIES - K307 FOR ENV=F FOR CP=2

ULTIMATE LOAD (BODY) (N)

DISPLACEMENT RATE

RT/LR EFFECT FOR F GROUP

☐R+0
○R+6
△R+29
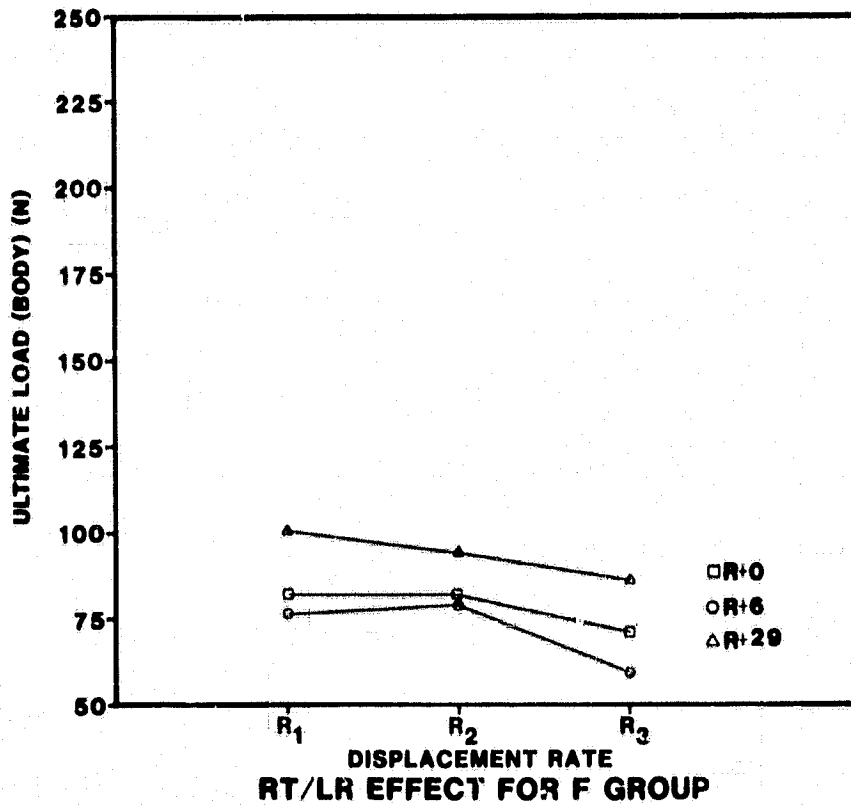
Figure 25

RAT VERTEBRAL BODIES - K307 FOR ENV=F FOR CP=3

ULTIMATE LOAD (BODY) (N)

DISPLACEMENT RATE

RT/LR EFFECT FOR F GROUP

☐R+0
○R+6
△R+29
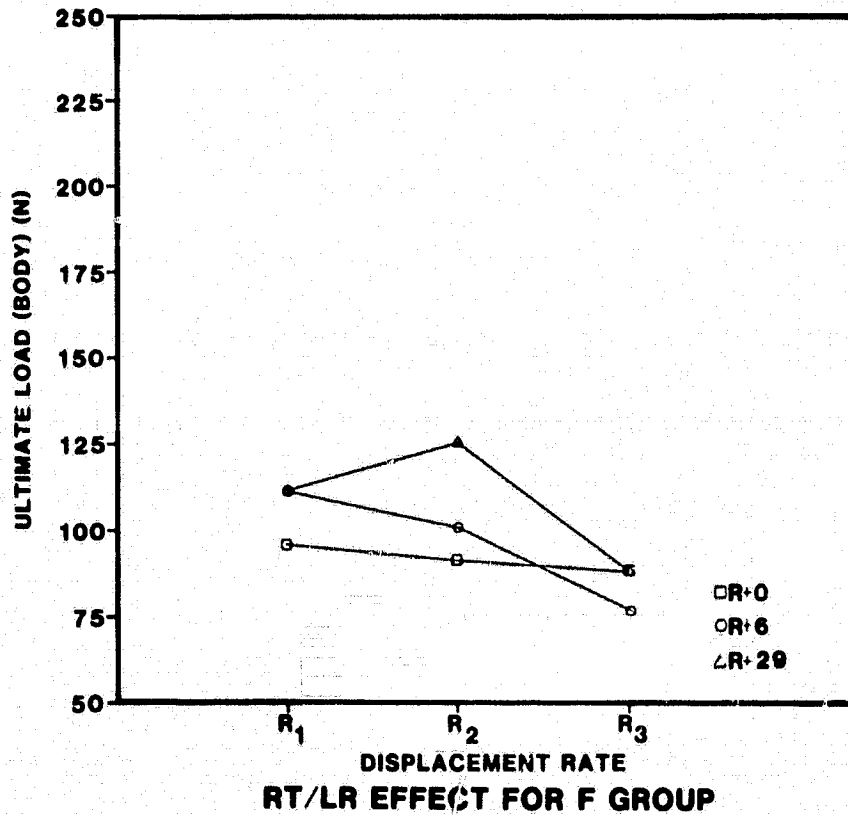
Figure 26

RAT VERTEBRAL BODIES - K307 FOR ENV=F FOR CP=4

RT/LR EFFECT FOR F GROUP
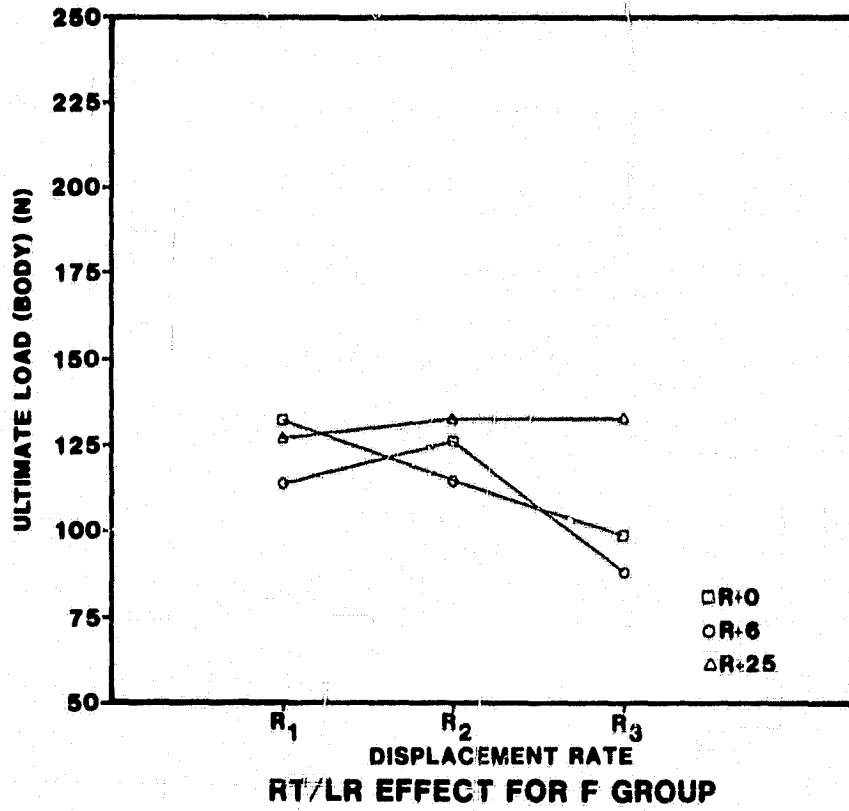
Figure 27

RAT VERTEBRAL BODIES - K307 FOR ENV=F FOR CP 5

RT/LR EFFECT FOR F GROUP

Figure 28

264

RAT VERTEBRAL BODIES – K307 FOR ENV–F FOR CP=6

RT/LR EFFECTS FOR F GROUP
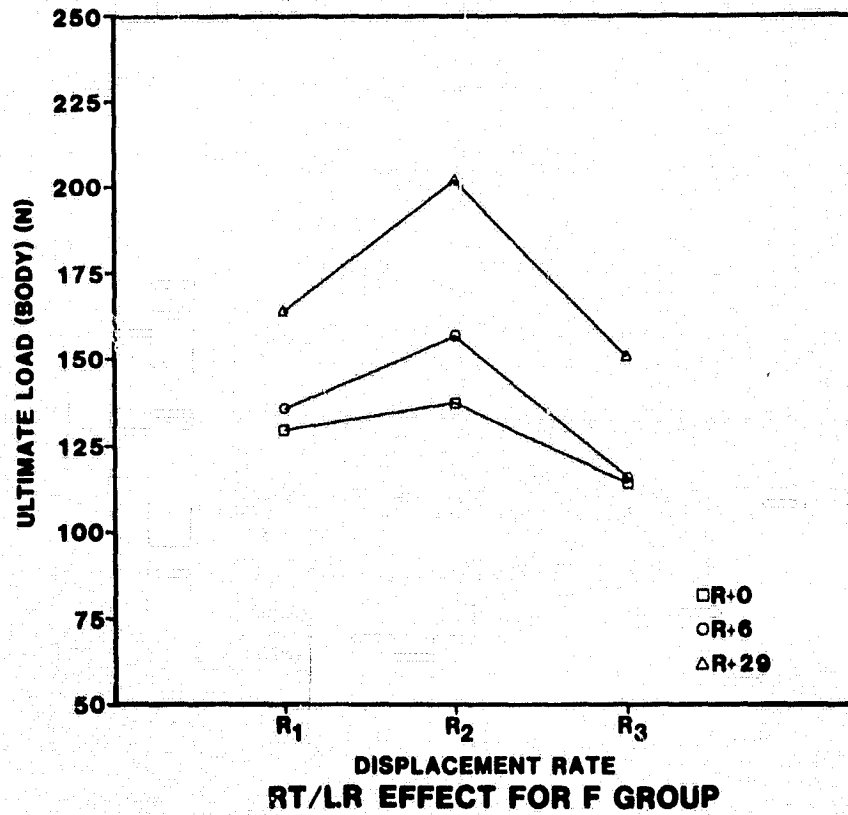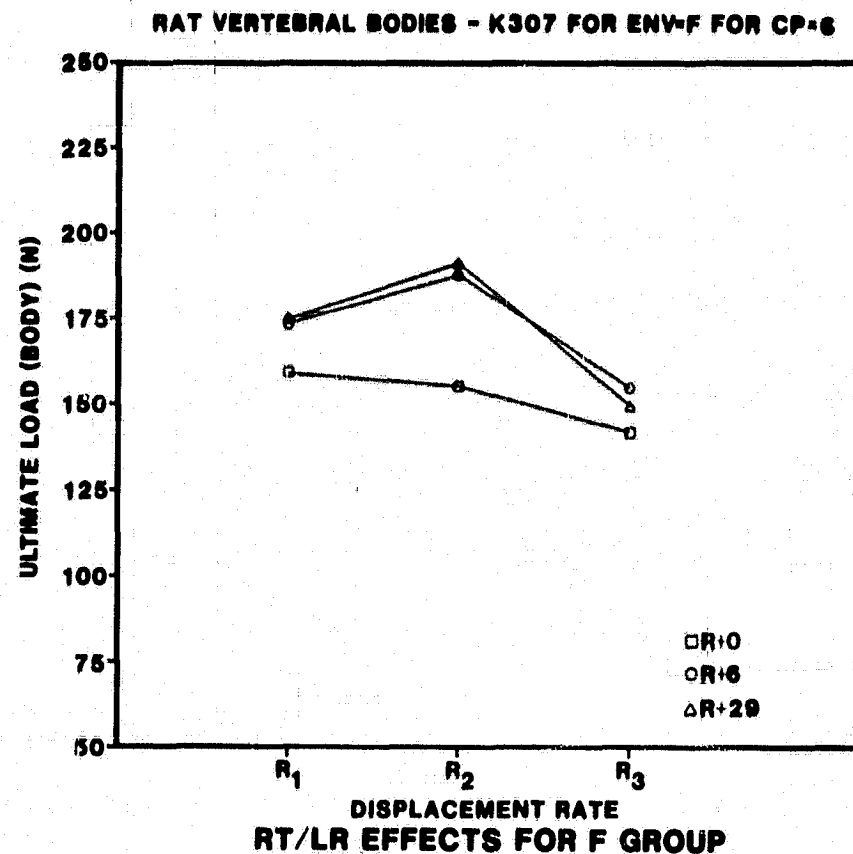
Figure 29

Because of the additional interaction term of RT*CP the effect of loading rate can not be averaged over all column positions. As can be seen from the graphical plots, the ultimate load was lower for the slower loading rate (R_3) and progressively higher for the R_2 and R_1 faster loading rates. In general, the R+0, R+6, and R+29 recovery time curves all decreased in ultimate load as loading rate decreased. Minor inconsistencies were noted at column positions 4, 5, and 6, where the ultimate load leveled off across loading rate or peaked at the R_2 loading rate. These plots also show that the R+29 recovery time curves exhibited greater ultimate loads, as a function of loading rate, than did the R+6 and R+0 curves.

265

By breaking down the vertebral body rat data into separate environmental groups of vivarium, synchronous and flight, it was possible to statistically analyze the data for recovery time effects. The results indicate that after a 29-day recovery period following flight, there was a statistically significant increase in bone strength approaching that of the vivarium or control group. The results relating to the synchronous group were not consistent, in that at the end of the 29-day recovery period the ultimate load data, in some cases, was greater than the ultimate load data of the vivarium.

COSMOS 1129
EXPERIMENT K-308

Automatic Analysis of Muscle Fibers from
Rats Subjected to Spaceflight

Kenneth R. Castleman, Ph.D.*
Luis A. Chui, M.D.**
Joseph P. Van Der Meulen, M.D.**

SUMMARY

The morphology of histochemically prepared muscle sections from the
gastrocnemius and plantaris muscles of flight and vivarium control
rats was studied quantitatively. Both fast-twitch and slow-twitch
fibers were significantly smaller in flight groups than in control
groups. Fibers in group 4F were somewhat larger than in 1F, presumably
due to growth after recovery. Fibers in 4V were slightly larger than
in 1V, presumably due to age. The slow fibers showed more spaceflight
induced size loss than fast fibers, suggesting they suffered more
from hypogravity. The proportion of slow fibers was also lower in the
flight groups, suggesting spaceflight induced fiber type conversion
from slow to fast.

_____

* Jet Propulsion Laboratory, Pasadena, California.

** USC School of Medicine, Los Angeles, California.

INTRODUCTION

Space flight and hypogravity are known to produce systemic and metabolic changes in animals and humans (1, 2). Even though the effects of weightlessness in various organ systems are well described, the pathophysiological mechanism is largely unknown. During adaptation to hypogravity during space flight, the musculoskeletal system is dynamically responsive to insufficient loading mechanism, leading to hypokinesia and hypodynamia. Decreases in body mass and leg volume have been described in manned space flights, resulting in loss of muscle bulk (3, 4).

Skeletal muscle is capable of two basic types of contraction. Some fibers utilize a glycolytic anaerobic energy mechanism. These fibers (fast twitch glycolytic) contract rapidly, but fatigue easily. Other fibers require an available oxygen supply since they utilize an oxidative metabolism for their energy (slow twitch oxidative). They contract more slowly and are resistant to fatigue. These fibers are important in maintaining posture against gravity, while fast twitch glycolytic fibers are required for quick, forceful movement (5). Upon close analysis, it becomes apparent that the above scheme is an over-simplification, and that all muscle fibers are not readily classified into one of only two distinct groups. In fact, there are fast twitch fibers having high level of enzymes for both glycolytic and oxidative metabolism. These fibers exhibit both fast contraction and fatigue-resistant characteristics. It has also become apparent that for any given fiber, the type of energy metabolism employed is not immutably fixed throughout its life. During fetal development for example, the fibers undergo type changes depending upon the type of innervation they

receive. More importantly, they change with exercise and with the demands put upon the muscle by the environment. Electrical stimulation of muscle can also change the contracting mechanism (6, 7, 8). These observations have far reaching implications for the effects of space flight on human and animal neuromuscular systems.

Previous flights in the COSMOS biosatellite series, involving similar exposures of rats to spaceflight conditions, have demonstrated atrophic and dystrophic changes in various muscles due to hypokinesis and hypogravity. On the 22-day COSMOS-605 flight the weight of the e.d.1. muscle was 12% lower in flight than vivarium animals, and fiber area was down by 13% (9). Changes in the soleus muscle were more pronounced, 32% down in weight and 22% down in fiber area. On those rats used in the radioisotope experiment the muscle weight changes were slightly larger: 18% for the e.d.1. and 37% for the soleus (10). Both muscles exhibited a decrease in strength and a slowing of the twitch response. In the soleus, contracting time was shorter in the flight animals (11).

On the 20.5 day COSMOS-690 flight, which included a 24 hour exposure to an 800 rad dose of radiation, the soleus showed a 25% weight deficit, and the gastrocnemius a 19% weight deficit when flight animals were compared with vivarium controls (12). In this experiment the e.d.1. showed no significant weight change. In the soleus the area of "red" fibers showed a 28.7% decrease while "intermediate" fiber area went down by 36.4%.

On COSMOS-782, the weight of the soleus was 38% lower in flight animals and 17% lower in the synchronous experiment than in vivarium controls (13). In all previous flights the large mixed-fiber muscles (quadriceps, biceps and, except as noted above, gastrocnemius) failed to show significant weight changes.

269

Muscle fiber size and type distribution were studied in the extensor digitorium longus (e.d.l.) muscles of 15 COSMOS-936 rats (14). Five flight stationary, five synchronous stationary, and five vivarium control animals were examined. Of the three groups, average fiber diameter was largest in the vivarium control animals, 7% smaller in synchronous control, and 17% smaller in the flight animals. Flight muscles appeared to be shorter than those of the other groups. Fiber number showed no significant difference. The e.d.l. contains predominantly "fast twitch" fibers. The "slow" fiber percentage was quite variable in these animals, and no statistically significant fiber type conversion was noted (14).

The effects of hypergravity have been studied in rats which spent the first 3 months of life in a 2g centrifuge. Fiber type conversion was observed in the soleus muscle which went from 84% slow fibers in controls (16% intermediate fibers) to 100% slow fibers in experimental animals (15). The soleus also showed a fiber diameter decrease in males. The plantaris muscle showed statistically significant fiber diameter increases in females and decreases in males.

MATERIALS AND METHODS

A total of 75 pathogen-free adult Wistar rats recovered from 18.5 days of orbital flight were included in the present study.

They were divided into three groups:

    Flight (F), 25 animals.

    Synchronous Control (S), 25 animals.

    Vivarium Control (V), 25 animals.

Seven animals of the flight groups were sacrificed at the recovery site within six hours of landing (R+0). Six were sacrificed six days later (R+6). Seven additional flight animals were also sacrificed six days later, but after immobilization stress. Finally, five flight animals were sacrificed twenty-nine days after recovery. Similar number of animals were obtained from Vivarium and Synchronous Control Groups.

The left gastrocnemius and plantaris muscles were carefully removed immediately after sacrifice by decapitation. Specimens were placed in pre-labeled and pre-chilled poly Q II scintillation vials (Beckman®) and immersed in liquid nitrogen for a period of approximately ten minutes. Vials containing muscle specimens properly labeled and color coded were stored in insulated containers, packed with dry ice and shipped to the University of Southern California, Neuromuscular Research Laboratory, and stored in a deep freezer for histochemical processing.

A. Histochemical Processing

Whole gastrocnemius and plantaris muscles were cryostat sectioned at 10 μm thick. Three consecutive serial sections were obtained for every 2000 μm interval. In addition to routine hematoxylin, eosin and trichrome histological stains, the following histochemical reactions were performed: reduced nicotinamide adenine dinucleotide tetrazolium reductase (NADH) (16), myofibrillar adenosine triphosphatase (ATP ase) incubated at ph 9.4 (17), 4.6 and 4.3 (18), and glycogen by periodic acid-Schiff (PAS) reagent. Fiber sizes were measured in sections processed for ATP ase at pH 4.6 .

B. Quantitative Analysis

Muscle histochemistry from all three groups of animals were analyzed in the Medical Image Analysis Facility at the Jet Propulsion Laboratory. This facility includes a microscope-mounted television camera capable of converting the specimen image into numerical form and feeding it into a computer for analysis. The digital image is a rectangular array of 512x512 optical density measurements. The operator selects for analysis a portion of the center section on the slide. The specimen image is digitized and processed in a PDP-11 minicomputer (19). The computer program isolates the individual fibers and measures the area, perimeter and average optical density of each. The operator corrects any inaccuracies in the automatic fiber isolation step. Fiber diameter D is computed as the diameter of that circle having the same area by the formula $D = 2\sqrt{A/\pi}$. This assumes that basically cylindrical fibers have been pushed into polygonal cross sectional shape by close packing, assuming that all fibers are cut normal to their axis. The fiber diameter measurement error is less than 3% (14).

The computer program produces a scatter plot showing how the fibers are distributed in diameter and optical density. The operator selects a density threshold which separates light (slow) from dark (fast) fibers and the program plots fiber diameter histograms (distribution curves) for both dark and light fibers. It also prints individual and mean fiber area and diameter measurements (19, 20).

Several non-overlapping fields are processed on the central section from each slide until from 200 to 500 fibers have been measured. Then mean fiber diameter, mean fiber area, and light fiber percentages are tabulated for each slide.

272

Cross sections of the gastrocnemius muscle were identified into
three distinct regions (I, II and III), primarily by the distribution
and clustering of dark and light fibers. Measurement of muscle fibers
of each of the regions was made according to the previously described
method (14).

RESULTS

Upon histological examination, all slides appeared essentially
normal. The PAS specimens showed no major accumulation of glycogen.
Loss of mitochondria in the NADH specimens was not observed. There were
no major cytoarchitectural changes, and necrotic changes and "moth
eaten" fibers were not seen. Morphometric analysis of muscle fibers
was obtained from the gastrocnemius only since this was the only
muscle containing enough slow fibers for comparison of both fiber
types. Table I shows fiber area measurements in square microns
(ATPase ph 4.6) from the region II. The flight animals showed a reduc-
tion in total area of both slow (dark) and fast (light) fibers.
However, the slow fibers were more affected as evidenced by the
decrease in slow-to-fast fiber area ratio. This is the region of the
muscle where fast and slow fibers are most nearly balanced, and it
demonstrates the observed trends quite well.

Table II indicates the percent changes compared by groups (flight
vs. control) and by regions. Both fiber types showed a significant
reduction in fiber area. With only two exceptions the proportion of
slow fibers was reduced by spaceflight. Finally, the ratio of slow
fiber area to fast fiber area was lower in the flight groups, indicating
that slow fibers suffer size loss more than do fast fibers.

Table III lists the quantitative data obtained from all three regions of the gastroc from four experimental groups. With few exceptions the fiber area, the slow fiber proportion and the ratio of slow to fast fiber area all increase in the order 1F, 4F, 1V, 4V. This suggests that the primary effect is spaceflight, with a secondary effect due to the post-flight activity of the 4F and the age of the 4V animals.

DISCUSSION

Animals subjected to hypogravity showed a significant reduction in fiber size for both fiber types. The mechanism of these changes is not clear and can only be postulated. Hypogravity produces insufficient loading of muscle, leading to hypokinesia (motion) and hypodynamia (force). This in turn produces trophic changes, particularly in antigravity muscles (or slow twitch oxidative fibers), decreased protein metabolism, negative nitrogen balance, etc., producing muscle atrophy as the final result, with the possible consequence of decreased muscle tone, strength and altered tolerance to physical work capacity. These observations have far reaching importance in prolonged manned space flights, where preventive measures could perhaps be achieved by designing appropriate exercise programs.

These results appear to give a snapshot of how muscle physiology adapts to the spaceflight environment. Slow fibers, important in maintaining posture against gravity, are little used in space, and their size, and even their proportion, are reduced by the adaptation process. Fast fibers also suffer a disuse atrophy, but to a lesser extent since they are still used for locomotion.

The conversion of fibers from slow to fast is particularly interesting since it has not previously been demonstrated in spaceflight.

ACKNOWLEDGEMENTS

REFERENCES

1. Pace, N. (1977): Weightlessness: A Matter of Gravity, New England Jour. Med. 297:32-37.

2. Rosenzweig, S. N. and Souza, K. A. (1975), Editors: Final Report of U.S. Experiment Flown on the Soviet Satellite Cosmos 936. NASA Technical Memorandum 78526.

3. Berry, C. A. (1971): Medical Results of Apollo 14 - Implications for Longer Duration of Space Flights. XXII Int. Astronaut. Congress, Brussels, Belgium.

4. Johnston, R. E., et al. (1975). Editors: Biomedical Results of Apollo; L. B. Johnson Space Center, NASA, Houston.

5. Burke, R. E. and Edgerton, V. R. (1975): Motor Unit Properties and Selective Involvement in Movement. Exercise and Sport Sciences Reviews, 3:31-81.

6. Close, R. I. (1972): Dynamic Properties of Mammalian Skeletal Muscles. Physiological Reviews, 52:129-197.

7. Van Der Meulen, J. P., et al. (1974): Use and Disuse of Muscle, Annals of the N.Y. Academy of Sciences 228:177-189.

8. Peckham, P. H., et al. (1970): Electrical Activation of Skeletal Muscle by Sequential Stimulation: The Nervous System and Electric Currents. Ed. Wulfsohn, N. L. and Sances, A., Plenium Press, N.Y., London, pp. 45-50.

9. Ilyina-Kakueva, E. I., et al. (1976): Space Flight Effects on the Skeletal Muscles of Rats. *Aviation, Space, and Environmental Medicine* 47:700-703.

10. Kazaryan, V. A., et al. (1977): Effect of Prolonged Weightlessness on Metabolism of Proteins in Red and White Skeletal Muscles of Rats. *Kosmicheskaya Biologiya I Aviakosmicheskaya Meditsina* 6:19-23.

11. Oganov, V. S. and Potapov, A. N. (1976): On the Mechanisms of Changes in Skeletal Muscles in the Weightless Environment. *Life Sciences on Space Research* XIV, Akademie-Verlag, Berlin.

12. Ilyina-Kakueva, E. I. and Portugalov, V. V. (1977): Combined Effect of Space Flight and Radiation on Skeletal Muscles of Rats. *Aviation, Space, and Environmental Medicine* 48:115-119.

13. Portugalov, V. V. (1976): Morphological and Cytochemical Study of the Organs and Tissues of Animals on Cosmos-782. Academy of Sciences of the USSR Report, Moscow.

14. Castleman, K. R., et al. (1978): Spaceflight Effects on Muscle Fibers: *Final Reports of U.S. Experiments Flown on Soviet Satellite Cosmos 936.* Rosenzweig, S. N. and Souza, K. A., Editors: NASA Technical Memorandum 78526 - pp. 224-289.

15. Martin, W. D. and Romond, E. H. (1975): Effects of Chronic Rotation and Hypergravity on Muscle Fibers of Soleus and Plantaris Muscles of the Rat. *Experimental Neurology* 49:758-771.

16. Barka, T. and Anderson, P. J. (1963): *Histochemistry: Theory, Practice and Bibliography,* N.Y. Harper & Row, Publishers.

17. Padykula, H. A. and Herman, E. (1955): The Specificity of Histochemical Method of ATPase: *J. Histochem. Cytochem,* 3:170-195.

18. Dubowitz, V. and Brooke, M. H. (1973): Histological and Histochemical Stains and Reactions, *Muscle Biopsy: A Modern Approach,* London, W. B. Saunders Co., Publishers, pp. 20.

19. Castleman, K. R., et al. (1976): Quantitative Muscle Biopsy Analysis. *Proceedings of the SPIE* 89:119.

20. Van Der Meulen, J. P., et al. (1977): Computer Assisted Quantitative Analysis of Muscle Biopsy, Preliminary Observations. *Neurology* 27:355.

Table I

This table compares the muscle fiber measurements from region II of the gastroc in IF and IV animals. ATPase reaction, pH 4.6 .

GASTROCNEMIUS REGION II

GROUP	NUMBER OF ANIMALS	AREA EXAMINED	FIBERS MEASURED	% SLOW FIBERS	SLOW FIBER AREA	FAST FIBER AREA	SLOW/FAST AREA RATIO
IV CONTROL	4	71.9 mm^2	2066	42.9%	3798 μ^2	3267 μ^2	1.157
IF FLIGHT	3	22.8 mm^2	894	38.9%	2480 μ^2	2602 μ^2	0.975

- 20.4% REDUCTION IN FAST FIBER AREA

- 34.7% REDUCTION IN SLOW FIBER AREA

- 15.7% DECREASE IN SLOW/FAST FIBER AREA RATIO

- 9.3 % DECREASE IN SLOW FIBER PROPORTION

Table II

This table shows the percentage changes in fiber parameters for various Flight/Control group comparisons. In all cases the control values are the basis for percentage changes. ATPase reaction, pH 4.6 .

GROUPS COMPARED	NUMBER OF RATS	No. FIBERS MEASURED	% SLOW FIBERS	SLOW FIBER AREA	FAST FIBER AREA	SLOW/FAST AREA RATIO
1F vs 1V (I)	5	1833	+35	-44	-32	-16
1F vs 1V (II)	7	2950	-9	-35	-20	-16
1F vs 1V (III)	6	3844	-20	-32	-26	-20
1,2,3F vs 1,2,3V (I)	12	3647	+28	-25	-13	-13
1,2,3F vs 1,2,3V (II)	17	4291	-2	-33	-13	-23
1,2,3F vs 1,2,3V (III)	16	7437	-20	-25	-30	-5

Table III

These are the mean values of the muscle fiber parameters tabulated by group. Included are the number of animals and the number of fibers analyzed in each group. ATPase reaction, pH 4.6 .

GROUP	REGION	RATS	FIBERS	SLOW FIBER AREA (μ^2)	FAST FIBER AREA (μ^2)	% SLOW	SLOW/FAST AREA RATIO
1F	I	3	1491	1644	2973	20.6	0.553
1V	I	3	981	2797	3967	19.4	0.705
1F	II	3	894	2480	2602	39.2	0.953
4F	II	3	838	3278	3721	43.8	0.881
1V	II	4	1621	3876	3271	44.7	1.185
4V	II	3	873	4153	3947	36.8	1.052
1F	III	4	2000	2365	2946	19.2	0.803
4F	III	3	658	3230	4989	24.5	0.647
1V	III	2	1844	3465	3379	22.3	1.025
4V	III	4	1425	3445	3627	21.1	0.950

K-310

THE EFFECT OF SPACEFLIGHT ON OSTEOGENESIS AND DENTINOGENESIS IN THE MANDIBLES OF RATS

David J. Simmons, Jean E. Russell
Washington University School of Medicine
Department of Surgery
Division of Orthopedic Surgery
St. Louis, Missouri

Frank Winter
Washington University School of Dental Medicine
Department of Physiology
St. Louis, Missouri

Gary D. Rosenberg
Indiana University-Purdue University
Department of Geology
Indianapolis, Indiana

William V. Walker
Washington University
St. Louis, Missouri

SUMMARY

Rats flown for 18.5d in the COSMOS 1129 Biosatellite exhibited normal rates
of dentinogenesis and osteogenesis in the body of the mandible during 0-G.
The total calcium, inorganic phosphorus and hydroxyproline levels in the
jaws and incisors of the flight rats were normal. Gravity density fraction-
ation studies suggested, however, that spaceflight caused a delay in the
normal maturation of bone mineral and matrix; normal values were reestablish-
ed by 6d postflight. The teeth were spared. The circadian and ultradian
patterns of dentin calcification were normal during spaceflight and recovery
periods, but the enamel rhythms displayed a greater amplitude of sulfur
concentrations and thus abnormal calcium:sulfur ratios only during exposure
to 0-G. We conclude that the rat mandible and teeth do not suffer the defi-
cits of bone formation common to weight-bearing parts of the skeleton during
spaceflight. The only derangements detected at 0-G were in the quality of
the matrix and mineral moieties.

INTRODUCTION

Efforts to understand how prolonged spaceflight effects changes in calcium homeostasis and bone formation-resorption have been pursued in laboratory rats during three joint NASA-Soviet Biosatellite Flights of 18.5-22d duration (COSMOS 782, 936, and 1129)(1-4). The appendicular weight bearing bones (tibias) suffered reduction in the rate of cortical bone growth and in femur bone strength. Quite unexplained was the fact that periosteal growth was diminished while endosteal growth remained unchanged. Bone resorption rates (specific osteoclast surfaces) were relatively normal. The COSMOS 936 biosatellite also included some animals maintained in a centrifuge which provided a 1G environment, and their skeletons were spared the deleterious effects of null gravity on bone strength. Healing of the periosteal growth deficit and restoration of long bone mechanical strength was noted in the 0-G group after a 25d post-flight recovery period in a Moscow vivarium. In the most recent COSMOS 1129 flight(September-October 1979), there was an opportunity to examine the effect of null gravity on the integrated growth and remodelling of a non-weight bearing bone-- the mandible and its teeth. How might 0-G affect tissues in a skeletal element which is only supplied with a large antigravity muscle(masseter)?

MATERIALS AND METHODS

Three groups of 5-7 SPF male rats(270-320g body weight) were injected with 1.0 mg/kg body weight Declomycin to mark forming and mineralizing surfaces of bone and dentin, 3d prior to being loaded into block modules of 5 cages(singly housed) mounted in a modified Vostok spacecraft. The animals were then launched into orbit for a period of 18.5d. The particu-

C-7

lar details of the flight and tetracycline labeling schedule have been described by Wronski et al(5). Water was supplied ad-lib, and they were fed 10g aliquots of a nutritionally defined paste diet four times per day. Control animals were maintained in a land bound mock-up of the biosatellite under nearly identical conditions, and these were subjected to simulated stresses of launch and recovery. Additional groups of (unstressed) control animals were maintained in a Moscow vivarium. The control groups and one group of flight rats received a second and/or third injection of Declomycin(1.0mg/kg) on the 6th and 27th days following recovery, and they were sacrificed 48h later. The total number of groups of animals were as follows:

Groups

1 Flight Basal
2 Synchronous Basal
3 Vivarium Controls
4 Synchronous Controls
5 Flight Rats

One group of 5 flight rats was used for analyses of circadian changes in (a) motor activity during the flight and recovery periods(6), and (b) the excretory patterns of Na^+, K^+, Ca^{++}, PO_4^{-3}, and hydroxyproline(OH-Pr)(7). These animals were subjected to a $180°$ inversion of the light-dark cycle after 10d at 0-G to test their ability to "resynchronize" their metabolic patterns. However, during the postflight test periods at R+3, R+8 and R+26, the animals each spent 3d in metabolism cages and were fed six times per day rather than the usual 4 times per day.

At autopsy, the mandibles were recovered, cleaned of soft tissues, and fixed in either 70% or 95% ethyl alcohol, for subsequent analysis of the

growth(tetracycline data) and matrix-mineral maturation.

Analysis of Growth

The left jaw was divided into 3 regions-- the premolar, molar and post-
molar areas. The premolar and postmolar areas were embedded undecalcified
in methylmethacrylate and sectioned transversely on a high speed rotary
saw at 50-60μm(Fig. 1). The molar region was sectioned in the frontal
plane at 10μm on a Jung Microtome to reveal the roots of the molar teeth,
and these sections were stained with the Goldner Method to reveal mineralized
bone and osteoid. All the sections were examined by UV microscopy to reveal
the distribution of the tetracycline time markers. The mineralization rate
(equal to the rates of appositional bone growth and dentinogenesis) was
estimated by measuring the distance between the tetracycline bands, and
dividing that value by the time interval(days) between injection. These
measurements around the roots of the molar teeth, based on Vignery and
Baron's model(8),provided information about the rate of tooth migration via
resorption on the anterior surface and formation on the posterior surface
of alveolar bone(see Tran Van Thuc et al in this Report). In addition,
they also measured the area of the periodontal ligament and the specific
surfaces of bone undergoing formation(osteoblast-covered) and resorption
(osteoclast-covered) with a Zeiss ocular grid.

Dentinogenesis was estimated in the portion of the mandibular incisor
that lay within the diastema, where the dentin was thick enough to record
a growth period of 19-21d. When the tetracycline labeling intervals were
longer than 21d, we used sections of the erupted portions of the teeth where
the dentin had formed almost exclusively during the flight period.

282

Matrix-Mineralization Maturation Rate

The incisor was removed from the right jaw and it was divided into 3 regions representing the distal region of tooth formation, the middle region of tooth maturation, and the coronal or erupted portion(Fig. 2). The teeth sectors and jaw bones were individually frozen, ground to a 40μm powder, and separated by a bromoform-toluene density gradient into 3 specific gravity fractions(1.3-1.9, 2.0-2.1, 2.2-2.9), which were analyzed for calcium(Ca), inorganic phosphorus(Pi), and hydroxyproline(OH-Pr). In the normal growing rat, most of the mineral and OH-Pr in bone and teeth are concentrated in the highest gradient density fractions(2.2-2.9). The less mature bone and tooth matrix-mineral is distributed in fractions 1.3-1.9 and 2.0-2.1. Thus, these analyses recorded a maturational profile for bone matrix and mineral(9).

Circadian Changes in Dentin-Enamel Formation

Polished slabs of the lower incisors were scanned across the labial surface at continuous 1.0μm intervals from the pulp to the enamel surface to measure the local variations in calcium, phosphorus and sulfur. Sulfur was used as an index to the glycosaminoglycans of dentin and to the keratin-like protein in enamel. A chlorapatite(10) with a weight percent of Ca and Pi of 53.89 and 41.00, respectively, served as the standard from which to calculate the Ca and P concentrations in the teeth. Figure 3 shows the track etched by the electron beam from a MAC-V microprobe(Monsanto Corp., St. Louis, Mo.); the diameter of the beam was 1.0μm. The data was refined by Fourier analysis to compute the normalized power spectra. The techniques used have been described by Rosenberg and Simmons(11-12), and they provide

estimates of the repeatability of rhythms of Ca, P, and S concentrations that may be present owing to circadian, ultradian, and infradian periodicities.

RESULTS

Dentinogenesis

At the mandibular diastema, the average preflight rate of dentinogenesis was 17-18μm/d(Fig. 4), and this was unchanged during the flight and post-flight recovery periods(Fig. 5) in the vivarium and synchronous control groups. However, the rates of dentinogenesis increased slightly during the recovery period in the control groups.

Osteogenesis

Body of the Mandible: No changes from the normal rate of osteogenesis was noted in the area of the mandibular diastema during spaceflight. The normal rate of growth of about 3-4μm/d was also maintained during the post-flight recovery period(Fig. 6). Growth in the groups of control animals proved to be the more variant, but generally the data showed the anticipated reduction in growth rates with age. Intergroup variations were also absent in the ossification of the post-molar mandibular ramus. Periosteal growth along the superior and inferior rami averaged 2-3μm/d, both during the flight and postflight recovery periods(Fig. 7).

These data suggested that spaceflight had no significant effect upon the appositional growth of the body of the rat mandible. These results, then, stand in sharp contrast to the data presented by Wronski et al(5), that bone formation rates in the weight-bearing bones(appendicular skeleton) were depressed 30-60%. In fact, however, the jaw bones were not entirely normal. There were distinct changes in the rates of remodeling of the alveolar bone

around the roots of the molar teeth(see Tran Van Thuc in this Report) and
in the maturational status of the bone mineral and collagen of the mandi-
bles which suggested that the rates of bone remodeling and bone maturation
were reduced.

Bone Maturation

When the jaws and each of the 3 regions of the lower incisor were ana-
lyzed for total Ca, PI and OH-Pr, we could not distinguish the flight from
the control animals by any change in their hard tissue chemistry(Fig. 8).
The illustrations also include, for comparison, data from animals of the
same age and sex which were fed Purina Laboratory block chow and tap water.
The density gradient fractionation studies indicated, however, that rat
alveolar bone was distinctly abnormal after spaceflight(Figs. 9-11). In
all flight rats, there was a highly significant diminution of bone collagen
and mineral moieties in the most dense mature fractions(2.2-2.9), with a
corresponding increase in the least dense, most immature fractions(1.3-1.9,
2.0-2.1). The highest density fractions of the flight rat bones had 30%
less mineral and collagen(OH-Pr) than the corresponding fractions from the
control rat bone. These changes suggested that there was a distinct deficit
in the flight animals-- that there was a delay in the maturation of the
collagen(lack of intramolecular cross links?) and apatite mineral. Impor-
tantly, these deficiencies tended to normalize after 6d at 1-G, and they
were fully corrected during the postflight recovery period of 29d(Figs.12-
15).

Similar changes were not apparent when the 3 regions of the teeth were
analyzed(Figs. 16-19)-- suggesting that the teeth were highly conserved

elements, i.e., vitally essential to life itself.

Microradiographs of the growth surfaces of the bones(Fig. 1) did not detect the mineral deficit associated with the period of null gravity, but they did reveal alternating bands of high and low density in rat incisor dentin(Fig. 20). There were no obvious differences between the flight and control rats in this regard. Given this difference in mineralization, an attempt was made to define the biorhythmical components of growth in the incisor dentin and enamel, since it was possible that spaceflight interfered with the normal rhythmic behavior of the odontoblasts and ameloblasts.

Biorhythmicity of Dentin and Enamel Formation(Electron microprobe)

(A) Dentin Formation: Fourier analysis of data derived from continuous 1.0μm traces with the electron microprobe from the pulp to the dentin-enamel junction revealed that there were repeatable Ca, P, and S peaks at intervals of about 5.0μm during both the flight and postflight recovery periods. Since labial dentin was deposited at a rate of 20μm/d, these 5.0μm periodicities must represent periods of formation/mineralization at times shorter than 24h(=ultradian), and multiples of this rhythm represented a circadian time period(=24h). Figure 21 shows that while the fluctuations in Ca and P were generally in-phase, the Ca and S concentrations were not always in-phase. The rhythms in the phosphorus concentration were the most regular. The obvious increase in the amplitude of Ca and S concentrations within 30.0μm of the pulp, i.e., the dentin formed during the last 24-36h of the flight period, may signal a disturbance associated with reentry-recovery.

(B) Enamel Formation: In contrast to dentin, the analyses indicated that

286

during exposure to 0-G, the concentration of S was much less regular than either phosphorus or calcium(Fig. 22). Wide variations in S concentration occur throughout the enamel in the flight group. These are absent in the vivarium controls, but they exist with a much lower amplitude(vs the flight group) in the synchronous controls. Nevertheless, even in the flight rats, the P concentrations exhibited persistent periodicities at 5.0µm intervals during the flight and recovery periods. If enamel is deposited at a rate of 10-15µm/d(13), then the data speak to the persistence of a normal biorhythmicity during spaceflight, involving 1 circadian period and 3 ultradian periods every 24h. Here too, the changes in Ca and P concentrations were usually in-phase, while the relationship between Ca and S was more variable.

Thus, these observations suggest that the enamel records a specific response to weightlessness during null gravity and that this is superimposed upon disturbances due to the 180° inversion of the light-dark cycle 10d after "lift-off," i.e., at mid-enamel thickness.

DISCUSSION

There were few direct measurable effects of spaceflight in the mandible of the rat. This suggests that, as opposed to the long bones which are weight-bearing parts, the non-weight bearing skeletal elements would tend to be unaffected-- even when supplied with powerful antigravity muscles. This was not surprising since the growth of the entire body of the rat mandible must be coordinated with the production of the incisor teeth which grow along a spiral axis. The lower incisors must appose after eruption if the animal is to continue eating and assure its survival. While the apposi-

tional growth of the body of the mandible is relatively normal, we did

detect changes in the maturation of bone collagen and mineral. Such

changes, involving a delay in the maturation of the collagen and mineral

fractions, is typical of some other skeletal problems, such as the derange-

ments in mineral metabolism common to uremic(9) and rachitic rats(14).

It was also notable that the rates of bone formation and resorption around

the roots of the molar teeth were slightly reduced(see Tran Van Thuc, this

Report). This might occur if there were a flight-related reduction in the

maturation of the osteoprogenitor cell population to the osteoblast class,

or in the generation of the monocytic-macrophagic cells which serve as the

precursors of osteoclasts. Roberts(15) noted that on the basis of nuclear:

cytoplasmic volume ratios(large ratios being typical of the mature osteo-

blast), there was a predominance of cells with a low volume ratio, i.e.,

more than the normal number of pre-osteoprogenitor cells in the space

around the roots of the maxillary molars. Thus, in the flight rats, there

seems to be a deficit of cell maturation, and this may have been due to

some alterations in blood corticosteroid levels and/or parathyroid gland

function(or end-organ response) during spaceflight.

Cann's estimates of whole body fecal and urinary calcium losses during

spaceflight(16) complement the histomorphometric assessment of the skeletons

which signal the significantly reduced rates of bone formation and resorption.

However, the histomorphometry indicates that these processes had been un-

coupled, such that there is a residual component of bone resorption(80% of

normal) which exceeds the rate of bone formation during flight. While the

weight-bearing long bones(5) and the vertebrae(17) seem to be the most

pointedly affected skeletal parts, an altered state of mineral metabolism certainly existed in the jaw bone. The aberrant picture of cell proliferation kinetics is apparently not limited to bone. Lymphocytes from crewmembers of Soyuz 6, 7,8, Skylab 2, 3, 4 and Apollo-Soyuz suffered failure of cell proliferation/maturation when challenged with mitogens(18).

While there appears to be little soft tissue evidence that spaceflight is chronically stressful(19), the hard tissue evidence is such that one must presume some degree of disturbance. Incisor enamel recorded widely fluctuating amplitudes of S concentration throughout its thickness. Tigranian and his coworkers(20) have emphasized the presence of stress at the time of reentry and recovery of the spacecraft(increased concentrations of circulating catecholamines, corticosterone and thyrotrophic hormone), and it is inviting to view the irregular patterns of Ca and S concentration in the dentin formed during this time in this light. The failure of bone and tooth cells to properly "process" the matrix and its mineral may be related to Matthew's demonstration of abnormal accumulations of mineral in epiphyseal plate chondrocytes(see Supplemental Report 3B). In other states of altered mineral metabolism, "extracellular lakes" of mineral have been described around osteocytes(21).

Our finding that stable or relatively stable biorhythms of calcium, phosphorus and sulfur persist in the dentin and enamel of the lower incisor during the spaceflight and recovery periods, despite the reversal of the light-dark cycles midway through the flight period, attests to the conservative nature of the teeth. The (motor) activity rhythm was also normal during spaceflight, but the rhythms of electrolyte and Ca, P, and OH-Pr excretion(7) and activity(6) were disturbed during the recovery period at 1-G. These

disturbances may relate more to alterations in caging and the feeding schedules upon which the regularity of the tooth Ca and P rhythms are highly dependent(22-26) than to any stress imposed by spaceflight, reentry, and recovery of the biosatellite. Rosenberg and Simmons(11,12) have reviewed the many evidences supporting the concept that the feeding schedule and resultant occlusal stress dictate the biorhythmicity of dentinogenesis.

In toto, the data we have presented suggest that the non-weight bearing bones of the skeleton will not escape the deleterious effects of spaceflight, but it is, rather, the quality of the bone which is impaired rather than the actual volume of the tissue or its mineralization status(=weight %).

REFERENCES

1. Holton, E.M. and D.J. Baylink. Final reports of U.S. experiments flown on the Soviet Satellite COSMOS 782(NASA TM-78525),(1978),pp.321-351.

2. Holton, E.M., R.T. Turner and D.J. Baylink. Final reports of experiments flown on the Soviet Satellite COSMOS 936(NASA TM-78536),(1978),pp. 135-178.

3. Spengler, D.M., E.R. Morey, D.R. Carter, R.T. Turner, and D.J. Baylink. Effect of spaceflight on bone strength. The Physiologist 22: 73-75(1979)

4. Morey, E.R. and D.J. Baylink. Inhibition of bone formation during space flight. Science 201: 1138-1141(1978)

5. Wronski, T.J., E.R. Morey, D.E. Philpott, R.T. Turner, D.J. Baylink, C.D. Arnaud, J.L. Matthews and W.S.S. Jee. Cosmos 1129: Spaceflight and bone changes. In: XXVIII Internat. Physiological Congress, Budapest, Hungary, Proc. Internat. Union Physiol. Sci., XIV: 281 only(1980).

6. Klimovitsky, V.Ya., E.A. Ilyin, V.S. Oganov, V.S. Magedov, G.G. Shlyk, L.M. Murashko, K. Hecht, M. Poppal, T. Schlegel, J. Kwarezki, S. Kotar, and B. Dembec. Studies of biorhythms in biosatellite experiments. In: XXVIII Internat. Physiol. Congress, Budapest, Hungary, Proc. Internat. Union Physiol. Sci., XIV: 165 only(1980)

7. Kwareckl, K., H. Deblec and Z. Koter. Rhythms of electrolytes and hydroxyproline excretion in urine of rats after 3 weeks weightlessness/Biosputnik Kosmos-1129. In: XXVIII Internat. Physiol. Congress, Budapest, Hungary. Proc. Internat. Union Physiol. Sci., XIV: 171 only(1980)

8. Vignery, A. and R. Baron. Dynamic histomorphometry of alveolar bone remodeling in the adult rat. Anat. Rec., 196: 191-200(1980)

9. Russell, J.E. and L.V. Avioli. Effect of experimental chronic renal insufficiency on bone minral and collagen maturation. J. Clin. Invest., 51: 3072-3079 (1972)

10. Young, E.J. and E.L. Munson. Fluor-chlor-oxy-apatite and sphene from Crystal Lode Pegmatite near Eagle, Colorado. Am. Naturalist, 51: 1476-1493 (1966)

11. Rosenberg, G.D. and D.J. Simmons. Rhythmic dentinogenesis in the rabbit incisor. I. Circadian, ultradian and infradian periods. Calcif. Tissue Internat. (1980), in press.

12. Rosenberg, G.D. and D.J. Simmons. Rhythmic dentinogenesis in the rabbit incisor. II. Allometric aspects. Calcif. Tissue Internat. (1980), in press.

13. Risnes, S. A method of calculating the speed of movement of ameloblasts during rat incisor amelogenesis. Arch. oral Biol., 24: 299-306(1979)

14. Dickson, I.R. and E. Kodicek. Effect of Vitamin D deficiency on bone formation in the chick. Biochem. J., 182: 429-435(1979)

15. Roberts, W.E. et al. Final Results- Cosmos 1129, K-305. Suppl. Report I(1980).

16. Cann, C.E., R.R. Adachi and E.R. Morey. Bone resorption and calcium absorption in rats during spaceflight. In: XXVIII Internat. Physiol. Congress, Budapest, Hungary, Proc. Internat. Union Physiol. Sci., XIV: 74 only (1980)

17. Kazarian, L.E.. Vertebral centra morphology and strength- Cosmos 1129. In: XXVIII Internat. Physiol. Congress, Budapest, Hungary. Proc. Internat. Union Physiol. Sci., XIV: 158 only (1980)

18. Cogoli, A. Effect of spaceflight on lymphocyte proliferation. In: XXVIII Internat. Physiol. Congress, Budapest, Hungary. Proc. Internat. Union Physiol. Sci., XIV: 84 only(1980)

19. Kaplansky, A.S., E.A. Savina, V.V. Portugalov, E.I. Ilyina-Kakueva, G.P. Stupakov, G.N. Durnova, E.I. Alekseev, G.I. Plakhuta-Plakutina, A.S. Pankova, V.N. Schvets, and V.I. Yakovleva. Weightlessness-induced morphological effects and stress reactions in rats flown aboard bio-satellites. In: XXVIII Internat. Physiol. Congress, Budapest, Hungary. Proc. Internat. Union Physiol. Sci., XIV: 156 only (1980)

20. Tigranian, R.A., L. Macho, R. Kvetnansky, S. Nemeth and N.F. Kalita. Stress metabolic aspects in space flight. In: XXVIII Internat. Physiol. Congress, Budapest, Hungary. Proc. Internat. Union Physiol. Sci.. XIV: 261 only (1980)

21. Weisbrode, S.E., C.C. Capen and A.W. Norman. Light-and electron-

microscopic evaluation of the effects of 1,25-dihydroxyvitamin D_3 on bone of thyroparathyroidectomized rats. Am. J. Path. 97: 247-260, (1980)

22. Staub, J.-F., A.-M. Perault-Staub and G. Milhaud. Endogenous nature of circadian rhythms in calcium metabolism. Am. J. Physiol., 237: R311-R317(1979)

23. Loutit, J.F. Diurnal variation in urinary excretion of calcium and strontium. Proc. Roy. Soc., B., 162: 458-472(1965)

24. Briscoe, A.M. and C. Ragan. Diurnal variations in calcium and magnesium excretion in man. Metabolism 15:1002-1010(1966)

25. Talmage, R.V., J.H. Roycroft and J.J.B. Anderson. Daily fluctuations in plasma calcium, phosphate and their radionuclide concentrations in the rat. Calcif. Tissue Research 17: 91-102(1975)

26. Kukreja, S.C., G.K. Hargis, E.N. Bowser, W.J. Henderson, E.W. Fishman and G.A. Williams. Role of adrenergic stimuli in parathyroid hormone secretion in man. J. Clin. Endocrinol. Metab., 40: 478-481 (1975)

293
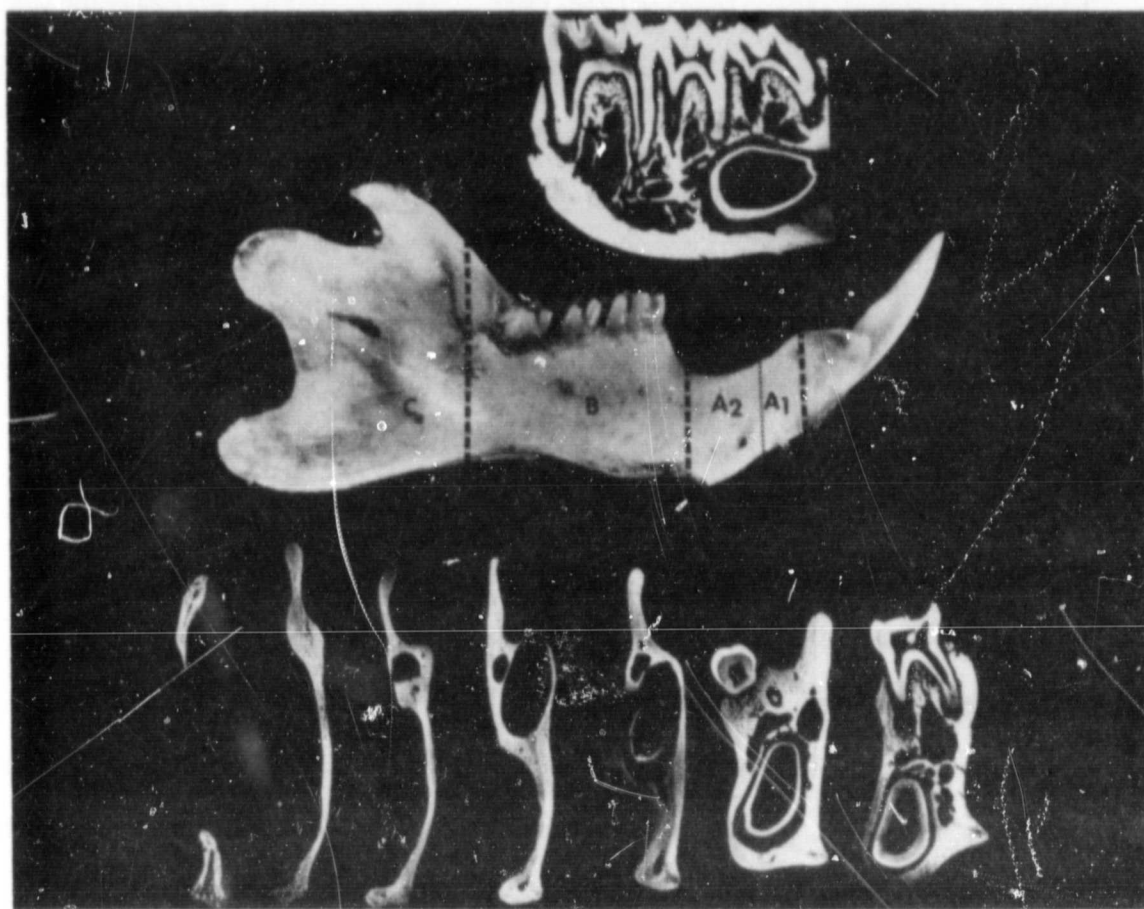
Figure 1

The mandible of an SPF rat, showing microradiographs of transverse
and frontal sections through the molar and postmolar regions.

A_1 = region of the diastema, transversely
sectioned to obtain tetracycline growth
data.

A_2 = region of the diastema used for electron
microprobe analyses of Ca, P, and S
concentration and biorhythmicity

B = molar region

C = postmolar region, treated as A_1

Rat #WR-49, (H.F. Winter Collection)
Mandibular Incisor, Scale X5
Male, 310 gm. body wt.
Calculations utilizing IER of 320 microns/day, ave. of 310 & 330
Herrman (1953) & Bourliere & Gourevitch (1952)
A.R. Ness, Advances in Oral Biology
(Academic Press) Vol. I, 1964.

3rd label
O Days, Recovery +23 days
10
2nd label
20
RECOVERY
30
1st label
FLIGHT
40
50
60
70
80
Pulp Closure at 61 Days, Dentinogenesis Rate = 1.05 mm Dentin/61 Days = 17.2 Microns/Day
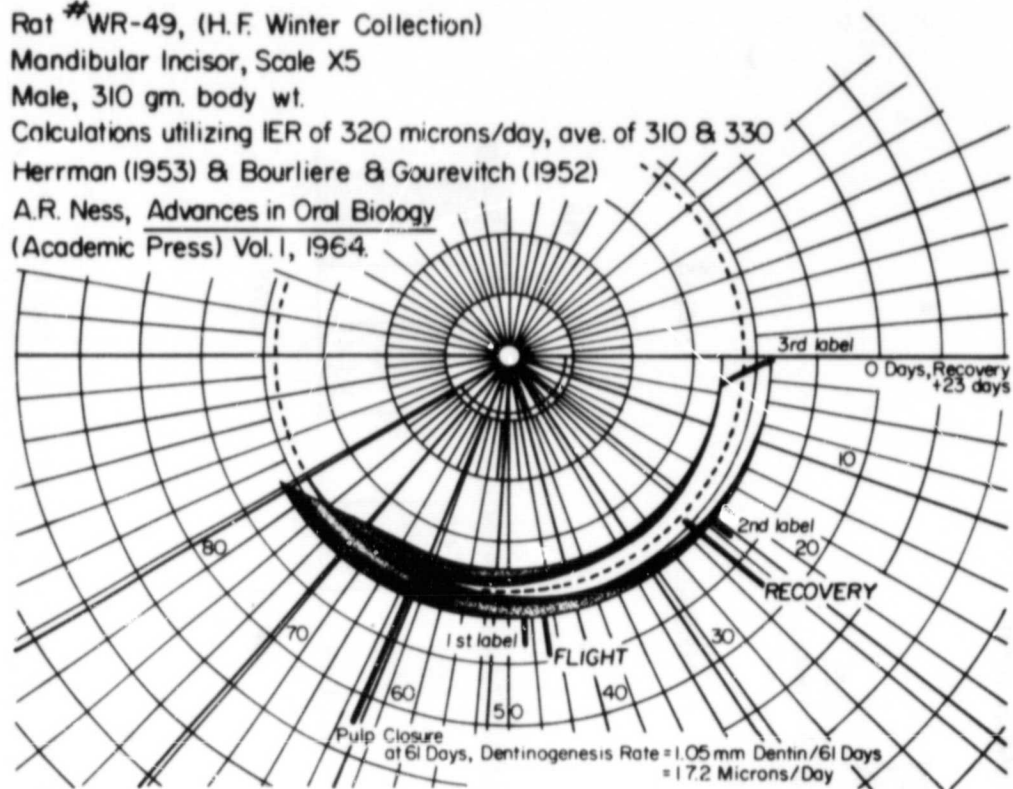
Figure 2

Scheme of growth of rat mandibular incisor and positions of tetracycline labels
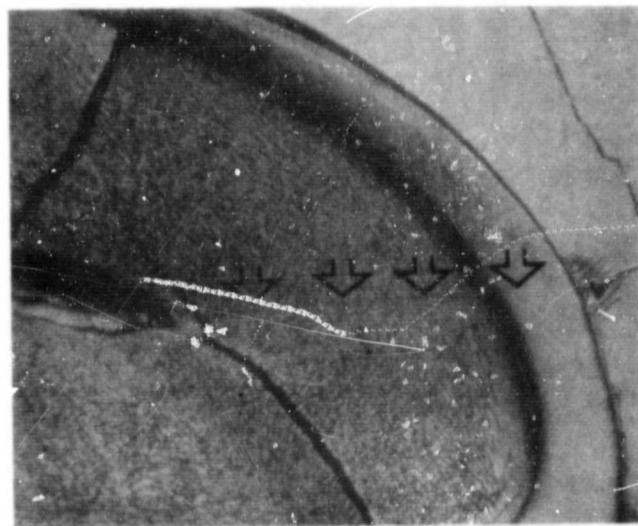
Figure 3

Photomicrograph of rat labial dentin-enamel, showing the etched track made by the 1.0μm beam of the electron microprobe.

295

DENTINOGENESIS RAT MANDIBULAR INCISOR (DIASTEMA)
(PRE-COSMOS 1129)
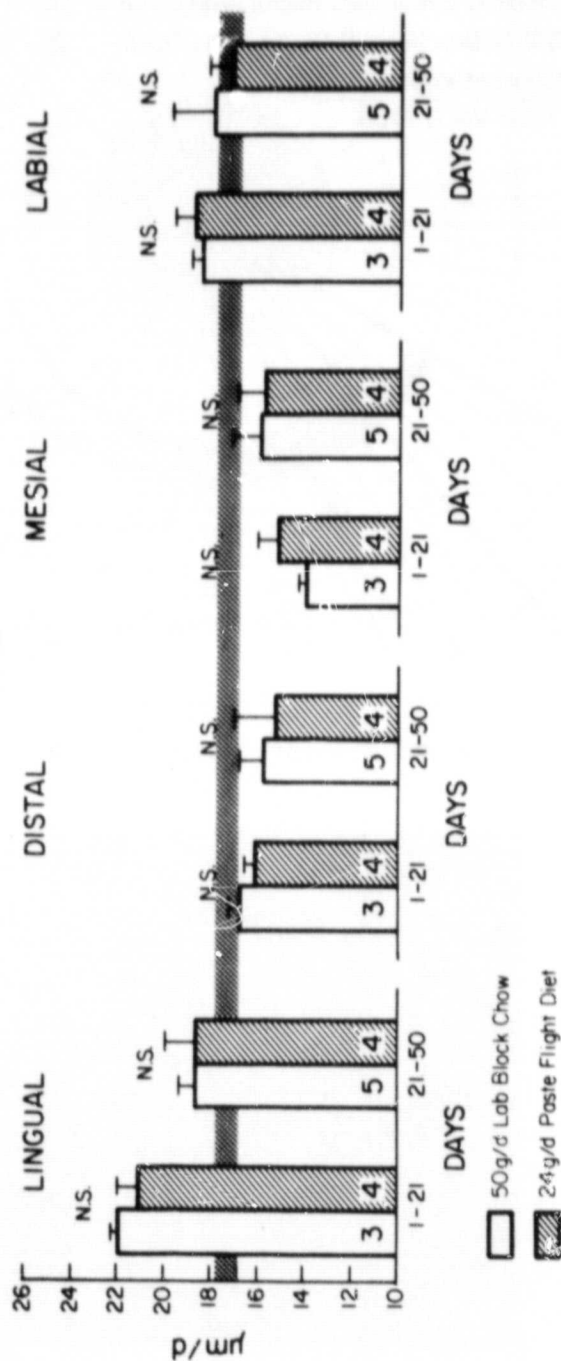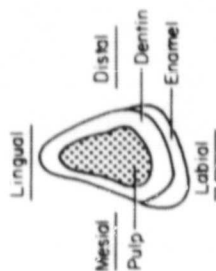
Figure 4

Schematic drawing of a cross section through the mandibular incisor of the rat at
the diastema. The bar graphs show the site-specific rates of dentinogenesis as
calculated from the tetracycline labeling patterns.

COSMOS 1129
DENTINOGENESIS- MANDIBULAR DIASTEMA

FB = flight basal
SB = synchronous basal control
V = vivarium control
S = synchronous control
F = flight
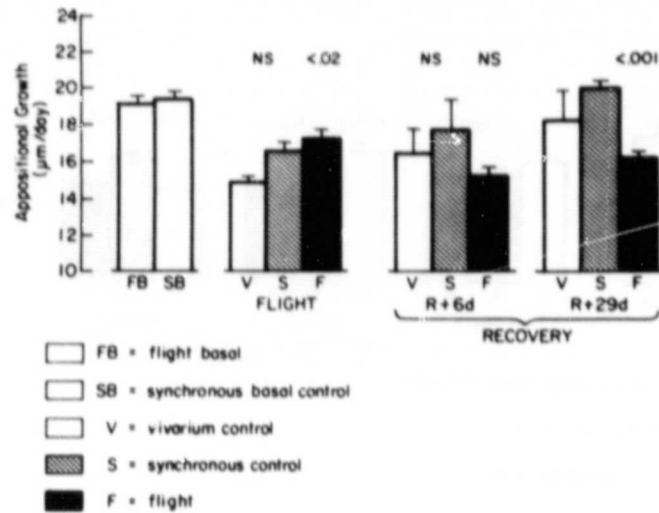
Figure 5

Calcification rates of dentin in the region of the mandibular diastema in rats during the Preflight, Flight and Postflight Recovery Periods.

COSMOS 1129
MANDIBULAR DIASTEMA- PERIOSTEAL

SB = synchronous basal control
V = vivarium control
S = synchronous control
F = flight
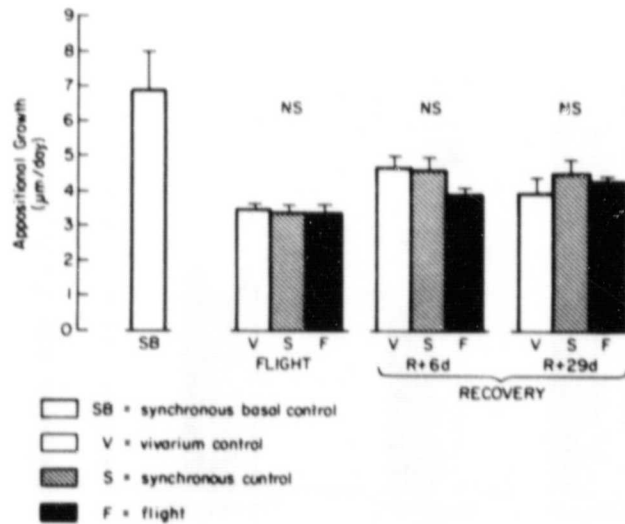
Figure 6

Calcification rates of bone in the region of the mandibular diastema in rats during the Preflight, Flight and Postflight Recovery Periods.

COSMOS 1129
POST-MOLAR MANDIBULAR RAMUS- PERIOSTEAL

SB = synchronous basal control

V = vivarium control

S = synchronous control
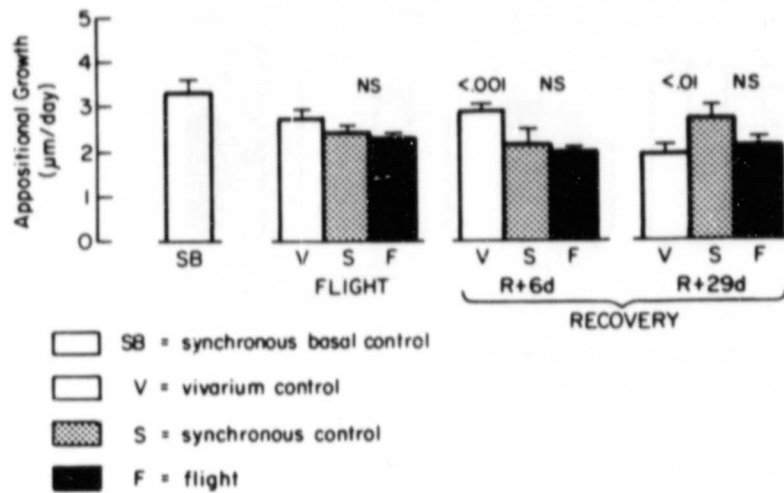
F = flight

Figure 7

Calcification rates of bone in the postmolar superior and inferior rami of the rat mandible during the Preflight, Flight, and Postflight Recovery Periods.

Total Mineral and Hydroxyproline Content of Rat Alveolar Bone
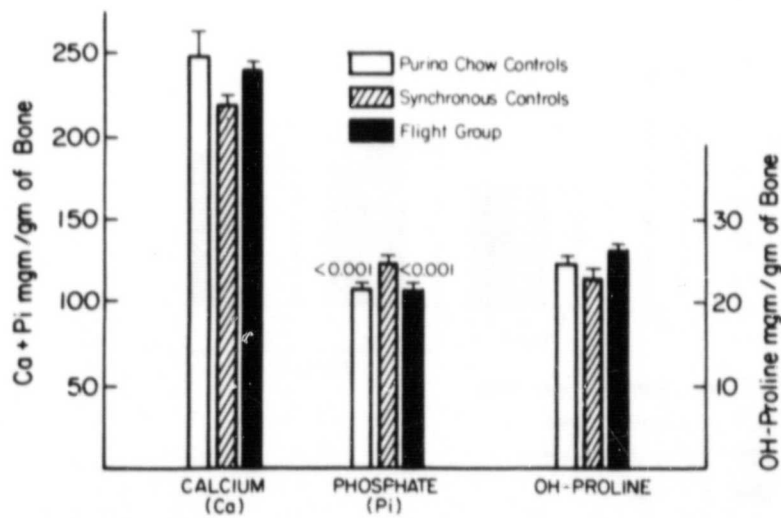
Figure 8

Total mineral and hydroxyproline content of alveolar bone of rats sacrificed immediately after an 18.5d spaceflight.

298

Density Gradient Fractionation of Rat Alveolar Bone Collagen (OH-Proline)
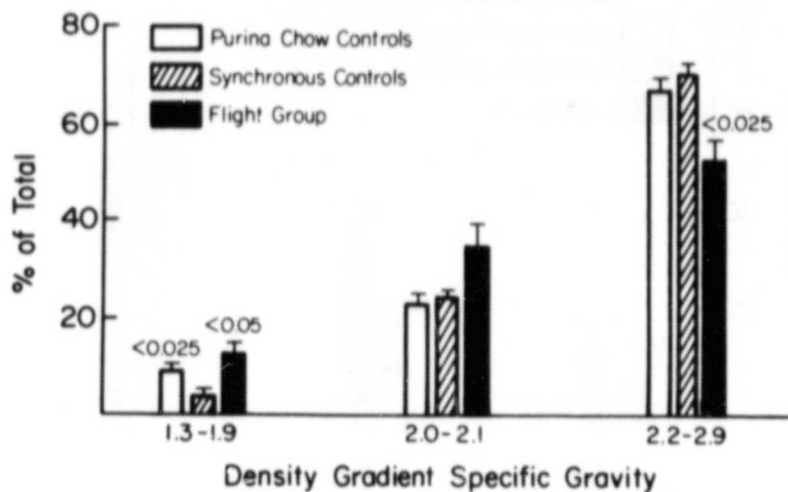
Figure 9

The distribution of collagen hydroxyproline in density gradient(specific gravity) fractions of the alveolar bone of rats sacrificed immediately after spaceflight vs that in several control groups.

Density Gradient Fractionation of Rat Alveolar Bone Total Calcium
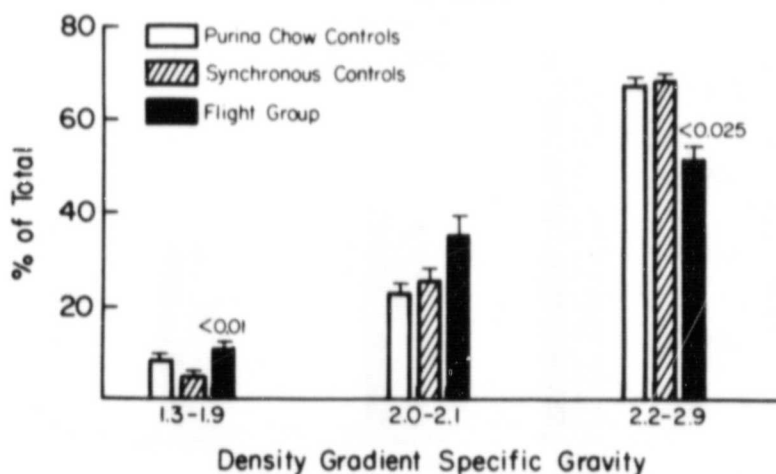
Figure 10

The distribution of calcium in specific gravity fractions of the alveolar bone of rats sacrificed immediately after spaceflight vs that in several control groups.

Density Gradient Fractionation of Rat Alveolar Bone
Inorganic Phosphate
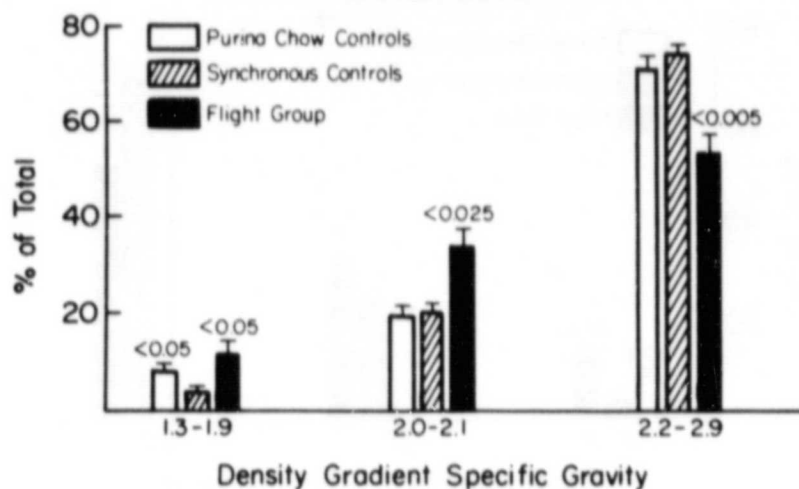
Figure 11

The distribution of inorganic phosphorus in specific gravity fractions of the alveolar bone of rats sacrificed immediately after spaceflight vs that in several control groups.

Total Mineral and Hydroxyproline Content
of Rat Alveolar Bone
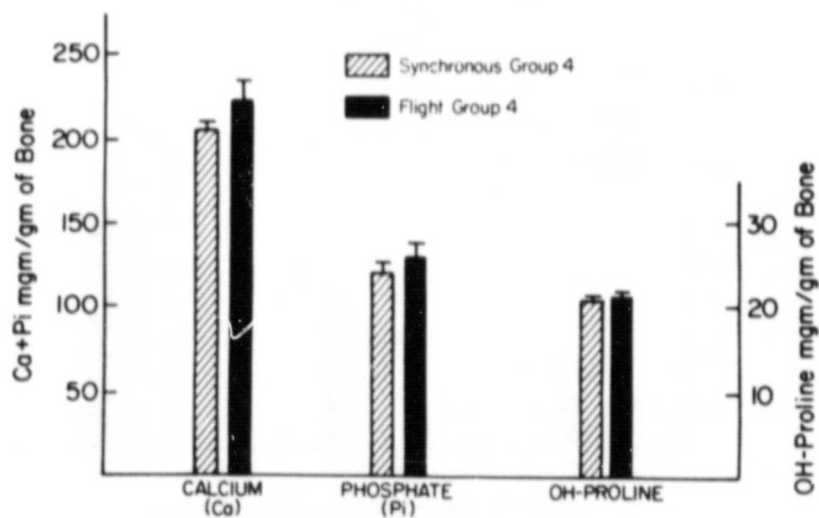
Figure 12

Total mineral and hydroxyproline content of alveolar bone of rats flown in space for 18.5d and sacrificed after a 29d recovery period at 1-G.

300

Density Gradient Fractionation of Rat Alveolar Bone
Collagen (OH-Proline)
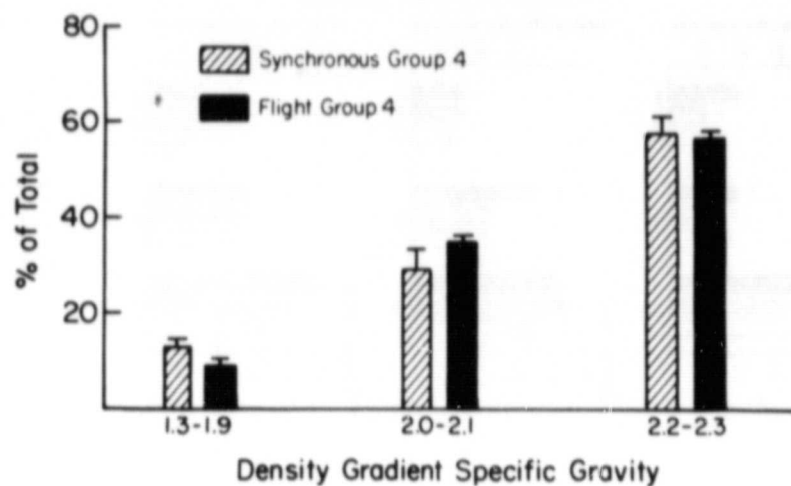
Figure 13

The distribution of hydroxyproline in specific gravity fractions of the alveolar bone of rats flown in space for 18.5d and sacrificed after a 29d recovery period at 1-G.

Density Gradient Fractionation of Rat Alveolar Bone
Total Calcium
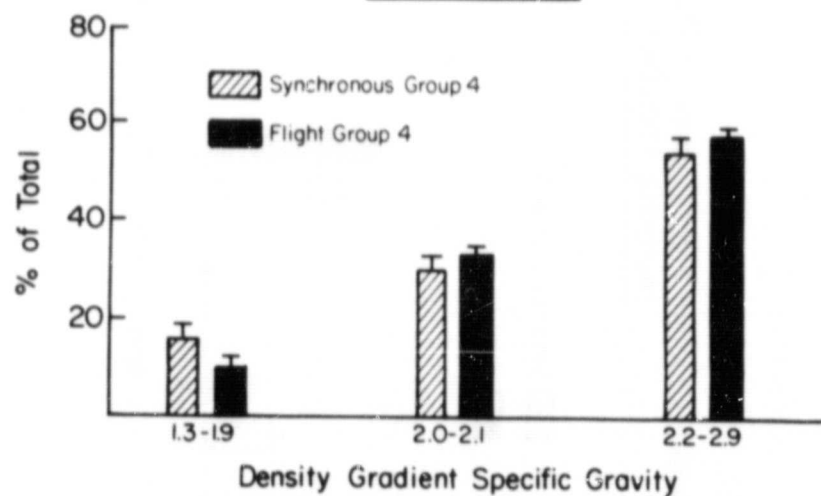
Figure 14

The distribution of calcium in specific gravity fractions of the alveolar bone of rats flown in space for 18.5d and sacrificed after a 29d recovery period at 1-G.

Total Mineral and Hydroxyproline Content of Rat Incisors
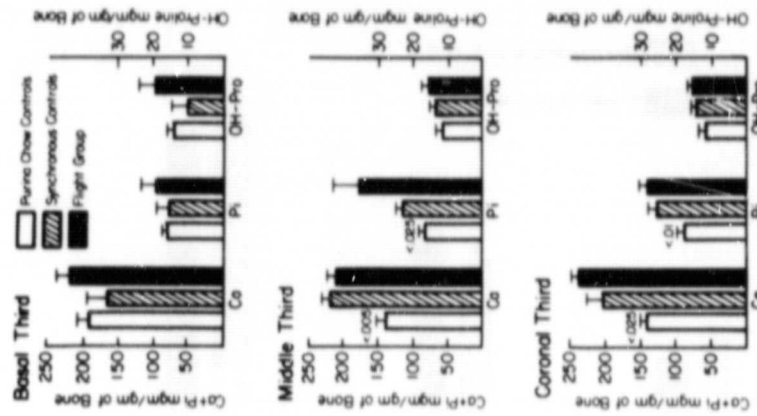
Figure 16

Total mineral and hydroxyproline content of the rat lower incisor in animals sacrificed immediately after an 18.5d exposure to 0-G.

Density Gradient Fractionation of Rat Alveolar Bone Inorganic Phosphate

Figure 15

The distribution of inorganic phosphorus in specific gravity fractions of the alveolar bones of rats flown in space for 18.5d and sacrificed after a 29d recovery period at 1-G.

Density Gradient Fractionation of Rat Incisors
Collagen (OH-Proline)

Figure 17

Distribution of hydroxyproline in specific gravity fractions of the lower incisors of rats sacrificed immediately after an 18.5d exposure to 0-G.

Density Gradient Fractionation of Rat Incisors
Total Calcium

Figure 18

Distribution of calcium in specific gravity fractions of the lower incisors of rats sacrificed immediately after an 18.5d exposure to 0-G.

Density Gradient Fractionation of Rat Incisors
Inorganic Phosphate

Figure 19

Distribution of inorganic phosphorus in specific gravity fractions of lower incisors of rats sacrificed immediately after an 18.5d exposure to 0-G.

303
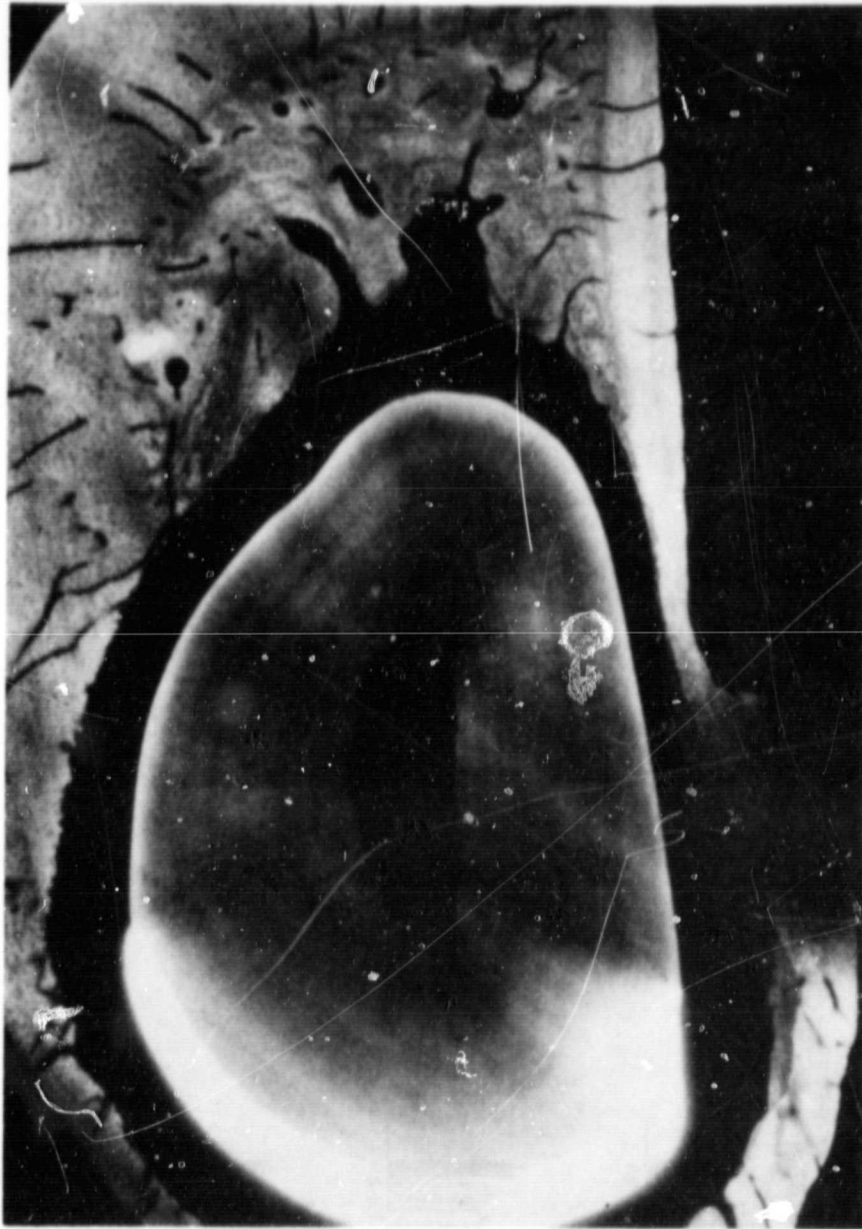
Figure 20

Microradiograph showing a cross section of a lower incisor and
investing bone in the region of the diastema of the mandible of
a rat exposed to 18.5d at 0-G. The appearance of the tissues
is normal. Note the alternating bands of highly and lowly
mineralized dentin laminae.

COSMOS 1129
Electron Microprobe Analysis of Dentin
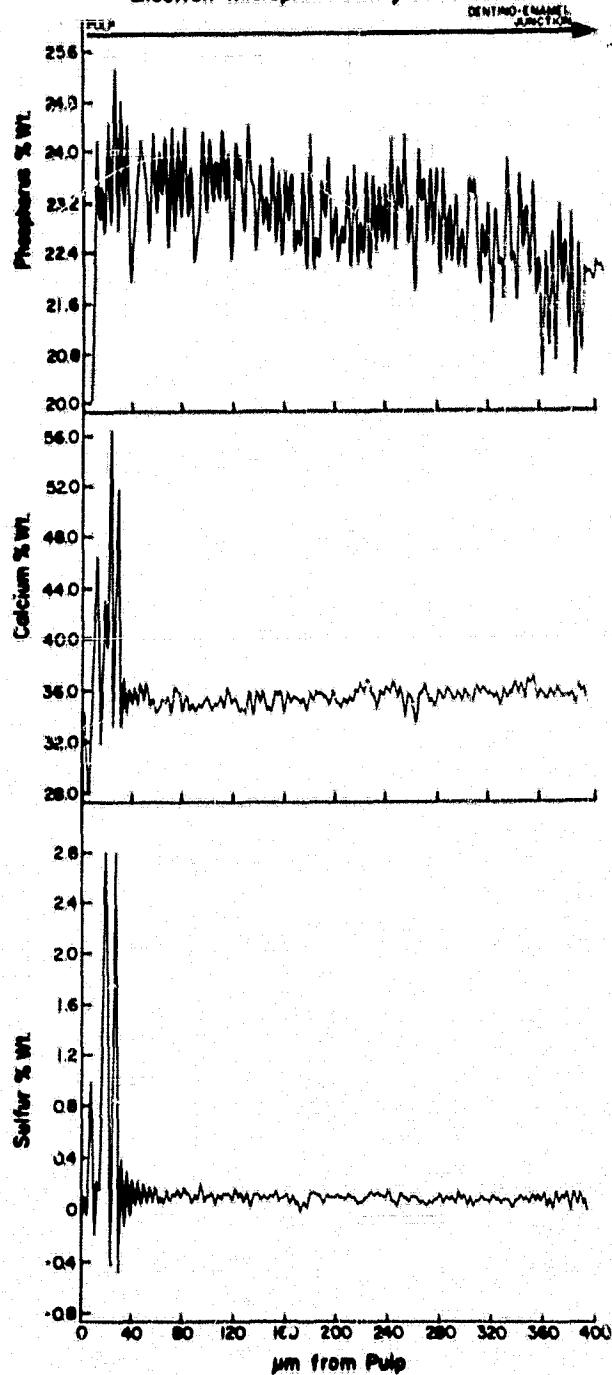
Figure 21

Recombinations(sum of all harmonics with a period≤ 4.5μm) of raw data for phosphorus, calcium and sulfur distribution in electron microprobe traverses(1.0μm intervals) across the labial surface of rat dentin. (Rat IF-I)

305
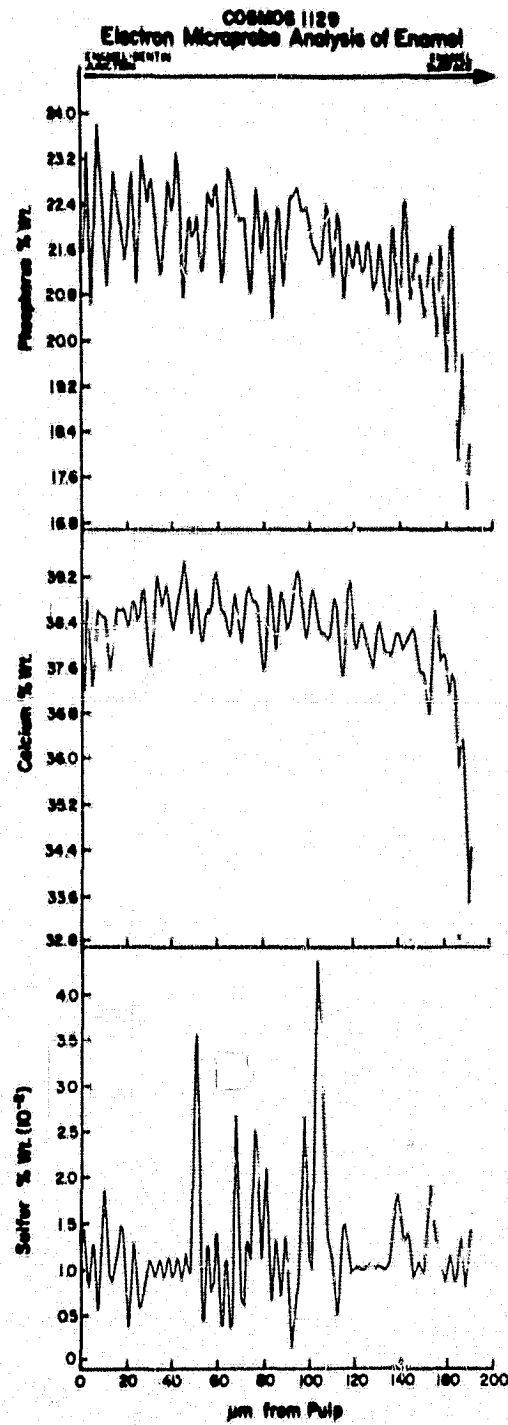
Figure 22

Recombinations(sum of all harmonics with a period ≤ 4.5μm) of
raw data for phosphorus, calcium and sulfur distribution in
electron microprobe traverses(1.0μm intervals) across rat
enamel in the region of the mandibular diastema.

K 310

The Effect of Space Flight on Osteogenesis and Dentinogenesis

in the Mandible of Rats

Supplement 1: The Effects of Space Flight on Alveolar Bone

Modeling and Remodeling in the Rat Mandible

P. Tran Van, A. Vignery and R. Baron

Departments of Internal Medicine and Cell Biology

Yale University School of Medicine

333 Cedar Street

New Haven, Connecticut 06510 U.S.A.

SUMMARY

The histomorphometric study of alveolar bone, a non-weight-bearing bone submitted mainly to the mechanical stimulations of mastication, showed that space flight decreases the remodeling activity but does not induce a negative balance between resorption and formation. The most dramatic effect of space flight has been observed along the periosteal surface, and especially in areas not contiguous with (covered with) masticatory muscles, where bone formation almost stopped completely during the flight period. This bone being submitted to the same mechanical forces in the flight animals and the controls (synchronous and vivarium) it is concluded that factors other than mechanical loading might be involved in the decreased bone formation during space flight.

INTRODUCTION

Metabolic studies of the Skylab astronauts during space flight concluded that there had been a significant increase in urinary calcium (1) similar to the observations made during bed rest immobilization. In the rat jaw bone, the highest density fraction in the flight rat had 30% less mineral and hydroxyproline (collagen) than the corresponding fraction in the control rat (2). Such data suggested a failure of bone mineral maturation. Microscopic examination of the long bones of male Wistar rats after about 20 days in space showed that the bone formation rate decreased about 40% compared with the control's (3). A decreased amount of trabecular bone near the cartilaginous growth plate was also noticed in space flight rats (4).

Following this information about bone loss and the lack of bone formation, our study has been concentrated on the dynamic histomorphometry technique described by Frost (5) and applied to the alveolar bone (6) to determine the extent and duration of each phase of the bone remodeling sequence, the mean calcification rate and the amount of bone mineralized per day. In the rat, alveolar bone remodeling is associated with the continuous drift of the teeth throughout the life of the animal (6,7). As the tooth drifts, there is one side of the socket which is in continuous bone formation (modeling side) and the opposite side shows alternative bone resorption and formation within small foci (remodeling side) (6). This model has already been used to study the cellular kinetics (7), function and origin of the bone cells (8,9) as well as the effects of calcitonin (10), parathyroid hormone (8,11), and the short and long term effects of occlusal hypofunction (12,13) on bone modeling and remodeling.

Under space flight conditions, and assuming the animals are eating normally, this bone should be subjected to only very slightly different mechanical

conditions which should not induce marked changes in bone remodeling if all other metabolic conditions are unchanged. On the other hand, if the changes observed by others in long bones (3) are due totally or in part to systemic changes, the alveolar bone remodeling should also be affected, and even more markedly considering its very high normal turnover rate (14).

MATERIALS AND METHODS

For a description of the experimental protocol and of the group of animals, refer to Cosmos 1129 experimental protocol. Our own procedure follows: The molar area was dissected out of the right lower jaws, fixed in alcohol 40% at 4°C, dehydrated in graded alcohol 70%, 90%, 100%, and embedded in methyl-methacrylate without decalcification. Horizontal sections, 4 microns thick, were prepared with a Jung K Microtome from the cervix to the apex of the root. One section out of every five in the middle part of the buccal root of the first molar was stained with Toluidine blue, pH 2.8. One section out of every five of these sections was prepared at a thickness of 8 microns, for fluorescent microscopic analysis. All measurements were made on the socket of the buccal root of the first molar.

The cellular measurements were made on four stained sections, using a Planimeter (MOP 3, Carl Zeiss, Germany), at 400 X magnification on a magnetic table. The following parameters were recorded:

- Extent of the remodeling side.

- Active resorption surface: interface between osteoclasts and bone.

- Reversal lacunae: extent of Howship's lacunae without osteoclasts and without osteoid tissue, lined with mononucleated cells.

- Remodeling formation: extent of lacunae lined with osteoid tissue along the remodeling side.

309

- Resting area or inactive surface: the bone surface covered neither by osteoclasts, nor osteoid tissue, nor Howship's lacunae.
- Number of osteoclasts on-bone and their number of nuclei.
- Number of osteoclasts off-bone and their number of nuclei.
- Osteoid thickness on the modeling side.

<u>Fluorescent label</u>: Measurements of tetracycline labelings were made on 4 x 5 inch black and white polaroid micrographs taken on a Univar microscope (Reichert, Austria) equipped with epifluorescence at 250 X magnification. Four sections 8 microns thick were measured on a magnetic table (MOP 3, Carl Zeiss, Germany) and the following parameters were recorded:

- The mean calcification rate per day.
- The volume of bone calcified per day.
- The bone porosity.
- The length of the modeling side.
- The length of the remodeling side.
- The volume of the periodontal ligament on the modeling side.
- The volume of the periodontal ligament on the remodeling side.
- The width of the periodontal ligament on the modeling side.
- The width of the periodontal ligament on the remodeling side.

All data are expressed in both relative values (%), absolute values (mm, mm^2, mm^3) and standard deviation of the mean calculated.

In addition, the mean calcification rate was also measured on the periosteum along the buccal surface of the mandible at 3 different sites, 2 of them in areas where the masticatory muscles are contiguous with the periosteum (m_2 and m_3) and one area where the periosteum is covered only by the gingival epithelium (m_1).

RESULTS

A. Alveolar bone remodeling

1. Preflight group (SB and FB, Table I)

The comparison of the preflight groups did not show any significant differences in the calcification rate and the total amount of bone calcified per day. There was, however, a significant increase in the number of osteoclasts and the extent of the resorbing surface ($p < 0.02$) and a decrease in the thickness of the osteoid seam along the modeling side ($p < 0.01$) in the FB group. These changes can be attributed to the stress of the training period.

2. Groups 1V, 1S and 1F (Table II, Figures 1, 2, 3)

The only change observed between the 1S and 1F group (flight effect) was a nearly significant decrease in the mean calcification rate ($0.10 > p > 0.05$). When compared to the vivarium animals (1V), this difference became clearly significant ($p < 0.05$). Concomitantly, a slight but not significant decrease was observed in all the resorption parameters in the space flight group of animals.

3. Postflight groups

a. Group 2S, 2V and 2F (Table III)

The tendencies observed in the previous groups of animals are maintained here. The only difference between the S and F group is a nearly significant ($0.10 > p > 0.05$) decrease in the mean calcification rate.

When comparing the F and V animals, this difference became significant ($p < 0.05$); moreover, other concomitant changes became significant: in the F group there was an increased resting surface ($p < 0.05$), an increased extent of labels on the modeling side ($p < 0.02$) and a markedly decreased thickness of the osteoid seam on the modeling side of the socket ($p < 0.01$). All these changes clearly indicate a decrease in the rate of the drift of the teeth in the flight group.

b. Groups 4S, 4V and 4F (Table IV)

Although the same tendencies were observed between the groups S and F, they were not significant. Only one unexplained significant decrease (p < 0.05) was observed in the osteoid surface of the remodeling side in the flight group. When comparing the F group to the V animals, the same differences were observed as previously in the groups 2: a decrease in the mean calcification rate (p < 0.02) and the amount of bone calcified per day (p < 0.01) as well as an increase in the osteoid thickness on the modeling side (p < 0.05) in the flight group. Altogether these results indicate a slower drift of the teeth in the postflight period as well as during the flight period itself.

When taking all these results into consideration (Fig. 4) it is possible to show a progressive decrease in the calcification rate as a function of age in the control animals. The synchronous group showed the same tendency but with a slower, although not significant, rate than the vivarium animals. The animals subjected to the flight showed a nearly or fully significant slower calcification rate than the synchronous or vivarium animals. However, these changes were not associated with any changes in periodontal ligament thickness and/or increased porosity of the alveolar bone, therefore indicating that they were due to a decrease in the speed of tooth drift (and consequently turnover rate or vice versa) and not to an imbalanced or abnormal bone formation per se.

B. Periosteal bone formation (Tables V and VI, Figure 5)

No differences were noted in the average calcification rate between the 3 areas that have been measured in the vivarium and/or synchronous groups. On the other hand, when the animals subjected to the space flight are taken into consideration, a very significant difference is observed between zones covered and not covered by muscles. Although the flight group shows a sig-

nificant decrease in bone calcification rate this effect is especially dramatic along the periosteal area not covered by muscle.

The recovery period showed the same trends as along the alveolar socket; bone formation along the periosteum was still very significantly lower than control during the first 6 days after the flight, but then returned to normal values.

DISCUSSION

The hypothesis which had to be tested in this study was that the changes in bone formation observed along the periosteum of space flight rat long bones (3) were essentially due to the lack of weight-bearing mechanical stimulation and not to a systemic factor. Alveolar bone remodeling was the ideal area of the skeleton in which to test this hypothesis because one would assume that weightlessness would have minimal effects in this non-weight-bearing bone upon which comparatively enormous mechanical pressures are exerted during the masticatory function. In addition, the existence of very accurately balanced bone modeling and remodeling activities associated with the physiological drift of the teeth, as well as of a very high turnover rate, make this bone very sensitive to slight and/or short term changes (14).

The results obtained in the present study showed the absence of effects of space flight upon the balance between bone formation and resorption in a bone where most of the mechanical stimulations have been maintained throughout the experiment. There was, however, a slight but constant decrease in the alveolar bone turnover rate. This decreased remodeling activity, although present in the synchronous groups of animals, living on earth under the exact space flight conditions but without weightlessness, was significantly lower in the space flight animals, even after a three week recovery period. It is not possible

to know if these changes were due to the slight difference in mechanical stimulation one would expect even in the jaws, or to a change in systemic factors.

In terms of bone remodeling activity, our results indicated a decrease in the birth rate of new Basic Multicellular Units (BMU) at the tissue level rather than an abnormal activity at the BMU or the cellular levels. Although the latter cannot be ruled out, there was, however, a good balance and a good coupling between resorption and formation. The changes observed by Roberts in the same animals (15), and suggesting a lack of conversion from osteoprogenitor cells to mature osteoblasts in the periodontal ligament facing the modeling side of the sockets, is therefore very likely due to a slowdown of the whole turnover rate and the physiological drift of the teeth, rather than to a primary defect in cell differentiation. However, the lack of recovery in the two postflight groups remains troublesome in this respect. As a matter of fact, both Roberts (15) and Morey and Baylink (3) studies indicated that the osteoblastic differentiation and activity returned to normal levels rapidly during the postflight periods. This discrepancy remains to be explained.

Of major interest are the results obtained along the periosteal surface of the alveolar bone. We observed at this site, like at all other sites in the skeleton and along the bone formation side of the tooth socket, a decrease in the average calcification rate in the flight group, despite a maintenance of mechanical stimulation. However, this decrease in bone formation was extremely dramatic in areas not contiguous with muscle and only moderate in areas contiguous with muscles. In both areas, it is possible to assume that the mechanical conditions, largely dominated by the masticatory function, are comparable in the flight and synchronous groups. Such local variations in the effects of space flight have never been mentioned before. Further studies

would be necessary to find out whether this differential decrease in the bone formation rate during space flight is the result of a combination of local and systemic factors, either endogenous or environmental. One is, however, driven to the conclusion that a factor other than mechanical loading is responsible for both the decreased turnover along the alveolar sockets and the decreased formation at the periosteal surface, marked differences being observed in this study between bones essentially subjected to the same mechanical conditions (synchronous vs. flight groups).

In conclusion, the alveolar bone remodeling rate, although decreased by the simulated space flight (synchronous controls), was significantly lower in the actual space flight groups. However, the balance between resorption and formation was not modified in this non-weight-bearing and still mechanically stimulated bone, excluding the existence of a systemic factor able to explain the otherwise observed osteopenia in weight-bearing bones.

REFERENCES

1. Whedon, C.D., L. Lutwak, P.C. Rambaut, M.W. Whittle, M.C. Smith, J. Reid, C.S. Leach, C.R. Stadler and D.D. Sanford. Mineral and nitrogen metabolic studies, experiment M071. In: Biomedical Results from Skylab, NASA SP-377, pp. 164-174 (1977).

2. Simmons, D.J., J.E. Russell, F. Winter, G.D. Rosenberg and W.V. Walker. Bone growth in the rat mandible during space flight. In: U.S. Preliminary Reports Cosmos 1129 (1979).

3. Morey, E.R. and D.J. Baylink. Inhibition of bone formation during space flight. Science 201:1138-1141 (1978).

4. Yagodovsky, V.S., L.A. Triftanidi and G.E. Gorokhova. Space flight effects on skeletal bones of rats. Av. Space Environ. Med. 47:734-738 (1976).

5. Frost, H.M. A method of analysis of trabecular bone dynamics. In: Bone Histomorphometry. P.J. Meunier, Ed., Lab Armour Montagu, Paris, pp. 445-476 (1977).

6. Baron, R. Remaniement de le lame cribriforme et des fibres desmodontales au cours de le migration physiologique. J. Biol. Buccale 1:151-171 (1973).

7. Roberts, W.E. Cell kinetic nature and diurnal periodicity of the rat periodontal ligament. Arch. Oral Biol. 20:465-471 (1975).

8. Roberts, W.E. Cell population dynamics of periodontal ligament stimulated with parathyroid extract. Am. J. Anat. 143:363-370 (1975).

9. Dorey, C.K. and K.L. Bicks. Ultrastructural analysis of glycosaminoglycan hydrolysis in the rat periodontal ligament. Calcif. Tiss. Res. 24:135-141 (1977).

10. Baron, R. and J.L. Saffar. A quantitative study of the effects of prolonged calcitonin treatment on alveolar bone remodeling in the golden hamster. Calcif. Tiss. Res. 22:265-274 (1977).

11. Duflot-Vignery, A. Etude quantitative des effets de le parathyroidectomie sur le remaniement osseux et le migration physiologique des dents chez le rat. J. Biol. Buccale 3:337-350 (1975).

12. Tran Van, P. and M. Mailland. Early response of periodontal ligament and alveolar bone to hypofunction in the rat. J. Dent. Res. 38:2261, Special Issue D (abstr.) (1979).

13. Levy, G. and M. Mailland. Etude quantitative des effets de hypofunction occlusale sur la largeur desmodontale et la resorption osteoclastique alveolaire chez le rat. J. Biol. Buccale 8:17-31 (1980).

14. Vignery, A. and R. Baron. Dynamic histomorphometry of alveolar bone remodeling in the adult rat. Anat. Rec. 196:191-200 (1980).

15. Roberts, W.E. and P.G. Mozsary. Effects of weightlessness on osteoblast differentiation in rat molar periodontium. In: U.S. Preliminary Reports Cosmos 1129 (1979).

TABLE I: BASAL GROUPS

Extent of the Different Activities Occurring Along the Remodeling Surface

	SB (5)		FB (5)	
	μ	%	μ	%
Perimeter of remodeling side	1185 ± 141		1158 ± 110	
Active resorption surface	76 ± 22	6 ± 1	175 ± 78	15 ± 7*
Reversal lacunae	552 ± 169	46 ± 9	593 ± 110	51 ± 8
Remodeling formation	104 ± 57	9 ± 5	60 ± 13	4 ± 1
Resting	453 ± 58	39 ± 6	341 ± 63	30 ± 6*
Total number of osteoclasts	18 ± 5		30 ± 14	
Total number of osteoclasts on-bone	12 ± 3		22 ± 9**	
Total number of nuclei of osteoclasts on-bone	15 ± 8		35 ± 13**	
Total number of osteoclasts off-bone	6 ± 4		8 ± 6	
Total number of nuclei of osteoclasts off-bone	11 ± 10		10 ± 8	
Osteoid thickness on the modeling side (μ)	7 ± 0.71		5.40 ± 0.55***	

Fluorescent Labels Measurements

	SB		FB	
Mean calcification rate/day (μ)	5.86 ± 1.79		5.41 ± 1.29	
Bone volume calcified/day $(mm^3) \times (10^{-3})$	3.69 ± 0.70		3.48 ± 0.48	
Bone density (%)	98	± 2	99	± 2
Length of modeling side (μ)	765	± 37	770	± 114
Length of remodeling side (μ)	1025	± 217	1163	± 321
Periodontal volume on the modeling side (mm^3)	48	± 4	46	± 4
Periodontal volume on the remodeling side (mm^3)	51	± 16	46	± 10
Periodontal width on the modeling side (μ)	77	± 8	73	± 7
Periodontal width on the remodeling side (μ)	59	± 11	51	± 7

* $p < 0.05$
** $p < 0.02$
*** $p < 0.01$

Extent of the Different Activities Occurring Along the Remodeling Surface

	IS (S) μ	%	IF (S) μ	%	IV (S) μ	%
Perimeter of remodeling side	1122 ± 106		1115 ± 64		1180 ± 125	
Active resorption surface	98 ± 42	9 ± 4	72 ± 31	6 ± 3	89 ± 36	7 ± 3
Reversal lacunae	442 ± 120	39 ± 8	499 ± 75	45 ± 5	565 ± 60	48 ± 6
Remodeling formation	98 ± 71	9 ± 7	74 ± 38	7 ± 4	105 ± 56	9 ± 5
Resting	485 ± 51	44 ± 6	469 ± 61	42 ± 6	422 ± 130	35 ± 8
Total number of osteoclasts	20 ± 5		19 ± 8		20 ± 6	
Total number of osteoclasts on-bone	15 ± 6		10 ± 4		11 ± 3	
Total number of nuclei of osteoclasts on-bone	15 ± 8		9 ± 7		18 ± 8	
Total number of osteoclasts off-bone	6 ± 2		9 ± 6		9 ± 4	
Total number of nuclei of osteoclasts off-bone	8 ± 3		10 ± 8		13 ± 7	
Osteoid thickness on the modeling side (μ)	5.66 ± 0.57		5.55 ± 0.73		6.15 ± 0.5	

Fluorescent Labels Measurements

	IS	IF	IV
Mean calcification rate/day (μ)	7.9 ± 0.8	6.8 ± 0.9*	7.6 ± 2.3+
Bone volume calcified/day (mm³) x (10⁻⁵)	4.7 ± 0.5	4.3 ± 0.4	5.0 ± 1.3
Bone density (%)	95.5 ± 1.7	95.7 ± 1.3	93 ± 2.6
Length of modeling side (μ)	721 ± 53	790 ± 89	833 ± 57
Length of remodeling side (μ)	1004 ± 157	955.17 ± 87	959 ± 113
Periodontal volume on the modeling side (mm³)	45 ± 4	51 ± 9	56 ± 7
Periodontal volume on the remodeling side (mm³)	44 ± 5	47 ± 6	46 ± 9
Periodontal width on the modeling side (μ)	77 ± 7	77 ± 5	81 ± 11
Periodontal width on the remodeling side (μ)	53 ± 11	59 ± 6	58 ± 5

* $0.10 > p > 0.05$ vs IS;   + $p < 0.05$ vs IF

318

TABLE III
Extent of the Different Activities Occurring Along the Remodeling Surface

	2S (5) μ	%	2F (5) μ	%	2V (5) μ	%
Perimeter of remodeling side	1064 ± 106		980 ± 125		1074 ± 30	
Active resorption surface	75 ± 49	7 ± 5	97 ± 33	10 ± 3	109 ± 31	10 ± 2
Reversal lacunae	473 ± 128	45 ± 8	367 ± 129	37 ± 9	487 ± 67	46 ± 7
Remodeling formation	75 ± 72	7 ± 7	83 ± 34	9 ± 5	98 ± 19	9 ± 2
Resting	432 ± 122	41 ± 6	433 ± 45	45 ± 5	380 ± 68+	36 ± 6
Total number of osteoclasts	18 ± 9		18 ± 4		21 ± 5	
Total number of osteoclasts on-bone	12 ± 8		14 ± 5		15 ± 4	
Total number of nuclei of osteoclasts on-bone	13 ± 12		14 ± 4		19 ± 5	
Total number of osteoclasts off-bone	6 ± 4		3 ± 2		7 ± 4	
Total number of nuclei of osteoclasts off-bone	7 ± 4		5 ± 3		10 ± 4	
Osteoid thickness on the modeling side (μ)	5 ± 1		4 ± 1		7 ± 1+++	

Fluorescent Labels Measurements

	2S	2F	2V
Mean calcification rate/day (μ)	6 ± 1	5 ± 1*	7 ± 2+
Bone volume calcified/day (mm³) x (10⁻³)	4 ± 0.3	4 ± 0.6	4 ± 1
Bone density (%)	95 ± 2	95 ± 2	96 ± 1
Length of modeling side (μ)	859 ± 66	883 ± 75	774 ± 16++
Length of remodeling side (μ)	872 ± 174	833 ± 137	966 ± 233
Periodontal volume on the modeling side (mm³)	50 ± 6	53 ± 7	45 ± 3
Periodontal volume on the remodeling side (mm³)	37 ± 13	36 ± 10	31 ± 5
Periodontal width on the modeling side (μ)	68 ± 13	70 ± 7	70 ± 7
Periodontal width on the remodeling side (μ)	51 ± 11	53 ± 8	42 ± 11

* $0.10 > p > 0.05$ vs 2S
+ $p < 0.05$, ++ $p < 0.02$, +++ $p < 0.01$ vs 2F

TABLE IV

Extent of the Different Activities Occurring Along the Remodeling Surface

	4S (4) μ	%	4F (5) μ	%	4V (4) μ	%
Perimeter of remodeling side	1110 ± 242		1076 ± 26		1119 ± 95	
Active resorption surface	79 ± 31	7 ± 2	63 ± 9	6 ± 1	72 ± 45	6 ± 3
Reversal lacunae	462 ± 174	40 ± 8	544 ± 112	51 ± 10	538 ± 108	48 ± 8
Remodeling formation	122 ± 39	11.5 ± 4	55 ± 35	5 ± 3*	126 ± 61	11 ± 5
Resting	447 ± 54	41 ± 7	414 ± 99	38 ± 10	382 ± 36	34 ± 4
Total number of osteoclasts	18 ± 4		15 ± 4		17 ± 10	
Total number of osteoclasts on-bone	12 ± 5		10 ± 2		11 ± 5	
Total number of nuclei of osteoclasts on-bone	14 ± 3		11 ± 7		11 ± 8	
Total number of osteoclasts off-bone	6 ± 0.5		5 ± 3		6 ± 6	
Total number of nuclei of osteoclasts off-bone	7 ± 3		8 ± 5		14 ± 14	
Osteoid thickness on the modeling side (μ)	5 ± 1		4 ± 1		6 ± 1+	

Fluorescent Labels Measurements

	4S		4F		4V	
Mean calcification rate/day (μ)	4.48 ±	0.74	3.94 ±	0.68	5.70 ±	1.08++
Bone volume calcified/day (mm³) x (10⁻³)	3.19 ±	0.76	2.79 ±	0.53	4.35 ±	0.67+++
Bone density (%)	95 ±	1	97 ±	2	96 ±	2
Length of modeling side (μ)	834 ±	120	794 ±	62	882 ±	83
Length of remodeling side (μ)	882 ±	259	947 ±	269	1120 ±	193
Periodontal volume on the modeling side (mm³)	53 ±	13	46 ±	5	53 ±	4
Periodontal volume on the remodeling side (mm³)	42 ±	13	44 ±	14	48 ±	9
Periodontal width on the modeling side (μ)	74 ±	9	69 ±	5	71 ±	8
Periodontal width on the remodeling side (μ)	58 ±	7	53 ±	5	55 ±	9

* $p < 0.05$ vs 4S

+ $p < 0.05$, ++ $p < 0.02$, +++ $p < 0.01$ vs 4F

TABLE V

Comparison of the mean calcification rate along the periosteal surface expressed in microns/day, without making distinctions between muscle covered and nonmuscle covered areas.

1V	1S	1F
2.76 ± 0.29	2.51 ± 0.30	1.71 ± 0.10***

*** $p < 0.001$

2V	2S	1F
2.36 ± 0.24	2.30 ± 0.32	1.14 ± 0.22***

*** $p < 0.001$

4V		4S		4F	
Flight time +6 days after reentry	6 days → 29 days after reentry	Flight time +6 days after reentry	6 days → 29 days after reentry	Flight time +6 days after reentry	6 days → 29 days after reentry
2.46 ± 0.7	1.90 ± 0.80	1.67 ± 0.67	1.88 ± 0.25	1.18 ± 0.26***	1.97 ± 0.24

*** $p < 0.001$

TABLE VI

Comparison of the calcification rate along the periosteal surface in the flight group in areas covered and not covered with masticatory muscles.

(The numbers represent the total amount of bone calcified during the flight period.)

	With Muscle	Without Muscle
1F	43.8 ± 4.93[a]	22.9 ± 4.62[b,c]
1S	54.30 ± 8.74	53.06 ± 6.18
1V	58.20 ± 9.44	61.2 ± 6.14

a) $p < 0.05$ vs. synchronous controls

b) $p < 0.001$ vs. muscle covered areas

c) $p < 0.0001$ vs. synchronous controls

FIGURE LEGENDS

Figures 1, 2 and 3

Buccal root of the first molar. Horizontal section X 100. Fluorescent labels. 8 μm thick section.

The left side of the socket, the modeling side (M) where continuous bone formation occurs is labeled (arrows) while the remodeling side (R) is not labeled.

Note a slight decrease in the amount of bone formed on the modeling side from the groups 1V (Fig. 1) to the group 1S (Fig. 2) and the group 1F (Fig. 3).

Figure 4

Effect of space flight on the calcification rate on the modeling side of the alveolar socket (a: $p < 0.05$ vs. S; b: $p < 0.05$ vs. V).

Figure 5

Effect of space flight on the calcification rate on the periosteal surface of the molar area (c: $p < 0.001$ vs. S).

CALCIFICATION RATE (µ /day)

Figure 4

**MEAN CALCIFICATION RATE
ON THE PERIOSTEAL SURFACE (µ /day)**

Figure 5

324
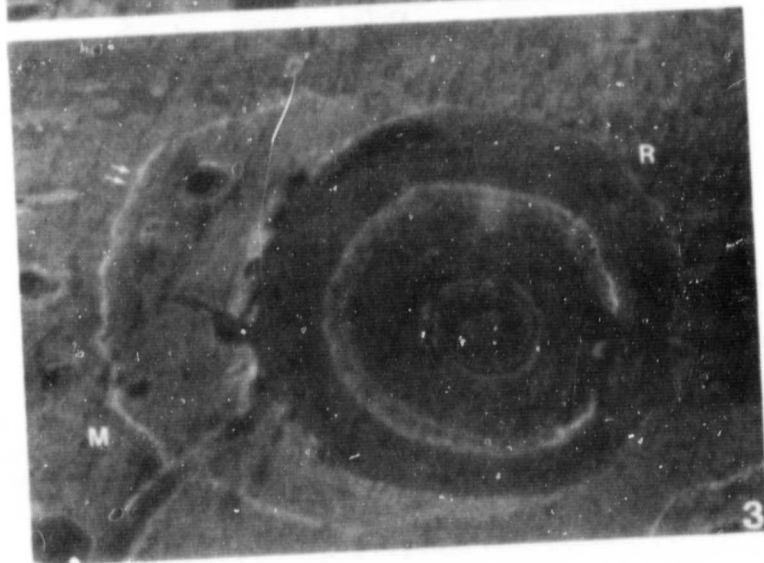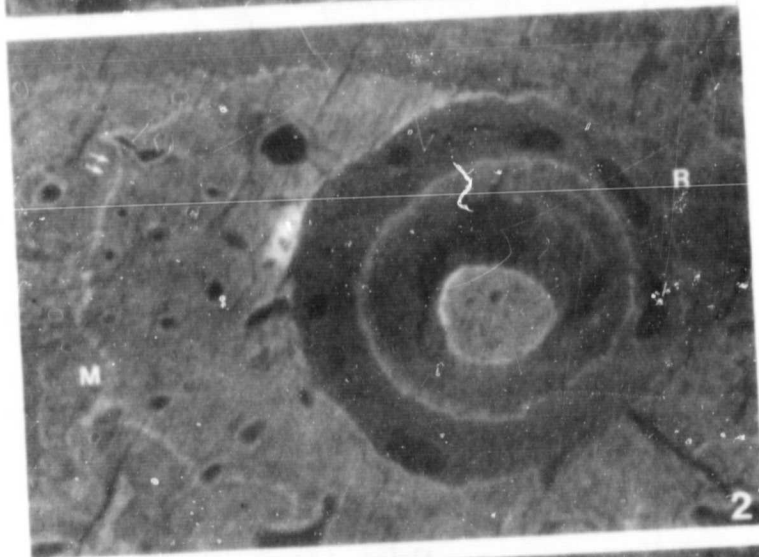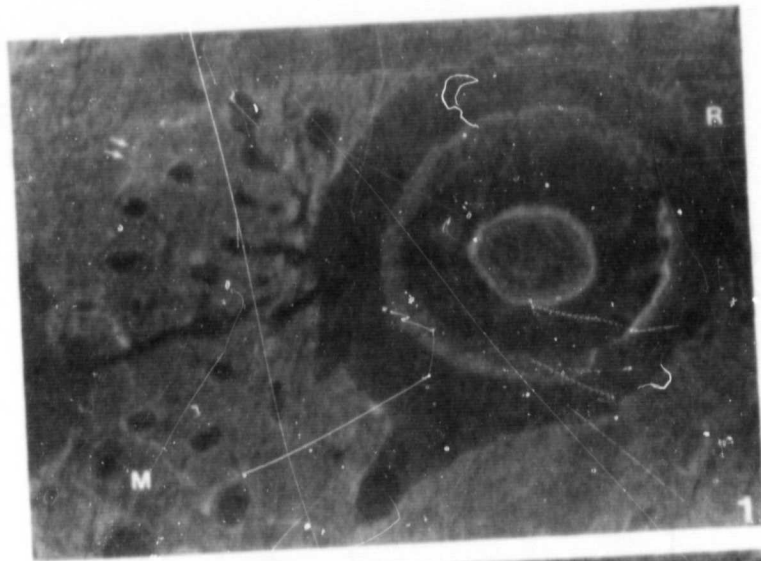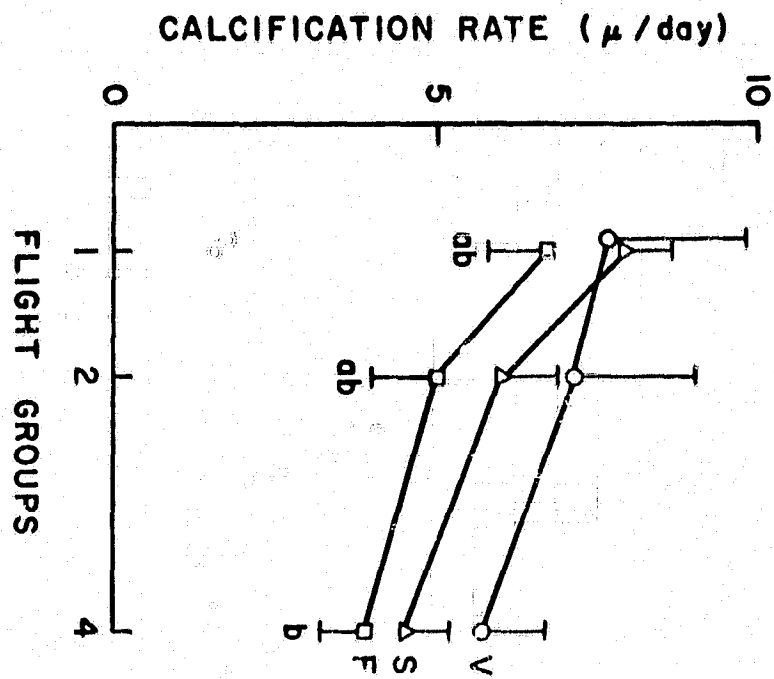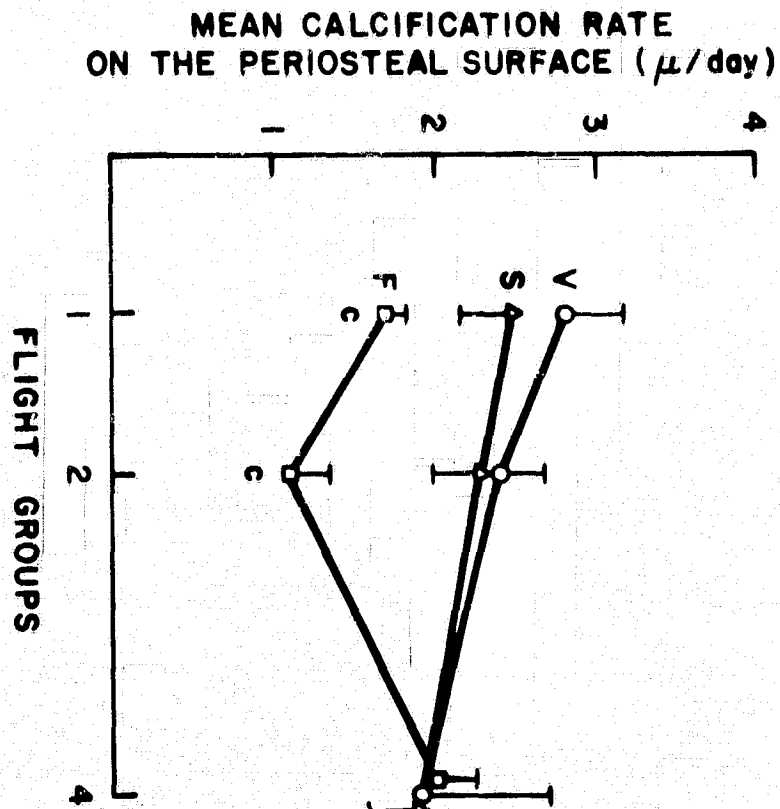
EXPERIMENT K-313: RAT AND QUAIL ONTOGENESIS

J. Richard Keefe, Ph.D.

BioSpace Incorporated

SUMMARY

The flight of Cosmos 1129 attempted to provide infor-
mation with respect to potential effects of Spaceflight
upon the processes of mammalian fertilization, implantation
and embryonic development. Five female and two male Wistar-
derived SPF rats were placed together on Day 2 of the 18.5
day flight in a common breeding chamber. Upon recovery, the
animals were weighed, housed separately and observed
for progressive pregnancy. By R+17, it was determined that
both flight and synchronous females were not carrying
normal pregnancies and three of the flight animals were
laparotomized. The uterus and ovaries were processed for
microscopic analyses. The two remaining flight females were
allowed to recover from the exploratory operation, rebred
with flight males and delivered normal litters.

As a control for potential transplacental effects that
might be interpreted as direct Spaceflight effects, a
series of fertilized Japanese Quail (Coturnix japonica)
eggs was flown on Cosmos 1129. Although all of the eggs
were adversely impacted by an inflight failure of the
incubator humidifier on flight Day 13, several embryos were
able to progress to a developmental stage equivalent to
that of a control 10-12 Day embryo.

INTRODUCTION

The studies of potential spaceflight effects upon
biological systems have been restricted among mammals to
adult males. Until the flight of Cosmos 1129, only two
female mammals had spent appreciable time in space – the
Soviet Cosmonaut Valentina Tereshkova and one experimental
Perognathus on Apollo 17.

Previous studies of vertebrate embryonic development
during spaceflight have been limited to non-mammalian
species with particular attention to fish and amphibian
eggs which require little in the way of special life-
-support systems.

In the only known spaceflight experiment involving
attempted fertilization in a vertebrate species, "Coworkers
of the Institute of General Genetics, USSR Academy of
Sciences" sent four guppies (six month old females after
the second spawning) on Kosmos 782. Two of the animals were
exposed to null gravity and two to the onboard gravity
control (0.6 G on the centrifuge) package on this 19.5 day
mission. The unnamed Soviet investigators concluded,
"Evidently, some flight factors inhibit the fertilization
of oocytes.", since they were unable to obtain evidence for
fertilization during the flight period in this rather
restricted experiment (1).

Studies on the development of Arbacia (Gemini III) and
Rana pipiens (Gemini VIII/Biosatellite II) by Young, Tremor
and coworkers have been restricted to ground-based
fertilization of eggs with the earliest flight exposure
commencing during second cleavage. Although brief in time
of spaceflight exposure, these studies clearly demonstrated
that differentiation to hatching in Rana is NOT adversely
affected by spaceflight factors (2).

On three separate flights, Scheld and coworkers flew
over 1400 developing embryos of Fundulus heteroclitus
(Skylab 3, ASTP and Kosmos 782). Due to preflight loading
restrictions, all of these embryos were at the mid-gastrula
stage or later at the time of lift-off. In each of these
experiments, embryogenesis continued at a slightly elevated
level, yielding normal hatchlings (3,4).

All of these embryological studies have demonstrated
the absence of any significant spaceflight effects upon
early-mid developmental stages. In several of these
studies, the embryos have proceded through the time of
hatching and have yielded a normal to slightly improved
hatch rate and normal ratio.

Two principal problems of embryonic development remain
to be studied under conditions of spaceflight.

1. The process of egg fertilization and the initial
stages of embryogenesis have not been successfully studied
during spaceflight.

327

2. The effects of spaceflight upon the processes of mammalian fertilization, implantation, placentation, embryogenesis and full fetal development have not been studied.

The absence of an effect of spaceflight upon the normal embryological development of free-floating aquatic eggs should not be extended to the more complicated mammalian species. In the mammalian system one must consider not only the DIRECT effects of spaceflight upon the developing embryo but must also consider the possible INDIRECT spaceflight effects brought about by the alterations in maternal physiology induced by null-gravity. Assuming that the female mammal will display the same set of alterations that have been demonstrated in the spaceflown male mammal, then the alterations in the endocrine, electrolyte, cardiovascular and musculo-skeletal systems could produce an INDIRECT effect of spaceflight upon the developing embryo/fetus by acting across the placenta. Any spaceflight experiment designed to study the processes of mammalian embryogenesis must take the potential indirect effects of null-gravity and stress acting across the placenta into the design philosophy.

The Principal Objectives of the K-313 Experiment flown on the COSMOS 1129 Flight were:

    I.   To determine the capability of a selected Mammalian species to undertake reproductive

processes, including copulation, fertilization, implantation, placentation and embryogenesis during Spaceflight exposure.

II. To separate potential spaceflight factors from indirect factors due to mater al stress.

III. To demonstrate the capability of Avian embryos to carry-out normal embryogenesis during spaceflight.

EXPERIMENTAL DESIGN

The K-313 experiment was originally designed to provide
pregnant female rats at the conclusion of the flight. These
rats were to be terminated on a schedule providing at least
two sets of embryos that had been conceived and undergone
embryogenesis under conditions of weightlessness. The
remaining pregnancies were to be allowed to go to term
delivery to determine possible effects of readaptation.
The Coturnix (Quail) component of K-313 would have provided
a comparison of direct vs indirect (transplacental) space-
flight effects as well as providing a basic understanding
of the ability of the Avian species to tolerate Null
Gravity exposure during embryogenesis.

Both flight and synchronous rat groups were provided a
dual chambered breeding cage constructed from a modified
Cosmos Bioblock (Figure 1). The males were housed in a
separate area from FD-3 (3 days preflight) to FD+2 at which
time the separator was opened and mingling allowed. A
total of eight feeding stations were provided for adminis-
tration of the flight paste diet, adlib water and activity
monitoring. The lid of the breeding cage was perforated to
enhance the airflow waste-handling system.

The flight and synchronous rats were to be placed upon
the flight paste diet for acclimation at FD-10 (55 gms/rat
once/day). At FD-3 five females were to be loaded into the

large compartment and two males into the smaller compartment of the breeding chamber (Figure 1). From FD-3 to the time of recovery, diet was to be administered at 6-hour intervals in the quantity of 55 gms diet/rat/day. Water was to be available adlibitum. At recovery, the animals were to be weighed, visually, inspected for pregnancy, and housed individually for transportation to and maintenance in the Moscow laboratories. All rats were to continue upon the paste diet through parturition.

The incubator designed for maintaining the Coturnix eggs during flight is illustrated in Figure 2 and consisted of an insulated chamber suspended by heavy-duty elastic shock cords from the mounting framework. Within the incubator chamber, the eggs were held between two perforated rubber strips which were matched to machined grooves on the inner and outer steel rings. The steel rings could be slightly adjusted to accomodate a minor variability in egg size. The five egg rings, each bearing 12 eggs, were capable of being rotated within the incubator housing thereby providing for a "turning" of the eggs before flight and throughout the synchronous control. Each egg was numbered and its position identified within the incubator by ring and position number.

The airflow within the incubator was from the core through the egg rings, with return along the outside of the rings. Provisions for maintaining a temperature of 37 C

and a relative humidity of 70-75 % were provided by the
source and monitors mounted in the core probe unit.

The Quail component of K-313 was to have provided the
following sets of parameters:

1. Loading of 60 fertilized Coturnix eggs into the
egg rings of the flight incubator at FD-3 with the
imposition of a controlled rate of rotation of the
egg rings to simulate a slow continuous egg rotation
during the preflight storage time.

2. Inflight rotation was not deemed necessary due
to the lack of a gravitational effect on the eggs.

3. Preflight and inflight egg storage temperatures
could not be reduced below the cabin ambient of
20-25 C.

4. Inflight activation of the incubator was to be on
FD+7 with the incubator to establish and maintain
conditions of 37 C and 70% RH.

5. The Synchronous control incubator was to provide
a continuous rate of egg ring rotation to simulate
the nullification of the gravity vector (similar to
that observed in the operation of a Clinostat).

MATERIALS AND METHODS

RATS: All rats were derived from the Czechoslovakian Institute of Sciences at Bratislava and were of a Wistar-derived SPF strain. All rats were born July 3-5 and weighed 234-300 g at the time of Flight experiment initiation.

QUAIL: Fertilized Japanese quail (Coturnix japonica) eggs were matched for size to fit the incubator egg rings (Figure 2) and stored for 5 days at 22 C. At T-3 the egg rings were loaded with 12 eggs/ring and five rings mounted into the flight incubator which was loaded into the Cosmos craft.

SACRIFICE SCHEDULE:

RATS: Depending upon the number of pregnant female rats recovered, alternative sampling of the litters was established with priorities as follows:

PRIORITY 1: Postnatal Day zero - sacrifice at birth.

PRIORITY 2: 10 Week Postnatal.

PRIORITY 3: 14 and 28 Days Postnatal.

PRIORITY 4: 5-7 Days Postnatal.

(Number pups/time dependent upon number and size of litters). Remaining pups were to be raised to sexual maturity for analysis of reproductive functions.

QUAIL: The flight load of 60 eggs was assumed to show 50 % viability with recovery site candling of eggs to be utilized to confirm this assumption. The sacrifice schedule was as follows:

1. R-0 (Day 12 embryos) - seven sacrifice at recovery.

2. R+5 - R+7 seven sacrificed at time of hatch.
Remaining live hatched quail were to be retained through
sexual maturity to determine suitability for postflight
breeding and normalcy of second generation.

Sacrifice was to be by decapitation with both the Rat
and Quail heads to be immediately immersed in a ten-fold
volume of Biostabilizer Fluid (see below) at 4 C. Samples
were to be stored and transported in the Biostabilizer fluid
to the U.S. laboratory for subsequent preparative steps.

BIOSTABILIZER FLUID: The composition and make-up of the
Biostabilizer fluid was as follows:

20.0 cc	8% Glutaraldehyde (pH 5.0/sealed under Nitrogen)
20.0 cc	8% Paraformaldehyde (freshly prepared)
2.0 cc	Dimethyl sulfoxide
42.8 cc	0.1 M Cacodylate buffer, pH 7.4 (see below)
10.0 cc	10% Acrolein solution

Preparation of the buffer solution: 3.198 gms of Sodium
cacodylate was dissolved in 100 cc of glass distilled water.
The pH was adjusted to 7.4 with 0.1 N HCl and the solution
was diluted to a final volume of 200 cc.

Upon arrival in the U.S. laboratory, each head was bissected
in the mid-line and the two halves divided further into
three portions as follows:

LEFT/RIGHT ANTERIOR: From tip of snout through middle
of the eye.

LEFT/RIGHT MID-PORTION: Middle of eye to behind the ear.

LEFT/RIGHT POSTERIOR: Containing cerebellum and temporo-mandibular joint and brainstem/neck.

Each portion of tissue was either poststabilized in Osmium tetroxide solution (1% in Cacodylate buffer) for three hours or transferred directly to the dehydration steps. Dehydration was in ascending concentrations of Ethanol followed by intermiscing with Propylene Oxide and embedding in either Araldite 502 or JB-4 mixtures. Sections were cut at 1 to 5 micra with glass knives, mounted in serial sequence upon thinly albumenized glass slides and stained for light microscopy with 0.25% Azure II in 0.5% Borax at 60 C for 3 mins.

Sections for electron microscopy were cut from selected block areas utilizing an LKB Ultratome equipped with a diamond knife. The 80 - 100 mμ sections were collected upon 75 x 300 mesh grids and stained with a combination Lead citrate Uranyl nitrate preparation prior to study with either a Siemens Elmskop I or a Philips 300 electron microscope.

PREFLIGHT STUDIES

WISTAR-SPF RATS:

To provide staged reference samples of embryos and pups, female Wistar-SPF rats were singly-placed with males and examined the following morning for vaginal plugs. The day of plug observation was termed Embryonic day 1 with conception arbitrarily assigned to 12:00 midnight. The females were shipped from the Pittsburg breeding facility to Cleveland by air on embryonic day 7 and tolerated the trip (no losses) well (truck to airport, two hour plane trip, truck to lab) for a total travel time of 6.5 hours on gestation day 8. Animals were singly housed, fed Purina Lab Chow adlib and maintained on a 12/12 (0800-2000) light cycle. Sample animals were sacrificed on Embryonic days 10, 12, 14, 16 and 18 while all term animals delivered normal litters (13 litters averaging 12.6 pups/litter). Eye opening in the neonates was on postnatal days 13 to 15. Samples from each set of embryos/fetuses were fixed in Bouins, 10% neutral buffered formalin (NBF) or Biostabilizer and processed for serial section/light microscopic studies to determine developmental correlates between peripheral vestibular structures and retinal development as well as to establish a staged series of specimens in each of three standard planes.

A series of preflight tests were carried out to determine any possible deleterious effects of cramped housing and USSR paste diet on the breeding of Czech Wistar-derived SPF rats. The tests included a mock-flight simulation in which 3 females and a male were housed for an 18-day period in a mock-flight cage of dimensions 6" high x 8" wide x 22" long. The cage was separated by a partition into a male compartment (floor area = 8" x 8") and a female compartment (area = 8" x 14"). On Mock flight-day 2 the divider was withdrawn and male-female interaction was possible. A similar cage was utilized for the Diet Controls (2 females and a male) fed Purina Lab Chow (ad lib). Both cages were provided with an open 1/4" mesh floor and solid sides. The tops of each cage were punched to provide for a movement of air in a vertical pattern. Each cage was elevated 2.5" above the waste collection tray to prevent coprophagy by the test animals.

The "Mock-Flight" animals were fed four times per day by injection of 10 gm aliquots of the USSR Paste diet into each of four feeding cups. Competition among the animals for the food was not observed although the animals appeared to be ravenously hungry at each feeding time. Feeding times were matched to the light cycle (12 hr light/12 hr dark) by rigid adherence to the following schedule:

0800 - Lights ON -feed

1400 - Mid-point Light cycle - Feed

2000 - Feed - Lights Off

0200 - Light On (2 Minutes) for Feed Administration

The Control cage was placed on the same Lab table two feet from the Experimental Cage. Room temperatures varied from 22 - 25 C. Room noise was at an absolute minimum.

Table 1 contains the experimental data generated by this Preflight study. The animals were housed singly and weighed daily at 2000 hours. For the first five days ALL animals were fed Purina Lab Chow. Two weeks before mockflight, the four animals randomly chosen to serve as experimentals were switched to the USSR paste diet, receiving 40 gms/day administered in 10 gm aliquots every six hours. The control animals continued on the Purina Lab Chow. All animals continued to be weighed daily at 2000 hours.

On T-2 (June 6) the animals were loaded into their respective cages. Each male was placed in the separate male compartment restrained from the females by a solid metal door. Once loaded into the cages, the animals were NOT HANDLED again until Recovery (R+0 on June 28). On T+2 (June 10), the metal dividers were removed. "Flight" and "Control" diets and the 12/12 light cycle continued during the 18 day mock-flight period.

Upon "Recovery" (June 28), each animal was weighed, visually inspected and housed singly with continuation of

respective diet regimen. Visual inspection revealed healthy animals with no signs of fighting in either group and confirmed that both of the "Control" females and two of the three "Flight" females were past mid-gestation. Births occurred on July 4 (2) and July 15 in the "Flight" group and on July 3 and 6 in the "Control" group. Figure 3 presents a summary diagram of weight profiles for the three "Flight" females during this simulation.

The post-partum decrease in maternal body weight demonstrated by E-1 and E-2 failed to show a turn around as was observed in both C-1 and C-2. This resulted from two problems:

1. The continuance until weaning of the Experimental animals on the USSR diet failed to provide adequate nutrition for the nursing mothers;

2. There was competition with the mother by the offspring for the administered paste diet. Such competition was NOT recognized until E-1 and E-2 continued to show significant weight losses.

The competition was recognized on R+25 (July 23) and, based upon observations in E-3 began about PN Day 8-10. All Experimental mothers were subsequently removed from their home

cages for diet administration, involving an approximate five minute interval of separation four times per day. The weight losses on all experimental animals continued but at a reduced level. Only E-1 failed to recover, becoming comatose and dying on R+26.

Cannibalism was NOT a problem in the Experimental group. Control mother C-1 destroyed the remaining members of her litter following litter size reduction on PN-6. Litter size reductions were attempted to balance out the nursing loads on the mothers and establish a comparison basis between the Experimental and Control litters (Table 2).

The USSR conducted a series of preflight Bioengineering tests that subjected the flight breeding cage with a nominal load of five female and two male rats to a simulated flight-duration. These tests were strictly tests of the Life Support systems of the breeding chamber and DID NOT include simulated lift-off or recovery stresses. In each of the tests, breeding, gestation time and litter size/sex ratio was normal (Personal Communication, Dr. L.V. Serova).

COTURNIX JAPONICA

The preflight testing in the Quail embryology experiment consisted of the following projects:

    1. Testing of stated preflight/inflight egg-holding temperature, relative humidity and rotation conditions on the subsequent development of the embryos.

2. Determination of egg viability, fertilization,
embryonic death rates and normalcy of development
in Coturnix under STANDARD and STATED conditions
of preflight holding and inflight holding/incubation.

3. Establishment of a series of staged Coturnix
embryos processed as proposed for the Cosmos mission
to serve as Ground-based controls.

Since the actual conditions for preflight storage and
handling were not known until immediately preflight, the
following parameters were utilized for this series of tests
(See Tables 3 and 4).

A. Incubator temperature = 37 C (36.1 - 37.8)

B. Relative humidity = 71 +/- 1%

C. Rotation of eggs = 3x daily

D. Preincubation Storage of Eggs:

1. Temperatures tested = 4-6, 10, 15, 20, 25 C.

2. Rotation tested = none, continuous or 3x daily.

3. Relative humidity = 40, 60, 70, 80 %.

E. Effect of egg freshness was tested by setting
batches of 100 eggs at selected times (0-14 days)
after laying.

During these tests eggs derived from several suppliers
as well as our own laying flock were utilized. In general,
the effect of shipping from distant suppliers with unknown
time and storage conditions enroute led us to base the majority
of our studies on our own flock. As an example, commercially

available eggs showed a fertility between 88.26% to 91.84% while our own flock consistently gave a greater then 95% fertility. Similar differences were observed in mortality rates.

Studies in our labs on another project indicated that continuous rotation of incubating chick eggs produced a more rapid development at 2 RPM while rotation at 10 RPM (14,400/day) caused serious developmental lags and numerous examples of multiple twinning (Egar and Keefe, unpublished results). Although not as extensive in scope, our preliminary results with Coturnix incubation demonstrate a similar pattern. For this reason the CONTINUOUS rotation rate was set to 2 RPM for the egg-storage and egg-rotation tests. We do NOT know the rate of rotation of the egg-rings in the Cosmos 1129 simulator.

The USSR conducted basic Bioengineering tests on the flight incubator to establish the adequacy of the life support systems. These Bioengineering tests DID NOT include simulated mechanical stresses of lift-off and recovery (Personal Communication, Dr. E.V. Shepelev).

EXPERIMENT EXECUTION ON COSMOS 1129

This portion of the report will be subdivided into four parts: flight rats/control rats/flight quail/control quail.

FLIGHT RATS: The flight breeding chamber with five female and two male Czech Wistar-derived SPF rats was loaded into the spacecraft three days before launch (09-22-79).

342

The divider separating males and females was removed on the 2nd flight day. We have no reports of unusual events in the Rat Ontogenesis experiment and assume that the temperature, relative humidity, air flow, waste handling and food administration systems functioned nominally as stated.

Upon recovery (FL/10-14:SY+VI/10-19), the animals were weighed and visually inspected for signs of pregnancy. Three of the flight females were felt to be pregnant although only two demonstrated a 20% increase from their preflight weights (Table 5). Two other flight females showed a slightly lower increase. The fifth animal demonstrated a negligible weight gain. However, ALL five of the flight females showed weight gains, attesting to the adequacy of the 55 gms/day diet. Both the synchronous control and vivarium females showed markedly larger weight increases (Table 5).

The animals were transferred to the Moscow laboratories and were housed individually. Administration of the flight paste diet continued but was supplemented with miscellaneous vegetables and rat chow. No weights were reported for days R+1,3,4,5 with daily weighings reported from R+6.

The three "pregnant" flight females and the synchronous animals showed only slight weight gains (Figures 4 and 5) compared with the Vivarium control group (Figure 6). When no births had occurred by R+17 and both the flight and

TABLE 5

WEIGHT GAINS OF RATS DURING 18.5 DAY FLIGHT PERIOD

FLIGHT	SYNCHRONOUS	VIVARIUM

FEMALES:weight gain (% increase)

1. 55 gm. (19%)	76 gm. (28%)	82 gm. (33%)
2. 52 gm. (20%)	84 gm. (30%)	70 gm. (27%)
3. 14 gm. (6%)	52 gm. (19%)	99 gm. (37%)
4. 36 gm. (14%)	58 gm. (22%)	95 gm. (33%)
5. 42 gm. (16%)	42 gm. (14%)	107 gm. (40%)

*** AVERAGES ***

39 gm. (15%)	62 gm. (23%)	90 gm (34%)

K-313 MALES (average gains):

46 gm.	54 gm.	59 gm.

(Weight data supplied by Dr. L. V. Serova)

synchronous females failed to show significant weight increases, the animals were laparotomized and the uteri and ovaries photographed. The intact uteri and ovaries were visually inspected and "triangular implantation sites" and "yellow bodies" (Corpora lutea) were tallied by gross observation. This data (supplied by Dr. Serova) is:

344

FLIGHT UTERI (BOTH HORNS/TWO ANIMALS):

26 "Implantation sites"

28 "Yellow bodies"

SYNCHRONOUS UTERI (BOTH HORNS/TWO ANIMALS):

23 "Implantation sites"

31 "Yellow bodies"

The uteri from the three "pregnant" flight rats and two synchronous rats were removed during animal sacrifice on R+17. The preparation of microscopic specimens from these uteri are in process by Dr. Serova. Two remaining flight females and the remaining synchronous animals were surgically restored and mated after a one-month recovery period.

The flight males were mated postflight with Vivarium females, and samples of the litters prepared as described under experimental materials. The litters from this pairing consisted of normal pups with average size and sex ratio. Flight males were also mated with the two recuperated flight females and produced litters. Samples from these litters have been received and histological studies are in progress.

CONTROL RATS: The controls for the rat portion of K-313 consisted of both Synchronous and Vivarium groups. The synchronous animals consisted of five females and two

males which were housed in an identical breeding chamber and subjected to the five-day delayed synchronous flight simulation, including diet regimen, housing, lift-off and recovery stresses. The divider separating the males and females was removed at Synchronous day 2.

Data on the pre- and postflight weights for the synchronous and vivarium females has been received from Dr. Serova and is presented in summary fashion in Figures 5 and 6. NONE of the synchronous females produced a successful pregnancy, although at least three of these have subsequently delivered normal litters of pups. The vivarium animals were housed in a single cage and all five females conceived and delivered litters on a standard 22-23 day gestation. Microscopic analyses of the pups derived from the vivarium and postflight breeding of flight and synchronous females reveal normal development in the peripheral vestibular, retinal and central nervous systems.

FLIGHT QUAIL: The 60 fertilized Coturnix eggs were loaded into the Cosmos craft on FD-3 and remained at cabin ambient temperature and relative humidity until FD+7. NO rotation of the egg rings was performed during the preflight period.

On FD+7 the incubator was activated and a temperature of 37 C with a relative humidity of 70% established. On FD+13 (incubation day 6) a failure of the humidifier caused

the relative humidity to drop to cabin ambient humidity at the elevated temperature (calculated to be 23-25% R.H.).

During the reentry phase of the flight, 40 of the 60 eggs were cracked. Analyses of the contents revealed that 20 of the eggs were either non-fertile or had failed to begin development. Of the remaining eggs, 23 ceased development at days 2-4, while 17 developed to day 7.5 - 12 stages (Figure 7). Representative samples of the dead embryos were fixed in Bouins solution and light microscopic analysis of serial sections confirms that the one flight embryo provided to us had been dead for 12-20 hours but had achieved a normal day 10 development in vestibular and retinal development at the time of death.

CONTROL QUAIL: The synchronous incubator was loaded with 60 eggs at SFD-3 and the egg rings rotated for the duration of the synchronous run. NO liftoff or recovery stresses were applied NOR was the incubator humidifier deactivated on Synchronous flight day 13 through Synchronous recovery.

The synchronous run produced the following results:

1. One non-fertile egg.

2. 18 dead embryos between days 2-6 incubation.

3. 19 live embryos at "recovery"(12-day incubation).

4. 14 live/unable to hatch.

5. 8 hatchlings.

Microscopic analyses of the Synchronous and Vivarium
Quail show normal retinal and vestibular development for
the respective ages of each animal (days 10 - 13).

RESULTS AND COMMENTARY

K-313 RAT ONTOGENESIS:

The results of the rat ontogenesis experiment have been
most unsettling.

1. All flight and synchronous females delivered
normal litters during the preflight period, thereby
assuring their fertility.

2. None of the flight or synchronous control
females gave birth as a result of breeding that occurred
during the flight phase of the experiment.

3. Flight males have subsequently sired litters
from both Vivarium and postoperative Flight females (see #4).

4. The one flight and two synchronous females that
have been bred following surgical examination have produced
viable litters with a normal size and sex ratio. Pups
derived from these litters demonstrate normal morpho-
logical development.

Whatever the limiting factor on the reproductive perfor-
mance of the flight and synchronous females it cannot be
attributed to direct spaceflight factors. The basic questions
of whether or not mammalian copulation, insemination, fertil-

ization, implantation, placentation and embryogenesis are
possible under the stressful conditions of spaceflight remain
unknowns.

The Life Support systems for the Rat Ontogenesis experi-
ment underwent extensive preflight testing by Soviet Scientists.
In their studies, using flight hardware and housing six
females/two males in the same volume that would house only
five females/two males during the flight phase, normal litters
resulted with a normal gestation interval (Pers.Com.,
Dr. Serova). Our own preflight simulation using a cage-model
with equivalent volume/animal also resulted in normal births.
Thus, crowding or an unusual grouping of animals does not
appear to be a limiting factor.

Similarly, the air-handling and food/water systems do
not appear to be responsible factors. In our preflight
simulations, the daily diet consisted of only 40 gms/day
while the amount available during the flight phase was
55 gms/day. It is significant that all female rats showed
a positive weight response during the flight period but that
their average inflight gain (39.6 gms on 94.5 kcal/day) was
less then the average inflight gain of the males from Groups
1-4 (46 gms on 68 kcal/day). Both the Synchronous and Vivarium
females showed a much larger weight increment over their
Group 1-4 counterparts (See Table 5 and Figure 8).

Simulations are being carried out by both Soviet
and American scientists in an effort to determine the restric-

tive factor that limited the Rat Ontogenesis eperiment on COSMOS 1129. However, only further studies of the processes of mammalian reproduction and embryogenesis under conditions of spaceflight can assure us that this fundamental and basic biological process will not be adversely affected by either the direct or indirect stresses of null gravity.

K-313 QUAIL ONTOGENESIS:

The Coturnix phase of K-313 demonstrated the hardiness of the Quail embryo under adverse conditions. The fertile flight eggs were exposed to at least three days of non-rotation at an elevated storage temperature (20-25 C), with a low ambient relative humidity, subjected to a set of significant lift-off stresses, seven more days of elevated storage temperatures before incubator activation and a failure in the flight incubator humidifier on incubator day 6 (FD+13). That none of the embryos survived beyond Embryonic day 12 is not surprising. That nearly one-third (17/60) developed beyond embryonic day 6 is remarkable (but see below).

Based upon examination of the external features and analyses of serial light microscopic sections of the one flight embryo that we have received (developmental stage equivalent to embryonic day 10), development under conditions of spaceflight appears to be normal.

However, with the elevated preflight and early inflight storage temperatures in this experiment, the Coturnix eggs may have been beyond the early stages of cleavage and gastrulation at the time of lift-off and orbital insertion. These stages are normally Day 1 stages for Coturnix and may have led to a moderately developed embryo by the time of incubator activation on Flight Day 7.

The Coturnix Synchronous control failed to simulate either lift-off or the reentry stresses and was maintained at the proper relative humidity throughout the entire "simulated-flight" interval and provided steady egg rotation during the preflight period.

Finally, the cause of the breakage of 2/3 of the flight eggs must be partially assigned to the failure of the flight incubator humidifier. The drop in relative humidty to a level of 23-25 % for a period of 6+ days must have led to a dehydration of the eggs and an increase in the fragility of the shell.

BIBLIOGRAPHY

----

(1) Gazenko,O.G., R.G.Butenko, B.A.Rubin and L.V.Belousov 1976
Preliminary Results of Studies on the Biosatellite
"KOSMOS-782" (Predvaritel'nyye rezul'taty issle-
dovaniy na biosputnike "Kosmos-782").NASA Technical
Translation, TT F 15,500, P76.

(2) Young,R.S.,J.W.Tremor,R.Willoughby,R.Corbett,K.A.Souza and
A.D.Sebesta 1971 The effect of weightlessness on
the dividing eggs of Rana pipiens, pp. 251 - 271.
IN: Saunder,J. (ED) "The Experiments of Biosatellite II"
NASA SP-204.

(3) Scheld,H.W.,J.F.Boyd,G.A.Bozarth,J.A.Conner,V.B.Eichler,
P.M.Fuller,R.B.Hoffman,J.R.Keefe,K.P.Kuchnow,
J.M.Oppenheimer,G.A.Salinas and R.J.vonBaumgarten 1976
Killifish hatching and orientation experiment MA-161,
PP.19-1 TO 19-14.IN:"Apollo-Soyuz Test Project:
Summary Science Report (NASA SP-412).

(4) Keefe,J.R.,H.W.Scheld,J.F.Boyd,P.M.Fuller and J.M.Oppenheimer
1978 Killifish Development in Zero-G on Cosmos 782:
Fundulus Experiment K-104, pp.179-199.IN: S.N.Rosenzweig
and K.A.Souza (EDS) "Final Reports of U.S. Experiments
Flown on the Soviet Satellite Cosmos 782"
NASA Technical Memorandum 78525.

(5) Egar,M.W. and J.R.Keefe (1980) Simulation of Null-gravity
by Continuous Rotation during Avian Development.
(Manuscript in preparation).

TABLE 1

DATE	DAY	FLIGHT DAY	GESTATION DAY(s)	EXPERIMENTALS FEMALES E-1	E-2	E-3	MALE E-0	CONTROLS FEMALES C-1	C-2	MALE C-0	PHASE
5-20 s		ALL RATS		201 L	185 L	202 L	258 L	205 L	218 L	293 L	WEIGHT
5-21 m		HOUSED		202 ↓	185 ↓	205 ↓	255 ↓	210 ↓	218 ↓	300 ↓	CHECK/
5-22 t		SINGLY		204 ↓	183 ↓	208 ↓	250 ↓	217 ↓	217 ↓	311 ↓	GROWTH
5-23 w		ALL adlib		207 ↓	183 ↓	212 ↓	269 ↓	217 ↓	223 ↓	313 ↓	CURVE
5-24 t		RAT CHOW		212 ↓	187 ↓	219 ↓	272 ↓	218 ↓	223 ↓	315 ↓	
5-25 f	T-14	ALL RATS		219 D	191 D	221 D	276 D	219 L	231 L	315 L	14-DAY
5-26 s	T-13	HOUSED		222 ↓	193 ↓	219 ↓	275 ↓	225 ↓	229 ↓	334 ↓	PREFLIGHT
5-27 s	T-12	SINGLY		220 ↓	184 ↓	212 ↓	271 ↓	223 ↓	232 ↓	340 ↓	HOLD
5-28 m	T-11			215 ↓	192 ↓	211 ↓	263 ↓	223 ↓	233 ↓	342 ↓	
5-29 t	T-10	D=USSR		212 ↓	197 ↓	208 ↓	270 ↓	226 ↓	237 ↓	346 ↓	
5-30 w	T-9	DIET		229 ↓	198 ↓	218 ↓	273 ↓	228 ↓	238 ↓	353 ↓	
5-31 t	T-8			229 ↓	201 ↓	222 ↓	277 ↓	231 ↓	237 ↓	341 ↓	
6-1 f	T-7	L=ad lib		235 ↓	204 ↓	224 ↓	281 ↓	231 ↓	240 ↓	363 ↓	
6-2 s	T-6	RAT CHOW		242 ↓	214 ↓	233 ↓	290 ↓	234 ↓	247 ↓	367 ↓	
6-3 s	T-5			239 ↓	208 ↓	227 ↓	284 ↓	241 ↓	243 ↓	382 ↓	
6-4 m	T-4			248 ↓	221 ↓	238 ↓	298 ↓	243 ↓	249 ↓	386 ↓	
6-5 t	T-3			248 ↓	220 ↓	238 ↓	296 ↓	241 ↓	249 ↓	390 ↓	
6-6 w	T-2			253 ↓	223 ↓	240 ↓	299 ↓	243 ↓	252 ↓	388 ↓	

** EXPERIMENTAL FLIGHT CAGE=3 female/1 male   CONTROL CAGE= 2 female/1 male **
** DIVIDERS SEPARATE FEMALE COMPARTMENT FROM MALE COMPARTMENT.DIETS CONTINUE**

DATE	DAY										PHASE
6-8 f	T-0	*** SIMULATED LIFT-OFF TIME ***									FLIGHT
6-9 s	T+1	*** USSR DIET = 10 gms/animal at 4 times/day ***									PHASE
6-10 s	T+2	*** DIVIDER PULLED IN BOTH CAGES - BREEDING POSSIBLE ***									BREEDING
		*** 6-8 thru 6-27 ANIMALS INFLIGHT-NO INFLIGHT WEIGHTS **									PHASE
		*** EXPERIMENTALS FED EVERY SIX HOURS ***									

DATE	DAY	FLIGHT DAY	GESTATION DAY(s)	E-1	E-2	E-3	E-0	C-1	C-2	C-0	PHASE
6-28 t	R+0		0↓17	326 D	290 D	308 D	364 D	324 L	372 L	485 L	RECOVERY
6-29 f	R+1		1↓18	335 ↓	304 ↓	318 ↓	370 ↓	345 ↓	390 ↓	469 ↓	PHASE
6-30 s	R+2		2↓19	339 ↓	308 ↓	317 ↓	371 ↓	350 ↓	400 ↓	477 ↓	
7-1 s	R+3		3↓20	343 ↓	312 ↓	316 ↓	372 ↓	355 ↓	409 ↓	484 ↓	ALL RATS
7-2 m	R+4		4↓21	354 ↓	325 ↓	319 ↓	380 ↓	369 ↓	430 ↓	478 ↓	HOUSED
7-3 t	R+5		5↓22	371 ↓	337 ↓	326 ↓	373 ↓	382 ↓	326***	483 ↓	SINGLY,
7-4 w	R+6		6↓22	327***	286***	339 ↓	384 ↓	397 ↓	320 ↓	489 ↓	WEIGHED
7-5 t	R+7		7↓22	322 ↓	281 ↓	333 ↓	386 ↓	403 ↓	312 ↓	489 ↓	DAILY.
7-6 f	R+8		8↓22	317 ↓	277 ↓	339 ↓	388 ↓	297***	310 ↓	490 ↓	
7-7 s	R+9		9↓22	311 ↓	269 ↓	340 ↓	382 ↓	296 ↓	313 ↓	498 ↓	DIETS
7-8 s	R+10		10↓22	318 ↓	264 ↓	348 ↓	383 ↓	301 ↓	308 ↓	506 ↓	CONTINUE
7-9 m	R+11		11↓22	308 ↓	259 ↓	350 ↓	386 ↓	292 ↓	308 ↓	503 ↓	
7-10 t	R+12		12↓22	312 ↓	270 ↓	365 ↓	395 ↓	268 ↓	319 ↓	505 ↓	
7-11 w	R+13		13↓22	295 ↓	253 ↓	362 ↓	385 ↓	268 ↓	291 ↓	499 ↓	
7-12 t	R+14		14↓22	295 ↓	251 ↓	377 ↓	397 ↓	291 ↓	311 ↓	505 ↓	
7-13 f	R+15		15↓22	303 ↓	251 ↓	390 ↓	394 ↓	293 ↓	287 ↓	501 ↓	
7-14 s	R+16		16↓22	287 ↓	245 ↓	404 ↓	394 ↓	306 ↓	316 ↓	504 ↓	
7-15 s	R+17		17↓22	285 ↓	245 ↓	343***	401 ↓	302 ↓	313 ↓	493 ↓	
7-16 m	R+18		18↓22	279 ↓	234 ↓	328 ↓	398 ↓	307 ↓	327 ↓	498 ↓	
7-17 t	R+19		19↓22	272 ↓	231 ↓	326 ↓	397 ↓	307 ↓	302 ↓	500 ↓	E1,E2,C2
7-18 w	R+20		20↓22	280 ↓	232 ↓	333 ↓	407 ↓	310 ↓	308 ↓	499 ↓	EYE OPEN
7-19 t	R+21		21↓22	271 ↓	227 ↓	327 ↓	405 ↓	307 ↓	295 ↓	503 ↓	
7-20 f	R+22		22	260 ↓	219 ↓	324 ↓	404 ↓	302 ↓	288 ↓	508 ↓	
7-21 s	R+23			256 ↓	214 ↓	321 ↓	406 ↓	318 ↓	328 ↓	519 ↓	
7-22 s	R+24			249 ↓	209 ↓	317 ↓	407 ↓	314 ↓	290 ↓	517 ↓	
7-23 m	R+25			245 ↓	205 ↓	308 ↓	408 ↓	311 ↓	308 ↓	513 ↓	
7-24 t	R+26			243ww	205ww	302 ↓	402 ↓	305 ↓	317ww	518 ↓	
7-25 w	R+27			----	203 L	300 ↓	405 ↓	310 ↓	314 L	514 ↓	
7-26 t	R+28			---	218 ↓	297 ↓	412 ↓	299 ↓	309 ↓	521 ↓	
7-27 f	R+29			---	238 ↓	291 .	437 ↓	287 ↓	300 ↓	529 ↓	
7-28 s	R+30			---	239 ↓	294 ↓	434 ↓	300 ↓	308 ↓	527 ↓	
7-29 s	R+31			---	244 ↓	290 ↓	436 ↓	308 ↓	313 ↓	531 ↓	E3-EYE
7-30 m	R+32			---	253 ↓	284 ↓	441 ↓	320 ↓	317 ↓	538 ↓	OPEN
7-31 t	R+33			---	255 ↓	271 ↓	441 ↓	315 ↓	313 ↓	522 ↓	
8-1 w	R+34			---	249 ↓	272 ↓	445 ↓	305 ↓	309 ↓	528 ↓	
8-2 t	R+35			---	258 ↓	266 ↓	447 ↓	318 ↓	317 ↓	532 ↓	
8-3 f	R+36			---	265 ↓	257 ↓	450 ↓	323 ↓	322 ↓	544 ↓	
8-4 s	R+37			---	261 ↓	244ww	451 ↓	.17 ↓	321 ↓	541 ↓	

LEGEND: *** = Birthdate; ww = Weaning; L = Lab Chow; D = Diet

TABLE 2
NEWBORN CZECH-WISTAR SPF RAT DATA

POSTNATAL DAY	E - 1 #	E - 1 AV/WT	E - 2 #	E - 2 AV/WT	E - 3 #	E - 3 AV/WT	C - 1 #	C - 1 AV/WT	C - 2 #	C - 2 AV/WT
1--->	7	6.41	10	5.95	14	4.79	16	5.98	16	6.09
2--->	7	7.50	10	6.82	14	5.22	16	7.03	16	6.84
3--->	7	8.20	10	7.81	14	5.88	16	7.93	15	7.57
4--->	6	9.43	6	9.77	6	7.25	16	8.30	6	8.78
5--->	6	9.95	6	10.92	6	8.28	15	8.11	6	9.27
6--->	6	9.83	6	12.77	6	9.78	--	----	6	9.20
7--->	6	11.23	6	13.95	6	11.15	--	-----	5	11.20
8--->	5	13.34	5	15.74	6	13.22	--	-----	4	12.73
9--->	5	15.06	5	17.72	6	15.15	==	====	4	14.53
10-->	5	16.20	5	19.44	6	16.03	--	-----	4	16.18
11-->	5	18.36	5	21.02	5	18.74	--	----	4	18.43
12-->	5	20.22	5	22.66	5	20.20	--	----	4	21.10
13-->	5	22.58	5	24.06	5	21.80	--	----	4	23.80
14-->	5	24.30	5	25.68	5	23.40	--	-----	4	26.88
15-->	4	27.23	4	27.55	5	24.40	--	-----	4	29.43
16-->	4	28.43	4	29.10	5	25.60	--	-----	4	30.60
17-->	4	30.25	4	31.00	5	27.40	--	-----	4	31.75
18-->	4	31.75	4	32.50	5	28.60	--	----	4	35.00
19-->	4	33.50	4	34.50	5	29.20	--	----	4	35.75
20-->	4	35.50	4	36.50	5	30.00	--	----	4	39.50
21-->	4	35.25	4	36.00	5	31.40	--	----	4	43.25

TABLE 4

QUAIL HATCHING RUNS

EGGS SOURCE	NO. SET	NO.EGG UNFERT	EGGS %FERT	EGGS LIVE	%LIVE	EGGS DEAD	%DEAD
1	176	16	91.84	96	48.97	84	46.66
2	247	29	86.26	123	49.79	95	45.57
BSI	500	21	95.8	259	51.8	220	45.92

HATCHING DATA FOR COTURNIX

HATCH DAY	INCUBATION DAY	SOURCE #1	SOURCE #2	SOURCE BSI	%HATCH
1	18	--	5	6	3.24 %
2	19	15	63	73	49.85 %
3	20	33	16	58	31.56 %
4	21	16	8	28	15.33 %
TOTALS-LIVE HATCH:		62	92	185	99.994
LIVE EMBRYO SAMPLE:		34	31	74	
TOTALS-EMBRYO/HATCH:		96	123	259	

(NOTE: TOTAL INCLUDES EMBRYO SAMPLES)
ON EMBRYONIC DAYS 6-14)

TABLE 3

EFFECT OF STORAGE CONDITIONS ON QUAIL EGG VIABILITY AND DEVELOPMENT
****

(ROTATED 3X/DAY>>><<REL.HUM.=50-55%)

SERIES	TEMP.	AGE	%SET	%HATCH
TEST 2	20 C	FRESH	100	53
TEST 3	20-22	10 D	100	6
TEST 4	10 C	10 D	100	44

(NO ROTATION >><<< REL.HUM.=50-55%)

SERIES	TEMP.	AGE	%SET	%HATCH
TEST 5	20-22	10 D	100	0
TEST 6	10 C	10 D	100	36

C1129 EGG STORAGE SIMULATION
(TEST 7 = CONTROL OF 12D AT 50% R.H.)
(TEST 8 = CONTIN.ROTATION (2 RPM))
(REL.HUM.=50%/2 DAY + 60%/10 DAY)

SERIES	TEMP.	AGE	%SET	%HATCH
TEST 7	20-22	12 D	100	3
TEST 8	20-22	2/10	100	8

FIGURE LEGENDS

Figures 3 through 6 have been normalized to display body weights of the female rats over identical time periods. The "inflight" period is reflected by the dashed lines since no actual weights were obtained during these time periods in any of the groups.

FIGURE 3 displays the weight curves of three female Czech Wistar rats during a preflight simulation in which they were maintained on 40 grams/animal/day paste diet. Breeding was possible following cage opening on day 22. Two of the animals delivered on day 46 and the third on day 57 (see Table 1). Note the slope of the dashed lines.

FIGURE 4 displays a plot of weight data from the five COSMOS 1129 flight females (data provided by Dr. L.V. Serova). Note the slope of the dashed lines (inflight portion) represents a continuation of the normal growth curve. Although these animals were provided with a paste diet of 55 grams/animal/day they showed only an average 15% weight increase during the flight period.

The weight decline in the immediate preflight period is unexplained and present in the synchronous and vivarium group data as well.

FIGURE 5: The weights of the five females of the synchronous group also show a continuation of the normal growth curve if the decrease immediately preflight is ignored.

FIGURE 6: The five females from the vivarium group demonstrate a marked slope during the "flight" period with prominent rises to parturi-

tion during the postflight period. Again, note the preflight decline in the weights of these animals although they were being maintained in the Vivarium.

FIGURE 7: Summary of the COSMOS 1129 Quail ontogenesis data (provided by Dr. E. Shepelev). The solid figures represent dead embryos (or non-fertile eggs), while the open circles at day 12 represent live synchronous group embryos at sacrifice. The 22 live synchronous embryos at day 18 represent 14 live but unable to hatch and 8 hatchlings.

Note the presence of 18 flight embryos that had achieved development ages comparable to normal day 8 to day 12 embryos.

FIGURE 8: A summary graph of the group means from each of the female rat groups displayed in Figures 3 - 6. COLUMN 1 is the starting weights; COLUMN 2 is the last preflight weight; COLUMN 3 is first weights postflight; COLUMN 4 represents termination weights (either at parturition or at maximum weight). The line above each bar represents one standard deviation.

Recall that weights in the preflight (COLUMN 2) period in the Flight, Synchronous and Vivarium groups all showed a decrease from the previous weighing period.

Figure 1

Figure 2

Figure 3. 1979 BioSpace COSMOS Simulation

Figure 4. COSMOS 1129 FLIGHT

360

COSMOS 1129 SYNC.

Body Weight (gm)

DAYS

5

COSMOS 1129 VIVARIUM

Body Weight (gm)

DAYS

6

COSMOS 1129 QUAIL

Figure 7

COSMOS 1129 Group Means
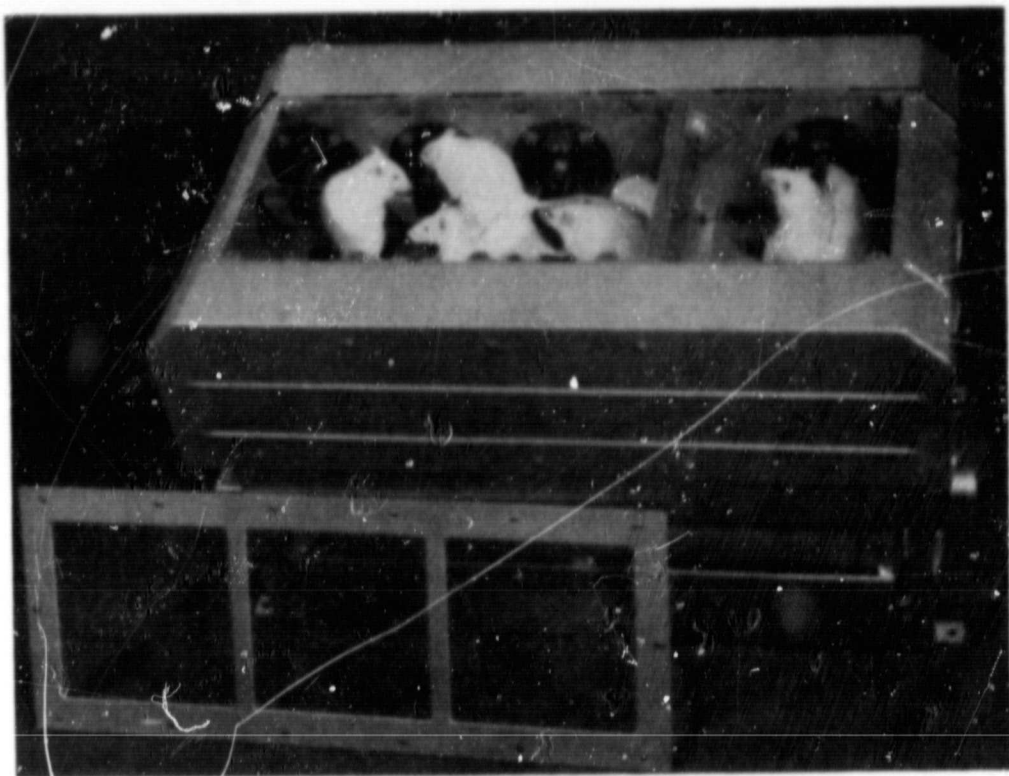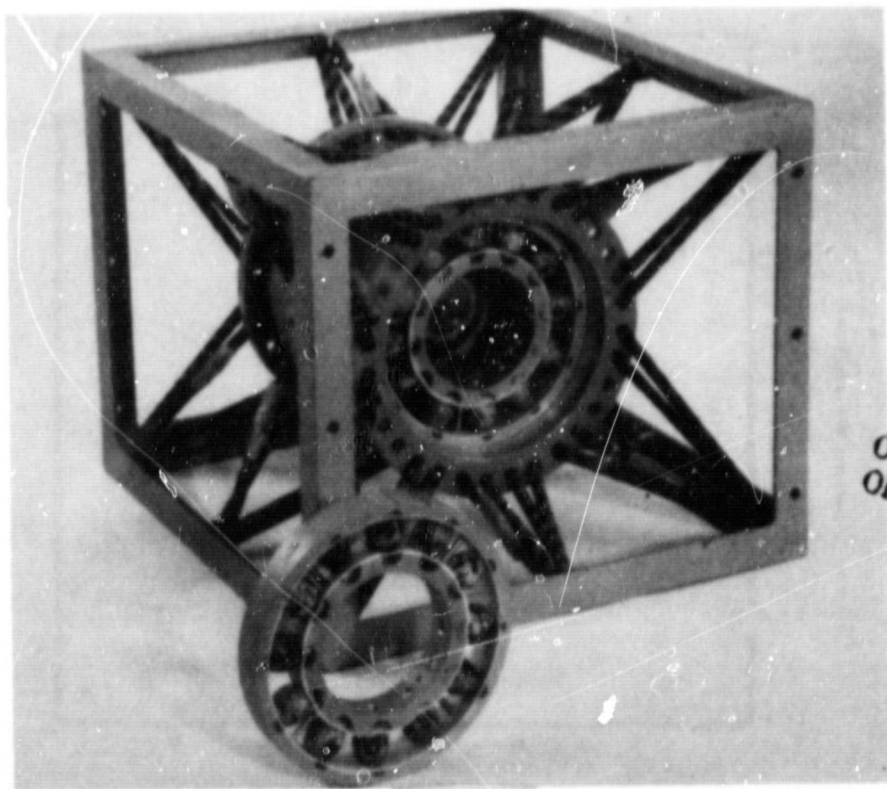
Figure 8
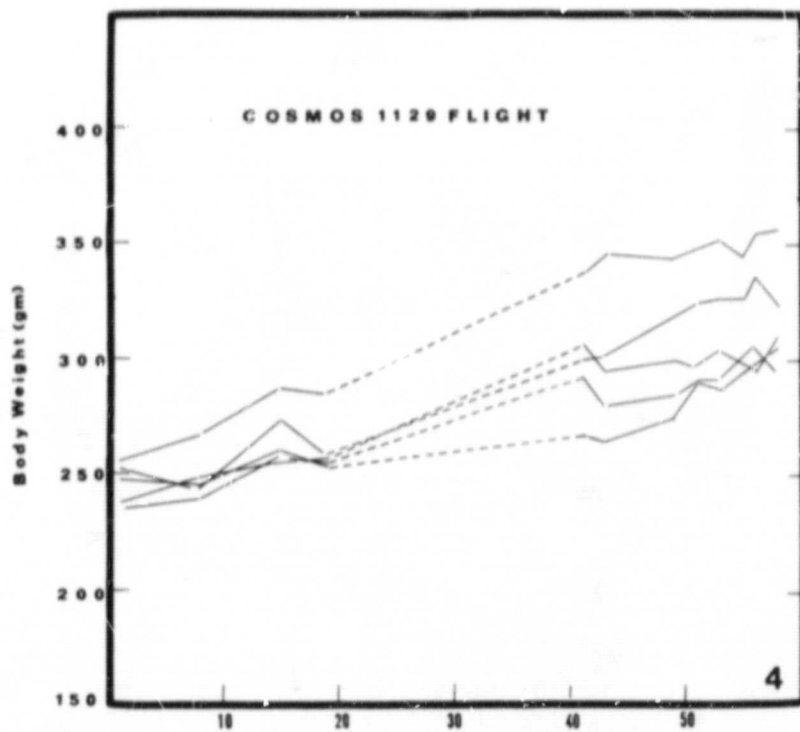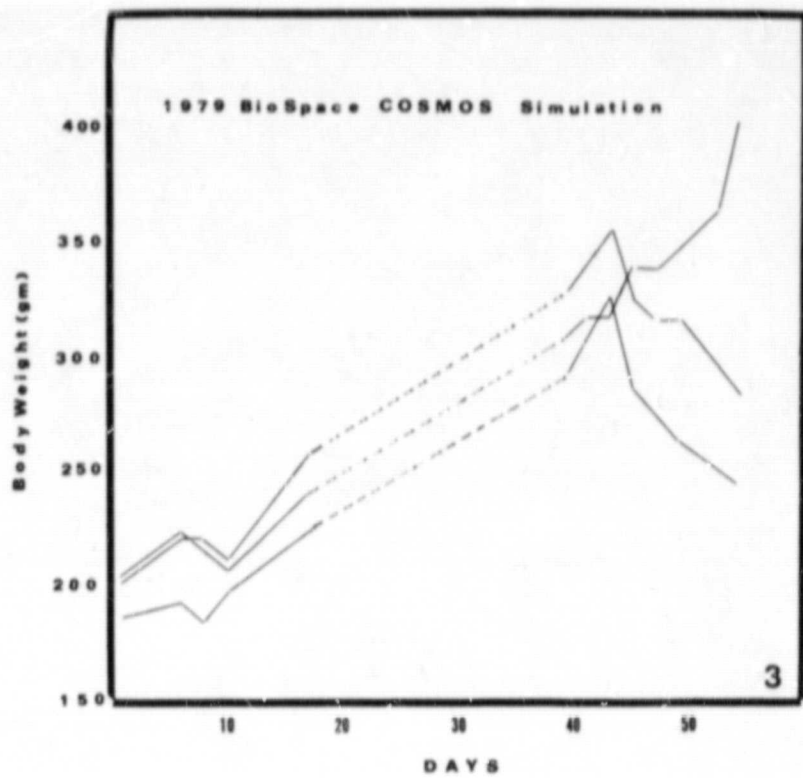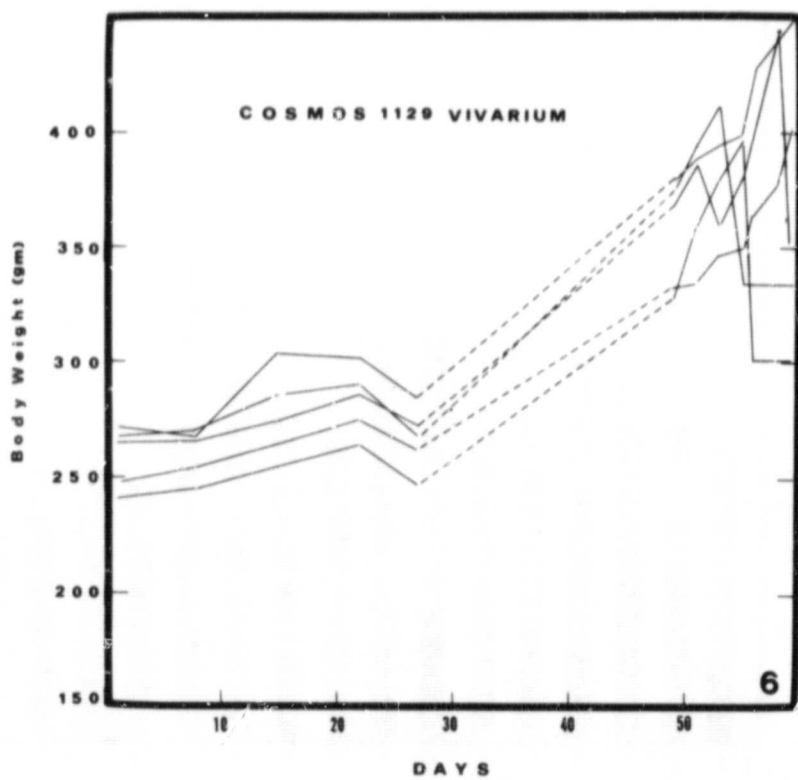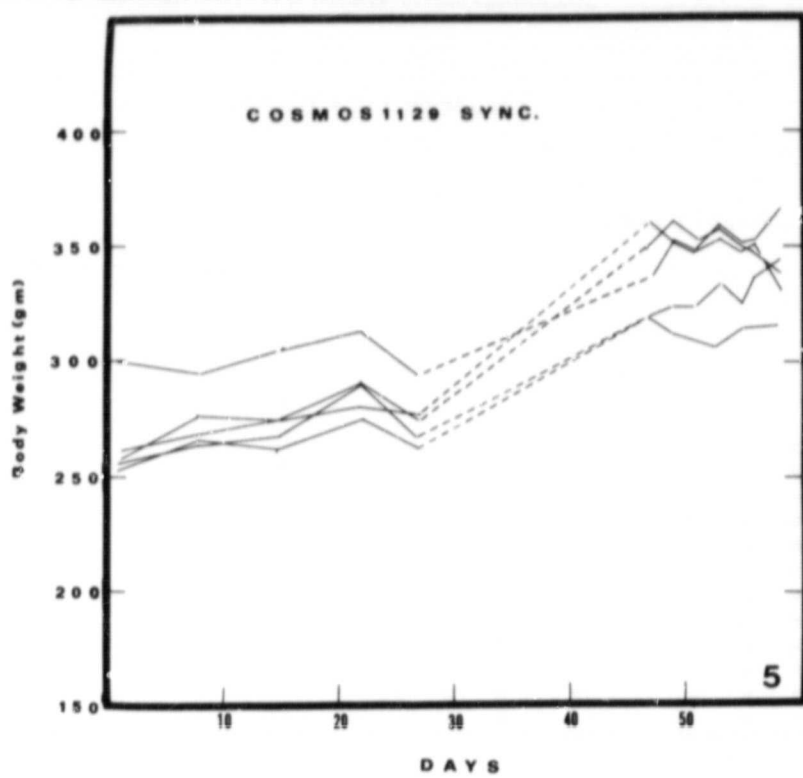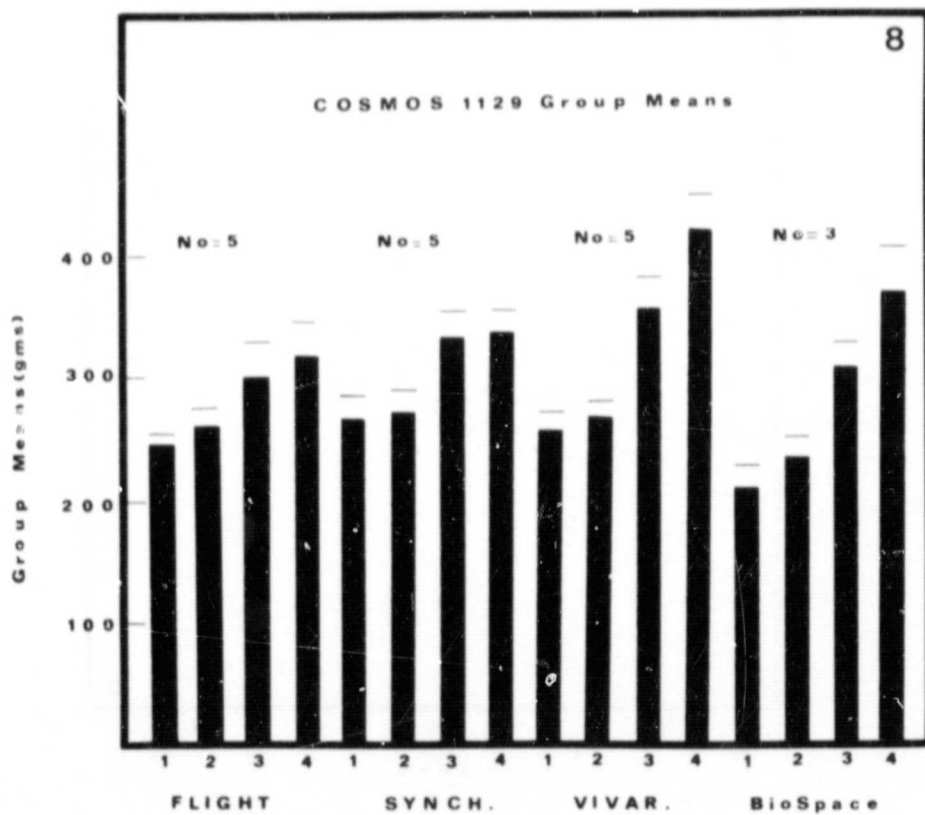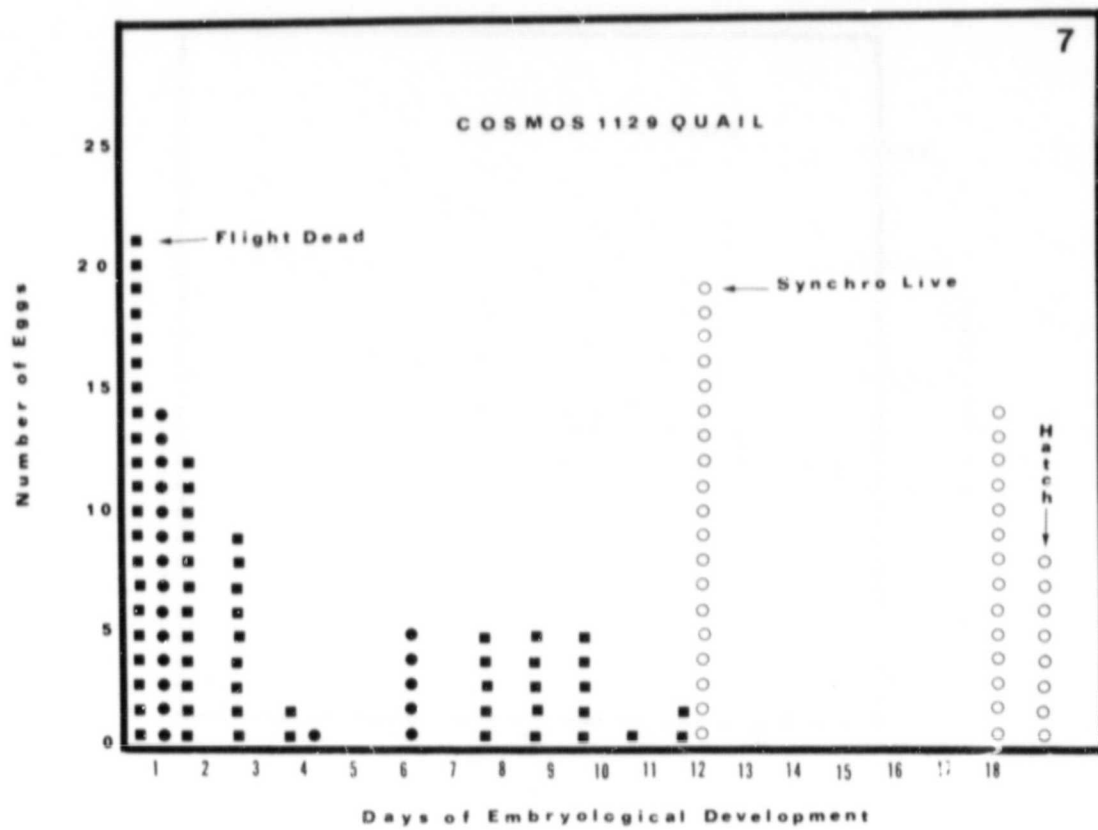
Cosmos 1129 Experiment K-314

Fetal and Neonatal Rat Bone and Joint Development
Following in Utero Spaceflight

E. E. Sabelman

University of California - San Francisco, CA

E. M. Holton

NASA-Ames Research Center, Moffett Field, CA

C. D. Arnaud

University of California - San Francisco, CA

SUMMARY

Infant rat limb specimens from Soviet and U.S. ground-based studies were
examined by radiography, macrophotography, histologic sectioning and stain-
ing and scanning electron microscopy. A comparison was conducted between
vivarium and flight-type diets suggesting that nutritional obesity may
adversely affect pregnancy. Data were obtained on maturation of ossif-
ication centers, orientation of collagen fibers in bone, tendon and liga-
ment, joint surface texture and spatial relationships of bones of the
hind limb. Computer reconstructions of the knee and hip show promise as
a means of investigating the etiology of congenital hip dislocation.

INTRODUCTION

The thrust of this study was altered by circumstances from the initial proposal to investigate effects prenatal exposure to spaceflight on rat limb development. Since no litters were born following in-flight impregnation, the only specimens were produced by vivarium and post-flight pregnancies. Although it was not possible to test the experiment hypotheses, these specimens have provided insight into developmental processes and time sequences. An effort was made to measure differences between groups of specimens attributable to maternal housing, diet or stress, which must be compensated for in future mammalian embryology experiments in space.

Spaceflight affords an opportunity to test the contribution of gravity to the fetal development or pre-adaptation of limb structures essential to weightbearing and locomotion of the postnatal animal. Although mechanisms have been proposed for the detection of gravity vector by individual somatic cells [1,2], our present hypothesis is that limb growth in the near-term fetus is influenced by muscle action and mechanical loading as in postnatal life. Evidence exists that prevention of active motion in utero by genetic muscular dysfunction [3] or injection of paralytic drugs [4,5] results in retardation of muscle and tendon growth, flattening and adhesion of articular surfaces and failure of morphological differentiation of bones. Similar effects are seen post-natally in cases of joint immobilization [6], bone resection [7], nerve section [8] and periosteal circumsection [9]. Magnitudes of effects of lack of gravitational stimuli are not anticipated to be as great as those

caused by paralysis, since fetal muscle action is uninhibited but altered from isotonic to isometric mode [10] by maternal fluid shift, internal organ displacement, stance or activity [11]. Since spaceflight effects potentially may be masked by birth order [12], litter size [13], maternal diet [14,15] or stress [16,17], knowledge of such variables is essential to the interpretation of data from specimens exposed to orbital conditions.

Because all specimens received from the USSR were from one week old or younger animals, most analytic work was concentrated on material of this age range. Of 27 variables initially identified as potentially sensitive to spaceflight effects, 14 were selected for detailed study by histomorphometry, polarized light microscopy, scanning electron microscopy (SEM) and X-ray photogrammetry. Four variables were combined for evaluation using a rat hind limb skeletal maturity index published by Highes and Tanner [18].

METHODS and MATERIALS

Soviet Specimens

Hind limb specimens dissected and fixed according to the K-314 protocol were received from the USSR in two batches. The first group comprised 24 to 36 hour postnatal offspring of matings of flight and synchronous males with vivarium females; eleven right and four left limbs were included, with skin removed to mid-tibia. Dissection artifacts were confined to one instance each of absence of the femoral head, damage to tibia muscles and laceration of the foot. State of microscopic preservation was

compromised by freezing during shipment. The second group comprised 15 hind limbs, divided equally among litters sired by flight, synchronous and vivarium males.   Age of the flight and vivarium-derived specimens was 2 1/2 or 3 days postnatal (24 days post-conception), while the synchronous litter was 4 days postnatal (28 days post-conception) and had correspondingly higher body weight. Six specimens were left and nine were right limbs. All were grossly normal except for several cases of foot laceration due to forceps pressure during dissection. Two specimens lacked the femoral head, while two included the hemipelvis and part of the spine.

Domestic Specimens

Both left and right hind limbs of 46 infant Simonsen Wistar rats were obtained at ages of 1 to 15 days. This material was used for refinement of tissue processing and analysis techniques. In addition, some animals were given prenatal and/or postnatal bone mineralization labels (tetracyclines [19], lead acetate [20] or tritiated thymidine [21]).

Dr. J. R. Keefe obtained five Czech Wistar females from the Soviets and simulated the Cosmos 1129 housing, diet and mating schedule on three females and one male. Offspring were killed at ages of 1 to 13 days and fixed in 10% formalin. Of 39 carcasses sent to Ames Research Center from this experiment, 27 pairs of hind limbs were processed for histology and comprise part of the baseline data pool for comparison with Soviet specimens.

An additional five female Czech Wistars with two males were located at Ames Research Center to establish a breeding colony. Both hind limbs of 30 offspring of this group aged 2 to 24 days were included in the baseline pool.

Diet Comparison

Three first-generation Czech Wistar females were fed a paste diet prepared according to the Soviet flight diet recipe. Ingredients differed slightly: the nutrient yeast contained unspecified quantities of vitamins in addition to those added in accordance with the recipe; also, the sunflower seed oil was probably less viscous than that used by the Soviets. The Soviet instructions specified Pasteurization for one hour at 100°C following mixing; to reproduce the consistency of samples, it was necessary to Pasteurize for two hours, followed by refrigeration and blending.

The female rats were acclimatized to 45 gm/day paste diet for 14 days before mating, and continued at this level until birth (or sacrifice if birth was delayed). After parturition the dose was increased to 60 gm/day. If sacrificed, the females were dissected, abnormalities in internal organs and adipose tissue were noted, and the ovaries and uteri were preserved in glutaraldehyde-based "triple fix". The two remaining first-generation females, plus second- and third-generation animals maintained continuously on standard lab chow were later sacrificed as controls.

Histology Processing

Domestic specimens, consisting of both hind limbs, sacral spine and tail, and single Soviet hind limbs were preserved in refrigerated glutaraldehyde-based "triple fix" [22]. After separation into single limbs and cleaning of skin and fat, specimens were superficially examined and macrophotographed at 3X.

The second step in processing was contact radiography on Kodak Type M film at 38 kV, 225 mA and 1 sec. exposure, using density and dimensional

scales on the film [23]. Radiographs were used as references to compensate for shrinkage or displacement artifacts during subsequent processing. Measurements of tibial and femoral cortical length were made with a 10X magnifying reticle. Radiographic density was measured using an image analysis system consisting of a Sierra Scientific camera, Spatial Data Systems "Eyecom 108PT" video-digitizer terminal and DEC PDP 11/34 computer. Skeletal maturity was evaluated by the method of Hughes and Tanner [18], in which shape and relative dimensions of ossification centers in the femur, tibia, calcaneum, metatarsals and proximal phalanges are assigned values on a scale of 0-15, which are summed to yield a maturity index for the whole limb.

An optional step was clearing to render bulk muscle transparent for visualization of bones in whole specimens. The method employed was successive changes of 1% KOH [24] with alizarin red S added to the last change to stain calcified bone [25]; alkali clearing was detrimental to cellular microstructure and unable to remove a yellow pigment left by the fixative. Further processing was primarily dehydration in graded ethanol solutions, clearing in cedarwood oil and paraffin embedding [26], although sample specimens were processed by polyethylene glycol embedding without dehydration [27] and by glycol methacrylate embedding [28] to reduce shrinkage artifacts.

Three sectioning orientations were employed: (a) whole length longitudinal sections, (b) cross-sections after pre-cutting at mid-tibia and mid-femur, and (c) longitudinal sections of hip, knee and foot with tibia and femur diaphyses excised and cross-sectioned. Serial sections were typically cut at 10 μm on an AO Model 820 microtome and mounted 5 or 10 per

slide with notation of any missing sections. Stains included routine hematoxylin-eosin [26], picro-Sirius Red F3BA for collagen fibers [29] and toluidine blue-safranin O for mucopolysaccharides in cartilage [30].

A computer program for three-dimensional reconstruction from serial sections similar to that of Sullivan [31] was used for qualitative evaluation of knee, hip and tibia-fibula geometry. The input program "RECONI" was written in FORTRAN for use on the video image analysis system with input from a Zeiss "Ultraphot" microscope and Cohu Model 4400 camera. Elements of the video image such as bone, cartilage, ligament or muscle were outlined using the Eyecom terminal joystick under normal, crossed polaroid or ultraviolet illumination and the outline vertices were stored in disc memory. Approximately every fourth section in a series of up to 200 sections was scanned. The output program "RECONO" retrieved the outline data and displayed them as a stack of color-coded filled or outlined plane polygons rotated horizontally or vertically at a selected angle.

Specimens selected for SEM processing were either dehydrated or freed from embedding medium, depending on extent of previous processing. They were then air-dried from xylene or critical-point dried in CO_2, mounted on stubs using conductive adhesive, coated with 18 nm Pt-Au by vacuum evaporation, and viewed on a AMR Model 1200 scanning electron microscope.

RESULTS

Diet Comparison

Of the three animals fed simulated Soviet paste diet, only one car-

369

ried a pregnancy to term; the litter included several weak pups out of 11 total. One female either resorbed early or did not implant embryos; she later developed cardiovascular lesions thought to be unrelated to diet. The third female gained weight until gestation day 21; at sacrifice three days later, she was found to have an extreme quantity of abdominal (14.9% of body weight) and subdermal fat. Mean wet weight abdominal fat to body ratio for females of comparable age fed standard lab chow was 6.4 ±1.2%. The uterus was slightly enlarged but no resorbing fetuses were evident, indicating resorption occurred earlier than implied by weight gain.

Radiographic Measurements

Data obtained from X-ray images comprised (a) femoral and tibial cortex lengths, (b) skeletal maturity indices [18], and (c) computer-generated optical density histograms.

Tibial cortex length (L) for specimens up to 6 days old was found to be related to body weight (W) by the regression equation:

$$L = .026 \ W + .25$$

with Soviet, Dr. Keefe's and Ames specimens having >99% probability of deriving from the same population at ages under 2 days. In animals older than 6 days, ratio of bone length to body weight declined, reflecting increasing robusticity and muscle growth [32]. Ratios of bone length [14,33] and ash weight [34] to body weight cited in the literature are based on caliper measurements of older specimens with calcified epiphyses, but when extrapolated are approximately parallel (Figure 1).

Mean skeletal maturity scores are given in Figure 2 and compared to scores for black hooded rats given by Hughes and Tanner [18]. The values

for Soviet specimens are depressed 10-15% due to difficulty of positioning caused by fixation-induced rigidity; an additional radiograph perpendicular to the foot would have aided in identifying phalanges and metatarsals. Because of the small number of specimens, males and females were included in each age group; other researchers [18,35] have found females to mature significantly faster after the tenth postnatal day, implying variance would be less if males and females were separated. Femoral head and proximal tibial ossification centers evident in microscopic sections generally did not contain enough calcified material to appear on radiographs until times corresponding to published values [35,36].

Histograms of radiographic density based on contrast-enhanced areas circumscribing the femur or tibia-fibula (Figure 3) illustrate the difficulty of interpreting density data. In some cases (Figure 4 A, B) a bimodal distribution may be inferred, corresponding to marrow and cortex densities. Triple peaks may reflect densities of marrow, cancellous and cortical bone, in increasing order (Figure 4 D, H). However, a major source of error exists in rotation causing the tibia and fibula to overlap, with consequent reduced area and spurious high density peaks (Figure 4 F). Additional artifacts occurred if the radiographic background was unevenly exposed or reflections caused highlights during digitization.

Gross Observations

No overt anatomical abnormalities were noted in domestic or Soviet specimens. A possible exception is histologic evidence of a blood-filled cyst in the popliteal region of one Wistar newborn; this may be merely an extreme variation in the branching of the femoral artery. Three categories

of developmental defect were specifically sought: (a) ectodermal-mesenchymal cell interactions, capable of causing skeletal absence [37], (b) collagen synthesis defects (chondrodysplasias) causing bone length retardation [38], and (c) late fetal and postnatal foot deformities [39]. The specimens were fixed in a variety of flexed positions, which prevented assessment of subtle joint defects (e.g.: varus-valgus angle of the ankle).

Body weight was a gross measurement available for all specimens, at least as an average for the litter. Figure 5 shows weight vs. age (postnatal) for values from the literature compared to animals from Soviet, Dr. Keefe and Ames sources. Weights of offspring whose dams were fed Soviet paste diet do not differ significantly until after day 15 from controls fed standard diet [40]. Slight differences between males and females are evident at birth, but do not reach statistical significance until day 30 or 35 [32]. An early paper records birth weights substantially lower than some modern strains, implying an effect of selective breeding [41].

Histologic Observations

Spatial relationship and morphology of bones were most easily observed in cleared alizarin-stained specimens (Figure 6). Quantitative measurements of tibial axis curvature and tibio-fibular fusion were made from serial longitudinal or cross-sections. The centroid of the tibia at different levels from proximal to distal was compared to a straight line through the centroids of the epiphyseal plates. The centroid of the fibula was inferred to the same nominal tibial axis (Figure 7). Sample specimens aged 2 to 6 days were examined and indicate that changes during this span can be repeatably measured and placed on a time scale from earliest

372

appearance of these bones through adulthood [42]. Accurate three-dimensional reconstructions require a reference axis exterior to both tibia and fibula; fiducial marks on the surface of the paraffin embedment [43] did not remain in register after mounting on slides.

Tendon and ligament insertions of primary interest were the patellar tendon/tibial crest (Figure 8), the ligamentum teres/femoral head and the ilio-femoral ligament/greater trochanter (Figure 9); a secondary interest was the Achilles tendon/calcaneum. Maturation of the insertion can be measured by the location of the insertion margins relative to the proximal or distal ends of the bone [44]. In animals less than two days old insertions tended to merge with the perichondrium rather than penetrate into underlying cartilage or bone. Older insertions had gradual transitions from tendon to fibrocartilage to bone as described in the literature [45,46].

Relative parallelism or co-linearity of tendon fibers as well as limited information on cross-sectional area was derived from Sirius Red stained longitudinal sections under polarized illumination. Patellar tendon thickness was .31 ±.11 mm at 1-2 days and .49 ±.21 at 4 days, implying rapid growth of the quadriceps muscle. The anterior cruciate ligament increased in thickness relatively little during this period (.15 ±.07 vs. .17 ±.09 mm, from mid-sagittal sections of at least 4 specimens). Collagen fiber crimping [47] was seen in the patellar ligament; fibers in the anterior cruciate were straight as a result of fixation flexion, and in the posterior cruciate were often folded out of the section plane.

Articular cartilage is considered to be sensitive to alterations in

compressive stress and motion [6]. Thickness and structure of the articular layer are distinguished from deeper hyaline cartilage by staining properties [48] and direction of collagen fibers [49]. Animals younger than 7 days tend to have little difference between articular and adjacent periosteal collagen fibers (Figure 10), while post-ambulatory animals have more distinctive orientation and substructure; during the same period chondrocyte shape changes from ovoid to flattened [50].

Epiphyseal plate properties of interest included angle relative to the bone axis, width and zone depth (Table 1). Widths of distal femoral and proximal tibial growth plates increased as expected with age [51]. The depth of all zones (resting, proliferating, hypertrophic, primary and secondary spongiosa [21]) was not measured, however, the primary (calcified cartilage) zone was compared to the sum of the proliferating, hypertrophic and primary zones. Both width and depth of the plates increase relatively slowly until 9 days of age; after appearance of secondary ossification centers the calcifying cartilage layer is expected to increase relative to the plate as a whole [52,53] although this is not evident in these animals. Epiphyseal ossification centers in the femoral head, distal femoral condyles and proximal tibia appeared prior to published times in about one-third of domestic specimens [35,36], but remained disorganized and uncalcified, consisting of hypertrophic chondrocyte lacunae, until vascularization occurred. Angle of the plate relative to bone axis is predicted to change with alteration of force vector across the associated joint as the animals become ambulatory [56,57]. The plate angle is too indefinite prior to appearance of the secondary ossification center, but can be seen in the assymmetry of the proximal femoral plate at the

374

C-5

greater trochanter (Figure 9).

Serial Section Reconstruction

Computer-generated reconstructions were made of up to six tissues of
the hip, knee and distal tibia-fibula. In the knee (Figures 11, 12) this
technique shows that the menisci are relatively large in animals less
than three days old, and recede toward the joint capsule wall as they ma-
ture [58]. The proximal-distal oriented collagen fibers of the capsule
and patellar ligament as seen under polarized illumination do not merge
with the tangential fibers of the menisci, suggesting that the latter are
under radial pressure or hoop stress [59]. The patella resides deep to
the highly linearly oriented tensile fibers of the patellar tendon, which
continue uninterrupted until inserting in the tibial crest [46]; the loose
connective tissue surrounding the remainder of the patella spreads out
in the tibial and femoral perichondrium.

Reconstructions of the tibial and fibular diaphyses have been unable
to depict changes in tibial axis due to lack of a reference axis, but
show that the fibular axis is helical relative to the tibia until it
approaches the site of impending fusion [60] (Figure 7).

The hip is sufficiently complex that six components were not adequate
to completely describe it. The "RECONO" program permits outlining some
components while shading others, to aid viewing the morphology of the
femur exclusive of surrounding tissue [61] (Figure 13). The ability to
view the femoral head from various angles is useful in determining spher-
icity and congruity with the acetabular cavity[62]. Other views show the
ligamentum teres to insert into a fossa of the tri-radiate cartilage in

sections near the maximum diameter of the femoral head, but to extend toward the acetabular labrum in more distal sections [63] (Figure 14).

The coxal ligaments include the ilio-femoral, which with the gluteus medius wraps around the trochanter near the femoral neck axis, to merge dorsally with the piriformis and distally with loose fibers spread over the acetabular rim [64] (Figure 15). The obturator muscle terminates in the concave area between the femoral neck and trochanter, with facial fibers making up part of the joint capsule between the trochanter and acetabular rim. The visceral wall of the innominate consists of highly oriented collagen fibers (whether a thickened periosteum or an independent fibrous sheath is uncertain); distinct regions of fibrocartilage and hyaline cartilage in neonatal animals (Figure 16) between the innominate sheath and the acetabular socket become merged into bone in the mature animal. These structures appear to provide the biomechanical stability necessary to the function of the hip and also permit the motion essential to development of a rotating rather than sliding joint. If the ligaments positioning the femoral head are weak relative to the tensile elements of the acetabulum during this phase, the joint may be predisposed to congenital dislocation[63,65,66].Continued refinement of the computer reconstruction technique should aid in determining the critical factors in hip development [43].

Scanning Electron Microscopy

SEM is well suited for observation of joint surfaces, ligaments and metaphyseal trabeculae, since shrinkage artifacts aid in exposing these regions. Striations in the articular surface (Figure 17) indicate that

cartilage cells are shallow and matrix sparse relative to mature specimens [49]. Projections into the joint space were not seen, implying that the joints were mobile. Cells adhering to the surface may have been introduced during processing, but more likely were detached synovial lining cells or migrating macrophages. The synovial membrane could be visualized but its surface was easily damaged during dissection (Figure 18). The texture of the meniscal fibrocartilage was distinct from adjacent ligament, with prominent cell lacunae which could be indicators of state of mechanical stress [57]. Marrow cavities in some metatarsals were nearly cell-free (Figure 19); although possibly a processing artifact, this could imply that marrow cavitation was so recent that blood-forming cells had not yet populated the region. Cells of the epiphyseal plate were not examined in detail, but were distinguishable as to zone under SEM [67]; similar zones were seen in ligament insertions [68].

DISCUSSION and RECOMMENDATIONS

Diet Effects

The results of the simulated paste diet feeding study are equivocal due to the small number of animals and possible differences from the Soviet paste diet. Feeding studies using actual Soviet diet are continuing at Ames Research Center. Since both Dr. Keefe's animals and the subjects of the Soviet "engineering study" were able to carry litters of normal size to term, the diet is unlikely to be solely responsible for lack of viable litters in flight and synchronous Cosmos 1129 females. However, the most notable abnormality in the Ames diet study was elevated

abdominal fat, which was also noted by Dr. Serova in dissection of three flight females. Preliminary results of the Cosmos 1129 body composition study [69] show visceral fat in flight and synchronous males approximately double that in vivarium controls. Wet abdominal fat weights given in the Soviet preliminary report are lower since organ fat is not included, but the ratio is similar. Hence, males as well as females are subject to excess fat buildup when fed paste diet of this composition.

Although the diet supports life and weight gain of animals, it may be subtly influencing results of other Cosmos experiments comparing flight and synchronous groups with vivarium controls. For example, an unusual amount of adipose tissue was noted in bone marrow of Cosmos 782 rats [55]. Besides reducing the cell population available for bone growth, particularly in the secondary spongiosa [55], the volume and precursor cell population participating in erythrocyte formation was probably affected.

Skeletal Maturation and Morphology

Radiography [18] and clearing/alizarin staining [25] are adequate means of quantifying time of appearance and growth of ossification centers. These morphologic indicators are corroborated by biochemical measurements of calcium utilization [70]. Abnormality occurrence rates of 0.5% of normal specimens can be reliably detected [25].

Our initial presumption that skeletal maturation was unaffected by factors other than genetic programming and functional loading excluded a number of significant variables. In fetal and neonatal rodents, these include: (a) tri-iodothyronine [71], (b) thyroxine and thiouracil [72], (c) nutritional body weight variations [14], (d) maternal protein def-

378

iciencies [73], (e) transplacental cortisone [74], (f) pituitary hormones [75] and (g) noise [16]. In older growing rodents, known factors are: (h) hypoxia [76], (i) exercise [77], (j) hypergravity [78], (k) resorption inhibitors [54] and (l) chronic vibration [79]. These factors presumably act by modulating the same routes of cell differentiation and metabolism as determine the responses to function and gravity [60,81]. Some or all of these factors may be present in fetuses due to the dietary, social or physical environment of Cosmos females. Hence, thorough control and preflight simulation of mission parameters are imperative if gravitational responses are to be identified.

Specimen Processing

Experience has suggested several modifications of the protocol for initial specimen acquisition that should be applied to future experiments. A single fixative should not be expected to provide ideal preservation for multiple end uses; rather, where rapid fixation is required, as for SEM or TEM, small needle biopsies of regions such as articular cartilage or epiphyseal plate during dissection of fresh tissue, and placed in a minimal volume of "triple fix". SEM may alternatively be enhanced by liquid nitrogen freezing of articular surface biopsies, followed by freeze-drying [82]. The remainder of the specimen should then be pinned in a standard flexed position and preserved in a simple fixative such as 10% buffered formalin; this method would facilitate room-temperature storage with less chance of freezing damage in transit.

In processing of specimens after receipt from the USSR, greater attention should be paid to extracting quantitative information from cleared

specimens, and/or using clearing methods less damaging to microstructure. No convenient solution has been found to the problem of reference axes for serial sections; perhaps biopsy sites or markers affixed to the specimen surface would suffice.

The pool of baseline data on body weights, bone lengths and ossification centers vs. age is approaching the size at which reliable strain-specific growth curves can be established [83,84]. With standardization of fixed joint flexure, similar standard curves could be derived for position-sensitive features such as bone tuberosities and tendon insertions [44,85].

Because of unknown degrees of sensitivity of bone and joint maturation of Czech Wistars to such factors as litter size [13,74,86], gestation age [32], uterine position or birth order [12] relative to other strains [87], this data should be gathered for all specimens, in addition to the age and weight at sacrifice provided for Cosmos 1129 material. Certainly, the environmental parameters to which flight and synchronous control groups were exposed, such as noise [16], vibration [79] and possible hypoxia [76] should be measured during all future simulations or space missions.

REFERENCES

1. Pollard, E. C. Theoretical studies on living systems in the absence of mechanical stress. J. Theoret. Biol. 8:113-123 (1965).

2. Dragomir, C. T. and S. A. Cananau. Distribution of subcellular components under gravity changes; the special conditions of the dystrophic cell. J.Theoret Biol. 65: 209-213 (1977).

3. Pai, A. C. Developmental genetics of a lethal mutation, muscular dysgenesis (mdg) in the mouse; 1. Genetic analysis and gross morphology. Devel.Biol. 11:82-92 (1965).

4. Beckham, C., Dimond, R. and Greenlee, T. K., Jr. The role of movement in the development of a digital flexor tendon. Am. J. Anat. 150: 443-460 (1977).

5. Shoro, A. A. Intra-uterine growth retardation and limb deformities produced by neuromuscular blocking agents in the rat fetus. J. Anat. 123: 341-350 (1977).

6. Hall, M. C., Cartilage changes after experimental immobilization of the knee joint of the young rat. J. Bone Joint Surg. 45A: 36-44(1963).

7. Doyle, W. J. Antagonistic compensation as a function of reduced weight bearing. Acta Anat. 95: 1-7 (1976).

8. Thaxter, T. H., R. A. Mann and C. E. Anderson. Degeneration of immobilized knee joints in rats. J.Bone Joint Surg. 47A: 567-585 (1965).

9. Harkness, E. M. and W. D. Trotter. Growth of transplants of rat humerus following circumferential division of the periosteum. J. Anat. 126: 275-289 (1978).

10. Sevastikoglou, J. A., S.-E. Larsson, S. Mattsson, R. Lemberg, V. Thomaidis and T. S. Lindholm. Localised disuse osteoporosis: Experimental studies in the adult rat. Acta Chir. Scand. suppl. 467: 40-47 (1976).

11. Goss, R. J. The Physiology of Growth, ch. 24: From embryo to adult. New York: Academic Press (1978).

12. Barr, M. Jr., Jensh, R. P. and Brent, R. L. Prenatal growth in the albino rat: Effects of number, intrauterine position and resorptions. Am. J. Anat. 128: 413-428 (1970).

13. Solomon, S. and H. H. Bengele. Growth rates and organ weights of rats. Biol. Neonate 22: 222-229 (1973).

14. Dickerson, J. W. T. and E. M. Widdowson. Some effects of accelerating growth: II. Skeletal development. Proc. Roy. Soc. (London) 152-B: 207-217 (1960).

15. Martin, R. B. Effects of different commercial diets on several orthopedic experiments. Clin. Orthop. Rel. Res. 138: 271 (1979).

16. Geber, W. F. Inhibition of fetal osteogenesis by maternal noise stress. Fed. Proc. 32: 2101-2104 (1973).

17. Barlow, S.M., A. F. Knight and F. M. Sullivan. Delay in postnatal growth and development of offspring produced by maternal restraint stress during pregnancy in the rat. Teratology 18: 211-218 (1978).

18. Hughes, P. C. R. and J. M. Tanner. The assessment of skeletal maturity in the growing rat. J. Anat. 106: 371-402 (1970).

19. Tam, C. S., R. Reed and B. Cruickshank. Bone growth kinetics: I. Modifications of the tetracycline labelling technique. J. Path. 113: 27-38 (1974).

20. Schneider, B. J. Lead acetate as a vital marker for the analysis of bone growth. Am.J. Phys. Anthrop. 29: 197-200 (1968).

21. Kember, N. F. Cell kinetics and the control of growth in long bones. Cell Tissue Kinet. 11: 477-485 (1978).

22. Corbett, R., D. E. Philpott and S. Black. Prolonged fixation studies for spaceflight. Proc. 31st Ann. Electron Microscopy Soc. Amer., New Orleans, La., C. J. Arceneaux, ed. (1973).

23. Becks, H. and H. M. Evans. Atlas of the Skeletal Development of the Rat (Long-Evans Strain). San Francisco: Am. Inst. Dent. Med. (1953).

24. Jensh, R. P. and Brent, R. L. Rapid schedules for KOH clearing and alizarin red S staining of fetal rat bone. Stain Tech. 41: 179-183 (1966).

25. Fritz, H. and R. Hess. Ossification of the rat and mouse skeleton in the perinatal period. Teratology 3: 331-338 (1970).

26. Preece, A. A Manual for Histologic Technicians. Boston: Little, Brown (2nd ed.: 1965).

27. Reid, J. D. and D. Taylor. An improved method for embedding tissues, using polyethylene glycols, with incorporation of low-viscosity nitrocellulose. Am. J. Clin. Path. 41: 513-516 (1964).

28. Bennett, H. S., A. D. Wyrick and S. W. Lee. Science and art in preparing tissues embedded in plastic for light microscopy, with special reference to glycol methylacrylate, glass knives and simple stains. Stain Tech. 51: 71 ff (1976).

29. Puchtler, H., F. S. Waldrop and L. S. Valentine. Polarization micro-scopic studies of connective tissues stained with picro-sirius red F3BA. *Beitr. Path.* 150: 174-187 (1978).

30. Rosenberg, L. Chemical basis for the histological use of safranin O in the study of articular cartilage. *J. Bone Joint Surg.* 53A: 69-82 (1971).

31. Sullivan, P. G. A method for the study of jaw growth using a computer-based three-dimensional recording technique. *J. Anat.* 112: 457-470 (1972).

32. Hughes, P. C. R. and J. M. Tanner. A longitudinal study of the growth of the black-hooded rat: methods of measurement and rates of growth for skull, limbs, pelvis, nose-rump and tail lengths. *J. Anat.* 106: 349-370 (1970).

33. Aries, L. J. Experimental analysis of the growth pattern and rates of appositional and longitudinal growth in the rat femur. *Surg. Gyn. Obstet.* 72: 679-689 (1941).

34. Zucker, T. F. and L. M. Zucker. Bone growth in the rat as related to age and body weight. *Am. J. Physiol.* 146: 585-592 (1946).

35. Spark, C. and A. B. Dawson. The order and time of appearance of centers of ossification in the fore and hind limbs of the albino rat, with special reference to the possible influence of the sex factor. *Am. J. Anat.* 41: 411-445 (1928).

36. Shrader, R. E. and F. J. Zeman. Skeletal development in rats as affected by maternal protein deprivation and postnatal food supply. *J. Nutr.* 103: 792-801 (1973).

37. Lewis, J. Growth and determination in the developing limb. *Vertebrate Limb and Somite Morphogenesis* (3rd Symp. Brit. Soc. For Devel. Biol.), D. A. Ede, J. R. Hinchliffe and M. Balls, eds. Cambridge Univ. Press. pp. 215-228 (1977).

38. Shambaugh, J. and W. A. Elmer. Analysis of glycosaminoglycans during chondrogenesis of normal and brachypod mouse limb mesenchyme. *J. Embryol. exp. Morphol.* 56: 225-238 (1980).

39. Ippolito, E. and I. G. Ponsetti. Congenital club foot in the human fetus. *J. Bone Joint Surg.* 62A: 8-22 (1980).

40. Keefe, J. R. Studies of rat and quail ontogenesis during the flight of Cosmos 1129. *US/USSR Biological Satellite Program: US Preliminary Reports* (1980).

41. King, H. D. On the weight of the albino rat at birth and the factors that influence it. *Anat. Rec.* 9: 213-231 (1915).

42. Bhaskar, S. N., J. P. Weinmann, I. Schour and R. O. Greep. The growth pattern of the tibia in normal and ia rats. Am. J. Anat. 86: 439-477 (1950).

43. Gaunt, W. A. Microreconstruction. London: Pitman Medical (1971).

44. Grant, P. G., Buschang, P. H. and Drolet, D. W. Positional relationships of structures attached to long bones during growth. Acta Anat. 102: 378-384 (1978).

45. Greenlee, T. K. and R. Ross. The development of the rat flexor digital tendon, a fine structure study. J. Ultrastr. Res. 18: 354-376 (1967).

46. Badi, M. H. Calcification and ossification of fibrocartilage in the attachment of the patellar ligament in the rat. J. Anat. 112: 415-421 (1972).

47. Kastelic, J., A. Galeski and E. Baer. The multicomposite structure of tendon. Conn. Tiss. Res. 6: 11-23 (1978).

48. Cole, M. B. Jr., and J. Ellinger. Cytochemistry of the glycosaminoglycan network in articular cartilage of neo-natal rats. Proc. 25th Orthop. Res. Soc., San Francisco, Cal. p. 228 (1979).

49. Speer, D. P. and L. Dahners. The collagenous architecture of articular cartilage. Clin. Orthop. Rel. Res. 139: 268-275 (1979).

50. Durkin, J. F., J. T. Irving and J. D. Heeley. Observations of rat tibial articular cartilage during maturation. Archs. Oral Biol. 16: 827-829 (1971).

51. Heft, J. Growth of the epiphyseal plate in circumference. Acta Anat. 82: 420-436 (1972).

52. Hansson, L. I., K. Menander-Sellman, A. Stenström and K.-G. Thorngren. Rate of normal longitudinal bone growth in the rat. Calcif. Tiss. Res. 10: 238-251 (1972).

53. Kalayjian, D. B. and R. R. Cooper. Osteogenesis of the epiphysis. Clin. Orthop. Rel. Res. 85: 242-256 (1972).

54. Schenk, R., W. A. Merz, R. Mühlbauer, R. G. G. Russell and H. Fleisch. Effect of Ethane-1-hydroxy-1,1-diphosphonate (EHDP) and dichloromethylene diphosphonate (Cl_2MDP) on the calcification and resorption of cartilage and bone in the tibial epiphysis and metaphysis of rats. Calcif. Tiss. Res. 11: 196-214 (1973).

55. Asling, C. W. Endochondral osteogenesis; medullary bone turnover. Final Reports of U.S. Experiments Flown on the Soviet Satellite Cosmos 782, NASA TM-78525. pp. 276-291 (1978).

56. Smith, J. W. The relationship of epiphyseal plates to stress in some bones of the lower limb. J. Anat. 96: 58-78 (1962).

57. Lerchenthal, C. H. The connection between the morphology of bone and mechanical stimuli. Israel J. Med. Sci. 7: 451-452 (1971).

58. Haines, R. W. The development of joints. J. Anat. 81: 33-55 (1947).

59. Whillis, J. The development of synovial joints. J. Anat. 74: 277-283 (1940).

60. Moss, M. L. A functional analysis of fusion of the tibia and fibula in the rat and mouse. Acta Anat. 97: 321-332 (1977).

61. Pratt, C. W. M. Postnatal changes in the shaft of the rat's femur. J. Anat. 93: 309-322 (1959).

62. Scherrer, P. K. and B. M. Hillberry. Piecewise mathematical representation of articular surfaces. J. Biomech. 12: 301-311 (1979).

63. Ippolito, E., Y. Ishii and I. V. Ponsetti. Histologic, Histochemical and ultrastructural studies of the hip joint capsule and ligamentum teres in congenital dislocation of the hip. Clin. Orthop. Rel. Res. 146: 246-258 (1980).

64. Green, E. C. Anatomy of the Rat (Trans. Am. Phil. Soc., no. 27) Philadelphia (1935).

65. Hirotani, H., S. Morishita and K. Ishida. Femoral head cartilage in immature rats; the normal and dislocated hips. Proc. 25th Ann. Orthop. Res. Soc., San Francisco, Cal., p. 106 (1979).

66. Rális, Z. and B. McKibbin. Changes in shape of the human hip joint during its development and their relation to its stability. J. Bone Joint Surg. 55B: 780-785 (1973).

67. Bozdech, Z. and V. Horn. The morphology of growth cartilage using the scanning electron microscope. Acta Orthop. Scand. 46: 561-568 (1975).

68. Cooper, R. R. and S. Misol. Tendon and ligament insertion, a light and electron microscopic study. J. Bone Joint Surg. 52A: 1-20 (1970).

69. Ushakov, A., G. C. Pitts, N. Pace and A. H. Smith. Effect of weightlessness on body composition in the rat. US/USSR Biological Satellite Program: US Preliminary Reports (1980).

70. Kuftinec, M. M. and Miller, S. A. Bone growth in the neonatal rat: II. Biochemical aspects of bone mineral incorporation. Calcif. Tiss. Res. 17: 183-188 (1975).

71. Walker, D. G. An assay of the skeletogenic effect of L-triiodothyronine and its acetic acid analogue in immature rats. Johns Hopkins Hosp. Bull. 101: 101-110 (1957).

72. Noback, C. R., J. C. Barnett and H. S. Kupperman. The time of appearance of ossification centers in the rat as influenced by injections of thyroxin, thiouracil, estradiol and testosterone propionate. Anat. Rec. 103: 49-64 (1949).

73. Shrader, R. E. and F. J. Zeman. Skeletal development in rats as affected by maternal protein deprivation and postnatal food supply. J. Nutr. 103: 792-801 (1973).

74. Ornoy, A. Transplacental effects of cortisone and vitamin D_2 on the osteogenesis and ossification of fetal long bones in rats. Israel J. Med. Sci. 7: 540-543 (1971).

75. Williams, J. P. G. and P. C. R. Hughes. Hormonal regulation of postnatal limb growth in mammals. Vertebrate Limb and Somite Morphogenesis, 3rd Symp. Brit. Soc. for Devel. Biol. D. A. Ede, J. R. Hinchliffe and M. Balls, eds. Cambridge Univ. Press. pp. 281-292 (1977).

76. Hunter, C. and E. J. Clegg. Changes in skeletal proportions of the rat in response to hypoxic stress. J. Anat. 114: 201-219 (1973).

77. Kiiskinen, A. Physical training and connective tissues in young mice: physical properties of Achilles tendons and long bones. Growth 41: 123-137 (1977).

78. Smith, S. D. Femoral development in chronically centrifuged rats. Aviat. Space Environ. Med. 48: 828-835 (1977).

79. Jankovich, J. P. The effects of mechanical vibration on bone development in the rat. J. Biomech. 5: 241-250 (1972).

80. Hall, B. K. Developmental and Cellular Skeletal Biology. New York: Academic Press (1978).

81. Friedenstein, A. J. Precursor cells of mechanocytes. Int'l Rev. Cytol. 47: 327-359 (1976).

82. Draenert, Y. and K. Draenert. Freeze-drying of articular cartilage; investigation of rat femoral heads by SEM. Scanning 2: 57-71 (1979).

83. Grover, N. B., M. Bloch and J. Gross. Computer analysis of growth of rats. Growth 34: 145-152 (1970).

84. Hirschfeld, W. J. Time series and exponential smoothing methods applied to the analysis and prediction of growth. _Growth_ 34: 129-143 (1970).

85. Walnut, T. H. A mathematical analysis of the changes in the size and shape of bones during growth. _Growth_ 31: 217-230 (1967).

86. Goedbloed, J. F. Embryonic and postnatal growth of rat and mouse: V. Prenatal growth of organs and tissues, general principles: allometric growth, absence of growth and the genetic regulation of the growth process. _Acta Anat._ 98: 162-182 (1977).

87. Curley, J. J. and A. Pelas. Comparative studies of litters obtained from Long-Evans and Sprague-Dawley rat stocks. _Lab. Anim. Care_ 19: 716-719 (1969).

88. Acheson, R. M., M. N. MacIntyre and E. Oldham. Techniques in longitudinal studies of the skeletal development of the rat. _Brit. J. Nutr._ 13: 283-292 (1959).

FIGURE 1: RADIOGRAPHIC FEMORAL & TIBIAL CORTEX LENGTH
(anterior proximal to mid-distal epiphyseal plate)
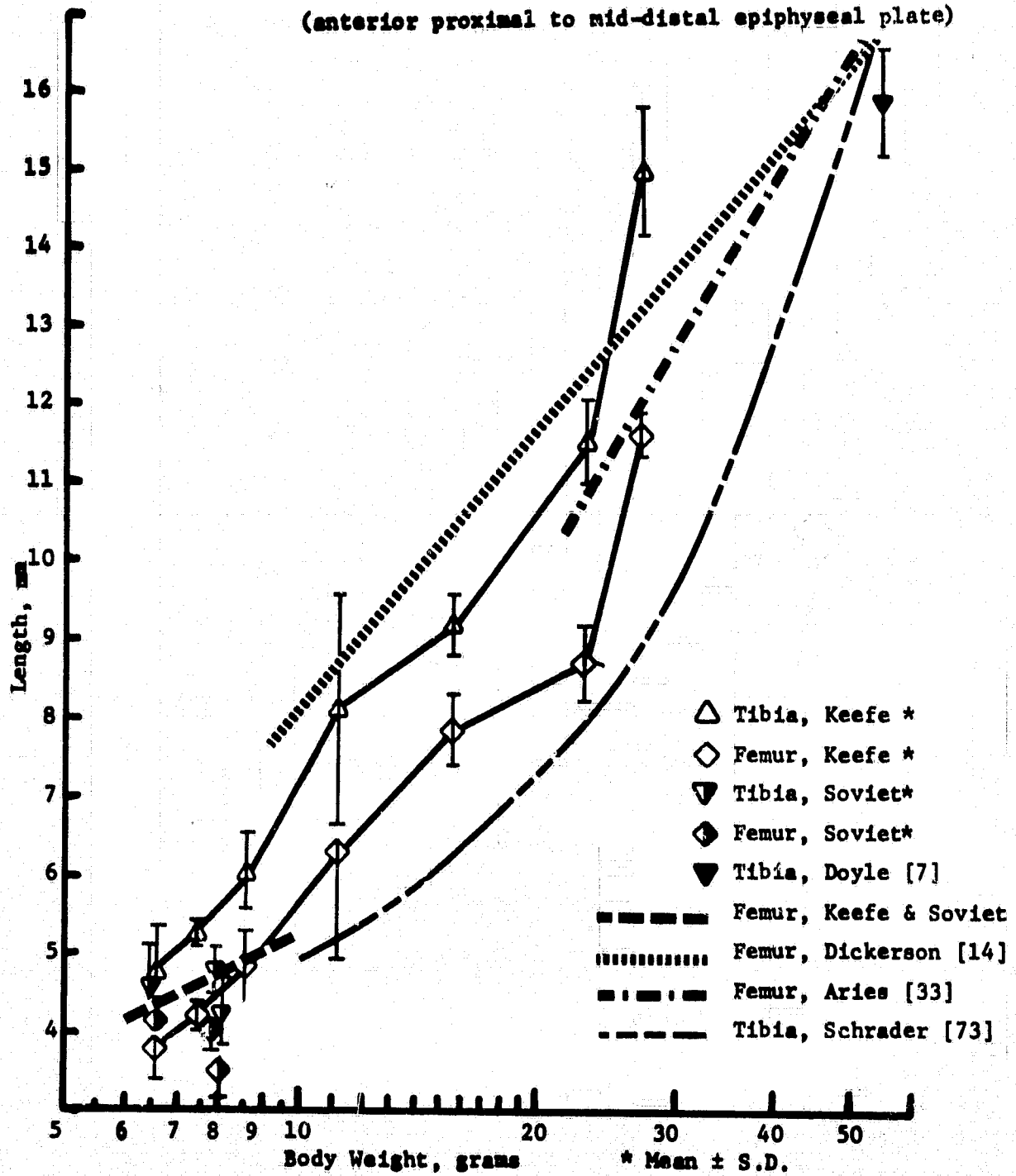
FIGURE 2: HINDLIMB SKELETAL MATURITY SCORES
(maximum possible: 159)

Legend:

▽ Czech rat, Keefe *

◇ Czech Rat, Soviet *

—◯— Hooded rat, Hughes & Tanner [18] *

* Mean ± S.D.

Postnatal age, days

Approximate post-conception age, days
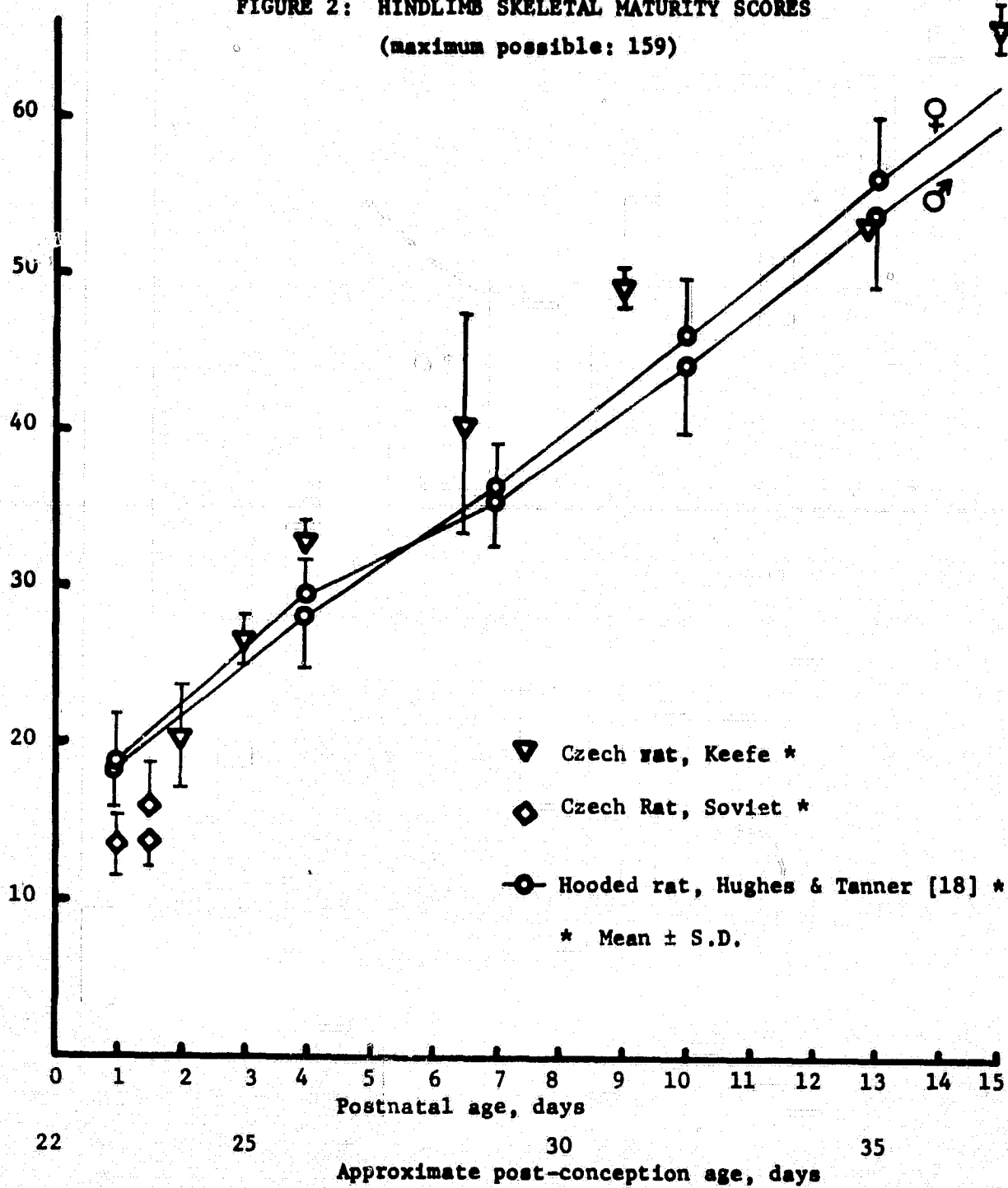
FIGURE 3: ENLARGED CONTRAST-ENHANCED RADIOGRAPH
2 day old Keefe Czech Wistar (KE3.1L) scale in cm.

The proximal metaphysis of the femur (F) is denser than
the distal and is skewed toward the trochanter. The
tibial proximal metaphysis (PM) is also denser than the
distal, which overlaps the fibula. The tibial diaphysis
(D) contains a region of primary osteons. The calcaneal
ossification center is present (C); no secondary centers
are visible.
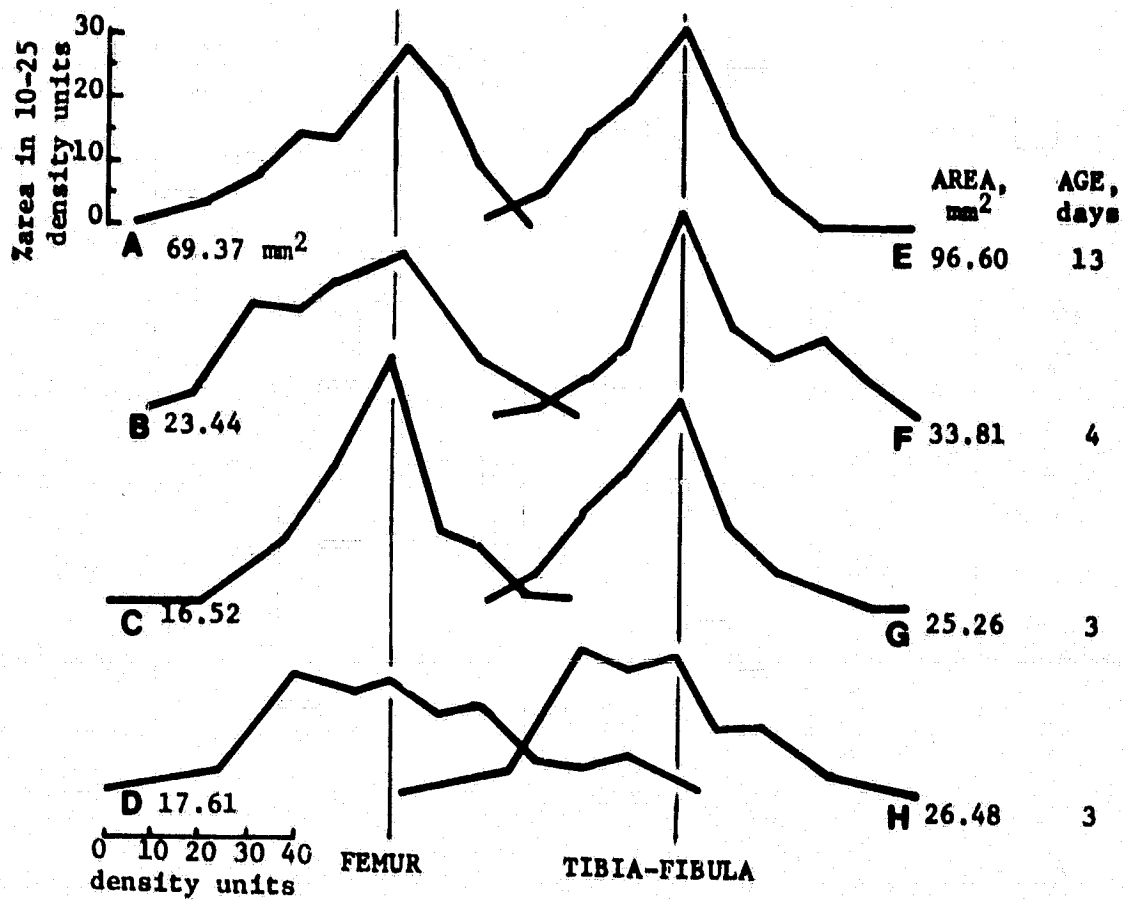
FIGURE 4: RELATIVE RADIOGRAPHIC DENSITY (Keefe specimens)

FIGURE 5: JUVENILE RAT BODY WEIGHT

Czech Wistar, Soviet
Czech Wistar, Ames
Czech Wistar, Keefe standard diet
Czech Wistar, Keefe paste diet
Hooded, Hughes & Tanner [32]
Sprague-Dawley (litter of 4) Shrader [36]
Sprague-Dawley, Acheson, et al [88]
Sprague-Dawley, Curley & Pelas [87]
Long-Evans, Curley & Pelas [87]

Postnatal age, days

Body Weight, grams

FIGURE 6: CLEARED ALIZARIN STAINED HIND LIMB
4 day old Keefe Czech Wistar (KC1.11L)

Modeling is occurring at the greater trochanter (GT) and
metaphyses of the femur and at the tibial crest (TC).
The ilium (Il) and ischium (Is) are flattened. Ossif-
ication centers of the foot include the primary (and
possibly secondary) calcaneum (C), 4 metatarsals (Mt),
and 4 proximal and distal phalanges (P). The meniscal
fibrocartilage (M) is revealed by expansion of the
joint space due to cartilage shrinkage.

FIGURE 7: BONE CURVATURE AND SPATIAL RELATIONSHIP MEASUREMENT

P-D: Nominal tibial axis, through centroids of proximal (P)
      and distal (D) epiphyseal plates
T: Centroid of tibial cross-section
F: Centroid of fibular cross-section
A: Intersection of nominal axis with section plane

FIGURE 6: CLEARED ALIZARIN STAINED HIND LIMB
4 day old Keefe Czech Wistar (KC1.11L)

Modeling is occurring at the greater trochanter (GT) and
metaphyses of the femur and at the tibial crest (TC).
The ilium (Il) and ischium (Is) are flattened. Ossif-
ication centers of the foot include the primary (and
possibly secondary) calcaneum (C), 4 metatarsals (Mt),
and 4 proximal and distal phalanges (P). The meniscal
fibrocartilage (M) is revealed by expansion of the
joint space due to cartilage shrinkage.

FIGURE 7: BONE CURVATURE AND SPATIAL RELATIONSHIP MEASUREMENT

P-D: Nominal tibial axis, through centroids of proximal (P) and distal (D) epiphyseal plates

T: Centroid of tibial cross-section

F: Centroid of fibular cross-section

A: Intersection of nominal axis with section plane

FIGURE 8: KNEE JOINT AND PATELLA
  sagittal section, 10 μm, Sirius Red, polarized illumination
  2 day old Soviet Czech Wistar (SF3.2L, sl. 16)

  Colinear collagen is seen in superficial patellar (PL) and
  posterior cruciate (PC) ligaments. Patella (P), femur (F)
  and tibial (T) cartilages are not birefringent. Deep to
  the patellar ligament is vascular synovial (SM) and loose
  connective tissue originating in the patellar rim.

FIGURE 9: HIP JOINT
  coronal section, 10 μm, H&E
  1 day old Wistar (TA2-.2d.1L, sl. 19)

  The distal branch of the ligamentum teres (LT) does not
  join the femoral head at this level. The ilio-femoral ligament
  (I-L) and gluteus medius (GM) in the superficial greater
  trochanter (GT). The gemellus (Gs) and obturator internans
  (OI) insert near the femoral neck.
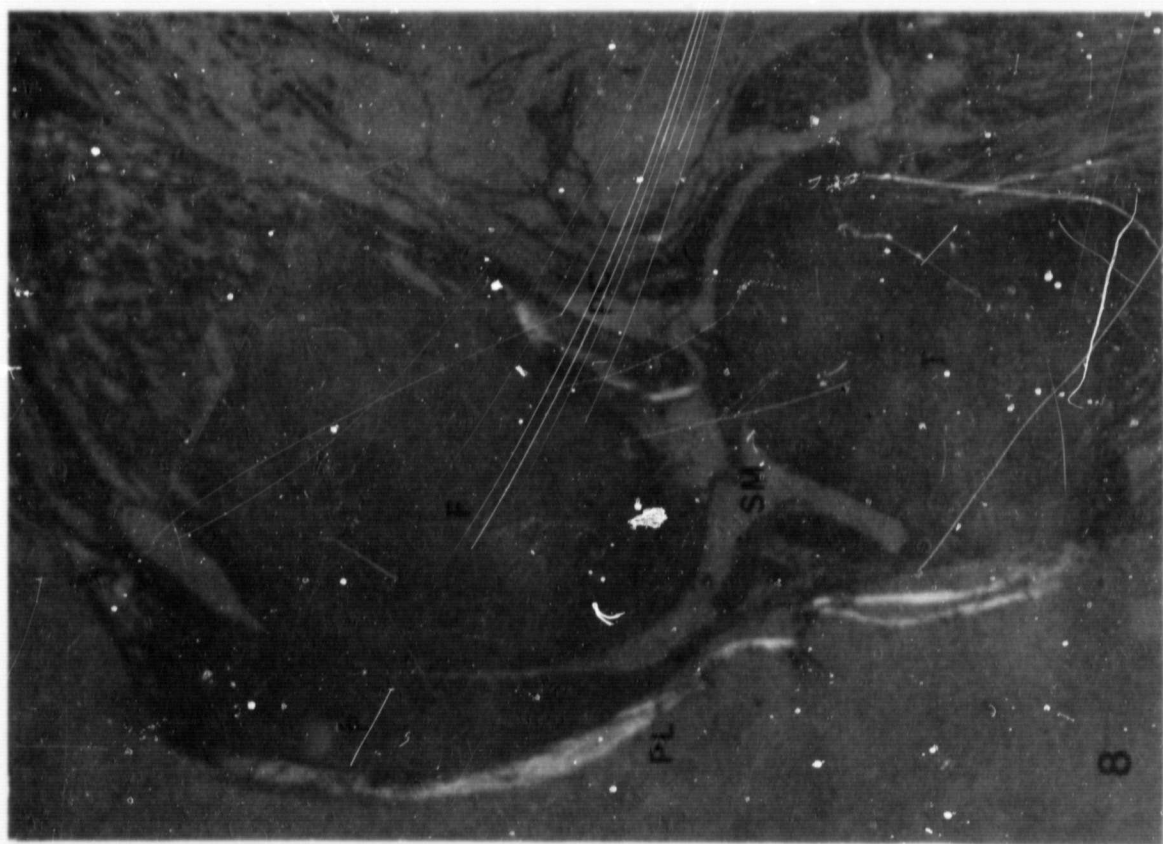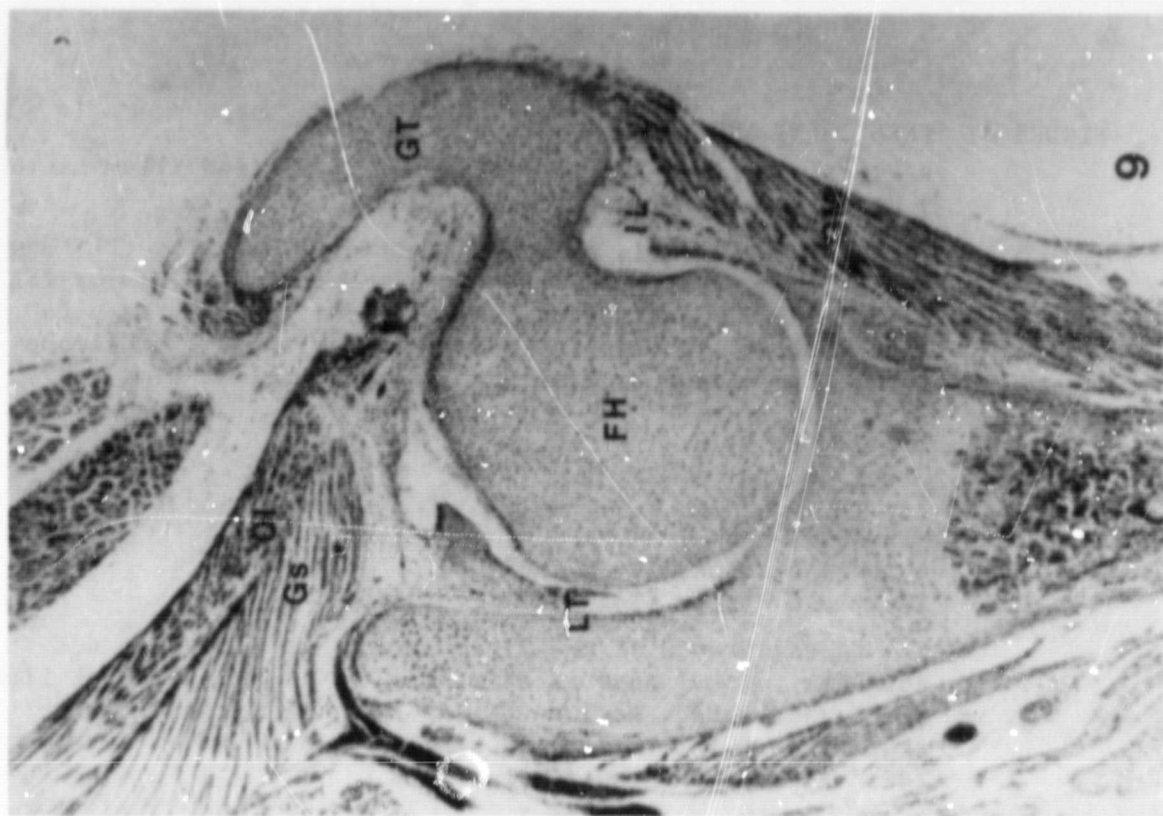
FIGURE 10: KNEE AND PROXIMAL TIBIA
Lateral parasagittal section, 10 μm, H&E
3 day old Keefe Czech Wistar (KE2.1L, sl. 4)

A: OVERVIEW

Fm   Femur
Tb   Tibia (condyle only)
Fb   Fibula
Jc   Joint capsule wall
M   Meniscus
EP   Distal femoral epiphyseal plate

B: DETAIL OF ARTICULAR SURFACE

A   Articular cartilage zone
H   Hyaline epiphyseal cartilage
P   Perichondrium

FIGURE 11: COMPUTER RECONSTRUCTION OF KNEE
60° view angle, 3 pixels/section spacing
3 day old Keefe Czech Wistar (KE2.3L)

PL   Patelar ligament and joint capsule (birefringent) - outlined
P   Patella - solid gray
M   Meniscus - white
F   Femur - outlined
T   Tibia - outlined

FIGURE 12: COMPUTER RECONSTRUCTION OF KNEE
60° view angle, 2 pixels/section
30 hour old Soviet Czech Wistar (SF3.3R)

PL   Patellar ligament - solid white
P   Patella - solid gray
M   Meniscus - outlined

FIGURE 13: COMPUTER RECONSTRUCTION OF FEMUR
72° view angle, 3 pixels/section
1 day old Wistar (TA2-12D.1L)

FH   Femoral head cartilage - light gray
GT   Greater trochanter and periosteum (birefringent) - dark gray
Il   Iliac component of acetabulum - white outline

397

398
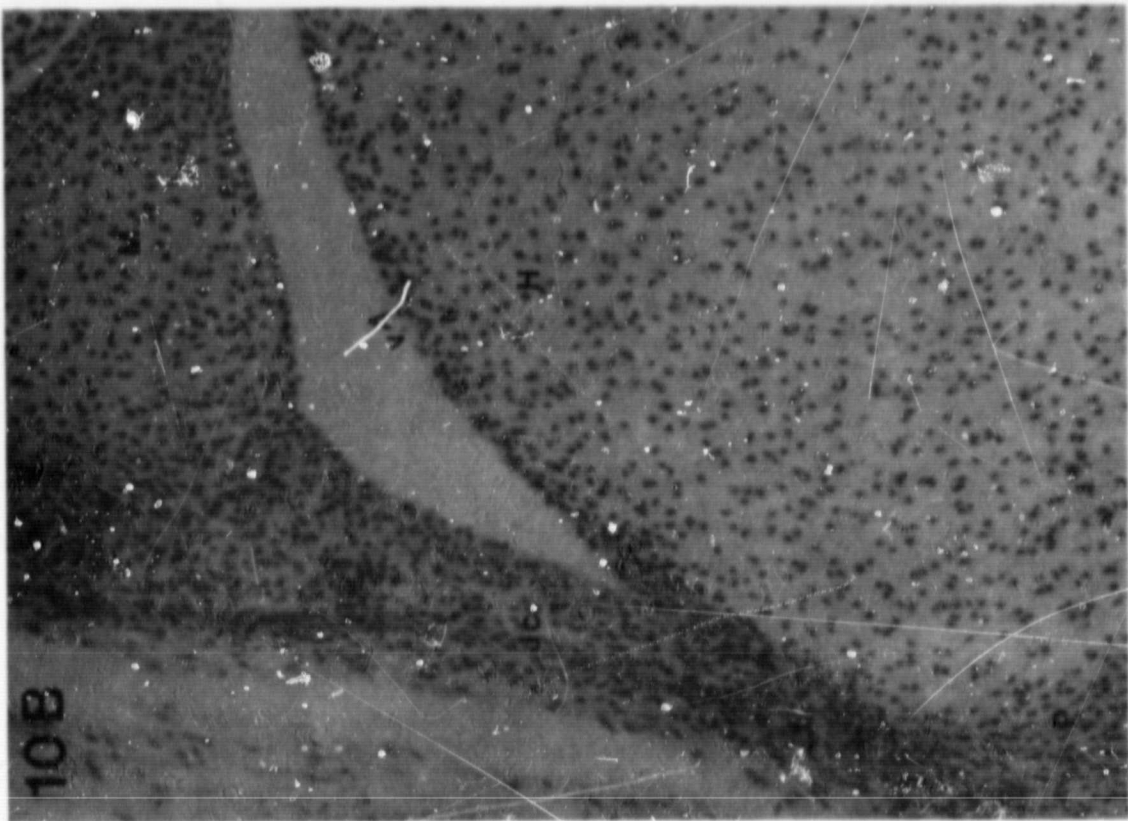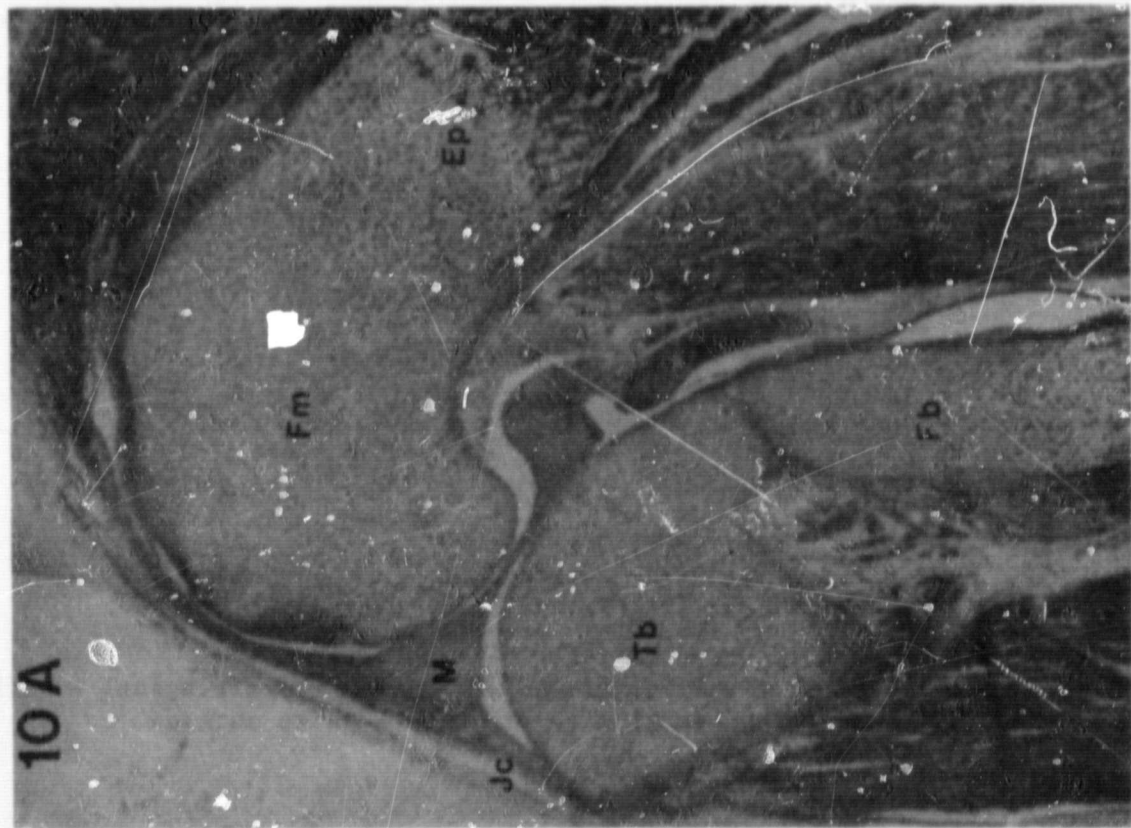
TABLE 1: CZECH RAT EPIPHYSEAL PLATE PROPERTIES (mean ± SD)

SOURCE	AGE, days	DIST. FEMORAL PLATE WIDTH, mm	PROX. TIBIA PLATE WIDTH	TOTAL PLATE HEIGHT, mm	CALC. CARTILAGE HEIGHT
Soviet	1-2	.94	.98 ± .08	.88	.17
Keefe	2-3	1.23 ± .12	1.11 ± .15		
	4			.83 ± .11	.16 ± .04
	6-7	1.09 ± .13	1.29 ± .13		
Ames	9	1.59 ± .22	1.90 ± .32	1.00 ± .05	.24 ± .01
Schenk, et al [54]	25-30			.51 ± .02	
+ EHDP				1.85 ± .13	
Asling [55] flight	85			.97 ± .22*	.32 ± .002*
synchronous				1.34 ± .18*	.55 ± .005*
vivarium				2.93 ± .20*	.82 ± .002*

* mean ± SE

FIGURE 14:   COMPUTER RECONSTRUCTION OF HIP
              60° view angle, 3 pixels/section
              30 hour old Soviet Czech Wistar (SF3.1R)

              FH   Femoral head – gray outline
              IL   Ilio-femoral ligament (Birefringent) – dark gray
              Gm   Gemellus and associated joint capsule (biref.) – white
                    Arrows point to sagittal plane (s) and distally (d)

FIGURE 15:   COMPUTER RECONSTRUCTION OF HIP; same specimen as Figure 14

              ~70° view angle, 4 pixels/section

              FH   Femoral head – gray
              LT   Ligamentum teres (birefringent) – white
                    O   Origin in femoral head
                    I   Insertion in acetabular labrum
              Ac   Acetabular components – gray outline
                    Arrows point to sagittal plane (s) and distally (d)

FIGURE 16:   COMPUTER RECONSTRUCTION OF ACETABULUM (FEMUR OMITTED)
              3 day old Keefe Czech Wistar (KE2.1L)
              60° view angle, 4 pixels/section

              FC   Fibrocartilage (birefringent) – light gray
              HC   Hyaline cartilage – dark and medium gray
              IW   Visceral wall of ilium (birefringent) – white outline
              Ob   Obturator group – gray outline

FIGURE 17:   KNEE, TIBIA AND FIBULA, SEM
              1 day old Sprague-Dawley (H4.1L)

         A: OVERVIEW

              FA   Popliteal plexus of femoral artery
              PC   Posterior cruciate ligament
              Ep   Proximal tibial epiphyseal plate
              SS   Secondary spongiosa
              FO   Femoral epiphyseal ossification center (hypertrophic)
              Fb   Fibula
              Gc   Gastrocnemius
              Ta   Talus
              Mt   Metatarsals

         B: DETAIL OF KNEE ARTICULAR SURFACE AND MENISCUS

400

402
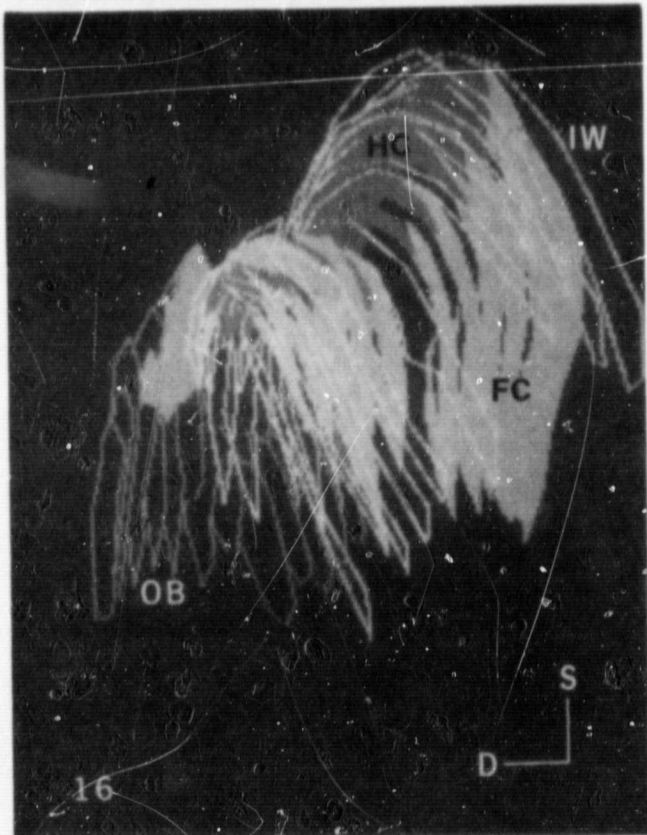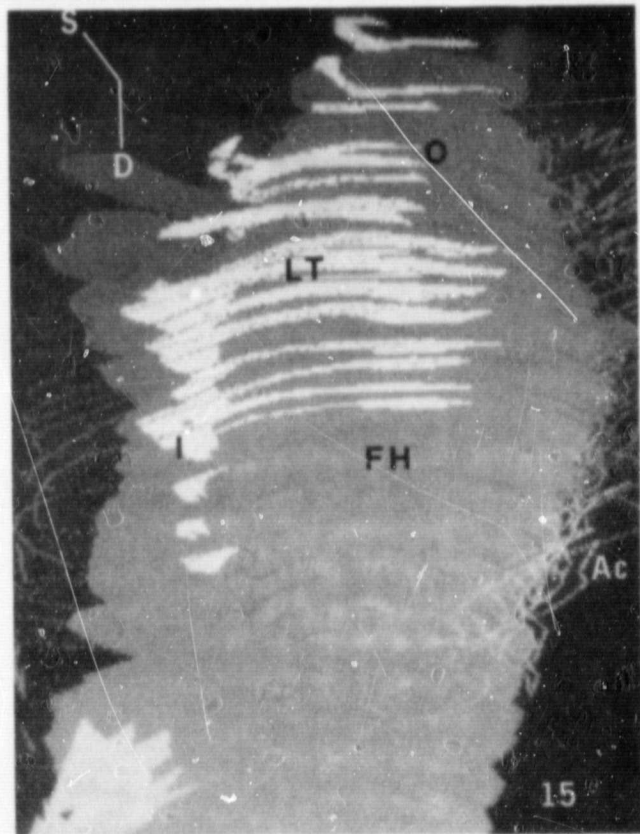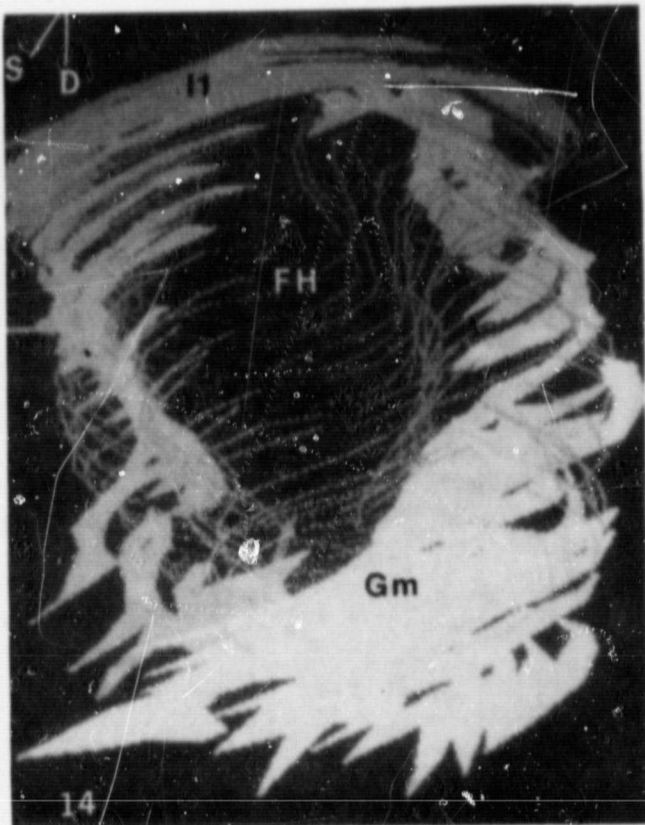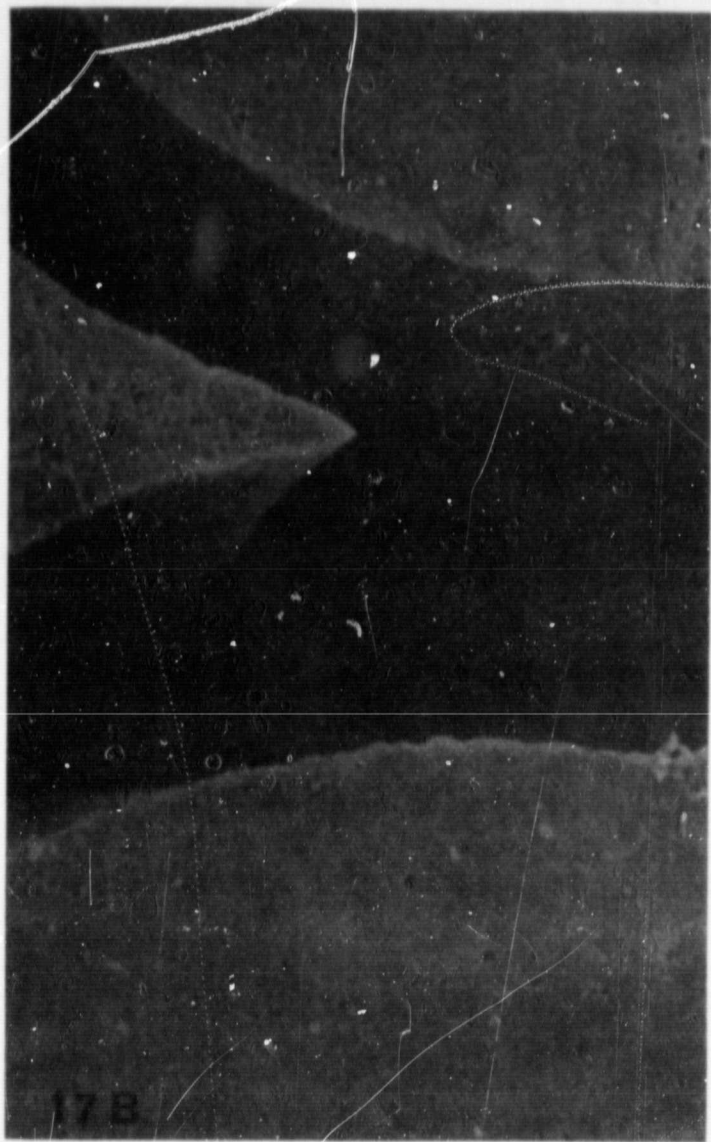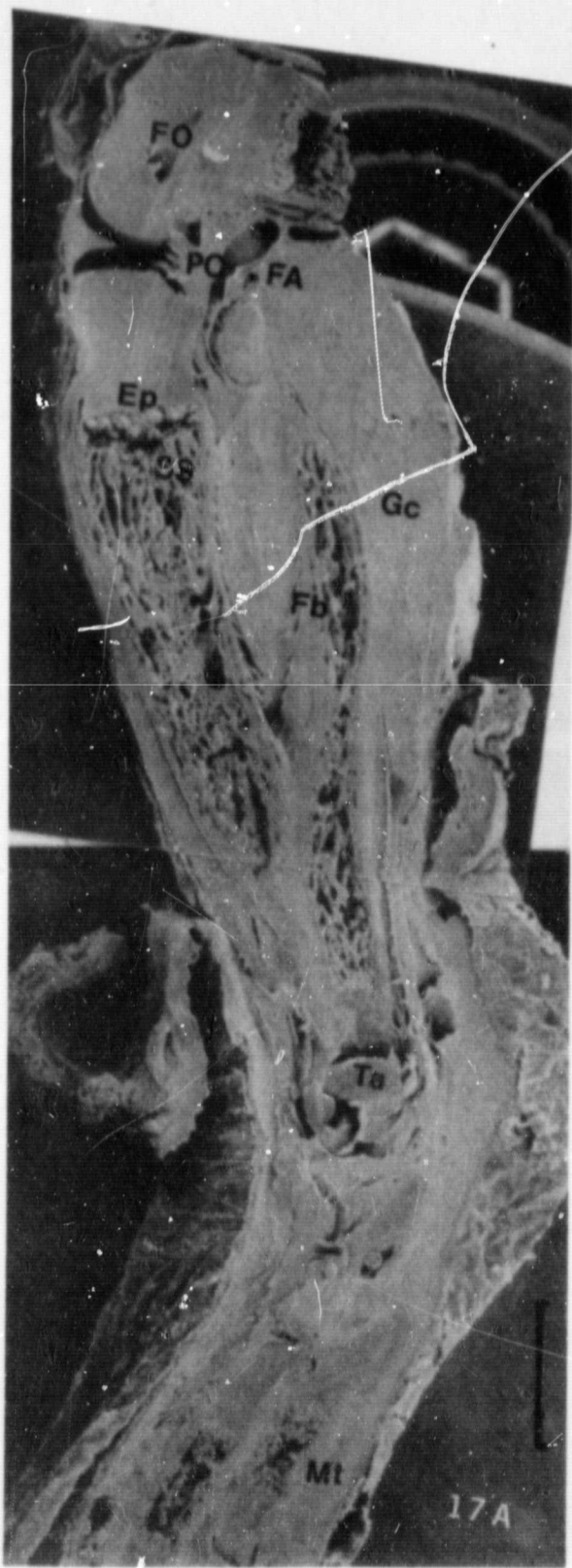
FIGURE 18:   ANKLE SYNOVIAL TISSUE, SEM (same specimen as Figure 17)

    TE   Distal tibial epiphyseal cartilage
    SM   Synovial membrane folds
    Ta   Talus, cartilage

FIGURE 19:   METATARSAL MEDULLARY CAVITY, SEM
             2 day old Keefe Czech Wistar (KE2.3L)

    HZ   Hypertrophic cell zone of proximal epiphyseal plate
    PS   Primary spongiosa
    SS   Secondary spongiosa
    HM   Hematopoietic marrow
    DP   Distal epiphyseal plate

404
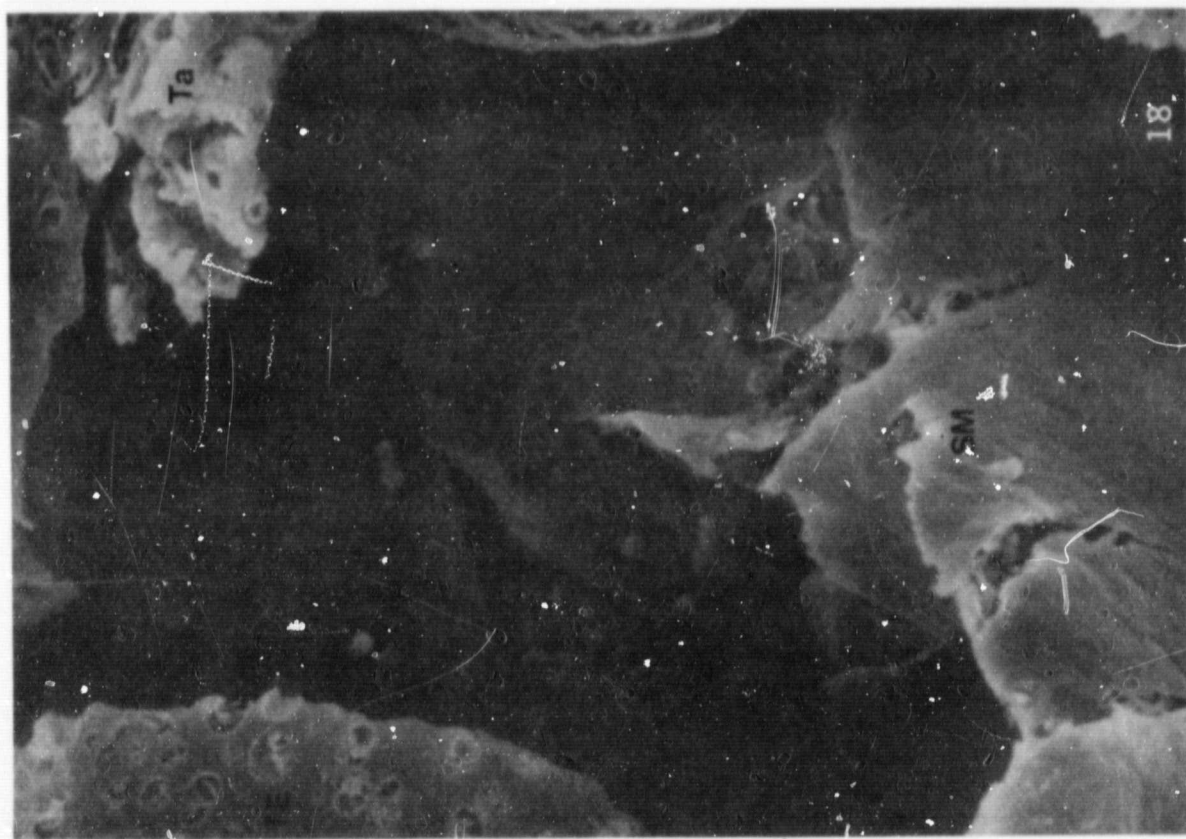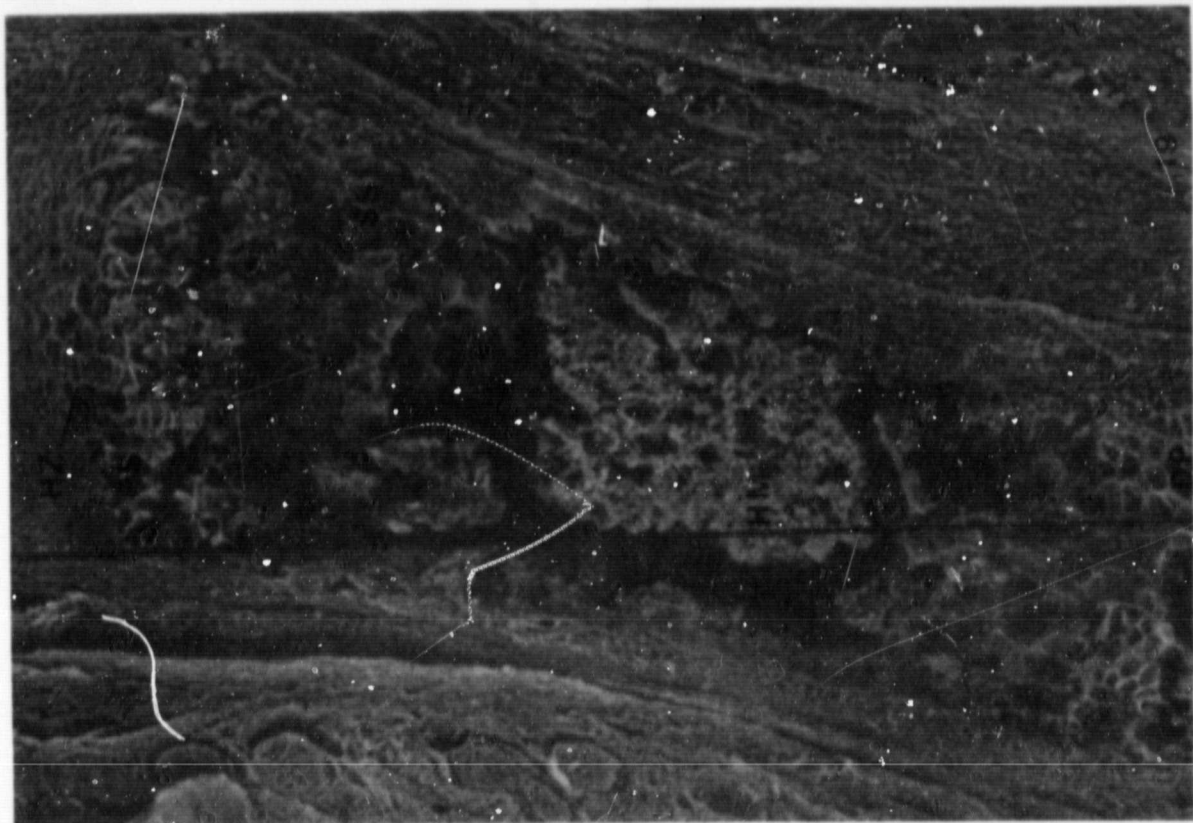
Experiment K 315

STUDIES OF THE NASAL MUCOSA

Lisbeth M. Kraft

Ames Research Center
National Aeronautics and Space Administration
Moffett Field, California

SUMMARY

The posterior regions of the olfactory nasal mucosa of rats flown on Cosmos 1129 failed to reveal histopathological changes. These results are at variance with those of the Apollo XVII Biocore experiment in which severe necrotic olfactory mucosal lesions were seen in flight animals only. In the anterior aspect of the nasal cavity of the Cosmos 1129 rats, however, focal lesions of moderate severity and variable extent were seen. These were consistent in character with that of a mild virus infection, which, it is postulated, was self-limiting. The infection was present in all groups of animals: flight, synchronous and vivarium control.

INTRODUCTION

The basis for examining the nasal mucosa of Cosmos 1129 rats resides in the extensive lesions that were seen in the olfactory, but not the respiratory, nasal mucosa of rodents, pocket mice (Perognathus longimembris), in the Biocore experiment that flew on board Apollo XVII in 1971. Those lesions, observed upon termination of the mission, were not found in any of numerous control pocket mice examined. Conjecture as to the causation of the lesions did not lead to a satisfactory conclusion at that time (1).

The present study was conducted to determine if similar lesions may occur in other rodents as a consequence of spaceflight. A further rationale involved the fact that the olfactory sense in rodents influences mating behavior (2), and successful mating was essential for the rat ontogenesis experiment included in the Cosmos 1129 payload. Thus, should nasal olfactory lesions develop during flight, with, presumably, impaired olfactory sense, they might be a contributing cause of failure to mate, should that indeed have been the case. If no lesions developed in the rats, then the etiology of the alterations in the Biocore pocket mice would remain an open question.

This report includes only the results of investigations in the Cosmos 1129 rats. Retrospective studies in the Biocore mice, stimulated by present results, will be reported separately (Kraft, L. M., D'Amelio, F. E., D'Amelio, E., Broderson, R. J., and Hierholzer. J., in preparation).

MATERIALS AND METHODS

Specimens from 54 rats were examined. The number of animals and the groups to which they belonged are:

Group	Days after recovery	Flight (F)	Synchronous (S)	Vivarium (V)
		Number of rats		
1	0	7	7	7
2	6	6	6	6
4	29	5	5	5

Specimens consisted of the remainder of the head after removal of brain, pituitary, eyes, and mandible. Cold fixative (3% glutaraldehyde, 1% paraformaldehyde, and 0.5% 1,5 difluoro-2,4 dinitrobenzene in 0.1 M sodium cacodylate buffer, pH 7.3, at approximately 900 mOsm) was instilled into the nostrils after which the specimen was immersed in the same fixative and

maintained at 4°C. The mean time interval between sacrifice and fixation of the specimens was 19.4 min (11-30 min).

Upon receipt in the laboratory, excess tissue was trimmed from the specimen of one flight animal of Group 1, decalcified in 10% hydrochloric acid in 10% formalin for 7-8 hours at room temperature, and processed for paraffin embedding. This was done in order to determine if it would be necessary to process the tissues of any of the other animals for electron microscopy. Subsequently, all specimens were treated in the manner just described.

After decalcification, before processing for embedding, each specimen was divided coronally into three segments. An anterior cut was made 2 mm behind the lingual eruption line of the incisors, and a posterior cut was made just behind the third molar. Sections 6 μm thick were made beginning at the posterior aspect of the anterior segment and at the anterior aspect of the posterior segment. In this way, respiratory mucosa, predominating in the anterior, and olfactory mucosa, more abundant in the posterior portion of the specimen, could be studied without having to make numerous serial or step sections.

Sections were stained with hematoxylin and eosin (H&E) and by the periodic acid Schiff (PAS) method. The middle of the three nasal segments was not sectioned. It was retained for further processing in the event that provocative results

requiring confirmation or augmentation would be found in the other segments.

In evaluating the tissues microscopically, slides were read without knowing the identity of the tissues until all had been examined. Any lesions found were scored on the basis of their severity and extent.

RESULTS

Olfactory Mucosa - Posterior Nasal Segment

Light microscopic observations in both H&E and PAS preparations failed to uncover lesions comparable with those of the Biocore pocket mice in this nasal segment of all 54 rats on Cosmos 1129. The olfactory mucosa appeared entirely normal, and the various groups of animals were indistinguishable from each other in this respect.

Respiratory and Olfactory Mucosa - Anterior Nasal Segment

In the anterior segment of the specimen, some inflammatory foci could be seen in the mucosa, both respiratory and olfactory, in all animals. These are depicted in Fig. 1 and 2. Assigning values from 1 to 3 on the basis of severity and extent resulted in the data seen in Table 1. The individual and mean scores for each group of animals suggest that both the flight and synchronous control rats showed the most severe and extensive lesions at the time of spacecraft recovery, while all other

409

groups did not differ markedly from each other. The method of
evaluation and the small number of animals per group did not, in
our opinion, warrant statistical treatment of the results.

DISCUSSION

Lesions similar to those in the Biocore flight animals were
not found in any of the Cosmos 1129 rats. Thus it is clear that
the etiology of the former is still in doubt.

With regard to the nasal lesions in the Cosmos 1129 rats,
it appears that the colony was infected with a mild respiratory
disease. Perhaps a pneumonitis might also be found in some of
the animals. Based on temporal considerations, the infection may
have been self-limiting, since group 1 flight and synchronous
controls showed the highest incidence and severity of lesions,
group 2 rats were intermediate in this regard, and group 4
demonstrated predominantly mild lesions. Since the vivarium
control animals cohabited with each other in standard cages
throughout the duration of the mission and thereafter whereas the
flight and synchronous control animals were housed separately,
they cannot be similarly evaluated. Yet it is clear from the
incidence of the lesions, that the vivarium controls were
undergoing an enzootic at the same time, i.e. the infection was
present in the colony before the flight.

This is not to say that the animals are not to be

considered specific pathogen free (SPF), for it is only reasonable to expect SPF animals to become infected from random sources after they leave the SPF environment. In any case, the results seem to illustrate the effect that stress, as exemplified by actual or simulated spaceflight, may have on an enzootic infection, even though it may be subclinical in character.

REFERENCES

1. Kraft, L.M., F.S. Vogel, B. Lloyd, E.V. Benton, M.R.Cruty, W. Haymaker, H.A. Leon, J. Billingham, C.E. Turnbill, V. Teas, B.C. Look, K. Suri, J. Miquel, W.W. Ashley, A.R. Behnke, Jr., T. Samorajski, O.T. Bailey, and W. Zeman. The effects of cosmic particle radiation on pocket mice aboard Apollo XVII. IX. Results of examination of the nasal mucosa. Aviat. Space Environ. Med. 46:561-568 (1975).

2. Pfaff, D. and C. Pfaffman. Behavioral and electro-physiological responses of male rats to female rat urine odors. Olfaction and Taste, III. C. Pfaffman, ed. The Rockefeller University Press, New York. (1968).

TABLE 1

LESION SCORES - ANTERIOR NASAL SEGMENT

Group	Rat Number							Mean Score
	1	2	3	4	5	6	7	
1F	3*	3	2	3	3	3	3	2.86
2F	2	1	2	2	1	2		1.67
4F	1	1	1	1	1			1.0
1S	3	3	2	1	3	2	1	2.14
2S	1	2	3	1	2	2		1.83
4S	1	1	1	2	1			1.2
1V	2	1	1	1	1	2	2	1.43
2V	2	3	1	1	1	2		1.67
4V	1	3	1	1	2			1.6

*3 = moderately severe and extensive

2 = of intermediate severity and extent

1 = minimally severe and extensive

Figure 1. Mucosal lesion in anterior nasal cavity. The focal
nature of a typical lesion is demonstrated. Note the
normal epithelium in the lower half of the field. The
bar represents 20 μm.
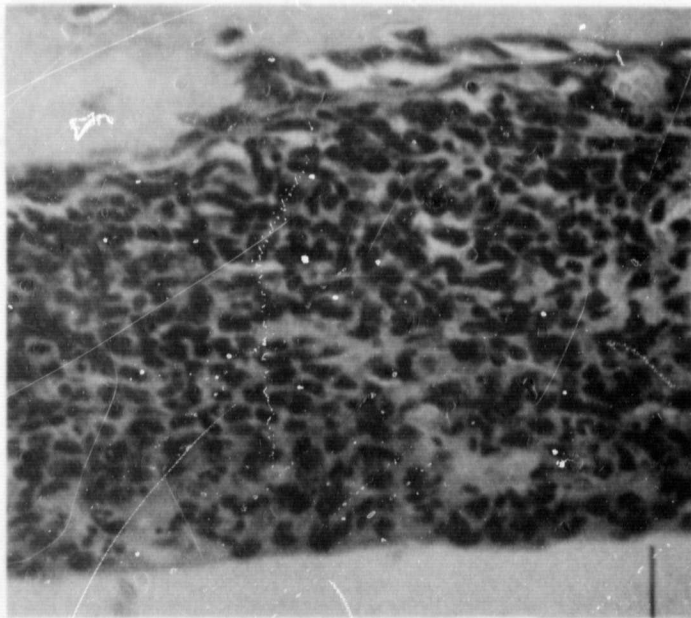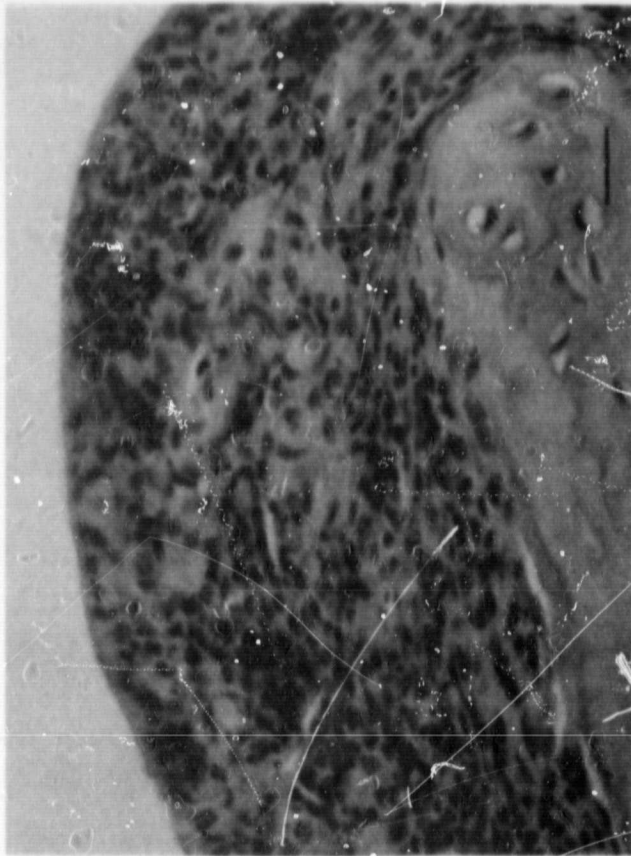
Figure 2A

Figure 2B

Figure 2. Numerous polymorphonuclear and mononuclear cells
together with a few necrotic cells obscuring the normal
architecture of the mucosa are depicted. Inflamatory
cells can be seen in both the affected epithelium as well
as in the lamina propria. Frank ulceration is not seen.
The bars represent 20 μm.

A. Rat number 2 from group 2V. The lesion is in the
nasal septum.

B. Rat number 6 from group 1F. The affected mucosa
on a nasal turbinate is shown.

414

K-316

EFFECTS OF WEIGHTLESSNESS ON BODY COMPOSITION IN THE RAT

by

A.S. Ushakov[1], T.A. Smirnova[1], G.C. Pitts[2], N. Pace[3], and A.H. Smith[4]

[1]Institute Of Biomedical Problems, Moscow 117113, USSR.

[2]Department Of Physiology, School Of Medicine, University Of Virginia, Charlottesville, VA 22908.

[3]Environmental Physiology Laboratory, University of California, Berkeley, CA 94720.

[4]Department Of Animal Physiology, University Of California, Davis, CA 95616.

SUMMARY

Cosmos 1129 included 5 male rats dedicated to K-316. These were sacrificed 32-36 hr after recovery, dissected into 3 major compartments (musculo-skeletal system, skin, and pooled viscera) and compared with 5 Synchronous Controls on the ground in flight-type hardware. In this comparison the Flight Group showed: a 6.7% reduction in total body water probably attributable to a 36.2% reduction in the extracellular compartment, reductions of 6.6% in musculo-skeletal water and 17.2% in skin water, an apparent shift of some water from skin to viscera, and a 20% reduction in bone mineral mass. Among organ fresh masses there was a 7.5% increase in kidneys and a 14.0% decrease in spleen.

INTRODUCTION

In general, environmental physiology evaluates organismic responses to changes in environmental parameters. Among such parameters, change in the chronic acceleration field (ΔG) is new in an evolutionary sense; i.e., physiologically significant changes in G have probably never occurred during the evolution of life on earth. While organisms have evolved defenses against changes in temperature, altitude, osmotic pressure, insolation, etc., they have had no need or opportunity to evolve defenses against ΔG. Thus, it comes as no surprise that ΔG perturbs body composition to a degree not seen with changes in most other environmental factors.

Among the various body compartments, the fat-free body mass (FFBM) in the adult rat resists perturbation by a variety of environmental factors, ΔG being a striking exception (1). An increase in ΔG caused by chronic centrifugation results in a prompt decrease in FFBM to a new steady state level (2), a response which is not altered by the ingestion of excess calories or protein (3). Thus, body composition parameters which resist perturbation by most environmental factors are clearly sensitive to ΔG.

Weightlessness represents a virtual extinction of the acceleration field. It is of basic physiological interest and has obvious applicability to space medicine. We report here on the body composition responses of the adult rat to weightlessness of 18.5 days duration.

METHODS

The albino rats used were Wistar-derived males, specific pathogen free, from the colony of the Institute of Experimental Endocrinology

416

of the Slovakian Academy of Sciences, Bratislava, Czechoslovakia and
~84 days old and 304-318g in body mass at launch. Five of these were
placed in the spacecraft (Flight Group) and five in flight-type hardware
at terrestrial gravity (Synchronous Control Group). The cages for
individual rats were cylindrical, 9.5 cm. diameter and 26 cm. long.
Body wastes were carried to a trap by air flow. The Synchronous Control
Group was subjected to the physical transients of launch and reentry.
These transients were presented serially rather than simultaneously and
with a 6-day lag behind the Flight Group.

The rats were fed a balanced diet based on casein, cornstarch,
sucrose, sunflower seed oil, dried brewers yeast and comprehensive
mixtures of salts and vitamins with enough water added to make a paste.
Each rat received 10g of this diet every 6 hours, providing a daily
ration of 40g or 68.7 kcal (1.72 kcal/g). Virtually all of this was
consumed. All rats were started on the flight diet 10 days before
launch. Water was available ad libitum.

The Flight Group arrived at the Institute in Moscow 32 hours after
touchdown, having been fed as scheduled during this interval. Killing
and dissection began immediately, with the last Flight animal being
killed ~36 hours after touchdown and dissected during the succeeding hour.
Sacrifice was by ethyl ether inhalation. The procedures used for dis-
section and analyses were those developed at the Environmental Physiology
Laboratory, University of California, Berkeley (4). The dissection
involved separation and weighing of 15 individual organs and organ
systems. Determination of water content (freeze-drying) and of fat
content (Soxhlet extraction) were carried out separately on 3 major

body compartments: skinned, eviscerated carcass, i.e., musculo-skeletal system (designated "carcass"); skin; and all other components pooled (designated "viscera"). Summation of these 3 compartments yielded whole body water, fat, and solids. The dried defatted residues from each rat were ground, combined, and mixed to provide a homogeneous whole-body powder for subsequent analyses. Aliquots were analyzed for: nitrogen, potassium, calcium, phosphorus, magnesium, and sodium.

The following calculations were employed(45). Net body mass = total body mass - fur, gut content, and urine. Intracellular water content = 0.73 x body cell mass. Extracellular water content = total body water - intracellular water. Body protein = 6.25 x body nitrogen. Body cell mass = 8.9 x body potassium. Bone mineral = 2.93 x body calcium.

The statistical significance of the differences between the two groups was evaluated with the t test (6). The criterion for rejecting the null hypothesis was P < .05.

RESULTS

Composition of the major body compartments is presented in Table 1. In general we shall comment on those differences which are statistically significant, in each case considering the relative position of the Flight Group.

The net body mass was reduced 3.9% in the Flight Group. To account for this one would consider the two major compartments, the fat and the fat-free. While fat did not contribute to the difference, the total fat-free body mass was reduced 5.8%. The compartment within the fat-free mass primarily responsible for this was the skin, which was 14.6%

lower in the Flight Group. Changes in the fat-free mass can be attributable to either or both water or dry fat-free material (solids). In this case the reduction in fat-free skin must be attributed largely to a 17.2% reduction in its water content. But there was also a 6.6% reduction of water in the carcass, and carcass plus skin accounted for the 6.7% reduction in total body water of the Flight Group. This total water reduction appeared to be restricted to the extracellular compartment and resulted in the following changes in fractional distribution. The fraction of the total water contained within viscera of the Flight Group went up 7.4% and that within skin went down 11.1%, representing a net shift from skin to viscera. Water as a fraction of the individual fat-free component masses went down in the total body, carcass, and skin. Finally, body sodium was down 11.3% and bone mineral (calculated from calcium) was down 22.1% in the Flight Group.

By contrast with the above we see that organ fresh masses (Table 2) showed few statistically significant changes, i.e., kidneys were increased 7.5% and spleen was reduced 14.0% in the Flight Group. While these two changes corroborate the results obtained by others (7) we have no explanation for them.

DISCUSSION

Some questions concerning the validity of these data should be discussed. First, did the values reached in orbit represent steady states or transients, i.e., was the 18.5 day exposure of sufficient duration? Chronic centrifugation of adult rats changes the FFBM to a new lower value which appears to be regulated and is characteristic of the new G-lev (2,3). If one imposes 4.15G ($\Delta G = 3.15$) in this way,

419

the loss in live mass may be ~50g and in FFBM ~30g and both are completed within 10 days of exposure. In the present case the change in acceleration provided by the mission was Δ1G. It appears highly probably that by the end of the 18.5 day exposure there was a steady state in body composition.

Second, did the 32-36 hrs. at terrestrial gravity between recovery and sacrifice evoke a reversal of the condition typical of weightlessness? The chronically centrifuged rats upon return to 1G show a reversal of the centrifugation-induced changes. During the first 7 days at 1G they regained ~70% of the live mass lost at 4.15G (2). It appears reasonable that they might have regained 15-20% in the 1 1/2 days being considered here. Thus, while the changes reported in Table 1 might have been greater if recorded just before reentry, we believe they reflect true effects of weightlessness.

One response reported in rats during the second day after reentry from earth orbit was an edema of skeletal muscles observed histologically (8). This should increase the carcass water content. If this response was present in our Flight Group, it did not offset the observed reduction in carcass water (Table 1).

The agreement between our rat data and those observed in weightless man gives us further confidence in the validity of our observations. Following exposure to weightlessness both species showed: a loss in total (or net) body mass (9), a loss in bone mineral (10), a loss in total body water (11), and a loss in extracellular fluid volume (11).

The data in Table 1 can be used to make several additional calculations as checks on reliability and internal consistency, as follows.

The protein fraction of the fat-free body calculated from Table 1 is 21.7% for the Flight and 20.9% for the Control Group. The value reported for adult rats at 1G is 22.0% (12). The reduction in bone mineral found in the Flight Group can be calculated from either calcium or phosphorus (13), and the values obtained (-22.1% and -18.2% respectively) are in agreement. Changes in extracellular fluid volume can be calculated from changes in body sodium. Flight Group minus Control Group yielded -0.037g of sodium corresponding to -11.5g of extracellular water. This agrees well with the Flight Group reduction in total body water (-14.0g).

Finally, our results support: the validity of the rat as an experimental model for gravitational studies (since it obviously responds physiologically to unloading from gravity), and the usefulness of the body composition approach to gravitational physiology.

REFERENCES

1. Pitts, G.C. Physiologic regulation of body energy storage. <u>Metab.</u> 27:469-478 (1978).

2. Pitts, G.C., L.S. Bull and J. Oyama. Effect of chronic centrifugation on body composition in the rat. <u>Am. J. Physiol.</u> 223:1044-1048 (1972).

3. Pitts, G.C., L.S. Bull and J. Oyama. Regulation of body mass in rats exposed to chronic acceleration. <u>Am. J. Physiol.</u> 228:714-717 (1975).

4. Pace, N., D.F. Rahlmann and A.H. Smith. Methodology for estimation of total body composition in laboratory mammals. Environmental Physiology Laboratory, University of California, Berkeley. <u>EPL</u> 79-1 (1979).

5. Pace, N., D.F. Rahlmann, A.M. Kodama and A.H. Smith. Body composition changes in monkeys during long-term exposure to high acceleration fields. <u>Life Sci. Space Res.</u>16;71-76 (1978).

6. Sokal, R.R. and F.J. Rohlf. Biometry. San Francisco:W.H. Freeman and Co. (1969).

7. Portugalov, V.V., E.A. Savina, A.S. Kaplansky, V.I. Yakavleva, G.I. Plakhuta-Plakutina, A.S. Pankova, P.I. Katunyan, M.G. Shubich and S.A. Buvailo. Effect of space flight factors on the mammal: experimental-morphological study. <u>Aviat. Space Environ. Med.</u> 47:813-816 (1976).

8. Il'ina-Kakueva, YE.I., N.V. Petrova and V.V Portugalov. The effect of space flight on the skeletal musculature and nerve apparatus of the muscles. In: The Effects of Dynamic Factors of Space Flight

on Animal Organisms, edited by A.M. Genin. Washington, D.C.:National Aeronautics and Space Administration (1979) p. 100-106.

9. Thornton, W.E. and J. Ord. Physiological mass measurements in Skylab. In: Biomedical Results from Skylab, edited by R.S. Johnston and L.F. Dietlein. Washington, D.C.:National Aeronautics and Space Administration (1977) chapt. 19, p. 175-182.

10. Smith, M.C., Jr., P.C. Rambaut, J.M. Vogel and M.W. Whittle. Bone mineral measurement--experiment M078. In: Biomedical Results from Skylab, edited by R.S. Johnston and L.F. Dietlein. Washington, D.C.: National Aeronautics and Space Administration (1977) chapt. 20, p. 183-190.

11. Leach, C.S. and P.C. Rambaut. Biochemical responses of the Skylab crewmen: an overview. In: Biomedical Results from Skylab, edited by R.S. Johnston and L.F. Dietlein. Washington, D.C.:National Aeronautics and Space Administration (1977) chapt. 23, p. 204-216.

12. Pace, N. and E.N. Rathbun. Studies on body composition. III. The body water and chemically combined nitrogen content in relation to fat content. J. Biol. Chem. 158:685-691 (1945).

13. Neuman, W.F. and M.W. Neuman. The Chemical Dynamics of Bone Mineral. Chicago:University of Chicago (1958) p. 49.

TABLE 1. Composition of major body compartments.

Masses (g)	Flight Group		Control Group		Difference Col. 2 - Col. 4		P
	Mean	CV	Mean	CV	Grams	Z	
Total Body	349.06	3.8	358.87	1.7	-9.80	-2.7	0.17
Net Body	+331.38	3.0	344.68	1.0	-13.30	-3.9	0.024
Fat:							
Body	59.74	6.7	56.33	13.4	+3.41	+6.0	0.40
Carcass	19.67	7.1	17.70	20.6	+1.97	+11.1	0.29
Viscera	25.71	9.5	23.70	13.3	+2.01	+8.4	0.29
Skin	14.36	23.3	14.93	9.6	-0.57	-3.9	0.73
Fat-Free:							
Body	+271.64	4.5	288.35	2.9	-16.71	-5.8	0.036
Carcass	162.97	5.6	172.21	2.6	-9.24	-5.4	0.074
Viscera	46.89	6.8	46.80	2.9	+0.09	+0.2	0.96
Skin	+38.58	4.4	45.21	8.1	-6.63	-14.6	0.006
Dry Fat-Free:							
Body	76.11	4.4	78.80	3.5	-2.69	-3.4	0.21
Carcass	51.22	5.4	52.61	3.4	-1.39	-2.6	0.37
Viscera	11.95	4.3	11.96	2.0	-0.01	-0.1	0.95
Skin	12.94	5.4	14.23	8.2	-1.29	-9.0	0.068
Water:							
Body	+195.53	4.6	209.55	2.7	-14.02	-6.7	0.018
Carcass	+111.75	5.7	119.60	2.3	-7.85	-6.6	0.035
Viscera	34.94	7.9	34.84	3.4	+0.10	+0.3	0.94
Skin	+25.64	4.3	30.98	8.2	-5.34	-17.2	0.003
Intracellular	150.56	5.4	139.08	6.6	+11.48	+8.3	0.069
Extracellular	+44.97	17.4	70.47	6.8	-25.50	-36.2	<.001
Body Magnesium	0.117	3.1	0.119	11.5	-0.002	-2.0	0.72
Body Sodium	+0.290	4.8	0.327	3.1	-0.037	-11.3	0.001
Body Potassium	0.905	5.4	0.836	6.6	+0.069	+8.3	0.069
Body Calcium	+2.86	7.8	3.67	10.5	-0.81	-22.1	0.003

Table 1. Concluded.

		CV		CV		%	p
Body Phosphorus	1.98	7.5	2.29	12.9	-0.31	-13.5	0.071
Body Protein	58.94	4.9	60.21	3.6	-1.27	-2.1	0.45
Body Cell Mass	206.25	5.4	190.52	6.6	+15.73	+8.3	0.069
Bone Mineral →	8.37	7.7	10.75	10.5	-2.38	-22.1	0.003
Fractions (%)							
[Component H₂O/Total H₂O] x 100:							
Carcass	57.13	1.6	57.08	1.5	+0.05	+0.1	0.93
Viscera ←	17.87	5.9	16.63	2.8	+1.24	+7.4	0.044
Skin ←	13.13	5.3	14.77	5.5	-1.64	-11.1	0.009
[Component H₂O/Fat-Free Component] x 100:							
Body →	71.98	0.3	72.67	0.4	-0.69	-0.9	0.004
Carcass →	68.56	0.5	69.45	0.6	-0.89	-1.3	0.004
Viscera	74.47	1.1	74.42	0.6	+0.05	+0.1	>.90
Skin →	66.48	1.1	68.53	0.7	-2.05	-3.0	<.001
[Component fat/Total fat] x 100:							
Carcass	33.04	9.6	31.18	8.8	+1.86	+6.0	0.35
Viscera	43.04	7.3	42.10	3.4	+0.94	+2.2	0.56
Skin	23.91	18.1	26.72	9.7	-2.81	-10.5	0.24

The arrows to the left of column 2 identify the differences between the Flight Group and Control Group which are statistically significant. The direction of the arrow indicates the relative position of the Flight Group mean. CV = coefficient of variation.

TABLE 2. Organ fresh masses.

	Flight Group		Control Group		Difference Col. 2 - Col. 4		
	Mean	CV	Mean	CV	Grams	%	P
Liver	19.03	9.9	17.13	7.1	+1.90	+11.0	0.095
GI Tract	16.02	5.8	15.64	3.9	+0.38	+ 2.5	0.46
Genitalia	12.01	11.5	12.85	4.7	-0.84	- 6.5	0.25
Kidneys	2.94	5.5	2.72	5.2	+0.22	+ 7.9	0.056
Brain	1.99	2.0	1.95	5.9	+0.04	+ 1.7	0.55
Resp. Tract	1.94	6.9	1.87	7.8	+0.07	+ 3.5	0.48
Heart	1.23	10.8	1.24	9.9	-0.01	- 0.8	0.92
Spleen	↓ 0.57	6.9	0.66	7.5	-0.08	-13.4	0.014
Bladder	0.15	14.9	0.17	20.7	-0.02	- 7.2	0.53
Adrenals	0.113	15.4	0.122	10.3	-0.009	- 7.7	0.36
Thyroid	0.022	26.4	0.020	21.8	+0.002	+11.9	0.49

The GI tract, heart and possibly the respiratory tract, as dissected and weighed, had varying amounts of adipose tissue associated with them. The other organs were relatively clean of adipose tissue. For other notes, see Table 1.

K-317

BONE RESORPTION IN RATS DURING SPACEFLIGHT

Christopher E. Cann, Ph.D.

Department of Radiology

University of California

San Francisco, California 94143

Richard R. Adachi

Biomedical Research Division

NASA-Ames Research Center

Moffett Field, California 94035

SUMMARY

Bone resorption was measured directly in flight and synchronous control rats during Cosmos 1129. Continuous tracer administration techniques were used, with replacement of dietary calcium with isotopically enriched ^{40}Ca and measurement by neutron activation analysis of the ^{48}Ca released by the skeleton. There is no large change in bone resorption in rats at the end of 20 days of spaceflight as has been found for bone formation. Based on the time course of changes, the measured 20-25% decrease in resorption is probably secondary to a decrease in total body calcium turnover. The excretion of sodium, potassium and zinc all increase during flight, sodium and potassium to a level 4-5 times control values.

INTRODUCTION

Calcium metabolism is altered in weightlessness. Bone loss occurs and urinary calcium output is increased in humans (1) and there is a significant decrease of tibial bone formation rate in young rats (2,3). These changes which occur during spaceflight are similar to changes observed in immobilized humans (4,5) and monkeys (6), but the underlying causes of these changes are not known. A primary defect in the development of immobilization osteoporosis in adults appears to be an unexplained increase in bone resorption coupled with a mineralization defect, leading to a rapid loss of bone. The sequence of metabolic changes which occurs after this postulated increase in bone resorption includes a slight increase in serum calcium and phosphorus. The homeostatic response to this change in serum calcium involves changes in circulating levels of parathyroid hormone and the active metabolites of vitamin D. Calcium turnover and urinary calcium output increase. This increased calcium excretion coupled with a decline in intestinal calcium absorption produces a strongly negative calcium balance. In paralyzed patients and bed-rested subjects, this process appears to be self-limiting. Following the initial rapid loss of bone, calcium turnover and urinary output decrease to below-normal values. This chronic phase of immobilization osteoporosis appears to be a state of rarefied bone with a low turnover rate. Remobilization in adults does not appear to completely correct the bone mass defect, so that adult bone loss due to immobilization or weightlessness may be irreversible.

The characteristics of immobilization osteoporosis are quite different in young, growing patients or animals. Bone turnover in a juvenile skeleton

is qualitatively different from that in an adult skeleton. Adult bone is characterized primarily by remodeling activity, in which existing bone is resorbed by osteoclasts and then replaced by osteoblasts, with no net change in bone mass or spatial orientation of the bone. In contrast, juvenile bone changes are composed of two processes: 1) growth and modeling, and 2) remodeling. The growth and modeling component includes periosteal apposition, endosteal resorption and apposition, and growth in the epiphyseal-metaphyseal regions of the bones, and dominates bone turnover until the skeleton matures. During this time of growth, bone formation exceeds bone resorption by a significant amount so that net body calcium balance is positive. Little data exists on the quantitative values of bone formation and resorption in juveniles, and even less on the effects of immobilization or weightlessness on these parameters. Experiments on previous Cosmos flights have shown that bone formation in the tibia is depressed in young, growing rats (2), but no direct information has been obtained about bone resorption, or any of the other calcium metabolic parameters such as excretion, absorption or net calcium balance. The basis for the present study was to determine the response of calcium homeostasis and bone to weightlessness.

Calcium tracer kinetic methods were used in this study, using non-radioactive calcium isotopes as tracers. Natural calcium is a mixture of the stable isotopes $^{40,42,43,44,46,48}Ca$ in varying percentages, with ^{40}Ca making up the largest fraction (96.94%). The other stable calcium isotopes are present in relatively small amounts, such as ^{46}Ca at 0.0033% and ^{48}Ca at 0.185%. Natural calcium can therefore be considered a bulk isotope (^{40}Ca) labeled with small quantities of stable isotopic tracers (^{46}Ca, ^{48}Ca). In this way, one can consider also that all the skeletal calcium of man or any

other animal is labeled with these stable isotopic tracers, and bone break-down or resorption can be measured directly if one measures the rate of re-lease of one of these tracers from bone into the serum/extracellular fluid pool. The only continuous sources of calcium into the serum pool are bone and the diet (Fig. 1). In the normal situation, both bone and dietary calcium are made up of natural calcium, and thus both are labeled with stable isotopic tracers such as ^{48}Ca. If one removes ^{48}Ca from the diet, however, then it is distinguished from bone calcium by this lack of tracer. This is done by re-placing natural dietary calcium with isotopically-separated ~100% ^{40}Ca. As calcium is excreted from the serum, it is replaced by calcium coming from both bone and the diet, but the only source of ^{48}Ca is the bone. Therefore, the amount of ^{48}Ca in the serum or muscle will fall to a value which represents the fraction of calcium turnover coming directly from bone (Fig. 2).

The primary measurements made in the Cosmos 1129 tracer studies were the ratio of ^{48}Ca to total calcium in muscle (or serum) and the excreta. Continuous tracer administration calcium kinetic methods were used. Bone resorption was measured directly as the release from the skeleton of the stable calcium isotope ^{48}Ca. Endogenous calcium excretion was also measured. The excretion of sodium, potassium, magnesium and zinc was determined to com-pare with the calcium results as an indicator of overall mineral homeostasis.

METHODS AND PROCEDURES

Subject material

A total of 10 rats were used in this study: 5 rats from the flight group killed immediately postflight (1F1-5) and their 5 synchronous controls (1S1-5). Specimens received from the Soviets following flight were the rib cage (left and right sides) from each animal and approximately 50% of each 2-day excreta

collection from each animal. A total of 10 rib cages and 102 fecal specimens were received. The muscle from each rib cage was used as an indicator of tracer activity in the serum because it has been shown that muscle calcium equilibrates rapidly with serum calcium in tracer studies (7).

Diet preparation

In order to use the continuous calcium tracer methods outlined in the introduction, natural dietary calcium had to be replaced with stable, isotopically-separated ^{40}Ca. The major source of calcium in the Soviet flight paste diet was calcium carbonate ($CaCO_3$). When the diet was prepared for the 1F and 1S groups of rats, the natural $CaCO_3$ was replaced with the chemically identical $^{40}CaCO_3$ (99.991% ^{40}Ca, < 0.001% ^{48}Ca). This diet was indistinguishable from the normal paste diet except in its ^{48}Ca content which was approximately zero. Animals were started on this diet at the time of loading into the flight hardware.

Sample preparation

Approximately 50% of each 2-day pooled excreta collection was received dry in a polyethylene vial. These specimens represented pooled urine and feces due to the manner in which excreta collection was done. Virtually all calcium excretion in the rat is through the feces, however, with less than 1 mg/day in the urine. For this reason separation of urine from feces in calcium metabolic studies is not critical and for the purposes of this study the pooled excreta will be referred to as "feces". Each sample was weighed, ground in a mortar and pestle, and dried at 110°C. An aliquot of the dried powder was accurately weighed ($\pm$0.1 mg) into a crucible for ashing. 0.1-0.2 gm of feces was used, depending upon amount received for each sample. Feces

431

were ashed at $600^\circ C$ for 48 hours and the ash was weighed (±0.1 mg). The ash was dissolved in $12N$ HNO_3, taken to dryness, and the residue dissolved in HNO_3 and diluted to either 25 ml or 50 ml depending on sample size. This was the stock solution on which mineral and calcium tracer measurements were made.

The rib cage (left and right sides) of each animal was received frozen. The specimens were thawed and the intercostal muscles were dissected out from between the third and eleventh ribs. Extreme care was taken in the dissection to be sure that no cartilage or bone was included in the muscle samples. To do this only 60-70% of the total musculature was used. Rib cages from left and right sides of each animal were treated as separate specimens, providing a total of 20 samples. Each muscle specimen was placed into a crucible, dried, weighed, ashed at $600^\circ C$ and weighed again to determine ash content. The ashed samples were then dissolved in HNO_3 for tracer analysis.

Tracer and chemical analysis

Total calcium, magnesium, sodium, potassium and zinc were determined in each fecal sample solution using atomic absorption spectrophotometry. Results were expressed in terms of mg of each mineral per gram of dried fecal material and total mg per 2-day collection period.

A 10 ml aliquot of each stock fecal solution was taken for calcium tracer measurements. The sample was adjusted to pH 4-5 with $8N$ NH_4OH. 3 ml of saturated ammonium oxalate (($NH_4)_2C_2O_4$) was added to each solution to precipitate calcium as CaC_2O_4. Solutions were centrifuged and supernate discarded. The precipitate was washed, redissolved and reprecipitated, washed again and finally dissolved in $4N$ HNO_3. 1.00 ml of this solution was used for neutron activation analysis determination of ^{48}Ca content, and

432

and total calcium was determined by atomic absorption on an aliquot of the remaining solution.

Neutron activation analysis for ^{48}Ca was done at the Berkeley Research Reactor, University of California, Berkeley. Each prepared sample was paired with a standard containing a known quantity of ^{48}Ca and irradiated in the Flexorabbit facility of the BRR for 10 minutes at a thermal neutron flux of 1.0×10^{13} $cm^{-2}sec^{-1}$. ^{49}Ca ($t\frac{1}{2}$ 8.7 minutes) was produced by the reaction $^{48}Ca(n,\gamma)^{49}Ca$. Two minutes after irradiation, the samples were counted for 5 minutes (real time) with a high efficiency Ge(Li) detector coupled to a 4096-channel pulse height analyzer. Standards were counted in the same geometry immediately after the sample count was completed. Live counting time of the system was determined using pulser electronics. The intensity of the 3084 keV photopeak from ^{49}Ca was determined in each spectrum using the computer code SAMPO. The quantity of ^{48}Ca in each specimen was determined from sample and standard photopeak intensities, decay times and counting times, and the known standard mass of ^{48}Ca.

RESULTS

The results of the mineral analyses of the excreta calcium, magnesium, sodium, potassium, zinc and ash are presented graphically in Figure 3. Each data point is the mean of the values obtained for the 5 rats in the flight and synchronous control groups. The points are plotted in 2-day collection periods without correcting for actual endogenous excretion periods. Results are expressed in mg per gram of dried feces for the minerals and percent of dry feces for ash. Total fecal material excreted by flight and control groups was not significantly different when averaged over the whole

flight period (10 collections). When averaged over collection periods 2-9, however, the synchronous control animals excreted approximately 14% more feces than flight animals (1.24 g/day vs. 1.09 g/day).

Bone resorption expressed as the fraction of the exchangeable calcium pool coming from bone was 0.690 ± 0.089 in flight animals vs. 0.675 ± 0.085 in controls, measured at the end of the flight period. Fecal excretion of ^{48}Ca/total Ca was 0.159 ± 0.011 for the flight rats and 0.157 ± 0.006 for control rats at the end of the flight period. Endogenous excretion of calcium, based on the measured ^{48}Ca/total Ca ratio and measured total calcium excretion was $29.0 \pm 3.1 \mu g$ ^{48}Ca/day in flight animals and $37.4 \pm 3.2 \mu g$ ^{48}Ca/day in control animals. Bone resorption rate at the end of the flight period was 15.7 mg Ca/day in the flight rats and 20.2 mg Ca/day in the controls.

DISCUSSION

Bone formation in rats is known to be decreased during spaceflight. In normal mineral homeostasis, a decrease in bone formation will lead to a decrease in bone resorption as well, so that bone mass will be maintained. If bone resorption either proceeds at its normal rate or increases, then bone mass will be lost at a rate which is proportional to the difference between formation rate and resorption rate. Estimates of the kinetics of the decrease in bone formation in the rat during spaceflight (3) suggest that formation decreases linearly with time, finally virtually ceasing at 11-12 days of flight. In contrast, the kinetics of bone resorption measured during this experiment as calcium excretion (Fig. 3), suggest that the breakdown of bone in flight rats is maintained at the same level as in control rats until 10-12 days into flight, then starts to decrease, reaching a level which is

20-25% below that for synchronous controls at the end of the flight period. It is significant that resorption normalized by calcium turnover does not decrease during flight, so that the decrease seen in the bone resorption rate is probably secondary to a decrease in total body calcium turnover. These results indicate that in rats during spaceflight, as in immobilized humans, bone formation and bone resorption are uncoupled, and the difference in their rates should lead to significantly less bone mass for flight animals compared to controls. Of particular interest may be the fact that while the bone resorption rate decreases during flight, it is still 75-80% of normal at the end of flight. This may indicate that bone loss on even longer flights will continue unless some method can be found to either turn off resorption completely or turn on formation again.

The excretion of minerals other than calcium show some interesting patterns. Sodium and potassium are virtually identical in their excretion with a consistent rise even until the end of flight when levels were 4-5 times normal. Whether this is decreased absorption or increased endogenous excretion is not known, although a rise of this magnitude would be expected to be due to increased excretion. Zinc excretion is the most consistent of all the elements in the control rats, and in the flight rats shows a rapid rise followed by a gradual fall back to near-normal values.

The continual imbalance of bone formation and breakdown and the large excretion of other minerals from the body during spaceflight indicate that mineral homeostasis does not adapt to weightlessness at least within the time frame studied in this experiment, and that the long-term consequences of weightlessness are not yet known.

ACKNOWLEDGEMENTS

REFERENCES

1. Whedon GD, L Lutwak, PC Rambaut, MW Whittle, MC Smith, J Reid, C Leach, CR Stadler, DD Sanford. 1977. Mineral and nitrogen metabolic studies, experiment M071. In Biomedical Results of Skylab, NASA SP-377, p 164-174.

2. Morey ER and DJ Baylink. Inhibition of Bone Formation During Space Flight. Science 201:1138-1141 (1978).

3. Holton EM, RT Turner, DJ Baylink. 1978. Quantitative Analysis of Selected Bone Parameters. In Final Reports of US Experiments Flown on the Soviet Satellite Cosmos 936, NASA TM-78525, p 135-178.

4. Heaney RP. Radiocalcium metabolism in disuse osteoporosis in man. Amer. J. Med 33:188-200 (1962).

5. Minaire P, P Meunier, C Edouard, J Bernard, P Courpron, J Bourret. Quantitative histological data on disuse osteoporosis. Calcif. Tiss. Res. 17:57-73 (1974).

6. Cann CE and DR Young. Calcium metabolism in disuse osteoporosis in monkeys: continuous tracer and pulse tracer kinetics (abst). Calcif. Tiss. Internat. 28:162 (1979).

7. Cann CE: Unpublished results.
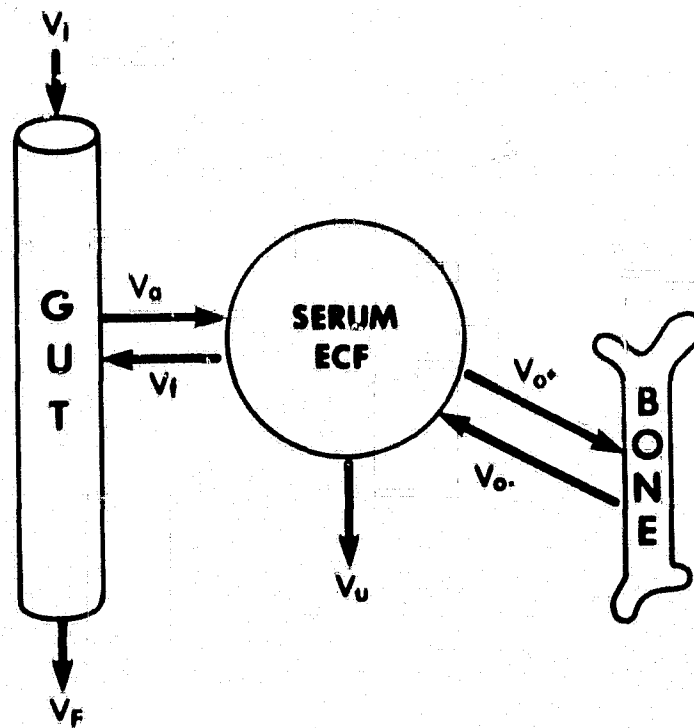
Figure 1. Schematic representation of calcium movement in the body. Calcium enters the serum pool from bone and intestine and leaves via the urine, feces, and bone formation.
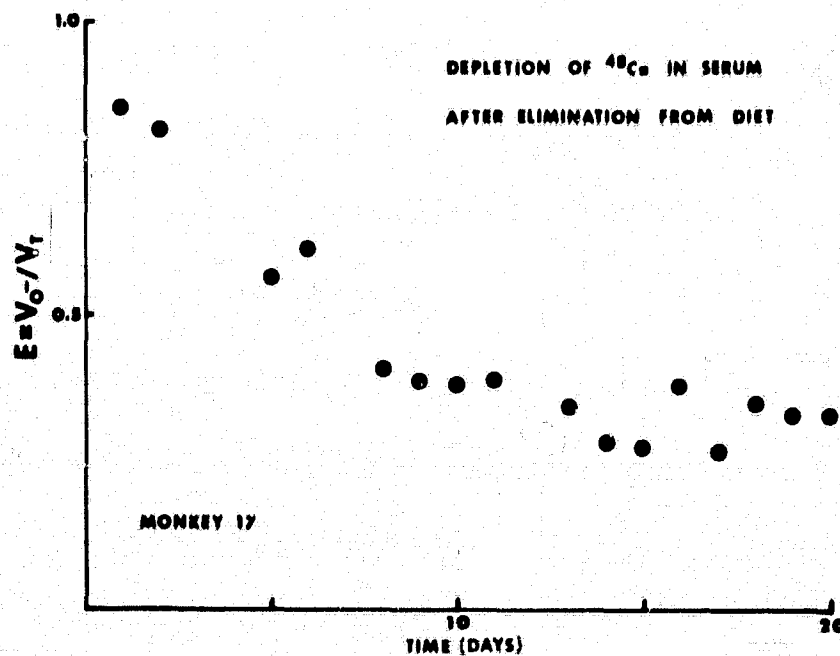

Figure 2. Disappearance of ^{48}Ca from the serum of a monkey with time after elimination from the diet. Asymptotic value represents the fraction of exchangeable calcium coming from bone (6).

437

MINERAL EXCRETION IN RATS DURING SPACEFLIGHT
(Dry weight basis)
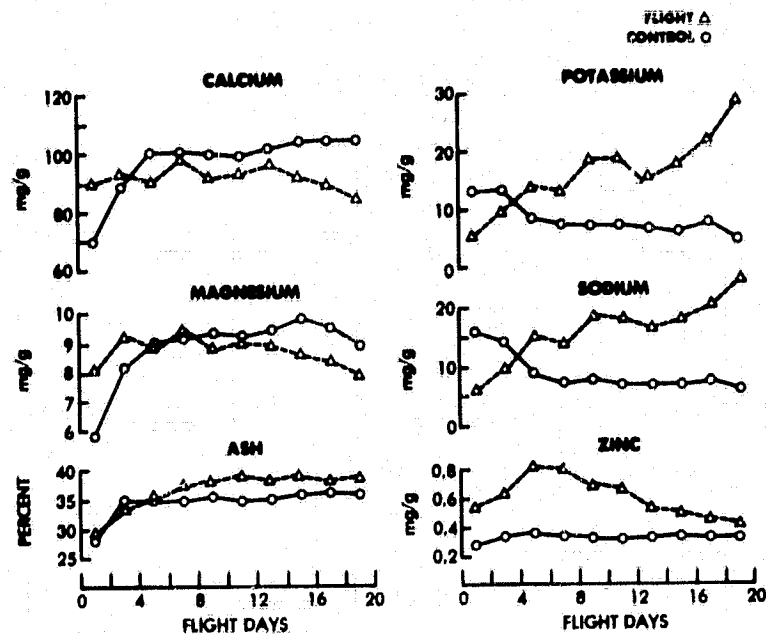
Figure 3. Excretion of Ca, Mg, K, Na, and Zn by flight and control rats. All values are expressed on a dry weight basis.